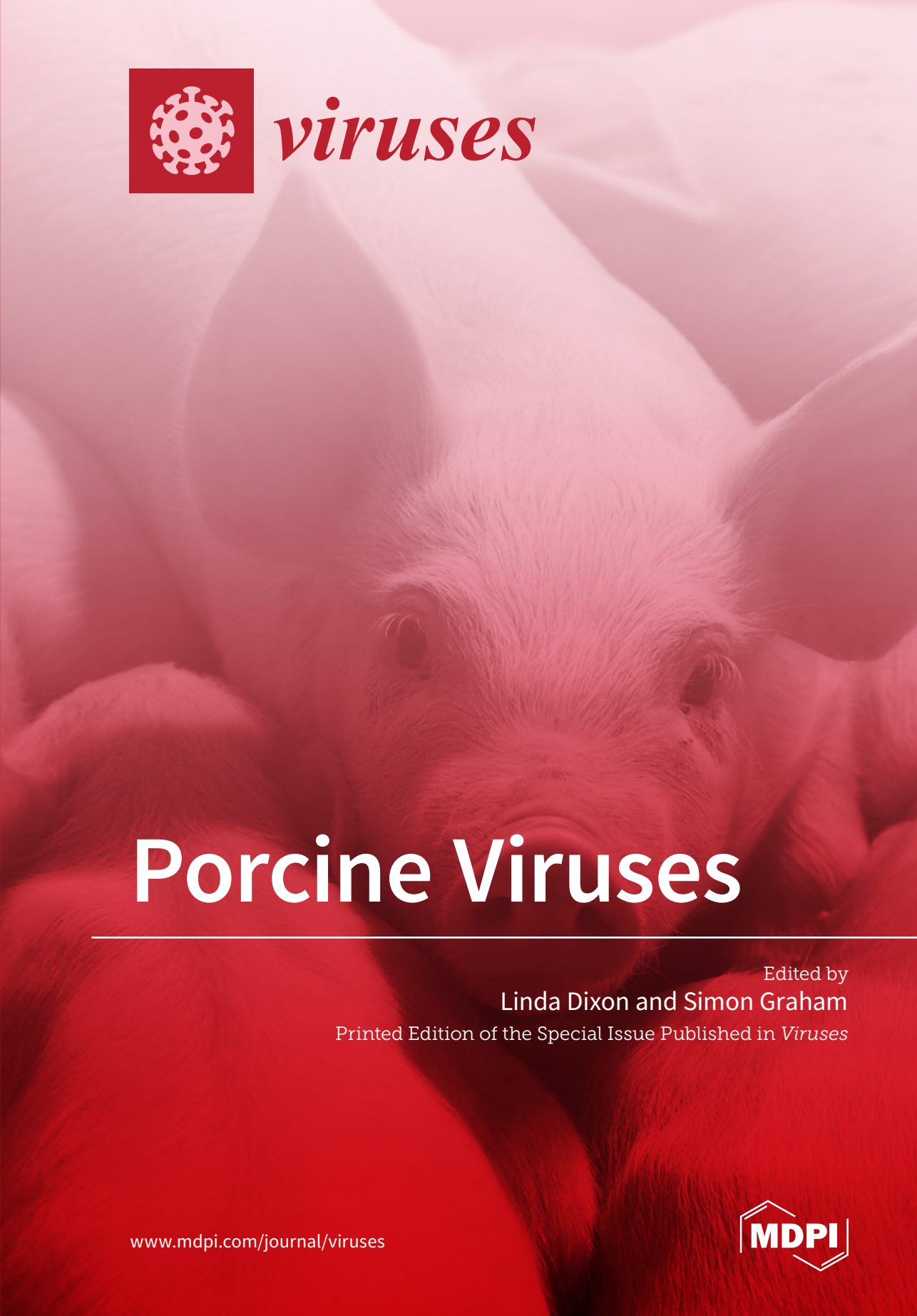

viruses

Porcine Viruses

Edited by
Linda Dixon and Simon Graham

Printed Edition of the Special Issue Published in *Viruses*

www.mdpi.com/journal/viruses

MDPI

Porcine Viruses

Special Issue Editors
Linda Dixon
Simon Graham

MDPI • Basel • Beijing • Wuhan • Barcelona • Belgrade

Special Issue Editors
Linda Dixon
The Pirbright Institute
UK

Simon Graham
The Pirbright Institute
UK

Editorial Office
MDPI AG
St. Alban-Anlage 66
Basel, Switzerland

This edition is a reprint of the Special Issue published online in the open access journal *Viruses* (ISSN 1999-4915) from 2016–2017 (available at: http://www.mdpi.com/journal/viruses/special_issues/porcine_viruses).

For citation purposes, cite each article independently as indicated on the article page online and as indicated below:

Author 1; Author 2. Article title. *Journal Name* **Year**, *Article number*, page range.

First Edition 2017

ISBN 978-3-03842-472-7 (Pbk)
ISBN 978-3-03842-473-4 (PDF)

Articles in this volume are Open Access and distributed under the Creative Commons Attribution license (CC BY), which allows users to download, copy and build upon published articles even for commercial purposes, as long as the author and publisher are properly credited, which ensures maximum dissemination and a wider impact of our publications. The book taken as a whole is © 2017 MDPI, Basel, Switzerland, distributed under the terms and conditions of the Creative Commons license CC BY-NC-ND (http://creativecommons.org/licenses/by-nc-nd/4.0/).

Table of Contents

About the Special Issue Editors vii

Preface to "Porcine Viruses" ix

Sandra Blome, Christoph Staubach, Julia Henke, Jolene Carlson and Martin Beer
Classical Swine Fever—An Updated Review
Reprinted from: *Viruses* **2017**, *9*(4), 86; doi: 10.3390/v9040086 1

Jean-Pierre Frossard, Sylvia Grierson, Tanya Cheney, Falko Steinbach, Bhudipa Choudhury and Susanna Williamson
UK Pigs at the Time of Slaughter: Investigation into the Correlation of Infection with PRRSV and HEV
Reprinted from: *Viruses* **2017**, *9*(6), 110; doi: 10.3390/v9060110 26

Inmaculada Galindo and Covadonga Alonso
African Swine Fever Virus: A Review
Reprinted from: *Viruses* **2017**, *9*(5), 103; doi: 10.3390/v9050103 35

Obdulio García-Nicolás, Meret E. Ricklin, Matthias Liniger, Nathalie J. Vielle, Sylvie Python, Philippe Souque, Pierre Charneau and Artur Summerfield
A Japanese Encephalitis Virus Vaccine Inducing Antibodies Strongly Enhancing In Vitro Infection Is Protective in Pigs
Reprinted from: *Viruses* **2017**, *9*(5), 124; doi: 10.3390/v9050124 45

Anbu K. Karuppannan and Tanja Opriessnig
Porcine Circovirus Type 2 (PCV2) Vaccines in the Context of Current Molecular Epidemiology
Reprinted from: *Viruses* **2017**, *9*(5), 99; doi: 10.3390/v9050099 60

Michael C. Rahe and Michael P. Murtaugh
Mechanisms of Adaptive Immunity to Porcine Reproductive and Respiratory Syndrome Virus
Reprinted from: *Viruses* **2017**, *9*(6), 148; doi: 10.3390/v9060148 75

Elma Tchilian and Barbara Holzer
Harnessing Local Immunity for an Effective Universal Swine Influenza Vaccine
Reprinted from: *Viruses* **2017**, *9*(5), 98; doi: 10.3390/v9050098 94

Anastasia N. Vlasova, Joshua O. Amimo and Linda J. Saif
Porcine Rotaviruses: Epidemiology, Immune Responses and Control Strategies
Reprinted from: *Viruses* **2017**, *9*(3), 48; doi: 10.3390/v9030048 109

Yen-Chen Chang, Chi-Fei Kao, Chia-Yu Chang, Chian-Ren Jeng, Pei-Shiue Tsai, Victor Fei Pang, Hue-Ying Chiou, Ju-Yi Peng, Ivan-Chen Cheng and Hui-Wen Chang
Evaluation and Comparison of the Pathogenicity and Host Immune Responses Induced by a G2b Taiwan Porcine Epidemic Diarrhea Virus (Strain Pintung 52) and Its Highly Cell-Culture Passaged Strain in Conventional 5-Week-Old Pigs
Reprinted from: *Viruses* **2017**, *9*(5), 121; doi: 10.3390/v9050121 136

Miguel Ángel Cuesta-Geijo, Lucía Barrado-Gil, Inmaculada Galindo, Raquel Muñoz-Moreno and Covadonga Alonso
Redistribution of Endosomal Membranes to the African Swine Fever Virus Replication Site
Reprinted from: *Viruses* **2017**, *9*(6), 133; doi: 10.3390/v9060133.....151

Joachim Denner and Annette Mankertz
Porcine Circoviruses and Xenotransplantation
Reprinted from: *Viruses* **2017**, *9*(4), 83; doi: 10.3390/v9040083.....163

Hui Dong, Xin Zhang, Hongyan Shi, Jianfei Chen, Da Shi, Yunnuan Zhu and Li Feng
Characterization of an Immunodominant Epitope in the Endodomain of the Coronavirus Membrane Protein
Reprinted from: *Viruses* **2016**, *8*(12), 327; doi: 10.3390/v8120327.....176

Alyssa B. Evans, Hyelee Loyd, Jenelle R. Dunkelberger, Sarah van Tol, Marcus J. Bolton, Karin S. Dorman, Jack C. M. Dekkers and Susan Carpenter
Antigenic and Biological Characterization of ORF2–6 Variants at Early Times Following PRRSV Infection
Reprinted from: *Viruses* **2017**, *9*(5), 113; doi: 10.3390/v9050113.....192

Xiaozhen Guo, Mengjia Zhang, Xiaoqian Zhang, Xin Tan, Hengke Guo, Wei Zeng, Guokai Yan, Atta Muhammad Memon, Zhonghua Li, Yinxing Zhu, Bingzhou Zhang, Xugang Ku, Meizhou Wu, Shengxian Fan and Qigai He
Porcine Epidemic Diarrhea Virus Induces Autophagy to Benefit Its Replication
Reprinted from: *Viruses* **2017**, *9*(3), 53; doi: 10.3390/v9030053.....212

Raquel A. Leme, Alice F. Alfieri and Amauri A. Alfieri
Update on Senecavirus Infection in Pigs
Reprinted from: *Viruses* **2017**, *9*(7), 170; doi: 10.3390/v9070170.....228

Su Li, Jinghan Wang, Qian Yang, Muhammad Naveed Anwar, Shaoxiong Yu and Hua-Ji Qiu
Complex Virus–Host Interactions Involved in the Regulation of Classical Swine Fever Virus Replication: A Minireview
Reprinted from: *Viruses* **2017**, *9*(7), 171; doi: 10.3390/v9070171.....242

Vladimir A. Morozov, Gerd Heinrichs and Joachim Denner
Effective Detection of Porcine Cytomegalovirus Using Non-Invasively Taken Samples from Piglets
Reprinted from: *Viruses* **2017**, *9*(1), 9; doi: 10.3390/v9010009.....257

Leopold K. Mulumba–Mfumu, Jenna E. Achenbach, Matthew R. Mauldin, Linda K. Dixon, Curé Georges Tshilenge, Etienne Thiry, Noelia Moreno, Esther Blanco, Claude Saegerman, Charles E. Lamien and Adama Diallo
Genetic Assessment of African Swine Fever Isolates Involved in Outbreaks in the Democratic Republic of Congo between 2005 and 2012 Reveals Co-Circulation of p72 Genotypes I, IX and XIV, Including 19 Variants
Reprinted from: *Viruses* **2017**, *9*(2), 31; doi: 10.3390/v9020031.....271

Wen Shi, Wenlu Fan, Jing Bai, Yandong Tang, Li Wang, Yanping Jiang, Lijie Tang, Min Liu, Wen Cui, Yigang Xu and Yijing Li
TMPRSS2 and MSPL Facilitate Trypsin-Independent Porcine Epidemic Diarrhea Virus Replication in Vero Cells
Reprinted from: *Viruses* **2017**, *9*(5), 114; doi: 10.3390/v9050114.....286

Wen Shi, Shuo Jia, Haiyuan Zhao, Jiyuan Yin, Xiaona Wang, Meiling Yu, Sunting Ma, Yang Wu, Ying Chen, Wenlu Fan, Yigang Xu and Yijing Li
Novel Approach for Isolation and Identification of Porcine Epidemic Diarrhea Virus (PEDV) Strain NJ Using Porcine Intestinal Epithelial Cells
Reprinted from: *Viruses* **2017**, *9*(1), 19; doi: 10.3390/v9010019.....303

About the Special Issue Editors

Simon Graham, Group Leader and Senior Lecturer, received his PhD from the Liverpool School of Tropical Medicine, where he developed a cattle model for testing vaccines against onchocerciasis. After post-doctoral positions working on vaccine development for Theilerioses at the Centre for Tropical Veterinary Medicine, Edinburgh, and the International Livestock Research Institute, Kenya, Simon joined the Virology Department of the Animal and Plant Health Agency, Weybridge, as a research fellow in immunology. In 2014, he took up the joint position of Group Leader (Porcine reproductive and respiratory syndrome, PRRS Immunology) at The Pirbright Institute and Senior Lecturer in Veterinary Immunology, within the School of Veterinary Medicine at the University of Surrey. Simon's research is focused on improving our understanding of the interactions of the PRRS virus with the porcine immune system and the development of improved vaccines.

Linda Dixon, Group Leader, received her PhD in Molecular Biology at Edinburgh University. She carried out postdoctoral research at Edinburgh University and The Friedrich Miescher Institute, Basel, Switzerland. Linda joined the Pirbright Institute to lead a group working on African swine fever virus (ASFV). Her research interests include functional genomics of ASFV and in particular the characterization of virus proteins which inhibit host defenses including type I interferon and cell death pathways. The role of these proteins on manipulation of host responses during virus infection of macrophages and infection in pigs is of particular interest. Linda is also actively engaged in development of vaccines for ASFV.

Preface to "Porcine Viruses"

Pig production is the fastest growing segment of the global livestock sector. Intensification of pig production has resulted in significant changes to traditional pig husbandry practices. Combined with urbanization and ease of travel and transport, these changes have led to an environment conducive to increased emergence and spread of viral diseases. The past decade alone has seen the global emergence and re-emergence of porcine viruses with devastating consequences: For example, in 2006, highly pathogenic porcine reproductive and respiratory syndrome viruses (PRRSV) spread rapidly across Southeast Asia killing millions of animals; since its introduction into the Caucasus in 2007, the African swine fever virus has steadily spread to Eastern Europe; and in 2013–2014, over 8 million pigs died when virulent porcine epidemic diarrhea virus (PEDV) swept across North America. In this Special Issue, we will explore our understanding of porcine viruses and how this may be exploited to improve the control of these pathogens of economic and agricultural significance.

Linda Dixon and Simon Graham
Special Issue Editors

viruses

MDPI

Review

Classical Swine Fever—An Updated Review

Sandra Blome [1,*], Christoph Staubach [2], Julia Henke [1], Jolene Carlson [1] and Martin Beer [1]

[1] Friedrich-Loeffler-Institut, Institute of Diagnostic Virology, Suedufer 10, 17493 Greifswald, Germany; julia.henke@fli.de (J.H.); jolene.carlson@fli.de (J.C.); martin.beer@fli.de (M.B.)

[2] Friedrich-Loeffler-Institut, Institute of Epidemiology, Suedufer 10, 17493 Greifswald, Germany; christoph.staubach@fli.de

* Correspondence: sandra.blome@fli.de; Tel.: +49-38351-7-1144

Academic Editors: Linda Dixon and Simon Graham
Received: 8 March 2017; Accepted: 13 April 2017; Published: 21 April 2017

Abstract: Classical swine fever (CSF) remains one of the most important transboundary viral diseases of swine worldwide. The causative agent is CSF virus, a small, enveloped RNA virus of the genus *Pestivirus*. Based on partial sequences, three genotypes can be distinguished that do not, however, directly correlate with virulence. Depending on both virus and host factors, a wide range of clinical syndromes can be observed and thus, laboratory confirmation is mandatory. To this means, both direct and indirect methods are utilized with an increasing degree of commercialization. Both infections in domestic pigs and wild boar are of great relevance; and wild boars are a reservoir host transmitting the virus sporadically also to pig farms. Control strategies for epidemic outbreaks in free countries are mainly based on classical intervention measures; i.e., quarantine and strict culling of affected herds. In these countries, vaccination is only an emergency option. However, live vaccines are used for controlling the disease in endemically infected regions in Asia, Eastern Europe, the Americas, and some African countries. Here, we will provide a concise, updated review on virus properties, clinical signs and pathology, epidemiology, pathogenesis and immune responses, diagnosis and vaccination possibilities.

Keywords: porcine viruses; *Pestivirus*; classical swine fever; clinical signs; pathogenesis; epidemiology; diagnosis; control; vaccination; marker strategy

1. Introduction

Classical swine fever (CSF) is one of the most important viral diseases of domestic pigs and wild boar. It has tremendous impact on animal health and pig industry and is therefore notifiable to the World Organization for Animal Health (OIE) [1]. After implementation of strict control measures, several countries succeeded in eradicating CSF. Nevertheless, in most parts of the world with significant pig production, CSF is at least sporadically present. Endemicity can be assumed in several countries of South and Central America, parts of Eastern Europe and neighboring countries, as well as Asia, including India. Little is known about the African situation.

A binding legal framework exists for the surveillance and control in most countries. Integral parts of the control measures are timely and reliable diagnosis, stamping out of infected herds, establishment of restriction zones, movement restrictions, and tracing of possible contacts. Prophylactic vaccination and other treatments are often also strictly prohibited. However, in Europe, where affected wild boar populations were shown to be an important reservoir for the virus, and acted as a source for reintroduction into the domestic pig population [2,3], emergency vaccination of wild boar has been practiced to control the disease [4–7]. Emergency vaccination is also among the options to combat CSF in domestic animals. Furthermore, vaccination is still in use to reduce the disease burden in endemically affected countries.

Design of control measures and risk assessment depends on the knowledge of factors that influence disease dynamics and epidemiology. For this purpose, the presented review aims at providing an updated overview on the disease and the underlying mechanisms but also control and diagnostic options.

2. Virus Properties

2.1. Virus Organization and Replication

Classical swine fever virus (CSFV) belongs to the genus *Pestivirus* within the *Flaviviridae* family [1]. Other members of this genus are *Bovine viral diarrhea virus* 1 and 2 (BVDV-1 and -2), *Border disease virus* (BDV) and a growing number of unclassified and so-called atypical pestiviruses, from giraffe-virus over HoBi-like viruses to recently discovered Bungowannah virus and atypical porcine pestivirus [2–13].

The enveloped viral particles consist of four structural proteins, namely the core protein (C), and envelope glycoproteins E1, E2, and E^{rns} [14–18]. The core encloses the positive single-stranded RNA genome of approximately 12.3 kb [19–22] which is translated into one polyprotein. The coding region is flanked by non-translated regions (NTR) at both ends. Co- and post-translational processing of the precursor protein by viral and cellular proteases results in 13 mature proteins, the above-mentioned structural proteins and non-structural proteins N^{pro}, p7, NS2-3, NS2, NS3, NS4A, NS4B, NS5A, and NS5B. The latter have various functions in the viral replication, e.g., NS5B represents the RNA-dependent RNA polymerase [23] and NS3 acts as protease [24,25].

Virus replication takes place in the cytoplasm after receptor mediated endocytosis and does normally not lead to a cytopathic effect in cell culture (naturally occurring CSFV strains were found to be non-cytopathic) [26]. A putative receptor is the porcine complement regulatory protein cluster of differentiation (CD) 46 that was shown to play a major role in CSFV attachment, together with heparan sulfates [27]. Upon cell culture adaptation an increased usage of heparin sulfates is observed for cell-virus interaction [28]. The mutation responsible for the adaptation lies within the E^{rns} encoding region [8], namely in the C-terminus where a Ser residue is replaced by an Arg residue at amino acid 476 in the polyprotein of CSFV.

In any case, glycoproteins E2 and E^{rns} are necessary for viral attachment [9,10], and the initial contact with the host cell is mediated through the E^{rns} which interacts with glycosaminoglycans [10,11]. For receptor binding and subsequent endocytosis, the E2-E1 heterodimer is essential [12]. After fusion of the virus envelope with the endosomal membrane, the virus core is released into the cytoplasm [13–15]. Thereafter, viral RNA is released into the cytoplasm and translation takes place. The binding of ribosomes at the rough endoplasmatic reticulum is realized through an internal ribosomal entry site (IRES) at the 5′ NTR, which allows a cap-independent translation [16–18]. The processing of the resulting viral polyprotein precursor occurs with the help of viral and cellular proteases [19]. Initially, autoproteinase N^{pro} is cleaved from the polyprotein [20,21]. Subsequently, cellular proteases cleave the C-protein and E^{rns}, E1 and E2, E2 and p7 as well as NS2-3. NS2-3 is then partially processed through the autocatalytic cysteine protease activity of NS2 into NS2 and NS3. In this way NS2 generates its own C-terminal ending [22,23]. The serine protease activity of NS3 leads to the cleavage of the rest of the NS3-NS5 region [24]. While replication progresses, negative-stranded RNA is generated, which serves as template for the synthesis of the positive stranded RNA. The positive stranded RNA is then packed into the capsid [25]. Virion assembly and maturation takes place in the endoplasmatic reticulum and the Golgi apparatus after which the progeny virions bud at the cell membrane through exocytosis [26,27].

2.2. Tenacity and Virus Inactivation

The survival of CSFV under different ambient conditions varies considerably and is influenced especially by the temperature but also by the matrix in which it is found. Generally, survival times

are higher under cold, moist and protein rich conditions [28]. The dependence of viral survival and temperature is well studied [29–31].

For animal disease control, survival in excretions (left in the pen or stored as slurry) and stability in meat products are crucial parameters. For CSFV in excretions, survival times were demonstrated that range from a few days at room temperature to several weeks at 5 °C [32]. If temperatures are higher than 35 °C, survival times are dramatically reduced, and inactivation occurs in hours or even minutes from temperatures above 50 °C [33]. This is an important factor when biogas plants and other industry parts are discussed. Along the same lines, Botner and Belsham [34] could show that survival of CSFV in slurry was short when heated and remained infective for weeks at cool temperature. Turner showed that complete inactivation was achieved at 60 °C for 3 min under lab conditions [35]. However, homogeneity of the mixture that is to be inactivated and thus temperature distribution is crucial [36]. For contaminated pig pens, this can mean virus survival for at least several days [37] to one month under cold winter conditions [38]. Under laboratory conditions, freeze-thawing has a negative impact on viral titers which can however be prevented by some chemical compounds such as dimethyl sulfoxide [39]. With regard to pH values, CSFV is relatively stable between pH 5 and 10. Half-lives at low pH levels are temperature dependent with mean half-lives that are more than ten-fold lower at room temperature compared to 4 °C (70 h at 4 °C compared to 5 h at 21 °C for pH 3). Overall variability is high and shows some strain dependence [40]. Another important matrix is meat or downstream products. Farez and Morley [30] report virus survival over years in meat frozen at −70 °C and of days to years in different meat products. Survival of 4.5 years in frozen meat was also reported by Edgar (reviewed in the EFSA scientific report 2009, [28]). Curing and smoking alone have little effect on the virus while higher temperatures readily inactivate the virus [31]. Survival times of more than 75 days were reported for salami [41] and over 120 days for Iberian loins or shoulders [42].

2.3. Genetic Diversity and Virulence Factors

Classical swine fever virus strains can be divided into three genotypes with three to four sub-genotypes. The most recently added sub-genotype 1.4 was only very recently described for CSFV strains from Cuba. These strains had so far been placed into sub-genotype 1.2 but formed a distinct cluster when compared based on longer genome fragments, e.g., full-length E2, N^{pro}, C, E1, and E^{rns} [43]. Further divisions that have been proposed concern sub-genotypes 2.1 and 2.3 [44–47]. However, these systems of clusters or clades were not further harmonized and did not enter routine use. The genetic diversity does not result in true serotypes and does not impact vaccine efficacy. In general, CSFV is highly stable, especially for an RNA virus [48].

Up to very recently, phylogenetic studies were mainly based on two short fragments, namely a 150 nucleotide (nt) fragment of the 5′NTR and a 190 nt fragment of the E2 encoding region [49]. Moreover, a 409 nt fragment of the region coding for the polymerase gene NS5B was employed [50]. With the advent of affordable sequencing technologies for longer fragments or even full genomes, in-detail analyses are now more often based on more than the traditional fragments. The European Union (EU) Reference Laboratory for CSF nowadays recommends using full-length E2 encoding sequences for reliable CSFV phylogenies [51]. The latter resulted, e.g., in the designation of the above-mentioned new sub-genotype 1.4. Full-length sequences are being employed for quasispecies analyses, investigation of virulence determinants but also high resolution molecular epidemiology [52–55].

The distribution of genotypes shows a distinct geographical pattern [50,56]: Whereas isolates belonging to group 3 seem to occur solely in Asia, all European CSFV isolates of the 1990s and later belonged to one of the subgroups within group 2 (2.1, 2.2, or 2.3) [45,51,57–64] and were clearly distinct from former CSF reference viruses, which belong to group 1 [50,65]. On the global scale, the most prevalent genotype over the last decades was undoubtedly genotype 2 [66]. However, all field isolates from the American continent belong to genotype 1 with only 1.1 strains from Argentina, Brazil, Colombia, and Mexico; 1.3 strains from Honduras and Guatemala; and the above-mentioned

sub-genotype 1.4 strains from Cuba [43,67–69]. Little is known about the CSF situation in Africa and the Middle East. Exceptions are the 2005 outbreak in South Africa and the 2009 outbreak in Israel that were both caused by 2.1 CSFV strains [70,71]. Reports from India are increasingly detailed and demonstrate that sub-genotypes 1.1, 2.1, and 2.2 are co-circulating [72–79]. This changes the historical situation where genotype 1.1 strains predominated. From Nepal, strains of sub-genotype 2.2 were reported [80]. The situation in China is characterized by high variability of strains that belong mainly to sub-genotypes 1.1, 2.1, 2.2, and 2.3 [81–84]. Taiwan is also experiencing a change in sub-genotypes. It seems that the historical 3.4 strains are replaced by the Chinese 2.1 strains [85]. However, Taiwanese reports include all the above-mentioned sub-genotypes [85–87]. Sub-genotype 2.1 and 2.2 strains are also reported from Laos [88,89]. From Korea, strains of sub-genotypes 3.2 and 2.1 were reported [44], and, for Japan, indications exist that genotype 3 is found [90]. Generally, endemicity is accompanied or driven by strains of moderate or low virulence. These strains have been found in several regions with long-term circulation of CSFV (e.g., Cuba [91]), and mathematical models have shown that these strains may represent the viral optimum for long-term persistence [92]. An overview of the genotype distribution is provided in Figure 1.

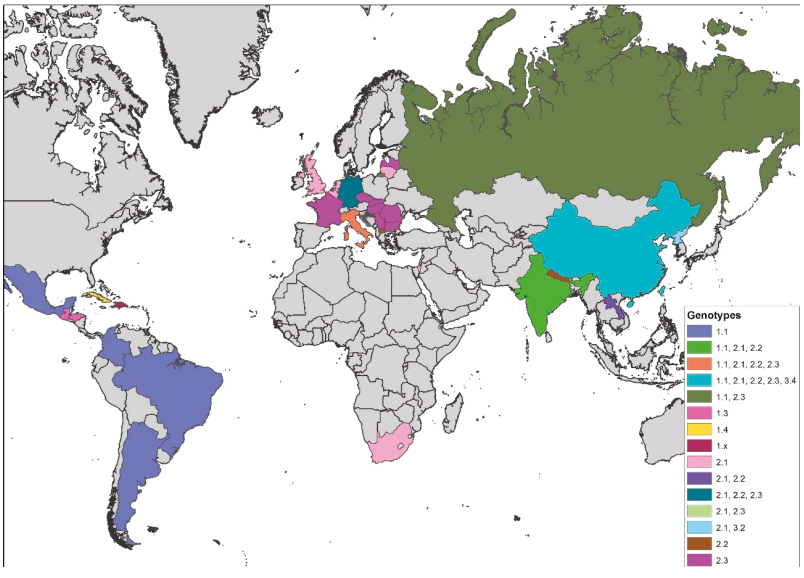

Figure 1. Global distribution of classical swine fever virus (CSFV) sub-genotypes (map based on Global Administrative Areas (GADM database 2.8; November 2015)).

European CSFV sequences were collected and made available through the semi-public CSF-database (DB) at the EU and OIE reference laboratory for CSF in Hannover, Germany [49,93–95]. Since the Institute of Virology became European Reference Laboratory for CSF more than 30 years ago, the virus isolates involved in European outbreaks but also other accessible sequence data were collected and stored. The database includes the above-mentioned fragments and also partial NS5B, full E2, and full-length CSFV sequences. It also allows automated typing and retrieval of sequences for in-detail analyses [95].

The search for virulence markers indicated a role of the N^{pro} [96], the E2 [97], the ribonuclease activity and dimerization of the E^{rns} [98,99], and NS4B [100]. Furthermore, glycosylation of structural proteins was shown to affect virulence [101–105]. However, these determinants are still far from being understood and do not seem to be transferrable among strains. Even the direct comparison of vaccine

strains and their virulent ancestors did not reveal clear pattern [100,106]. Investigations into the role of quasispecies composition did not lead to the establishment of a clear correlation between variability and virulence [52]. There were also no predictors for different disease courses found [107].

3. Clinical Signs and Pathomorphological Lesions

Classical swine fever can be divided into the following forms of the disease: an acute (transient or lethal), a chronic and a persistent course, which usually requires infection during pregnancy [65]. In general, the same clinical signs are seen in both domestic pigs and wild boar, and show up after an incubation period of four to seven (seldom 10) days after the infection. The progression is dependent on strain virulence, host responses, and secondary infections and may vary considerably. However, infection of young pigs (weaners) with a moderately virulent CSFV strain may serve as an example for the acute disease course: During the first two weeks upon infection, the acute phase is characterized by unspecific (often referred to as "atypical") clinical signs like high fever, anorexia, gastrointestinal symptoms, general weakness, and conjunctivitis [108]. Around two to four weeks after infection neurological signs can occur including incoordination, paresis, paralysis and convulsions. At the same time, skin hemorrhages or cyanosis can appear in different locations of the body such as the ears, limbs, and ventral abdomen. These late signs are the textbook cases and are therefore referred to as "typical" CSF signs. Examples of clinical signs can be found in Figure 2.

In acute-lethal courses, death usually occurs 2–4 weeks after CSFV infection. Mortality can reach up to 100% from 10 to 30 days depending on the age of the animal and the virulence of the virus strain [65,109–111]. Due to the immunosuppressive character of CSF infection, severe respiratory and gastrointestinal secondary infections can complicate the disease course and overlay the CSF signs. This is particularly important for clinical diagnosis. Infections with highly virulent CSFV strains such as "Margarita" or "Koslov" (the ones that are often used for vaccine testing) show a less age-dependent clinical course and may result in 100% mortality in all age classes of animals and severe neurological signs within 7 to 10 days (see, e.g., [112]).

Chronic course occurs when an infected pig is not able to mount an adequate immune response. In general, only non-specific clinical signs are observed in infected animals like remittent fever, depression, wasting and diffuse dermatitis (see Figure 3). It is acknowledged opinion that all chronically infected animals will eventually die. However, they can live for month in which they constantly shed high amounts of virus. Affected animals may develop antibodies that are in some cases only intermittently present and do not effect viral clearance. This, together with persistent infection, can play a role especially for affected wild boar populations [113–115], but also in endemically affected regions with constant virus circulation. Host rather than viral factors seem to play a role for the establishment of chronic infection [107].

When infection occurs during pregnancy, the virus can also infect the fetus in the womb due to its ability to pass the placental barrier which in turn might lead to persistent infection in the piglets. While the sows often show only mild clinical signs, an infection depending on the stage of gestation, leads to absorption or mummification of the fetuses and to abortions or stillbirth [114,116–123]. When infected between days 50 and 70 of pregnancy, an immunotolerance phenomenon can be induced and persistently infected offspring are born. The problem is that those piglets seem to be healthy and survive for several months but die due to the so-called late onset form of CSF. During that period they shed high viral loads which are sufficient for transmission. Recent studies discuss that persisting infection can also be induced when infecting newborn piglets within the first eight hours of life or even 48 h after birth [124,125]. This was shown to impact on the efficacy of vaccines and may complicate control in endemically affected countries.

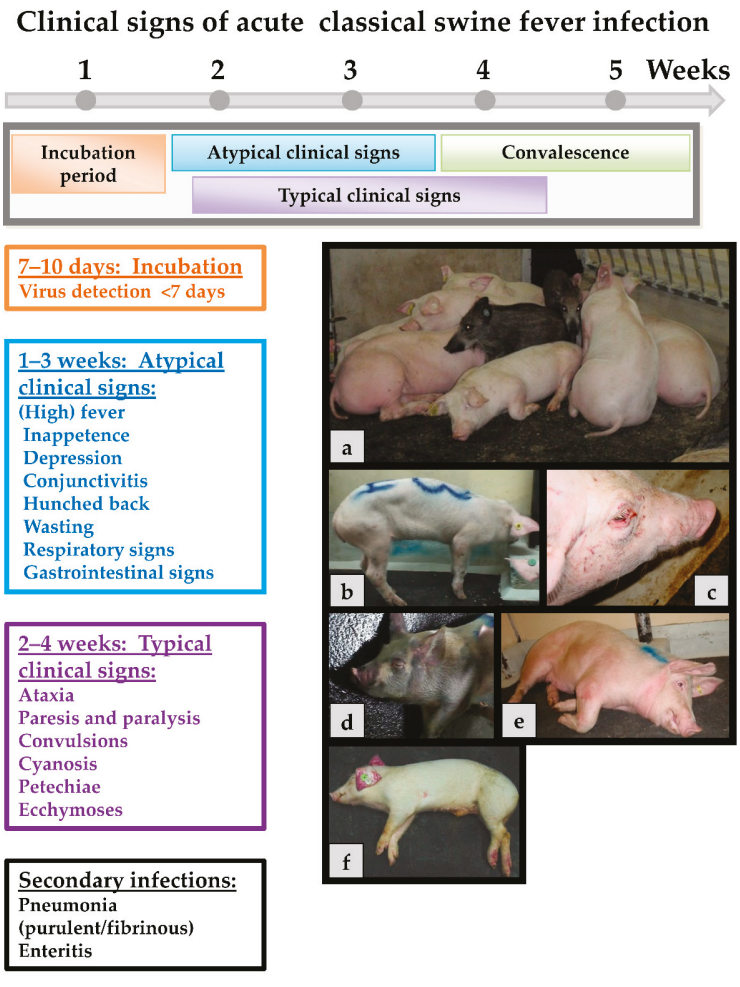

Figure 2. Acute CSFV infection with moderately virulent strains. The incubation period in most cases is from 7 to 10 days. Atypical clinical signs range from one to two weeks. Typical clinical signs occur around 2 to 4 weeks. The convalescent period is from 3 to 4 weeks. Death can occur as late as five weeks post-infection. (**a**) Swine are huddling, 10–15 days post-infection; (**b**) swine are presenting with hunched back; (**c**) severe conjunctivitis; (**d**) severe cyanosis of the skin around the face, ears, and limbs; (**e**) neurological signs, swine was unable to stand; and (**f**) dead swine with classic cyanosis of the ears.

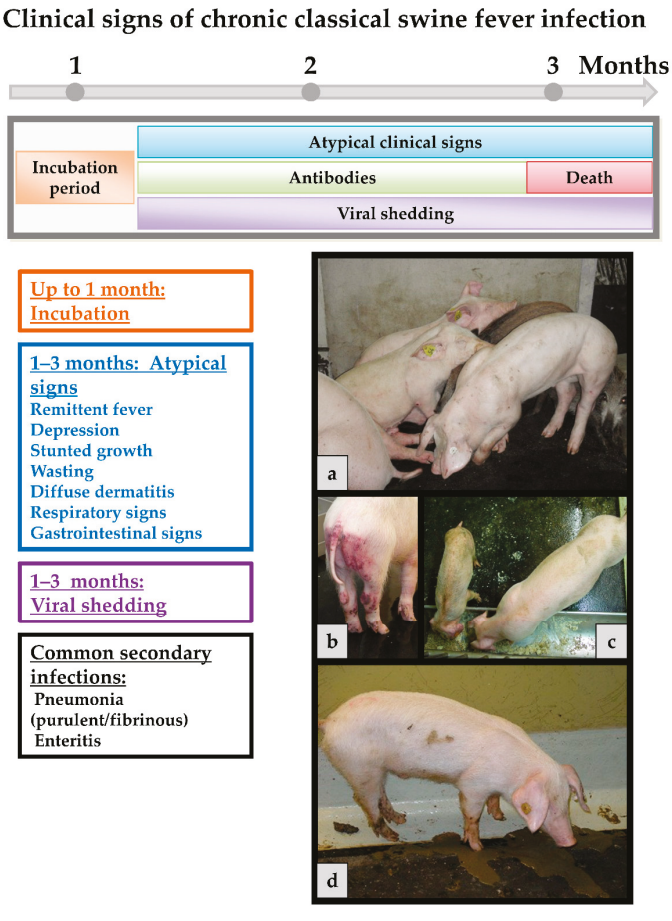

Figure 3. Chronic CSFV infection. The incubation period is the same as with the acute course. However, it may take up to a month until they are truly recognized. Atypical clinical signs can be present throughout and until death, occurring up to three months or even later after the infection. Antibodies can be detected at low levels after two weeks or later but do usually not persist. Viral shedding is observed from about four days post infection till the death of the animal. (**a**) Pigs are depressed, hunched over, and anorexic; (**b**) pig with petechial bleedings and ecchymosis in the anogenital region; (**c**) stunted and wasting pig beside a normally developed one of the same age; and (**d**) pig with diarrhea, shedding high viral loads until death.

The pathological findings (Figure 4) depend on the course of the viral infection. In the acute course of CSF, pathology often reveals enlarged lymph nodes, hemorrhages and petechiae on serosal and mucosal surfaces of different organs such as the, lungs, kidneys, intestines and urinary bladder. Tonsillitis, necrotic ulcers in the intestines, lesions in the lymphoreticular system, and non-purulent encephalitis can be observed [126] Splenic infarctions can occur and are considered pathognomic for CSF [127]. Infected piglets develop leukopenia, thrombocytopenia and immunosuppression, which increases the risk for secondary infections and thus to diseases of the gastrointestinal and respiratory system [128]. In the chronic form, pathological lesions include atrophy of the thymus, depletion of the lymphoid organs, necrosis and ulceration of the small intestine, colon, and ileocecal valve. It is important to consider that these clinical signs and pathological lesions should be considered as

differentials for a number of swine pathogens. These unspecific clinical signs and lesions can vary among animals depending on host factors and the virulence of the CSFV strain. Often, the age, breed and immune status play a role in the outcome of the disease [65,108,129].

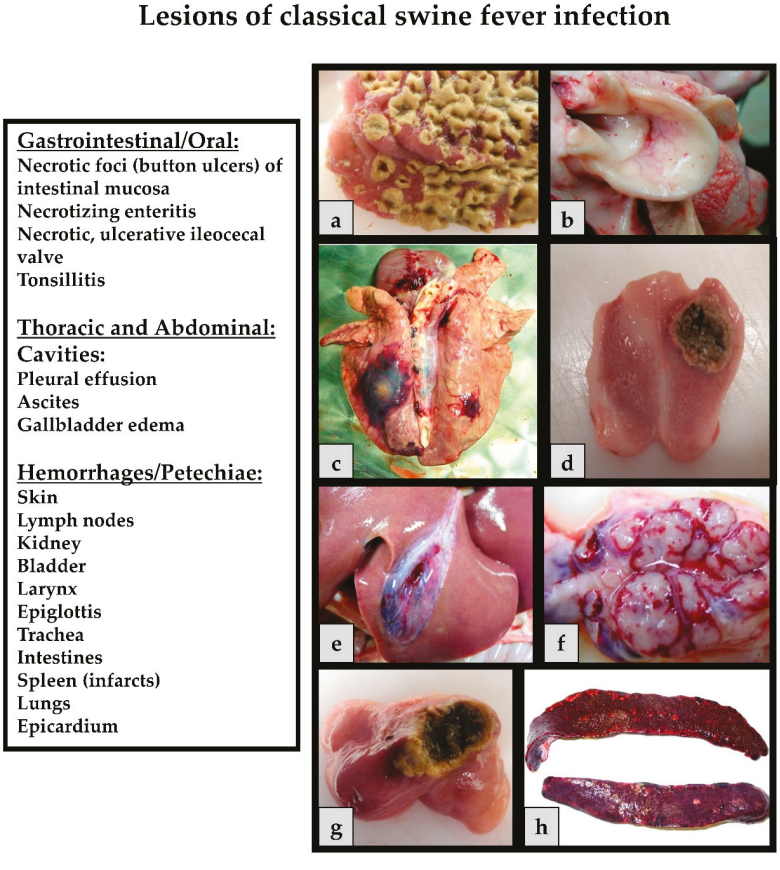

Figure 4. CSF related lesions: (**a**) Diphtheroid-necrotizing enteritis; (**b**) hemorrhages on the epiglottis; (**c**) severe secondary infections of the lung (*Actinobacillus pleuropneumoniae*); (**d**) necrotic tonsillitis with an ulcer; (**e**) gallbladder edema; (**f**) hemorrhagic lymph node; (**g**) necrotizing ileocecal valve; and (**h**) splenic infarcts.

4. Pathogenesis and Immune Responses

As mentioned above, clinical signs of CSFV infections can vary considerably from peracute deaths to unapparent courses depending on virulence of the virus strain involved and different (partly unknown) host factors [65]. Unspecific clinical signs predominate, and differentiation from several other infectious diseases of swine is only possibly based on laboratory diagnosis. Acute-lethal forms can be viral hemorrhagic fever-like with severe thrombocytopenia, pulmonary edema, petechial bleedings, and increased vascular leakage [130]. Cytokine involvement is discussed for many lesions observed in acute CSF [131].

Infection with CSFV is followed by primary replication in the tonsils and subsequently spread to surrounding lymphoid tissues [132]. The virus reaches the regional lymph nodes through lymphatic vessels. Here further replication takes place and the virus is spread via blood to secondary replication

sites such as spleen, bone marrow, and visceral lymph nodes [133–135]. Apoptotic reactions as well as phagocytic and secretory activation can be observed in several macrophage populations [136–144]. These activated macrophages seem to play a crucial role in (immuno-)pathogenesis while direct damage by the virus could be almost excluded for many lesions occurring in the course of CSFV infection. Moreover, dendritic cells are targeted and disturbance of the interferon system contributes to the pathogenesis [136–140]. There seems to be a correlation between high interferon (IFN)-α in the serum and disease severity and virulence of the strain involved [140,141]. High IFN-α concentrations are found as early as two days post infection, prior to the onset of clinical symptoms [112]. These findings are confirmed by microarray analyses of peripheral blood monocytic cells derived from CSFV-infected pigs [142].

Especially in the acute-lethal course, CSF is accompanied by severe lymphopenia and resulting immunosuppression as well as granulocytopenia [143–146]. Moreover, a marked thrombocytopenia starts very early after infection [147–149]. The mechanisms leading to this platelet decrease are not yet understood but disseminated intravascular coagulation (DIC), degeneration of megakaryocytes, bone marrow lesions, and accelerated deterioration have been discussed [130]. In addition, massive activation and subsequent phagocytosis of platelets has been discussed as an etiological factor [147] while DIC related correlates were not observed upon infection with a genotype 2.3 CSFV strain [150]. At least in vitro, endothelial cells are also activated and expression levels of pro-inflammatory and pro-coagulatory factors are increased [151]. The pathogenic mechanism involved in hemorrhagic lesions include damage of endothelial cells, causal involvement of thrombocytopenia (and DIC), erythrodiapedesis, and capillary vasodilatation and increased permeability [146,148,149,152,153]. However, several factors remain unclear and studies with different strains have given conflicting results.

Despite the immunopathogenesis of most CSF-related lesions, pigs recovering from CSFV infection mount an effective immune response with E2-specific antibodies detectable after 10–14 days. The E2 antibodies are able to neutralize CSFV in vitro and induce protective immune responses [154,155]. These antibodies and protection against re-infection persist probably livelong. In addition to E2, antibodies are raised against the E^{rns} and the non-structural protein NS3 [156,157]. Immunization with live attenuated CSFV can be efficient as early as 3–5 days post vaccination [158–160]. Thus, protection is possible without neutralizing antibodies and even before specific T-cell responses can be seen. Despite the fact that this very early protection is far from being understood, IFN-γ secreting T-cells seem to play a role [161–163].

5. Epidemiology

Susceptible hosts are different members of the *Suidae* family, particularly domestic pigs (*Sus scrofa domesticus*) and European wild boar (*Sus scrofa scrofa*) [113,164]. Moreover, the susceptibility of common warthogs (*Phacochoerus africanus*) and bushpigs (*Potamochoerus larvatus*) was recently demonstrated [165].

Classical swine fever virus can be transmitted both horizontally and vertically. Horizontal transmission takes places through direct or indirect contact between infected and susceptible pigs. Important indirect routes include feeding of virus contaminated garbage/swill and mechanical transmission via contact to humans or agricultural and veterinary equipment [127]. Aerogenic transmission was reported under experimental conditions [166–168], and it can probably play a role for within herd transmission [169].

Upon contact, infection usually occurs through the oronasal route, or less frequently via conjunctiva, mucus membranes, skin abrasions, insemination, and the use of contaminated instruments [170–173]. Infected pigs show high-titer viremia and shed virus at least from the beginning of clinical disease until death or specific antibodies have developed. The main excretion routes are by saliva, lacrimal secretions, urine, feces, and semen [127,135,173]. As mentioned above, chronically infected pigs shed the virus continuously or intermittently until death [65]. Vertical transmission from

pregnant sows to fetuses is possible throughout all stages of gestation and can lead to persistently infected offspring (see above).

Classical swine fever affected wild boar populations can serve as reservoir of the virus and present a constant risk for domestic pigs. Fritzemeier et al. [2] could show that almost 60% of the primary CSF outbreaks in Germany between 1993 and 1998 were linked to infected wild boar. This link was particularly important for holdings with low biosecurity or problems in biosafety management.

Over the last decades, a decreasing virulence was observed for the CSFV strains involved in many outbreaks among wild boar and domestic pigs. In Europe, the most prevalent genotype 2.3 strains showed moderate virulence with a highly age-dependent clinical picture and rather unspecific clinical pictures in older animals (see above). These strains showed potential to establish endemicity in affected wild boar populations rather than showing the self-limiting behavior of the historical highly virulent CSFV strains. It was discussed whether these strains are somewhat the ideally adapted variants of CSFV for long-term perpetuation in wildlife [92].

In endemically affected countries with official but imperfect vaccination, circulation of less virulent CSFV strains is often masked by partial protection. In combination with management and biosecurity issues (swill feeding, contacts, shared equipment), the virus is maintained over prolonged periods in the domestic pig population.

6. Diagnosis

Rapid and reliable diagnosis is of utmost importance for the timely implementation of control measures against CSF. On the international level, laboratory methods as well as sampling and shipping guidelines can be found in the OIE Manual of Diagnostic Tests and Vaccines for Terrestrial Animals and the respective EU Diagnostic Manual (European Commission Decision 2002/106/EC).

For CSFV, primary detection is performed using well established real-time reverse transcription polymerase chain reaction (RT-qPCR) systems [174–183], of which many are available commercially. Recently, field applicable RT-PCRs [184] but also alternatives have been designed such as loop-mediated isothermal amplification (LAMP) assays [185–190], primer-probe energy transfer RT-qPCR [191,192] or recently insulated isothermal RT-qPCR [193]. Moreover, CSFV can be isolated on different permanent cell lines such as porcine kidney cell lines PK15 or SK6 (Technical Annex to Commission Decision 2002/106/EC). In addition, detection of antigen on fixed cryosections of tissues is possible using fluorescence antibody or immune-peroxidase assays [194,195]. The available antigen ELISAs are recommended for the use with herd-based testing only. While the sensitivity of panpesti-specific assays (based on the E^{rns}) is usually at least comparable with virus isolation, most CSF specific assays lack sensitivity [196]. Serological screening can be performed using different commercially available E2 antibody enzyme-linked immunosorbent assays (ELISAs). In addition, neutralization assays allow, to a certain extent, differentiation of pestivirus antibodies and are used for confirmation [197].

Reliable DIVA (differentiation of infected and vaccinated animals) assays are needed when using DIVA vaccines. Commercially available tests that can accompany both E2 subunit vaccines and chimeric vaccines such as "CP7_E2alf", target the detection of antibodies directed against glycoprotein E^{rns} [196,198,199]. Recently, additional diagnostic tests have been developed. One is a double-antigen ELISA format that was recently commercialized [200], another is an ELISA with a screening and a confirmation part [201]: Moreover, a microsphere immunoassay was also developed as a confirmatory test [202].

Due to the increased sensitivity of diagnostic tools (especially RT-qPCR), vaccine virus detections are quite common in oral vaccination campaigns of wild boar and vaccination programs of domestic pigs. For this reason, different RT-qPCR systems have been developed and tested, these allow differentiation between vaccine and field viruses (genetic DIVA) [203–208].

Sampling can be the bottleneck of swine fever diagnosis, especially in the case of wild boar, but also in remote areas. For this reason, alternative sampling strategies and sample matrices have been tested for CSF (often combined with African swine fever sampling) especially for wildlife specimens

and under rural conditions [209–212]. However, most of them are not yet in routine use and need further validation.

7. Vaccination

Highly efficacious and safe live-attenuated CSF vaccines have existed for decades [160]. The underlying virus strains (e.g., the C-strain of CSFV, the Lapinized Philippines Coronel, the Thiverval or the Japanese guinea-pig exaltation negative GPE strain) were attenuated through serial passages in animals (rabbits) or cell culture. These vaccines have been implemented in mandatory control programs that led, together with strict hygiene measures, to the eradication of CSF from several regions of the world [213]. At this time, they are still in use in several Asian countries including China [84], countries of South and Central America, Trans-Caucasian Countries, and Eastern Europe (see Table 1). In 2016, 22 countries officially reported mandatory vaccination campaigns (OIE WAHIS [214]).

In addition, these vaccines were also adapted to a bait format for oral immunization of wild boar [6,215,216] and were recently explored for the vaccination of domestic pigs under backyard conditions [217–219]. While these vaccines usually have outstanding virtues in terms of onset, spectrum and duration of immunity [158,220–223], the main drawback is the lack of a serological marker concept [160] that would allow differentiation of field virus infected from vaccinated animals (DIVA concept). This is usually less important in endemically affected countries where prophylactic vaccination is carried out to reduce the disease burden and to ensure product safety. In general, there are also no legal obligations to use a certain type of vaccine for an emergency vaccination scenario. However, due to the trade restrictions that are imposed on pigs vaccinated with conventional live attenuated vaccines, only DIVA vaccines are considered a feasible option for domestic pigs [224]. Up to very recently, only E2 subunit marker (DIVA) vaccines were available on the market (at present, one E2 marker vaccine is commercially available, Porcilis® Pesti, MSD Animal Health, Unterschleißheim, Germany). These vaccines are safe and were shown to provide clinical protection and limit the spread of CSF [225–235]. However, they show drawbacks especially in terms of early protection [160,236] and protection against transplacental transmission [237]. Due to these problems, emergency vaccination was hardly implemented in domestic pigs (one exception being Romania). Several research groups have therefore sought to develop a next-generation marker vaccine candidate that would ideally answer all demands with regard to safety, efficacy, DIVA potential, and marketability [238]. Among the concepts that have been investigated are different vector vaccines based on vaccinia virus, pseudorabies virus or adenoviruses. Other vaccine designs include recombinant attenuated vaccines with chimeric constructs, subunit vaccines based on different expression systems, and RNA/DNA vaccines (recently reviewed by Blome et al., [239]. In 2014, the European Medicines Agency (EMA) licensed one of the chimeric marker vaccine candidates, "CP7_E2alf", after extensive testing in the framework of an EU-funded research project [159,240–257]. This new marker vaccine is still under investigation and could be a powerful tool for both emergency vaccination of domestic pigs and also wild boar.

Oral emergency vaccination of wild boar with baits has proven to be a potent tool to control the disease in wildlife and to safeguard domestic pigs [3]. For this purpose, the above-mentioned C-strain formulations have been used in several European countries including Germany and France. To further optimize the strategy, a DIVA vaccine such as "CP7_E2alf" could be used. The latter was already tested for use in wild boar under both laboratory and field conditions and could be a medium term option [241,246,251].

Table 1. CSF vaccination: Countries that reported official vaccination campaigns through World Organization for Animal Health (OIE) in 2016 (their last reported outbreaks are presented in brackets; no reports for some countries since 2005) (WAHIS Interface [214]).

Country	Last reported CSF outbreak
Albania	no reports
Armenia	2006
Azerbaijan	no reports
Belarus	no reports
Bosnia and Herzegovina	2007
Bulgaria (wb)	2009 wb
China	2015
Colombia	2016
Cuba	2016
Dominican Republic	2016
Ecuador	2016
Macedonia	2008
Georgia	no reports
Hong Kong	2005
Madagascar	2016
Moldova	(no reports)
Mongolia	2016
Myanmar	2015
Peru	2016
Philippines	2016
Russia	2016
Ukraine	2015

Wb: Wild boar.

Conflicts of Interest: The authors were involved in the design and testing of some of the vaccines and received third party funds to carry out the studies (industry funding and EU framework programs FP6 and FP7 under grant agreement numbers 227003 CP-FP and SSPE-CT-2003-501559). No other conflicts of interest exist.

References

1. Edwards, S.; Fukusho, A.; Lefevre, P.C.; Lipowski, A.; Pejsak, Z.; Roehe, P.; Westergaard, J. Classical swine fever: The global situation. *Vet. Microbiol.* **2000**, *73*, 103–119. [CrossRef]
2. Fritzemeier, J.; Teuffert, J.; Greiser-Wilke, I.; Staubach, C.; Schlüter, H.; Moennig, V. Epidemiology of classical swine fever in germany in the 1990s. *Vet. Microbiol.* **2000**, *77*, 29–41. [CrossRef]
3. Rossi, S.; Staubach, C.; Blome, S.; Guberti, V.; Thulke, H.H.; Vos, A.; Koenen, F.; Le Potier, M.F. Controlling of csfv in european wild boar using oral vaccination: A review. *Front. Microbiol.* **2015**, *6*, 1141. [CrossRef] [PubMed]
4. Rossi, S.; Pol, F.; Forot, B.; Masse-Provin, N.; Rigaux, S.; Bronner, A.; Le Potier, M.F. Preventive vaccination contributes to control classical swine fever in wild boar (*Sus scrofa* sp.). *Vet. Microbiol.* **2010**, *142*, 99–107. [CrossRef] [PubMed]
5. von Rüden, S.; Staubach, C.; Kaden, V.; Hess, R.G.; Blicke, J.; Kühne, S.; Sonnenburg, J.; Fröhlich, A.; Teuffert, J.; Moennig, V. Retrospective analysis of the oral immunisation of wild boar populations against classical swine fever virus (csfv) in region Eifel of Rhineland-Palatinate. *Vet. Microbiol.* **2008**, *132*, 29–38. [CrossRef] [PubMed]
6. Kaden, V.; Heyne, H.; Kiupel, H.; Letz, W.; Kern, B.; Lemmer, U.; Gossger, K.; Rothe, A.; Böhme, H.; Tyrpe, P. Oral immunisation of wild boar against classical swine fever: Concluding analysis of the recent field trials in Germany. *Berl. Munch. Tierarztl. Wochenschr.* **2002**, *115*, 179–185. [PubMed]
7. Blome, S.; Gabriel, C.; Staubach, C.; Leifer, I.; Strebelow, G.; Beer, M. Genetic differentiation of infected from vaccinated animals after implementation of an emergency vaccination strategy against classical swine fever in wild boar. *Vet. Microbiol.* **2011**, *153*, 373–376. [CrossRef] [PubMed]

8. Hulst, M.M.; van Gennip, H.G.; Moormann, R.J. Passage of classical swine fever virus in cultured swine kidney cells selects virus variants that bind to heparan sulfate due to a single amino acid change in envelope protein E^{rns}. *J. Virol.* **2000**, *74*, 9553–9561. [CrossRef] [PubMed]
9. Weiland, E.; Ahl, R.; Stark, R.; Weiland, F.; Thiel, H.J. A second envelope glycoprotein mediates neutralization of a pestivirus, hog cholera virus. *J. Virol.* **1992**, *66*, 3677–3682. [PubMed]
10. Iqbal, M.; Flick-Smith, H.; McCauley, J.W. Interactions of bovine viral diarrhoea virus glycoprotein E^{rns} with cell surface glycosaminoglycans. *J. Gen. Virol.* **2000**, *81*, 451–459. [CrossRef] [PubMed]
11. Hulst, M.M.; van Gennip, H.G.; Vlot, A.C.; Schooten, E.; de Smit, A.J.; Moormann, R.J. Interaction of classical swine fever virus with membrane-associated heparan sulfate: Role for virus replication in vivo and virulence. *J. Virol.* **2001**, *75*, 9585–9595. [CrossRef] [PubMed]
12. Wang, Z.; Nie, Y.; Wang, P.; Ding, M.; Deng, H. Characterization of classical swine fever virus entry by using pseudotyped viruses: E1 and E2 are sufficient to mediate viral entry. *Virology* **2004**, *330*, 332–341. [CrossRef] [PubMed]
13. Donis, R.O. Molecular biology of bovine viral diarrhea virus and its interactions with the host. *Vet. Clin. N. Am. Food Anim. Pract.* **1995**, *11*, 393–423. [CrossRef]
14. Krey, T.; Thiel, H.J.; Rümenapf, T. Acid-resistant bovine pestivirus requires activation for ph-triggered fusion during entry. *J. Virol.* **2005**, *79*, 4191–4200. [CrossRef] [PubMed]
15. Lecot, S.; Belouzard, S.; Dubuisson, J.; Rouille, Y. Bovine viral diarrhea virus entry is dependent on clathrin-mediated endocytosis. *J. Virol.* **2005**, *79*, 10826–10829. [CrossRef] [PubMed]
16. Rijnbrand, R.; van der Straaten, T.; van Rijn, P.A.; Spaan, W.J.; Bredenbeek, P.J. Internal entry of ribosomes is directed by the 5′ noncoding region of classical swine fever virus and is dependent on the presence of an RNA pseudoknot upstream of the initiation codon. *J. Virol.* **1997**, *71*, 451–457. [PubMed]
17. Pestova, T.V.; Hellen, C.U. Internal initiation of translation of bovine viral diarrhea virus RNA. *Virology* **1999**, *258*, 249–256. [CrossRef] [PubMed]
18. Poole, T.L.; Wang, C.; Popp, R.A.; Potgieter, L.N.; Siddiqui, A.; Collett, M.S. Pestivirus translation initiation occurs by internal ribosome entry. *Virology* **1995**, *206*, 750–754. [CrossRef]
19. Rümenapf, T.; Unger, G.; Strauss, J.H.; Thiel, H.J. Processing of the envelope glycoproteins of pestiviruses. *J. Virol.* **1993**, *67*, 3288–3294. [PubMed]
20. Stark, R.; Meyers, G.; Rümenapf, T.; Thiel, H.J. Processing of pestivirus polyprotein: Cleavage site between autoprotease and nucleocapsid protein of classical swine fever virus. *J. Virol.* **1993**, *67*, 7088–7095. [PubMed]
21. Wiskerchen, M.; Belzer, S.K.; Collett, M.S. Pestivirus gene expression: The first protein product of the bovine viral diarrhea virus large open reading frame, p20, possesses proteolytic activity. *J. Virol.* **1991**, *65*, 4508–4514. [PubMed]
22. Lackner, T.; Müller, A.; Pankraz, A.; Becher, P.; Thiel, H.J.; Gorbalenya, A.E.; Tautz, N. Temporal modulation of an autoprotease is crucial for replication and pathogenicity of an rna virus. *J. Virol.* **2004**, *78*, 10765–10775. [CrossRef] [PubMed]
23. Lackner, T.; Thiel, H.J.; Tautz, N. Dissection of a viral autoprotease elucidates a function of a cellular chaperone in proteolysis. *Proc. Natl. Acad. Sci. USA* **2006**, *103*, 1510–1515. [CrossRef] [PubMed]
24. Tautz, N.; Elbers, K.; Stoll, D.; Meyers, G.; Thiel, H.J. Serine protease of pestiviruses: Determination of cleavage sites. *J. Virol.* **1997**, *71*, 5415–5422. [PubMed]
25. Gong, Y.; Trowbridge, R.; Macnaughton, T.B.; Westaway, E.G.; Shannon, A.D.; Gowans, E.J. Characterization of RNA synthesis during a one-step growth curve and of the replication mechanism of bovine viral diarrhoea virus. *J. Gen. Virol.* **1996**, *77*, 2729–2736. [CrossRef] [PubMed]
26. Gray, E.W.; Nettleton, P.F. The ultrastructure of cell cultures infected with border disease and bovine virus diarrhoea viruses. *J. Gen. Virol.* **1987**, *68*, 2339–2346. [CrossRef] [PubMed]
27. Ohmann, H.B. Electron microscopy of bovine virus diarrhoea virus. *Rev. Sci. Tech.* **1990**, *9*, 61–73. [CrossRef] [PubMed]
28. Kramer, M.; Staubach, C.; Koenen, F.; Haegeman, A.; Pol, F.; Le Potier, M.F.; Greiser-Wilke, I. Scientific review on Classical Swine Fever. *EFSA Support. Publ.* **2009**, *6*. [CrossRef]
29. Wijnker, J.J.; Depner, K.R.; Berends, B.R. Inactivation of classical swine fever virus in porcine casing preserved in salt. *Int. J. Food Microbiol.* **2008**, *128*, 411–413. [CrossRef] [PubMed]
30. Farez, S.; Morley, R.S. Potential animal health hazards of pork and pork products. *Rev. Sci. Tech.* **1997**, *16*, 65–78. [CrossRef] [PubMed]

31. Edwards, S. Survival and inactivation of classical swine fever virus. *Vet. Microbiol.* **2000**, *73*, 175–181. [CrossRef]
32. Weesendorp, E.; Stegeman, A.; Loeffen, W.L. Survival of classical swine fever virus at various temperatures in faeces and urine derived from experimentally infected pigs. *Vet. Microbiol.* **2008**, *132*, 249–259. [CrossRef] [PubMed]
33. Haas, B.; Ahl, R.; Böhm, R.; Strauch, D. Inactivation of viruses in liquid manure. *Rev. Sci. Tech.* **1995**, *14*, 435–445. [CrossRef] [PubMed]
34. Botner, A.; Belsham, G.J. Virus survival in slurry: Analysis of the stability of foot-and-mouth disease, classical swine fever, bovine viral diarrhoea and swine influenza viruses. *Vet. Microbiol.* **2012**, *157*, 41–49. [CrossRef] [PubMed]
35. Turner, C.; Williams, S.M.; Cumby, T.R. The inactivation of foot and mouth disease, aujeszky's disease and classical swine fever viruses in pig slurry. *J. Appl. Microbiol.* **2000**, *89*, 760–767. [CrossRef] [PubMed]
36. Gale, P. Risks to farm animals from pathogens in composted catering waste containing meat. *Vet. Rec.* **2004**, *155*, 77–82. [CrossRef] [PubMed]
37. Artois, M.; Depner, K.R.; Guberti, V.; Hars, J.; Rossi, S.; Rutili, D. Classical swine fever (hog cholera) in wild boar in Europe. *Rev. Sci. Tech.* **2002**, *21*, 287–303. [CrossRef] [PubMed]
38. Harkness, J.W. Classical swine fever and its diagnosis: A current view. *Vet. Rec.* **1985**, *116*, 288–293. [CrossRef] [PubMed]
39. Tessler, J.; Stewart, W.C.; Kresse, J.I. Stabilization of hog cholera virus by dimethyl sulfoxide. *Can. J. Comp. Med.* **1975**, *39*, 472–473. [PubMed]
40. Depner, K.; Bauer, T.; Liess, B. Thermal and pH stability of pestiviruses. *Rev. Sci. Tech.* **1992**, *11*, 885–893. [CrossRef] [PubMed]
41. Panina, G.F.; Civardi, A.; Cordioli, P.; Massirio, I.; Scatozza, F.; Baldini, P.; Palmia, F. Survival of hog cholera virus (HCV) in sausage meat products (italian salami). *Int. J. Food Microbiol.* **1992**, *17*, 19–25. [CrossRef]
42. Mebus, C.; House, C.; Gonzalvo, F.R.; Pineda, J.; Tapiador, J.; Pire, J.; Bergada, J.; Yedloutschnig, R.; Sahu, S.; Becerra, V. Survival of foot-and-mouth disease, african swine fever, and hog cholera viruses in spanish serrano cured hams and Iberian cured hams, shoulders and loins. *Food Microbiol.* **1993**, *10*, 133–143. [CrossRef]
43. Postel, A.; Schmeiser, S.; Perera, C.L.; Rodriguez, L.J.; Frias-Lepoureau, M.T.; Becher, P. Classical swine fever virus isolates from Cuba form a new subgenotype 1.4. *Vet. Microbiol.* **2013**, *161*, 334–338. [CrossRef] [PubMed]
44. Cha, S.H.; Choi, E.J.; Park, J.H.; Yoon, S.R.; Kwon, J.H.; Yoon, K.J.; Song, J.Y. Phylogenetic characterization of classical swine fever viruses isolated in Korea between 1988 and 2003. *Virus Res.* **2007**, *126*, 256–261. [CrossRef] [PubMed]
45. Blome, S.; Grotha, I.; Moennig, V.; Greiser-Wilke, I. Classical swine fever virus in South-Eastern Europe—Retrospective analysis of the disease situation and molecular epidemiology. *Vet. Microbiol.* **2010**, *146*, 276–284. [CrossRef] [PubMed]
46. Chen, N.; Hu, H.; Zhang, Z.; Shuai, J.; Jiang, L.; Fang, W. Genetic diversity of the envelope glycoprotein E2 of classical swine fever virus: Recent isolates branched away from historical and vaccine strains. *Vet. Microbiol.* **2008**, *127*, 286–299. [CrossRef] [PubMed]
47. Jiang, D.L.; Liu, G.H.; Gong, W.J.; Li, R.C.; Hu, Y.F.; Tu, C.; Yu, X.L. Complete genome sequences of classical swine fever virus isolates belonging to a new subgenotype, 2.1c, from Hunan province, China. *Genome Announc.* **2013**, *28*, e00080. [CrossRef] [PubMed]
48. Vanderhallen, H.; Mittelholzer, C.; Hofmann, M.A.; Koenen, F. Classical swine fever virus is genetically stable in vitro and in vivo. *Arch. Virol.* **1999**, *144*, 1669–1677. [CrossRef] [PubMed]
49. Greiser-Wilke, I.; Dreier, S.; Haas, L.; Zimmermann, B. Genetic typing of classical swine fever viruses—A review. *Dtsch. Tierarztl. Wochenschr.* **2006**, *113*, 134–138. [PubMed]
50. Paton, D.J.; McGoldrick, A.; Greiser-Wilke, I.; Parchariyanon, S.; Song, J.Y.; Liou, P.P.; Stadejek, T.; Lowings, J.P.; Bjorklund, H.; Belak, S. Genetic typing of classical swine fever virus. *Vet. Microbiol.* **2000**, *73*, 137–157. [CrossRef]
51. Postel, A.; Schmeiser, S.; Bernau, J.; Meindl-Boehmer, A.; Pridotkas, G.; Dirbakova, Z.; Mojzis, M.; Becher, P. Improved strategy for phylogenetic analysis of classical swine fever virus based on full-length E2 encoding sequences. *Vet. Res.* **2012**, *43*, 50. [CrossRef] [PubMed]

52. Töpfer, A.; Höper, D.; Blome, S.; Beer, M.; Beerenwinkel, N.; Ruggli, N.; Leifer, I. Sequencing approach to analyze the role of quasispecies for classical swine fever. *Virology* **2013**, *438*, 14–19. [CrossRef] [PubMed]
53. Leifer, I.; Hoeper, D.; Blome, S.; Beer, M.; Ruggli, N. Clustering of classical swine fever virus isolates by codon pair bias. *BMC Res. Notes* **2011**, *4*, 521. [CrossRef] [PubMed]
54. Goller, K.V.; Gabriel, C.; Dimna, M.L.; Potier, M.F.; Rossi, S.; Staubach, C.; Merboth, M.; Beer, M.; Blome, S. Evolution and molecular epidemiology of classical swine fever virus during a multi-annual outbreak amongst european wild boar. *J. Gen. Virol.* **2016**, *97*, 639–645. [CrossRef] [PubMed]
55. Fahnoe, U.; Pedersen, A.G.; Risager, P.C.; Nielsen, J.; Belsham, G.J.; Höper, D.; Beer, M.; Rasmussen, T.B. Rescue of the highly virulent classical swine fever virus strain "Koslov" from cloned cDNA and first insights into genome variations relevant for virulence. *Virology* **2014**, *468–470*, 379–387. [CrossRef] [PubMed]
56. Björklund, H.; Lowings, P.; Stadejek, T.; Vilcek, S.; Greiser-Wilke, I.; Paton, D.; Belak, S. Phylogenetic comparison and molecular epidemiology of classical swine fever virus. *Virus Genes* **1999**, *19*, 189–195. [CrossRef] [PubMed]
57. Greiser-Wilke, I.; Fritzemeier, J.; Koenen, F.; Vanderhallen, H.; Rutili, D.; De Mia, G.M.; Romero, L.; Rosell, R.; Sanchez-Vizcaino, J.M.; San Gabriel, A. Molecular epidemiology of a large classical swine fever epidemic in the European Union in 1997–1998. *Vet. Microbiol.* **2000**, *77*, 17–27. [CrossRef]
58. Jemersic, L.; Greiser-Wilke, I.; Barlic-Maganja, D.; Lojkic, M.; Madic, J.; Terzic, S.; Grom, J. Genetic typing of recent classical swine fever virus isolates from Croatia. *Vet. Microbiol.* **2003**, *96*, 25–33. [CrossRef]
59. Bartak, P.; Greiser-Wilke, I. Genetic typing of classical swine fever virus isolates from the territory of the Czech Republic. *Vet. Microbiol.* **2000**, *77*, 59–70. [CrossRef]
60. Wonnemann, H.; Floegel-Niesmann, G.; Moennig, V.; Greiser-Wilke, I. Genetic typing of German isolates of classical swine fever virus. *Dtsch. Tierarztl. Wochenschr.* **2001**, *108*, 252–256. [PubMed]
61. Biagetti, M.; Greiser-Wilke, I.; Rutili, D. Molecular epidemiology of classical swine fever in Italy. *Vet. Microbiol.* **2001**, *83*, 205–215. [CrossRef]
62. Pol, F.; Rossi, S.; Mesplede, A.; Kuntz-Simon, G.; Le Potier, M.F. Two outbreaks of classical swine fever in wild boar in France. *Vet. Rec.* **2008**, *162*, 811–816. [CrossRef] [PubMed]
63. Leifer, I.; Hoffmann, B.; Höper, D.; Bruun Rasmussen, T.; Blome, S.; Strebelow, G.; Höreth-Böntgen, D.; Staubach, C.; Beer, M. Molecular epidemiology of current classical swine fever virus isolates of wild boar in germany. *J. Gen. Virol.* **2010**, *91*, 2687–2697. [CrossRef] [PubMed]
64. Simon, G.; Le Dimna, M.; Le Potier, M.F.; Pol, F. Molecular tracing of classical swine fever viruses isolated from wild boars and pigs in France from 2002 to 2011. *Vet. Microbiol.* **2013**, *166*, 631–638. [CrossRef] [PubMed]
65. Moennig, V.; Floegel-Niesmann, G.; Greiser-Wilke, I. Clinical signs and epidemiology of classical swine fever: A review of new knowledge. *Vet. J.* **2003**, *165*, 11–20. [CrossRef]
66. Beer, M.; Goller, K.V.; Staubach, C.; Blome, S. Genetic variability and distribution of classical swine fever virus. *Anim. Health Res. Rev.* **2015**, *16*, 33–39. [CrossRef] [PubMed]
67. Pereda, A.J.; Greiser-Wilke, I.; Schmitt, B.; Rincon, M.A.; Mogollon, J.D.; Sabogal, Z.Y.; Lora, A.M.; Sanguinetti, H.; Piccone, M.E. Phylogenetic analysis of classical swine fever virus (CSFV) field isolates from outbreaks in south and central America. *Virus Res.* **2005**, *110*, 111–118. [CrossRef] [PubMed]
68. Diaz de Arce, H.; Nunez, J.I.; Ganges, L.; Barreras, M.; Teresa Frias, M.; Sobrino, F. Molecular epidemiology of classical swine fever in Cuba. *Virus Res.* **1999**, *64*, 61–67. [CrossRef]
69. de Arce, H.D.; Ganges, L.; Barrera, M.; Naranjo, D.; Sobrino, F.; Frias, M.T.; Nunez, J.I. Origin and evolution of viruses causing classical swine fever in Cuba. *Virus Res.* **2005**, *112*, 123–131. [CrossRef] [PubMed]
70. Sandvik, T.; Crooke, H.; Drew, T.W.; Blome, S.; Greiser-Wilke, I.; Moennig, V.; Gous, T.A.; Gers, S.; Kitching, J.A.; Buhrmann, G.; et al. Classical swine fever in South Africa after 87 years' absence. *Vet. Rec.* **2005**, *157*, 267. [CrossRef] [PubMed]
71. David, D.; Edri, N.; Yakobson, B.A.; Bombarov, V.; King, R.; Davidson, I.; Pozzi, P.; Hadani, Y.; Bellaiche, M.; Schmeiser, S.; et al. Emergence of classical swine fever virus in Israel in 2009. *Vet. J.* **2011**, *190*, e146–e149. [CrossRef] [PubMed]
72. Barman, N.N.; Bora, D.P.; Khatoon, E.; Mandal, S.; Rakshit, A.; Rajbongshi, G.; Depner, K.; Chakraborty, A.; Kumar, S. Classical swine fever in wild hog: Report of its prevalence in northeast India. *Transbound. Emerg. Dis.* **2014**, *63*, 540–547. [CrossRef] [PubMed]

73. Roychoudhury, P.; Sarma, D.K.; Rajkhowa, S.; Munir, M.; Kuchipudi, S.V. Predominance of genotype 1.1 and emergence of genotype 2.2 classical swine fever viruses in north-eastern region of India. *Transbound. Emerg. Dis.* **2014**, *61* (Suppl. 1), 69–77. [CrossRef] [PubMed]
74. Patil, S.S.; Hemadri, D.; Shankar, B.P.; Raghavendra, A.G.; Veeresh, H.; Sindhoora, B.; Chandan, S.; Sreekala, K.; Gajendragad, M.R.; Prabhudas, K. Genetic typing of recent classical swine fever isolates from India. *Vet. Microbiol.* **2010**, *141*, 367–373. [CrossRef] [PubMed]
75. Patil, S.S.; Hemadri, D.; Veeresh, H.; Sreekala, K.; Gajendragad, M.R.; Prabhudas, K. Phylogenetic analysis of NS5B gene of classical swine fever virus isolates indicates plausible Chinese origin of Indian subgroup 2.2 viruses. *Virus Genes* **2012**, *44*, 104–108. [CrossRef] [PubMed]
76. Rajkhowa, T.K.; Hauhnar, L.; Lalrohlua, I.; Mohanarao, G.J. Emergence of 2.1. Subgenotype of classical swine fever virus in pig population of India in 2011. *Vet. Q.* **2014**, *34*, 224–228. [CrossRef] [PubMed]
77. Desai, G.S.; Sharma, A.; Kataria, R.S.; Barman, N.N.; Tiwari, A.K. 5′ UTR-based phylogenetic analysis of classical swine fever virus isolates from India. *Acta Virol.* **2010**, *54*, 79–82. [CrossRef] [PubMed]
78. Sarma, D.K.; Mishra, N.; Vilcek, S.; Rajukumar, K.; Behera, S.P.; Nema, R.K.; Dubey, P.; Dubey, S.C. Phylogenetic analysis of recent classical swine fever virus (CSFV) isolates from Assam, India. *Comp. Immunol. Microbiol. Infect. Dis.* **2011**, *34*, 11–15. [CrossRef] [PubMed]
79. Nandi, S.; Muthuchelvan, D.; Ahuja, A.; Bisht, S.; Chander, V.; Pandey, A.B.; Singh, R.K. Prevalence of classical swine fever virus in India: A 6-year study (2004–2010). *Transbound. Emerg. Dis.* **2011**, *58*, 461–463. [CrossRef] [PubMed]
80. Postel, A.; Jha, V.C.; Schmeiser, S.; Becher, P. First molecular identification and characterization of classical swine fever virus isolates from Nepal. *Arch. Virol.* **2013**, *158*, 207–210. [CrossRef] [PubMed]
81. An, T.Q.; Peng, J.M.; Tian, Z.J.; Zhao, H.Y.; Li, N.; Liu, Y.M.; Chen, J.Z.; Leng, C.L.; Sun, Y.; Chang, D.; et al. Pseudorabies virus variant in Bartha-K61-vaccinated pigs, China, 2012. *Emerg. Infect. Dis.* **2013**, *19*, 1749–1755. [CrossRef] [PubMed]
82. Afshar, A.; Dulac, G.C.; Dubuc, C.; Howard, T.H. Comparative evaluation of the fluorescent antibody test and microtiter immunoperoxidase assay for detection of bovine viral diarrhea virus from bull semen. *Can. J. Vet. Res.* **1991**, *55*, 91–93. [PubMed]
83. Luo, T.R.; Liao, S.H.; Wu, X.S.; Feng, L.; Yuan, Z.X.; Li, H.; Liang, J.J.; Meng, X.M.; Zhang, H.Y. Phylogenetic analysis of the *E2* gene of classical swine fever virus from the Guangxi province of southern China. *Virus Genes* **2011**, *42*, 347–354. [CrossRef] [PubMed]
84. Luo, Y.; Li, S.; Sun, Y.; Qiu, H.J. Classical swine fever in China: A minireview. *Vet. Microbiol.* **2014**, *172*, 1–6. [CrossRef] [PubMed]
85. Pan, C.H.; Jong, M.H.; Huang, T.S.; Liu, H.F.; Lin, S.Y.; Lai, S.S. Phylogenetic analysis of classical swine fever virus in Taiwan. *Arch. Virol.* **2005**, *150*, 1101–1119. [CrossRef] [PubMed]
86. Deng, M.C.; Huang, C.C.; Huang, T.S.; Chang, C.Y.; Lin, Y.J.; Chien, M.S.; Jong, M.H. Phylogenetic analysis of classical swine fever virus isolated from Taiwan. *Vet. Microbiol.* **2005**, *106*, 187–1893. [CrossRef] [PubMed]
87. Lin, Y.J.; Chien, M.S.; Deng, M.C.; Huang, C.C. Complete sequence of a subgroup 3.4 strain of classical swine fever virus from Taiwan. *Virus Genes* **2007**, *35*, 737–744. [CrossRef] [PubMed]
88. Blacksell, S.D.; Khounsy, S.; Boyle, D.B.; Gleeson, L.J.; Westbury, H.A.; Mackenzie, J.S. Genetic typing of classical swine fever viruses from Lao PDR by analysis of the 5' non-coding region. *Virus Genes* **2005**, *31*, 349–355. [CrossRef] [PubMed]
89. Blacksell, S.D.; Khounsy, S.; Boyle, D.B.; Greiser-Wilke, I.; Gleeson, L.J.; Westbury, H.A.; Mackenzie, J.S. Phylogenetic analysis of the *E2* gene of classical swine fever viruses from Lao PDR. *Virus Res.* **2004**, *104*, 87–92. [CrossRef] [PubMed]
90. Sakoda, Y.; Ozawa, S.; Damrongwatanapokin, S.; Sato, M.; Ishikawa, K.; Fukusho, A. Genetic heterogeneity of porcine and ruminant pestiviruses mainly isolated in Japan. *Vet. Microbiol.* **1999**, *65*, 75–86. [CrossRef]
91. Coronado, L.; Liniger, M.; Munoz-Gonzalez, S.; Postel, A.; Perez, L.J.; Perez-Simo, M.; Perera, C.L.; Frias-Lepoureau, M.T.; Rosell, R.; Grundhoff, A.; et al. Novel poly-uridine insertion in the 3' UTR and E2 amino acid substitutions in a low virulent classical swine fever virus. *Vet. Microbiol.* **2017**, *201*, 103–112. [CrossRef] [PubMed]
92. Lange, M.; Kramer-Schadt, S.; Blome, S.; Beer, M.; Thulke, H.H. Disease severity declines over time after a wild boar population has been affected by classical swine fever–legend or actual epidemiological process? *Prev. Vet. Med.* **2012**, *106*, 185–195. [CrossRef] [PubMed]

93. Dreier, S.; Zimmermann, B.; Moennig, V.; Greiser-Wilke, I. A sequence database allowing automated genotyping of classical swine fever virus isolates. *J. Virol. Methods* **2007**, *140*, 95–99. [CrossRef] [PubMed]
94. Greiser-Wilke, I.; Zimmermann, B.; Fritzemeier, J.; Floegel, G.; Moennig, V. Structure and presentation of a world wide web database of CSF virus isolates held at the EU reference laboratory. *Vet. Microbiol.* **2000**, *73*, 131–136. [CrossRef]
95. Postel, A.; Schmeiser, S.; Zimmermann, B.; Becher, P. The European classical swine fever virus database: Blueprint for a pathogen-specific sequence database with integrated sequence analysis tools. *Viruses* **2016**, *8*, 302. [CrossRef] [PubMed]
96. Mayer, D.; Hofmann, M.A.; Tratschin, J.D. Attenuation of classical swine fever virus by deletion of the viral N^{pro} gene. *Vaccine* **2004**, *22*, 317–328. [CrossRef] [PubMed]
97. Risatti, G.R.; Borca, M.V.; Kutish, G.F.; Lu, Z.; Holinka, L.G.; French, R.A.; Tulman, E.R.; Rock, D.L. The E2 glycoprotein of classical swine fever virus is a virulence determinant in swine. *J. Virol.* **2005**, *79*, 3787–3796. [CrossRef] [PubMed]
98. Tews, B.A.; Schurmann, E.M.; Meyers, G. Mutation of cysteine 171 of pestivirus E^{rns} RNase prevents homodimer formation and leads to attenuation of classical swine fever virus. *J. Virol.* **2009**, *83*, 4823–4834. [CrossRef] [PubMed]
99. Meyers, G.; Saalmüller, A.; Büttner, M. Mutations abrogating the RNAse activity in glycoprotein E^{rns} of the pestivirus classical swine fever virus lead to virus attenuation. *J. Virol.* **1999**, *73*, 10224–10235. [PubMed]
100. Tamura, T.; Sakoda, Y.; Yoshino, F.; Nomura, T.; Yamamoto, N.; Sato, Y.; Okamatsu, M.; Ruggli, N.; Kida, H. Selection of classical swine fever virus with enhanced pathogenicity reveals synergistic virulence determinants in E2 and NS4B. *J. Virol.* **2012**, *86*, 8602–8613. [CrossRef] [PubMed]
101. Risatti, G.R.; Holinka, L.G.; Fernandez Sainz, I.; Carrillo, C.; Kutish, G.F.; Lu, Z.; Zhu, J.; Rock, D.L.; Borca, M.V. Mutations in the carboxyl terminal region of E2 glycoprotein of classical swine fever virus are responsible for viral attenuation in swine. *Virology* **2007**, *364*, 371–382. [CrossRef] [PubMed]
102. Risatti, G.R.; Holinka, L.G.; Fernandez Sainz, I.; Carrillo, C.; Lu, Z.; Borca, M.V. *N*-linked glycosylation status of classical swine fever virus strain brescia E2 glycoprotein influences virulence in swine. *J. Virol.* **2007**, *81*, 924–933. [CrossRef] [PubMed]
103. Sainz, I.F.; Holinka, L.G.; Lu, Z.; Risatti, G.R.; Borca, M.V. Removal of a *N*-linked glycosylation site of classical swine fever virus strain Brescia E^{rns} glycoprotein affects virulence in swine. *Virology* **2008**, *370*, 122–129. [CrossRef] [PubMed]
104. Tang, F.; Pan, Z.; Zhang, C. The selection pressure analysis of classical swine fever virus envelope protein genes E^{rns} and E2. *Virus Res.* **2008**, *131*, 132–135. [CrossRef] [PubMed]
105. Wu, Z.; Wang, Q.; Feng, Q.; Liu, Y.; Teng, J.; Yu, A.C.; Chen, J. Correlation of the virulence of CSFV with evolutionary patterns of E2 glycoprotein. *Front. Biosci. (Elite Ed.)* **2010**, *2*, 204–220. [PubMed]
106. Ishikawa, K.; Nagai, H.; Katayama, K.; Tsutsui, M.; Tanabayashi, K.; Takeuchi, K.; Hishiyama, M.; Saitoh, A.; Takagi, M.; Gotoh, K.; et al. Comparison of the entire nucleotide and deduced amino acid sequences of the attenuated hog cholera vaccine strain GPE- and the wild-type parental strain ALD. *Arch. Virol.* **1995**, *140*, 1385–1391. [CrossRef] [PubMed]
107. Jenckel, M.; Blome, S.; Beer, M.; Höper, D. Quasispecies composition and diversity do not reveal any predictors for chronic classical swine fever virus infection. *Arch. Virol.* **2017**, *162*, 775–786. [CrossRef] [PubMed]
108. Petrov, A.; Blohm, U.; Beer, M.; Pietschmann, J.; Blome, S. Comparative analyses of host responses upon infection with moderately virulent classical swine fever virus in domestic pigs and wild boar. *Virol. J.* **2014**, *11*, 134. [CrossRef] [PubMed]
109. Bunzenthal, C. Determination of the virulence of classical swine fever virus isolates [Bestimmung der Virulenz von Virusisolaten der Klassischen Schweinepest]. Ph.D. Thesis, University of Veterinary Medicine Hannover, Foundation, Hannover, Germany, 2003.
110. Floegel-Niesmann, G.; Blome, S.; Gerss-Dülmer, H.; Bunzenthal, C.; Moennig, V. Virulence of classical swine fever virus isolates from Europe and other areas during 1996 until 2007. *Vet. Microbiol.* **2009**, *139*, 165–169. [CrossRef] [PubMed]
111. Floegel-Niesmann, G.; Bunzenthal, C.; Fischer, S.; Moennig, V. Virulence of recent and former classical swine fever virus isolates evaluated by their clinical and pathological signs. *J. Vet. Med. B Infect. Dis. Vet. Public Health* **2003**, *50*, 214–220. [CrossRef] [PubMed]

112. Tarradas, J.; de la Torre, M.E.; Rosell, R.; Perez, L.J.; Pujols, J.; Munoz, M.; Munoz, I.; Munoz, S.; Abad, X.; Domingo, M.; et al. The impact of CSFV on the immune response to control infection. *Virus Res.* **2014**, *185*, 82–91. [CrossRef] [PubMed]
113. Depner, K.R.; Müller, A.; Gruber, A.; Rodriguez, A.; Bickhardt, K.; Liess, B. Classical swine fever in wild boar (*Sus scrofa*)—Experimental infections and viral persistence. *Dtsch. Tierarztl. Wochenschr.* **1995**, *102*, 381–384. [PubMed]
114. Kaden, V.; Steyer, H.; Schnabel, J.; Bruer, W. Classical swine fever (CSF) in wild boar: The role of the transplacental infection in the perpetuation of CSF. *J. Vet. Med. B Infect. Dis. Vet. Public Health* **2005**, *52*, 161–164. [CrossRef] [PubMed]
115. Kern, B.; Depner, K.R.; Letz, W.; Rott, M.; Thalheim, S.; Nitschke, B.; Plagemann, R.; Liess, B. Incidence of classical swine fever (CSF) in wild boar in a densely populated area indicating CSF virus persistence as a mechanism for virus perpetuation. *Zentralbl. Veterinarmed. B* **1999**, *46*, 63–67. [CrossRef] [PubMed]
116. von Benten, K.; Trautwein, G.; Richter-Reichhelm, H.B.; Liess, B.; Frey, H.R. Experimental transplacental transmission of hog cholera virus in pigs. III. Histopathological findings in the fetus. *Zentralbl. Veterinarmed. B* **1980**, *27*, 714–724. [CrossRef] [PubMed]
117. Stewart, W.C.; Carbrey, E.A.; Kresse, J.I. Transplacental hog cholera infection in susceptible sows. *Am. J. Vet. Res.* **1973**, *34*, 637–640. [PubMed]
118. Stewart, W.C.; Carbrey, E.A.; Kresse, J.I. Transplacental hog cholera infection in immune sows. *Am. J. Vet. Res.* **1972**, *33*, 791–798. [PubMed]
119. Richter-Reichhelm, H.B.; Trautwein, G.; von Benten, K.; Liess, B.; Frey, H.R. Experimental transplacental transmission of hog cholera virus in pigs. II. Immunopathological findings in the fetus. *Zentralbl. Veterinarmed. B* **1980**, *27*, 243–252. [CrossRef] [PubMed]
120. Overby, E.; Eskildsen, M. *Transplacental Infection in Susceptible Gilts after Inoculation with: I. Lapinized Swine Fever Vaccine, II. Bovine Viral Diarrhoea Virus Strains*; Commission of the European Communities, DG Scientific and Technical Information and Information Management: Luxembourg, 1977; Volume EUR 5904.
121. Meyer, H.; Liess, B.; Frey, H.R.; Hermanns, W.; Trautwein, G. Experimental transplacental transmission of hog cholera virus in pigs. IV. Virological and serological studies in newborn piglets. *Zentralbl. Veterinarmed. B* **1981**, *28*, 659–668. [CrossRef] [PubMed]
122. Hermanns, W.; Trautwein, G.; Meyer, H.; Liess, B. Experimental transplacental transmission of hog cholera virus in pigs. V. Immunopathological findings in newborn pigs. *Zentralbl. Veterinarmed. B* **1981**, *28*, 669–683. [CrossRef] [PubMed]
123. Frey, H.R.; Liess, B.; Richter-Reichhelm, H.B.; von Benten, K.; Trautwein, G. Experimental transplacental transmission of hog cholera virus in pigs. I. Virological and serological studies. *Zentralbl. Veterinarmed. B* **1980**, *27*, 154–164. [CrossRef] [PubMed]
124. Cabezon, O.; Colom-Cadena, A.; Munoz-Gonzalez, S.; Perez-Simo, M.; Bohorquez, J.A.; Rosell, R.; Marco, I.; Domingo, M.; Lavin, S.; Ganges, L. Post-natal persistent infection with classical swine fever virus in wild boar: A strategy for viral maintenance? *Transbound. Emerg. Dis.* **2017**, *64*, 651–655. [CrossRef] [PubMed]
125. Munoz-Gonzalez, S.; Perez-Simo, M.; Munoz, M.; Bohorquez, J.A.; Rosell, R.; Summerfield, A.; Domingo, M.; Ruggli, N.; Ganges, L. Efficacy of a live attenuated vaccine in classical swine fever virus postnatally persistently infected pigs. *Vet. Res.* **2015**, *46*, 78. [CrossRef] [PubMed]
126. Gomez-Villamandos, J.C.; Garcia de Leaniz, I.; Nunez, A.; Salguero, F.J.; Ruiz-Villamor, E.; Romero-Trevejo, J.L.; Sanchez-Cordon, P.J. Neuropathologic study of experimental classical swine fever. *Vet. Pathol.* **2006**, *43*, 530–540. [CrossRef] [PubMed]
127. Van Oirschot, J.T. *Classial Swine Fever (Hog Cholera)*, 8th ed.; Straw, B.E., D'Allaire, S., Mengeling, W.L., Taylor, D.J., Eds.; Iowa State University Press: Ames, IA, USA, 1999; pp. 159–172.
128. Depner, K.R.; Lange, E.; Pontrakulpipat, S.; Fichtner, D. Does porcine reproductive and respiratory syndrome virus potentiate classical swine fever virus infection in weaner pigs? *Zentralbl. Veterinarmed. B* **1999**, *46*, 485–491. [CrossRef] [PubMed]
129. Kaden, V.; Ziegler, U.; Lange, E.; Dedek, J. Classical swine fever virus: Clinical, virological, serological and hematological findings after infection of domestic pigs and wild boars with the field isolate "Spante" originating from wild boar. *Berl. Munch. Tierarztl. Wochenschr.* **2000**, *113*, 412–416. [PubMed]

130. Gomez-Villamandos, J.C.; Carrasco, L.; Bautista, M.J.; Sierra, M.A.; Quezada, M.; Hervas, J.; Chacon Mde, L.; Ruiz-Villamor, E.; Salguero, F.J.; Sonchez-Cordon, P.J.; et al. African swine fever and classical swine fever: A review of the pathogenesis. *Dtsch. Tierarztl. Wochenschr.* **2003**, *110*, 165–169. [PubMed]
131. Lange, A.; Blome, S.; Moennig, V.; Greiser-Wilke, I. Pathogenesis of classical swine fever—Similarities to viral haemorrhagic fevers: A review. *Berl. Munch. Tierarztl. Wochenschr.* **2011**, *124*, 36–47. [PubMed]
132. Liess, B. Pathogenesis and epidemiology of hog cholera. *Ann. Rech. Vet.* **1987**, *18*, 139–145. [PubMed]
133. Dunne, H.W. *Hog Cholera*, 3rd ed.; Dunne, H.W., Ed.; The Iowa State University Press: Ames, IA, USA, 1970; Vol. Diseases of Swine; pp. 177–239.
134. Ressang, A.A. Studies on the pathogenesis of hog cholera. II. Virus distribution in tissue and the morphology of the immune response. *Zentralbl. Veterinarmed. B* **1973**, *20*, 272–288. [CrossRef] [PubMed]
135. Ressang, A.A. Studies on the pathogenesis of hog cholera. I. Demonstration of hog cholera virus subsequent to oral exposure. *Zentralbl. Veterinarmed. B* **1973**, *20*, 256–271. [CrossRef] [PubMed]
136. Bauhofer, O.; Summerfield, A.; McCullough, K.C.; Ruggli, N. Role of double-stranded RNA and N^{pro} of classical swine fever virus in the activation of monocyte-derived dendritic cells. *Virology* **2005**, *343*, 93–105. [CrossRef] [PubMed]
137. Carrasco, C.P.; Rigden, R.C.; Vincent, I.E.; Balmelli, C.; Ceppi, M.; Bauhofer, O.; Tache, V.; Hjertner, B.; McNeilly, F.; van Gennip, H.G.; et al. Interaction of classical swine fever virus with dendritic cells. *J. Gen. Virol.* **2004**, *85*, 1633–1641. [CrossRef] [PubMed]
138. Fiebach, A.R.; Guzylack-Piriou, L.; Python, S.; Summerfield, A.; Ruggli, N. Classical swine fever virus N^{pro} limits type I interferon induction in plasmacytoid dendritic cells by interacting with interferon regulatory factor 7. *J. Virol.* **2011**, *85*, 8002–8011. [CrossRef] [PubMed]
139. Jamin, A.; Gorin, S.; Cariolet, R.; Le Potier, M.F.; Kuntz-Simon, G. Classical swine fever virus induces activation of plasmacytoid and conventional dendritic cells in tonsil, blood, and spleen of infected pigs. *Vet. Res.* **2008**, *39*, 7. [CrossRef] [PubMed]
140. Summerfield, A.; Ruggli, N. Immune responses against classical swine fever virus: Between ignorance and lunacy. *Front. Vet. Sci.* **2015**, *2*, 10. [CrossRef] [PubMed]
141. Summerfield, A.; Alves, M.; Ruggli, N.; de Bruin, M.G.; McCullough, K.C. High IFN-α responses associated with depletion of lymphocytes and natural IFN-producing cells during classical swine fever. *J. Interferon Cytokine Res.* **2006**, *26*, 248–255. [CrossRef] [PubMed]
142. Renson, P.; Blanchard, Y.; Le Dimna, M.; Felix, H.; Cariolet, R.; Jestin, A.; Le Potier, M.F. Acute induction of cell death-related IFN stimulated genes (ISG) differentiates highly from moderately virulent CSFV strains. *Vet. Res.* **2010**, *41*, 7. [CrossRef] [PubMed]
143. Pauly, T.; König, M.; Thiel, H.J.; Saalmüller, A. Infection with classical swine fever virus: Effects on phenotype and immune responsiveness of porcine T lymphocytes. *J. Gen. Virol.* **1998**, *79*, 31–40. [CrossRef] [PubMed]
144. Summerfield, A.; Knoetig, S.M.; Tschudin, R.; McCullough, K.C. Pathogenesis of granulocytopenia and bone marrow atrophy during classical swine fever involves apoptosis and necrosis of uninfected cells. *Virology* **2000**, *272*, 50–60. [CrossRef] [PubMed]
145. Susa, M.; König, M.; Saalmüller, A.; Reddehase, M.J.; Thiel, H.J. Pathogenesis of classical swine fever: B-lymphocyte deficiency caused by hog cholera virus. *J. Virol.* **1992**, *66*, 1171–1175. [PubMed]
146. Trautwein, G. Classical swine fever and related infections. In *Pathology and Pathogenesis of the Disease*; Martinus Nijhoff: Boston, MA, USA, 1988; pp. 27–54.
147. Bautista, M.J.; Ruiz-Villamor, E.; Salguero, F.J.; Sanchez-Cordon, P.J.; Carrasco, L.; Gomez-Villamandos, J.C. Early platelet aggregation as a cause of thrombocytopenia in classical swine fever. *Vet. Pathol.* **2002**, *39*, 84–91. [CrossRef] [PubMed]
148. Heene, D.; Hoffmann-Fezer, G.; Müller-Berghaus, G.; Hoffmann, R.; Weiss, E.; Lasch, H.G. Coagulation disorders in acute hog cholera. *Beitr. Pathol.* **1971**, *144*, 259–271. [PubMed]
149. Weiss, E.; Teredesai, A.; Hoffmann, R.; Hoffmann-Fezer, G. Volume distribution and ultrastructure of platelets in acute hog cholera. *Thromb. Diath. Haemorrh.* **1973**, *30*, 371–380. [PubMed]
150. Blome, S.; Meindl-Böhmer, A.; Nowak, G.; Moennig, V. Disseminated intravascular coagulation does not play a major role in the pathogenesis of classical swine fever. *Vet. Microbiol.* **2013**, *162*, 360–368. [CrossRef] [PubMed]
151. Bensaude, E.; Turner, J.L.; Wakeley, P.R.; Sweetman, D.A.; Pardieu, C.; Drew, T.W.; Wileman, T.; Powell, P.P. Classical swine fever virus induces proinflammatory cytokines and tissue factor expression and inhibits

apoptosis and interferon synthesis during the establishment of long-term infection of porcine vascular endothelial cells. *J. Gen. Virol.* **2004**, *85*, 1029–1037. [CrossRef] [PubMed]
152. Gomez-Villamandos, J.C.; Ruiz-Villamor, E.; Bautista, M.J.; Quezada, M.; Sanchez, C.P.; Salguero, F.J.; Sierra, M.A. Pathogenesis of classical swine fever: Renal haemorrhages and erythrodiapedesis. *J. Comp. Pathol.* **2000**, *123*, 47–54. [CrossRef] [PubMed]
153. Hoffmann, R.; Hoffmann-Fezer, G.; Kimeto, B.; Weiss, E. Microthrombi as morphological evidence of consumption coagulopathy in acute hog cholera. *Zentralbl. Veterinarmed. B* **1971**, *18*, 710–718. [CrossRef] [PubMed]
154. Hulst, M.M.; Westra, D.F.; Wensvoort, G.; Moormann, R.J. Glycoprotein E1 of hog cholera virus expressed in insect cells protects swine from hog cholera. *J. Virol.* **1993**, *67*, 5435–5442. [PubMed]
155. Rümenapf, T.; Stark, R.; Meyers, G.; Thiel, H.J. Structural proteins of hog cholera virus expressed by vaccinia virus: Further characterization and induction of protective immunity. *J. Virol.* **1991**, *65*, 589–597. [PubMed]
156. König, M.; Lengsfeld, T.; Pauly, T.; Stark, R.; Thiel, H.J. Classical swine fever virus: Independent induction of protective immunity by two structural glycoproteins. *J. Virol.* **1995**, *69*, 6479–6486. [PubMed]
157. Paton, D.J.; Ibata, G.; Edwards, S.; Wensvoort, G. An ELISA detecting antibody to conserved pestivirus epitopes. *J. Virol. Methods* **1991**, *31*, 315–324. [CrossRef]
158. Graham, S.P.; Everett, H.E.; Haines, F.J.; Johns, H.L.; Sosan, O.A.; Salguero, F.J.; Clifford, D.J.; Steinbach, F.; Drew, T.W.; Crooke, H.R. Challenge of pigs with classical swine fever viruses after C-strain vaccination reveals remarkably rapid protection and insights into early immunity. *PLoS ONE* **2012**, *7*, e29310. [CrossRef] [PubMed]
159. Renson, P.; Le Dimna, M.; Keranflech, A.; Cariolet, R.; Koenen, F.; Le Potier, M.F. CP7_E2alf oral vaccination confers partial protection against early classical swine fever virus challenge and interferes with pathogeny-related cytokine responses. *Vet. Res.* **2013**, *44*, 9. [CrossRef] [PubMed]
160. van Oirschot, J.T. Vaccinology of classical swine fever: From lab to field. *Vet. Microbiol.* **2003**, *96*, 367–384. [CrossRef] [PubMed]
161. Graham, S.P.; Haines, F.J.; Johns, H.L.; Sosan, O.; La Rocca, S.A.; Lamp, B.; Rümenapf, T.; Everett, H.E.; Crooke, H.R. Characterisation of vaccine-induced, broadly cross-reactive IFN-γ secreting T cell responses that correlate with rapid protection against classical swine fever virus. *Vaccine* **2012**, *30*, 2742–2748. [CrossRef] [PubMed]
162. Tarradas, J.; Argilaguet, J.M.; Rosell, R.; Nofrarias, M.; Crisci, E.; Cordoba, L.; Perez-Martin, E.; Diaz, I.; Rodriguez, F.; Domingo, M.; et al. Interferon-γ induction correlates with protection by DNA vaccine expressing E2 glycoprotein against classical swine fever virus infection in domestic pigs. *Vet. Microbiol.* **2010**, *142*, 51–58. [CrossRef] [PubMed]
163. Ganges, L.; Barrera, M.; Nunez, J.I.; Blanco, I.; Frias, M.T.; Rodriguez, F.; Sobrino, F. A DNA vaccine expressing the E2 protein of classical swine fever virus elicits T cell responses that can prime for rapid antibody production and confer total protection upon viral challenge. *Vaccine* **2005**, *23*, 3741–3752. [CrossRef] [PubMed]
164. Blacksell, S.D.; Khounsy, S.; Van Aken, D.; Gleeson, L.J.; Westbury, H.A. Comparative susceptibility of indigenous and improved pig breeds to classical swine fever virus infection: Practical and epidemiological implications in a subsistence-based, developing country setting. *Trop. Anim. Health Prod.* **2006**, *38*, 467–474. [CrossRef] [PubMed]
165. Everett, H.; Crooke, H.; Gurrala, R.; Dwarka, R.; Kim, J.; Botha, B.; Lubisi, A.; Pardini, A.; Gers, S.; Vosloo, W.; et al. Experimental infection of common warthogs (*Phacochoerus africanus*) and bushpigs (*Potamochoerus larvatus*) with classical swine fever virus. I: Susceptibility and transmission. *Transbound. Emerg. Dis.* **2011**. [CrossRef] [PubMed]
166. Terpstra, C. Epizootiology of swine fever. *Vet. Q.* **1987**, *9* (Suppl. 1), 50S–60S. [CrossRef] [PubMed]
167. Weesendorp, E.; Landman, W.J.; Stegeman, A.; Loeffen, W.L. Detection and quantification of classical swine fever virus in air samples originating from infected pigs and experimentally produced aerosols. *Vet. Microbiol.* **2008**, *127*, 50–62. [CrossRef] [PubMed]
168. Weesendorp, E.; Stegeman, A.; Loeffen, W.L. Quantification of classical swine fever virus in aerosols originating from pigs infected with strains of high, moderate or low virulence. *Vet. Microbiol.* **2009**, *135*, 222–230. [CrossRef] [PubMed]

169. Laevens, H.; Koenen, F.; Deluyker, H.; de Kruif, A. Experimental infection of slaughter pigs with classical swine fever virus: Transmission of the virus, course of the disease and antibody response. *Vet. Rec.* **1999**, *145*, 243–248. [CrossRef] [PubMed]
170. de Smit, A.J.; Bouma, A.; Terpstra, C.; van Oirschot, J.T. Transmission of classical swine fever virus by artificial insemination. *Vet. Microbiol.* **1999**, *67*, 239–249. [CrossRef]
171. Floegel, G.; Wehrend, A.; Depner, K.R.; Fritzemeier, J.; Waberski, D.; Moennig, V. Detection of classical swine fever virus in semen of infected boars. *Vet. Microbiol.* **2000**, *77*, 109–116. [CrossRef]
172. Moennig, V.; Greiser-Wilke, I. Classical swine fever virus. In *Encyclopedia of Virology*; Mahy, B.W.J., van Regenmortel, M.H.V., Eds.; Elsevier: Amsterdam, The Netherlands, 2008; pp. 525–532.
173. Pasick, J. Classical swine fever. In *Foreign Animal Diseases*, 7th ed.; Brown, C., Torres, A., Eds.; Committee on Foreign and Emerging Diseases of the United States Animal Health Association, Boca Publications Group: Boca Raton, FL, USA, 2008; pp. 197–205.
174. Hoffmann, B.; Beer, M.; Reid, S.M.; Mertens, P.; Oura, C.A.; van Rijn, P.A.; Slomka, M.J.; Banks, J.; Brown, I.H.; Alexander, D.J.; et al. A review of RT-PCR technologies used in veterinary virology and disease control: Sensitive and specific diagnosis of five livestock diseases notifiable to the World Organisation for Animal Health. *Vet. Microbiol.* **2009**, *139*, 1–23. [CrossRef] [PubMed]
175. Hoffmann, B.; Beer, M.; Schelp, C.; Schirrmeier, H.; Depner, K. Validation of a real-time RT-PCR assay for sensitive and specific detection of classical swine fever. *J. Virol. Methods* **2005**, *130*, 36–44. [CrossRef] [PubMed]
176. Hoffmann, B.; Blome, S.; Bonilauri, P.; Fernandez-Pinero, J.; Greiser-Wilke, I.; Haegeman, A.; Isaksson, M.; Koenen, F.; Leblanc, N.; Leifer, I.; et al. Classical swine fever virus detection: Results of a real-time reverse transcription polymerase chain reaction ring trial conducted in the framework of the European network of excellence for epizootic disease diagnosis and control. *J. Vet. Diagn. Investig.* **2011**, *23*, 999–1004. [CrossRef] [PubMed]
177. Le Dimna, M.; Vrancken, R.; Koenen, F.; Bougeard, S.; Mesplede, A.; Hutet, E.; Kuntz-Simon, G.; Le Potier, M.F. Validation of two commercial real-time RT-PCR kits for rapid and specific diagnosis of classical swine fever virus. *J. Virol. Methods* **2008**, *147*, 136–142. [CrossRef] [PubMed]
178. Le Potier, M.F.; Le Dimna, M.; Kuntz-Simon, G.; Bougeard, S.; Mesplede, A. Validation of a real-time RT-PCR assay for rapid and specific diagnosis of classical swine fever virus. *Dev. Biol. (Basel)* **2006**, *126*, 179–186; discusssion 326–327. [PubMed]
179. Leifer, I.; Blome, S.; Beer, M.; Hoffmann, B. Development of a highly sensitive real-time RT-PCR protocol for the detection of classical swine fever virus independent of the 5′ untranslated region. *J. Virol. Methods* **2011**, *171*, 314–317. [CrossRef] [PubMed]
180. McGoldrick, A.; Lowings, J.P.; Ibata, G.; Sands, J.J.; Belak, S.; Paton, D.J. A novel approach to the detection of classical swine fever virus by RT-PCR with a fluorogenic probe (TaqMan). *J. Virol. Methods* **1998**, *72*, 125–135. [CrossRef]
181. Paton, D.J.; McGoldrick, A.; Belak, S.; Mittelholzer, C.; Koenen, F.; Vanderhallen, H.; Biagetti, M.; De Mia, G.M.; Stadejek, T.; Hofmann, M.A.; et al. Classical swine fever virus: A ring test to evaluate RT-PCR detection methods. *Vet. Microbiol.* **2000**, *73*, 159–174. [CrossRef]
182. Paton, D.J.; McGoldrick, A.; Bensaude, E.; Belak, S.; Mittelholzer, C.; Koenen, F.; Vanderhallen, H.; Greiser-Wilke, I.; Scheibner, H.; Stadejek, T.; et al. Classical swine fever virus: A second ring test to evaluate RT-PCR detection methods. *Vet. Microbiol.* **2000**, *77*, 71–81. [CrossRef]
183. Belak, S. Experiences of an oie collaborating centre in molecular diagnosis of transboundary animal diseases: A review. *Dev. Biol. (Basel)* **2007**, *128*, 103–112. [PubMed]
184. Liu, L.; Luo, Y.; Accensi, F.; Ganges, L.; Rodriguez, F.; Shan, H.; Stahl, K.; Qiu, H.J.; Belak, S. Pre-clinical evaluation of a real-time PCR assay on a portable instrument as a possible field diagnostic tool: Experiences from the testing of clinical samples for African and classical swine fever viruses. *Transbound. Emerg. Dis.* **2016**. [CrossRef] [PubMed]
185. Chen, H.T.; Zhang, J.; Ma, L.N.; Ma, Y.P.; Ding, Y.Z.; Liu, X.T.; Chen, L.; Ma, L.Q.; Zhang, Y.G.; Liu, Y.S. Rapid pre-clinical detection of classical swine fever by reverse transcription loop-mediated isothermal amplification. *Mol. Cell. Probes* **2009**, *23*, 71–74. [CrossRef] [PubMed]

186. Chen, L.; Fan, X.Z.; Wang, Q.; Xu, L.; Zhao, Q.Z.; Zhou, Y.C.; Liu, J.; Tang, B.; Zou, X.Q. A novel RT-LAMP assay for rapid and simple detection of classical swine fever virus. *Virol. Sin.* **2010**, *25*, 59–64. [CrossRef] [PubMed]
187. Chowdry, V.K.; Luo, Y.; Widen, F.; Qiu, H.J.; Shan, H.; Belak, S.; Liu, L. Development of a loop-mediated isothermal amplification assay combined with a lateral flow dipstick for rapid and simple detection of classical swine fever virus in the field. *J. Virol. Methods* **2014**, *197*, 14–18. [CrossRef] [PubMed]
188. Yin, S.; Shang, Y.; Zhou, G.; Tian, H.; Liu, Y.; Cai, X.; Liu, X. Development and evaluation of rapid detection of classical swine fever virus by reverse transcription loop-mediated isothermal amplification (RT-LAMP). *J. Biotechnol.* **2010**, *146*, 147–150. [CrossRef] [PubMed]
189. Zhang, X.J.; Han, Q.Y.; Sun, Y.; Belak, S.; Liu, L.; Qiu, H.J. Development of a loop-mediated isothermal amplification for visual detection of the HCLV vaccine against classical swine fever in China. *J. Virol. Methods* **2011**, *171*, 200–205. [CrossRef] [PubMed]
190. Zhang, X.J.; Sun, Y.; Liu, L.; Belak, S.; Qiu, H.J. Validation of a loop-mediated isothermal amplification assay for visualised detection of wild-type classical swine fever virus. *J. Virol. Methods* **2010**, *167*, 74–78. [CrossRef] [PubMed]
191. Liu, L.; Xia, H.; Belak, S.; Widen, F. Development of a primer-probe energy transfer real-time PCR assay for improved detection of classical swine fever virus. *J. Virol. Methods* **2009**, *160*, 69–73. [CrossRef] [PubMed]
192. Zhang, X.J.; Xia, H.; Everett, H.; Sosan, O.; Crooke, H.; Belak, S.; Widen, F.; Qiu, H.J.; Liu, L. Evaluation of a primer-probe energy transfer real-time PCR assay for detection of classical swine fever virus. *J. Virol. Methods* **2010**, *168*, 259–261. [CrossRef] [PubMed]
193. Lung, O.; Pasick, J.; Fisher, M.; Buchanan, C.; Erickson, A.; Ambagala, A. Insulated isothermal reverse transcriptase PCR (iiRT-PCR) for rapid and sensitive detection of classical swine fever virus. *Transbound. Emerg. Dis.* **2016**, *63*, e395–402. [CrossRef] [PubMed]
194. Turner, L.W.; Brown, L.N.; Carbrey, E.A.; Mengeling, W.L.; Perella, D.H.; Solorzano, R.F. Recommended minimum standards for the isolation and identification of hog cholera by the fluorescent antibody-cell culture technique. *Proc. Annu. Meet. U. S. Anim. Health Assoc.* **1968**, *72*, 444–447. [PubMed]
195. De Smit, A.J.; Eble, P.L.; de Kluijver, E.P.; Bloemraad, M.; Bouma, A. Laboratory experience during the classical swine fever virus epizootic in the Netherlands in 1997–1998. *Vet. Microbiol.* **2000**, *73*, 197–208. [CrossRef]
196. Blome, S.; Meindl-Böhmer, A.; Loeffen, W.; Thuer, B.; Moennig, V. Assessment of classical swine fever diagnostics and vaccine performance. *Rev. Sci. Tech.* **2006**, *25*, 1025–1038. [CrossRef] [PubMed]
197. Greiser-Wilke, I.; Blome, S.; Moennig, V. Diagnostic methods for detection of classical swine fever virus–status quo and new developments. *Vaccine* **2007**, *25*, 5524–5530. [CrossRef] [PubMed]
198. Floegel-Niesmann, G. Marker vaccines and companion diagnostic tests for classical swine fever. *Dev. Biol. (Basel)* **2003**, *114*, 185–191. [PubMed]
199. Floegel-Niesmann, G. Classical swine fever (CSF) marker vaccine. Trial III. Evaluation of discriminatory ELISAs. *Vet. Microbiol.* **2001**, *83*, 121–136. [CrossRef]
200. Meyer, D.; Fritsche, S.; Luo, Y.; Engemann, C.; Blome, S.; Beyerbach, M.; Chang, C.Y.; Qiu, H.J.; Becher, P.; Postel, A. The double-antigen ELISA concept for early detection of E^{rns} -specific classical swine fever virus antibodies and application as an accompanying test for differentiation of infected from marker vaccinated animals. *Transbound. Emerg. Dis.* **2017**. [CrossRef] [PubMed]
201. Aebischer, A.; Müller, M.; Hofmann, M.A. Two newly developed E^{rns}-based ELISAs allow the differentiation of classical swine fever virus-infected from marker-vaccinated animals and the discrimination of pestivirus antibodies. *Vet. Microbiol.* **2013**, *161*, 274–285. [CrossRef] [PubMed]
202. Xia, H.; Harimoorthy, R.; Vijayaraghavan, B.; Blome, S.; Widen, F.; Beer, M.; Belak, S.; Liu, L. Differentiation of classical swine fever virus infection from CP7_E2alf marker vaccination by a multiplex microsphere immunoassay. *Clin. Vaccine Immunol.* **2015**, *22*, 65–71. [CrossRef] [PubMed]
203. Huang, Y.L.; Pang, V.F.; Pan, C.H.; Chen, T.H.; Jong, M.H.; Huang, T.S.; Jeng, C.R. Development of a reverse transcription multiplex real-time PCR for the detection and genotyping of classical swine fever virus. *J. Virol. Methods* **2009**, *160*, 111–118. [CrossRef] [PubMed]
204. Leifer, I.; Depner, K.; Blome, S.; Le Potier, M.F.; Le Dimna, M.; Beer, M.; Hoffmann, B. Differentiation of C-strain "Riems" or CP7_E2alf vaccinated animals from animals infected by classical swine fever virus field strains using real-time RT-PCR. *J. Virol. Methods* **2009**, *158*, 114–122. [CrossRef] [PubMed]

205. Li, Y.; Zhao, J.J.; Li, N.; Shi, Z.; Cheng, D.; Zhu, Q.H.; Tu, C.; Tong, G.Z.; Qiu, H.J. A multiplex nested RT-PCR for the detection and differentiation of wild-type viruses from C-strain vaccine of classical swine fever virus. *J. Virol. Methods* **2007**, *143*, 16–22. [CrossRef] [PubMed]
206. Liu, L.; Hoffmann, B.; Baule, C.; Beer, M.; Belak, S.; Widen, F. Two real-time RT-PCR assays of classical swine fever virus, developed for the genetic differentiation of naturally infected from vaccinated wild boars. *J. Virol. Methods* **2009**, *159*, 131–133. [CrossRef] [PubMed]
207. Widen, F.; Everett, H.; Blome, S.; Fernandez Pinero, J.; Uttenthal, A.; Cortey, M.; von Rosen, T.; Tignon, M.; Liu, L. Comparison of two real-time RT-PCR assays for differentiation of C-strain vaccinated from classical swine fever infected pigs and wild boars. *Res. Vet. Sci.* **2014**, *97*, 455–457. [CrossRef] [PubMed]
208. Zhao, J.J.; Cheng, D.; Li, N.; Sun, Y.; Shi, Z.; Zhu, Q.H.; Tu, C.; Tong, G.Z.; Qiu, H.J. Evaluation of a multiplex real-time RT-PCR for quantitative and differential detection of wild-type viruses and C-strain vaccine of classical swine fever virus. *Vet. Microbiol.* **2008**, *126*, 1–10. [CrossRef] [PubMed]
209. Dietze, K.; Tucakov, A.; Engel, T.; Wirtz, S.; Depner, K.; Globig, A.; Kammerer, R.; Mouchantat, S. Rope-based oral fluid sampling for early detection of classical swine fever in domestic pigs at group level. *BMC Vet. Res.* **2017**, *13*, 5. [CrossRef] [PubMed]
210. Michaud, V.; Gil, P.; Kwiatek, O.; Prome, S.; Dixon, L.; Romero, L.; Le Potier, M.F.; Arias, M.; Couacy-Hymann, E.; Roger, F.; et al. Long-term storage at tropical temperature of dried-blood filter papers for detection and genotyping of RNA and DNA viruses by direct PCR. *J. Virol. Methods* **2007**, *146*, 257–265. [CrossRef] [PubMed]
211. Mouchantat, S.; Globig, A.; Böhle, W.; Petrov, A.; Strebelow, H.G.; Mettenleiter, T.C.; Depner, K. Novel rope-based sampling of classical swine fever shedding in a group of wild boar showing low contagiosity upon experimental infection with a classical swine fever field strain of genotype 2.3. *Vet. Microbiol.* **2014**, *170*, 425–429. [CrossRef] [PubMed]
212. Prickett, J.R.; Zimmerman, J.J. The development of oral fluid-based diagnostics and applications in veterinary medicine. *Anim. Health Res. Rev.* **2010**, *11*, 207–216. [CrossRef] [PubMed]
213. Greiser-Wilke, I.; Moennig, V. Vaccination against classical swine fever virus: Limitations and new strategies. *Anim. Health Res. Rev.* **2004**, *5*, 223–226. [CrossRef] [PubMed]
214. World Animal Health Information Database (WAHIS) Interface. Available online: http://www.oie.int/wahis_2/public/wahid.php/Diseasecontrol/measures (accessed 19 April 2017).
215. Kaden, V.; Lange, E.; Fischer, U.; Strebelow, G. Oral immunisation of wild boar against classical swine fever: Evaluation of the first field study in Germany. *Vet. Microbiol.* **2000**, *73*, 239–252. [CrossRef]
216. Kaden, V.; Lange, E.; Küster, H.; Müller, T.; Lange, B. An update on safety studies on the attenuated "RIEMSER Schweinepestoralvakzine" for vaccination of wild boar against classical swine fever. *Vet. Microbiol.* **2010**, *143*, 133–138. [CrossRef] [PubMed]
217. Milicevic, V.; Dietze, K.; Plavsic, B.; Tikvicki, M.; Pinto, J.; Depner, K. Oral vaccination of backyard pigs against classical swine fever. *Vet. Microbiol.* **2012**, *225*, 167–171. [CrossRef] [PubMed]
218. Dietze, K.; Milicevic, V.; Depner, K. Prospects of improved classical swine fever control in backyard pigs through oral vaccination. *Berl. Munch. Tierarztl. Wochenschr.* **2013**, *126*, 476–480. [PubMed]
219. Monger, V.R.; Stegeman, J.A.; Dukpa, K.; Gurung, R.B.; Loeffen, W.L. Evaluation of oral bait vaccine efficacy against classical swine fever in village backyard pig farms in Bhutan. *Transbound. Emerg. Dis.* **2016**, *63*, e211–e218. [CrossRef] [PubMed]
220. Dahle, J.; Liess, B. Assessment of safety and protective value of a cell culture modified strain "C" vaccine of hog cholera/classical swine fever virus. *Berl. Munch. Tierarztl. Wochenschr.* **1995**, *108*, 20–25. [PubMed]
221. Kaden, V.; Riebe, B. Classical swine fever (CSF): A historical review of research and vaccine production on the Isle of Riems. *Berl. Munch. Tierarztl. Wochenschr.* **2001**, *114*, 246–251. [PubMed]
222. Terpstra, C.; Woortmeyer, R.; Barteling, S.J. Development and properties of a cell culture produced vaccine for hog cholera based on the Chinese strain. *Dtsch. Tierarztl. Wochenschr.* **1990**, *97*, 77–79. [PubMed]
223. Ferrari, M. A tissue culture vaccine with lapinized Chinese (LC) strain of hog cholera virus (HCV). *Comp. Immunol. Microbiol. Infect. Dis.* **1992**, *15*, 221–228. [CrossRef]
224. Blome, S.; Gabriel, C.; Beer, M. Possibilities and limitations in veterinary vaccine development using the example of classical swine fever. *Berl. Munch. Tierarztl. Wochenschr.* **2013**, *126*, 481–490. [PubMed]
225. Ahrens, U.; Kaden, V.; Drexler, C.; Visser, N. Efficacy of the classical swine fever (CSF) marker vaccine Porcilis Pesti in pregnant sows. *Vet. Microbiol.* **2000**, *77*, 83–97. [CrossRef]

226. Bouma, A.; De Smit, A.J.; De Jong, M.C.; De Kluijver, E.P.; Moormann, R.J. Determination of the onset of the herd-immunity induced by the E2 sub-unit vaccine against classical swine fever virus. *Vaccine* **2000**, *18*, 1374–1381. [CrossRef]
227. Bouma, A.; de Smit, A.J.; de Kluijver, E.P.; Terpstra, C.; Moormann, R.J. Efficacy and stability of a subunit vaccine based on glycoprotein E2 of classical swine fever virus. *Vet. Microbiol.* **1999**, *66*, 101–114. [CrossRef]
228. de Smit, A.J.; Bouma, A.; de Kluijver, E.P.; Terpstra, C.; Moormann, R.J. Duration of the protection of an E2 subunit marker vaccine against classical swine fever after a single vaccination. *Vet. Microbiol.* **2001**, *78*, 307–317. [CrossRef]
229. de Smit, A.J.; Bouma, A.; de Kluijver, E.P.; Terpstra, C.; Moormann, R.J. Prevention of transplacental transmission of moderate-virulent classical swine fever virus after single or double vaccination with an E2 subunit vaccine. *Vet. Q.* **2000**, *22*, 150–153. [CrossRef] [PubMed]
230. Dewulf, J.; Laevens, H.; Koenen, F.; Vanderhallen, H.; Mintiens, K.; Deluyker, H.; de Kruif, A. An experimental infection with classical swine fever in E2 sub-unit marker-vaccine vaccinated and in non-vaccinated pigs. *Vaccine* **2000**, *19*, 475–482. [CrossRef]
231. Klinkenberg, D.; Moormann, R.J.; de Smit, A.J.; Bouma, A.; de Jong, M.C. Influence of maternal antibodies on efficacy of a subunit vaccine: Transmission of classical swine fever virus between pigs vaccinated at 2 weeks of age. *Vaccine* **2002**, *20*, 3005–3013. [CrossRef]
232. Lipowski, A.; Drexler, C.; Pejsak, Z. Safety and efficacy of a classical swine fever subunit vaccine in pregnant sows and their offspring. *Vet. Microbiol.* **2000**, *77*, 99–108. [CrossRef]
233. Moormann, R.J.; Bouma, A.; Kramps, J.A.; Terpstra, C.; De Smit, H.J. Development of a classical swine fever subunit marker vaccine and companion diagnostic test. *Vet. Microbiol.* **2000**, *73*, 209–219. [CrossRef]
234. van Aarle, P. Suitability of an E2 subunit vaccine of classical swine fever in combination with the E^{rns}-marker-test for eradication through vaccination. *Dev. Biol. (Basel)* **2003**, *114*, 193–200. [PubMed]
235. van Oirschot, J.T. DIVA vaccines that reduce virus transmission. *J. Biotechnol.* **1999**, *73*, 195–205. [CrossRef]
236. van Oirschot, J.T. Emergency vaccination against classical swine fever. *Dev. Biol. (Basel)* **2003**, *114*, 259–267. [PubMed]
237. Depner, K.R.; Bouma, A.; Koenen, F.; Klinkenberg, D.; Lange, E.; de Smit, H.; Vanderhallen, H. Classical swine fever (CSF) marker vaccine. Trial II. Challenge study in pregnant sows. *Vet. Microbiol.* **2001**, *83*, 107–120. [CrossRef]
238. Beer, M.; Reimann, I.; Hoffmann, B.; Depner, K. Novel marker vaccines against classical swine fever. *Vaccine* **2007**, *25*, 5665–5670. [CrossRef] [PubMed]
239. Blome, S.; Moss, C.; Reimann, I.; König, P.; Beer, M. Classical swine fever vaccines-state-of-the-art. *Vet. Microbiol.* **2017**, *201–204*. [CrossRef] [PubMed]
240. Blome, S.; Aebischer, A.; Lange, E.; Hofmann, M.; Leifer, I.; Loeffen, W.; Koenen, F.; Beer, M. Comparative evaluation of live marker vaccine candidates "CP7_E2alf" and "flc11" along with C-strain "Riems" after oral vaccination. *Vet. Microbiol.* **2012**, *158*, 42–59. [CrossRef] [PubMed]
241. Blome, S.; Gabriel, C.; Schmeiser, S.; Meyer, D.; Meindl-Böhmer, A.; Koenen, F.; Beer, M. Efficacy of marker vaccine candidate CP7_E2alf against challenge with classical swine fever virus isolates of different genotypes. *Vet. Microbiol.* **2014**, *169*, 8–17. [CrossRef] [PubMed]
242. Dräger, C.; Petrov, A.; Beer, M.; Teifke, J.P.; Blome, S. Classical swine fever virus marker vaccine strain CP7_E2alf: Shedding and dissemination studies in boars. *Vaccine* **2015**, *33*, 3100–3103. [CrossRef] [PubMed]
243. Dräger, C.; Schröder, C.; König, P.; Tegtmeyer, B.; Beer, M.; Blome, S. Efficacy of Suvaxyn CSF marker (CP7_E2alf) in the presence of pre-existing pestiviral antibodies against bovine viral diarrhea virus type 1. *Vaccine* **2016**, in press.
244. Eble, P.L.; Geurts, Y.; Quak, S.; Moonen-Leusen, H.W.; Blome, S.; Hofmann, M.A.; Koenen, F.; Beer, M.; Loeffen, W.L. Efficacy of chimeric pestivirus vaccine candidates against classical swine fever: Protection and DIVA characteristics. *Vet. Microbiol.* **2012**, *162*, 437–446. [CrossRef] [PubMed]
245. Eble, P.L.; Quak, S.; Geurts, Y.; Moonen-Leusen, H.W.; Loeffen, W.L. Efficacy of csf vaccine CP7_E2alf in piglets with maternally derived antibodies. *Vet. Microbiol.* **2014**, *174*, 27–38. [CrossRef] [PubMed]
246. Feliziani, F.; Blome, S.; Petrini, S.; Giammarioli, M.; Iscaro, C.; Severi, G.; Convito, L.; Pietschmann, J.; Beer, M.; De Mia, G.M. First assessment of classical swine fever marker vaccine candidate CP7_E2alf for oral immunization of wild boar under field conditions. *Vaccine* **2014**, *32*, 2050–2055. [CrossRef] [PubMed]

247. Gabriel, C.; Blome, S.; Urniza, A.; Juanola, S.; Koenen, F.; Beer, M. Towards licensing of CP7_E2alf as marker vaccine against classical swine fever-duration of immunity. *Vaccine* **2012**, *30*, 2928–2936. [CrossRef] [PubMed]
248. Goller, K.V.; Dräger, C.; Höper, D.; Beer, M.; Blome, S. Classical swine fever virus marker vaccine strain CP7_E2alf: Genetic stability in vitro and in vivo. *Arch. Virol.* **2015**, *160*, 3121–3125. [CrossRef] [PubMed]
249. König, P.; Blome, S.; Gabriel, C.; Reimann, I.; Beer, M. Innocuousness and safety of classical swine fever marker vaccine candidate CP7_E2alf in non-target and target species. *Vaccine* **2011**, *30*, 5–8. [CrossRef] [PubMed]
250. König, P.; Hoffmann, B.; Depner, K.R.; Reimann, I.; Teifke, J.P.; Beer, M. Detection of classical swine fever vaccine virus in blood and tissue samples of pigs vaccinated either with a conventional C-strain vaccine or a modified live marker vaccine. *Vet. Microbiol.* **2007**, *120*, 343–351. [CrossRef] [PubMed]
251. König, P.; Lange, E.; Reimann, I.; Beer, M. CP7_E2alf: A safe and efficient marker vaccine strain for oral immunisation of wild boar against classical swine fever virus (CSFV). *Vaccine* **2007**, *25*, 3391–3399. [CrossRef] [PubMed]
252. Leifer, I.; Lange, E.; Reimann, I.; Blome, S.; Juanola, S.; Duran, J.P.; Beer, M. Modified live marker vaccine candidate CP7_E2alf provides early onset of protection against lethal challenge infection with classical swine fever virus after both intramuscular and oral immunization. *Vaccine* **2009**, *27*, 6522–6529. [CrossRef] [PubMed]
253. Levai, R.; Barna, T.; Fabian, K.; Blome, S.; Belak, K.; Balint, A.; Koenen, F.; Kulcsar, G.; Farsang, A. Pre-registration efficacy study of a novel marker vaccine against classical swine fever on maternally derived antibody negative (MDA-) target animals. *Biologicals* **2015**, *14*, 1045–1056. [CrossRef] [PubMed]
254. Rangelova, D.; Nielsen, J.; Strandbygaard, B.; Koenen, F.; Blome, S.; Uttenthal, A. Efficacy of marker vaccine candidate CP7_E2alf in piglets with maternally derived C-strain antibodies. *Vaccine* **2012**, *30*, 6376–6381. [CrossRef] [PubMed]
255. Reimann, I.; Depner, K.; Trapp, S.; Beer, M. An avirulent chimeric *Pestivirus* with altered cell tropism protects pigs against lethal infection with classical swine fever virus. *Virology* **2004**, *322*, 143–157. [CrossRef] [PubMed]
256. Renson, P.; Le Dimna, M.; Gabriel, C.; Levai, R.; Blome, S.; Kulcsar, G.; Koenen, F.; Le Potier, M.F. Cytokine and immunoglobulin isotype profiles during CP7_E2alf vaccination against a challenge with the highly virulent Koslov strain of classical swine fever virus. *Res. Vet. Sci.* **2014**, *96*, 389–395. [CrossRef] [PubMed]
257. Farsang, A.; Levai, R.; Barna, T.; Fabian, K.; Blome, S.; Belak, K.; Balint, A.; Koenen, F.; Kulcsar, G. Pre-registration efficacy study of a novel marker vaccine against classical swine fever on maternally derived antibody positive (MDA+) target animals. *Biologicals* **2017**, *45*, 85–92. [CrossRef] [PubMed]

© 2017 by the authors. Licensee MDPI, Basel, Switzerland. This article is an open access article distributed under the terms and conditions of the Creative Commons Attribution (CC BY) license (http://creativecommons.org/licenses/by/4.0/).

viruses

MDPI

Article

UK Pigs at the Time of Slaughter: Investigation into the Correlation of Infection with PRRSV and HEV

Jean-Pierre Frossard [1,*], Sylvia Grierson [1,*], Tanya Cheney [1], Falko Steinbach [1], Bhudipa Choudhury [1] and Susanna Williamson [2]

[1] Animal and Plant Health Agency, Woodham Lane, New Haw, Surrey KT15 3NB, UK; tcheney87@hotmail.com (T.C.); Falko.Steinbach@apha.gsi.gov.uk (F.S.); Bhudipa.Choudhury@apha.gsi.gov.uk (B.C.)

[2] Surveillance Intelligence Unit, Animal and Plant Health Agency, Rougham Hill, Bury St Edmunds, Suffolk IP33 2RX, UK; Susanna.Williamson@apha.gsi.gov.uk

* Correspondence: jean-pierre.frossard@apha.gsi.gov.uk (J.-P.F.); Sylvia.Grierson@apha.gsi.gov.uk (S.G.); Tel.: +44-020-8026-9730 (J.-P.F.); +44-020-8415-2219 (S.G.)

Academic Editors: Linda Dixon and Simon Graham
Received: 29 March 2017; Accepted: 6 May 2017; Published: 9 June 2017

Abstract: Hepatitis E virus (HEV) and porcine reproductive and respiratory syndrome virus (PRRSV) and are both globally prevalent in the pig population. While HEV does not cause clinical disease in pigs, its zoonotic potential has raised concerns in the food safety sector. PRRS has become endemic in the United Kingdom (UK) since its introduction in 1991, and continues to cause considerable economic losses to the swine industry. A better understanding of the current prevalence and diversity of PRRSV and HEV in the UK, and their potential association, is needed to assess risks and target control measures appropriately. This study used plasma, tonsil, and cecal content samples previously collected from pigs in 14 abattoirs in England and Northern Ireland to study the prevalence of several pathogens including PRRSV and HEV. The diversity of PRRSV strains detected in these samples was analyzed by sequencing open reading frame 5 (*ORF5*), revealing no substantial difference in PRRSV strains from these clinically unaffected pigs relative to those from clinical cases of disease in the UK. Despite the potential immuno-modulatory effect of PRRSV infection, previously demonstrated to affect *Salmonella* and HEV shedding profiles, no significant association was found between positive PRRSV status and positive HEV status.

Keywords: porcine viruses; PRRSV; HEV; evolution and molecular epidemiology; co-infections

1. Introduction

Hepatitis E virus (HEV) is the cause of hepatitis E in humans, typically a self-limiting hepatitis but more serious in those with pre-existing liver conditions and in the immunocompromised [1]. In pigs, HEV infection alone does not cause clinical disease. HEV genotypes HEV-3 and HEV-4 are the cause of sporadic cases of hepatitis E in developed countries, and are ubiquitous in the pig population worldwide [2]. Hepatitis E is a foodborne zoonosis, for which pork or pork products from infected pigs is one of the risks identified in Europe [1,2] and consumption of processed pork products in the United Kingdom (UK) has been shown to be associated with an increased risk of acquiring HEV [3]. Hence, there is a need to better understand factors influencing HEV entering the food chain.

Porcine reproductive and respiratory syndrome virus (PRRSV) was first confirmed in the UK in 1991 and is now considered endemic [4]. The economic and welfare impacts of the disease are considerable, as both the breeder and grower segments of the pig industry are affected [5]. All PRRSV infections in the UK characterized to date have been identified as being caused by genotype 1 virus, but the genetic diversity of the virus is continually increasing [6]. The phylogenetic analyses

of UK PRRSV sequences have previously been based on data from samples submitted for diagnostic purposes, originating from clinical cases of PRRS, thereby possibly introducing a bias in our coverage of circulating strains. It is therefore possible that PRRSV strains circulating in apparently healthy pigs in the UK may represent a different subset from those causing disease.

PRRSV infection has been suggested to modulate pig immune responses, thereby rendering pigs more susceptible to other infections [7–9]. For example, previous studies have shown significant associations between PRRSV presence and *Salmonella* shedding [10]. Salines et al. [11] reported that experimental co-infection of HEV and PRRSV affected the dynamics of HEV infection. However, a direct immune-regulation in infected pigs could not be confirmed for genotype 1 PRRSV [12], rather suggesting a role for co-infection viruses influencing each other more directly. Moreover, less pathogenic strains of genotype 1 PRRSV seem to cause a more persistent infection than highly pathogenic ones which are better resolved by the immune response [13]. Notably, viruses closely related to the modified-live vaccine used in the UK have previously been found circulating on farms with clinical PRRS [6].

In 2013, an abattoir-based study was undertaken to estimate the prevalence of various pathogens including HEV and PRRSV in UK-reared pigs at slaughter and seroprevalence for PRRSV was 58.3% (362/621) [14], while HEV seroprevalence was 92.8% (584/629). Approximately 5.7% of pigs were HEV viremic (36/629) and around one in five pigs had evidence of an active HEV infection (129/629), with HEV RNA detected in serum or cecal contents [15]. To follow up these studies, we report here on (1) the investigation of PRRSV active infection (RNA in tonsil) using the same 2013 abattoir survey sample-set and (2) an analysis of the correlation of PRRSV and HEV infection in these pigs, which could be of significance for the control of both diseases and in informing farming practices for reducing HEV in the food chain.

2. Materials and Methods

The overall study design for the abattoir survey has been described previously [14]. Briefly, 626 qualifying pigs were sampled at 14 abattoirs in England and Northern Ireland, between January and May 2013. These pigs originated from 439 farms, with between 1 and 10 pigs from each. The majority of pigs were from farms in England (81.7%), followed by Northern Ireland (13.4%), Scotland (4.5%), and Wales (0.3%), which is representative of the UK pig population [16]. Of the samples collected from each selected carcass along the processing line, those relevant for the investigation of HEV and PRRSV were a blood sample (whole blood with ethylenediaminetetraacetic acid (EDTA)), tonsil, and the whole cecum.

Antibody to PRRSV had been detected in 362 of 621 plasma samples, with 11 additional samples being inconclusive [14]. Only 610 of these plasma samples were also analyzed for the presence of antibodies to HEV, with 354 of these being sero-positive for PRRSV. Tonsil samples from all seropositive or inconclusive pigs were then tested by a real-time reverse transcription polymerase chain reaction (RT-PCR) to detect PRRSV nucleic acid. The tonsils of four other pigs for which plasma samples—and hence enzyme-linked immunosorbent assay (ELISA) results—were missing were also tested by PCR, while for five seropositive animals the tonsil samples were not available, so a total of 372 tonsil samples were analyzed; only 358 of these animals also had matching HEV PCR data. RNA was extracted from the tonsil samples using the MagNA Pure LC DNA Isolation kit II (Tissue) following the manufacturer's instructions (Roche Diagnostics, Burgess Hill, UK), setting the sample volume to 110 μL and the elution volume to 200 μL. A real-time RT-PCR assay targeting the nucleocapsid (*ORF7*) gene of PRRSV and differentiating genotypes 1 and 2 was used [17] with a Stratagene Mx3000P QPCR System (Agilent Genomics, Wokingham, UK). Sequencing of the PRRSV open reading frame 5 (*ORF5*) gene was subsequently performed on nucleic acids from tonsil samples testing positive in the diagnostic PRRSV PCR to characterize the viruses present [6]. The PCR amplicons were purified using the Beckman AMPure solid phase reversible immobilisation (SPRI) technique (Beckman Coulter Ltd., High Wycombe, UK). Cycle sequencing was performed using forward and

reverse primers and ABI BigDye chemistry (Applied Biosystems Ltd., Warrington, UK) at the end of which the dye terminators were removed using Beckman CleanSEQ SPRI (Beckman Coulter Ltd., High Wycombe, UK). Samples were sequenced on an ABI capillary electrophoresis DNA analyser (Applied Biosystems Ltd., Warrington, UK) and the raw data analysed by ABI SeqScape software (Applied Biosystems Ltd., Warrington, UK). The resulting sequences were aligned with 48 reference sequences from GenBank, and with 431 other UK PRRSV *ORF5* sequences from samples submitted to the Animal and Plant Health Agency (APHA) for PRRS diagnostic testing between 1991 and 2014, using the ClustalW algorithm [18] in MEGA6 [19]. The phylogenetic tree was generated in MEGA6 using the neighbour-joining method [20], with the evolutionary distances being computed using the maximum composite likelihood method [21]. The sequences obtained were deposited in GenBank with accession numbers MF043094 to MF043116.

Existing data for PRRSV seropositivity [14] and HEV seropositivity and active infection [15] were collated with data obtained in this study for PRRSV active infection. Associations between the two viruses, or antibodies to them, in the same carcasses were investigated using χ^2 tests, with Stata v.12 (StataCorp, College Station, TX, USA). Collated data for PRRSV seropositivity and HEV seropositivity and active infection (RNA in plasma and/ or cecal contents) were available for 610 pigs. Collated data for PRRSV active infection (RNA in tonsil) and seropositivity and active infection for HEV were available for 358 pigs.

3. Results

3.1. Detection of Active PRRSV Infection at Slaughter Age

PRRSV RNA was detected in 31 of 372 tonsil samples. This corresponds to 8.3% of the PRRSV seropositive finisher pigs showing active PRRSV infection at slaughter. Importantly, all PCR-positive samples were of genotype 1 (European), which is endemic in the UK, and no genotype 2 virus, which is exotic to the UK, was detected. While the ELISA-positive pigs tested by PCR originated from farms in 24 counties, PCR-positive pigs were only identified from farms in eight of those counties. Almost two-thirds of the PCR-positive pigs were from farms in East Anglia or East Riding and North Lincolnshire. While seropositivity had been found to vary significantly between age groups ($p = 0.002$) with the highest level found in pigs aged less than six months (68.5%) and lowest in those aged >12 months (32.1%) [14], the prevalence of PRRSV RNA-positive tonsils was similar across the age groups (Table 1).

Table 1. Porcine reproductive and respiratory syndrome virus (PRRSV) polymerase chain reaction (PCR) results for 372 tonsil samples from PRRS seropositive or inconclusive animals, by age.

Age	Number Tested	Number Positive	% Positive
<6 months	34	4	11.8%
6–12 months	312	25	8.0%
>12 months	19	2	10.5%
Not known	7	0	0%

3.2. PRRSV Genetic Characterization

Sequencing of the *ORF5* PRRSV gene was undertaken on 29 of the 31 tonsil samples from which PRRSV RNA was detected. Two PCR-positive tonsils were not suitable for sequencing as there was insufficient viral nucleic acid in the samples. Six samples did not yield useable sequence data. All of the sequences confirm that the viruses belong to PRRSV genotype 1. Only three of the sequences may be considered to possibly originate from the currently licensed attenuated vaccine, with greater than 99% similarity between the sample and vaccine strain *ORF5* sequences (99.2%, 99.8%, and 100%).

The phylogenetic trees (Figure 1) illustrate the genetic diversity of the *ORF5* genes from the 23 samples in this study in comparison to the vaccine virus licensed in the UK at the time and 48 published reference sequences representing the different genotypes and subtypes (Figure 1A)

and in more detail, in the context of 431 previously sequenced viruses specifically from UK pigs between 1991 and 2014 (unpublished data) (Figure 1B). In the within-UK analysis, there is no clear association between geographic origin and the clade in which the PRRSV strains belong. All of the 23 sequences are found in clades where other UK strains were already identified, and no distinct clustering is observed.

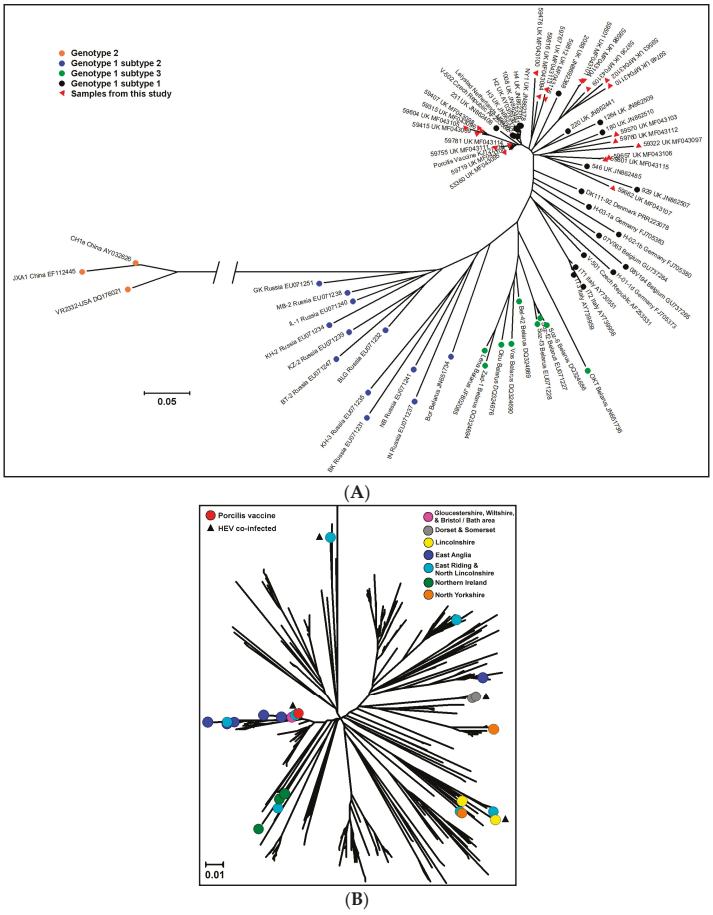

3.3. PRRSV and HEV Co-Infections

Analyses were performed to identify potential associations between PRRSV serology or PCR status (PRRSV RNA detected in tonsil sample) and HEV serology or PCR status (HEV RNA detected in serum or cecal contents). These are summarized in Tables 2 and 3. Of the six animals that were PCR positive for both HEV and PRRSV, one was less than six months old, three were six months of age, and two were greater than six months of age.

Table 2. Association of hepatitis E virus (HEV) with porcine reproductive and respiratory syndrome virus (PRRSV) seropositivity (from 610 plasma samples where both tests were performed).

Pathogen	Serology Status	HEV			
		Seropositive *n* (%)	**RNA + Plasma and/or Cecum *n* (%)**	**RNA + Plasma *n* (%)**	**RNA + Cecum *n* (%)**
PRRSV	Seronegative (n = 256)	235 (91.8)	62 (24.2)	20 (7.8)	50 (19.5)
	Seropositive (n = 354)	333 (94.1)	60 (17.0)	14 (4.0)	52 (14.7)
		p = 0.31	p = 0.03	p = 0.05	p = 0.13

Table 3. Association with porcine reproductive and respiratory syndrome virus (PRRSV) active infection (RNA detection in tonsil) (from 358 animals where PCR results for both PRRSV and hepatitis E virus (HEV) were available).

Pathogen	RNA Status	HEV			
		Seropositive *n* (%)	**RNA + Plasma and/or Cecum *n* (%)**	**RNA + Plasma *n* (%)**	**RNA + Cecum *n* (%)**
PRRSV	PCR negative (n = 327)	311 (95.1)	55 (16.8)	12 (3.7)	48 (14.7)
	PCR positive (n = 31)	26 (83.9)	6 (19.4)	2 (6.5)	5 (16.1)
		p = 0.01	p = 0.73	p = 0.45	p = 0.83

There was no evidence from this study that PRRSV infection, as detected by serology or PCR, increased the likelihood of HEV infection in pigs at the time of slaughter. The only associations identified suggested that for the pigs in this study, PRRSV seropositive animals were less likely (17.0% vs. 24.2%, p = 0.03) to be HEV PCR positive in plasma or cecum (Table 3); PRRSV seropositive animals were less likely (4.0% vs. 7.8%, p = 0.05) to be HEV PCR positive in plasma (Table 2); PRRSV PCR positive animals were less likely (83.9% vs. 95.1%, p = 0.01) to be HEV seropositive (Table 3).

4. Discussion

It has been suggested that infection with PRRSV renders pigs more susceptible to secondary bacterial [7,8,10,22] or viral [9,23] infections. In this study, we further investigated the active PRRSV infection at slaughter age and the association between PRRSV infection and an active HEV infection in pigs entering the food chain in the UK. Since the majority of UK pig farms that vaccinate against PRRSV use a live vaccine [24] it was considered that PRRSV in both the vaccinated and naturally infected pigs may modulate HEV infection.

The 2013 abattoir survey had found a prevalence of antibodies to PRRSV in slaughter-age pigs of 58.3% [14]. Antibody to vaccine and field PRRSV cannot be distinguished but vaccination of rearing pigs is less common than that of breeding pigs in the UK and is generally performed when there is an expectation of field PRRSV challenge during the rearing period. Therefore, seropositivity in finishers is considered a reasonable indicator of the presence of PRRSV infection on the respective rearing units. From the PRRSV seropositive pigs in the study, the prevalence of PRRS viral RNA in tonsils, where PRRSV may persist up to 130 days post infection [25], was 8.3%. As tonsils from most seronegative pigs were not tested by PCR, it is possible that detection of a few PRRSV-positive pigs in the early stages of infection were missed, although PRRSV RNA was not detected in any of the 28 tonsils from

seronegative pigs in a pilot study (data not shown). As the pigs were not showing obvious clinical signs, this is a significant finding, highlighting that a proportion of healthy pigs from PRRSV-infected units may be infectious at slaughter, and if still shedding virus, may be able to transmit the virus on to other farms, for example through contaminated vehicles [26], underlining the need for good biosecurity during and after transport to slaughter. These findings triggered the genetic characterization of the viruses in order to further evaluate the potential risks associated with their presence.

Overall, the sequences from the abattoir samples did not cluster separately from those from clinical cases submitted for diagnostic testing, and they appear to be representative of the overall diversity of PRRSV strains circulating in the UK. None of them was from an Eastern European subtype of genotype 1 PRRSV. Of the 23 successfully-sequenced viruses, three showed greater than 98.5% similarity to the modified-live vaccine used in the UK at the time. These 'vaccine-like' viruses may derive from vaccine virus, and have been identified in previous years, although at a lower rate [6], possibly because most samples previously sequenced were from disease outbreaks, whereas these were detected in clinically normal pigs. The other 20 viruses showed between 88.4% and 98.3% similarity to the vaccine sequence. Although the degree of genetic difference of a field PRRS virus from the vaccine strain cannot alone predict the degree of protection that would be afforded by the vaccine to infection by the field virus, nor allow for a determination of the strain's pathogenicity, these results further illustrate the diverse nature of field PRRSV in the UK. Interestingly, some of the viruses from this study are sufficiently similar to one another to be potentially linked epidemiologically, even when they originate from pigs from different geographic regions. Conversely, for two pigs from the same farm, the viruses detected in them did not show a great degree of similarity. There was no relation between four PRRSV sequences from animals co-infected with HEV (no sequence data was available for the other two), as they each grouped into different clusters in the phylogenetic analysis, one being homologous with the Porcilis PRRS vaccine strain sequence. The sequences from the abattoir samples did not cluster separately from those from clinical cases submitted for diagnostic testing, and they appear to fit within the overall diversity of PRRSV strains previously found to be circulating in the UK. The existence of infected slaughter-age pigs with the potential, if shedding, to transmit the virus to susceptible pigs is thereby confirmed.

We found no evidence in this study that exposure to, or infection with PRRSV enhanced HEV infection rates in pigs entering the food chain. Indeed, pigs exposed to PRRSV were less likely to be viremic ($p = 0.05$). The age-range of the six co-infected pigs identified reflected that of the overall population sampled. The calculated virus load in plasma for HEV showed no association with either PRRSV serology or PCR status (data not shown). Several other studies have specifically investigated PRRSV and HEV co-infection [11,27,28], some by experimental infection. One report of an association of co-infection with disease was restricted to investigation of a single pig [27]. Martelli et al. [28] found no association between these pathogens in an investigation of diagnostic submissions. The 2013 abattoir survey had investigated the presence of a number of other pathogens in clinically healthy pigs, but no evidence was found that the PRRSV-seropositive pigs were more likely to carry *Salmonella* or *Yersinia* or have antibodies to Toxoplasma [14]. Interestingly, Salines et al. [11] reported that experimental PRRSV and HEV co-infection did affect the HEV infection dynamics in five-week old pigs with no maternal antibody for these two endemic viruses. The simultaneous co-infection resulted in delays to both the latent period (13.4 vs. 7.1 days with HEV alone) and the humoral response (43.1 vs. 26.3 days) to HEV, as well as increasing the infectious period (48.6 vs. 9.7 days), in association with an increased HEV viral load. In contrast, several other studies have failed to demonstrate any association between PRRSV infection and the dynamics of other viral infections [13,28,29]. While the present study failed to show any positive association overall between PRRSV and HEV infections, this may be an age-dependent effect, and variation in the timing of the respective infections may also affect their outcomes. Future investigations of natural PRRSV and HEV co-infections should perhaps be directed towards younger pigs, since these were under-represented in this study, and may provide different outcomes. A field study showed that the majority of pigs were infected by 15 weeks of age [30]. Experimental infections

to further characterize PRRSV and HEV co-infections must consider non-simultaneous infections, as they may be more relevant to the situation in the field. Other viral co-infections such as porcine circovirus type 2 (PCV-2) and PRRSV or HEV also remain to be investigated, with at least one report of fatal disease associated with HEV and PCV-2 [31].

An active HEV infection in pigs entering the food chain is a potential risk to public health and there is a need to better understand factors that may influence this. The UK abattoir survey had found that one in five pigs had an active HEV infection as they entered the food chain [15]. This same finding of active HEV infections in slaughter-age pigs is found worldwide [32–35]. There was no evidence from the current study that PRRSV infection adversely affected the proportion of HEV infected pigs entering the food chain. Further studies are needed to investigate factors influencing the dynamics of HEV infection in the pig and within farms and that may then be used to inform means of reducing infection in slaughter-age pigs.

5. Conclusions

No association was found between PRRSV and HEV infections in the slaughter age pigs sampled. In addition, there was no difference in strain diversity of PRRSV sampled from clinically unaffected pigs in this study relative to those identified from clinical cases of disease in the UK.

Acknowledgments: The abattoir project was funded by Defra and the devolved administrations, the Food Standards Agency, Agriculture and Horticulture Development Board (ADHB) Pork (formerly the British Pig Executive), the Veterinary Medicines Directorate, Public Health England (formerly the Health Protection Agency), Public Health Wales, Quality Meat Scotland, and the Ulster Pork and Bacon Forum. The PRRSV testing was funded mainly from AHDB Pork and Defra (project ED1200 Scanning Surveillance for Diseases in Pigs in England and Wales). The authors thank the abattoirs for participating in this study, the Consortium for Pig and Public Health, FSA Operations, and DARD for collecting the samples. Richard Tedder and Samreen Ijaz from the Blood Borne Virus Unit, Public Health England are thanked for fruitful discussions and comments on the manuscript.

Author Contributions: S.W., B.C., and F.S. conceived and designed the experiments; S.G. performed the experiments; T.C., S.G., and J.-P.F. analyzed the data; J.-P.F., S.G., F.S., and B.C. wrote the paper.

Conflicts of Interest: The authors declare no conflict of interest. The funding sponsors had no role in the design of the study; in the collection, analyses, or interpretation of data; in the writing of the manuscript, and in the decision to publish the results.

References

1. Dalton, H.R.; Bendall, R.; Ijaz, S.; Banks, M. Hepatitis E: An emerging infection in developed countries. *Lancet Infect. Dis.* **2008**, *8*, 698–709. [CrossRef]
2. Pavio, N.; Meng, X.J.; Doceul, V. Zoonotic origin of hepatitis E. *Curr. Opin. Virol.* **2015**, *10*, 34–41. [CrossRef] [PubMed]
3. Said, B.; Ijaz, S.; Chand, M.A.; Kafatos, G.; Tedder, R.; Morgan, D. Hepatitis E virus in England and Wales: Indigenous infection is associated with the consumption of processed pork products. *Epidemiol. Infect.* **2014**, *142*, 1467–1475. [CrossRef] [PubMed]
4. Edwards, S.; Robertson, I.; Wilesmith, J.; Ryan, J.; Kilner, C.; Paton, D.; Drew, T.; Brown, I; Sands, J. PRRS (Blue Eared Pig Disease) in Great Britain. *Am. Assoc. Swine Pract. Newsl.* **1992**, *4*, 32–36.
5. Richardson, J.S. The cost of endemic disease in pig production. *Pig J.* **2011**, *65*, 10–17.
6. Frossard, J.P.; Hughes, G.J.; Westcott, D.G.; Naidu, B.; Williamson, S.; Woodger, N.G.A.; Steinbach, F.; Drew, T.W. Porcine reproductive and respiratory syndrome virus: Genetic diversity of recent British isolates. *Vet. Microbiol.* **2013**, *162*, 507–518. [CrossRef] [PubMed]
7. Riber, U.; Nielsen, J.; Lind, P. In utero infection with PRRS virus modulates cellular functions of blood monocytes and alveolar lung macrophages in piglets. *Vet. Immunol. Immunopathol.* **2004**, *99*, 169–177. [CrossRef] [PubMed]
8. Thanawongnuwech, R.; Brown, G.B.; Halbur, P.G.; Roth, J.A.; Royer, R.L.; Thacker, B.J. Pathogenesis of porcine reproductive and respiratory syndrome virus-induced increase in susceptibility in *Streptococcus suis* infection. *Vet. Pathol.* **2000**, *37*, 143–152. [CrossRef] [PubMed]

9. Li, H.; Yang, H. Infection of porcine reproductive and respiratory syndrome virus suppresses the antibody response to classical swine fever virus vaccination. *Vet. Microbiol.* **2003**, *95*, 295–301. [CrossRef]
10. Beloeil, P.A.; Fravalo, P.; Fablet, C.; Jolly, J.P.; Eveno, E.; Hascoet, Y.; Chauvin, C.; Salvat, G.; Madec, F. Risk factors for *Salmonella enterica* subsp *enterica* shedding by market-age pigs in French farrow-to-finish herds. *Prev. Vet. Med.* **2004**, *63*, 103–120. [CrossRef] [PubMed]
11. Salines, M.; Barnaud, E.; Andraud, M.; Eono, F.; Renson, P.; Bourry, O.; Pavio, N.; Rose, N. Hepatitis E virus chronic infection of swine co-infected with porcine reproductive and respiratory syndrome virus. *Vet. Res.* **2015**, *46*, 55. [CrossRef] [PubMed]
12. Salguero, F.J.; Frossard, J.P.; Rebel, J.M.; Stadejek, T.; Morgan, S.B.; Graham, S.P.; Steinbach, F. Host-pathogen interactions during porcine reproductive and respiratory syndrome virus 1 infection of piglets. *Virus Res.* **2015**, *202*, 135–143. [CrossRef] [PubMed]
13. Morgan, S.B.; Graham, S.P.; Salguero, F.J.; Sánchez Cordón, P.J.; Mokhtar, H.; Rebel, J.M.J.; Weesendorp, E.; Bodman-Smith, K.B.; Steinbach, F.; Frossard, J.P. Increased pathogenicity of European porcine reproductive and respiratory syndrome virus is associated with enhanced adaptive responses and viral clearance. *Vet. Microbiol.* **2013**, *163*, 13–22. [CrossRef] [PubMed]
14. Powell, L.F.; Cheney, T.E.A.; Williamson, S.; Guy, E.; Smith, R.P.; Davies, R.H. A prevalence study of *Salmonella* spp., *Yersinia* spp., *Toxoplasma gondii* and porcine reproductive and respiratory syndrome virus in UK pigs at slaughter. *Epidemiol. Infect.* **2016**, *144*, 1538–1549. [CrossRef] [PubMed]
15. Grierson, S.; Heaney, J.; Cheney, T.; Morgan, D.; Wyllie, S.; Powell, L.; Smith, D.; Ijaz, S.; Steinbach, F.; Choudhury, B.; et al. Prevalence of hepatitis E virus infection in pigs at the time of slaughter, United Kingdom, 2013. *Emerg. Infect. Dis.* **2015**, *21*, 1396–1401. [CrossRef] [PubMed]
16. *Zoonoses Report UK 2012*; Defra: London, UK, 2013. Available online: https://www.gov.uk/government/publications/zoonoses-report-uk-2012 (accessed on 10 May 2017).
17. Frossard, J.P.; Fearnley, C.; Naidu, B.; Errington, J.; Westcott, D.G.; Drew, T.W. Porcine reproductive and respiratory syndrome virus: Antigenic and molecular diversity of British isolates and implications for diagnosis. *Vet. Microbiol.* **2012**, *158*, 308–315. [CrossRef] [PubMed]
18. Thompson, J.D.; Higgins, D.G.; Gibson, T.J. CLUSTAL W: Improving the sensitivity of progressive multiple sequence alignment through sequence weighting, position-specific gap penalties and weight matrix choice. *Nucleic Acids. Res.* **1994**, *22*, 4673–4680. [CrossRef] [PubMed]
19. Tamura, K.; Stecher, G.; Peterson, D.; Filipski, A.; Kumar, S. MEGA6: Molecular evolutionary genetics analysis version 6.0. *Mol. Biol. Evol.* **2013**, *30*, 2725–2729. [CrossRef] [PubMed]
20. Saitou, N.; Nei, M. The neighbour-joining method: A new method for reconstructing phylogenetic trees. *Mol. Biol. Evol.* **1987**, *4*, 406–425. [PubMed]
21. Tamura, K.; Dudley, J.; Nei, M.; Kumar, S. MEGA4: Molecular evolutionary genetics analysis (MEGA) software version 4.0. *Mol. Biol. Evol.* **2007**, *24*, 1596–1599. [CrossRef] [PubMed]
22. Feng, W.H.; Laster, S.M.; Tompkins, M.; Brown, T.; Xu, J.S.; Altier, C.; Gomez, W.; Benfield, D.; McCaw, M.B. In utero infection by porcine reproductive and respiratory syndrome virus is sufficient to increase susceptibility of piglets to challenge by *Streptococcus suis* type II. *J. Virol.* **2001**, *75*, 4889–4895. [CrossRef] [PubMed]
23. Jung, K.; Renukaradhya, G.J.; Alekseev, K.P.; Fang, Y.; Tang, Y.; Saif, L.J. Porcine reproductive and respiratory syndrome virus modifies innate immunity and alters disease outcome in pigs subsequently infected with porcine respiratory coronavirus: Implications for respiratory viral co-infections. *J. Gen. Virol.* **2009**, *90*, 2713–2723. [CrossRef] [PubMed]
24. Velasova, M.; Alarcon, P.; Williamson, S.; Wieland, B. Risk factors for porcine reproductive and respiratory syndrome virus infection and resulting challenges for effective disease surveillance. *BMC Vet. Res.* **2012**, *8*, 184. [CrossRef] [PubMed]
25. Wills, R.W.; Doster, A.R.; Galeota, J.A.; Sur, J.H.; Osorio, F.A. Duration of infection and proportion of pigs persistently infected with porcine reproductive and respiratory syndrome virus. *J. Clin. Microbiol.* **2003**, *41*, 58–62. [CrossRef] [PubMed]
26. Dee, S.; Deen, J.; Otake, S.; Pijoan, C. An experimental model to evaluate the role of transport vehicles as a source of transmission of porcine reproductive and respiratory syndrome virus to susceptible pigs. *Can. J. Vet. Res.* **2004**, *68*, 128–133. [PubMed]

27. Mao, J.; Zhao, Y.; She, R.; Xiao, P.; Tian, J.; Chen, J. One case of swine hepatitis E virus and porcine reproductive and respiratory syndrome virus co-infection in weaned pigs. *Vir. J.* **2013**, *10*, 341. [CrossRef] [PubMed]
28. Martelli, F.; Toma, S.; Di Bartolo, I.; Caprioli, A.; Ruggeri, F.M.; Lelli, D.; Bonci, M.; Ostanello, F. Detection of hepatitis E virus (HEV) in Italian pigs displaying different pathological lesions. *Res. Vet. Sci.* **2010**, *88*, 492–496. [CrossRef] [PubMed]
29. De Bruin, M.G.; Samsom, J.N.; Voermans, J.J.; Van Rooij, E.M.; De Visser, Y.E.; Bianchi, A.T. Effects of a porcine reproductive and respiratory syndrome virus infection on the development of the immune response against pseudorabies virus. *Vet. Immunol. Immunopathol.* **2000**, *76*, 125–135. [CrossRef]
30. De Deus, N.; Casas, M.; Peralta, B.; Nofrarías, M.; Pina, S.; Martín, M.; Segalés, J. Hepatitis E virus infection dynamics and organic distribution in naturally infected pigs in a farrow-to-finish farm. *Vet. Microbiol.* **2008**, *132*, 19–28. [CrossRef] [PubMed]
31. Yang, Y.; Shi, R.; She, R.; Mao, J.; Zhao, Y.; Du, F.; Liu, C.; Liu, J.; Cheng, M.; Zhu, R.; et al. Fatal disease associated with swine hepatitis E virus and porcine circovirus 2 co-infection in four weaned pigs in China. *BMC Vet. Res.* **2015**, *11*, 77. [CrossRef] [PubMed]
32. Di Bartolo, I.; Diez-Valcarce, M.; Vasickova, P.; Kralik, P.; Hernandez, M.; Angeloni, G.; Ostanello, F.; Bouwknegt, M.; Rodríguez-Lázaro, D.; Pavlik, I.; et al. Hepatitis E virus in pork production chain in Czech Republic, Italy, and Spain, 2010. *Emerg. Infect. Dis.* **2012**, *18*, 1282–1289. [CrossRef] [PubMed]
33. Leblanc, D.; Poitras, E.; Gagné, M.J.; Ward, P.; Houde, A. Hepatitis E virus load in swine organs and tissues at slaughterhouse determined by real-time RT-PCR. *Int. J. Food Microbiol.* **2010**, *139*, 206–209. [CrossRef] [PubMed]
34. Dos Santos, D.R.; de Paula, V.S.; de Oliveira, J.M.; Marchevsky, R.S.; Pinto, M.A. Hepatitis E virus in swine and effluent samples from slaughterhouses in Brazil. *Vet. Microbiol.* **2011**, *149*, 236–241. [CrossRef] [PubMed]
35. Wang, X.J.; Zhao, Q.; Jiang, F.L.; Liu, B.Y.; Zhao, J.N.; Dang, L.; Sun, Y.N.; Mu, Y.; Xiao, S.Q.; Wang, C.B.; et al. Genetic characterization and serological prevalence of swine hepatitis E virus in Shandong province, China. *Vet. Microbiol.* **2014**, *172*, 415–424. [CrossRef] [PubMed]

© 2017 by the authors. Licensee MDPI, Basel, Switzerland. This article is an open access article distributed under the terms and conditions of the Creative Commons Attribution (CC BY) license (http://creativecommons.org/licenses/by/4.0/).

viruses

MDPI

Review

African Swine Fever Virus: A Review

Inmaculada Galindo and Covadonga Alonso *

Dpto. de Biotecnología, Instituto Nacional de Investigación y Tecnología Agraria y Alimentaria (INIA), Ctra. de la Coruña km 7.5, 28040 Madrid, Spain; galindo@inia.es
* Correspondence: calonso@inia.es

Academic Editors: Linda Dixon and Simon Graham
Received: 10 April 2017; Accepted: 4 May 2017; Published: 10 May 2017

Abstract: African swine fever (ASF) is a highly contagious viral disease of swine which causes high mortality, approaching 100%, in domestic pigs. ASF is caused by a large, double stranded DNA virus, ASF virus (ASFV), which replicates predominantly in the cytoplasm of macrophages and is the only member of the *Asfarviridae* family, genus *Asfivirus*. The natural hosts of this virus include wild suids and arthropod vectors of the *Ornithodoros* genus. The infection of ASFV in its reservoir hosts is usually asymptomatic and develops a persistent infection. In contrast, infection of domestic pigs leads to a lethal hemorrhagic fever for which there is no effective vaccine. Identification of ASFV genes involved in virulence and the characterization of mechanisms used by the virus to evade the immune response of the host are recognized as critical steps in the development of a vaccine. Moreover, the interplay of the viral products with host pathways, which are relevant for virus replication, provides the basic information needed for the identification of potential targets for the development of intervention strategies against this disease.

Keywords: African swine fever virus; ASFV; virus entry; endocytosis; endosomal pathway; host cell targets; cellular responses; ER stress; apoptosis; autophagy; A179L

1. Introduction

African swine fever (ASF) is a viral disease of swine that leads to a high mortality in domestic pigs while being asymptomatic in the natural suid reservoir hosts [1–3]. It causes important economic losses that are unavoidable in the absence of an effective vaccine and the available methods of disease control are the quarantine of the affected area and the slaughter of the infected animals [4]. ASF is caused by the ASF virus (ASFV), a double-stranded DNA virus with a complex molecular structure. It is the only member of the *Asfarviridae* family [5] and the only DNA virus transmitted by arthropods, soft ticks of the *Ornithodoros* genus [3,6]. Soft ticks (*Ornithodoros moubata*) are involved in the sylvatic transmission cycle of the virus in Africa and *O. erraticus* in Europe. The wild boar that suffers an acute disease similar to the domestic pig appears to be relevant in the transmission cycle in Europe.

The disease caused by this virus was first identified in Kenya in the 1920s [7]. Then, it was confined to Africa until it spread to Europe in the middle of the last century, and later to South America and the Caribbean. The disease was eradicated from Europe (except of Sardinia) at the 1990s via drastic control and eradication programs. However, in 2007, the disease spread again out of Africa into the Caucasus, especially Georgia, and in 2014 it reached the eastern territory of the European Union. The latest reports of the disease include an increasing list of EU countries, Poland and the three Baltic republics [8,9] and very recently Moldova [10]. Due to the absence of vaccines with protective efficacy, ASF represents a serious threat to all European countries. The epidemiological complexity of ASF has been clearly demonstrated in eastern and southern Africa, where genetic characterization of ASFV based on sequence variation in the C-terminal region of the B646L gene encoding the major capsid protein p72, revealed the presence of 22 genotypes [11,12]. Recently, a new genotype, genotype

XXIII, that shares a common ancestor with genotypes IX and X, which comprise isolates circulating in Eastern African countries and the Republic of Congo, has been described [13]. This review paper summarizes the current state of knowledge about ASFV.

2. African Swine Fever Virus

ASFV is a large, enveloped virus with icosahedral morphology and an average diameter of 200 nm. The viral genome consists of a single molecule of linear, covalently close-ended, double stranded DNA. The genomes of different isolates vary in length between 170 and 190 Kbp and encode between 151 and 167 open reading frames. ASFV replication cycle is mainly cytoplasmic, but the nucleus is also a site of viral DNA synthesis at early times [14,15]. The disassembly of the lamina network close to the sites where the viral genome starts its replication and the redistribution of several nuclear proteins suggests the existence of sophisticated mechanisms to regulate the nuclear machinery during viral infection [16].

Transcription of viral genes is strongly regulated. Four classes of mRNAs have been identified by their distinctive accumulation kinetics—including immediate–early, early, intermediate, and late transcripts. Immediate–early and early genes are expressed before the onset of DNA replication, whereas intermediate and late genes are expressed afterwards. The presence of intermediate genes suggests a cascade model for the regulation of ASFV gene expression [17,18]. Enzymes required for DNA replication are expressed immediately after virus entry into the cytoplasm from partially uncoated core particles and using enzymes and other factors packaged in virus particles [17–20]. Virus morphogenesis takes place in the viral factories where the main late phase of DNA replication also occurs.

3. Virion Structure

The ASFV particle has an icosahedral morphology composed of several concentric domains: the internal core formed by the central genome contains the nucleoid, which is coated by a thick protein layer named core shell; an inner lipid envelope surrounding the core; and finally the capsid, which is the outermost layer of the intracellular virions [21]. The extracellular virions possess an additional external envelope that is obtained when the virus buds out through the plasma membrane [22]. However, the importance of this envelope is unclear as it is not required for infectivity [23].

4. Viral Entry Mechanisms

The ASFV infectious cycle starts with the viral adsorption and entry into the host cell. Early studies on ASFV entry characterized this event as a low pH- and temperature-dependent process consistent with saturable and specific receptor-mediated endocytosis in Vero cells and porcine macrophages [24–27]. However, the receptor(s) for the virus still remain unknown. The limited cell tropism of ASFV suggests that a macrophage-specific receptor is required for infection. Successful infection of porcine macrophages and monocytes by ASFV correlates to the expression of the CD163 scavenger receptor, a hallmark of macrophage maturation. It was previously suggested as a potential virus receptor, as monoclonal antibodies against this molecule were able to block infection of primary alveolar macrophages [28]. However, more recent studies have demonstrated that CD163 is not necessary for infection with the Georgia 2007/1 virus isolates. Gene-edited pigs possessing a complete knockout of CD163 produced using the CRISPR/Cas9 system showed no differences in clinical signs, mortality, pathology, or viremia [29]. One conclusion from these studies was that CD163 may be necessary but insufficient for infection, suggesting that other macrophage surface proteins may participate in the infection process.

While there is support for receptor-dependent mechanisms of viral entry, such as clathrin-mediated dynamin-dependent endocytosis [30,31], there is also evidence that ASFV exploits other mechanisms, such as phagocytosis [32] and macropinocytosis [33,34]. Also, cholesterol is required

for a successful entry. These mechanisms occur both in the macrophage target cell and in Vero cells using viral isolates adapted to this cell line.

In addition, some ASFV proteins are involved in the entry mechanism such as p30, important for viral internalization, while other proteins such as p12 and p54 have been identified as potential viral attachment proteins [35–37].

5. ASFV Enters the Endosomal Pathway

ASFV infection by either pathway of entry should finally reach the endocytic pathway [38]. Once the virus has entered the endocytic pathway, it must pass through different endosome populations to achieve a successful infection (Figure 1). Endocytic pathway maturation is carefully orchestrated by proteins and lipids that are recruited to the endosomal membrane. Rab GTPase protein family is the major regulator of the endosomal maturation pathway, where each member of the Rab family is specifically located to a different endosomal compartment [39]. Incoming viruses are found in early endosomes (EE) labeled with Rab5 and EEA1 markers from very few minutes after adsorption. In fact, complete encapsidated virions are only found at the level of EE but not in other mature acidic compartments [38]. The inhibition of endosomal acidification with bafilomycin A1 prevents viral decapsidation and only under this condition it is possible to observe complete viruses inside multivesicular endosomes positive for CD63 and late endosomes expressing Rab7. In normal conditions, late endosomes harbor only viral cores lacking the capsid protein [38].

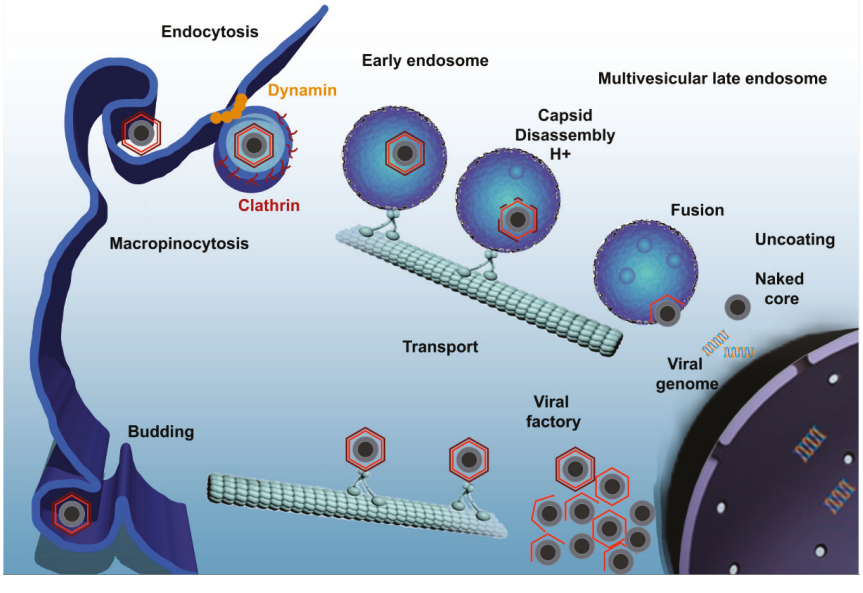

Figure 1. ASFV enters the host cell through a complex process involving dynamin- and clathrin-mediated endocytosis and macropinocytosis. Only few seconds later, ASFV progresses through the endocytic pathway and reaches mature endosomal compartments where viral decapsidation and fusion of the inner viral envelope with the endosomal membrane occurs. Newly synthesized virions are assembled in the viral factory and will exit the cell either by exocytosis budding at the plasma membrane or through the formation of apoptotic bodies.

Viral decapsidation occurs at the acidic intraluminal pH in mature endosomal compartments between 30 and 45 min post infection (mpi). Mature endosomal compartments are multivesicular

bodies expressing CD63 that are characterized by the presence of intraluminal vesicles and also, late endosomes expressing Rab7. Dependence on the endosomal maturation for sequential viral uncoating and penetration has been also described for other viruses [40,41]. Once decapsidated, virus particles expose the inner envelope which allows their interaction and subsequent fusion of this viral membrane with the limiting membrane of the endosomes and naked cores can be released into cytosol in order to start replication. This process is strongly dependent on the cholesterol efflux at the endosomal membrane. In fact, blocking cholesterol transport at this level causes retention of virions inside endosomes, inhibiting infection progression [42]. The inner envelope viral protein pE248R is also involved in viral fusion. This protein shares sequence similarity with some members of the poxviral entry/fusion complex [34].

Other inhibitors of endosome maturation such as wortmannin, a phosphatidylinositol 3 (PI3)-kinase inhibitor that blocks early endosome fusion, and nocodazole, an inhibitor that disturbs microtubule-dependent endosomal transport also prevent ASFV infection [38].

6. ASFV Gene Expression and DNA Replication

Incoming ASFV virions should reach their replication site in the perinuclear area close to the microtubule organizing center (MTOC) [43]. Immediate early and early genes are expressed before the onset of DNA replication. Both DNA chains are alternatives used as the coding strand. This is possible due to the action of several enzymes involved in viral transcription that are packed in the viral core. Following DNA replication, the transcription of intermediate and late genes begins. ASFV commits approximately 20% of its genome to encode genes involved in the transcription and modification of its mRNAs. This transcriptional machinery gives to ASFV a relative independence from its host and an accurate positional and temporal control of its gene expression [44]. The existence of a nuclear stage in the replication of ASFV DNA has been determined by in situ hybridization and autoradiography in thin sections of infected cells, although the precise role of the nucleus in viral replication remains unclear. Sedimentation analysis of replicating viral DNA in alkaline sucrose gradients has shown that small DNA fragments are pulse-labeled in the nucleus at early times in the replication of the viral DNA, whereas larger molecules are synthesized in the cytoplasm at later times. The replicative intermediates that are synthesized both in the nucleus and cytoplasm of ASFV-infected cells consist of head to head concatemers. It is possible that the nucleus may provide small transcripts or other factors required for priming virus replication or that an early stage of virus DNA replication should take place [15].

7. Formation of the Viral Factory

Microtubules are required for the transport of the virus to perinuclear area, where replication takes place. Integrity of microtubules is required for the formation of viral factories [45] and virus particles are found associated to stabilized microtubules at entry [46]. Also, nocodazole, which interferes with the polymerization of microtubule filaments, prevents the correct formation of factories [43,47–49]. Structural protein p54 interacts with the dynein motor protein during virus infection and could constitute a molecular mechanism for microtubule-mediated virus transport [43].

The viral factory, localized in the cytoplasm close to the nucleus, can be described as a single and large perinuclear area at the MTOC. On this site, viral proteins and DNA are accumulated and newly synthesized virions are assembled. A cage made of intermediate filament vimentin surrounds the viral factory likely to prevent the sensing of viral components into the cytoplasm and concentrate structural proteins at sites of assembly [50]. There are many features shared between aggresomes and VFs. However, neither HDAC6 nor Bag3 are required for factory formation, suggesting that aggresomes and viral factories are not the same structures [51].

Formation of viral replication sites depends on several cellular determinants. For example, Rho GTPase inhibitors produce an abnormal viral factory size with the accumulation of envelope precursors and immature virions [46]. This specialized site at the MTOC, contains viral DNA, most of the viral

proteins, immature and mature virions, and also abundant virus-induced membranes. Viral factories contain precursors that develop into icosahedral intermediates by the assembly of the icosahedral capsid and the core shell domain. The last step of virion morphogenesis will be the encapsidation of DNA giving rise to mature virions. Finally, the newly formed virus leaves the factory and is transported to the cell surface by kinesin where it is released by budding [50]. Extracellular virus is covered by an additional external envelope that is acquired during this budding process [22].

8. ER Stress and Unfolded Protein Response

The virus modifies and interacts with cellular pathways in response to infection. The endoplasmic reticulum (ER) is an essential organelle for ASFV replication and maturation and a large number of viral proteins are synthesized in infected cells and accumulated in the ER during the viral life cycle. This process can trigger ER stress and the unfolded protein response (UPR) of the host cell as the induction of caspase 12 indicates [52]. Viruses have evolved various mechanisms to counteract these cellular responses that would limit or inhibit viral replication. This response is a regulatory program that upregulates a large number of genes, such as ER chaperones and ER-associated degradation (ERAD) components, which increase the folding capacity of the ER. ASFV induces the upregulation of the chaperones calnexin and calreticulin, but not ERp57, PDI [52], or BiP/Grp78 [52,53]. Moreover, ASFV induces selectively the transcription factor 6 (ATF6) signaling pathway of the UPR, but not the protein kinase-like ER kinase (PERK) or the inositol-requiring enzyme 1 (IRE1) pathways. Thus, the capacity of ASFV to regulate the UPR signaling cascade may prevent the effects that are detrimental to the infection, while maintaining those that are beneficial. Importantly, viral protein DP71L is involved in ATF4 downregulation and in CHOP inhibition [54]. DP71L, homolog of the neurovirulence factor ICP34.5 of HSV-1 and the cellular gene GADD34, binds to catalytic subunit of protein phosphatase 1 (PP1) and causes the dephosphorylation of eukaryotic translation initiation factor 2 alpha (eIF2 α), thereby preventing the inhibition of protein synthesis produced by ER stress and the UPR [55].

9. ASFV and Apoptosis

ER stress after ASFV infection is reflected by the activation of caspase 12, which follows similar temporal dynamics to the activation of mitochondrial caspase 9 and effector caspase 3 [52]. Apoptosis represents an important innate cellular mechanism to prevent virus infection, and many viruses have developed strategies for inhibiting or delaying this cellular response in turn [56]. Thus, ASFV A179L gene encodes an homolog of antiapoptotic Bcl-2 protein to prolong host cell survival until the replication of the viral genome is completed [57]. This viral Bcl-2 is expressed both at early and late times after infection and inhibits the action of several pro-apoptotic BH3-only proteins, known to be rapid inducers of apoptosis, such as activated Bid, BimL, BimS, BimEL, Bad, Bmf, Bik, Puma, and DP5 [58]. Another ASFV gene, A224L, encodes a member of the family of apoptosis inhibitors known as IAP proteins and is able to inhibit caspase activation and to promote cell survival [59,60]. Viral IAP not only blocks caspase-3 activation but also activates NF-κB [61]. It is interesting that the virus encodes an IκB-like molecule (A238L) that interferes with NF-κB activation [62]. A238L and A224L are expressed at different times during ASFV infection, this suggests that ASFV requires a low NF-κB activity at early times of infection to avoid immune responses but a higher activity at late times, probably to prevent apoptosis as the cellular systems are abused [61]. At very late stages of ASFV infection, infected cells undergo apoptosis [63] and show the characteristic morphological changes of programmed cell death, including typical membrane blebbing of the infected cell that led to the formation of numerous vesicles containing virus [45] and this could be an efficient system for virus spread.

10. ASFV and Autophagy

A179L, the viral Bcl2 homolog of African swine fever virus, not only interacts with pro-apoptotic Bcl2 family proteins to inhibit apoptosis but also inhibits autophagy by interacting with Beclin1

through its BH3 homology domain. ASFV is armed to counteract elimination by autophagy as other DNA viruses. An example of that is the HSV-1 ICP34.5 protein, which inhibits autophagy by targeting Beclin1 [64]. ASFV encodes a protein homologous to ICP34.5, which exerts other functions. ASFV DP71L inhibits the ER stress response activating PP1/protein phosphatase 1 [55]. However, in contrast to HSV-1 ICP34.5, it does not interact with Beclin1 [65].

In fact, ASFV infection does not induce LC3 activation or autophagosome formation in Vero cells [65]. Autophagy is a relevant cellular defense mechanism that allows the orderly degradation and recycling of cellular components. Autophagy eliminates intracellular pathogens and has a crucial role for innate and adaptive immune responses. Some DNA viruses, such as ASFV and HSV-1, have developed strategies to keep this cellular response under control to prevent the degradation of newly assembled virions. In contrast, most RNA viruses have been reported to induce autophagy in infected cells, and in several cases autophagy may enhance viral replication [66].

11. ASFV Egress

The mature particle is transported from the virus factories to the cell surface through a microtubule-mediated mechanism [48] depending on the motor protein conventional kinesin [67] and on the capsid protein pE120R [68]. Once on the cell surface, particles exit the host cell by budding at the membrane, acquiring an additional envelope [22]. Both intracellular and extracellular viruses are infectious but structurally and antigenically different [68], and this could have important implications in the host immune response against ASFV.

12. Potential Vaccines and Antivirals

Previous attempts to develop vaccines against ASFV have failed to induce protective immunity. Currently, there are several reports of the protection elicited by experimental vaccines based in live attenuated ASFV (LAV) containing single or double gene deletions in the genome [69] and other different approaches, including DNA vaccines [70,71]. Some of them might turn into successful vaccine candidates. Nowadays, a vaccine to be used in the field should meet a number of requirements. Any potential ASFV vaccine should include markers for differentiation between infected or vaccinated animals that allows for DIVA diagnostics. Also, vaccine production could not be possible because of the lack of a cell line supporting the replication of attenuated vaccine viruses without modifying the virus virulence. At present, wild boars were found to be major players of disease spread in both the Baltics and Poland. Hence, a live vaccine given as bait for these animals could be crucial to limit disease spread. In the current scenario, a vaccine would make possible to eradicate the disease together with infection surveillance by diagnostics. Available diagnostic methods allow both virus detection and also detection of antibodies for identification of survivors and asymptomatic carriers [72].

Until an effective vaccine is developed, the possibility of using antivirals remains. Antiviral strategies have been extensively applied in human infections but can be used in animal health. Antivirals are useful for an early control of virus spread after an outbreak. In addition, the combination of antivirals with vaccination protocols could be applied to elicit the immune response required for effective protection against the disease. Here, we have reviewed potential molecular targets to be considered as targets for antivirals. Antivirals against ASFV described include resveratrol and oxyresveratrol [73], microalgae [74], cholesterol lowering drugs [46] or inhibitors of cholesterol transport [42], antitumoral lauryl-gallate [75], anticonvulsivant valproic acid [75], dynamin inhibitors [38], fluoroquinolones [76], serine protease inhibitors [52], specific peptides [77], and miscelanea [32]. These could be eventually applied in a quick response to reduce susceptible animals in order to create 'safe areas' around the outbreaks and thus control the spread of the infection.

Acknowledgments: This work was funded by grant AGL2015-69598-R of the Ministerio de Economía, Industria y Competitividad of Spain.

Conflicts of Interest: The authors declare no conflict of interest.

References

1. Parker, J.; Plowright, W.; Pierce, M.A. The epizootiology of african swine fever in Africa. *Vet. Rec.* **1969**, *85*, 668–674. [PubMed]
2. Thomson, G.R.; Gainaru, M.D.; van Dellen, A.F. Experimental infection of warthos (*Phacochoerus aethiopicus*) with african swine fever virus. *Onderstepoort J. Vet. Res.* **1980**, *47*, 19–22. [PubMed]
3. Anderson, E.C.; Hutchings, G.H.; Mukarati, N.; Wilkinson, P.J. African swine fever virus infection of the bushpig (*Potamochoerus porcus*) and its significance in the epidemiology of the disease. *Vet. Microbiol.* **1998**, *62*, 1–15. [CrossRef]
4. Penrith, M.L.; Vosloo, W. Review of african swine fever: Transmission, spread and control. *J. S. Afr. Vet. Assoc.* **2009**, *80*, 58–62. [CrossRef] [PubMed]
5. Dixon, L.K.; Escribano, J.M.; Martins, C.; Rock, D.L.; Salas, M.L.; Wilkinson, P.J. Asfarviridae. In *Virus Taxonomy. VIIIth Report of the ICTV*; Fauquet, C.M., Mayo, M.A., Maniloff, J., Desselberger, U., Ball, L.A., Eds.; Elsevier/Academic Press: London, UK, 2005; pp. 135–143.
6. Kleiboeker, S.B.; Scoles, G.A.; Burrage, T.G.; Sur, J. African swine fever virus replication in the midgut epithelium is required for infection of ornithodoros ticks. *J. Virol.* **1999**, *73*, 8587–8598. [PubMed]
7. Montgomery, R.E. On a form of swine fever occurring in british east Africa (Kenya Colony). *J. Comp. Pathol. Ther.* **1921**, *34*, 159–191. [CrossRef]
8. Wozniakowski, G.; Kozak, E.; Kowalczyk, A.; Lyjak, M.; Pomorska-Mol, M.; Niemczuk, K.; Pejsak, Z. Current status of african swine fever virus in a population of wild boar in eastern Poland (2014–2015). *Arch. Virol.* **2016**, *161*, 189–195. [CrossRef] [PubMed]
9. Pejsak, Z.; Truszczynski, M.; Niemczuk, K.; Kozak, E.; Markowska-Daniel, I. Epidemiology of african swine fever in Poland since the detection of the first case. *Pol. J. Vet. Sci.* **2014**, *17*, 665–672. [CrossRef] [PubMed]
10. OIE-WAHID. World Animal Health Information Database (Wahid) [Database on the Internet]. World Organisation for Animal Health (OIE), 2017. [Cited World Animal Health Information System (WAHIS)]. Available online: http://www.Oie.Int/wahis/public.Php?Page=home (accessed on 27 March 2017).
11. Boshoff, C.I.; Bastos, A.D.; Gerber, L.J.; Vosloo, W. Genetic characterisation of african swine fever viruses from outbreaks in southern Africa (1973–1999). *Vet. Microbiol.* **2007**, *121*, 45–55. [CrossRef] [PubMed]
12. Bastos, A.D.; Penrith, M.L.; Cruciere, C.; Edrich, J.L.; Hutchings, G.; Roger, F.; Couacy-Hymann, E.; Thomson, G.R. Genotyping field strains of african swine fever virus by partial p72 gene characterisation. *Arch. Virol.* **2003**, *148*, 693–706. [CrossRef] [PubMed]
13. Achenbach, J.E.; Gallardo, C.; Nieto-Pelegrin, E.; Rivera-Arroyo, B.; Degefa-Negi, T.; Arias, M.; Jenberie, S.; Mulisa, D.D.; Gizaw, D.; Gelaye, E.; et al. Identification of a new genotype of african swine fever virus in domestic pigs from Ethiopia. *Transbound. Emerg. Dis.* **2016**. [CrossRef] [PubMed]
14. Garcia-Beato, R.; Salas, M.L.; Vinuela, E.; Salas, J. Role of the host cell nucleus in the replication of African swine fever virus DNA. *Virology* **1992**, *188*, 637–649. [CrossRef]
15. Rojo, G.; Garcia-Beato, R.; Vinuela, E.; Salas, M.L.; Salas, J. Replication of african swine fever virus DNA in infected cells. *Virology* **1999**, *257*, 524–536. [CrossRef] [PubMed]
16. Ballester, M.; Rodriguez-Carino, C.; Perez, M.; Gallardo, C.; Rodriguez, J.M.; Salas, M.L.; Rodriguez, F. Disruption of nuclear organization during the initial phase of african swine fever virus infection. *J. Virol.* **2011**, *85*, 8263–8269. [CrossRef] [PubMed]
17. Almazan, F.; Rodriguez, J.M.; Andres, G.; Perez, R.; Vinuela, E.; Rodriguez, J.F. Transcriptional analysis of multigene family 110 of african swine fever virus. *J. Virol.* **1992**, *66*, 6655–6667. [PubMed]
18. Rodriguez, J.M.; Salas, M.L.; Vinuela, E. Intermediate class of mRNAs in African swine fever virus. *J. Virol.* **1996**, *70*, 8584–8589. [PubMed]
19. Almazan, F.; Rodriguez, J.M.; Angulo, A.; Vinuela, E.; Rodriguez, J.F. Transcriptional mapping of a late gene coding for the p12 attachment protein of African swine fever virus. *J. Virol.* **1993**, *67*, 553–556. [PubMed]
20. Salas, M.L.; Kuznar, J.; Vinuela, E. Polyadenylation, methylation, and capping of the RNA synthesized in vitro by African swine fever virus. *Virology* **1981**, *113*, 484–491. [CrossRef]
21. Salas, M.L.; Andres, G. African swine fever virus morphogenesis. *Virus Res.* **2013**, *173*, 29–41. [CrossRef] [PubMed]
22. Breese, S.S., Jr.; de Boer, C.J. Electron microscope observations of African swine fever virus in tissue culture cells. *Virology* **1966**, *28*, 420–428. [CrossRef]

23. Schloer, G.M. Polypeptides and structure of African swine fever virus. *Virus Res.* **1985**, *3*, 295–310. [CrossRef]
24. Valdeira, M.L.; Geraldes, A. Morphological study on the entry of African swine fever virus into cells. *Biol. Cell* **1985**, *55*, 35–40. [CrossRef] [PubMed]
25. Alcami, A.; Carrascosa, A.L.; Vinuela, E. Interaction of African swine fever virus with macrophages. *Virus Res.* **1990**, *17*, 93–104. [CrossRef]
26. Alcami, A.; Carrascosa, A.L.; Vinuela, E. The entry of African swine fever virus into vero cells. *Virology* **1989**, *171*, 68–75. [CrossRef]
27. Alcami, A.; Carrascosa, A.L.; Vinuela, E. Saturable binding sites mediate the entry of African swine fever virus into vero cells. *Virology* **1989**, *168*, 393–398. [CrossRef]
28. Sanchez-Torres, C.; Gomez-Puertas, P.; Gomez-del-Moral, M.; Alonso, F.; Escribano, J.M.; Ezquerra, A.; Dominguez, J. Expression of porcine cd163 on monocytes/macrophages correlates with permissiveness to African swine fever infection. *Arch. Virol.* **2003**, *148*, 2307–2323. [CrossRef] [PubMed]
29. Popescu, L.; Gaudreault, N.N.; Whitworth, K.M.; Murgia, M.V.; Nietfeld, J.C.; Mileham, A.; Samuel, M.; Wells, K.D.; Prather, R.S.; Rowland, R.R. Genetically edited pigs lacking cd163 show no resistance following infection with the African swine fever virus isolate, georgia 2007/1. *Virology* **2017**, *501*, 102–106. [CrossRef] [PubMed]
30. Galindo, I.; Cuesta-Geijo, M.A.; Hlavova, K.; Munoz-Moreno, R.; Barrado-Gil, L.; Dominguez, J.; Alonso, C. African swine fever virus infects macrophages, the natural host cells, via clathrin and cholesterol-dependent endocytosis. *Virus Res.* **2015**, *200*, 45–55. [CrossRef] [PubMed]
31. Hernaez, B.; Alonso, C. Dynamin and clathrin-dependent endocytosis in African swine fever virus entry. *J. Virol.* **2010**, *84*, 2100–2109. [CrossRef] [PubMed]
32. Basta, S.; Gerber, H.; Schaub, A.; Summerfield, A.; McCullough, K.C. Cellular processes essential for African swine fever virus to infect and replicate in primary macrophages. *Vet. Microbiol.* **2010**, *140*, 9–17. [CrossRef] [PubMed]
33. Sanchez, E.G.; Quintas, A.; Perez-Nunez, D.; Nogal, M.; Barroso, S.; Carrascosa, A.L.; Revilla, Y. African swine fever virus uses macropinocytosis to enter host cells. *PLoS Pathog.* **2012**, *8*, e1002754. [CrossRef] [PubMed]
34. Hernaez, B.; Guerra, M.; Salas, M.L.; Andres, G. African swine fever virus undergoes outer envelope disruption, capsid disassembly and inner envelope fusion before core release from multivesicular endosomes. *PLoS Pathog.* **2016**, *12*, e1005595. [CrossRef] [PubMed]
35. Gomez-Puertas, P.; Rodriguez, F.; Oviedo, J.M.; Brun, A.; Alonso, C.; Escribano, J.M. The african swine fever virus proteins p54 and p30 are involved in two distinct steps of virus attachment and both contribute to the antibody-mediated protective immune response. *Virology* **1998**, *243*, 461–471. [CrossRef] [PubMed]
36. Angulo, A.; Vinuela, E.; Alcami, A. Comparison of the sequence of the gene encoding African swine fever virus attachment protein p12 from field virus isolates and viruses passaged in tissue culture. *J. Virol.* **1992**, *66*, 3869–3872. [PubMed]
37. Angulo, A.; Vinuela, E.; Alcami, A. Inhibition of African swine fever virus binding and infectivity by purified recombinant virus attachment protein p12. *J. Virol.* **1993**, *67*, 5463–5471. [PubMed]
38. Cuesta-Geijo, M.A.; Galindo, I.; Hernaez, B.; Quetglas, J.I.; Dalmau-Mena, I.; Alonso, C. Endosomal maturation, Rab7 GTPase and phosphoinositides in African swine fever virus entry. *PLoS ONE* **2012**, *7*, e48853. [CrossRef] [PubMed]
39. Stenmark, H. Rab GTPases as coordinators of vesicle traffic. *Nat. Rev. Mol. Cell Biol.* **2009**, *10*, 513–525. [CrossRef] [PubMed]
40. Lozach, P.Y.; Mancini, R.; Bitto, D.; Meier, R.; Oestereich, L.; Overby, A.K.; Pettersson, R.F.; Helenius, A. Entry of bunyaviruses into mammalian cells. *Cell Host Microbe* **2010**, *7*, 488–499. [CrossRef] [PubMed]
41. Pasqual, G.; Rojek, J.M.; Masin, M.; Chatton, J.Y.; Kunz, S. Old world arenaviruses enter the host cell via the multivesicular body and depend on the endosomal sorting complex required for transport. *PLoS Pathog.* **2011**, *7*, e1002232. [CrossRef]
42. Cuesta-Geijo, M.A.; Chiappi, M.; Galindo, I.; Barrado-Gil, L.; Munoz-Moreno, R.; Carrascosa, J.L.; Alonso, C. Cholesterol flux is required for endosomal progression of african swine fever virions during the initial establishment of infection. *J. Virol.* **2015**, *90*, 1534–1543. [CrossRef] [PubMed]

43. Alonso, C.; Miskin, J.; Hernaez, B.; Fernandez-Zapatero, P.; Soto, L.; Canto, C.; Rodriguez-Crespo, I.; Dixon, L.; Escribano, J.M. African swine fever virus protein p54 interacts with the microtubular motor complex through direct binding to light-chain dynein. *J. Virol.* **2001**, *75*, 9819–9827. [CrossRef] [PubMed]
44. Rodriguez, J.M.; Salas, M.L. African swine fever virus transcription. *Virus Res.* **2013**, *173*, 15–28. [CrossRef] [PubMed]
45. Hernaez, B.; Escribano, J.M.; Alonso, C. Visualization of the African swine fever virus infection in living cells by incorporation into the virus particle of green fluorescent protein-p54 membrane protein chimera. *Virology* **2006**, *350*, 1–14. [CrossRef] [PubMed]
46. Quetglas, J.I.; Hernaez, B.; Galindo, I.; Munoz-Moreno, R.; Cuesta-Geijo, M.A.; Alonso, C. Small Rho GTPases and cholesterol biosynthetic pathway intermediates in African swine fever virus infection. *J. Virol.* **2012**, *86*, 1758–1767. [CrossRef] [PubMed]
47. Carvalho, Z.G.; de Matos, A.P.; Rodrigues-Pousada, C. Association of African swine fever virus with the cytoskeleton. *Virus Res.* **1988**, *11*, 175–192. [CrossRef]
48. De Matos, A.P.; Carvalho, Z.G. African swine fever virus interaction with microtubules. *Biol. Cell* **1993**, *78*, 229–234. [CrossRef]
49. Heath, C.M.; Windsor, M.; Wileman, T. Aggresomes resemble sites specialized for virus assembly. *J. Cell Biol.* **2001**, *153*, 449–455. [CrossRef] [PubMed]
50. Stefanovic, S.; Windsor, M.; Nagata, K.I.; Inagaki, M.; Wileman, T. Vimentin rearrangement during African swine fever virus infection involves retrograde transport along microtubules and phosphorylation of vimentin by calcium calmodulin kinase II. *J. Virol.* **2005**, *79*, 11766–11775. [CrossRef] [PubMed]
51. Munoz-Moreno, R.; Barrado-Gil, L.; Galindo, I.; Alonso, C. Analysis of HDAC6 and BAG3-aggresome pathways in African swine fever viral factory formation. *Viruses* **2015**, *7*, 1823–1831. [CrossRef] [PubMed]
52. Galindo, I.; Hernaez, B.; Munoz-Moreno, R.; Cuesta-Geijo, M.A.; Dalmau-Mena, I.; Alonso, C. The ATF6 branch of unfolded protein response and apoptosis are activated to promote African swine fever virus infection. *Cell Death Dis.* **2012**, *3*, e341. [CrossRef] [PubMed]
53. Netherton, C.L.; Parsley, J.C.; Wileman, T. African swine fever virus inhibits induction of the stress-induced proapoptotic transcription factor CHOP/GADD153. *J. Virol.* **2004**, *78*, 10825–10828. [CrossRef] [PubMed]
54. Zhang, F.; Moon, A.; Childs, K.; Goodbourn, S.; Dixon, L.K. The African swine fever virus DP71L protein recruits the protein phosphatase 1 catalytic subunit to dephosphorylate eIF2alpha and inhibits chop induction but is dispensable for these activities during virus infection. *J. Virol.* **2010**, *84*, 10681–10689. [CrossRef] [PubMed]
55. Rivera, J.; Abrams, C.; Hernaez, B.; Alcazar, A.; Escribano, J.M.; Dixon, L.; Alonso, C. The MyD116 African swine fever virus homologue interacts with the catalytic subunit of protein phosphatase 1 and activates its phosphatase activity. *J. Virol.* **2007**, *81*, 2923–2929. [CrossRef] [PubMed]
56. Benedict, C.A.; Norris, P.S.; Ware, C.F. To kill or be killed: Viral evasion of apoptosis. *Nat. Immunol.* **2002**, *3*, 1013–1018. [CrossRef] [PubMed]
57. Brun, A.; Rivas, C.; Esteban, M.; Escribano, J.M.; Alonso, C. African swine fever virus gene *a179l*, a viral homologue of *BCL-2*, protects cells from programmed cell death. *Virology* **1996**, *225*, 227–230. [CrossRef] [PubMed]
58. Galindo, I.; Hernaez, B.; Diaz-Gil, G.; Escribano, J.M.; Alonso, C. A179l, a viral BCL-2 homologue, targets the core BCL-2 apoptotic machinery and its upstream BH3 activators with selective binding restrictions for bid and noxa. *Virology* **2008**, *375*, 561–572. [CrossRef] [PubMed]
59. Chacon, M.R.; Almazan, F.; Nogal, M.L.; Vinuela, E.; Rodriguez, J.F. The African swine fever virus IAP homolog is a late structural polypeptide. *Virology* **1995**, *214*, 670–674. [CrossRef] [PubMed]
60. Nogal, M.L.; Gonzalez de Buitrago, G.; Rodriguez, C.; Cubelos, B.; Carrascosa, A.L.; Salas, M.L.; Revilla, Y. African swine fever virus IAP homologue inhibits caspase activation and promotes cell survival in mammalian cells. *J. Virol.* **2001**, *75*, 2535–2543. [CrossRef] [PubMed]
61. Rodriguez, C.I.; Nogal, M.L.; Carrascosa, A.L.; Salas, M.L.; Fresno, M.; Revilla, Y. African swine fever virus IAP-like protein induces the activation of nuclear factor kappa B. *J. Virol.* **2002**, *76*, 3936–3942. [CrossRef] [PubMed]
62. Revilla, Y.; Callejo, M.; Rodriguez, J.M.; Culebras, E.; Nogal, M.L.; Salas, M.L.; Vinuela, E.; Fresno, M. Inhibition of nuclear factor kappa b activation by a virus-encoded I kappa b-like protein. *J. Biol. Chem.* **1998**, *273*, 5405–5411. [CrossRef] [PubMed]

63. Ramiro-Ibanez, F.; Ortega, A.; Brun, A.; Escribano, J.M.; Alonso, C. Apoptosis: A mechanism of cell killing and lymphoid organ impairment during acute african swine fever virus infection. *J. Gen. Virol.* **1996**, *77*, 2209–2219. [CrossRef] [PubMed]
64. Orvedahl, A.; Alexander, D.; Talloczy, Z.; Sun, Q.; Wei, Y.; Zhang, W.; Burns, D.; Leib, D.A.; Levine, B. HSV-1 ICP34.5 confers neurovirulence by targeting the Beclin 1 autophagy protein. *Cell Host Microbe* **2007**, *1*, 23–35. [CrossRef] [PubMed]
65. Hernaez, B.; Cabezas, M.; Munoz-Moreno, R.; Galindo, I.; Cuesta-Geijo, M.A.; Alonso, C. A179l, a new viral Bcl2 homolog targeting Beclin 1 autophagy related protein. *Curr. Mol. Med.* **2013**, *13*, 305–316. [CrossRef] [PubMed]
66. Klionsky, D.J. Guidelines for the use and interpretation of assays for monitoring autophagy (3rd edition). *Autophagy* **2016**, *12*, 1–222. [CrossRef] [PubMed]
67. Jouvenet, N.; Monaghan, P.; Way, M.; Wileman, T. Transport of african swine fever virus from assembly sites to the plasma membrane is dependent on microtubules and conventional kinesin. *J. Virol.* **2004**, *78*, 7990–8001. [CrossRef] [PubMed]
68. Andres, G.; Garcia-Escudero, R.; Vinuela, E.; Salas, M.L.; Rodriguez, J.M. African swine fever virus structural protein pE120R is essential for virus transport from assembly sites to plasma membrane but not for infectivity. *J. Virol.* **2001**, *75*, 6758–6768. [CrossRef] [PubMed]
69. O'Donnell, V.; Risatti, G.R.; Holinka, L.G.; Krug, P.W.; Carlson, J.; Velazquez-Salinas, L.; Azzinaro, P.A.; Gladue, D.P.; Borca, M.V. Simultaneous deletion of the 9gl and uk genes from the African swine fever virus georgia 2007 isolate offers increased safety and protection against homologous challenge. *J. Virol.* **2017**, *91*, e01760-16.
70. Lacasta, A.; Ballester, M.; Monteagudo, P.L.; Rodriguez, J.M.; Salas, M.L.; Accensi, F.; Pina-Pedrero, S.; Bensaid, A.; Argilaguet, J.; Lopez-Soria, S.; et al. Expression library immunization can confer protection against lethal challenge with african swine fever virus. *J. Virol.* **2014**, *88*, 13322–13332. [CrossRef] [PubMed]
71. Reis, A.L.; Abrams, C.C.; Goatley, L.C.; Netherton, C.; Chapman, D.G.; Sanchez-Cordon, P.; Dixon, L.K. Deletion of African swine fever virus interferon inhibitors from the genome of a virulent isolate reduces virulence in domestic pigs and induces a protective response. *Vaccine* **2016**, *34*, 4698–4705. [CrossRef] [PubMed]
72. Cubillos, C.; Gomez-Sebastian, S.; Moreno, N.; Nunez, M.C.; Mulumba-Mfumu, L.K.; Quembo, C.J.; Heath, L.; Etter, E.M.; Jori, F.; Escribano, J.M.; et al. African swine fever virus serodiagnosis: A general review with a focus on the analyses of african serum samples. *Virus Res.* **2013**, *173*, 159–167. [CrossRef] [PubMed]
73. Galindo, I.; Hernaez, B.; Berna, J.; Fenoll, J.; Cenis, J.L.; Escribano, J.M.; Alonso, C. Comparative inhibitory activity of the stilbenes resveratrol and oxyresveratrol on african swine fever virus replication. *Antivir. Res.* **2011**, *91*, 57–63. [CrossRef] [PubMed]
74. Fabregas, J.; Garcia, D.; Fernandez-Alonso, M.; Rocha, A.I.; Gomez-Puertas, P.; Escribano, J.M.; Otero, A.; Coll, J.M. In vitro inhibition of the replication of haemorrhagic septicaemia virus (VHSV) and African swine fever virus (ASFV) by extracts from marine microalgae. *Antivir. Res.* **1999**, *44*, 67–73. [CrossRef]
75. Hurtado, C.; Bustos, M.J.; Sabina, P.; Nogal, M.L.; Granja, A.G.; Gonzalez, M.E.; Gonzalez-Porque, P.; Revilla, Y.; Carrascosa, A.L. Antiviral activity of lauryl gallate against animal viruses. *Antivir. Ther.* **2008**, *13*, 909–917. [PubMed]
76. Mottola, C.; Freitas, F.B.; Simoes, M.; Martins, C.; Leitao, A.; Ferreira, F. In vitro antiviral activity of fluoroquinolones against African swine fever virus. *Vet. Microbiol.* **2013**, *165*, 86–94. [CrossRef] [PubMed]
77. Hernaez, B.; Tarrago, T.; Giralt, E.; Escribano, J.M.; Alonso, C. Small peptide inhibitors disrupt a high-affinity interaction between cytoplasmic dynein and a viral cargo protein. *J. Virol.* **2010**, *84*, 10792–10801. [CrossRef] [PubMed]

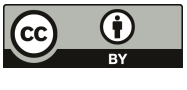

© 2017 by the authors. Licensee MDPI, Basel, Switzerland. This article is an open access article distributed under the terms and conditions of the Creative Commons Attribution (CC BY) license (http://creativecommons.org/licenses/by/4.0/).

viruses

MDPI

Article

A Japanese Encephalitis Virus Vaccine Inducing Antibodies Strongly Enhancing In Vitro Infection Is Protective in Pigs

Obdulio García-Nicolás [1,2], Meret E. Ricklin [1,2], Matthias Liniger [1,2], Nathalie J. Vielle [1,2], Sylvie Python [1,2], Philippe Souque [3], Pierre Charneau [3] and Artur Summerfield [1,2,*]

1 Institute of Virology and Immunology, Sensemattstrasse 293, 3147 Mittelhäusern, Switzerland; obdulio.garcia-nicolas@ivi.admin.ch (O.G.-N.); meret.ricklin@gmail.com (M.E.R.); matthias.liniger@ivi.admin.ch (M.L.); nathalie.vielle@ivi.admin.ch (N.J.V.); sylvie.python@ivi.admin.ch (S.P.)

2 Department of Infectious Diseases and Immunopathology, Vetsuisse Faculty, University of Bern, Länggassstrasse 122, 3001 Bern, Switzerland

3 Virologie Moléculaire et Vaccinologie, Institut Pasteur, 75015 Paris, France; pierre.charneau@pasteur.fr (P.S.); pierre.charneau@pasteur.fr (P.C.)

* Correspondence: artur.summerfield@ivi.admin.ch; Tel.: +41-58-469-9377

Academic Editors: Linda Dixon and Simon Graham
Received: 5 April 2017; Accepted: 18 May 2017; Published: 22 May 2017

Abstract: The Japanese encephalitis virus (JEV) is responsible for zoonotic severe viral encephalitis transmitted by Culex mosquitoes. Although birds are reservoirs, pigs play a role as amplifying hosts, and are affected in particular through reproductive failure. Here, we show that a lentiviral JEV vector, expressing JEV prM and E proteins (TRIP/JEV.prME), but not JEV infection induces strong antibody-dependent enhancement (ADE) activities for infection of macrophages. Such antibodies strongly promoted infection via Fc receptors. ADE was found at both neutralizing and non-neutralizing serum dilutions. Nevertheless, in vivo JEV challenge of pigs demonstrated comparable protection induced by the TRIP/JEV.prME vaccine or heterologous JEV infection. Thus, either ADE antibodies cause no harm in the presence of neutralizing antibodies or may even have protective effects in vivo in pigs. Additionally, we found that both pre-infected and vaccinated pigs were not fully protected as low levels of viral RNA were found in lymphoid and nervous system tissue in some animals. Strikingly, the virus from the pre-infection persisted in the tonsils throughout the experiment. Finally, despite the vaccination challenge, viral RNA was detected in the oronasal swabs in all vaccinated pigs. These latter data are relevant when JEV vaccination is employed in pigs.

Keywords: Japanese encephalitis virus; antibody-dependent enhancement of infection; Fc receptor; lentiviral vector vaccine; vaccine-induced protection; persistence; mucosal virus shedding

1. Introduction

Japanese encephalitis (JE), a mosquito-borne zoonotic viral disease endemic in parts of East Asia, Southeast Asia and Australasia, is considered the most important human viral encephalitis associated with fatality and severe sequelae [1–4]. Every year, 50,000 to 175,000 clinical JE cases in humans are reported, but it is estimated that less than 1% of infected people develop encephalitis [3,5]. Nevertheless, lethality in these cases can be up to 30%, and approximately 50% of surviving patients present long-term neurologic sequelae [3,5]. In addition, for pigs, JEV infection is of high relevance in endemic regions. Although the infection in adult swine is asymptomatic, it represents a significant cause of reproductive problems. Infection of pregnant sows can result in abortion, still-birth and birth defects. Furthermore, infected piglets can display fatal neurological disease [6].

The JE virus (JEV) is a positive single-stranded RNA virus belonging to the genus flavivirus, and encodes a polyprotein processed into three structural proteins being the capsid (C), the precursor membrane (prM), the envelope (E), and seven non-structural proteins (NS1-NS5) [4]. After virus assembly, virions undergo a maturation, in which prM is cleaved to generate M, and this process is required for viral entry into cells [4]. JEV is classified in five different genotypes G1–G5 [7,8]. In the last century, G3 was the dominant genotype and is now being replaced by G1 [9,10]. Recently, G5 strains have also re-emerged in China and South Korea [11,12].

Neutralizing antibodies targeting the E protein play a central role in immunological protection against JEV [13–16]. On the other side, antibodies have also been suspected to enhance disease in certain flavivirus infection, in particular, Dengue virus infection leading to severe hemorrhagic fever [17,18]. The proposed mechanism of antibody-dependent enhancement (ADE) of infection is based on virion-antibody complexes binding to FcγR expressing cells such as macrophages, resulting in enhancement of infection rather than neutralization [19]. In vivo ADE has also been described for flaviviruses closely related to JEV such as Murray Valley encephalitis virus in a mouse model [20]. There is also evidence that antibodies can enhance JE under certain conditions in a murine model [21].

Mosquitoes belonging to the Culex genus act as main vectors for JEV, while wild water birds represent the main vertebrate reservoir. Nevertheless, as pigs are highly susceptible to JEV infection and develop a relatively high viremia for several days, they can play an important role in the ecology of the virus as amplifying hosts [1,3,8,22]. This contrasts with horses and humans which may develop fatal disease but do not contribute to further transmission of JEV to mosquitoes or other species [3]. Considering this situation, vaccination of pigs against JEV is and has been widely practiced in certain countries such as Japan and South Korea [6].

Up to now, JEV remained endemic mainly in Southeast Asia but climate warming, globalization and virus adaptation to new arthropod vectors could result in the emergence of JEV in other parts of the world, as it has occurred for West Nile virus and Zika virus. Furthermore, we have recently shown that, under experimental conditions, the virus can transmit between pigs by contact and is secreted in oronasal fluids for a prolonged period of time [23]. This indicates a potential of JEV to spread and circulate even in areas with a climate unfavorable to the virus transmission by mosquitos. An additional concern is that JEV has a particularly high tropism for the tonsils and can persist in this tissue for several weeks [23,24], providing a possible mechanism of virus overwintering in the pig population. For these reasons and because vaccination represents an efficient countermeasure against JEV, we have recently developed a novel vaccine based on a lentiviral TRIP/JEV which expressed JEV G3 prM and E proteins (TRIP/JEV.prME) [25].

Considering the possible involvement of ADE during flavivirus infections, the present study investigated ADE activities of sera from TRIP/JEV.prME-immunized compared to JEV-infected pigs. To our surprise, we found particularly high levels of ADE with sera following TRIP/JEV.prME vaccination. This in vitro ADE of infection was found with macrophages and an Fc receptor (FcR) expressing kidney cell line. However, despite these responses, the TRIP/JEV.prME vaccine was found to induce protective immunity as demonstrated in a heterologous challenge infection in pigs.

2. Materials and Methods

2.1. Monocyte-Derived Macrophages

Blood was obtained from specific pathogen free (SPF) Swiss Large White pigs. The blood sampling was approved by the cantonal ethical committee for animal experiments, license #BE88/14. Peripheral blood mononuclear cells (PBMC) were isolated using ficoll-paque density centrifugation (1.077 g/L; GE Healthcare Life Sciences, Dübendorf, Switzerland). Monocytes were sorted as CD172a+ cells using monoclonal antibody (mAb), clone 74-22-15A (hybridoma kindly provided by Dr. A. Saalmüller, Veterinary University of Vienna, Austria) and magnetic cell sorting with LS columns and the MACS (magnetic cell sorting) system (Miltenyi Biotec GmbH, Bergisch Gladbach, Germany). Macrophages

were generated as previously described [26]. Briefly, monocytes were cultured at 5×10^5 cell/mL in Dulbecco's modified Eagle's medium (DMEM) containing Glutamax (ThermoFisher Scientific, Zug, Switzerland) supplemented with 10% of specific pathogen-free porcine serum (produced in-house), seeded in 24-well culture plates and incubated for three days at 39 °C and 5% CO_2.

2.2. Generation of CD16 Expressing SK6 Cells

For generation of CD16 expressing SK6 cells, a lentivirus (LV) expression system using plasmids obtained from the laboratory of Dr. Didier Trono (Ecole Polytechnique Federale de Lausanne, Switzerland) or through Addgene (Cambridge MA, USA) [27,28] was employed to co-express FcγRIIIa and the common γ-chain. This is required for stable expression of CD16 on the cell surface (unpublished results). Porcine FcγRIIIa (FCGR3A, GenBank AF372453.1) and porcine FcR common γ-chain (FCER1G; NCBI NM_001001265.1) were cloned into the lentiviral transfer plasmid pWPT-GFP. FCGR3A and FCER1G were amplified from cDNA obtained from porcine PBMCs using the oligonucleotides pCD16_F (5′-CTACCTACGCGTCACCATGTGGCAGCTGCTGTCACC-3′) and pCD16_R (5′-TGCCGTCGACTTATCCTCCTTTGTCCTGCGG-3′) or pFceRI_F (5′-CTACCTACGCGTCAC CATGATTCCAGCAGTGGTCTTGC-3′) and pFceRI_R (5′-TGCCCTCGAGTTACTGTGGTGGTTTCTC ATGC-3′). The MluI and SalI fragment containing FCGR3A and the MluI and XhoI fragment containing FCER1G were cloned into the MluI and SalI sites of the pWPT-GFP vector, resulting in pWPT-FCGR3A and pWPT-FCER1G. The nucleotide sequences of the plasmid inserts were verified by automated DNA sequencing using the ABI 3130 Genetic Analyzer (Life Technologies, Zug, Switzerland).

In order to generate two different lentiviruses (expressing FCGR3A or FCER1G), HEK293T cells were transfected with the envelope plasmid (pMD2.G), the packaging plasmid (pCMV-R8.74) and the pWPT-FCGR3A or pWPT-FCER1G plasmids using standard calcium phosphate precipitation. Medium was changed after overnight incubation at 37 °C and the supernatant harvested after 48 h, centrifuged (350× *g*, 10 min) and filtered. The virus was purified and enriched by centrifugation on a 20% sucrose cushion at 100,000× *g* for 90 min at 4 °C. SK6 cells were transduced twice with 1:100 dilutions of the purified lentiviruses in 1 mL serum free medium of a T25 cell culture flask followed by culture overnight at 37 °C and medium change between the transductions. After 5 days, cells were stained with anti-CD16 mAb G7 (Becton Dickinson, Basel, Switzerland) and sorted by flow cytometry (FACSAria, Becton Dickinson) to obtain >95% pure CD16+ SK6 cells. The cells termed SK6-CD16 were then expanded and stored in liquid nitrogen for further proliferation. CD16 expression was found to remain stable over at least five passages.

2.3. Viruses

The following JEV strains were used: JEV Laos (G1; CNS769_Laos_2009; [23,29]) kindly provided by Prof. Remi Charrel, Aix-Marseille Université, Marseille, France; JEV Nakayama strain (G3; National Collection of Pathogenic Viruses, Salisbury, UK); JEV S-g5/NS-g3, which represents a chimeric G3/G5 expressing the structural proteins of the G5 strain XZ0934 fused to the nonstructural proteins of JEV G3 RP-9 [25], was kindly obtained from Dr. Philipp Despres, Université de La Réunion, France). All JEV strains were propagated in Vero cells in G-MEM BHK-21 medium (ThermoFisher Scientific) supplemented with 2% fetal bovine serum (FBS; Biowest, Nuaillé, France) and cultured at 37 °C and 5% CO_2. Virus titrations were determined using Vero cells. Infected cells were detected using immunoperoxidase monolayer assay (IPMA) with the anti-flavivirus E mAb 4G2 (ATCC). Titers were calculated and expressed as 50% tissue culture infective dose per mL (TCID50/mL).

2.4. Antibody-Dependent Enhancement of Infection

A collection of sera from previously published work was employed (Table 1). This included sera from pigs vaccinated with the lentiviral vector-based vaccine expressing prM and E of G5 strain XZ0934 (TRIP/JEV.prME) [25]. In addition, we also used sera from pigs infected with JEV G1 Laos

and G3 Nakayama strains and collected at 11 days post infection (p.i.) [24]. As negative control, naïve serum from SPF pigs was included.

Table 1. Sera collection employed for antibody-dependent enhancement (ADE) experiments.

Serum	JEV Strain	$FRNT_{50}$
JEV G1 antisera	G1	1:80
	G3	1:320
	G3/G5	1:160
JEV G3 antisera	G1	1:20
	G3	1:320–640
	G3/G5	1:80
TRIP/JEV.prME antisera	G1	1:40
	G3	1:160
	G3/G5	1:60

JEV: Japanese encephalitis virus; $FRNT_{50}$: focus 50% reduction neutralization test.

To test the ADE of these sera, different serum dilutions were incubated during 30 min at 37 °C with an equal volume of viral suspension at a dose of 0.1 $TCID_{50}$/cell, followed by addition to porcine macrophages or SK6-CD16 cells. To verify JEV strain-dependent differences, ADE of infection mediated by the anti-flavivirus E protein mAb 4G2 was tested using the murine J744A.1 macrophages cell line (ATCC, cultured in DMEM supplemented with 10% FBS). After incubation for 1 h at 37 °C, the cells were washed and fresh medium was added. After 24 h, the cells were then analyzed for expression of JEV E protein using flow cytometry. To this end, cells in suspension were fixed with 4% (*w*/*v*) paraformaldehyde during 10 min at room temperature, followed by washing and permeabilization with 0.3% (*w*/*v*) saponin in PBS in presence of anti-flavivirus E protein mAb 4G2 for 15 min on ice. After washing, anti-mouse Alexa 647 fluochrome conjugate (ThermoFisher Scientific) was added for 15 min and the cells were acquired on a FACSCantoII (Becton Dickinson). For analysis, Flowjo V.9.1 software (Treestars, Inc., Ashland, OR, USA) was used. Dead cells were excluded by electronic gating in forward/side scatter plots, followed by exclusion of doublets.

2.5. Vaccination Challenge Experiment

The pig immunization/challenge experiment was conducted according to Swiss animal welfare regulations and approved by the cantonal ethical committee of Bern (approval number BE 118-13). Five-week-old SPF Swiss Landrace piglets from our own in-house breeding were randomly allocated into three different groups of three animals each. Prior to the first immunization, the animals were left one week for adaptation. The first group was immunized with the TRIP/JEV.prME lentiviral vector produced as previously described [25]. These pigs received 10^5 transduction units (TU) diluted in 0.5 mL in DMEM intramuscularly, followed by booster immunization after three weeks. The second group was intradermally inoculated with JEV G1 Laos at 10^5 $TCID_{50}$ diluted in DMEM. The third group of animals was intradermally inoculated with DMEM as control. The sera were collected before vaccination/infection, and then once a week. Thirty-six days after the first TRIP/JEV.prME vaccination or JEV Laos infection, all pigs were challenged with JEV G3 Nakayama at 10^3 $TCID_{50}$ using oro-nasal administration. Thereafter, clinical signs and body temperature were checked and blood taken daily until the end of the study at 10 days post-challenge.

2.6. Virological Analyses

For reverse transcription quantitative polymerase chain reaction (RT-qPCR) based quantification of viral RNA, 1.5 mL tubes were filled with 500 µL of minimum essential medium (MEM; ThermoFisher Scientific) and weighed before and after filling of the organs samples. Samples were lysed with a BulletBlender (Next Advanced Inc., Averill Park, NY, USA), and after centrifugation, the supernatants

were transferred into new tubes and immediately frozen at −80 °C for storage. After thawing, each sample was spiked with a defined amount of enhanced green fluorescent protein (eGFP) RNA. Then, RNA extraction was performed using the QIAmp viral RNA extraction kit (Qiagen AG, Hombrechtikon, Switzerland) following the manufacturer's instructions. RT-qPCR of the highly conserved 3′ NTR of the JEV genome was performed as previously described [30]. With the aim to discriminate between JEV G1 Laos and JEV G3 Nakayama strains, specific sets of primers and probes were designed and RT-qPCR conditions optimized (Table 2). RT-qPCR used the SuperScript III Platinium One-Step qRT-PCR system (ThermoFisher Scientific) with ROX (carboxy-x-rhodamine) reference dye according to manufacturer's instructions, and where run in a 7500 Applied Biosystems Real-time PCR machine (ThermoFisher Scientific). The thermal cycling setup was 30 min at 50 °C for the RT step, then qPCR steps which included 2 min at 95 °C for enzyme activation, and 50 cycles of denaturation at 95 °C during 15 s, annealing at 60 °C for 30 s and extension at 72 °C for 30 s. Samples were taken as positive only with the cycle threshold (CT) value of the internal eGFP control was lower than 28. Viral load was quantified relatively by using RNA from a stock of Nakayama JEV with a known titer as a standard. The stock was serially diluted tenfold, RNA was extracted, and CT values were determined to draw a standard curve (correlation coefficient R = 0.99). CT values above 40 were defined as negative. The CT value corresponding to 1 TCID50 was defined as 1 RNA unit (U). Using this standard, the CT values of our samples were transformed into relative quantities as RNA U/mL. Organ samples were corrected for their weight and data calculated as relative RNA quantities in U/mg.

Table 2. Primer and probe sets employed for JEV reverse transcription-quantitative PCR (RT-qPCR).

Specificity		Primer and Probe Sequence (5′-3′)	Concentration (nM)
3′ NTR JEV	forward	GGTGTAAGGACTAGAGGTTAGAGG	200
	reverse	ATTCCCAGGTGTCAATATGCTGTT	200
	probe	FAM-CCCGTGGAAACAACATCATGCGGC-BHQ-1	100
JEV G1 Laos	forward	GACAGGATAAAGTCATGTGCGT	200
	reverse	CCTGACGTTGGTCTTTCAAC	200
	probe	FAM-CCGTCTCGGAAGCAGGTCCC-BHQ-1	100
JEV G3 Nakayama	forward	CAGGGTCATCTAGTGTGATTTAAGG	1600
	reverse	CAGTCCTCCTGGGACTGAGA	1600
	probe	FAM-TGCTGGCCTGACTCCATATGCA-BHQ-1	200

Infectious virus quantification was determined by titration on Vero cells as previously described [23].

2.7. Serum Neutralization Assay

Neutralizing antibodies against JEV were determined by focus reduction neutralization test (FRNT) on Vero cells as previously described [25]. Briefly, pig sera were two-fold serially diluted starting in 1:5 serum dilution, and incubated with 100 focus-forming units (FFU) of JEV for 30 min at 37 °C and then added to Vero cells for 1h at 37 °C. After removal of the inoculum and washing once, DMEM supplemented with 2% FBS was added and culture at 37 °C. Infected cells were fixed, permeabilized and stained as described above using the 4G2 mAb. The highest serum dilution which reduced the FFU by 50% was defined as the end-point titer and expressed as $FRNT_{50}$/mL.

2.8. Statistics

Statistical analyses for the ADE of infection were tested using two-way ANOVA followed by Dunnets's multiple comparison test (variables were serum dilution and serum origin). For neutralizing antibodies, data was Log2 transformed and *p*-values determined using two-way ANOVA and Sidak's multiple comparison (variables were time p.i. and serum origin). All tests were made with GraphPad Prism 7 (GraphPad Software version 7.0b, La Jolla, San Diego, CA, USA). Alpha was set to 0.05; * $p < 0.05$, ** $p < 0.002$, *** $p < 0.001$.

3. Results

3.1. TRIP/JEV.prME Induces ADE of Macrophage Infection

To test a possible ADE of infection in macrophages, sera from TRIP/JEV.prME-immunized and JEV-infected pigs were incubated at different concentrations with JEV G3 Nakayama, and infectivity tested for monocyte-derived macrophages. Our results demonstrated that, while no statistically significant ADE was found with the immune serum from the JEV-infected animals, sera from TRIP/JEV.prME-immunized animals ($FRNT_{50}$ 1:160) strongly promoted infection by JEV, even at high dilutions (Figure 1).

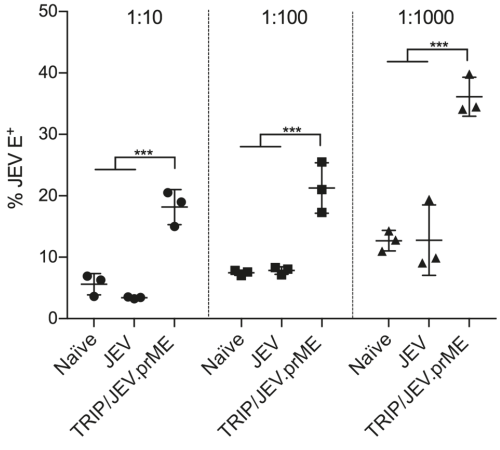

Figure 1. Antibody-dependent enhancement (ADE) of macrophage infection. Sera from piglets immunized with lentiviral vector TRIP/JEV which expressed JEV G3 prM and E proteins (TRIP/JEV.prME) or infected with Japanese encephalitis virus (JEV) G3 Nakayama (focus 50% reduction neutralization test; FRNT50 1:160 and 1:320, respectively) were 10-fold diluted (from 1:10 to 1:1000) and incubated with JEV G3 Nakayama at multiplicity of infection (MOI) 0.1 of 50% tissue culture infective dose per mL (TCID50) per cell during 30 min at 37 °C, and then added to the cells. The percentage of cells expressing JEV E protein as a measure of ADE of infection in macrophages is shown. Statistical significance was calculated using a two-way ANOVA followed by Dunnets's multiple comparison. The results are representative of triplicate cultures repeated in three independent experiments. * $p < 0.05$, ** $p < 0.002$, *** $p < 0.001$.

3.2. TRIP/JEV.prME-Antibodies Strongly Enhance JEV Infection of Cells Expressing FcγRIII

Considering the ADE of infection by JEV opsonized with TRIP/JEV.prME serum in macrophages, we tested if similar observations could be made using the porcine kidney cell line SK6 engineered to express porcine FcγRIII (SK6-CD16). To this end, we compared sera from TRIP/JEV.prME-vaccinated pigs with sera from pigs infected with JEV G1 (Laos) and G3 (Nakayama). These sera were tested against JEV G1 (Figure 2a), JEV G3 (Figure 2b) and against JEV G5/G3 (homologous prM/E to the TRIP/JEV.prME vector).

The data obtained confirmed the very potent ADE activity of the TRIP/JEV.prME sera in enhancing infection with all three JEV genotypes. Its efficiency was also demonstrated by the fact that ADE was even seen at serum dilutions of 1:10,000 although the neutralizing titers of this serum was 1:40 against JEV G1 Laos and 1:160 against both JEV G3 Nakayama and the chimeric G3/G5 JEV [25]. Only for the Nakayama strain was there was a clear reduction of ADE at this serum dilution (Figure 2b).

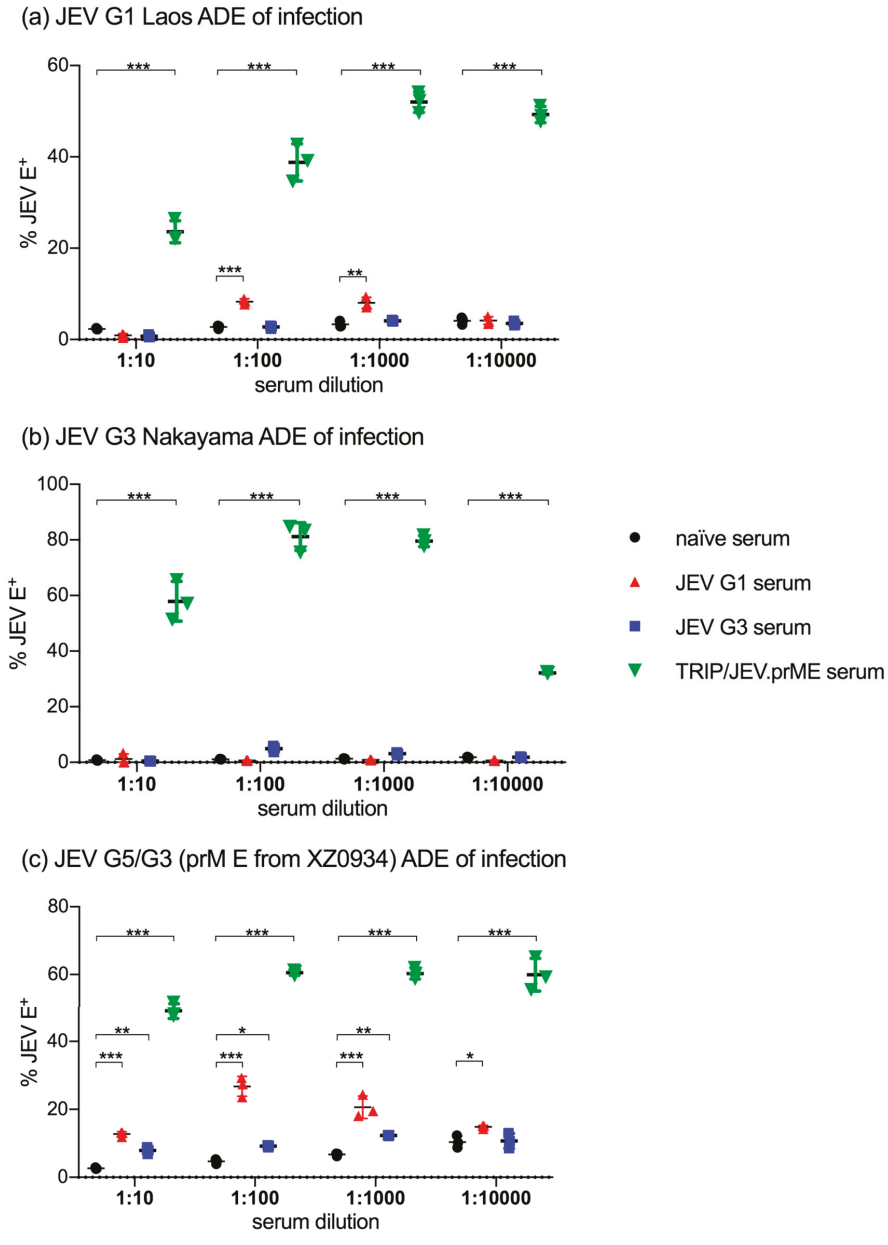

Figure 2. ADE of infection in SK6-CD16 cells. Sera from TRIP/JEV.prME-immunized, JEV Laos- and JEV Nakayama-infected pigs were tested for ADE activity in the porcine kidney cell line SK6 expressing CD16. ADE of infection was tested as described in Figure 1 using (**a**) JEV G1 Laos; (**b**) JEV G3 Nakayama and (**c**) JEV G5/G3, representing a chimeric virus expressing a G5 prM/E. The percentage of infected cells was determined after 24 h. Statistical significance was calculated using a two-way ANOVA followed by Dunnets's multiple comparison. The results are representative of triplicate cultures repeated in two independent experiments. * $p < 0.05$, ** $p < 0.002$, *** $p < 0.001$.

In contrast to this, the ADE activity of various sera from JEV-infected pigs was absent or much lower. Anti-JEV G1 Laos serum had a moderately but statistically significant ADE activity for a homologous virus (Figure 2a), no activity of JEV G3 Nakayama (Figure 2b), but relatively strong ADE activity for the G5/G3 chimeric virus (Figure 2c). Anti-JEV G3 Nakayama serum had no ADE activity for JEV G1 Laos (Figure 2a) and the homologous virus (Figure 2b), but significantly enhanced infection by G5/G3 JEV (Figure 2c). These results were in accordance with experiments investigating the ability of the anti-flavivirus E protein mAb4G2 to enhance infection of murine J744A.1 macrophages. The strongest ADE activity was found with the JEV G5/G3 chimeric virus and no enhanced infection by JEV G3 Nakayama (Figure S1).

There results indicate that also viral factors, which are independent of the antigenic relationship to the serum, determine the infectivity of opsonized virus. On the other hand, the fact that Laos-immunized but not Nakayama-immunized pigs developed ADE antibodies against a homologous virus, demonstrates strain-dependent differences in the ability to induce ADE antibodies in pigs.

3.3. Antibody Responses Induced by TRIP/JEV.prME Vaccine and JEV Infection

Considering the strong ADE of infection induced by the TRIP/JEV.prME vaccine but not following JEV infection, we decided to compare the protection induced by the vaccine to that following JEV G1 Laos infection. We selected G3 Nakayama strain as a challenge virus as ADE of infection by this virus was only enhanced with TRIP/JEV.prME antisera (Figure 2b).

All three pigs infected with JEV G1 Laos strain became viremic as early as one day p.i. and remained positive for viral RNA until 7–8 days p.i. (Figure 3a), comparable to previously published results [23].

All three animals seroconverted after one week and developed serum neutralizing antibodies against homologous and heterologous JEV G1 Laos and G3 Nakayama strains (Figure 3b). This coincided with the end of the viremia. Between days 14 and 28 p.i., the neutralizing antibodies further increased. Surprisingly, at these time points, titers were even higher against the heterologous JEV G3 strain. Nevertheless, at the time of challenge infection (day 36), there was no statistical significance between the neutralization of the Laos and Nakayama strains.

Piglets immunized with TRIP/JEV.prME lentiviral vector also developed neutralizing antibodies but at a slower and weaker rate (Figure 3c). Again, neutralization activity against the Nakayama strain was found to be more potent than against the Laos strain. At day 36 post vaccination, titers were between 160 and 320 with all pigs.

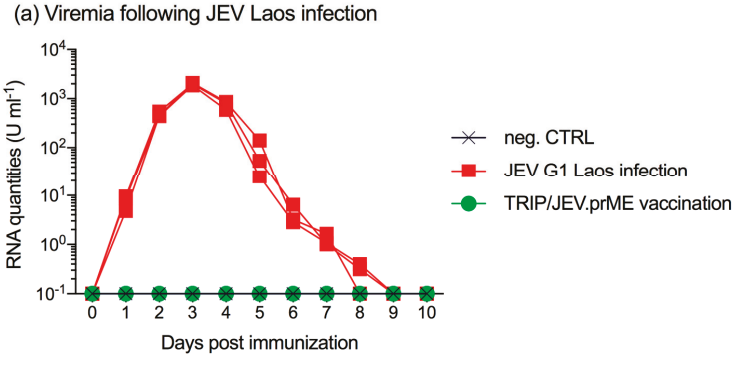

Figure 3. *Cont.*

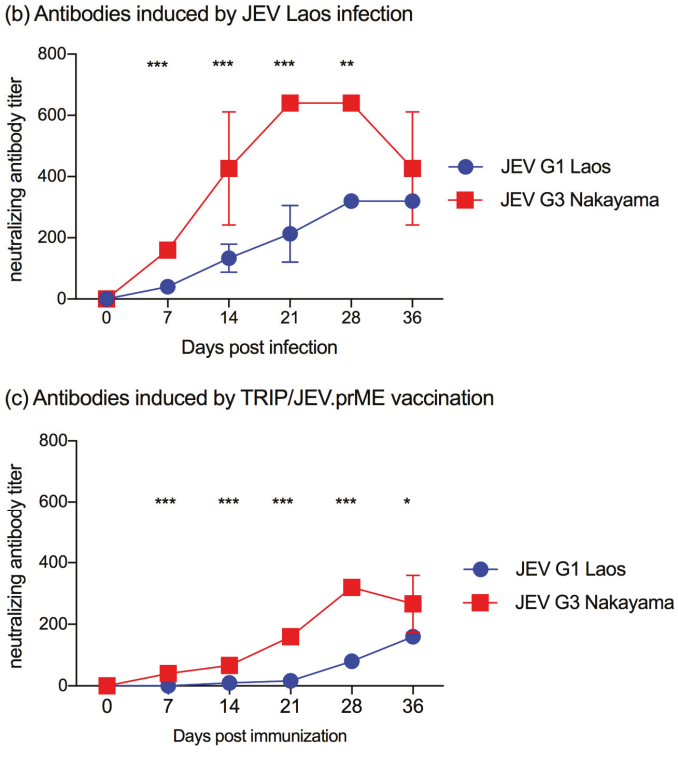

Figure 3. Neutralizing antibody response in piglets immunized with JEV G1 Laos or TRIP/JEV.prME. Groups of three pigs were either infected with JEV Laos or immunized with TRIP/JEV.prME or mock-inoculated, and serum was collected at the indicated time points (*x*-axis). (**a**) viral RNA load determined by RT-qPCR in sera from all nine animals; (**b**) JEV Laos- and (**c**) TRIP/JEV.prME-induced neutralizing antibody responses of sera against homologous JEV Laos (blue circles) and JEV Nakayama (red squares). Mean and standard deviations are shown. Statistical significance was determined after Log2 transformation of the data using two-way ANOVA and Sidak's multiple comparison. * $p < 0.05$, ** $p < 0.002$, *** $p < 0.001$.

3.4. TRIP/JEV.prME Vaccine and Previous JEV Infection Induce Protection against Viremia

At day 36 post vaccination, all nine animals were challenge infected with JEV G3 Nakayama. Only animals from the unvaccinated control group developed viremia in terms of viral RNA detection in the serum. This started in two pigs at 3–4 days p.i. and lasted for 4–6 days. In one animal, viremia was only found 10 days p.i. (Figure 4a). The virus infection did not induce clinical signs with the exception of fever in one of the control animals at days 8 and 9 p.i. (Figure 4b).

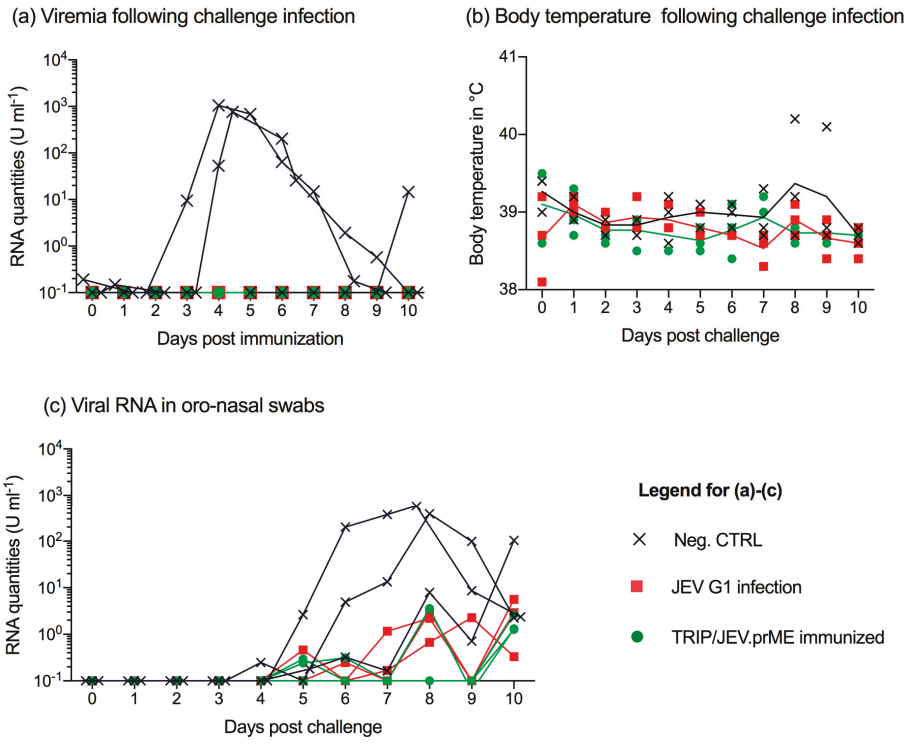

Figure 4. TRIP/JEV.prME vaccine and previous JEV infection induce protection but do not prevent virus shedding. Groups of three pigs were either mock-inoculated (Neg. CTRL, cross), immunized by previous infection with JEV Laos (red square) or vaccinated with TRIP/JEV.prME (green circle), and then challenged infected with JEV G3 Nakayama. Data post challenge is shown. (**a**) viral RNA loads determined by RT-qPCR in sera from all nine animals; (**b**) body temperature; (**c**) viral RNA load in oro-nasal swabs collected daily.

3.5. JEV Immunization Does Not Completely Prevent Oro-Nasal Shedding of Challenge Virus

Considering the ability of JEV to shed through oro-nasal secretions, which can result in vector-free transmission by contact [23], we collected oro-nasal swabs and tested them by RT-qPCR (Figure 4c). Animals from the control group shed virus from 4 to 10 days p.i. Interestingly, we detected low but clearly detectable JEV RNA in many oro-nasal swabs samples from all pigs previously infected with JEV G1 Laos or vaccinated with TRIP/JEV.prME (Figure 4c).

3.6. JEV Immunization Does Not Provide Sterile Immunity

At 10 days p.i., all animals were euthanized and various tissues analyzed for viral RNA. In the negative control group, the two viremic animals had high levels of JEV RNA in lymphoid tissues including the tonsils, the lymph node and the continuous Peyer's patches of the terminal ileum (Figure 5a). Similar to previous studies [23,24], these pigs also had high viral RNA quantities in the neocortex, the thalamus and the striatum. The third animal in this group, which only became viremic at 10 days p.i., also had viral RNA in lymphatic tissues, thalamus and brain stem but reaching much lower levels (blue crosses).

In the JEV G1 pre-infected group, viral RNA was found in the tonsils and ileum of all pigs and in lymph nodes of two pigs. Furthermore, one animal also had a virus in the jejunum, the trachea, nasal

cavity, although at very low levels (Figure 5b). In pigs immunized with TRIP/JEV.prME lentiviral vector, low levels of viral RNA were found in the lymph node, ileum, jejunum, nasal cavity, olfactory bulb, striatum and brain stem. One animal was negative in all tissues (Figure 5c).

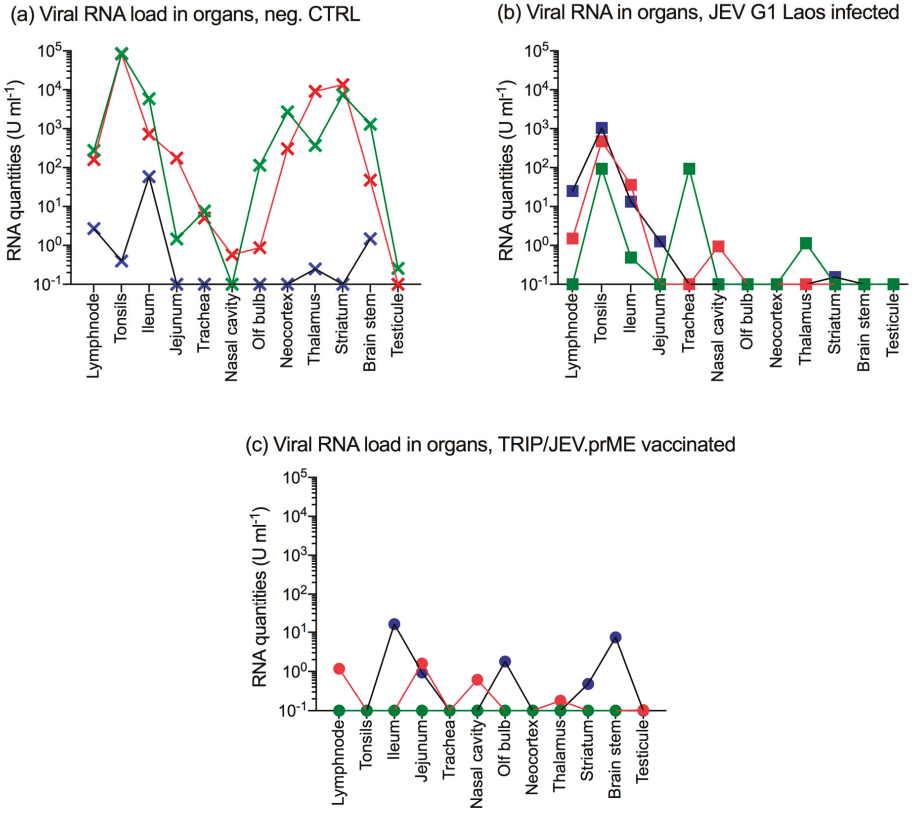

Figure 5. TRIP/JEV.prME vaccine or previous JEV infection induce protection but do not prevent organ infection. Groups of three pigs were either unvaccinated/infected (negative control; Neg. CTRL, crosses), immunized by previous infection with JEV Laos (squares) or vaccinated with TRIP/JEV.prME (circles), and then challenge infected with JEV G3 Nakayama. At 10 days p.i., the animals were euthanized and organ samples tested for viral RNA by RTqPCR. (**a**) viral RNA load in pigs from the Neg. CTRL group; (**b**) viral RNA load from the JEV Laos pre-infected group; (**c**) viral RNA load from the TRIP/JEVprME-vaccinated group.

3.7. JEV G1 Persistence after JEV G3 Challenge

Considering the relatively high viral loads in the tonsils found in the JEV Laos-preinfected group, and the previously described ability of JEV to persist for several weeks in the tonsils [23], we re-analyzed these samples with a set of primers and probes which discriminate between JEV G1 Laos (first infection) and JEV G3 Nakayama (challenge virus). For all three animals, these strain-specific RT-qPCR's were only positive for JEV G1 Laos demonstrating the long-term persistence for least 46 days, even following challenge infection with a heterologous JEV strain. As expected, only Nakayama-specific viral transcripts were found in the unvaccinated (Neg. CTRL) group (Table 3).

Considering these results, we also re-tested all swabs using the strain-specific RT-qPCR. Interestingly, only the RT-qPCR detecting JEV G3 Nakayama was positive, demonstrating that the shed virus was originating from the challenge infection.

Table 3. JEV Nakayama and JEV Laos viral RNA loads in tonsils at 10 days post challenge

Group/Pig Number [1]	Nakayama-Specific RT-qPCR	Laos-Specific RT-qPCR
Neg. CTRL, #1516	5.2×10^0	negative
Neg. CTRL, #1517	4.6×10^5	negative
Neg. CTRL, #1518	2.0×10^5	negative
JEV G1, #1512	negative	3.2×10^1
JEV G1, #1513	negative	1.7×10^1
JEV G1, #1521	negative	2.9×10^0

[1] groups as defined in Figure 4.

4. Discussion

In the present study, we have discovered that the TRIP/JEV.prME, in contrast to JEV infection, induced very high levels of antibodies with ADE activity. Considering the possible importance of ADE of disease during certain flavivirus infections, we decided to test the protective value of this vaccine and found it to be at least as protective as a previous JEV infection.

For flaviviruses, ADE can occur through various mechanisms. Using West Nile virus (WNV) as model, it was demonstrated that ADE may occur when antibodies concentration does not achieve the minimum stoichiometric threshold for viral neutralization. This explains that ADE is often seen at sub-neutralizing antibody concentrations [31]. Nevertheless, the sera from the TRIP/JEV.prME immunized animals also strongly enhanced infection at concentrations clearly above the neutralization titers. An alternative explanation would be that the TRIP/JEV.prME vaccine induces antibodies with a particular specificity causing high ADE activity. For instance, antibodies against the prM protein are known to mediate ADE [32,33]. In fact, our previous work showed that TRIP/JEV.prME immunized animals developed antibodies against both E and prM proteins [25]. Alternatively or additionally, the TRIP/JEV.prME vaccine may induce antibodies against the fusion loop of the E protein, also known to cause ADE [34]. We also have no indication that the strong ADE activity could be related to differences in antibody isotypes induced by the TRIP/JEV.prME vaccine, as these were similar to those from JEV infected pigs [25]. Future studies would be required to identify the targets of the antibodies induced by the TRIP/JEV.prME vaccine.

In our study, we also observed differences in the susceptibility of three different JEV virus strains to ADE. It is well known that immature virions express prM on their surface, making them susceptible to ADE [35]. Although the cleavage of prM is important for maturation of virions to full infectivity, this process is often incomplete, showing substantial variability between viruses [36]. Therefore, virus preparations are typically a mixture of immature and mature virions, and even the passage history of a virus can have an effect on in vitro ADE [31,37]. These possible differences in virus structure between strains also influence virus neutralization [38], which may explain why the heterologous virus was more efficiently neutralized in the present work. For this study, we used virus preparations produced in Vero cells, described to produce many immature virions expressing prM [39,40].

The observation that the TRIP/JEV.prME vaccine protects is in line with other studies showing that antibodies causing ADE in vitro can be protective. This has been demonstrated for antibodies against the fusion loop in a WNV murine model [41]. Furthermore, no association was found between the levels of anti-prM antibodies and the severity of Dengue in human beings [42].

The in vivo trial performed in this study confirmed and complemented two important findings related to JEV infection in pigs. First, we confirmed that JEV can persist long term in the tonsils of infected pigs as previously described [23]. In the present study, persistence was found for at least 46 days, even after a second heterologous challenge infection expected to boost antiviral immunity.

This indicates that the virus is well hidden from neutralizing antibodies and cytotoxic T-cells. Second, we also confirmed the oro-nasal virus shedding peaking clearly after the viremia. This means that the highest degree of shedding occurs when the pigs are basically no longer viremic. We also found a low degree of virus shedding in vaccinated animals, although these were never viremic. It appears that the source of the virus detected in the oronasal swabs was not the tonsils. The virus detected in the tonsil was exclusively JEV Laos G1 utilized for the first immunization, whereas only the challenge virus (Nakayama) was found in the swabs. Clearly, more research addressing the source of the virus in oronasal secretion, which is probably local, is required.

In accordance with our previous work, experimental JEV infection under our defined conditions induced no or only mild signs of disease [23,24]. In the present study, the animals were also older compared to our previous work explaining the complete lack of clinical signs. Nevertheless, similar to previous results, JEV RNA was readily detected in CNS tissues and lymphoid tissues with the highest viral RNA loads were found in the tonsils. An important observation was also that previous infection or vaccination did not prevent secondary infection of pigs. Even if the oro-nasal viral shedding was low in immunized pigs, these animals may still be able to transmit the virus to other pigs in close contact. This is based on our work showing that 10 $TCID_{50}$ given oro-nasally is sufficient to infect pigs [23]. Future studies are required to address if transmission can occur under such conditions and the role of contact transmission in field situations.

5. Conclusions

The present study demonstrates that a viral vector vaccine based on prM and E protein expression induces high levels of antibodies that strongly enhance infection of FcγR expressing cells, but still provides protection comparable to a natural infection. This has implications for vaccine design against JEV and other flaviviruses. Furthermore, our data on virus persistence and shedding are of relevance for JEV ecology and pig vaccination.

Supplementary Materials: The following are available online at www.mdpi.com/1999-4915/9/5/124/s1, Figure S1: ADE of infection in murine macrophages J744A.1 cells.

Acknowledgments: We are grateful to Beatrice Zumkehr for technical help, Daniel Brechbühl for animal care as well as to Urs Pauli and Monika Gsell-Albert for biosafety support. We thank Remi Charrel and Antoine Nougairede (Aix-Marseille Université, Marseille, France) for providing the JEV strain Laos, and Philippe Desprès (Université de La Reunion, France) for providing JEV S-g5/NS-g3. This work was supported by the European Union's Seventh Framework Program for research, technological development and demonstration under Grant No. 278433-PREDEMICS.

Author Contributions: O.G.N. was responsible for design of the study, data acquisition, data analysis, and drafting the manuscript; MER completed design of the study, critical review of the manuscript; M.L., N.J.V., and S.P. were responsible for data acquisition and data analysis; P.C. designed the study and provided vaccines; and AS designed the study, completed data analysis, and finalized the manuscript. All authors read and approved the manuscript.

Conflicts of Interest: The authors declare no conflict of interest.

References

1. Weaver, S.C.; Barrett, A.D. Transmission cycles, host range, evolution and emergence of arboviral disease. *Nat. Rev. Microbiol.* **2004**, *2*, 789–801. [CrossRef] [PubMed]
2. Van den Hurk, A.F.; Ritchie, S.A.; Mackenzie, J.S. Ecology and geographical expansion of Japanese encephalitis virus. *Annu. Rev. Entomol.* **2009**, *54*, 17–35. [CrossRef] [PubMed]
3. Impoinvil, D.E.; Baylis, M.; Solomon, T. Japanese encephalitis: On the One Health agenda. *Curr. Top. Microbiol. Immunol.* **2013**, *365*, 205–247. [PubMed]
4. Yun, S.I.; Lee, Y.M. Japanese encephalitis: The virus and vaccines. *Hum. Vaccines Immunother.* **2014**, *10*, 263–279. [CrossRef] [PubMed]

5. Campbell, G.L.; Hills, S.L.; Fischer, M.; Jacobson, J.A.; Hoke, C.H.; Hombach, J.M.; Marfin, A.A.; Solomon, T.; Tsai, T.F.; Tsu, V.D.; et al. Estimated global incidence of Japanese encephalitis: A systematic review. *Bull. World Health Organ.* **2011**, *89*, 766–774. [CrossRef] [PubMed]
6. Mansfield, K.L.; Hernandez-Triana, L.M.; Banyard, A.C.; Fooks, A.R.; Johnson, N. Japanese encephalitis virus infection, diagnosis and control in domestic animals. *Vet. Microbiol.* **2017**, *201*, 85–92. [CrossRef] [PubMed]
7. Le Flohic, G.; Porphyre, V.; Barbazan, P.; Gonzalez, J.P. Review of climate, landscape, and viral genetics as drivers of the Japanese encephalitis virus ecology. *PLoS Negl. Trop. Dis.* **2013**, *7*, e2208. [CrossRef] [PubMed]
8. Go, Y.Y.; Balasuriya, U.B.; Lee, C.K. Zoonotic encephalitides caused by arboviruses: Transmission and epidemiology of alphaviruses and flaviviruses. *Clin. Exp. Vaccine Res.* **2014**, *3*, 58–77. [CrossRef] [PubMed]
9. Gao, X.; Liu, H.; Wang, H.; Fu, S.; Guo, Z.; Liang, G. Southernmost Asia is the source of Japanese encephalitis virus (genotype 1) diversity from which the viruses disperse and evolve throughout Asia. *PLoS Negl. Trop. Dis.* **2013**, *7*, e2459. [CrossRef] [PubMed]
10. Schuh, A.J.; Ward, M.J.; Brown, A.J.; Barrett, A.D. Phylogeography of Japanese encephalitis virus: Genotype is associated with climate. *PLoS Negl. Trop. Dis.* **2013**, *7*, e2411. [CrossRef] [PubMed]
11. Takhampunya, R.; Kim, H.C.; Tippayachai, B.; Kengluecha, A.; Klein, T.A.; Lee, W.J.; Grieco, J.; Evans, B.P. Emergence of Japanese encephalitis virus genotype V in the Republic of Korea. *Virol. J.* **2011**, *8*, 449. [CrossRef] [PubMed]
12. Li, M.H.; Fu, S.H.; Chen, W.X.; Wang, H.Y.; Guo, Y.H.; Liu, Q.Y.; Li, Y.X.; Luo, H.M.; Da, W.; Duo Ji, D.Z.; et al. Genotype V Japanese encephalitis virus is emerging. *PLoS Negl. Trop. Dis.* **2011**, *5*, e1231. [CrossRef] [PubMed]
13. Dubischar-Kastner, K.; Kanesa-Thasan, N. Vaccinating against Japanese encephalitis virus: What have we learned from recent clinical trials? *Expert. Rev. Vaccines* **2012**, *11*, 1159–1161. [CrossRef] [PubMed]
14. Larena, M.; Prow, N.A.; Hall, R.A.; Petrovsky, N.; Lobigs, M. JE-ADVAX vaccine protection against Japanese encephalitis virus mediated by memory B cells in the absence of CD8(+) T cells and pre-exposure neutralizing antibody. *J. Virol.* **2013**, *87*, 4395–4402. [CrossRef] [PubMed]
15. Kimura-Kuroda, J.; Yasui, K. Protection of mice against Japanese encephalitis virus by passive administration with monoclonal antibodies. *J. Immunol.* **1988**, *141*, 3606–3610. [PubMed]
16. Van Gessel, Y.; Klade, C.S.; Putnak, R.; Formica, A.; Krasaesub, S.; Spruth, M.; Cena, B.; Tungtaeng, A.; Gettayacamin, M.; Dewasthaly, S. Correlation of protection against Japanese encephalitis virus and JE vaccine (IXIARO((R)) induced neutralizing antibody titers. *Vaccine* **2011**, *29*, 5925–5931. [CrossRef] [PubMed]
17. Murphy, B.R.; Whitehead, S.S. Immune response to dengue virus and prospects for a vaccine. *Annu. Rev. Immunol.* **2011**, *29*, 587–619. [CrossRef] [PubMed]
18. Durbin, A.P. Dengue Antibody and Zika: Friend or Foe? *Trends Immunol.* **2016**, *37*, 635–636. [CrossRef] [PubMed]
19. Taylor, A.; Foo, S.S.; Bruzzone, R.; Dinh, L.V.; King, N.J.; Mahalingam, S. Fc receptors in antibody-dependent enhancement of viral infections. *Immunol. Rev.* **2015**, *268*, 340–364. [CrossRef] [PubMed]
20. Wallace, M.J.; Smith, D.W.; Broom, A.K.; Mackenzie, J.S.; Hall, R.A.; Shellam, G.R.; McMinn, P.C. Antibody-dependent enhancement of Murray Valley encephalitis virus virulence in mice. *J. Gen. Virol.* **2003**, *84*, 1723–1728. [CrossRef] [PubMed]
21. Gould, E.A.; Buckley, A. Antibody-dependent enhancement of yellow fever and Japanese encephalitis virus neurovirulence. *J. Gen. Virol.* **1989**, *70*, 1605–1608. [CrossRef] [PubMed]
22. Scherer, W.F.; Moyer, J.T.; Izumi, T.; Gresser, I.; Mc, C.J. Ecologic studies of Japanese encephalitis virus in Japan. VI. Swine infection. *Am. J. Trop. Med. Hyg.* **1959**, *8*, 698–706. [CrossRef] [PubMed]
23. Ricklin, M.E.; Garcia-Nicolas, O.; Brechbuhl, D.; Python, S.; Zumkehr, B.; Nougairede, A.; Charrel, R.N.; Posthaus, H.; Oevermann, A.; Summerfield, A. Vector-free transmission and persistence of Japanese encephalitis virus in pigs. *Nat. Commun.* **2016**, *7*, 10832. [CrossRef] [PubMed]
24. Ricklin, M.E.; Garcia-Nicolas, O.; Brechbuhl, D.; Python, S.; Zumkehr, B.; Posthaus, H.; Oevermann, A.; Summerfield, A. Japanese encephalitis virus tropism in experimentally infected pigs. *Vet. Res.* **2016**, *47*, 34. [CrossRef] [PubMed]
25. De Wispelaere, M.; Ricklin, M.; Souque, P.; Frenkiel, M.P.; Paulous, S.; Garcia-Nicolas, O.; Summerfield, A.; Charneau, P.; Despres, P.A. Lentiviral Vector Expressing Japanese Encephalitis Virus-like Particles Elicits Broad Neutralizing Antibody Response in Pigs. *PLoS Negl. Trop. Dis.* **2015**, *9*, e0004081. [CrossRef] [PubMed]

26. Garcia-Nicolas, O.; Baumann, A.; Vielle, N.J.; Gomez-Laguna, J.; Quereda, J.J.; Pallares, F.J.; Ramis, G.; Carrasco, L.; Summerfield, A. Virulence and genotype-associated infectivity of interferon-treated macrophages by porcine reproductive and respiratory syndrome viruses. *Virus Res.* **2014**, *179*, 204–211. [CrossRef] [PubMed]
27. Alves, M.P.; Neuhaus, V.; Guzylack-Piriou, L.; Ruggli, N.; McCullough, K.C.; Summerfield, A. Toll-like receptor 7 and MyD88 knockdown by lentivirus-mediated RNA interference to porcine dendritic cell subsets. *Gene Ther.* **2007**, *14*, 836–844. [CrossRef] [PubMed]
28. Zufferey, R.; Dull, T.; Mandel, R.J.; Bukovsky, A.; Quiroz, D.; Naldini, L.; Trono, D. Self-inactivating lentivirus vector for safe and efficient in vivo gene delivery. *J. Virol.* **1998**, *72*, 9873–9880. [PubMed]
29. Aubry, F.; Vongsouvath, M.; Nougairede, A.; Phetsouvanh, R.; Sibounheuang, B.; Charrel, R.; Rattanavong, S.; Phommasone, K.; Sengvilaipraserth, O.; de Lamballerie, X.; et al. Complete Genome of a Genotype I Japanese Encephalitis Virus Isolated from a Patient with Encephalitis in Vientiane, Lao PDR. *Genome Announc.* **2013**, *1*, 1. [CrossRef] [PubMed]
30. Yang, D.K.; Kweon, C.H.; Kim, B.H.; Lim, S.I.; Kim, S.H.; Kwon, J.H.; Han, H.R. TaqMan reverse transcription polymerase chain reaction for the detection of Japanese encephalitis virus. *J. Vet. Sci.* **2004**, *5*, 345–351. [PubMed]
31. Pierson, T.C.; Xu, Q.; Nelson, S.; Oliphant, T.; Nybakken, G.E.; Fremont, D.H.; Diamond, M.S. The stoichiometry of antibody-mediated neutralization and enhancement of West Nile virus infection. *Cell. Host Microbe* **2007**, *1*, 135–145. [CrossRef] [PubMed]
32. Dejnirattisai, W.; Jumnainsong, A.; Onsirisakul, N.; Fitton, P.; Vasanawathana, S.; Limpitikul, W.; Puttikhunt, C.; Edwards, C.; Duangchinda, T.; Supasa, S.; et al. Cross-reacting antibodies enhance dengue virus infection in humans. *Science* **2010**, *328*, 745–748. [CrossRef] [PubMed]
33. Rodenhuis-Zybert, I.A.; van der Schaar, H.M.; da Silva Voorham, J.M.; van der Ende-Metselaar, H.; Lei, H.Y.; Wilschut, J.; Smit, J.M. Immature dengue virus: A veiled pathogen? *PLoS Pathog.* **2010**, *6*, e1000718. [CrossRef] [PubMed]
34. Dejnirattisai, W.; Supasa, P.; Wongwiwat, W.; Rouvinski, A.; Barba-Spaeth, G.; Duangchinda, T.; Sakuntabhai, A.; Cao-Lormeau, V.M.; Malasit, P.; Rey, F.A.; et al. Dengue virus sero-cross-reactivity drives antibody-dependent enhancement of infection with zika virus. *Nat. Immunol.* **2016**, *17*, 1102–1108. [CrossRef] [PubMed]
35. Nelson, S.; Jost, C.A.; Xu, Q.; Ess, J.; Martin, J.E.; Oliphant, T.; Whitehead, S.S.; Durbin, A.P.; Graham, B.S.; Diamond, M.S.; et al. Maturation of West Nile virus modulates sensitivity to antibody-mediated neutralization. *PLoS Pathog.* **2008**, *4*, e1000060. [CrossRef] [PubMed]
36. Pierson, T.C.; Diamond, M.S. Degrees of maturity: The complex structure and biology of flaviviruses. *Curr. Opin. Virol.* **2012**, *2*, 168–175. [CrossRef] [PubMed]
37. Wikan, N.; Libsittikul, S.; Yoksan, S.; Auewarakul, P.; Smith, D.R. Delayed antibody dependent enhancement of low passage dengue virus 4 isolates. *BMC Res. Notes* **2015**, *8*, 399. [CrossRef] [PubMed]
38. Dowd, K.A.; Mukherjee, S.; Kuhn, R.J.; Pierson, T.C. Combined effects of the structural heterogeneity and dynamics of flaviviruses on antibody recognition. *J. Virol.* **2014**, *88*, 11726–11737. [CrossRef] [PubMed]
39. He, R.T.; Innis, B.L.; Nisalak, A.; Usawattanakul, W.; Wang, S.; Kalayanarooj, S.; Anderson, R. Antibodies that block virus attachment to Vero cells are a major component of the human neutralizing antibody response against dengue virus type 2. *J. Med. Virol.* **1995**, *45*, 451–461. [CrossRef] [PubMed]
40. Putnak, R.; Barvir, D.A.; Burrous, J.M.; Dubois, D.R.; D'Andrea, V.M.; Hoke, C.H.; Sadoff, J.C.; Eckels, K.H. Development of a purified, inactivated, dengue-2 virus vaccine prototype in Vero cells: Immunogenicity and protection in mice and rhesus monkeys. *J. Infect. Dis.* **1996**, *174*, 1176–1184. [CrossRef] [PubMed]
41. Vogt, M.R.; Dowd, K.A.; Engle, M.; Tesh, R.B.; Johnson, S.; Pierson, T.C.; Diamond, M.S. Poorly neutralizing cross-reactive antibodies against the fusion loop of West Nile virus envelope protein protect in vivo via Fcgamma receptor and complement-dependent effector mechanisms. *J. Virol.* **2011**, *85*, 11567–11580. [CrossRef] [PubMed]
42. Rodenhuis-Zybert, I.A.; da Silva Voorham, J.M.; Torres, S.; van de Pol, D.; Smit, J.M. Antibodies against immature virions are not a discriminating factor for dengue disease severity. *PLoS Negl. Trop. Dis.* **2015**, *9*, e0003564. [CrossRef] [PubMed]

© 2017 by the authors. Licensee MDPI, Basel, Switzerland. This article is an open access article distributed under the terms and conditions of the Creative Commons Attribution (CC BY) license (http://creativecommons.org/licenses/by/4.0/).

viruses

MDPI

Review

Porcine Circovirus Type 2 (PCV2) Vaccines in the Context of Current Molecular Epidemiology

Anbu K. Karuppannan [1] and Tanja Opriessnig [1,2,*]

[1] Department of Veterinary Diagnostic and Production Animal Medicine, College of Veterinary Medicine, Iowa State University, Ames, IA 50011, USA; akkarup@iastate.edu

[2] The Roslin Institute and the Royal (Dick) School of Veterinary Studies, University of Edinburgh, Midlothian EH25 9RG, UK

* Correspondence: Tanja.Opriessnig@roslin.ed.ac.uk or tanjaopr@iastate.edu; Tel.: +44-0-131-651-9177

Academic Editors: Linda Dixon and Simon Graham
Received: 3 March 2017; Accepted: 28 April 2017; Published: 6 May 2017

Abstract: Porcine circovirus type 2 (PCV2) is an economically important swine pathogen and, although small, it has the highest evolution rate among DNA viruses. Since the discovery of PCV2 in the late 1990s, this minimalistic virus with a 1.7 kb single-stranded DNA genome and two indispensable genes has become one of the most important porcine pathogens, and presently is subjected to the highest volume of prophylactic intervention in the form of vaccines in global swine production. PCV2 can currently be divided into five different genotypes, PCV2a through PCV2e. It is well documented that PCV2 continues to evolve, which is reflected by changes in the prevalence of genotypes. During 2006, commercial vaccines for PCV2 were introduced on a large scale in a pig population mainly infected with PCV2b. Since 2012, the PCV2d genotype has essentially replaced the previously predominant PCV2b genotype in North America and similar trends are also documented in other geographic regions such as China and South Korea. This is the second major PCV2 genotype shift since the discovery of the virus. The potential increase in virulence of the emergent PCV2 genotype and the efficacy of the current vaccines derived from PCV2a genotype against the PCV2d genotype viruses has received considerable attention. This review attempts to synthesize the understanding of PCV2 biology, experimental studies on the antigenic variability, and molecular epidemiological analysis of the evolution of PCV2 genotypes.

Keywords: PCV2; epidemiology; pigs; vaccination

1. Introduction

Infectious disease plays an important role in pig production and prevention is often essential to minimize economic losses. Since the discovery of porcine circovirus type 2 (PCV2) in 1998 [1,2], this small, circular, non-enveloped DNA virus is recognized as one of the most important pathogens of the pig population worldwide. Porcine circovirus (PCV) was first observed as a contaminant in pig kidney cell line in 1974, and in 1982 the 17-nm single-stranded DNA virus with a circular genome was described in more detail [3,4]. The initial name of the virus, PCV, was changed to PCV type 1 (PCV1) in 1998 [5] to differentiate this non-pathogenic virus type from its pathogenic variant PCV2. For many years, PCV1 was considered widespread as antibodies to this virus were found in farmed pigs as well as wild boars, however, no disease association was noted [6,7]. A number of field surveys and experimental inoculations of PCV1 were reported from Canada, the UK and continental Europe, which all showed the absence of pathogenesis in pigs infected with PCV1. In the mid-1990s, the novel PCV2 with a restriction fragment length pattern (RFLP) of 422 was identified and subsequently associated with post-weaning multi-systemic wasting syndrome (PMWS) in Canada [1]. PMWS is characterized by poor weight gain, wasting and general symptoms such as dyspnea, pallor, diarrhea

and icterus [8]. These initial finding led to the almost simultaneous identification of PCV2 in diseased pigs in different geographical regions including North America, the UK and France [2]. All these viruses had more than 95% genetic similarity, but were different from PCV1 and hence were named PCV2 [5]. Subsequent studies on the prevalence of PCV2 in the wild pig population indicated its ubiquitous nature [9,10]. A picture of PCV2 as a pig pathogen commonly present in association with other viruses or bacteria became obvious [11,12]. Apart from PMWS, many PCV2 infection-associated clinical conditions such as respiratory symptoms, congenital tremors, enteritis, dermatitis, nephropathy and reproductive issues were described and later grouped as porcine circovirus-associated diseases (PCV-AD) in North America [13] and porcine circovirus diseases (PCVD) in Europe [14]. High PCV2 viremia and viral load in tissues, granulomatous inflammation, depletion of lymphocytes and dysfunction of the lymphoid system causing immunosuppression were characterized as the hallmarks of severe PCV2 infection [15–18]. Defying Koch's postulates, experimental reproduction of PCV-AD proved to be difficult and inconsistent and PCV2 was acknowledged, amidst skepticism, as necessary but not sufficient to elicit PCV-AD [12,19,20]. The importance of co-infection or at least a mitogenic trigger to host lymphocytes was understood to be an essential part of the development of severe PCV-AD [21,22]. Experimental co-infection of pigs with PCV2 along with other common swine pathogens consistently resulted in PMWS [12,23–26]. The first commercial vaccines became available in 2004 in Europe and in 2006 in North America, and have since received wide acceptance among pig farmers worldwide. The decrease in morbidity and improved production efficiency after the adoption of PCV2 vaccines unambiguously emphasized the adverse impact of PCV2 on the health of pigs [27]. PCV2 vaccines are now the single most-selling prophylactic agent in porcine husbandry. Besides clinical disease, the impact of sub-clinical infection of PCV2 on the health of farmed pigs and production parameters has been documented [28]. A wealth of knowledge of various aspects of PCV2 such as its evolution and phylogeny, immune response, interaction of viral proteins with host cellular proteins, and efficacy of its vaccines has been accumulated. This review will focus on the recent developments in antigenic variability, molecular epidemiology and diagnosis of PCV2 infections as well as current challenges in controlling PCV2 infections.

2. Virus Replication and Genes

The genome architecture of PCV1 and PCV2 is very minimalistic; among the seven predicted open reading frames (ORFs), only ORF1 and ORF2, which encode for the replicase (Rep) proteins and the capsid (Cap) protein, respectively, are indispensable for virus propagation [29,30]. The ORF1 gene, essential for the replication of the circoviral genome, is present on the sense strand of the encapsulated single-stranded DNA (ssDNA) genome and produces several splice variants of which Rep and Rep' are the largest [31–34]. The genome of PCV2 has a conserved stem loop structure present in diverse ssDNA viruses that infect eukaryotes [35]. The Rep and Rep' proteins bind to a octanucleotide motif on the genome, near the stem loop structure present proximal to the ORF1 gene, and mediates the genome replication through their nicking and joining enzymatic activity [33,36,37]. However, the Rep proteins do not have any polymerase activity and recruit host DNA polymerases and factors, expressed by host cells during the S-phase of cell cycle, to mediate PCV genome replication by rolling circle replication mechanism [38,39]. The ORF2 gene of PCV2 is transcribed from the complimentary strand in the replicative form of the virus to produce a 233 amino acid capsid protein [32,40,41]. PCV1 and PCV2 are icosahedral virions without envelope, and 60 capsomeres form the virus. Porcine circoviruses are thought to have originated from a recombination event between a plant nanovirus and an animal picornavirus, deduced by the conserved stem loop structure at the origin of replication of circovirus and the homology of Rep proteins [42,43].

Despite its minimalistic design, the search for a specific genetic determinant of pathogenicity or virulence of PCV2 has been elusive. Chimeric viruses with ORF1 from the nonpathogenic PCV1 and ORF2 from the pathogenic PCV2 are not pathogenic and elicit protective immune response against a subsequent challenge with PCV2 [44–47]. The ORF3 gene, encoded on the antisense strand of the PCV2

genome, potentially encodes a 105-amino acid protein implicated in inducing apoptosis of infected cells and has been ascribed to have a role in PCV2 pathogenesis amidst opposing views [48–51]. Recently, an interesting study has depicted latent and productive PCV2 infection in the corticomedullary junction of the thymus, leading to the dysregulation of T cell maturation [52]. The study suggests that early life PCV2 infection of the thymus could lead to the recognition of PCV2 as self, later leading to a negative selection of PCV2-specific T cells. In addition, the study also suggests the development of adaptive tolerance in peripheral T cells to PCV2 antigens. Overall, the role of the capsid protein in enhancing the fitness of PCV2 replication at the cellular level and the spread of the virus in the host population, with widespread preexisting seroconversion against PCV2, is arguably an important factor in determining the pathogenicity and virulence of the virus. Experimental evidence shows that subtle changes in the PCV2 capsid protein can increase its fitness at the cellular level and increase its virulence in infected pigs [53,54]. Recent field observations have brought the role of the capsid protein in the molecular epidemiology of PCV2 into light [55–59].

3. Molecular Epidemiology

Analysis of PCV1 and PCV2 evolutionary trends estimates the time to most recent common ancestor (TMRCA) approximately to the later part of the nineteenth century or the beginning of the twentieth century, as well as subsequent independent evolution in spite of co-circulation [55–60]. A convention on the sub-classification of PCV2 into genotypes was accepted in 2008 based on the then prevalent diversity in the ORF2 nucleotide and a p-distance of 0.035, which was the criteria used to delineate the PCV2 genotypes [61]. To date, studies of PCV2 genomes based on the above criteria identify three major genotypes; PCV2a, PCV2b and PCV2d, and two genotypes; PCV2c and PCV2e, with low prevalence [55,58,62–65]. Examination of archived tissue revealed that PCV2 was circulating among domesticated pigs as early as the 1960s in the US and Germany, the 1970s in Northern Ireland and Switzerland, and from 1980s in the UK and Denmark [53,66–69]. Since its discovery, two major changes in the prevalence of circulating genotypes of PCV2 have been observed, which are described as "genotype shifts" [55]. The prevalent PCV2a genotype was replaced by the PCV2b genotype in the mid-2000s, with a purported increase in virulence [55,57,70–72]. In recent years, the PCV2d genotype (earlier known as mutant PCV2b) has been increasing in prevalence in major pork producing areas, including the United States, Europe, China, Korea and South America [55,56,58,73]. It is interesting that the first genotype shift slightly predates the widespread vaccination against PCV2, while the recent genotype shift is noticed in the presence of widespread vaccination. The PCV2 is recognized for its estimated evolutionary rate of 1.2×10^{-3} substitutions/site/year, the highest among comparable DNA viruses [58,60,74]. It should be noted that ORF2 has a higher rate of evolution than the whole genome of PCV2 [58,65], which could be due to the constraints imposed by deleterious mutations in the ORF1 gene with its alternately spliced variants. Interestingly, the evolutionary rate for PCV1, which displays very low genetic diversity, is estimated to be around 1.15×10^{-5} substitutions/site/year [75]. Studies to estimate the putative temporal origin of the major PCV2 genotypes are summarized in Table 1.

Table 1. Estimated time of origin of the main porcine circovirus type 2 (PCV2) genotypes and earliest specimen retrieved.

Genotype	Estimated Time of Divergence (Reference)	Earliest Archived Tissue Identification
PCV2a	1966 (1945–1983) [60] 1964 (1948–1974) [55]	1962 [68]
PCV2b	1989 (1980–1995) [60] 1973 (1952–1996) [55]	1979 [69]
PCV2d	1986 (1971–1996) [58]	Genbank Accession Number JX512856, 1999 from a healthy herd [52,58]

Global trade in breeding pigs, semen and pork products have contributed to the worldwide dissemination of PCV2 [55,60] to the extent that PCV2c, for long considered to be confined to Denmark,

and PCV2d, thought to be a newly divergent genotype, have been isolated in wild boars in the Brazilian Pantanal [76] and are speculated to have be transmitted to the wild boars by peccaries, which are also documented to harbor the PCV2 virus [77].

The patterns in PCV2 genome evolution could have been driven by factors such as natural mutational bias, restraints on genetic variability owing to the topology of its transcripts and genes in overlapping arrangements [34,40,41], evolution for enhanced replication and transmission fitness at the cellular level [53,54], and evolution under immune selective pressure [59,74], either natural or vaccine-induced [78]. As a related point of much practical implications, some reports indicate that the virulence of the different genotypes is similar, while others contend this view [79–82]. Isolation of recombinant PCV2 genomes, which must have arisen from co-infecting PCV2 genotypes, is a common event in domestic pigs and wild boars [55,83–86]. Interestingly, recombination breakpoints are found more frequently in the intergenic regions and to a lesser extent in the ORF1 and ORF2 genes. The ORF2 encoded capsid protein is the primary target for the immune system, hence it is naturally under selective pressure from the immune system, as observed by the higher rate of mutation in this gene [58,61]. The case for PCV2 evolution under vaccine pressure, discussed in the next section, is made by comparing the ORF2 amino acid content of PCV2 isolates from pig populations prior to and after the introduction of vaccines, and also by comparing the isolates from unvaccinated farmed pigs, wild boars, and free ranging pigs [74,87–89]. The latter comparison is potentially confounded by limited dataset owing to the scarcity of farms not vaccinating against PCV2 and the free transmission of PCV2 from vaccinated pigs and unvaccinated pigs [74].

4. PCV2 Vaccines

The main commercial vaccines available to date are derived from the PCV2a genotype or its capsid protein [13], and are acknowledged as highly successful in decreasing the disease burden found prior to the introduction of the vaccine. The current vaccines are efficient in inducing humoral and cell-mediated immunity against PCV2 [90–92]. In North America, the PCV2a genotype has gradually been replaced by the PCV2b genotype since 2005 [72], followed by the recent replacement of the PCV2b genotype by the PCV2d genotype as the most prevalent [59]. Despite the health benefits and production parameter improvements associated with the current PCV2 vaccines and its almost universal use in the United States, PCV2 infection is yet widespread among the vaccinated population. An epidemiological study of serum and tissue samples in 2012 showed 7.7% positive for PCV2a and 8.4% positive for PCV2b viral DNA [89], and approximately one in four pigs showed detectable PCV2 viremia, with a break up of 11.3% PCV2a, 29% PCV2b and 71.8% PCV2d, in a recently published study [59]. Another recent study reports a decrease in the prevalence and viremia level of PCV2a and PCV2b in field pig serum collected from 12 states in the United States in 2012 compared to data from the pre-vaccination period of 2006 [93], indicating that vaccines are effective in controlling the virus load in individual pigs and the PCV2 prevalence on a per site basis. The distribution of PCV2 genotypes continues to evolve in the vaccinated population, as reflected by the change in genotype prevalence to PCV2d [59]. Concurrent infection with PCV2a and PCV2b genotypes is thought to be a potentiating factor in the development of clinical disease and PCV-AD cases, with concurrent PCV2a and PCV2b infections also being observed in the field [94].

The immuno-dominant epitopes on the 233 amino acid capsid protein of PCV2, recognized by antibodies from PCV2-infected pigs, are characterized into distinct A, B, C and D regions, which approximately correspond to amino acid segments 65–87, 113–139, 169–183 and few C-terminal amino acids, respectively [95,96]. Signature motifs on the capsid protein can distinguish between PCV2 genotypes, with the emerging PCV2d genotype harboring an extra lysine residue at the C-terminal end at position 234, and PCV2e coding for 238 amino acids with an additional five amino acids at the C-terminal end [59,97]. The characterization of the atomic structure of the PCV2 virus enabled a better understanding of the previously deduced antigenic domains of the viral capsid protein [98]. The immuno-dominant region spanning amino acids 163–180 in the capsid protein of PCV2 is

implicated to function as a decoy epitope, resulting in the production of non-neutralizing antibodies against PCV2 [82,99]. Non-neutralizing antibodies against this epitope region were not elicited by PCV2 vaccines but found in serum from PCV-AD-diagnosed pigs, and this epitope has been suggested as a basis to develop serological assays to predict the protective capacity of antibody response against PCV2. Another study demonstrated the existence of antigenic differences in the virus particle structure between PCV2 genotypes, utilizing panels of neutralizing mouse monoclonal antibodies against epitopes in the capsid [100]. The variation of a single amino acid between PCV2a and PCV2b was able to abolish the neutralizing activity of a monoclonal antibody against the PCV2b genotype [101], and a similar effect was observed in another study [102]. These findings highlight the potential of minor variations in the capsid protein that can cumulatively lead to escape from a vaccine-induced immune response. In line with this, PCV2d, which varies from PCV2a by 23 amino acids, most of which fall in or near the epitope A and the decoy epitope regions, was isolated in many apparent vaccine failure cases worldwide [103–107]. Variations in PCV2d capsid protein were found in the conformational epitope regions, loop BC (epitope A) and loop CT, by in silico analysis, and are thought to cause changes in the antigenic structure on the viral surface, enabling improved binding of the PCV2d virus to the host cell and enabling it to escape preexisting immunity [108]. Earlier experimental evidence also showed that the C-terminal epitope D, which is located on the viral surface, is a target for neutralizing antibodies and, interestingly, the PCV2d genotype has an extra lysine residue at its very C-terminal end [95]. Assuming proper vaccination practices are followed in every instance, the current predominant prevalence of PCV2d, which is estimated to have diverged before the introduction of widespread PCV2 vaccines, could potentially reflect the lack of a thorough immunological protection against this genotype by current vaccines. Molecular epidemiological studies to analyze the evolution of PCV2 strains under vaccine pressure have surmised that the capsid protein amino acids in field isolates display divergence from the antigenic determinants in the PCV2a-based vaccine strains, clearly in the case of PCV2a and less so in the case of PCV2b and PCV2d [74,87,88]. These studies also show that the PCV2 population is shrinking in genetic diversity after the introduction of vaccines, mirroring their decrease in prevalence. However, controlled experimental studies and field trials show that PCV2a-based vaccines and a PCV2b-based vaccine confer adequate cross protection against clinical disease upon challenge with PCV2a, PCV2b and PCV2d genotype viruses and improve average daily weight gain [104,109–115]. These observations show that the current vaccines are adequate in preventing clinical disease in most instances; however, they may represent a "leaky vaccine" situation. This is a terminology used in the field of vaccinology to refer to vaccines which tend to decrease the transmission rate and infection rate on a per exposure basis, such as in a vaccine trial or in the presence of good biosecurity, but may not confer protection under conditions of repeated exposure and the influence of other cofactors [116]. Therefore, current vaccines may be able to minimize PCV2d replication but not abolish it. Experimental evidence from controlled studies also suggest that a homologous vaccine for PCV2b may be better than a heterologous vaccine in decreasing the viremia after concurrent PCV2a and PCV2b challenge, even if both vaccines prevent the development of lesions [78]. Similar differential viremia or viral shedding upon heterologous genotype challenge following PCV2a- or PCV2b-based vaccination has also been recorded in other studies, which are summarized in Table 2 [109,117].

The current situation warrants more long-term experimentation with homologous vs heterologous PCV2 vaccines and even multi-genotype vaccines with an aim to simultaneously control the emergence of the PCV2d genotype and the reemergence of PCV2a and PCV2b genotypes.

Table 2. Comparison of viral load inhibition by heterologous PCV2 genotype vaccines.

Study No.	Vaccine Genotype	Challenge Genotype	Co-Infecting Agent, If Any	Comments on Viremia
1	PCV2b	PCV2a PCV2b	None None	Viral load in lymph nodes of vaccinated pigs at 21 days after challenge with PCV2a was higher compared to pigs challenged with PCV2b (statistical significance not known) [109]
2	PCV2a PCV2b	PCV2b	PRRSV, PPV	Compared to unvaccinated control pigs, the inhibition of serum viral load after challenge was 25% with the PCV2a vaccine and 100% with the PCV2b vaccine [78]
3	PCV2a PCV2d	PCV2d	PRRSV	92.2% inhibition of serum viral load with a PCV2a vaccine and 100% inhibition of serum viral load with a PCV2d vaccine on day 49 after challenge [113]
4	PCV2a	PCV2b	None	Vaccinated challenged and vaccinated contact pigs displayed approximately one log decrease in viral load; however, the viral load was higher than 10^4 genome copies per mL of serum until 42 days after inoculation [115]
5	PCV2b PCV2d	PCV2b	None	One out of the five pigs vaccinated with a PCV2d vaccine displayed detectable viral load at 21 days after challenge, compared to none in the PCV2b vaccine group [118]
6	PCV2a	PCV2d	None	Viral load after PCV2d challenge was reduced by one log or more in vaccinated pigs; however, serum viremia and shedding of virus were observed at 21 days after challenge in vaccinated pigs [110]

PRRSV: Porcine reproductive and respiratory syndrome virus; PPV: Porcine parvovirus.

Notable among recent efforts in improving the current vaccines against PCV2 is the development of marker vaccines, which will allow the differentiation of infected and vaccinated pigs, with engineered foreign epitopes at the C-terminal end of the capsid protein and vaccines incorporating the PCV2b capsid protein [70,109,119]. A recent novel vaccine candidate, probably the most innovative PCV2 vaccine candidate yet, was developed by the molecular breeding of ORF2 genes of many PCV2 genotypes and the creation of a mosaic ORF2 gene with 234 amino acids which was cloned into the backbone of PCV1 ORF1 [120]. The selected chimeric virus candidate in this study, PCV1-3cl14, displayed wide heterologous immune response and conferred good protection upon heterologous challenge [120]. However, this study lacks information on how the novel chimeric vaccine candidate compares with other commercial and experimental PCV2a or PCV2b vaccines in eliciting neutralizing antibody response and the prevention of viremia and lesions. In addition, further experiments in this direction, perhaps with a directed engineering of a mosaic virus instead of the traditional random molecular breeding approach, used in the above study, would be very interesting. An improvement of current models of vaccine evaluation strategies, similar to the views of Ragonnet et al. [121], should also be seriously considered in light of factors such as the enzootic nature of PCV2, concurrent multi genotype infections, other immuno-suppressing co-infections such as porcine reproductive and respiratory syndrome virus (PRRSV), classical swine fever virus (CSFV) and the presence of feral and wild reservoirs. The reservoir population is a niche where PCV2 diversification could be still ongoing without vaccine-induced immune pressure. Many other factors which may influence the efficacy of a vaccine such as host genetics, inherent difference among the commercial vaccines, time and frequency of vaccine administration, and interference from maternal antibodies are not commented upon here [119,122].

5. Diagnosis

Diagnosis of PCV2 as the principal etiology of disease has been centered on the detection of hallmark histopathological lesions of histiocytic infiltration, lymphoid depletion and associated PCV2 antigens/PCV2 genome [13]. Analysis of histological sections for the amount and distribution of PCV2 in suspected tissues by immunohistochemistry and in situ hybridization is considered the gold standard for a diagnosis of PCV-AD. Currently, many commercial enzyme-linked immunosorbent assay (ELISA) kits to detect PCV2 antigens and PCV2-specific antibodies are available and routinely utilized in diagnostic labs. The ELISAs to detect antibodies against PCV2 are of two types, indirect

ELISAs and competitive blocking ELISAs [13]. Prior to the advent of these kits, immunofluorescence assay and immune peroxidase monolayer assay were widely used to detect PCV2-specific antibodies and to identify infective PCV2 viruses [13]. Serological assays to detect PCV2-specific antibodies have been adapted to various platforms including microbead-based assays such as Luminex, which allow for the detection of antibodies against other pathogens simultaneously [123]. As PCV2 infection is considered ubiquitous, and since most pigs are vaccinated against PCV2 at an early age, majority of the farmed pigs in developed countries have antibodies against PCV2.

Neutralization assay to detect PCV2-specific antibodies is a technique of high utility, but it is prolonged and laborious and requires fluorescent labelled antibodies and a cell culture capable laboratory to perform the assay. For the routine and rapid diagnosis of samples, conventional polymerase chain reaction (PCR) assays followed by RFLP is helpful. The discovery of PCV2 as a pathogen, and that of PCV2b as an emergent genotype, were triggered by variations in RFLP patterns [1,72]. The latter was a change from RFLP type 422 to RFLP type 321. PCR followed by Sanger sequencing has greatly contributed to the accumulation of the current wealth of knowledge on the molecular epidemiology of PCV2. However, similar to seroconversion to PCV2, the ubiquitous and enzootic nature of PCV2 makes this assay redundant in the current setting. The PCR assay has been superseded by quantitative PCR (qPCR) assays to estimate the viral genome copy numbers as a measure of the viral load in body fluids and tissue samples. The qPCR is of high utility in detecting the etiology during laboratory disease investigation, especially in cases of reproductive failure where the viral load in fetuses is a very useful indicator. Another variation of this technique is based on fluorescent probe-based PCRs, such as Taqman probes, which enable to specifically detect PCV2 genotypes and also allow for the detection of multiple genotypes of PCV2 and other pathogens in a single reaction. Automated sample processing and fluorescent probe-based PCR assays have revolutionized the diagnostic capacity and information available to investigate clinical cases. Unlike PCR-based assays, which need prior sequence information and primers, next generation sequencing techniques (NGS) have made it possible to obtain information on PCV2 molecular epidemiology along with co-infecting pathogens and also have enabled the unmasking of any potential associations not hitherto known. The PCV2 research community is yet to catch up with this technology, reflected by the scarcity of reports in the public domain utilizing this technique [87].

In light of the current scenario, where the genotype prevalence switch from PCV2b to PCV2d is thought to be occurring worldwide, it is important to develop assays capable of detecting and measuring changes in the immune response. ELISA-based assays to differentially identify the genotype of infecting PCV2 would be of high utility. Current methods of utilizing sequence information to study the molecular epidemiology do not enable the direct understanding of changes in immunological parameters of the emerging genotype(s). Developing serological assays to study changes in the neutralization profiles in the serum of PCV2 infected or vaccinated pigs, such as immune response against the decoy epitope [82], is essential. Utilization of PEPSCAN, phage display or protein array-based serological assays at a sufficient resolution to quantify immune response against specific epitopes of the PCV2 capsid protein could improve our understanding of the interplay between different PCV2 vaccines and genotypes [74,95,96,108]. Development of competitive blocking ELISA with panels of specific peptide epitopes from the capsid protein of different PCV2 genotypes and complimentary monoclonal antibodies would enable precise monitoring of the shifts in epitope-specific immune responses. Accumulation of more knowledge on neutralization profiles of the different PCV2 genotype capsids will help this effort. Establishment of a dedicated, peer-reviewed, curated database for PCV2, similar to the PRRSV and influenza virus databases, is essential to bolster the efforts of the PCV2 research community.

6. Conclusions

PCV2 made a dramatic appearance towards the end of last century and soon became recognized as the most important pig pathogen, which was followed by the rapid development of successful vaccines,

utilizing multiple approaches ranging from inactivated PCV2 vaccines to baculovirus expressed recombinant capsid protein-based vaccines. Until a few years ago, PCV2 was considered a successfully controlled emergent pathogen. However, the worldwide second genotype shift to PCV2d and a debated increase in associated virulence and vaccine failures has raised alarm. As a biological problem, PCV2 is a fascinating puzzle of minimal dimensions, which is not yet completely unraveled. Unambiguously deciphering its molecular evolution and epidemiology is a daunting task, given its ubiquitous nature and expanding genetic spectrum. Understanding the forces behind the emergence of PCV2d as the most prevalent genotype is of prime importance. The recent report of porcine circovirus 3 (PCV3) in the US [124,125], with a 2000 bp genome, is probably an indication of the plasticity of the circoviral genomes. The use of vaccines in PCV2 is perhaps one of biggest success stories in veterinary vaccines; however, it is clear that vaccines are no replacement for good biosecurity programs in intensive pig husbandry.

Acknowledgments: Funding was provided by the Biotechnology and Biological Sciences Research Council (BBSRC) Institute Strategic Programme Grant awarded to the Roslin Institute (BB/J004324/1; BBS/E/D/20241864).

Conflicts of Interest: None of the authors of this paper has a financial or personal relationship with other people or organizations that could inappropriately influence or bias the content of the paper.

References

1. Nayar, G.P.; Hamel, A.; Lin, L. Detection and characterization of porcine circovirus associated with postweaning multisystemic wasting syndrome in pigs. *Can. Vet. J.* **1997**, *38*, 385–386. [PubMed]
2. Allan, G.M.; McNeilly, F.; Kennedy, S.; Daft, B.; Clarke, E.G.; Ellis, J.A.; Haines, D.M.; Meehan, B.M.; Adair, B.M. Isolation of porcine circovirus-like viruses from pigs with a wasting disease in the USA and europe. *J. Vet. Diagn. Investig.* **1998**, *10*, 3–10. [CrossRef] [PubMed]
3. Tischer, I.; Gelderblom, H.; Vettermann, W.; Koch, M.A. A very small porcine virus with circular single-stranded DNA. *Nature* **1982**, *295*, 64–66. [CrossRef] [PubMed]
4. Tischer, I.; Rasch, R.; Tochtermann, G. Characterization of papovavirus-and picornavirus-like particles in permanent pig kidney cell lines. *Zentralbl. Bakteriol. Orig. A* **1974**, *226*, 153–167. [PubMed]
5. Meehan, B.M.; McNeilly, F.; Todd, D.; Kennedy, S.; Jewhurst, V.A.; Ellis, J.A.; Hassard, L.E.; Clark, E.G.; Haines, D.M.; Allan, G.M. Characterization of novel circovirus DNAs associated with wasting syndromes in pigs. *J. Gen. Virol.* **1998**, *79*, 2171–2179. [CrossRef] [PubMed]
6. Allan, G.M.; McNeilly, F.; Cassidy, J.P.; Reilly, G.A.; Adair, B.; Ellis, W.A.; McNulty, M.S. Pathogenesis of porcine circovirus; experimental infections of colostrum deprived piglets and examination of pig foetal material. *Vet. Microbiol.* **1995**, *44*, 49–64. [CrossRef]
7. Tischer, I.; Bode, L.; Peters, D.; Pociuli, S.; Germann, B. Distribution of antibodies to porcine circovirus in swine populations of different breeding farms. *Arch. Virol.* **1995**, *140*, 737–743. [CrossRef] [PubMed]
8. Harding, J.C.S.; Clark, E.G. Recognizing and diagnosing postweaning multisystemic wasting syndrome (PMWS). *Swine Health Prod.* **1997**, *5*, 201–203.
9. Schulze, C.; Neumann, G.; Grutze, I.; Engelhardt, A.; Mirle, C.; Ehlert, F.; Hlinak, A. Case report: Porcine circovirus type 2 infection in an European wild boar (*Sus scrofa*) in the state of Brandenburg, Germany. *Dtsch. Tierarztl. Wochenschr.* **2003**, *110*, 426–428. (In German). [PubMed]
10. Vicente, J.; Segales, J.; Hofle, U.; Balasch, M.; Plana-Duran, J.; Domingo, M.; Gortazar, C. Epidemiological study on porcine circovirus type 2 (PCV2) infection in the European wild boar (*Sus scrofa*). *Vet. Res.* **2004**, *35*, 243–253. [CrossRef] [PubMed]
11. Ellis, J.A.; Bratanich, A.; Clark, E.G.; Allan, G.; Meehan, B.; Haines, D.M.; Harding, J.; West, K.H.; Krakowka, S.; Konoby, C.; et al. Coinfection by porcine circoviruses and porcine parvovirus in pigs with naturally acquired postweaning multisystemic wasting syndrome. *J. Vet. Diagn. Investig.* **2000**, *12*, 21–27. [CrossRef] [PubMed]
12. Krakowka, S.; Ellis, J.A.; Meehan, B.; Kennedy, S.; McNeilly, F.; Allan, G. Viral wasting syndrome of swine: Experimental reproduction of postweaning multisystemic wasting syndrome in gnotobiotic swine by coinfection with porcine circovirus 2 and porcine parvovirus. *Vet. Pathol.* **2000**, *37*, 254–263. [CrossRef] [PubMed]

13. Opriessnig, T.; Meng, X.J.; Halbur, P.G. Porcine circovirus type 2 associated disease: Update on current terminology, clinical manifestations, pathogenesis, diagnosis, and intervention strategies. *J. Vet. Diagn. Investig.* **2007**, *19*, 591–615. [CrossRef] [PubMed]
14. Segales, J.; Allan, G.M.; Domingo, M. Porcine circovirus diseases. *Anim. Health Res. Rev.* **2005**, *6*, 119–142. [CrossRef] [PubMed]
15. Darwich, L.; Segales, J.; Domingo, M.; Mateu, E. Changes in $CD4^+$, $CD8^+$, $CD4^+$ $CD8^+$, and immunoglobulin M-positive peripheral blood mononuclear cells of postweaning multisystemic wasting syndrome-affected pigs and age-matched uninfected wasted and healthy pigs correlate with lesions and porcine circovirus type 2 load in lymphoid tissues. *Clin. Diagn. Lab. Immunol.* **2002**, *9*, 236–242. [PubMed]
16. Krakowka, S.; Ellis, J.A.; McNeilly, F.; Gilpin, D.; Meehan, B.; McCullough, K.; Allan, G. Immunologic features of porcine circovirus type 2 infection. *Viral. Immunol.* **2002**, *15*, 567–582. [CrossRef] [PubMed]
17. Rosell, C.; Segales, J.; Plana-Duran, J.; Balasch, M.; Rodriguez-Arrioja, G.M.; Kennedy, S.; Allan, G.M.; McNeilly, F.; Latimer, K.S.; Domingo, M. Pathological, immunohistochemical, and in-situ hybridization studies of natural cases of postweaning multisystemic wasting syndrome (PMWS) in pigs. *J. Comp. Pathol.* **1999**, *120*, 59–78. [CrossRef] [PubMed]
18. Segales, J.; Domingo, M.; Chianini, F.; Majo, N.; Dominguez, J.; Darwich, L.; Mateu, E. Immunosuppression in postweaning multisystemic wasting syndrome affected pigs. *Vet. Microbiol.* **2004**, *98*, 151–158. [CrossRef] [PubMed]
19. Albina, E.; Truong, C.; Hutet, E.; Blanchard, P.; Cariolet, R.; L'Hospitalier, R.; Mahe, D.; Allee, C.; Morvan, H.; Amenna, N.; et al. An experimental model for post-weaning multisystemic wasting syndrome (PMWS) in growing piglets. *J. Comp. Pathol.* **2001**, *125*, 292–303. [CrossRef] [PubMed]
20. Allan, G.M.; Kennedy, S.; McNeilly, F.; Foster, J.C.; Ellis, J.A.; Krakowka, S.J.; Meehan, B.M.; Adair, B.M. Experimental reproduction of severe wasting disease by co-infection of pigs with porcine circovirus and porcine parvovirus. *J. Comp. Pathol.* **1999**, *121*, 1–11. [CrossRef] [PubMed]
21. Darwich, L.; Segales, J.; Mateu, E. Pathogenesis of postweaning multisystemic wasting syndrome caused by porcine circovirus 2: An immune riddle. *Arch. Virol.* **2004**, *149*, 857–874. [CrossRef] [PubMed]
22. Krakowka, S.; Ellis, J.A.; McNeilly, F.; Ringler, S.; Rings, D.M.; Allan, G. Activation of the immune system is the pivotal event in the production of wasting disease in pigs infected with porcine circovirus-2 (PCV-2). *Vet. Pathol.* **2001**, *38*, 31–42. [CrossRef] [PubMed]
23. Opriessnig, T.; Fenaux, M.; Yu, S.; Evans, R.B.; Cavanaugh, D.; Gallup, J.M.; Pallares, F.J.; Thacker, E.L.; Lager, K.M.; Meng, X.J.; et al. Effect of porcine parvovirus vaccination on the development of PMWS in segregated early weaned pigs coinfected with type 2 porcine circovirus and porcine parvovirus. *Vet. Microbiol.* **2004**, *98*, 209–220. [CrossRef] [PubMed]
24. Harms, P.A.; Sorden, S.D.; Halbur, P.G.; Bolin, S.R.; Lager, K.M.; Morozov, I.; Paul, P.S. Experimental reproduction of severe disease in CD/CD pigs concurrently infected with type 2 porcine circovirus and porcine reproductive and respiratory syndrome virus. *Vet. Pathol.* **2001**, *38*, 528–539. [CrossRef] [PubMed]
25. Opriessnig, T.; Madson, D.M.; Roof, M.; Layton, S.M.; Ramamoorthy, S.; Meng, X.J.; Halbur, P.G. Experimental reproduction of porcine circovirus type 2 (PCV2)-associated enteritis in pigs infected with PCV2 alone or concurrently with lawsonia intracellularis or salmonella typhimurium. *J. Comp. Pathol.* **2011**, *145*, 261–270. [CrossRef] [PubMed]
26. Opriessnig, T.; Halbur, P.G. Concurrent infections are important for expression of porcine circovirus associated disease. *Virus Res.* **2012**, *164*, 20–32. [CrossRef] [PubMed]
27. Ellis, J. Porcine circovirus. *Vet. Pathol.* **2014**, *51*, 315–327. [CrossRef] [PubMed]
28. Alarcon, P.; Rushton, J.; Wieland, B. Cost of post-weaning multi-systemic wasting syndrome and porcine circovirus type-2 subclinical infection in England—An economic disease model. *Prev. Vet. Med.* **2013**, *110*, 88–102. [CrossRef] [PubMed]
29. Hamel, A.L.; Lin, L.L.; Nayar, G.S. Nucleotide sequence of porcine circovirus associated with postweaning multisystemic wasting syndrome in pigs. *J. Virol.* **1998**, *72*, 5262–5267. [PubMed]
30. Mankertz, A.; Mankertz, J.; Wolf, K.; Buhk, H.J. Identification of a protein essential for replication of porcine circovirus. *J. Gen. Virol.* **1998**, *79*, 381–384. [CrossRef] [PubMed]
31. Mankertz, A.; Persson, F.; Mankertz, J.; Blaess, G.; Buhk, H.J. Mapping and characterization of the origin of DNA replication of porcine circovirus. *J. Virol.* **1997**, *71*, 2562–2566. [PubMed]

32. Mankertz, J.; Buhk, H.J.; Blaess, G.; Mankertz, A. Transcription analysis of porcine circovirus (PCV). *Virus Genes* **1998**, *16*, 267–276. [CrossRef] [PubMed]
33. Steinfeldt, T.; Finsterbusch, T.; Mankertz, A. Rep and rep' protein of porcine circovirus type 1 bind to the origin of replication in vitro. *Virology* **2001**, *291*, 152–160. [CrossRef] [PubMed]
34. Cheung, A.K. The essential and nonessential transcription units for viral protein synthesis and DNA replication of porcine circovirus type 2. *Virology* **2003**, *313*, 452–459. [CrossRef]
35. Rosario, K.; Duffy, S.; Breitbart, M. A field guide to eukaryotic circular single-stranded DNA viruses: Insights gained from metagenomics. *Arch. Virol.* **2012**, *157*, 1851–1871. [CrossRef] [PubMed]
36. Steinfeldt, T.; Finsterbusch, T.; Mankertz, A. Demonstration of nicking/joining activity at the origin of DNA replication associated with the rep and rep' proteins of porcine circovirus type 1. *J. Virol.* **2006**, *80*, 6225–6234. [CrossRef] [PubMed]
37. Cheung, A.K. Identification of an octanucleotide motif sequence essential for viral protein, DNA, and progeny virus biosynthesis at the origin of DNA replication of porcine circovirus type 2. *Virology* **2004**, *324*, 28–36. [CrossRef] [PubMed]
38. Gassmann, M.; Focher, F.; Buhk, H.J.; Ferrari, E.; Spadari, S.; Hubscher, U. Replication of single-stranded porcine circovirus DNA by DNA polymerases alpha and delta. *Biochim. Biophys. Acta* **1988**, *951*, 280–289. [CrossRef]
39. Cheung, A.K. Rolling-circle replication of an animal circovirus genome in a theta-replicating bacterial plasmid in *Escherichia coli*. *J. Virol.* **2006**, *80*, 8686–8694. [CrossRef] [PubMed]
40. Cheung, A.K. Comparative analysis of the transcriptional patterns of pathogenic and nonpathogenic porcine circoviruses. *Virology* **2003**, *310*, 41–49. [CrossRef]
41. Cheung, A.K. Transcriptional analysis of porcine circovirus type 2. *Virology* **2003**, *305*, 168–180. [CrossRef] [PubMed]
42. Gibbs, M.J.; Weiller, G.F. Evidence that a plant virus switched hosts to infect a vertebrate and then recombined with a vertebrate-infecting virus. *Proc. Natl. Acad. Sci. USA* **1999**, *96*, 8022–8027. [CrossRef] [PubMed]
43. Meehan, B.M.; Creelan, J.L.; McNulty, M.S.; Todd, D. Sequence of porcine circovirus DNA: Affinities with plant circoviruses. *J. Gen. Virol.* **1997**, *78*, 221–227. [CrossRef] [PubMed]
44. Fenaux, M.; Opriessnig, T.; Halbur, P.G.; Elvinger, F.; Meng, X.J. A chimeric porcine circovirus (PCV) with the immunogenic capsid gene of the pathogenic PCV type 2 (PCV2) cloned into the genomic backbone of the nonpathogenic PCV1 induces protective immunity against PCV2 infection in pigs. *J. Virol.* **2004**, *78*, 6297–6303. [CrossRef] [PubMed]
45. Fenaux, M.; Opriessnig, T.; Halbur, P.G.; Meng, X.J. Immunogenicity and pathogenicity of chimeric infectious DNA clones of pathogenic porcine circovirus type 2 (PCV2) and nonpathogenic PCV1 in weanling pigs. *J. Virol.* **2003**, *77*, 11232–11243. [CrossRef] [PubMed]
46. Gillespie, J.; Juhan, N.M.; DiCristina, J.; Key, K.F.; Ramamoorthy, S.; Meng, X.J. A genetically engineered chimeric vaccine against porcine circovirus type 2 (PCV2) is genetically stable in vitro and in vivo. *Vaccine* **2008**, *26*, 4231–4236. [CrossRef] [PubMed]
47. Hemann, M.; Beach, N.M.; Meng, X.J.; Halbur, P.G.; Opriessnig, T. Vaccination with inactivated or live-attenuated chimeric PCV1–2 results in decreased viremia in challenge-exposed pigs and may reduce transmission of PCV2. *Vet. Microbiol.* **2012**, *158*, 180–186. [CrossRef] [PubMed]
48. Chaiyakul, M.; Hsu, K.; Dardari, R.; Marshall, F.; Czub, M. Cytotoxicity of ORF3 proteins from a nonpathogenic and a pathogenic porcine circovirus. *J. Virol.* **2010**, *84*, 11440–11447. [CrossRef] [PubMed]
49. Juhan, N.M.; LeRoith, T.; Opriessnig, T.; Meng, X.J. The open reading frame 3 (ORF3) of porcine circovirus type 2 (PCV2) is dispensable for virus infection but evidence of reduced pathogenicity is limited in pigs infected by an ORF3-null PCV2 mutant. *Virus Res.* **2010**, *147*, 60–66. [CrossRef] [PubMed]
50. Karuppannan, A.K.; Jong, M.H.; Lee, S.H.; Zhu, Y.; Selvaraj, M.; Lau, J.; Jia, Q.; Kwang, J. Attenuation of porcine circovirus 2 in spf piglets by abrogation of ORF3 function. *Virology* **2009**, *383*, 338–347. [CrossRef] [PubMed]
51. Liu, J.; Chen, I.; Du, Q.; Chua, H.; Kwang, J. The orf3 protein of porcine circovirus type 2 is involved in viral pathogenesis in vivo. *J. Virol.* **2006**, *80*, 5065–5073. [CrossRef] [PubMed]

52. Klausmann, S.; Sydler, T.; Summerfield, A.; Lewis, F.I.; Weilenmann, R.; Sidler, X.; Brugnera, E. T-cell reprogramming through targeted CD4-coreceptor and T-cell receptor expression on maturing thymocytes by latent *Circoviridae* family member porcine circovirus type 2 cell infections in the thymus. *Emerg. Microbes Infect.* **2015**, *4*, e15. [CrossRef] [PubMed]
53. Krakowka, S.; Allan, G.; Ellis, J.; Hamberg, A.; Charreyre, C.; Kaufmann, E.; Brooks, C.; Meehan, B. A nine-base nucleotide sequence in the porcine circovirus type 2 (PCV2) nucleocapsid gene determines viral replication and virulence. *Virus Res.* **2012**, *164*, 90–99. [CrossRef] [PubMed]
54. Fenaux, M.; Opriessnig, T.; Halbur, P.G.; Elvinger, F.; Meng, X.J. Two amino acid mutations in the capsid protein of type 2 porcine circovirus (PCV2) enhanced PCV2 replication in vitro and attenuated the virus in vivo. *J. Virol.* **2004**, *78*, 13440–13446. [CrossRef] [PubMed]
55. Franzo, G.; Cortey, M.; Segalés, J.; Hughes, J.; Drigo, M. Phylodynamic analysis of porcine circovirus type 2 reveals global waves of emerging genotypes and the circulation of recombinant forms. *Mol. Phylogen. Evolut.* **2016**, *100*, 269–280. [CrossRef] [PubMed]
56. Kwon, T.; Lee, D.-U.; Yoo, S.J.; Je, S.H.; Shin, J.Y.; Lyoo, Y.S. Genotypic diversity of porcine circovirus type 2 (PCV2) and genotype shift to PCV2d in korean pig population. *Virus Res.* **2017**, *228*, 24–29. [CrossRef] [PubMed]
57. Constans, M.; Ssemadaali, M.; Kolyvushko, O.; Ramamoorthy, S. Antigenic determinants of possible vaccine escape by porcine circovirus subtype 2b viruses. *Bioinform. Biol. Insights* **2015**, *9*, 1–12. [PubMed]
58. Xiao, C.-T.; Halbur, P.G.; Opriessnig, T. Global molecular genetic analysis of porcine circovirus type 2 (PCV2) sequences confirms the presence of four main PCV2 genotypes and reveals a rapid increase of PCV2d. *J. Gen. Virol.* **2015**, *96*, 1830–1841. [CrossRef] [PubMed]
59. Xiao, C.-T.; Harmon, K.M.; Halbur, P.G.; Opriessnig, T. PCV2d-2 is the predominant type of PCV2 DNA in pig samples collected in the U.S. During 2014–2016. *Vet. Microbiol.* **2016**, *197*, 72–77. [CrossRef] [PubMed]
60. Firth, C.; Charleston, M.A.; Duffy, S.; Shapiro, B.; Holmes, E.C. Insights into the evolutionary history of an emerging livestock pathogen: Porcine circovirus 2. *J. Virol.* **2009**, *83*, 12813–12821. [CrossRef] [PubMed]
61. Segales, J.; Olvera, A.; Grau-Roma, L.; Charreyre, C.; Nauwynck, H.; Larsen, L.; Dupont, K.; McCullough, K.; Ellis, J.; Krakowka, S.; et al. PCV-2 genotype definition and nomenclature. *Vet. Rec.* **2008**, *162*, 867–868. [CrossRef] [PubMed]
62. Davies, B.; Wang, X.; Dvorak, C.M.; Marthaler, D.; Murtaugh, M.P. Diagnostic phylogenetics reveals a new porcine circovirus 2 cluster. *Virus Res.* **2016**, *217*, 32–37. [CrossRef] [PubMed]
63. Dupont, K.; Nielsen, E.O.; Baekbo, P.; Larsen, L.E. Genomic analysis of PCV2 isolates from Danish archives and a current PMWS case-control study supports a shift in genotypes with time. *Vet. Microbiol.* **2008**, *128*, 56–64. [CrossRef] [PubMed]
64. Harmon, K.M.; Gauger, P.C.; Zhang, J.; Pineyro, P.E.; Dunn, D.D.; Chriswell, A.J. Whole-genome sequences of novel porcine circovirus type 2 viruses detected in swine from Mexico and the United States. *Genome Announc.* **2015**, *3*, e01315. [CrossRef] [PubMed]
65. Olvera, A.; Cortey, M.; Segales, J. Molecular evolution of porcine circovirus type 2 genomes: Phylogeny and clonality. *Virology* **2007**, *357*, 175–185. [CrossRef] [PubMed]
66. Choi, J.; Stevenson, G.W.; Kiupel, M.; Harrach, B.; Anothayanontha, L.; Kanitz, C.L.; Mittal, S.K. Sequence analysis of old and new strains of porcine circovirus associated with congenital tremors in pigs and their comparison with strains involved with postweaning multisystemic wasting syndrome. *Can. J. Vet. Res.* **2002**, *66*, 217–224. [PubMed]
67. Grierson, S.S.; King, D.P.; Sandvik, T.; Hicks, D.; Spencer, Y.; Drew, T.W.; Banks, M. Detection and genetic typing of type 2 porcine circoviruses in archived pig tissues from the UK. *Arch. Virol.* **2004**, *149*, 1171–1183. [CrossRef] [PubMed]
68. Jacobsen, B.; Krueger, L.; Seeliger, F.; Bruegmann, M.; Segales, J.; Baumgaertner, W. Retrospective study on the occurrence of porcine circovirus 2 infection and associated entities in northern Germany. *Vet. Microbiol.* **2009**, *138*, 27–33. [CrossRef] [PubMed]
69. Wiederkehr, D.D.; Sydler, T.; Buergi, E.; Haessig, M.; Zimmermann, D.; Pospischil, A.; Brugnera, E.; Sidler, X. A new emerging genotype subgroup within PCV-2b dominates the PMWS epizooty in Switzerland. *Vet. Microbiol.* **2009**, *136*, 27–35. [CrossRef] [PubMed]
70. Beach, N.M.; Meng, X.J. Efficacy and future prospects of commercially available and experimental vaccines against porcine circovirus type 2 (PCV2). *Virus Res.* **2012**, *164*, 33–42. [CrossRef] [PubMed]

71. Carman, S.; Cai, H.Y.; DeLay, J.; Youssef, S.A.; McEwen, B.J.; Gagnon, C.A.; Tremblay, D.; Hazlett, M.; Lusis, P.; Fairles, J.; et al. The emergence of a new strain of porcine circovirus-2 in Ontario and Quebec swine and its association with severe porcine circovirus associated disease—2004–2006. *Can. J. Vet. Res.* **2008**, *72*, 259–268. [PubMed]
72. Carman, S.; McEwen, B.; DeLay, J.; van Dreumel, T.; Lusis, P.; Cai, H.; Fairles, J. Porcine circovirus-2 associated disease in swine in Ontario (2004 to 2005). *Can. Vet. J.* **2006**, *47*, 761–762. [PubMed]
73. Guo, L.J.; Lu, Y.H.; Wei, Y.W.; Huang, L.P.; Liu, C.M. Porcine circovirus type 2 (PCV2): Genetic variation and newly emerging genotypes in China. *Virol. J.* **2010**, *7*, 273. [CrossRef] [PubMed]
74. Franzo, G.; Tucciarone, C.M.; Cecchinato, M.; Drigo, M. Porcine circovirus type 2 (PCV2) evolution before and after the vaccination introduction: A large scale epidemiological study. *Sci. Rep.* **2016**, *6*, 39458. [CrossRef] [PubMed]
75. Cortey, M.; Segalés, J. Low levels of diversity among genomes of porcine circovirus type 1 (PCV1) points to differential adaptive selection between porcine circoviruses. *Virology* **2012**, *422*, 161–164. [CrossRef] [PubMed]
76. Franzo, G.; Cortey, M.; Castro, A.M.M.G.D.; Piovezan, U.; Szabo, M.P.J.; Drigo, M.; Segalés, J.; Richtzenhain, L.J. Genetic characterisation of Porcine circovirus type 2 (PCV2) strains from feral pigs in the Brazilian Pantanal: An opportunity to reconstruct the history of PCV2 evolution. *Vet. Microbiol.* **2015**, *178*, 158–162. [CrossRef] [PubMed]
77. De Castro, A.M.; Brombila, T.; Bersano, J.G.; Soares, H.S.; Silva, S.O.; Minervino, A.H.; Ogata, R.A.; Gennari, S.M.; Richtzenhain, L.J. Swine infectious agents in *Tayassu pecari* and *Pecari tajacu* tissue samples from Brazil. *J. Wildl. Dis.* **2014**, *50*, 205–209. [CrossRef] [PubMed]
78. Opriessnig, T.; O'Neill, K.; Gerber, P.F.; de Castro, A.M.; Gimenez-Lirola, L.G.; Beach, N.M.; Zhou, L.; Meng, X.J.; Wang, C.; Halbur, P.G. A PCV2 vaccine based on genotype 2b is more effective than a 2a-based vaccine to protect against PCV2b or combined PCV2a/2b viremia in pigs with concurrent PCV2, PRRSV and PPV infection. *Vaccine* **2013**, *31*, 487–494. [CrossRef] [PubMed]
79. Grau-Roma, L.; Crisci, E.; Sibila, M.; Lopez-Soria, S.; Nofrarias, M.; Cortey, M.; Fraile, L.; Olvera, A.; Segales, J. A proposal on porcine circovirus type 2 (PCV2) genotype definition and their relation with postweaning multisystemic wasting syndrome (PMWS) occurrence. *Vet. Microbiol.* **2008**, *128*, 23–35. [CrossRef] [PubMed]
80. Guo, L.; Fu, Y.; Wang, Y.; Lu, Y.; Wei, Y.; Tang, Q.; Fan, P.; Liu, J.; Zhang, L.; Zhang, F.; et al. A porcine circovirus type 2 (PCV2) mutant with 234 amino acids in capsid protein showed more virulence in vivo, compared with classical PCV2a/b strain. *PLoS ONE* **2012**, *7*, e41463. [CrossRef] [PubMed]
81. Opriessnig, T.; Xiao, C.T.; Gerber, P.F.; Halbur, P.G.; Matzinger, S.R.; Meng, X.J. Mutant USA strain of porcine circovirus type 2 (mPCV2) exhibits similar virulence to the classical PCV2a and PCV2b strains in caesarean-derived, colostrum-deprived pigs. *J. Gen. Virol.* **2014**, *95*, 2495–2503. [CrossRef] [PubMed]
82. Trible, B.R.; Suddith, A.W.; Kerrigan, M.A.; Cino-Ozuna, A.G.; Hesse, R.A.; Rowland, R.R. Recognition of the different structural forms of the capsid protein determines the outcome following infection with porcine circovirus type 2. *J. Virol.* **2012**, *86*, 13508–13514. [CrossRef] [PubMed]
83. Cadar, D.; Cságola, A.; Lőrincz, M.; Tombácz, K.; Spînu, M.; Tuboly, T. Detection of natural inter- and intra-genotype recombination events revealed by *cap* gene analysis and decreasing prevalence of PCV2 in wild boars. *Infect. Gen. Evolut.* **2012**, *12*, 420–427. [CrossRef] [PubMed]
84. Cai, L.; Han, X.; Ni, J.; Yu, X.; Zhou, Z.; Zhai, X.; Chen, X.; Tian, K. Natural recombinants derived from different patterns of recombination between two PCV2b parental strains. *Virus Res.* **2011**, *158*, 281–288. [CrossRef] [PubMed]
85. Hesse, R.; Kerrigan, M.; Rowland, R.R. Evidence for recombination between PCV2a and PCV2b in the field. *Virus Res.* **2008**, *132*, 201–207. [CrossRef] [PubMed]
86. Lefebvre, D.J.; Van Doorsselaere, J.; Delputte, P.L.; Nauwynck, H.J. Recombination of two porcine circovirus type 2 strains. *Arch. Virol.* **2009**, *154*, 875–879. [CrossRef] [PubMed]
87. Kekarainen, T.; Gonzalez, A.; Llorens, A.; Segales, J. Genetic variability of porcine circovirus 2 in vaccinating and non-vaccinating commercial farms. *J. Gen. Virol.* **2014**, *95*, 1734–1742. [CrossRef] [PubMed]
88. Reiner, G.; Hofmeister, R.; Willems, H. Genetic variability of porcine circovirus 2 (PCV2) field isolates from vaccinated and non-vaccinated pig herds in Germany. *Vet. Microbiol.* **2015**, *180*, 41–48. [CrossRef] [PubMed]

89. Shen, H.G.; Halbur, P.G.; Opriessnig, T. Prevalence and phylogenetic analysis of the current porcine circovirus 2 genotypes after implementation of widespread vaccination programmes in the USA. *J. Gen. Virol.* **2012**, *93*, 1345–1355. [CrossRef] [PubMed]
90. Fort, M.; Sibila, M.; Nofrarías, M.; Pérez-Martín, E.; Olvera, A.; Mateu, E.; Segalés, J. Evaluation of cell-mediated immune responses against porcine circovirus type 2 (PCV2) Cap and Rep proteins after vaccination with a commercial PCV2 sub-unit vaccine. *Vet. Immunol. Immunopathol.* **2012**, *150*, 128–132. [CrossRef] [PubMed]
91. Fort, M.; Sibila, M.; Pérez-Martín, E.; Nofrarías, M.; Mateu, E.; Segalés, J. One dose of a porcine circovirus 2 (PCV2) sub-unit vaccine administered to 3-week-old conventional piglets elicits cell-mediated immunity and significantly reduces PCV2 viremia in an experimental model. *Vaccine* **2009**, *27*, 4031–4037. [CrossRef] [PubMed]
92. Kekarainen, T.; McCullough, K.; Fort, M.; Fossum, C.; Segalés, J.; Allan, G.M. Immune responses and vaccine-induced immunity against porcine circovirus type 2. *Vet. Immunol. Immunopathol.* **2010**, *136*, 185–193. [CrossRef] [PubMed]
93. Dvorak, C.M.; Yang, Y.; Haley, C.; Sharma, N.; Murtaugh, M.P. National reduction in porcine circovirus type 2 prevalence following introduction of vaccination. *Vet. Microbiol.* **2016**, *189*, 86–90. [CrossRef] [PubMed]
94. Gerber, P.F.; Johnson, J.; Shen, H.; Striegel, D.; Xiao, C.-T.; Halbur, P.G.; Opriessnig, T. Association of concurrent porcine circovirus (PCV) 2a and 2b infection with PCV associated disease in vaccinated pigs. *Res. Vet. Sci.* **2013**, *95*, 775–781. [CrossRef] [PubMed]
95. Lekcharoensuk, P.; Morozov, I.; Paul, P.S.; Thangthumniyom, N.; Wajjawalku, W.; Meng, X.J. Epitope mapping of the major capsid protein of type 2 porcine circovirus (PCV2) by using chimeric PCV1 and PCV2. *J. Virol.* **2004**, *78*, 8135–8145. [CrossRef] [PubMed]
96. Mahe, D.; Blanchard, P.; Truong, C.; Arnauld, C.; Le Cann, P.; Cariolet, R.; Madec, F.; Albina, E.; Jestin, A. Differential recognition of ORF2 protein from type 1 and type 2 porcine circoviruses and identification of immunorelevant epitopes. *J. Gen. Virol.* **2000**, *81*, 1815–1824. [CrossRef] [PubMed]
97. Opriessnig, T.; Xiao, C.T.; Gerber, P.F.; Halbur, P.G. Emergence of a novel mutant PCV2b variant associated with clinical PCVAD in two vaccinated pig farms in the U.S. Concurrently infected with PPV2. *Vet. Microbiol.* **2013**, *163*, 177–183. [CrossRef] [PubMed]
98. Khayat, R.; Brunn, N.; Speir, J.A.; Hardham, J.M.; Ankenbauer, R.G.; Schneemann, A.; Johnson, J.E. The 2.3-angstrom structure of porcine circovirus 2. *J. Virol.* **2011**, *85*, 7856–7862. [CrossRef] [PubMed]
99. Trible, B.R.; Kerrigan, M.; Crossland, N.; Potter, M.; Faaberg, K.; Hesse, R.; Rowland, R.R. Antibody recognition of porcine circovirus type 2 capsid protein epitopes after vaccination, infection, and disease. *Clin. Vaccine Immunol.* **2011**, *18*, 749–757. [CrossRef] [PubMed]
100. Saha, D.; Huang, L.; Bussalleu, E.; Lefebvre, D.J.; Fort, M.; Van Doorsselaere, J.; Nauwynck, H.J. Antigenic subtyping and epitopes' competition analysis of porcine circovirus type 2 using monoclonal antibodies. *Vet. Microbiol.* **2012**, *157*, 13–22. [CrossRef] [PubMed]
101. Huang, L.P.; Lu, Y.H.; Wei, Y.W.; Guo, L.J.; Liu, C.M. Identification of one critical amino acid that determines a conformational neutralizing epitope in the capsid protein of porcine circovirus type 2. *BMC Microbiol.* **2011**, *11*, 188. [CrossRef] [PubMed]
102. Saha, D.; Lefebvre, D.J.; Ooms, K.; Huang, L.; Delputte, P.L.; Van Doorsselaere, J.; Nauwynck, H.J. Single amino acid mutations in the capsid switch the neutralization phenotype of porcine circovirus 2. *J. Gen. Virol.* **2012**, *93*, 1548–1555. [CrossRef] [PubMed]
103. Franzo, G.; Cortey, M.; Segales, J.; Hughes, J.; Drigo, M. Phylodynamic analysis of porcine circovirus type 2: Methodological approach and datasets. *Data Brief* **2016**, *8*, 549–552. [CrossRef] [PubMed]
104. Jeong, J.; Park, C.; Choi, K.; Chae, C. Comparison of three commercial one-dose porcine circovirus type 2 (PCV2) vaccines in a herd with concurrent circulation of PCV2b and mutant PCV2b. *Vet. Microbiol.* **2015**, *177*, 43–52. [CrossRef] [PubMed]
105. Salgado, R.L.; Vidigal, P.M.; de Souza, L.F.; Onofre, T.S.; Gonzaga, N.F.; Eller, M.R.; Bressan, G.C.; Fietto, J.L.; Almeida, M.R.; Silva Junior, A. Identification of an emergent porcine circovirus-2 in vaccinated pigs from a Brazilian farm during a postweaning multisystemic wasting syndrome outbreak. *Genome Announc.* **2014**, *2*, e00163-14. [CrossRef] [PubMed]

106. Seo, H.W.; Park, C.; Kang, I.; Choi, K.; Jeong, J.; Park, S.-J.; Chae, C. Genetic and antigenic characterization of a newly emerging porcine circovirus type 2b mutant first isolated in cases of vaccine failure in Korea. *Arch. Virol.* **2014**, *159*, 3107–3111. [CrossRef] [PubMed]
107. Xiao, C.T.; Halbur, P.G.; Opriessnig, T. Complete genome sequence of a novel porcine circovirus type 2b variant present in cases of vaccine failures in the united states. *J. Virol.* **2012**, *86*, 12469. [CrossRef] [PubMed]
108. Zhan, Y.; Wang, N.; Zhu, Z.; Wang, Z.; Wang, A.; Deng, Z.; Yang, Y. In silico analyses of antigenicity and surface structure variation of an emerging porcine circovirus genotype 2b mutant, prevalent in southern China from 2013 to 2015. *J. Gen. Virol.* **2016**, *97*, 922–933. [CrossRef] [PubMed]
109. Beach, N.M.; Ramamoorthy, S.; Opriessnig, T.; Wu, S.Q.; Meng, X.J. Novel chimeric porcine circovirus (PCV) with the capsid gene of the emerging PCV2b subtype cloned in the genomic backbone of the non-pathogenic PCV1 is attenuated in vivo and induces protective and cross-protective immunity against PCV2b and PCV2a subtypes in pigs. *Vaccine* **2010**, *29*, 221–232. [PubMed]
110. Opriessnig, T.; Xiao, C.-T.; Halbur, P.G.; Gerber, P.F.; Matzinger, S.R.; Meng, X.-J. A commercial porcine circovirus (PCV) type 2a-based vaccine reduces PCV2d viremia and shedding and prevents PCV2d transmission to naïve pigs under experimental conditions. *Vaccine* **2017**, *35*, 248–254. [CrossRef] [PubMed]
111. Chae, C. Commercial porcine circovirus type 2 vaccines: Efficacy and clinical application. *Vet. J.* **2012**, *194*, 151–157. [CrossRef] [PubMed]
112. Opriessnig, T.; Gerber, P.F.; Xiao, C.-T.; Halbur, P.G.; Matzinger, S.R.; Meng, X.-J. Commercial PCV2a-based vaccines are effective in protecting naturally PCV2b-infected finisher pigs against experimental challenge with a 2012 mutant PCV2. *Vaccine* **2014**, *32*, 4342–4348. [CrossRef] [PubMed]
113. Opriessnig, T.; Gerber, P.F.; Xiao, C.-T.; Mogler, M.; Halbur, P.G. A commercial vaccine based on PCV2a and an experimental vaccine based on a variant mPCV2b are both effective in protecting pigs against challenge with a 2013 U.S. variant mPCV2b strain. *Vaccine* **2014**, *32*, 230–237. [CrossRef] [PubMed]
114. Opriessnig, T.; Gomes-Neto, J.C.; Hemann, M.; Shen, H.G.; Beach, N.M.; Huang, Y.; Halbur, P.G.; Meng, X.J. An experimental live chimeric porcine circovirus 1-2a vaccine decreases porcine circovirus 2b viremia when administered intramuscularly or orally in a porcine circovirus 2b and porcine reproductive and respiratory syndrome virus dual-challenge model. *Microbiol. Immunol.* **2011**, *55*, 863–873. [CrossRef] [PubMed]
115. Rose, N.; Andraud, M.; Bigault, L.; Jestin, A.; Grasland, B. A commercial PCV2a-based vaccine significantly reduces PCV2b transmission in experimental conditions. *Vaccine* **2016**, *34*, 3738–3745. [CrossRef] [PubMed]
116. Edlefsen, P.T. Leaky vaccines protect highly exposed recipients at a lower rate: Implications for vaccine efficacy estimation and sieve analysis. *Comput. Math. Methods Med.* **2014**, *2014*, 1–12. [CrossRef] [PubMed]
117. Fort, M.; Sibila, M.; Allepuz, A.; Mateu, E.; Roerink, F.; Segales, J. Porcine circovirus type 2 (PCV2) vaccination of conventional pigs prevents viremia against PCV2 isolates of different genotypes and geographic origins. *Vaccine* **2008**, *26*, 1063–1071. [CrossRef] [PubMed]
118. Li, J.; Yu, T.; Zhang, F.; Wang, X.; Zhou, J.; Gao, X.; Gao, S.; Liu, X. Inactivated chimeric porcine circovirus (PCV) 1–2 vaccines based on genotypes 2b and 2d exhibit similar immunological effectiveness in protecting pigs against challenge with PCV2b strain 0233. *Arch. Virol.* **2017**, *162*, 235–246. [CrossRef] [PubMed]
119. Afghah, Z.; Webb, B.; Meng, X.-J.; Ramamoorthy, S. Ten years of PCV2 vaccines and vaccination: Is eradication a possibility? *Vet. Microbiol.* **2016**. [CrossRef] [PubMed]
120. Matzinger, S.R.; Opriessnig, T.; Xiao, C.T.; Catanzaro, N.; Beach, N.M.; Slade, D.E.; Nitzel, G.P.; Meng, X.J. A chimeric virus created by DNA shuffling of the capsid genes of different subtypes of porcine circovirus type 2 (PCV2) in the backbone of the non-pathogenic PCV1 induces protective immunity against the predominant PCV2b and the emerging PCV2d in pigs. *Virology* **2016**, *498*, 82–93. [CrossRef] [PubMed]
121. Ragonnet, R.; Trauer, J.M.; Denholm, J.T.; Geard, N.L.; Hellard, M.; McBryde, E.S. Vaccination programs for endemic infections: Modelling real versus apparent impacts of vaccine and infection characteristics. *Sci. Rep.* **2015**, *5*, 15468. [CrossRef] [PubMed]
122. Da Silva, N.; Carriquiry, A.; O'Neill, K.; Opriessnig, T.; O'Connor, A.M. Mixed treatment comparison meta-analysis of porcine circovirus type 2 (PCV2) vaccines used in piglets. *Prev. Vet. Med.* **2014**, *117*, 413–424. [CrossRef] [PubMed]
123. Lin, K.; Wang, C.; Murtaugh, M.P.; Ramamoorthy, S. Multiplex method for simultaneous serological detection of porcine reproductive and respiratory syndrome virus and porcine circovirus type 2. *J. Clin. Microbiol.* **2011**, *49*, 3184–3190. [CrossRef] [PubMed]

124. Palinski, R.; Piñeyro, P.; Shang, P.; Yuan, F.; Guo, R.; Fang, Y.; Byers, E.; Hause, B.M.; McFadden, G. A novel porcine circovirus distantly related to known circoviruses is associated with porcine dermatitis and nephropathy syndrome and reproductive failure. *J. Virol.* **2017**, *91*, e01816–e01879. [CrossRef] [PubMed]
125. Phan, T.G.; Giannitti, F.; Rossow, S.; Marthaler, D.; Knutson, T.; Li, L.; Deng, X.; Resende, T.; Vannucci, F.; Delwart, E. Detection of a novel circovirus PCV3 in pigs with cardiac and multi-systemic inflammation. *Virol. J.* **2016**, *13*, 184. [CrossRef] [PubMed]

© 2017 by the authors. Licensee MDPI, Basel, Switzerland. This article is an open access article distributed under the terms and conditions of the Creative Commons Attribution (CC BY) license (http://creativecommons.org/licenses/by/4.0/).

viruses

MDPI

Review

Mechanisms of Adaptive Immunity to Porcine Reproductive and Respiratory Syndrome Virus

Michael C. Rahe * and Michael P. Murtaugh

Department of Veterinary and Biomedical Sciences, University of Minnesota, 1971 Commonwealth Avenue, St. Paul, MN 55108, USA; murta001@umn.edu

* Correspondence: rahex008@umn.edu; Tel.: +1-563-599-7268

Academic Editors: Linda Dixon and Simon Graham
Received: 31 March 2017; Accepted: 7 June 2017; Published: 13 June 2017

Abstract: The adaptive immune response is necessary for the development of protective immunity against infectious diseases. Porcine reproductive and respiratory syndrome virus (PRRSV), a genetically heterogeneous and rapidly evolving RNA virus, is the most burdensome pathogen of swine health and wellbeing worldwide. Viral infection induces antigen-specific immunity that ultimately clears the infection. However, the resulting immune memory, induced by virulent or attenuated vaccine viruses, is inconsistently protective against diverse viral strains. The immunological mechanisms by which primary and memory protection are generated and used are not well understood. Here, we summarize current knowledge regarding cellular and humoral components of the adaptive immune response to PRRSV infection that mediate primary and memory immune protection against viruses.

Keywords: PRRSV; T cell; B cell; NK cell; neutralizing antibody; porcine; memory; adaptive immune response

1. Introduction

Porcine reproductive and respiratory syndrome virus (PRRSV) is the most severe enemy of porcine health and wellbeing. The highly mutable, enveloped, RNA virus was discovered nearly 30 years ago but, while extensive research has been carried out and many vaccines have been developed, there is still no reproducible immunological intervention that develops a broadly protective immune response against virulent PRRSV.

PRRS disease was first described on farms in North Carolina in the USA at the end of the 1980s. Outbreaks were marked by reproductive losses, post-weaning pneumonia, and increased mortality in growing pigs. Initial efforts to identify an etiological agent responsible for the new disease syndrome were unsuccessful, leading to the disease being temporarily designated mystery swine disease (MSD) in North America. Koch's postulates for MSD were fulfilled in 1991 with a previously unidentified RNA virus discovered in Europe, named Lelystad virus [1,2]. The discovery was quickly followed by isolation of the virus, initially referred to as swine infertility and respiratory syndrome virus or SIRS virus, in North America [3].

The name PRRSV was introduced in 1992 and encompasses PRRSV-1 (genotypes first isolated in Europe) and PRRSV-2 (genotypes first isolated in North America) [4,5]. Today, both virus types are globally distributed, with PRRSV-1 viruses predominantly in Europe and PRRSV-2 viruses largely in North America, Asia and South America [6]. Recent discovery of multiple arteriviral nucleotide sequences in nonhuman primates has led to a reclassification of PRRSV as two distinct viruses, PRRSV-1 and PRRSV-2 [7]. Here, we use the generic PRRSV to refer broadly to both viruses when evidence indicates that are equivalent, and the specific PRRSV-1 and PRRSV-2 is used when a distinction is desired. The reasoning is based on the many similarities of the two viruses in fine details of genome structure and organization, transcriptional strategy, host preference, clinical signs of disease, and

anti-viral immunity [7–11]. In particular, chimeric PRRSV consisting of PRRSV-1 open reading frames (ORFs) 2–5 in a background of PRRSV-2 are fully viable, showing as well that the molecular signals for transcription and translation are preserved [12].

PRRSV has a positive-sense, single-stranded RNA genome of approximately 15 kb designated to the *Arteriviridae* family. The virus encodes at least 10 functional ORFs. ORF1a and 1b encode two large polyproteins which are cleaved into 14 non-structural proteins [13]. There are eight known structural proteins encoded by ORF2a, ORF2b, ORF3–7 and ORF5a [14–16]. PRRSV is one of the most rapidly mutating RNA viruses known, with considerable genetic variation within both PRRSV-1 and PRRSV-2, based on ORF5 phylogenetic analysis [10,17]. This impressive genetic diversity makes the development of a broadly protective immune response to vaccination difficult to achieve. After infection, the virus can endure and replicate in the host, depending on immune status and PRRSV strain, for a period of at least 150 days [18]. Therefore, contrary to being labeled repeatedly as a persistent pathogen, animals are capable of eventually clearing PRRSV. However, the components of the immune system responsible for the development of sterilizing immunity are not completely understood or have yet to be discovered. Here, we will discuss several aspects of PRRSV antigen-specific and protective immunity which have yet to be elucidated while focusing on potential areas of further investigation. Readers interested in additional reviews of PRRSV literature related to immunity are directed to the following articles [11,19].

2. The Targets of Infection

PRRSV infects cells of the macrophage/monocyte lineage, including dendritic cells [20–23]. Permissive cells express Cluster of Differentiation (CD)163, a hemoglobin-haptoglobin scavenger, which is the necessary receptor for PRRSV infection and replication [24–26]. Macrophages and dendritic cells are common members of the mononuclear phagocyte system that plays a varied, and important, role in many aspects of tissue remodeling, development, immunity and immunopathology [27]. Classically designated as part of the innate immune system, these leukocytes are critical for the development of a productive adaptive immune response. Macrophages and, particularly, dendritic cells take up and present antigen to T cells and B cells, thus initiating an adaptive immune response against the presented antigen [28,29]. If a pathogen is able to infect and destroy, manipulate, or maintain itself within macrophages or dendritic cells, it then has the potential to modulate the immune response into a favorable situation for its own replication and survival.

Therefore, many pathogens employ strategies for macrophage infection as a way to make the host more amenable to infection. Recent research into *Mycobacterium tuberculosis* (Mtb) has shown that, after phagocytosis, the bacterium arrests phagosome maturation and intra-phagosome lipolysis resulting in Mtb survival and an increased supply of nutrients for growth [30,31]. Human immunodeficiency virus (HIV) infects macrophages to establish reservoirs within the host for the chronic stage of the disease when $CD4^+$ T cells are largely depleted and neutralizing antibodies may be present [32–34]. *Leishmania major* is a protozoan which infects phagocytes to subvert the immune system. The parasite expresses glycoprotein (gp)63, a multifaceted surface-expressed pathogenicity factor that is responsible for preventing antigen presentation and killing by natural killer (NK) cells [35–37]. Indeed, there are many more examples of burdensome pathogens which target phagocytic cells, especially macrophages and dendritic cells, in an attempt to gain a foothold within the immune system and allow for unchecked survival and replication [38–40]. PRRSV is one of these pathogens.

The ability of PRRSV to subvert the immune system has not been investigated as extensively as more prominent pathogens of humans, such as HIV. PRRSV has been shown to inhibit the production, or the downstream effects, of type 1 interferons, particularly interferon (IFN)-α, on intracellular signaling [41–48]. Interestingly, multiple PRRSV proteins (nonstructural protein (nsp) 1, nsp2, nsp4, nsp5, nsp11 and nucleocapsid) have been reported to possess interferon inhibiting abilities.

In addition, a number of in vivo experiments have reproduced earlier in vitro findings showing that interferon-α is inhibited during the early stages of PRRSV infection [47,49,50]. While the impact of type 1 interferon suppression is likely to create a favorable environment for the virus to replicate

and survive in phagocytic cells, it is still unclear what effect, if any, suppression of type 1 interferon activity has on the adaptive immune response to infection [51]. Future investigations could clarify the relative contributions of viral proteins on modulation of interferon production and their impacts on viral growth, survival, and the subsequent development of the adaptive immune response.

Apart from interfering with interferon expression, PRRSV has also displayed the in vitro ability to subvert the immune system by spreading from cell to cell. Recent work has uncovered the ability of the virus to spread infectious viral RNA, several replicases, and certain structural proteins between cells via intercellular nanotubules [52,53]. While this activity theoretically allows for PRRSV to avoid neutralizing antibodies, the presence and significance of this mechanism in PRRSV pathogenesis has yet to be fully elucidated. Future studies are needed to determine if this process operates in naturally permissive macrophages and dendritic cells, if it can be interrupted, for example by intracellular antibodies, and what effect it might have on viral propagation [54,55].

Vaccines depend upon innate immune stimulation to promote effective adaptive immune response to antigen, resulting in production of antibodies and cytotoxic T cell responses. The ability of a pathogen to successfully infect and replicate within innate immune cells makes the development of a protective immune response more difficult. As a result, the generation of effective vaccines against pathogens that target immune cells is fraught with challenges. Extensive variation in viral genetics, primary immune responses, and cross-protection indicates that much remains to be learned about cellular pathogenesis in order to arrive at better immunological solutions.

3. Immunosuppression

Immunosuppression refers to suppression of the immune system and its ability to fight infection. HIV and infectious bursal disease virus are examples of viral infections that destroy entire lymphoid cell populations that ablate or disable adaptive immune responses. Lymphoproliferative cancers block cellular differentiation and deprive the body of mature, effector lymphocytes, thus causing immunosuppression in a different manner. PRRSV does neither; infection does not lead to severe lymphoid depletion or ablation, and it does not interfere profoundly with lymphocyte differentiation or maturation. Leukocyte perturbations in lymphoid tissues are associated with PRRSV infection, suggesting that adaptive immunity might be weakened, though not destroyed [56–61].

The immune system also maintains peripheral tolerance to self and commensal bacteria through immunosuppressive mechanisms that include regulatory T cells (Tregs), characterized as $CD4^+CD25^+$Forkhead box p3 $(Foxp3)^+$ T lymphocytes [62]. Treg suppressive properties were discovered when thymectomized or Treg-depleted mice succumbed to autoimmune reactions [63,64]. Tregs suppress effector and effector memory T cell proliferation by cytokine deprivation leading to polyclonal apoptosis, and by suppression of antigen presenting cells by cytotoxic T lymphocyte-associated antigen-4 (CTLA-4) and other mechanisms [62]. Studies in PRRSV infections give an ambiguous picture about the role of Tregs. PRRSV-2 strains are reported to induce a strong Treg response which included transforming growth factor (TGF)β-1 secretion in vitro as well as in vivo [65,66]. Other studies did not show Treg responses to infection with either PRRSV-1 or PRRSV-2 [67,68]. Interleukin-10 (IL-10), an immunosuppressive cytokine expressed by various cell types including Tregs, was induced by PRRSV-2 vaccination in weaned pigs in one study, but was not induced in weaned or adult pigs in another study [69]. Additional in vitro and in vivo studies reported IL-10 mRNA transcription and cytokine production after PRRSV infection [70–72]. However, kinetic analysis in serum of viremic pigs of various ages showed that elevated IL-10 levels were primarily a function of age and were not associated with infection status [69]. The only exception was in weaned pigs infected with a virulent virus, in which a transient increase was associated with viral pathogenesis [69].

On balance, the immunological evidence for PRRSV inducing a state of immunosuppression does not appear to be compelling. Secondary infections following PRRS disease outbreak in swine herds, suggesting a reduced ability to fight infection, is an alternative indicator of immunosuppression. An early study showed concurrent pulmonary bacterial infections in 58% of 221 PRRS cases [73].

However, the study did not determine if bacterial infections were present before the PRRS outbreaks. The immunosuppression question also was addressed in more controlled settings using dual infection models with PRRSV and various bacterial species. A summary of published literature in 2003 showed no predisposition to bacterial disease in 8 of 15 coinfection models, three ambiguous outcomes, and four cases in which severity of disease was increased [74]. More recent studies found a positive association between PRRSV infection and replication of porcine circovirus 2 (PCV2) or swine influenza virus [75,76].

It is possible that bacterial infections in swine herds increase following PRRS outbreaks due an increased burden of viral infection on host resilience to pathogen burden. Subclinical viral and bacterial infections are common, with PCV2, *Salmonella enterica*, *Haemophilus parasuis*, various *Mycoplasma* species, *Leptospira*, and *Escherichia coli* being examples. Control of infection is maintained by a combination of immune resistance to microbial replication and tissue tolerance to damage. In a coinfection model of influenza virus and *Legionella pneumophila*, it was clearly demonstrated that *L. pneumophila* infection was subclinical in healthy mice, but was lethal in the presence of influenza virus [77]. Overwhelming disease was due to loss of tissue resilience, since the bacterial load was unchanged [77]. This model might account for mortalities observed in experimental swine following PRRSV exposure [78]. Given the variable results of PRRSV coinfection models in swine and an alternative mechanism for increased disease in PRRSV-infected herds, generalized immunosuppression does not appear to be a key feature of PRRSV pathogenesis.

PRRSV, like many viruses, has developed countermeasures to host immune responses that enable it to survive and replicate for extended periods of time before the infection is resolved. PRRSV modulation of intracellular antiviral defense mechanisms has been reviewed extensively [79]. The effects of PRRSV infection on adaptive immune response, i.e., antigen-specific T cell, B cell, and antibody responses, are less well characterized. The antiviral response of T cells to PRRSV, examined primarily by the IFNγ enzyme-linked immunospot (ELISPOT), appears to develop slowly over a period of weeks, and is not associated with changes in viral loads in blood or in infected lung and lymphoid tissues [80,81]. Peripheral blood mononuclear cells (PBMC) from young, weaned pigs show limited IFNγ responses even when stimulated by phytohemagluttinin, which might account for the low anti-PRRSV responsiveness after re-stimulation in vitro [69]. However, PBMC from growing pigs and mature sows, which showed higher levels of IFNγ sensitivity, still showed limited responsiveness [69]. These findings indicate that PRRSV may interfere with specific cell-mediated immunity, but more direct evidence is needed for a fuller understanding.

By contrast, the interaction of PRRSV with pigs does not appear to retard or attenuate the development of humoral immunity or B cell differentiation. Induction of antibody responses to PRRSV proteins, both structural and non-structural, occurred in the same time frame as antibody responses to keyhole limpet hemocyanin (KLH), an irrelevant protein antigen [51]. The antibody response to KLH was also the same in the presence or absence of PRRSV infection [51]. Similarly, PRRSV infection did not inhibit cellular or humoral immune protection in response to pseudorabies virus vaccination [82]. Thus, the adaptive B cell response is not delayed or suppressed by PRRSV.

An extended viremia and prolonged survival in lymphoid tissues is characteristic of PRRSV infection. These features show that PRRSV has mechanisms of immune avoidance that are not present in viruses such as influenza virus and foot and mouth disease virus, in which sterilizing immunity is achieved within 10–14 days. It appears from the findings of field observations and experimental investigations that some type of PRRSV-specific T cell interference is present, whereas specific B cell inhibition or a generalized state of immunosuppression are not immunological hallmarks of PRRSV infection.

4. Antibody Response

4.1. Neutralizing Antibody Response

The antibody response to PRRSV typically dominates discussions of PRRSV immunity, as neutralizing antibodies are the crucial component of immune-mediated protection against most

viral infections [83,84]. As a result, shortly after the identification of PRRSV as the causative agent of Mystery Swine Disease, there was a strong push to identify the presence and dynamic response of neutralizing antibodies against PRRSV and then to characterize their specificity for PRRSV variants. Early work suggested that neutralizing antibodies against homologous PRRSV could be found as early as 9–11 days after inoculation [85]. However, this was likely the non-affinity matured immunoglobulin (Ig)M response, as anti-swine IgM ablated the previously observed neutralizing activity. Subsequent research showed that the high affinity neutralizing IgG response, detected at around 28–42 days post-inoculation, is specific for the inoculating virus with partial neutralizing activity against heterologous viruses [86–90].

Following the identification of PRRSV neutralizing antibodies, the effectiveness of immunoglobulins in protecting against infection was evaluated with passive transfer studies. These experiments displayed the effectiveness of neutralizing antibodies at preventing clinical infection and disease against homologous challenge [91,92]. However, these studies also showed that immune protection can be quite limited, especially between PRRSV-1 and PRRSV-2 [93]. Within PRRSV-1 or PRRSV-2, protection against homologous inoculation is consistently solid, whereas protection against heterologous challenge is variable for unclear reasons [93–95]. However, genetic similarity, based primarily on ORF5 sequence comparisons, shows no relationship with degree of protection [96]. These results appeared to explain the potential field problem, in which vaccinated or live virus inoculated animals become infected with a variant PRRSV genetically different enough from the inoculating strain to evade the immune system, propagate, and then cause disease. Hence, ever since the mutability, antigenic variability, and resultant immunological elusiveness of PRRSV were first appreciated, a broadly neutralizing antibody response to PRRSV has been coveted by immunologists and practitioners [97].

Recent research shows that there are animals capable of developing a broadly neutralizing antibody response to genetically disparate viruses [9,98]. However, this immune capability has only been found in a proportion of animals in groups of similar genetics age, sex, and exposure history [9]. The seemingly random ability of some animals to develop broadly neutralizing antibodies suggests that the inherent variation of the adaptive immune response may play a role in conferring broadly neutralizing capabilities to certain animals. Investigations into this ability are needed at the lymphocyte level and while the obvious target is the B cell, T cells cannot be overlooked, as the induction of a humoral immune response requires antigen-specific T cell driven help [99,100]. Therefore, animals able to develop a strong neutralizing antibody response would require both B cells and T cells that are capable of recognizing neutralizing epitopes.

The conditions needed to achieve cross-neutralizing antibody production are not known, but may involve multiple exposures to the same or different virus isolates. Sows with high titered, broadly neutralizing antibodies were found in herds with multiple exposures to virulent field viruses [9]. In an experimental study, cross-neutralization was reported in animals exposed first to a PRRSV vaccine strain followed by homologous or heterologous virus challenge [86]. However, the majority of data analyzed were below the neutralization assay cutoff. Duration of viremia, up to 42 days, was linked with increased breadth of neutralizing antibodies following a single viral infection [101]. However, since cross-neutralization activity and titer data were not presented, it was not possible to further interpret the results. The animals were not subsequently challenged, so it is not known if the cross-neutralizing activity in serum was predictive of protection. Other studies showed that significant neutralizing antibody responses are not commonly observed during viremic infection of young pigs, as well as in adult sows [69,102–104].

Recently, vaccinology research in HIV has shown that sequential immunizations, tailored for specific stages of the immune response, may be useful for inducing broadly neutralizing antibodies [105–107]. The approach is based on the finding that early immune responses to HIV resulted in neutralizing antibodies against the circulating virus which quickly led to immune escape of the virus and the ineffectiveness of generated antibodies. The antibody-resistant virus then stimulated a secondary antibody response which again selected for antibody resistant virus. This virus-antibody

hide and seek continued, eventually resulting in the selection of several neutralization targets of the virus as well as the generation of broadly neutralizing antibodies [108–110]. Cloning of the antibodies showed that somatic mutations are generally necessary for antibody neutralizing capabilities against HIV-1 [111,112]. These findings have shown that the B cell response of the host adapts in the germinal center as the virus evolves, suggesting that tailored sequential immunization could lead to the development of a broadly neutralizing antibody response [113].

The consistent generation of a broadly neutralizing antibody response to PRRSV on the herd level has evaded the swine health industry since the emergence of PRRSV. There are multiple proposed mechanisms by which PRRSV may evade or inhibit the development, or the effectiveness, of a neutralizing antibody response, such as glycan shielding of envelope glycoprotein (GP)3 or GP5 [114,115], the existence of decoy epitopes in GP5 [116], lymphocyte dysregulation [79], and inhibition of the innate immune response [117]. Comprehension of defense mechanisms employed by PRRSV makes the development of a broadly neutralizing immune response appear to be a daunting task. However, as previously shown, some animals are capable of developing such a response. Simply, the key to adapting the immune phenomenon of some animals to a vaccine capable of inducing broadly protective immunity in many animals lies in identifying conserved epitopes on surface proteins which are necessary for infection.

While the purported targets of neutralization have been extensively discussed in recent reviews, it is worth noting that several epitopes on the membrane (M) protein, GP5, GP2, GP3, and GP4, have been shown, or implicated, to harbor neutralizing activity [114,116,118–124]. However, knocking out only CD163 in the pig is sufficient to render animals non-susceptible to PRRSV infection and replication [24,25,125]. It is proposed that following endocytosis, CD163 associates with the virus within the endosome, resulting in uncoating of the virus and the release of the viral genome into the cellular cytoplasm [126]. Since CD163 is necessary for viral infection and replication, the logical next step is to identify the conserved regions of viral surface proteins, most likely the minor glycoproteins (GP2, GP3, and GP4), that interact with CD163 [124,127].

4.2. Non-Neutralizing Antibody Response

Traditionally, the non-neutralizing antibody response to PRRSV has been considered useful only for its ability to identify if an animal had been exposed and seroconverted to virus. Indeed, there are many structural and non-structural proteins of PRRSV which make this possible through their ability to induce a robust humoral immune response [15,80,102]. However, recent research on other pathogens has shown that non-neutralizing antibodies may play a much larger role in immunity than was previously appreciated [128–131]. Alternative antibody functions, such as antibody dependent cell-mediated cytotoxicity (ADCC), antibody-dependent complement-mediated cytotoxicity (CDC), and antibody-dependent complement-mediated virolysis may be important in the clearance of virus and virally infected cells from an animal. To our knowledge, there are only two published papers investigating non-neutralizing antibody functions in the context of PRRSV infection [59,132]. Both of these in vitro studies utilized a PRRSV-1 virus and failed to find an effect of ADCC and CDC on infected cells. However, experiments focused on PRRSV-2 viruses with extended time points beyond 12 h are warranted. A more extensive review of non-neutralizing antibody functions can be found in the cited review [133].

5. The B Cell Response

If antibodies are the most important effectors of the immune system against viral infection, then B cells that make the antibodies are the most important cells. Previous research on the interaction between PRRSV and the porcine B cell is contradictory. It has recently been suggested that PRRSV infection results in lymphocyte apoptosis and immune impairment [61]. Several sources have shown that PRRSV largely or exclusively induces a specific humoral response to infection [51,134]. Other studies report that PRRSV infection results primarily in polyclonal B cell activation leading

to hypergammaglobulinemia and the development of immune complexes [135–138]. The majority of work describing infection leading to polyclonal activation and hypergammaglobulinemia was performed in germ-free isolator piglets. This model is very effective for comparing B cell and antibody repertoire development in the fetus, as the germ-free status of the pigs removes many of the variables present when experiments are performed on conventionally reared animals [139]. However, these animals are deprived of the microflora and maternal antibodies to which conventional animals are exposed. As a result, the translation of immunological outcomes observed in isolator pigs to conventional pigs must be performed with caution. Studies in mice show that the immune systems of specific-pathogen free laboratory mice are similar to neonatal human immune systems, whereas feral mice displayed immune systems more comparable to adult humans. Effectively, the immune systems of germ-free animals may not display "normal" immune system phenotypes due to the lack of exposure to microflora [140,141].

The development of protective humoral immunity, after vaccination or exposure to a pathogen, is dependent upon two lines of defense. The first immune defense is secreted antibodies, first from short-lived and then from long-lived, plasma cells residing somewhere in the body (Figure 1). The second line of defense is memory B cells (Figure 1). Memory cells are sentinels against reinfection which are activated upon antigen recognition to proliferate and differentiate into antibody secreting plasma cells, thus rapidly boosting circulating antibody titers with high affinity class switched antibodies [142].

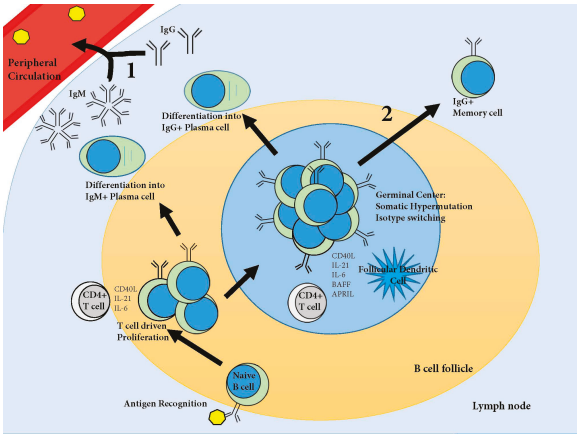

Figure 1. Development of systemic humoral immunity. Naive B cells move through the B cell follicles of the secondary lymphoid organs searching for antigens specific for their B cell receptors (BCR, surface immunoglobulin). Upon antigen recognition, the BCR is endocytosed, the antigen is degraded and then presented on the surface of the cell via Major Histocompatibility Complex (MHC)II. The B cell then migrates to the periphery of the B cell follicle searching for a Cluster of Differentiation (CD)4^+ T cell specific for the same antigen. Upon T cell recognition of the MHCII presented antigen, the T cell stimulates the B cell by cytokine driven proliferation. The B cell proliferates and differentiates, some cells become immunoglobulin (Ig)M producing plasma cells, and other cells migrate into the B cell follicle where, with the help of cytokines from $CD4^+$ follicular helper T cells and follicular dendritic cells, a germinal center is formed. In the germinal center, B cells proliferate and undergo somatic hypermutation and isotype switching. Affinity matured B cells then leave the germinal center as either IgG^+ plasma cells or IgG^+ memory cells. These cells constitute the first two lines of defense against reinfection: (1) affinity matured antibodies produced by plasma cells; and (2) memory cells which boost antibody titers upon antigen recognition. For an in depth review of this process based on data in humans and mice, please refer to Taylor et al. [143]. APRIL: a proliferation-inducing ligand; BAFF: B-cell-activating factor of the TNF family; IL: interleukin.

Currently, there is scant research on the memory B cell response to PRRSV. Strong memory responses have been shown against nsp2, nsp7, N, and the 3′ end of GP5 [51,144]. The specific memory B cells are abundant in tonsil, lymph nodes draining the lungs and reproductive tract, and spleen. Unfortunately, there are many questions about the porcine memory response to PRRSV which have yet to be answered, including if memory cell kinetics closely mimic antibody kinetics, the response of PRRSV-specific memory pools upon homologous or heterologous viral challenge, and the importance of these cells in conferring protection against challenge. The development of sensitive and specific reagents, such as B cell tetramers, is a first step in being able to answer these critical questions. Additionally, it is possible that the key to understanding the broadly neutralizing response to PRRSV lies within circulating or lymphoid organ resident memory B cells. The potential to investigate these cells for identification of heavy and light chain antibody sequences is reviewed in Rahe and Murtaugh [133].

Plasma Cells

Plasma cells are terminally differentiated B cells responsible for making antibodies. Apart from the immature plasmablast, two types of plasma cells have been defined in the mouse and human [145,146]. Short-lived plasma cells quickly boost antibody titers while long-lived plasma cells maintain circulating antibody titers in the face of continual antibody degradation. Mulupuri et al. identified PRRSV-specific plasma cells in several secondary lymphoid organs, such as the spleen, tonsil, sternal lymph node, and inguinal lymph node [51]. Interestingly, no PRRSV-specific or KLH-specific plasma cells were found in the bone marrow of immune pigs [51]. This was surprising, as the bone marrow has been long considered as the reservoir for long-lived plasma cells in both mice and humans [147–149]. It then begs the question, do pigs have long-lived plasma cells and, if so, where do they reside? Mulupuri et al. found PRRSV and KLH specific plasma cells in secondary lymphoid organs 120 days after inoculation [51]. However, these cells may not be "long lived" as the prolonged viremia of PRRSV may result in a somewhat continuous stimulation of memory B cells resulting in the appearance of this plasma cell population in secondary lymphoid organs.

It seems unlikely that pigs do not have long lived plasma cells, as the half-life of porcine antibodies in serum is, on average, approximately nine days [150,151]. Therefore, without long lived plasma cells, pigs would quickly lose humoral protection as antibody titers waned. The identification of the anatomic location as well as the understanding of mechanisms for inducing a strong long lived plasma cell response may be important for future vaccine design as well as comprehending host–pathogen interactions.

6. T Cell Response

Interestingly, even though neutralizing antibodies have historically garnered the majority of attention in PRRSV immunology, it is well-known that pigs readily control infection in the absence of neutralizing antibodies. Furthermore, viremia is reported in the presence of neutralizing antibodies [152,153]. Therefore, there must be other facets of the immune system which effectively function to control infection and eliminate PRRSV from the host. While some of this activity may be attributed to non-neutralizing functions of antibodies, the T cell response to infection demands further investigation. A recent PRRS immunity review summarized previous research on functional T cell subsets, and PRRSV epitope targets, as well as gaps in T cell immunity [11]. Here, we provide context for the understanding of novel results that have not been comprehensively reviewed.

Early research on the T cell response to PRRSV identified a large, transient decrease in the $CD4^+/CD8^+$ T cell ratio early, usually within the first week, in the course of infection [154]. The change in this ratio could have been due to a temporary loss of $CD4^+$ cells through apoptosis or to an increase in $CD8^+$ cells due to antigen-specific proliferation [154]. The importance of these findings for clearance of PRRSV or protection from infection were not known at the time, and other explanations, such as fluxes in cell populations between spleen, other lymphoid tissues, and blood could not be discounted.

Experiments to address the helper T cell type 1/helper T cell type 2 (Th1/Th2) paradigm in the pig showed that PRRSV induced a strong Th1 response, as expected, identified in vivo by an increased expression of Th1-specification factor Tbx21(T-bet) in $CD4^+$ cells [155]. However, the finding is at odds with previously reports indicating that PRRSV infection results in the production of IL-10, a cytokine classically associated with a Th2 phenotype. Similarly, monocyte-derived dendritic cells (Mo-DCs) infected with PRRSV down regulate swine leukocyte antigen (SLA)-I, SLA-II, CD40 and CD80 as well as promote IL-10 secretion over IL-12 secretion [156]. Delineation of the Th1/Th2 response to PRRSV, elucidation of Th1/Th2-specific cytokine markers in swine, as well as identifying associated cytokine responses of dendritic cells within secondary lymphoid organs where T cell proliferation and differentiation is most likely to occur, would help to resolve these outstanding questions [157].

The Th17 cell has classically been identified, in mouse and human, as playing an important role in extracellular bacterial immunity through the production of the pro-inflammatory cytokines, IL-17A, IL-17F, and IL-22 [158,159]. IL-17 producing Th17 cells are known to exist in the pig [160]. The importance of this T cell subset in the context of PRRSV infection has recently been investigated. A strain of Chinese highly pathogenic PRRSV (HP-PRRSV) appeared to suppress Th17 cells in the peripheral blood and lungs of pigs, resulting in an increased susceptibility to secondary bacterial infections [56]. Remarkably, the effect was PRRSV strain-specific, as a non-HP PRRSV strain failed to elicit the same response. Future research into the T cell response to PRRSV, especially with T cell tetramers and functional ELISPOTs, will be essential for the characterization of both $CD4^+$ and $CD8^+$ antigen specific T cells. Understanding how antigen-specific T cells interact with both infected and uninfected antigen presenting macrophages and dendritic cells will be helpful for advancing the field of PRRSV immunity.

7. Natural Killer Cell Response

The natural killer cell is an innate lymphoid cell which can have a profound impact on adaptive immunity, but is also able to induce an early and rapid innate response against pathogens through a variety of mechanisms. NK cells produce cytokines, such as IFNγ, show cytotoxic activity against infected cells not expressing MHCI, can induce dendritic cell maturation, and effect the destruction of infected cells in ADCC [161]. However, NK cells may deploy even more extensive and important functions in porcine immunity than are currently realized.

An early clue that NK cells were involved in innate responses to PRRSV was a sharp peak in serum IFNγ shortly after infection [162]. The acute response was attributed to NK cells, as the result was deemed too early for a T cell response, and suggested that decreased viral burdens in the lung prior to humoral or T cell responses could be due to the function of NK cells. However, it is known that porcine macrophages are also capable of producing IFNγ in the presence of PRRSV infection [163,164]. Furthermore, PRRSV appears to suppress the NK cell response without significantly affecting NK cell numbers [165–168]. The cause of this suppression has yet to be determined, although viral proteins, rather than soluble factors from cells, may be responsible [59]. Potential roles of additional NK cell functions, such as ADCC, in PRRSV immunity are poorly understood [133].

8. Conclusions

PRRSV has tormented the health and wellbeing of swine worldwide since its discovery in the late 1980s. Unfortunately, after almost 30 years of research into the porcine immune response to PRRSV, there is still no effective means for inducing a broadly protective immune response at the herd level. The reasons for this failure are not completely known, but presumably include mechanisms by which the virus subverts the immune system. The ability of the virus to rapidly mutate while not losing fitness challenges the host immune system to keep pace. At the same time, infection of macrophages, a key player in immunoregulation, challenges both innate and adaptive immune cell mobilization as well as induction of a coordinated response that is needed for effective control and elimination of the virus.

Fortunately, foundational advances in the understanding of viral pathogenesis and immunity are enabling more informative investigations. The identification of CD163 as the necessary and sufficient receptor for infection supports the implications of broadly neutralizing antibodies that a conserved target is present on all PRRSV. Understanding how PRRSV surface glycoproteins interact with CD163 should lead to the identification of conserved epitopes which are necessary for infection. If, as appears to be the case, there is only one conserved way into the cell, then there must be a conserved viral sequence, or structure, which enables viral entry. Furthermore, the knowledge that pigs eventually develop sterilizing immunity, if given enough time, supports the concept that conserved epitopes exist on the virus. Therefore, the study of mature animals, which have cleared the virus, may provide the key to understanding how the immune system eventually gets the upper hand on the virus and cures infection.

Even with seminal advances in several aspects of the study of PRRSV, there remains much to be understood and clarified. Currently, the published literature presents conflicting views on many aspects of PRRSV adaptive immunity, especially related to T and B cell responses and the production, or inhibition, of cytokines in the face of infection. The continued development of antigen-specific reagents, of high sensitivity and specificity, is needed for understanding how the host responds to PRRSV infection. Furthermore, it is important that future PRRSV studies focus on the relevant host animal, the conventional pig. While the study of this outbred animal species is perhaps challenging at times, it affords the ability to study the host–pathogen interaction in the only species in which the virus naturally interacts. Additionally, knowledge gained about the immunology of conventional pigs will accelerate immunological elucidation of other pig–pathogen interactions.

In conclusion, PRRSV continues to be the most burdensome pathogen of pigs worldwide, due to its propensity for immune evasion and manipulation. However, the continued study of the porcine immune response to infection, with improved reagents and methods, will illuminate those aspects of the host–pathogen interaction that are now hidden. It is through these discoveries that the complex question that is PRRSV will finally be answered.

Acknowledgments: The authors were supported in part by Agriculture and Food Research Initiative Competitive Grant No. 2016-67015-24928 from the USDA National Institute of Food and Agriculture and NIH award T32 OD010993 for support of M.C.R.

Conflicts of Interest: The authors declare no conflicts of interest.

References

1. Wensvoort, G.; Terpstra, C.; Pol, J.M.; ter Laak, E.A.; Bloemraad, M.; de Kluyver, E.P.; Kragten, C.; van Buiten, L.; den Besten, A.; Wagenaar, F. Mystery swine disease in The Netherlands: The isolation of Lelystad virus. *Vet. Q.* **1991**, *13*, 121–130. [CrossRef] [PubMed]
2. Terpstra, C.; Wensvoort, G.; Pol, J.M. Experimental reproduction of porcine epidemic abortion and respiratory syndrome (mystery swine disease) by infection with lelystad virus: Koch's postulates fulfilled. *Vet. Q.* **1991**, *13*, 131–136. [CrossRef] [PubMed]
3. Collins, J.E.; Benfield, D.A.; Christianson, W.T.; Harris, L.; Hennings, J.C.; Shaw, D.P.; Goyal, S.M.; McCullough, S.; Morrison, R.B.; Joo, H.S. Isolation of swine infertility and respiratory syndrome virus (isolate ATCC VR-2332) in North America and experimental reproduction of the disease in gnotobiotic pigs. *J. Vet. Diagn. Investig.* **1992**, *4*, 117–126. [CrossRef] [PubMed]
4. Nelsen, C.J.; Murtaugh, M.P.; Faaberg, K.S. Porcine reproductive and respiratory syndrome virus comparison: Divergent evolution on two continents. *J. Virol.* **1999**, *73*, 270–280. [PubMed]
5. Allende, R.; Lewis, T.L.; Lu, Z.; Rock, D.L.; Kutish, G.F.; Ali, A.; Doster, A.R.; Osorio, F.A. North American and European porcine reproductive and respiratory syndrome viruses differ in non-structural protein coding regions. *J. Gen. Virol.* **1999**, *80*, 307–315. [CrossRef] [PubMed]
6. Zimmerman, J.; Benfield, D.; Dee, S.; Murtaugh, M.; Stadejek, T.; Stevenson, G.; Torremorell, M. Porcine reproductive and respiratory syndrome virus (porcine arterivirus). In *Diseases of Swine*, 10th ed.; John Wiley & Sons Ltd.: West Sussex, UK, 2012.

7. Kuhn, J.H.; Lauck, M.; Bailey, A.L.; Shchetinin, A.M.; Vishnevskaya, T.V.; Bào, Y.; Ng, T.F.; LeBreton, M.; Schneider, B.S.; Gillis, A.; et al. Reorganization and expansion of the nidoviral family *Arteriviridae*. *Arch. Virol.* **2016**, *161*, 755–768. [CrossRef] [PubMed]
8. Meulenberg, J.J. PRRSV, the virus. *Vet. Res.* **2000**, *31*, 11–21. [CrossRef] [PubMed]
9. Robinson, S.R.; Li, J.; Nelson, E.A.; Murtaugh, M.P. Broadly neutralizing antibodies against the rapidly evolving porcine reproductive and respiratory syndrome virus. *Virus Res.* **2015**, *203*, 56–65. [CrossRef] [PubMed]
10. Murtaugh, M.P.; Stadejek, T.; Abrahante, J.E.; Lam, T.T.; Leung, F.C. The ever-expanding diversity of porcine reproductive and respiratory syndrome virus. *Virus Res.* **2010**, *154*, 18–30. [CrossRef] [PubMed]
11. Loving, C.L.; Osorio, F.A.; Murtaugh, M.P.; Zuckermann, F.A. Innate and adaptive immunity against porcine reproductive and respiratory syndrome virus. *Vet. Immunol. Immunopathol.* **2015**, *167*, 1–14. [CrossRef] [PubMed]
12. Tian, D.; Zheng, H.; Zhang, R.; Zhuang, J.; Yuan, S. Chimeric porcine reproductive and respiratory syndrome viruses reveal full function of genotype 1 envelope proteins in the backbone of genotype 2. *Virology* **2011**, *412*, 1–8. [CrossRef] [PubMed]
13. Fang, Y.; Snijder, E.J. The PRRSV replicase: Exploring the multifunctionality of an intriguing set of nonstructural proteins. *Virus Res.* **2010**, *154*, 61–76. [CrossRef] [PubMed]
14. Dea, S.; Gagnon, C.A.; Mardassi, H.; Pirzadeh, B.; Rogan, D. Current knowledge on the structural proteins of porcine reproductive and respiratory syndrome (PRRS) virus: Comparison of the North American and European isolates. *Arch. Virol.* **2000**, *145*, 659–688. [CrossRef] [PubMed]
15. Johnson, C.R.; Griggs, T.F.; Gnanandarajah, J.; Murtaugh, M.P. Novel structural protein in porcine reproductive and respiratory syndrome virus encoded by an alternative ORF5 present in all arteriviruses. *J. Gen. Virol.* **2011**, *92*, 1107–1116. [CrossRef] [PubMed]
16. Meulenberg, J.J.; van Nieuwstadt, A.P.; van Essen-Zandbergen, A.; Bos-de Ruijter, J.N.; Langeveld, J.P.; Meloen, R.H. Localization and fine mapping of antigenic sites on the nucleocapsid protein N of porcine reproductive and respiratory syndrome virus with monoclonal antibodies. *Virology* **1998**, *252*, 106–114. [CrossRef] [PubMed]
17. Brar, M.S.; Shi, M.; Murtaugh, M.P.; Leung, F.C. Evolutionary diversification of type 2 porcine reproductive and respiratory syndrome virus. *J. Gen. Virol.* **2015**, *96*, 1570–1580. [CrossRef] [PubMed]
18. Allende, R.; Laegreid, W.W.; Kutish, G.F.; Galeota, J.A.; Wills, R.W.; Osorio, F.A. Porcine reproductive and respiratory syndrome virus: Description of persistence in individual pigs upon experimental infection. *J. Virol.* **2000**, *74*, 10834–10837. [CrossRef] [PubMed]
19. Lunney, J.K.; Fang, Y.; Ladinig, A.; Chen, N.; Li, Y.; Rowland, B.; Renukaradhya, G.J. Porcine reproductive and respiratory syndrome virus (PRRSV): Pathogenesis and interaction with the immune system. *Annu. Rev. Anim. Biosci.* **2016**, *4*, 129–154. [CrossRef] [PubMed]
20. Lawson, S.R.; Rossow, K.D.; Collins, J.E.; Benfield, D.A.; Rowland, R.R. Porcine reproductive and respiratory syndrome virus infection of gnotobiotic pigs: Sites of virus replication and co-localization with MAC-387 staining at 21 days post-infection. *Virus Res.* **1997**, *51*, 105–113. [CrossRef]
21. Duan, X.; Nauwynck, H.J.; Pensaert, M.B. Virus quantification and identification of cellular targets in the lungs and lymphoid tissues of pigs at different time intervals after inoculation with porcine reproductive and respiratory syndrome virus (PRRSV). *Vet. Microbiol.* **1997**, *56*, 9–19. [CrossRef]
22. Kim, H.S.; Kwang, J.; Yoon, I.J.; Joo, H.S.; Frey, M.L. Enhanced replication of porcine reproductive and respiratory syndrome (PRRS) virus in a homogeneous subpopulation of MA-104 cell line. *Arch. Virol.* **1993**, *133*, 477–483. [CrossRef] [PubMed]
23. Park, J.Y.; Kim, H.S.; Seo, S.H. Characterization of interaction between porcine reproductive and respiratory syndrome virus and porcine dendritic cells. *J. Microbiol. Biotechnol.* **2008**, *18*, 1709–1716. [PubMed]
24. Whitworth, K.M.; Rowland, R.R.; Ewen, C.L.; Trible, B.R.; Kerrigan, M.A.; Cino-Ozuna, A.G.; Samuel, M.S.; Lightner, J.E.; McLaren, D.G.; Mileham, A.J.; et al. Gene-edited pigs are protected from porcine reproductive and respiratory syndrome virus. *Nat. Biotechnol.* **2016**, *34*, 20–22. [CrossRef] [PubMed]
25. Prather, R.S.; Whitworth, K.M.; Schommer, S.K.; Wells, K.D. Genetic engineering alveolar macrophages for host resistance to PRRSV. *Vet. Microbiol.* **2017**. [CrossRef] [PubMed]

26. Gao, L.; Guo, X.K.; Wang, L.; Zhang, Q.; Li, N.; Chen, X.X.; Wang, Y.; Feng, W.H. MicroRNA 181 suppresses porcine reproductive and respiratory syndrome virus (PRRSV) infection by targeting PRRSV receptor CD163. *J. Virol.* **2013**, *87*, 8808–8812. [CrossRef] [PubMed]
27. Hume, D.A. Macrophages as APC and the dendritic cell myth. *J. Immunol.* **2008**, *181*, 5829–5835. [CrossRef] [PubMed]
28. Batista, F.D.; Harwood, N.E. The who, how and where of antigen presentation to B cells. *Nat. Rev. Immunol.* **2009**, *9*, 15–27. [CrossRef] [PubMed]
29. Katz, D.H.; Unanue, E.R. Critical role of determinant presentation in the induction of specific responses in immunocompetent lymphocytes. *J. Exp. Med.* **1973**, *137*, 967–990. [CrossRef] [PubMed]
30. Podinovskaia, M.; Lee, W.; Caldwell, S.; Russell, D.G. Infection of macrophages with *Mycobacterium tuberculosis* induces global modifications to phagosomal function. *Cell. Microbiol.* **2013**, *15*, 843–859. [CrossRef] [PubMed]
31. Kalam, H.; Fontana, M.F.; Kumar, D. Alternate splicing of transcripts shape macrophage response to *Mycobacterium tuberculosis* infection. *PLoS Pathog.* **2017**, *13*, e1006236. [CrossRef] [PubMed]
32. Abbas, W.; Tariq, M.; Iqbal, M.; Kumar, A.; Herbein, G. Eradication of HIV-1 from the macrophage reservoir: An uncertain goal? *Viruses* **2015**, *7*, 1578–1598. [CrossRef] [PubMed]
33. Koppensteiner, H.; Brack-Werner, R.; Schindler, M. Macrophages and their relevance in human immunodeficiency virus type I infection. *Retrovirology* **2012**, *9*, 82. [CrossRef] [PubMed]
34. Koppensteiner, H.; Banning, C.; Schneider, C.; Hohenberg, H.; Schindler, M. Macrophage internal HIV-1 is protected from neutralizing antibodies. *J. Virol.* **2012**, *86*, 2826–2836. [CrossRef] [PubMed]
35. Moradin, N.; Descoteaux, A. Leishmania promastigotes: Building a safe niche within macrophages. *Front. Cell. Infect. Microbiol.* **2012**, *2*, 121. [CrossRef] [PubMed]
36. Matheoud, D.; Moradin, N.; Bellemare-Pelletier, A.; Shio, M.T.; Hong, W.J.; Olivier, M.; Gagnon, E.; Desjardins, M.; Descoteaux, A. Leishmania evades host immunity by inhibiting antigen cross-presentation through direct cleavage of the SNARE VAMP8. *Cell Host Microbe* **2013**, *14*, 15–25. [CrossRef] [PubMed]
37. Ghosh, J.; Bose, M.; Roy, S.; Bhattacharyya, S.N. *Leishmania donovani* targets Dicer1 to downregulate miR-122, lower serum cholesterol, and facilitate murine liver infection. *Cell Host Microbe* **2013**, *13*, 277–288. [CrossRef] [PubMed]
38. Lam, G.Y.; Czuczman, M.A.; Higgins, D.E.; Brumell, J.H. Interactions of *Listeria* monocytogenes with the autophagy system of host cells. *Adv. Immunol.* **2012**, *113*, 7–18. [PubMed]
39. Lee, J.W.; Lee, E.J. Regulation and function of the *Salmonella* MgtC virulence protein. *J. Microbiol.* **2015**, *53*, 667–672. [CrossRef] [PubMed]
40. Laksono, B.M.; de Vries, R.D.; McQuaid, S.; Duprex, W.P.; de Swart, R.L. Measles virus host invasion and pathogenesis. *Viruses* **2016**, *8*, 210. [CrossRef] [PubMed]
41. Yang, L.; Zhang, Y.J. Antagonizing cytokine-mediated JAK-STAT signaling by porcine reproductive and respiratory syndrome virus. *Vet. Microbiol.* **2016**. [CrossRef] [PubMed]
42. Yang, L.; Wang, R.; Ma, Z.; Xiao, Y.; Nan, Y.; Wang, Y.; Lin, S.; Zhang, Y.J. Porcine reproductive and respiratory syndrome virus antagonizes JAK/STAT3 signaling via Nsp5 by inducing STAT3 degradation. *J. Virol.* **2016**, *91*, e02087–e02116.
43. Huang, C.; Zhang, Q.; Guo, X.K.; Yu, Z.B.; Xu, A.T.; Tang, J.; Feng, W.H. Porcine reproductive and respiratory syndrome virus nonstructural protein 4 antagonizes beta interferon expression by targeting the NF-κB essential modulator. *J. Virol.* **2014**, *88*, 10934–10945. [CrossRef] [PubMed]
44. Beura, L.K.; Sarkar, S.N.; Kwon, B.; Subramaniam, S.; Jones, C.; Pattnaik, A.K.; Osorio, F.A. Porcine reproductive and respiratory syndrome virus nonstructural protein 1b modulates host innate immune response by antagonizing IRF3 activation. *J. Virol.* **2010**, *84*, 1574–1584. [CrossRef] [PubMed]
45. Sun, Z.; Li, Y.; Ransburgh, R.; Snijder, E.J.; Fang, Y. Nonstructural protein 2 of porcine reproductive and respiratory syndrome virus inhibits the antiviral function of interferon-stimulated gene 15. *J. Virol.* **2012**, *86*, 3839–3850. [CrossRef] [PubMed]
46. Sun, Y.; Ke, H.; Han, M.; Chen, N.; Fang, W.; Yoo, D. Nonstructural protein 11 of porcine reproductive and respiratory syndrome virus suppresses both MAVS and RIG-I expression as one of the mechanisms to antagonize type I interferon production. *PLoS ONE* **2016**, *11*, e0168314. [CrossRef] [PubMed]

47. Albina, E.; Carrat, C.; Charley, B. Interferon-alpha response to swine arterivirus (PoAV), the porcine reproductive and respiratory syndrome virus. *J. Interferon Cytokine Res.* **1998**, *18*, 485–490. [CrossRef] [PubMed]
48. Badaoui, B.; Tuggle, C.K.; Hu, Z.; Reecy, J.M.; Ait-Ali, T.; Anselmo, A.; Botti, S. Pig immune response to general stimulus and to porcine reproductive and respiratory syndrome virus infection: A meta-analysis approach. *BMC Genom.* **2013**, *14*, 220. [CrossRef] [PubMed]
49. Buddaert, W.; Van Reeth, K.; Pensaert, M. In vivo and in vitro interferon (IFN) studies with the porcine reproductive and respiratory syndrome virus (PRRSV). *Adv. Exp. Med. Biol.* **1998**, *440*, 461–467. [PubMed]
50. Van Reeth, K.; Labarque, G.; Nauwynck, H.; Pensaert, M. Differential production of proinflammatory cytokines in the pig lung during different respiratory virus infections: Correlations with pathogenicity. *Res. Vet. Sci.* **1999**, *67*, 47–52. [CrossRef] [PubMed]
51. Mulupuri, P.; Zimmerman, J.J.; Hermann, J.; Johnson, C.R.; Cano, J.P.; Yu, W.; Dee, S.A.; Murtaugh, M.P. Antigen-specific B-cell responses to porcine reproductive and respiratory syndrome virus infection. *J. Virol.* **2008**, *82*, 358–370. [CrossRef] [PubMed]
52. Guo, R.; Katz, B.B.; Tomich, J.M.; Gallagher, T.; Fang, Y. Porcine reproductive and respiratory syndrome virus utilizes nanotubes for intercellular spread. *J. Virol.* **2016**, *90*, 5163–5175. [CrossRef] [PubMed]
53. Cafruny, W.A.; Duman, R.G.; Wong, G.H.; Said, S.; Ward-Demo, P.; Rowland, R.R.; Nelson, E.A. Porcine reproductive and respiratory syndrome virus (PRRSV) infection spreads by cell-to-cell transfer in cultured MARC-145 cells, is dependent on an intact cytoskeleton, and is suppressed by drug-targeting of cell permissiveness to virus infection. *Virol. J.* **2006**, *3*, 90. [CrossRef] [PubMed]
54. Corthésy, B.; Benureau, Y.; Perrier, C.; Fourgeux, C.; Parez, N.; Greenberg, H.; Schwartz-Cornil, I. Rotavirus anti-VP6 secretory immunoglobulin A contributes to protection via intracellular neutralization but not via immune exclusion. *J. Virol.* **2006**, *80*, 10692–10699. [CrossRef] [PubMed]
55. Bai, Y.; Ye, L.; Tesar, D.B.; Song, H.; Zhao, D.; Björkman, P.J.; Roopenian, D.C.; Zhu, X. Intracellular neutralization of viral infection in polarized epithelial cells by neonatal Fc receptor (FcRn)-mediated IgG transport. *Proc. Natl. Acad. Sci. USA* **2011**, *108*, 18406–18411. [CrossRef] [PubMed]
56. Zhang, L.; Zhou, L.; Ge, X.; Guo, X.; Han, J.; Yang, H. The Chinese highly pathogenic porcine reproductive and respiratory syndrome virus infection suppresses Th17 cells response in vivo. *Vet. Microbiol.* **2016**, *189*, 75–85. [CrossRef] [PubMed]
57. Amarilla, S.P.; Gómez-Laguna, J.; Carrasco, L.; Rodríguez-Gómez, I.M.; Caridad Y Ocerín, J.M.; Graham, S.P.; Frossard, J.P.; Steinbach, F.; Salguero, F.J. Thymic depletion of lymphocytes is associated with the virulence of PRRSV-1 strains. *Vet. Microbiol.* **2016**, *188*, 47–58. [CrossRef] [PubMed]
58. Li, Y.; Wang, G.; Liu, Y.; Tu, Y.; He, Y.; Wang, Z.; Han, Z.; Li, L.; Li, A.; Tao, Y.; et al. Identification of apoptotic cells in the thymus of piglets infected with highly pathogenic porcine reproductive and respiratory syndrome virus. *Virus Res.* **2014**, *189*, 29–33. [CrossRef] [PubMed]
59. Cao, J.; Grauwet, K.; Vermeulen, B.; Devriendt, B.; Jiang, P.; Favoreel, H.; Nauwynck, H. Suppression of NK cell-mediated cytotoxicity against PRRSV-infected porcine alveolar macrophages in vitro. *Vet. Microbiol.* **2013**, *164*, 261–269. [CrossRef] [PubMed]
60. Sinkora, M.; Butler, J.E.; Lager, K.M.; Potockova, H.; Sinkorova, J. The comparative profile of lymphoid cells and the T and B cell spectratype of germ-free piglets infected with viruses SIV, PRRSV or PCV2. *Vet. Res.* **2014**, *45*, 91. [CrossRef] [PubMed]
61. Gómez-Laguna, J.; Salguero, F.J.; Fernández de Marco, M.; Barranco, I.; Rodríguez-Gómez, I.M.; Quezada, M.; Carrasco, L. Type 2 porcine reproductive and respiratory syndrome virus infection mediated apoptosis in B- and T-cell areas in lymphoid organs of experimentally infected pigs. *Transbound. Emerg. Dis.* **2013**, *60*, 273–278. [CrossRef] [PubMed]
62. Pandiyan, P.; Zheng, L.; Lenardo, M.J. The molecular mechanisms of regulatory T cell immunosuppression. *Front. Immunol.* **2011**, *2*, 60. [CrossRef] [PubMed]
63. Sakaguchi, S.; Takahashi, T.; Nishizuka, Y. Study on cellular events in post-thymectomy autoimmune oophoritis in mice. II. Requirement of Lyt-1 cells in normal female mice for the prevention of oophoritis. *J. Exp. Med.* **1982**, *156*, 1577–1586. [CrossRef] [PubMed]
64. Sakaguchi, S.; Toda, M.; Asano, M.; Itoh, M.; Morse, S.S.; Sakaguchi, N. T cell-mediated maintenance of natural self-tolerance: Its breakdown as a possible cause of various autoimmune diseases. *J. Autoimmun.* **1996**, *9*, 211–220. [CrossRef] [PubMed]

65. Silva-Campa, E.; Flores-Mendoza, L.; Reséndiz, M.; Pinelli-Saavedra, A.; Mata-Haro, V.; Mwangi, W.; Hernández, J. Induction of T helper 3 regulatory cells by dendritic cells infected with porcine reproductive and respiratory syndrome virus. *Virology* **2009**, *387*, 373–379. [CrossRef] [PubMed]
66. Wongyanin, P.; Buranapraditkun, S.; Chokeshai-Usaha, K.; Thanawonguwech, R.; Suradhat, S. Induction of inducible CD4+CD25+Foxp3+ regulatory T lymphocytes by porcine reproductive and respiratory syndrome virus (PRRSV). *Vet. Immunol. Immunopathol.* **2010**, *133*, 170–182. [CrossRef] [PubMed]
67. Rodríguez-Gómez, I.M.; Käser, T.; Gómez-Laguna, J.; Lamp, B.; Sinn, L.; Rümenapf, T.; Carrasco, L.; Saalmüller, A.; Gerner, W. PRRSV-infected monocyte-derived dendritic cells express high levels of SLA-DR and CD80/86 but do not stimulate PRRSV-naïve regulatory T cells to proliferate. *Vet. Res.* **2015**, *46*, 54. [CrossRef] [PubMed]
68. Silva-Campa, E.; Cordoba, L.; Fraile, L.; Flores-Mendoza, L.; Montoya, M.; Hernández, J. European genotype of porcine reproductive and respiratory syndrome (PRRSV) infects monocyte-derived dendritic cells but does not induce Treg cells. *Virology* **2010**, *396*, 264–271. [CrossRef] [PubMed]
69. Klinge, K.L.; Vaughn, E.M.; Roof, M.B.; Bautista, E.M.; Murtaugh, M.P. Age-dependent resistance to porcine reproductive and respiratory syndrome virus replication in swine. *Virol. J.* **2009**, *6*, 177. [CrossRef] [PubMed]
70. Suradhat, S.; Thanawongnuwech, R. Upregulation of interleukin-10 gene expression in the leukocytes of pigs infected with porcine reproductive and respiratory syndrome virus. *J. Gen. Virol.* **2003**, *84*, 2755–2760. [CrossRef] [PubMed]
71. García-Nicolás, O.; Quereda, J.J.; Gómez-Laguna, J.; Salguero, F.J.; Carrasco, L.; Ramis, G.; Pallarés, F.J. Cytokines transcript levels in lung and lymphoid organs during genotype 1 porcine reproductive and respiratory syndrome virus (PRRSV) infection. *Vet. Immunol. Immunopathol.* **2014**, *160*, 26–40. [CrossRef] [PubMed]
72. Gómez-Laguna, J.; Salguero, F.J.; De Marco, M.F.; Pallarés, F.J.; Bernabé, A.; Carrasco, L. Changes in lymphocyte subsets and cytokines during European porcine reproductive and respiratory syndrome: Increased expression of IL-12 and IL-10 and proliferation of CD4-CD8^{high}. *Viral. Immunol.* **2009**, *22*, 261–271. [CrossRef] [PubMed]
73. Zeman, D. Concurrent respiratory infections in 221 cases of PRRS virus pneumonia. *J. Swine Health Prod.* **1996**, *4*, 143–145.
74. Halbur, P. *"PRRS Plus"—PRRSV Infection in Combination with Other Agents*; National Pork Board: Des Moines, IA, USA, 2003; pp. 19–24.
75. Sinha, A.; Shen, H.G.; Schalk, S.; Beach, N.M.; Huang, Y.W.; Meng, X.J.; Halbur, P.G.; Opriessnig, T. Porcine reproductive and respiratory syndrome virus (PRRSV) influences infection dynamics of porcine circovirus type 2 (PCV2) subtypes PCV2a and PCV2b by prolonging PCV2 viremia and shedding. *Vet. Microbiol.* **2011**, *152*, 235–246. [CrossRef] [PubMed]
76. Dobrescu, I.; Levast, B.; Lai, K.; Delgado-Ortega, M.; Walker, S.; Banman, S.; Townsend, H.; Simon, G.; Zhou, Y.; Gerdts, V.; et al. In vitro and ex vivo analyses of co-infections with swine influenza and porcine reproductive and respiratory syndrome viruses. *Vet. Microbiol.* **2014**, *169*, 18–32. [CrossRef] [PubMed]
77. Jamieson, A.M.; Pasman, L.; Yu, S.; Gamradt, P.; Homer, R.J.; Decker, T.; Medzhitov, R. Role of tissue protection in lethal respiratory viral-bacterial coinfection. *Science* **2013**, *340*, 1230–1234. [CrossRef] [PubMed]
78. Johnson, W.; Roof, M.; Vaughn, E.; Christopher-Hennings, J.; Johnson, C.R.; Murtaugh, M.P. Pathogenic and humoral immune responses to porcine reproductive and respiratory syndrome virus (PRRSV) are related to viral load in acute infection. *Vet. Immunol. Immunopathol.* **2004**, *102*, 233–247. [CrossRef] [PubMed]
79. Butler, J.E.; Lager, K.M.; Golde, W.; Faaberg, K.S.; Sinkora, M.; Loving, C.; Zhang, Y.I. Porcine reproductive and respiratory syndrome (PRRS): An immune dysregulatory pandemic. *Immunol. Res.* **2014**, *59*, 81–108. [CrossRef] [PubMed]
80. Brown, E.; Lawson, S.; Welbon, C.; Gnanandarajah, J.; Li, J.; Murtaugh, M.P.; Nelson, E.A.; Molina, R.M.; Zimmerman, J.J.; Rowland, R.R.; et al. Antibody response to porcine reproductive and respiratory syndrome virus (PRRSV) nonstructural proteins and implications for diagnostic detection and differentiation of PRRSV types I and II. *Clin. Vaccine Immunol.* **2009**, *16*, 628–635. [CrossRef] [PubMed]
81. Xiao, Z.; Batista, L.; Dee, S.; Halbur, P.; Murtaugh, M.P. The level of virus-specific T-cell and macrophage recruitment in porcine reproductive and respiratory syndrome virus infection in pigs is independent of virus load. *J. Virol.* **2004**, *78*, 5923–5933. [CrossRef] [PubMed]

82. De Bruin, M.G.; Samsom, J.N.; Voermans, J.J.; van Rooij, E.M.; De Visser, Y.E.; Bianchi, A.T. Effects of a porcine reproductive and respiratory syndrome virus infection on the development of the immune response against pseudorabies virus. *Vet. Immunol. Immunopathol.* **2000**, *76*, 125–135. [CrossRef]
83. Burton, D.R. Antibodies, viruses and vaccines. *Nat. Rev. Immunol.* **2002**, *2*, 706–713. [CrossRef] [PubMed]
84. Plotkin, S.A. Correlates of protection induced by vaccination. *Clin. Vaccine Immunol.* **2010**, *17*, 1055–1065. [CrossRef] [PubMed]
85. Yoon, I.J.; Joo, H.S.; Goyal, S.M.; Molitor, T.W. A modified serum neutralization test for the detection of antibody to porcine reproductive and respiratory syndrome virus in swine sera. *J. Vet. Diagn. Investig.* **1994**, *6*, 289–292. [CrossRef] [PubMed]
86. Li, X.; Galliher-Beckley, A.; Pappan, L.; Trible, B.; Kerrigan, M.; Beck, A.; Hesse, R.; Blecha, F.; Nietfeld, J.C.; Rowland, R.R.; et al. Comparison of host immune responses to homologous and heterologous type II porcine reproductive and respiratory syndrome virus (PRRSV) challenge in vaccinated and unvaccinated pigs. *Biomed. Res. Int.* **2014**, *2014*, 416727. [CrossRef] [PubMed]
87. Labarque, G.G.; Nauwynck, H.J.; Van Reeth, K.; Pensaert, M.B. Effect of cellular changes and onset of humoral immunity on the replication of porcine reproductive and respiratory syndrome virus in the lungs of pigs. *J. Gen. Virol.* **2000**, *81*, 1327–1334. [CrossRef] [PubMed]
88. Correas, I.; Osorio, F.A.; Steffen, D.; Pattnaik, A.K.; Vu, H.L. Cross reactivity of immune responses to porcine reproductive and respiratory syndrome virus infection. *Vaccine* **2017**, *35*, 782–788. [CrossRef] [PubMed]
89. Bilodeau, R.; Archambault, D.; Vézina, S.A.; Sauvageau, R.; Fournier, M.; Dea, S. Persistence of porcine reproductive and respiratory syndrome virus infection in a swine operation. *Can. J. Vet. Res.* **1994**, *58*, 291–298. [PubMed]
90. Loemba, H.D.; Mounir, S.; Mardassi, H.; Archambault, D.; Dea, S. Kinetics of humoral immune response to the major structural proteins of the porcine reproductive and respiratory syndrome virus. *Arch. Virol.* **1996**, *141*, 751–761. [CrossRef] [PubMed]
91. Lopez, O.J.; Oliveira, M.F.; Garcia, E.A.; Kwon, B.J.; Doster, A.; Osorio, F.A. Protection against porcine reproductive and respiratory syndrome virus (PRRSV) infection through passive transfer of PRRSV-neutralizing antibodies is dose dependent. *Clin. Vaccine Immunol.* **2007**, *14*, 269–275. [CrossRef] [PubMed]
92. Osorio, F.A.; Galeota, J.A.; Nelson, E.; Brodersen, B.; Doster, A.; Wills, R.; Zuckermann, F.; Laegreid, W.W. Passive transfer of virus-specific antibodies confers protection against reproductive failure induced by a virulent strain of porcine reproductive and respiratory syndrome virus and establishes sterilizing immunity. *Virology* **2002**, *302*, 9–20. [CrossRef] [PubMed]
93. Choi, K.; Park, C.; Jeong, J.; Chae, C. Comparison of protection provided by type 1 and type 2 porcine reproductive and respiratory syndrome field viruses against homologous and heterologous challenge. *Vet. Microbiol.* **2016**, *191*, 72–81. [CrossRef] [PubMed]
94. Wang, G.; Yu, Y.; Zhang, C.; Tu, Y.; Tong, J.; Liu, Y.; Chang, Y.; Jiang, C.; Wang, S.; Zhou, E.M.; et al. Immune responses to modified live virus vaccines developed from classical or highly pathogenic PRRSV following challenge with a highly pathogenic PRRSV strain. *Dev. Comp. Immunol.* **2016**, *62*, 1–7. [CrossRef] [PubMed]
95. Lager, K.M.; Mengeling, W.L.; Brockmeier, S.L. Evaluation of protective immunity in gilts inoculated with the NADC-8 isolate of porcine reproductive and respiratory syndrome virus (PRRSV) and challenge-exposed with an antigenically distinct PRRSV isolate. *Am. J. Vet. Res.* **1999**, *60*, 1022–1027. [PubMed]
96. Opriessnig, T.; Pallares, F.; Nilubol, D.; Vincent, A.; Thacker, E.; Vaughn, E.; Roof, M.; Halbur, P. Genomic homology of ORF 5 gene sequence between modified live vaccine virus and porcine reproductive and respiratory syndrome virus challenge isolates is not predictive of vaccine efficacy. *J. Swine Health Prod.* **2005**, *13*, 246–253.
97. Dea, S.; Gagnon, C.A.; Mardassi, H.; Milane, G. Antigenic variability among North American and European strains of porcine reproductive and respiratory syndrome virus as defined by monoclonal antibodies to the matrix protein. *J. Clin. Microbiol.* **1996**, *34*, 1488–1493. [PubMed]
98. Trible, B.R.; Popescu, L.N.; Monday, N.; Calvert, J.G.; Rowland, R.R. A single amino acid deletion in the matrix protein of porcine reproductive and respiratory syndrome virus confers resistance to a polyclonal swine antibody with broadly neutralizing activity. *J. Virol.* **2015**, *89*, 6515–6520. [CrossRef] [PubMed]
99. Schimpl, A.; Wecker, E. Stimulation of IgG antibody response in vitro by T cell-replacing factor. *J. Exp. Med.* **1973**, *137*, 547–552. [CrossRef] [PubMed]

100. Singer, A.; Hodes, R.J. Mechanisms of T cell-B cell interaction. *Annu. Rev. Immunol.* **1983**, *1*, 211–241. [CrossRef] [PubMed]
101. Islam, Z.U.; Bishop, S.C.; Savill, N.J.; Rowland, R.R.; Lunney, J.K.; Trible, B.; Doeschl-Wilson, A.B. Quantitative analysis of porcine reproductive and respiratory syndrome (PRRS) viremia profiles from experimental infection: A statistical modelling approach. *PLoS ONE* **2013**, *8*, e83567. [CrossRef] [PubMed]
102. Molina, R.M.; Cha, S.H.; Chittick, W.; Lawson, S.; Murtaugh, M.P.; Nelson, E.A.; Christopher-Hennings, J.; Yoon, K.J.; Evans, R.; Rowland, R.R.; et al. Immune response against porcine reproductive and respiratory syndrome virus during acute and chronic infection. *Vet. Immunol. Immunopathol.* **2008**, *126*, 283–292. [CrossRef] [PubMed]
103. Mateu, E.; Diaz, I. The challenge of PRRS immunology. *Vet. J.* **2008**, *177*, 345–351. [CrossRef] [PubMed]
104. Nelson, E.A.; Christopher-Hennings, J.; Benfield, D.A. Serum immune responses to the proteins of porcine reproductive and respiratory syndrome (PRRS) virus. *J. Vet. Diagn. Investig.* **1994**, *6*, 410–415. [CrossRef] [PubMed]
105. Dosenovic, P.; von Boehmer, L.; Escolano, A.; Jardine, J.; Freund, N.T.; Gitlin, A.D.; McGuire, A.T.; Kulp, D.W.; Oliveira, T.; Scharf, L.; et al. Immunization for HIV-1 broadly neutralizing antibodies in human Ig knockin mice. *Cell* **2015**, *161*, 1505–1515. [CrossRef] [PubMed]
106. Sanders, R.W.; van Gils, M.J.; Derking, R.; Sok, D.; Ketas, T.J.; Burger, J.A.; Ozorowski, G.; Cupo, A.; Simonich, C.; Goo, L.; et al. HIV-1 vaccines. HIV-1 neutralizing antibodies induced by native-like envelope trimers. *Science* **2015**, *349*, 156–161. [CrossRef] [PubMed]
107. Jardine, J.G.; Kulp, D.W.; Havenar-Daughton, C.; Sarkar, A.; Briney, B.; Sok, D.; Sesterhenn, F.; Ereño-Orbea, J.; Kalyuzhniy, O.; Deresa, I.; et al. HIV-1 broadly neutralizing antibody precursor B cells revealed by germline-targeting immunogen. *Science* **2016**, *351*, 1458–1463. [CrossRef] [PubMed]
108. Bonsignori, M.; Hwang, K.K.; Chen, X.; Tsao, C.Y.; Morris, L.; Gray, E.; Marshall, D.J.; Crump, J.A.; Kapiga, S.H.; Sam, N.E.; et al. Analysis of a clonal lineage of HIV-1 envelope V2/V3 conformational epitope-specific broadly neutralizing antibodies and their inferred unmutated common ancestors. *J. Virol.* **2011**, *85*, 9998–10009. [CrossRef] [PubMed]
109. Bonsignori, M.; Zhou, T.; Sheng, Z.; Chen, L.; Gao, F.; Joyce, M.G.; Ozorowski, G.; Chuang, G.Y.; Schramm, C.A.; Wiehe, K.; et al. Maturation pathway from germline to broad HIV-1 neutralizer of a CD4-mimic antibody. *Cell* **2016**, *165*, 449–463. [CrossRef] [PubMed]
110. MacLeod, D.T.; Choi, N.M.; Briney, B.; Garces, F.; Ver, L.S.; Landais, E.; Murrell, B.; Wrin, T.; Kilembe, W.; Liang, C.H.; et al. Early antibody lineage diversification and independent limb maturation lead to broad HIV-1 neutralization targeting the Env high-mannose patch. *Immunity* **2016**, *44*, 1215–1226. [CrossRef] [PubMed]
111. Scheid, J.F.; Mouquet, H.; Feldhahn, N.; Seaman, M.S.; Velinzon, K.; Pietzsch, J.; Ott, R.G.; Anthony, R.M.; Zebroski, H.; Hurley, A.; et al. Broad diversity of neutralizing antibodies isolated from memory B cells in HIV-infected individuals. *Nature* **2009**, *458*, 636–640. [CrossRef] [PubMed]
112. Jardine, J.; Julien, J.P.; Menis, S.; Ota, T.; Kalyuzhniy, O.; McGuire, A.; Sok, D.; Huang, P.S.; MacPherson, S.; Jones, M.; et al. Rational HIV immunogen design to target specific germline B cell receptors. *Science* **2013**, *340*, 711–716. [CrossRef] [PubMed]
113. Escolano, A.; Dosenovic, P.; Nussenzweig, M.C. Progress toward active or passive HIV-1 vaccination. *J. Exp. Med.* **2017**, *214*, 3–16. [CrossRef] [PubMed]
114. Vu, H.L.; Kwon, B.; Yoon, K.J.; Laegreid, W.W.; Pattnaik, A.K.; Osorio, F.A. Immune evasion of porcine reproductive and respiratory syndrome virus through glycan shielding involves both glycoprotein 5 as well as glycoprotein 3. *J. Virol.* **2011**, *85*, 5555–5564. [CrossRef] [PubMed]
115. Ansari, I.H.; Kwon, B.; Osorio, F.A.; Pattnaik, A.K. Influence of N-linked glycosylation of porcine reproductive and respiratory syndrome virus GP5 on virus infectivity, antigenicity, and ability to induce neutralizing antibodies. *J. Virol.* **2006**, *80*, 3994–4004. [CrossRef] [PubMed]
116. Ostrowski, M.; Galeota, J.A.; Jar, A.M.; Platt, K.B.; Osorio, F.A.; Lopez, O.J. Identification of neutralizing and nonneutralizing epitopes in the porcine reproductive and respiratory syndrome virus GP5 ectodomain. *J. Virol.* **2002**, *76*, 4241–4250. [CrossRef] [PubMed]
117. Sang, Y.; Rowland, R.R.; Blecha, F. Interaction between innate immunity and porcine reproductive and respiratory syndrome virus. *Anim. Health Res. Rev.* **2011**, *12*, 149–167. [CrossRef] [PubMed]

118. Plagemann, P.G.; Rowland, R.R.; Faaberg, K.S. The primary neutralization epitope of porcine respiratory and reproductive syndrome virus strain VR-2332 is located in the middle of the GP5 ectodomain. *Arch. Virol.* **2002**, *147*, 2327–2347. [CrossRef] [PubMed]
119. Cancel-Tirado, S.M.; Evans, R.B.; Yoon, K.J. Monoclonal antibody analysis of porcine reproductive and respiratory syndrome virus epitopes associated with antibody-dependent enhancement and neutralization of virus infection. *Vet. Immunol. Immunopathol.* **2004**, *102*, 249–262. [CrossRef] [PubMed]
120. Delputte, P.L.; Meerts, P.; Costers, S.; Nauwynck, H.J. Effect of virus-specific antibodies on attachment, internalization and infection of porcine reproductive and respiratory syndrome virus in primary macrophages. *Vet. Immunol. Immunopathol.* **2004**, *102*, 179–188. [CrossRef] [PubMed]
121. Vanhee, M.; Van Breedam, W.; Costers, S.; Geldhof, M.; Noppe, Y.; Nauwynck, H. Characterization of antigenic regions in the porcine reproductive and respiratory syndrome virus by the use of peptide-specific serum antibodies. *Vaccine* **2011**, *29*, 4794–4804. [CrossRef] [PubMed]
122. Costers, S.; Lefebvre, D.J.; Van Doorsselaere, J.; Vanhee, M.; Delputte, P.L.; Nauwynck, H.J. GP4 of porcine reproductive and respiratory syndrome virus contains a neutralizing epitope that is susceptible to immunoselection in vitro. *Arch. Virol.* **2010**, *155*, 371–378. [CrossRef] [PubMed]
123. Zhou, L.; Ni, Y.Y.; Piñeyro, P.; Sanford, B.J.; Cossaboom, C.M.; Dryman, B.A.; Huang, Y.W.; Cao, D.J.; Meng, X.J. DNA shuffling of the GP3 genes of porcine reproductive and respiratory syndrome virus (PRRSV) produces a chimeric virus with an improved cross-neutralizing ability against a heterologous PRRSV strain. *Virology* **2012**, *434*, 96–109. [CrossRef] [PubMed]
124. Das, P.B.; Dinh, P.X.; Ansari, I.H.; de Lima, M.; Osorio, F.A.; Pattnaik, A.K. The minor envelope glycoproteins GP2a and GP4 of porcine reproductive and respiratory syndrome virus interact with the receptor CD163. *J. Virol.* **2010**, *84*, 1731–1740. [CrossRef] [PubMed]
125. Burkard, C.; Lillico, S.G.; Reid, E.; Jackson, B.; Mileham, A.J.; Ait-Ali, T.; Whitelaw, C.B.; Archibald, A.L. Precision engineering for PRRSV resistance in pigs: Macrophages from genome edited pigs lacking CD163 SRCR5 domain are fully resistant to both PRRSV genotypes while maintaining biological function. *PLoS Pathog.* **2017**, *13*, e1006206. [CrossRef] [PubMed]
126. Van Breedam, W.; Delputte, P.L.; Van Gorp, H.; Misinzo, G.; Vanderheijden, N.; Duan, X.; Nauwynck, H.J. Porcine reproductive and respiratory syndrome virus entry into the porcine macrophage. *J. Gen. Virol.* **2010**, *91*, 1659–1667. [CrossRef] [PubMed]
127. Tian, D.; Wei, Z.; Zevenhoven-Dobbe, J.C.; Liu, R.; Tong, G.; Snijder, E.J.; Yuan, S. Arterivirus minor envelope proteins are a major determinant of viral tropism in cell culture. *J. Virol.* **2012**, *86*, 3701–3712. [CrossRef] [PubMed]
128. Von Bredow, B.; Arias, J.F.; Heyer, L.N.; Moldt, B.; Le, K.; Robinson, J.E.; Zolla-Pazner, S.; Burton, D.R.; Evans, D.T. Comparison of antibody-dependent cell-mediated cytotoxicity and virus neutralization by HIV-1 Env-specific monoclonal antibodies. *J. Virol.* **2016**, *90*, 6127–6139. [CrossRef] [PubMed]
129. Ackerman, M.E.; Alter, G. Opportunities to exploit non-neutralizing HIV-specific antibody activity. *Curr. HIV Res.* **2013**, *11*, 365–377. [CrossRef] [PubMed]
130. Long, L.; Jia, M.; Fan, X.; Liang, H.; Wang, J.; Zhu, L.; Xie, Z.; Shen, T. Non-neutralizing epitopes induce robust HCV-specific antibody-dependent $CD56^{+}$ NK cell responses in chronic HCV-infected patients. *Clin. Exp. Immunol.* **2017**, *189*, 92–102. [CrossRef] [PubMed]
131. Wong, S.S.; Duan, S.; DeBeauchamp, J.; Zanin, M.; Kercher, L.; Sonnberg, S.; Fabrizio, T.; Jeevan, T.; Crumpton, J.C.; Oshansky, C.; et al. The immune correlates of protection for an avian influenza H5N1 vaccine in the ferret model using oil-in-water adjuvants. *Sci. Rep.* **2017**, *7*, 44727. [CrossRef] [PubMed]
132. Costers, S.; Delputte, P.L.; Nauwynck, H.J. Porcine reproductive and respiratory syndrome virus-infected alveolar macrophages contain no detectable levels of viral proteins in their plasma membrane and are protected against antibody-dependent, complement-mediated cell lysis. *J. Gen. Virol.* **2006**, *87*, 2341–2351. [CrossRef] [PubMed]
133. Rahe, M.; Murtaugh, M. Effector mechanisms of humoral immunity to porcine reproductive and respiratory syndrome virus. *Vet. Immunol. Immunopathol.* **2017**, *186*, 13–17. [CrossRef] [PubMed]
134. Lamontagne, L.; Page, C.; Larochelle, R.; Longtin, D.; Magar, R. Polyclonal activation of B cells occurs in lymphoid organs from porcine reproductive and respiratory syndrome virus (PRRSV)-infected pigs. *Vet. Immunol. Immunopathol.* **2001**, *82*, 165–182. [CrossRef]

135. Lemke, C.D.; Haynes, J.S.; Spaete, R.; Adolphson, D.; Vorwald, A.; Lager, K.; Butler, J.E. Lymphoid hyperplasia resulting in immune dysregulation is caused by porcine reproductive and respiratory syndrome virus infection in neonatal pigs. *J. Immunol.* **2004**, *172*, 1916–1925. [CrossRef] [PubMed]
136. Butler, J.E.; Wertz, N.; Weber, P.; Lager, K.M. Porcine reproductive and respiratory syndrome virus subverts repertoire development by proliferation of germline-encoded B cells of all isotypes bearing hydrophobic heavy chain CDR3. *J. Immunol.* **2008**, *180*, 2347–2356. [CrossRef] [PubMed]
137. Plagemann, P.G.; Rowland, R.R.; Cafruny, W.A. Polyclonal hypergammaglobulinemia and formation of hydrophobic immune complexes in porcine reproductive and respiratory syndrome virus-infected and uninfected pigs. *Viral. Immunol.* **2005**, *18*, 138–147. [CrossRef] [PubMed]
138. Sun, X.; Wertz, N.; Lager, K.M.; Butler, J.E. Antibody repertoire development in fetal and neonatal piglets. XV. Porcine circovirus type 2 infection differentially affects serum IgG levels and antibodies to ORF2 in piglets free from other environmental factors. *Vaccine* **2012**, *31*, 141–148. [CrossRef] [PubMed]
139. Butler, J.E.; Sun, J.; Weber, P.; Ford, S.P.; Rehakova, Z.; Sinkora, J.; Lager, K. Antibody repertoire development in fetal and neonatal piglets. IV. Switch recombination, primarily in fetal thymus, occurs independent of environmental antigen and is only weakly associated with repertoire diversification. *J. Immunol.* **2001**, *167*, 3239–3249. [CrossRef] [PubMed]
140. Beura, L.K.; Hamilton, S.E.; Bi, K.; Schenkel, J.M.; Odumade, O.A.; Casey, K.A.; Thompson, E.A.; Fraser, K.A.; Rosato, P.C.; Filali-Mouhim, A.; et al. Normalizing the environment recapitulates adult human immune traits in laboratory mice. *Nature* **2016**, *532*, 512–516. [CrossRef] [PubMed]
141. Graham, D.M. Dirty mice might make better models. *Lab. Anim.* **2016**, *45*, 198. [CrossRef] [PubMed]
142. Ahmed, R.; Gray, D. Immunological memory and protective immunity: Understanding their relation. *Science* **1996**, *272*, 54–60. [CrossRef] [PubMed]
143. Taylor, J.J.; Jenkins, M.K.; Pape, K.A. Heterogeneity in the differentiation and function of memory B cells. *Trends Immunol.* **2012**, *33*, 590–597. [CrossRef] [PubMed]
144. Rahe, M.C.; Murtaugh, M.P. Interleukin-21 drives proliferation and differentiation of porcine memory B cells into antibody secreting cells. *PLoS ONE* **2017**, *12*, e0171171. [CrossRef] [PubMed]
145. Slifka, M.K.; Antia, R.; Whitmire, J.K.; Ahmed, R. Humoral immunity due to long-lived plasma cells. *Immunity* **1998**, *8*, 363–372. [CrossRef]
146. Radbruch, A.; Muehlinghaus, G.; Luger, E.O.; Inamine, A.; Smith, K.G.; Dörner, T.; Hiepe, F. Competence and competition: The challenge of becoming a long-lived plasma cell. *Nat. Rev. Immunol.* **2006**, *6*, 741–750. [CrossRef] [PubMed]
147. McMillan, R.; Longmire, R.L.; Yelenosky, R.; Lang, J.E.; Heath, V.; Craddock, C.G. Immunoglobulin synthesis by human lymphoid tissues: Normal bone marrow as a major site of IgG production. *J. Immunol.* **1972**, *109*, 1386–1394. [PubMed]
148. Benner, R.; Meima, F.; van der Meulen, G.M.; van Muiswinkel, W.B. Antibody formation in mouse bone marrow. I. Evidence for the development of plaque-forming cells in situ. *Immunology* **1974**, *26*, 247–255. [PubMed]
149. Slifka, M.K.; Matloubian, M.; Ahmed, R. Bone marrow is a major site of long-term antibody production after acute viral infection. *J. Virol.* **1995**, *69*, 1895–1902. [PubMed]
150. Curtis, J.; Bourne, F.J. Half-lives of immunoglobulins IgG, IgA and IgM in the serum of new-born pigs. *Immunology* **1973**, *24*, 147–155. [PubMed]
151. Polo, J.; Campbell, J.M.; Crenshaw, J.; Rodríguez, C.; Pujol, N.; Navarro, N.; Pujols, J. Half-life of porcine antibodies absorbed from a colostrum supplement containing porcine immunoglobulins. *J. Anim. Sci.* **2012**, *90* (Suppl. 4), 308–310. [CrossRef] [PubMed]
152. Fontanella, E.; Ma, Z.; Zhang, Y.; de Castro, A.M.; Shen, H.; Halbur, P.G.; Opriessnig, T. An interferon inducing porcine reproductive and respiratory syndrome virus vaccine candidate elicits protection against challenge with the heterologous virulent type 2 strain VR-2385 in pigs. *Vaccine* **2017**, *35*, 125–131. [CrossRef] [PubMed]
153. Batista, L.; Pijoan, C.; Dee, S.; Olin, M.; Molitor, T.; Joo, H.S.; Xiao, Z.; Murtaugh, M. Virological and immunological responses to porcine reproductive and respiratory syndrome virus in a large population of gilts. *Can. J. Vet. Res.* **2004**, *68*, 267–273. [PubMed]

154. Shimizu, M.; Yamada, S.; Kawashima, K.; Ohashi, S.; Shimizu, S.; Ogawa, T. Changes of lymphocyte subpopulations in pigs infected with porcine reproductive and respiratory syndrome (PRRS) virus. *Vet. Immunol. Immunopathol.* **1996**, *50*, 19–27. [CrossRef]
155. Ebner, F.; Rausch, S.; Scharek-Tedin, L.; Pieper, R.; Burwinkel, M.; Zentek, J.; Hartmann, S. A novel lineage transcription factor based analysis reveals differences in T helper cell subpopulation development in infected and intrauterine growth restricted (IUGR) piglets. *Dev. Comp. Immunol.* **2014**, *46*, 333–340. [CrossRef] [PubMed]
156. Liu, J.; Wei, S.; Liu, L.; Shan, F.; Zhao, Y.; Shen, G. The role of porcine reproductive and respiratory syndrome virus infection in immune phenotype and Th1/Th2 balance of dendritic cells. *Dev. Comp. Immunol.* **2016**, *65*, 245–252. [CrossRef] [PubMed]
157. Murtaugh, M.P.; Johnson, C.R.; Xiao, Z.; Scamurra, R.W.; Zhou, Y. Species specialization in cytokine biology: Is interleukin-4 central to the T_H1–T_H2 paradigm in swine? *Dev. Comp. Immunol.* **2009**, *33*, 344–352. [CrossRef] [PubMed]
158. Liang, S.C.; Tan, X.Y.; Luxenberg, D.P.; Karim, R.; Dunussi-Joannopoulos, K.; Collins, M.; Fouser, L.A. Interleukin (IL)-22 and Il-17 are coexpressed by Th17 cells and cooperatively enhance expression of antimicrobial peptides. *J. Exp. Med.* **2006**, *203*, 2271–2279. [CrossRef] [PubMed]
159. Kudva, A.; Scheller, E.V.; Robinson, K.M.; Crowe, C.R.; Choi, S.M.; Slight, S.R.; Khader, S.A.; Dubin, P.J.; Enelow, R.I.; Kolls, J.K.; et al. Influenza A inhibits Th17-mediated host defense against bacterial pneumonia in mice. *J. Immunol.* **2011**, *186*, 1666–1674. [CrossRef] [PubMed]
160. Pilon, C.; Levast, B.; Meurens, F.; Le Vern, Y.; Kerboeuf, D.; Salmon, H.; Velge-Roussel, F.; Lebranchu, Y.; Baron, C. CD40 engagement strongly induces CD25 expression on porcine dendritic cells and polarizes the T cell immune response toward Th1. *Mol. Immunol.* **2009**, *46*, 437–447. [CrossRef] [PubMed]
161. Shekhar, S.; Yang, X. Natural killer cells in host defense against veterinary pathogens. *Vet. Immunol. Immunopathol.* **2015**, *168*, 30–34. [CrossRef] [PubMed]
162. Wesley, R.D.; Lager, K.M.; Kehrli, M.E. Infection with porcine reproductive and respiratory syndrome virus stimulates an early gamma interferon response in the serum of pigs. *Can. J. Vet. Res.* **2006**, *70*, 176–182. [PubMed]
163. Choi, C.; Cho, W.S.; Kim, B.; Chae, C. Expression of interferon-gamma and tumour necrosis factor-alpha in pigs experimentally infected with porcine reproductive and respiratory syndrome virus (PRRSV). *J. Comp. Pathol.* **2002**, *127*, 106–113. [CrossRef] [PubMed]
164. Thanawongnuwech, R.; Rungsipipat, A.; Disatian, S.; Saiyasombat, R.; Napakanaporn, S.; Halbur, P.G. Immunohistochemical staining of IFN-γ positive cells in porcine reproductive and respiratory syndrome virus-infected lungs. *Vet. Immunol. Immunopathol.* **2003**, *91*, 73–77. [CrossRef]
165. Jung, K.; Renukaradhya, G.J.; Alekseev, K.P.; Fang, Y.; Tang, Y.; Saif, L.J. Porcine reproductive and respiratory syndrome virus modifies innate immunity and alters disease outcome in pigs subsequently infected with porcine respiratory coronavirus: Implications for respiratory viral co-infections. *J. Gen. Virol.* **2009**, *90*, 2713–2723. [CrossRef] [PubMed]
166. Renukaradhya, G.J.; Alekseev, K.; Jung, K.; Fang, Y.; Saif, L.J. Porcine reproductive and respiratory syndrome virus-induced immunosuppression exacerbates the inflammatory response to porcine respiratory coronavirus in pigs. *Viral. Immunol.* **2010**, *23*, 457–466. [CrossRef] [PubMed]
167. Dwivedi, V.; Manickam, C.; Binjawadagi, B.; Linhares, D.; Murtaugh, M.P.; Renukaradhya, G.J. Evaluation of immune responses to porcine reproductive and respiratory syndrome virus in pigs during early stage of infection under farm conditions. *Virol. J.* **2012**, *9*, 45. [CrossRef] [PubMed]
168. Manickam, C.; Dwivedi, V.; Patterson, R.; Papenfuss, T.; Renukaradhya, G.J. Porcine reproductive and respiratory syndrome virus induces pronounced immune modulatory responses at mucosal tissues in the parental vaccine strain VR2332 infected pigs. *Vet. Microbiol.* **2013**, *162*, 68–77. [CrossRef] [PubMed]

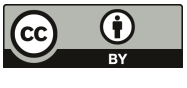

© 2017 by the authors. Licensee MDPI, Basel, Switzerland. This article is an open access article distributed under the terms and conditions of the Creative Commons Attribution (CC BY) license (http://creativecommons.org/licenses/by/4.0/).

viruses

MDPI

Review

Harnessing Local Immunity for an Effective Universal Swine Influenza Vaccine

Elma Tchilian * and Barbara Holzer

The Pirbright Institute, Woking, Surrey GU24 0NF, UK; barbara.holzer@pirbright.ac.uk
* Correspondence: elma.tchilian@pirbright.ac.uk

Academic Editor: Eric O. Freed
Received: 20 March 2017; Accepted: 28 April 2017; Published: 5 May 2017

Abstract: Influenza A virus infections are a global health threat to humans and are endemic in pigs, contributing to decreased weight gain and suboptimal reproductive performance. Pigs are also a source of new viruses of mixed swine, avian, and human origin, potentially capable of initiating human pandemics. Current inactivated vaccines induce neutralising antibody against the immunising strain but rapid escape occurs through antigenic drift of the surface glycoproteins. However, it is known that prior infection provides a degree of cross-protective immunity mediated by cellular immune mechanisms directed at the more conserved internal viral proteins. Here we review new data that emphasises the importance of local immunity in cross-protection and the role of the recently defined tissue-resident memory T cells, as well as locally-produced, and sometimes cross-reactive, antibody. Optimal induction of local immunity may require aerosol delivery of live vaccines, but it remains unclear how long protective local immunity persists. Nevertheless, a universal vaccine might be extremely useful for disease prevention in the face of a pandemic. As a natural host for influenza A viruses, pigs are both a target for a universal vaccine and an excellent model for developing human influenza vaccines.

Keywords: Swine influenza; local lung immunity; lung tissue resident memory T cells; universal influenza vaccines; heterosubtypic immunity

1. Introduction

Influenza A virus infection is a global health threat to livestock and humans, causing substantial mortality and morbidity. H1N1 and H3N2 influenza viruses are endemic in pigs and humans in addition to H1N2 in pigs. Since human origin viruses, or viruses containing human origin gene segments, frequently adapt to transmit efficiently in pigs [1,2], the pig is a source of new viruses capable of initiating epidemics or pandemics in humans of mixed swine, human, and avian origin [3]. As both pigs and humans are readily infected with influenza A viruses of similar subtype, the pig is a robust and appropriate model for investigating both swine and human disease. Like humans, pigs are outbred, and physiologically, anatomically, and immunologically similar to humans. The porcine lung also resembles the human in terms of its tracheobronchial tree structure, lung physiology, morphology, and distribution of receptors bound by influenza viruses [4,5].

Swine influenza virus (SI) infection exhibits a spectrum of clinical signs, ranging from inapparent disease to fever, with overt respiratory signs and disease severity is increased significantly by secondary bacterial infection. SI contributes to sub-optimal reproductive performance and is occasionally associated with fever-induced abortion in sows. Immunisation may be a cost effective control measure to combat SI, but the rapid evolution of the virus is a major obstacle SI diversity is reviewed in [1,6,7]. Not all countries with SI use vaccines to control disease. Current UK policy does not involve immunisation against SI, although it is used in some European countries and widely in the US. While

it will be difficult to convince government and livestock keepers to invest in control measures for a disease causing insidious losses without providing clear economic and welfare benefits, with pig production intensifying worldwide it is likely that an improved immunisation strategy for SI would result in more countries relying on vaccines to control disease.

Parenterally-administered inactivated vaccines against SI, widely used in the US, are strain-specific and protection correlates with the presence of neutralising antibodies. The most commonly used are whole inactivated virus (WIV) administered with oil-in-water adjuvants, non-replicating alphavirus RNA particle, or autogenous vaccines. For autogenous vaccines the vaccine organism(s) must come from the herd in which the vaccine is to be used, and they accounted for more than half of all SI vaccine doses released for sale in 2008. Recent reviews by Sandbulte et al. [8] and Vincent et al. [6] provide comprehensive information on currently used vaccines in the field in the US. In Europe, RESPIPORC FLU 3 (IDT Biologika, Dessau-Rasslau, Germany) and Gripovac (Merial, Lyon, France) against H1N1, H1N2, and H3N2 circulating SI viruses are used in approximately 5–25% of the pig farms in Belgium, Denmark, France, Spain, Italy, Poland, and Germany.

However, these vaccines do not protect against new viral strains and show poor efficacy in the field because of the evolution of the virus [9]. This lack of efficacy against mismatched strains has two consequences: (1) it requires frequent reformulation and production of influenza vaccines based on the prediction of strains that may circulate. While virological surveillance for human influenza A and B viruses is the cornerstone of the World Health Organisation vaccine selection process, a similar strategy for pig (and other) animal influenza vaccines is still lacking; and (2) in the event of the emergence of a completely novel reassortant virus, there is little or no efficacy leaving both swine and humans at high risk of infection with potential for pandemic spread. A further problem of WIV with oil-in-water adjuvants is enhanced respiratory disease and increased pathology, associated with immune complexes of low avidity or non-neutralising antibodies. Vaccine-associated enhanced respiratory disease (VAERD) has been observed in pigs when heterologous SI infection occurs after immunisation with mismatched WIV [10–13]. WIVs are also commonly used in pregnant sows to prevent SI infection in piglets [14]. In these circumstances, maternally derived antibodies can be detected in piglets up to 14 weeks after birth and levels correlate with protection against homologous infections [12]. However, after heterologous challenge WIV induced maternally-derived antibodies were associated with enhanced clinical signs [15].

2. Universal Influenza Vaccine/Heterotypic Immunity

A cross-protective "universal vaccine" would be an enormous advantage in preventing SI in pigs and reducing the zoonotic threat. The development of a "universal" or broadly protective influenza A vaccine depends on inducing immune responses to conserved components of the virus that either prevent infection or limit replication of virus after infection has occurred. The classical broad immunity detected in convalescent animals and humans is dominated by the latter, mediated by cross-reactive CD4 and CD8 T lymphocytes [16]. The phenomenon was first observed after the isolation of human influenza in the 1930s when ferrets that had recovered from swine influenza were immune to the human virus but did not make detectable cross-neutralising antibodies [17,18]. The term "partial heterotypic immunity" (also called "heterosubtypic") was introduced by Schulman and Kilbourne in 1965 who observed that mice infected with a H1N1 strain and subsequently challenged with a lethal H2N2 virus, had reduced viral titers in the lung, milder lung pathology, and decreased mortality in the absence of neutralizing antibodies [18]. Since then, studies in multiple animal models including non-human primates have observed reduction in viral load, lung pathology, weight loss and decreased mortality, but not infection, in the absence of detectable cross-neutralizing antibodies (reviewed in [19,20]).

Experimental infection and recovery from SI infection in pigs has also been shown to completely or partially protect against infection with another type of SI [21–24]. Post-infection immunity to H1N1 and/or H3N2 viruses conferred cross protection against H1N2 in pigs [23], in the absence of detectable haemagglutination inhibition and virus neutralising antibodies, although inhibitory anti-neuraminidase

(NA) antibodies were detected prior to infection with H1N2. In contrast a double vaccination with an inactivated H1N1 and H3N2 based vaccine did not confer significant cross-protection [25], highlighting the importance of active virus replication for the induction of heterosubtypic immunity in pigs, directed towards the conserved internal proteins [26]. In line with these findings partial protection was observed in pigs with infection-induced immunity against avian-like H1N1 upon challenge with H3N2, whereas pandemic (pdm)H1N1-immune pigs were not protected because the pdmH1N1 has a different set of internal genes from the challenge strain [22]. In another study pigs previously infected with H1N1, and subsequently challenged with H3N2, did not get fever, showed reduced virus shedding, and showed no transmission to contact pigs [21]. The observed heterosubtypic protection occurred in the absence of cross-reactive haemagglutination inhibition antibodies after primary infection, but correlated with increased serum immunoglobulins (Ig)G antibody levels against the conserved extracellular domain of matrix protein 2 (M2) and nasal nucleoprotein (NP)-specific IgA antibodies. In addition, increased numbers of CD8 T cells were observed in the lungs of pigs previously infected with H1N1 and challenged with H3N2. The extent of heterosubtypic protection varies greatly between studies partly because of the immunisation/challenge strategies used, as well as the degree of conservation of the internal genes between the strains used for immunisation and challenge.

In this review we shall discuss the importance of local lung immunity and the feasibility of making an effective SI universal vaccine.

3. Respiratory Tract Immunisation

For optimum induction of heterotypic immunity in experimental animals, virus infection of the lung is required, as opposed to infection of the upper respiratory tract or other peripheral sites [27,28]. Immunisation via the respiratory tract has been shown to be a highly effective means of immunising against influenza. A recent murine study that evaluated the capacity of inactivated influenza vaccine or live attenuated influenza vaccine (LAIV) to induce protective lung response showed that site specific productive infection is required. Interestingly intra-nasal administration of inactivated vaccine or parenteral administration of LAIV failed to elicit protective T cell responses, confirming the requirement for respiratory targeting of LAIV to establish cross-protection [29]. Experimentally, immunisation via the respiratory tract is also highly protective against several other pulmonary diseases in livestock, including bovine tuberculosis [30,31], respiratory syncytial virus in cattle [32] and porcine reproductive and respiratory syndrome virus [33].

Although it is clear that local mucosal immunity is critical for protection against respiratory tract diseases in most cases it is not known what part of the respiratory tract should be targeted to induce optimal protection. Even in non-human primates and humans, where a common respiratory mucosal system has been postulated [34,35], so that immunisation of any part of the respiratory tract might be expected to protect the whole tract, it is not clear whether immunisation of the upper (URT) or lower respiratory tract (LRT) is more effective. A number of studies in mice and ferrets with influenza vaccines show that the LRT is the best target for inhaled influenza vaccination [36,37]. Targeting the LRT and URT by inhalation with the candidate universal influenza vaccine S-FLU (a non-replicating, pseudotyped influenza virus where the viral RNA (vRNA) encoding the haemagglutinin (HA) was inactivated by suppression of the HA signal sequence) resulted in a high degree of cross-protection against H1 and H3 influenza strains in mice [38]. This confirms the studies of Lau et al. [27] showing that protection of mice from H5N1 influenza by LAIV requires delivery of vaccine to the lung as opposed to the URT alone. Neutralising Ab were not induced by S-FLU immunisation of mice, ferrets, or pigs [38–40], but strong local lung cellular immune responses were detected, which correlated with protection against challenge. S-FLU coated with H1 or H5 HA has also been administered to pigs to the LRT by aerosol or intra-tracheal methods [40]. The aerosol method was the most efficient in reducing virus titre in nasal swabs and lung tissue after live virus challenge with pandemic H1N1 virus in pigs [40]. Similar comparisons between intra-tracheal and aerosol delivery have been performed with

adenoviral vectored TB [30] or Ebola vaccines [41] in non-human primates and, in both cases, aerosol delivery offered superior protection compared to other mucosal routes.

4. Live Attenuated Influenza Vaccines

Currently, cold-adapted LAIVs administered by nasal spray, targeting the URT, have been approved for equine (FluAvert, MSD Animal Health, Milton Keynes, UK) and human species (FluMist/Fluenz, MedImmune Gaithersburg, MD, Maryland, US). Studies in young children suggest that LAIV is more protective than inactivated influenza vaccines in those not previously exposed to influenza or influenza vaccines, due to increased vaccine-induced T cell and/or secretory IgA responses. In adults with extensive and partially cross-reactive pre-existing influenza immunity, LAIV boosting of secretory IgA reactive with HA and non-HA antigenic targets expressed by circulating influenza strains, may be an important additional mechanism of vaccine-induced immunity [42]. FluMist was introduced for infants in the UK in 2013, although because of troubling results of recent effectiveness studies, it will not be used during the 2016–2017 vaccination season in the US. The reason for the apparent decreased effectiveness of LAIV as compared with the efficacy shown in the original studies is unclear [43], but it could be related to repeated immunisations and increased baseline immunity, which might interfere with vaccine-virus replication [44].

Experimental LAIV vaccines delivered by the intranasal route have been shown to be protective in pigs [45–48]. Eight segment SI virus harbouring two different HA (H1 and H3) was generated by replacement of the ectodomain of the NA with the ectodomain of a second HA (H3), thus creating a virus displaying two different HAs (H1 and H3) on the surface [49]. The resulting vaccine was attenuated in pigs and conferred reduction of fever and other clinical signs as well as decreasing gross lesions in the lungs after challenge with both H1 and H3 SI viruses. LAIVs carrying an elastase cleavage site [50,51], NS1 truncations [24], or temperature-sensitive mutations in the polymerase basic protein (PB) 2 and PB1 segments [45,47] all provide degrees of cross-protection after challenge with antigenically distinct viruses but from the same subtype. Sterilizing immunity with no transmission to naïve pigs, was achieved with the temperature sensitive LAIV as opposed to the NS1 truncated LAIV where transmission was not prevented [45]. Considerably high IgA antibody responses in nasal washes and bronchoalveolar lavage (BAL) against whole virus were found in LAIV-immunised pigs compared to inactivated vaccine groups. The elevated IgA levels alone did not determine sterilizing immunity as both tested LAIV vaccines induced equal titers, but only one prevented transmission, suggesting additional requirements for protection, such as induction of cell-mediated immunity [45]. Partial heterosubtypic protection with the LAIV vaccine carrying the elastase cleavage site was observed when the vaccine was administered in a prime/boost regime and challenged either intratracheally [50] or intranasally [46]. As in other studies with LAIV vaccines, cross reactive IgG in serum and IgA in BAL and nasal mucosa were detected. IFNγ secretion by lymph node cells could be induced by exposure to the heterologous challenge strain, suggesting that cell-mediated immunity was also involved in the cross protective effect. Similarly, in NS-1-truncated LAIV immunised animals, heterosubtypic T cell priming against the challenge strain was observed [24], however immune responses waned at 7–8 weeks post immunisation and recall responses of LAIV-immunised pigs were in general lower when compared to wild type-infected pigs or not different from naïve pigs. These results suggest that although LAIV offer partial cross-protection it is less efficient than infection with a live virus.

Clearly the route of delivery is very important for induction of local immunity. Intranasal delivery of a LAIV vaccine was more efficient in inducing mucosal antibodies when compared to intramuscular delivery [48]. It may also be that intra-nasal delivery in pigs is effective because a small proportion of the administered dose reaches some of the lung lobes, albeit most of the material delivered intra-nasally is deposited in the stomach and oesophagus [52]. Whether LAIVs will have much enhanced protective efficacy if deliberately delivered to the LRT requires thorough investigation to determine whether this is more efficient in inducing both homologous and heterologous protection against SI in pigs. However, despite major advances in aerosol vaccine delivery in humans [53] and some examples of

local delivery to livestock, no practical devices for aerosol delivery are yet available for farm animals in the field.

5. Safety and Danger of Re-Assortment of LAIV

LAIV given as a large droplet aerosol to the URT in humans still requires updating to keep pace with antigenic drift, implying that type specific antibody is the main mechanism of protection. By contrast when administered to the LRT in mice and ferrets it can act as a "universal" influenza vaccine by inducing a multi-component response that is cross-protective between group I (H5N1) and group 2 (H7N9) influenza viruses [39,54]. However, administration of LAIV by small droplet aerosol to the lung in humans (or other species) is strongly discouraged by the manufacturer [55], due to concerns that replication is not completely restricted at 37 °C. In addition pre-pandemic versions of LAIV contain full length versions of vRNAs encoding potentially pandemic HAs, which could reassort into seasonal influenza viruses in cases of dual infection. Similarly reassortment of LAIVs with wild-type swine strains is possible. Furthermore, mixing of different vaccines from different sources is common in the field and if two LAIV vaccines were to be mixed prior to administration to pigs, there is a chance that a wild type SI will be generated with gene segments derived from unmodified gene segments in each LAIV vaccine. This might lead to even more diversity of swine IAV strains or strains with increased zoonotic potential [6].

The universal vaccine candidate, S-FLU was designed to overcome these objections. It is based on the suppression of HA signal sequence, most of the coding sequence of the HA viral RNA is deleted. HA protein is provided from a transfected cell line by pseudotyping. This design allows infection by S-FLU to occur once only and replication of vaccine in the lung or nose is prevented, but all of the conserved viral proteins are expressed in the cytosol of S-FLU infected cells and available for antigen presentation to T lymphocytes [56]. S-FLU cannot replicate in the lung due to lack of a viable HA vRNA, and cannot donate a viable vRNA encoding HA because it does not contain any genetic information from the potentially pandemic virus, being only coated in HA protein. Another single-replication cycle universal vaccine candidate RedeeFlu (FluGen Inc, Madison, WI, USA) is based on the partial deletion of the M2 gene [57] and shown to elicit humoral, mucosal, and cell mediated immunity. The vaccine induced sterilising immunity to homosubtypic challenge, but although it protected mice against lethal heterosubtypic challenge it did not prevent viral replication in nasal turbinates and lung.

6. Immunological Mechanisms of Heterotypic Protection

Investigation of the immunological mechanisms mediating the cross protective heterotypic immunity in animal models revealed the role of CD8 and CD4 T-cells and has been reviewed in [20]. The specificity of the protective effect correlates with the conserved viral core antigens recognised by T cells [16,58,59] and protection can be transferred in mice with core protein-specific T cells, particularly class I restricted cytotoxic T lymphocytes [60,61]. A recent prospective study in humans also showed this correlation between cross-reactive CD8 T cell responses and protection from symptomatic infection during the H1N1 influenza pandemic [62,63], confirming earlier work from experimental challenges with influenza virus in humans [59,64].

Similar CD8 systemic responses against the internal NP and M proteins were induced in both pigs and humans after intra-muscular immunisation with a candidate universal Modified Vaccinia Ankara vaccine encoding NP and M1 proteins [65]. This vaccine has been tested in co-administration regimes with either HA protein or following prime boost with a chimpanzee adeno vector also expressing NP and M1 and was shown to induce T cell responses to NP and M1 in pigs. However, no challenge was performed. Whether CD8 cells induced by parenteral immunisation would have the same protective effect as CD8 cells induced by local pulmonary infection or immunisation remains to be established, although there are ongoing efforts to induce mucosal responses through systemic parenteral immunisation in other diseases [66,67]. Alternatively harnessing simultaneously both local

and systemic immunity might be an optimal strategy as immunisation against tuberculosis in mice and non-human primates has demonstrated [68,69].

However, despite the wealth of evidence for both CD4 and CD8 T cell mediated cross-protection in mice and humans, studies in pigs are very scarce. An immunoinformatic tool for predicting swine T cell epitopes identified highly conserved class I and class II epitopes among seven SI strains prevalent in US pig herds. The class I peptides were restricted to the external proteins, while responses to class II peptides were focused on epitopes derived from the internal proteins [70]. This is in contrast to humans in whom most cross-reactive CD8 and CD4 T cell epitopes are derived from internal influenza virus proteins. SI class I epitopes were also identified and tetramers developed in pigs following four repeated immunisations with different SI strains in incomplete Freund's adjuvant [71]. Further studies will be needed to evaluate whether epitope based vaccines will be able to reduce viral burden and morbidity.

The only studies analysing local and systemic immune responses following infection with SI by the pulmonary route, albeit intra-tracheal infection with high dose H1N2, revealed multifunctional T cells with diverse cytokine profiles and in vitro reactivity against heterologous influenza strains, supporting their potential to combat heterologous influenza virus infections in pigs [72,73]. Low frequency SI specific IFNγ producing CD4 and CD8 cells were detected in the lungs four days post-infection, reaching a peak at nine days post infection. At six weeks post-infection CD4 and CD8 memory T cells had accumulated in the lung tissues, but it is not known which epitopes these cells are targeting. Neither is it known whether natural infection induces cells which recognise the informatically defined epitopes.

7. Tissue-Resident Memory T Cells

T cell memory was previously considered to be mediated by recirculating memory cells able to pass from the blood to tissues and back to the blood via the lymph. It was not thought that the cells remained in tissues for more than few hours, nor that they divide in non-lymphoid tissues. However recent overwhelming evidence indicates the importance of local tissue-resident memory T cells (T_{RM}) in protective immunity. T_{RM} are a newly-defined subset of memory T cells generated following primary infection in tissues such as the respiratory tract, gastrointestinal tract and skin and they persist at these sites after the pathogen has been cleared by the immune response [74,75]. Upon subsequent infection, pathogen-specific T_{RM} cells mount a rapid local response that is independent of T cell recruitment from the blood. Surprisingly, sessile T_{RM} greatly outnumber recirculating T cells within non-lymphoid tissues [76]. They express homing molecules such as the integrin CD103 and the activation marker CD69, the latter indicating that these cells are dividing and likely express effector function. However, there is some phenotypic heterogeneity and overlap of phenotype with cells in blood and lymphoid tissues, so that T_{RM} are best defined by their inaccessibility from the blood stream. This has been elegantly demonstrated by the intravenous administration of labelled antibody, which identifies all intra-vascular, but not tissue-resident cells [76] and by experiments which prevent efflux of cells from lymph nodes so that recirculating cells cannot reach the tissues [77,78].

It is increasingly evident that lung T_{RM} play a major role in protective immunity against respiratory tract infections. In mice both CD4 and CD8 lung T_{RM}, induced by immunisation via the respiratory tract, mediate immunity against heterosubtypic influenza strains, enhancing viral clearance and survival after lethal challenge [29,77,79,80]. Influenza-specific T_{RM} are also present in most healthy humans [81,82]. After pneumonectomy for isolated tumours, histologically normal human lung tissue far from the tumours contains both CD4 and CD8 cells with diverse T cell receptors (TCR) that express CD69, produce TNFα and IFNγ and proliferate in response to influenza virus. T_{RM} were also found in a large survey of human tissues [83] and in BAL after respiratory syncytial virus infection [84].

The effector functions of T_{RM} remain incompletely understood, but may involve: (1) direct killing of pathogen-infected cells; (2) release of cytokines that render the surrounding environment non-permissive for pathogen replication; and (3) promoting recruitment of infection-fighting cells

from the circulation [75]. The only studies on the duration of cross reactive immunity mediated by T_{RM} have been performed in mice and have shown that heterosubtypic immunity was substantially reduced after seven months [77].

The few studies that have investigated how T_{RM} cells are induced and maintained have used mouse models. Factors necessary for the induction of T_{RM} are not currently well understood but both the route of antigen encounter and the nature of the antigen itself may play a crucial role [29]. However, despite these advances in mice and although T_{RM} cells have been identified in the human lung, we currently understand very little about the role of T_{RM} in any other species, how they are generated in response to infection or vaccination, or how best to induce them. There is no information on T_{RM} in pigs or other livestock, but it is to be expected that they play an important role in protection against SI in these species.

8. Mucosal Associated Invariant T Cells

Although conventional T cells are clearly important, the mucosal immune system contains other cell populations whose functions are less clear. One such population is the recently discovered mucosal associated invariant T cells (MAITs), which exhibit properties of both innate and adaptive cells, as do natural killer T cells and gamma delta T cells (reviewed in [85–87]). They are highly enriched in mucosal sites, including lungs, intestines and liver, but are also present in the periphery where they can make up between 1–10% of the total circulating lymphocytes. In humans, MAITs express the Va7.2-Ja33 chain of the T cell receptor, make up to ~10% of blood CD8 cells and detect riboflavin metabolites bound to the non-polymorphic major histocompatibility complex (MHC) class-I related protein, MR1.

MAITs are associated with protection from bacterial infections, but recently were shown to be activated by influenza virus through mechanisms independent of MR1-TCR engagement and mediated through IL-18 combined with IL-12, IL-15, and/or interferon-α/β, which are expressed by a range of antigen presenting cells and monocytes [88]. The importance of MAITs in influenza is suggested by the correlation of patient survival with a ~2.5 fold increase in total MAITs cell numbers. Here too, MAIT activation was highly dependent on secondary cytokine stimulation derived from monocytes and activation is primarily, but not entirely, IL18-dependent [89]. MAITs have been identified in sheep and cattle, but there is no published data on pigs, nor has the role of MAITs in SI been defined.

9. Antibody Mediated Cross-Protective Immunity

Protective humoral responses to influenza are usually associated with antibodies against its surface glycoproteins HA and NA and in the last decade many laboratories identified broadly cross-protective antibodies directed against the highly-conserved HA stalk domain that showed different levels of cross-reactivity towards group 1 [90–92], group 2 [93–95] or both group 1 and 2 viruses [96–99]. Multiple studies have shown that in vivo efficacy of broadly cross neutralising anti-stalk antibodies is dependent on Fc-dependent mechanisms, like antibody-dependent cytotoxicity, antibody-dependent cellular phagocytosis, and complement-dependent cytotoxicity. A problem related to the development of anti-stem antibodies is their variable neutralising potency against viruses belonging to different subtypes and the existence of natural escape mutants, although some exhibit unprecedented breadth and potency [100]. Vaccine strategies targeting antibodies to the conserved stalk region of HA involve "headless" HA although responses were suboptimal, probably because removal of the head domain destroyed important conformational epitopes, or destabilized the stem domain in such a way that it was no longer able to elicit protective antibody responses. An alternative approach uses a vaccine consisting of a chimeric HA structure made of the conserved HA stem domain of an H1 or H3 strain of influenza, capped with the HA head domain from an exotic zoonotic influenza strain that has not been previously encountered by the human population, most likely directing the recall responses to stimulate pre-existing stem-reactive memory B cells (reviewed in [101,102]).

A recent mouse study suggests that memory B cells specific for broadly neutralizing epitopes may reside in the lungs instead of in circulation or in secondary lymphoid organs. These lung-resident memory B cells were highly mutated, and were generated as a result of local persistent germinal centres that are responding to prolonged exposure to viral antigens found in the lung. These tissue-resident memory B cells provided robust protection against a drifted virus in a secondary challenge model, confirming their importance in generating a cross-reactive, broadly neutralizing antibody response against influenza [103]. Although these findings have not yet been confirmed in humans or livestock, it does suggest a role for tissue-resident memory B cells in providing broadly-neutralizing responses.

IgA has been implicated in host protection against influenza in several studies [104,105]. Polymeric forms of IgA in nasal washes from adults vaccinated intranasally with a WIV are very potent in neutralizing influenza virus [106]. Interestingly IgA can also intercept antigen within epithelial cells [107] and for example, in that way NP-specific IgA in the nasal mucosa in pigs after SI infection may contribute to virus clearance [21]. HA-specific IgA antibody responses in the nasal washes have been detected as early as four days after intranasal or intratracheal inoculation with SI in 50% of pigs [108]. Cells isolated from the nasal turbinates and lymphoid tissue of the soft palate were tested for their ability to secrete influenza virus-specific IgA or IgG [109]. Notably those cells produced IgA, whereas significantly less cells produced IgG. Most likely IgA-producing cells can also be isolated in pigs from the lungs as high titres of IgA were found in the BAL fluid. In mice protection from influenza correlated with influenza-specific IgA and IgG antibody secreting cells in the lung at the time of challenge [110]. Therefore, it is quite likely that a major contributor to the protective efficacy of LAIV vaccine is IgA produced in the local mucosa.

Recently the breadth and magnitude of Ab response directed against HA and NA has been determined in mice, guinea pigs and ferrets following sequential infections with H1N1 or H3N2 influenza viruses [111]. Guinea pigs developed high titres of broadly cross-reactive antibodies, while mice and ferrets exhibited narrower responses. When these were compared to the antibody responses after infection of humans with H1N1 or H3N2 a markedly broad response was found, with the cross-reactivity profiles dependent on the viral strain first encountered during childhood (original antigenic sin). Re-analysis of the Cleveland Family Study which monitored families before and during the pandemic of 1957 where a subtype shift from H1N1 to H2N2 occurred, did show significantly lower incident rates during the pandemic in adults that contracted symptomatic influenza before, compared to children [112]. Recently it was shown that childhood hemagglutinin imprinting conferred lifelong protection against severe infection and death from novel HA as long as the virus belonged to the same phylogenetic group as the one encountered first in an individual's life [113]. Better understanding of cross-reactive immunity in humans is important for the development of universal vaccine strategies that are designed to boost pre-existing antibodies to protective levels. However, there is surprising lack of information about the landscape of the antibody response in pigs, which are exposed to multiple SI and very often are infected with one or more different SI subtypes without overt disease, a situation that may reflect better the immune responses in humans with pre-existing immunity and a complicated history of exposure to influenza viruses.

However, the role of antibodies in protection needs further evaluation and caution, because of some evidence for enhancement of disease by antibody. VAERD was associated with the presence of high titre cross-reacting non-neutralizing antibodies targeting the conserved stem HA2 domain at a site adjacent to the fusion peptide. In the absence of neutralizing antibodies against the HA1 globular head of pdmH1N1, HA2 antibodies increased virus infection of MDCK cells in vitro and enhanced membrane fusion [114]. However, VAERD is mainly associated with WIV administered with oil-in-water adjuvant parenterally, and has not been reported after LAIV administration by the mucosal route [115]. Although an immune response against mismatched HA protein alone was enough to cause VAERD [116], it has been shown recently that NA inhibiting antibodies to the homologous NA were sufficient to abrogate it [117]. There clearly is a need to determine the relative contribution of all types of anti-influenza antibodies, rather than focusing only on those to the HA stem.

10. Conclusions

The global influenza community is in urgent need of a universal influenza vaccine capable of inducing durable cross-protection against a broad spectrum of influenza virus strains. Harnessing local T cell immunity is essential for the development of a practical and effective universal influenza vaccine. Vaccines that induce T cell mediated immunity reduce disease severity and may reduce or prevent transmission, but do not prevent infection. The evaluation, licensure and deployment of a vaccine not designed to prevent infection, but to limit the severity of disease, will be challenging, as it must show comparable or better efficacy than current vaccines. However, universal vaccines might substantially reduce the severity of infection and limit the spread of disease during outbreaks and could be used 'off the shelf' early in an outbreak or pandemic, before strain-matched vaccines are available. In contrast a universal vaccine based on antibody responses would prevent infection and broadly-neutralizing antibodies specific for the conserved stem domain of the HA have shown promise both from a therapeutic perspective, as well as for guiding vaccine design efforts. Since most studies of human broadly-neutralizing monoclonal antibodies have focused primarily on B cells isolated from blood samples, a focus on lung-resident memory B cells may provide greater insight into how to generate broadly neutralizing antibodies. Future delivery strategies must consider how to best boost lung-resident memory B cells to elicit potent broadly protective responses. Combining both approaches would be a viable strategy and only field trials will show whether a universal vaccine could induce sufficient herd immunity to be useful. It is important to be aware of the limitations of the animal models used to study universal vaccines. It is challenging to scale up from 25 g mice to 70 kg humans. Pigs of 10 to 60 kg approach the weight of humans and, therefore, have great potential as a translation tool for therapeutics, such as antibodies and vaccines. Swine are also natural hosts of influenza viruses and play a critical role in the emergence and epidemiology of novel and potentially zoonotic influenza viruses. They are, therefore, a powerful model to study immunity to influenza.

Conflicts of Interest: The authors disclose no conflict of interest.

References

1. Watson, S.J.; Langat, P.; Reid, S.M.; Lam, T.T.; Cotten, M.; Kelly, M.; Van Reeth, K.; Qiu, Y.; Simon, G.; Bonin, E.; et al. Molecular epidemiology and evolution of influenza viruses circulating within European swine between 2009 and 2013. *J. Virol.* **2015**, *89*, 9920–9931. [CrossRef] [PubMed]
2. Nelson, M.I.; Vincent, A.L. Reverse zoonosis of influenza to swine: New perspectives on the human-animal interface. *Trends Microbiol.* **2015**, *23*, 142–153. [CrossRef] [PubMed]
3. Smith, G.J.D.; Vijaykrishna, D.; Bahl, J.; Lycett, S.J.; Worobey, M.; Pybus, O.G.; Ma, S.K.; Cheung, C.L.; Raghwani, J.; Bhatt, S.; et al. Origins and evolutionary genomics of the 2009 swine-origin H1N1 influenza a epidemic. *Nature* **2009**, *459*, 1122–1125. [CrossRef] [PubMed]
4. Rajao, D.S.; Vincent, A.L. Swine as a model for influenza A virus infection and immunity. *ILAR J.* **2015**, *56*, 44–52. [CrossRef] [PubMed]
5. Janke, B.H. Influenza A virus infections in swine: Pathogenesis and diagnosis. *Vet. Pathol.* **2014**, *51*, 410–426. [CrossRef] [PubMed]
6. Vincent, A.L.; Perez, D.R.; Rajao, D.; Anderson, T.K.; Abente, E.J.; Walia, R.R.; Lewis, N.S. Influenza A virus vaccines for swine. *Vet. Microbiol.* **2016**. [CrossRef] [PubMed]
7. Lewis, N.S.; Russell, C.A. The global antigenic diversity of swine influenza A viruses. *Elife* **2016**, *5*, e12217. [CrossRef] [PubMed]
8. Sandbulte, M.R.; Spickler, A.R.; Zaabel, P.K.; Roth, J.A. Optimal use of vaccines for control of influenza A virus in swine. *Vaccines* **2015**, *3*, 22–73. [CrossRef] [PubMed]
9. Rahn, J.; Hoffmann, D.; Harder, T.C.; Beer, M. Vaccines against influenza A viruses in poultry and swine: Status and future developments. *Vaccine* **2015**, *33*, 2414–2424. [CrossRef] [PubMed]
10. Gauger, P.C.; Vincent, A.L.; Loving, C.L.; Lager, K.M.; Janke, B.H.; Kehrli, M.E.; Roth, J.A. Enhanced pneumonia and disease in pigs vaccinated with an inactivated human-like (delta-cluster) H1N2 vaccine and challenged with pandemic 2009 H1N1 influenza virus. *Vaccine* **2011**, *29*, 2712–2719. [CrossRef] [PubMed]

11. Gauger, P.C.; Vincent, A.L.; Loving, C.L.; Henningson, J.N.; Lager, K.M.; Janke, B.H.; Kehrli, M.E., Jr.; Roth, J.A. Kinetics of lung lesion development and pro-inflammatory cytokine response in pigs with vaccine-associated enhanced respiratory disease induced by challenge with pandemic (2009) A/H1N1 influenza virus. *Vet. Pathol.* **2012**, *49*, 900–912. [CrossRef] [PubMed]
12. Kitikoon, P.; Nilubol, D.; Erickson, B.J.; Janke, B.H.; Hoover, T.C.; Sornsen, S.A.; Thacker, E.L. The immune response and maternal antibody interference to a heterologous H1N1 swine influenza virus infection following vaccination. *Vet. Immunol. Immunopathol.* **2006**, *112*, 117–128. [CrossRef] [PubMed]
13. Souza, C.K.; Rajao, D.S.; Loving, C.L.; Gauger, P.C.; Perez, D.R. Age at vaccination and timing of infection do not alter vaccine-associated enhanced respiratory disease in influenza a virus-infected pigs. *Clin. Vaccine Immunol.* **2016**, *23*, 470–482. [CrossRef] [PubMed]
14. Vincent, A.L.; Ma, W.; Lager, K.M.; Janke, B.H.; Richt, J.A. Swine influenza viruses a north american perspective. *Adv. Virus Res.* **2008**, *72*, 127–154. [PubMed]
15. Rajao, D.S.; Sandbulte, M.R.; Gauger, P.C.; Kitikoon, P.; Platt, R.; Roth, J.A.; Perez, D.R.; Loving, C.L.; Vincent, A.L. Heterologous challenge in the presence of maternally-derived antibodies results in vaccine-associated enhanced respiratory disease in weaned piglets. *Virology* **2016**, *491*, 79–88. [CrossRef] [PubMed]
16. Doherty, P.C.; Kelso, A. Toward a broadly protective influenza vaccine. *J. Clin. Invest.* **2008**, *118*, 3273–3275. [CrossRef] [PubMed]
17. Francis, T.; Shope, R.E. Neutralization tests with sera of convalescent or immunized animals and the viruses of swine and human influenza. *J. Exp. Med.* **1936**, *63*, 645–653. [CrossRef] [PubMed]
18. Schulman, J.L.; Kilbourne, E.D. Induction of partial specific heterotypic immunity in mice by a single infection with influenza a virus. *J. Bacteriol.* **1965**, *89*, 170–174. [PubMed]
19. Epstein, S.L.; Price, G.E. Cross-protective immunity to influenza A viruses. *Expert Rev. Vaccines* **2010**, *9*, 1325–1341. [CrossRef] [PubMed]
20. Sridhar, S. Heterosubtypic T-cell immunity to influenza in humans: Challenges for universal T-cell influenza vaccines. *Front. Immunol.* **2016**, *7*, 195. [CrossRef] [PubMed]
21. Heinen, P.P.; de Boer-Luijtze, E.A.; Bianchi, A.T. Respiratory and systemic humoral and cellular immune responses of pigs to a heterosubtypic influenza a virus infection. *J. Gen. Virol.* **2001**, *82*, 2697–2707. [CrossRef] [PubMed]
22. Qiu, Y.; De Hert, K.; Van Reeth, K. Cross-protection against european swine influenza viruses in the context of infection immunity against the 2009 pandemic H1N1 virus: Studies in the pig model of influenza. *Vet. Res.* **2015**, *46*, 105. [CrossRef] [PubMed]
23. Van Reeth, K.; Gregory, V.; Hay, A.; Pensaert, M. Protection against a european h1n2 swine influenza virus in pigs previously infected with H1N1 and/or H3N2 subtypes. *Vaccine* **2003**, *21*, 1375–1381. [CrossRef]
24. Kappes, M.A.; Sandbulte, M.R.; Platt, R.; Wang, C.; Lager, K.M.; Henningson, J.N.; Lorusso, A.; Vincent, A.L.; Loving, C.L.; Roth, J.A.; et al. Vaccination with NS1-truncated H3N2 swine influenza virus primes T cells and confers cross-protection against an H1N1 heterosubtypic challenge in pigs. *Vaccine* **2012**, *30*, 280–288. [CrossRef] [PubMed]
25. Van Reeth, K.; Van Gucht, S.; Pensaert, M. Investigations of the efficacy of european H1N1- and H3N2-based swine influenza vaccines against the novel h1n2 subtype. *Veterinary Record* **2003**, *153*, 9–13. [CrossRef] [PubMed]
26. Reeth, K.V.; Brown, I.; Essen, S.; Pensaert, M. Genetic relationships, serological cross-reaction and cross-protection between H1N2 and other influenza a virus subtypes endemic in european pigs. *Virus Res.* **2004**, *103*, 115–124. [CrossRef] [PubMed]
27. Lau, Y.F.; Wright, A.R.; Subbarao, K. The contribution of systemic and pulmonary immune effectors to vaccine-induced protection from H5N1 influenza virus infection. *J. Virol.* **2012**, *86*, 5089–5098. [CrossRef] [PubMed]
28. S, F.d.S.G.; Donnelley, M. Studies in experimental immunology of influenza. Iv. The protective value of active immunization. *Aust. J. Exp. Biol. Med. Sci.* **1950**, *28*, 61–75.
29. Zens, K.D.; Chen, J.K.; Farber, D.L. Vaccine-generated lung tissue-resident memory T cells provide heterosubtypic protection to influenza infection. *JCI Insight* **2016**, *1*. [CrossRef] [PubMed]
30. Jeyanathan, M.; Shao, Z.; Yu, X.; Harkness, R.; Jiang, R.; Li, J.; Xing, Z.; Zhu, T. Adhu5ag85a respiratory mucosal boost immunization enhances protection against pulmonary tuberculosis in BCG-primed non-human primates. *PLoS ONE* **2015**, *10*, e0135009. [CrossRef] [PubMed]

31. Dean, G.S.; Clifford, D.; Whelan, A.O.; Tchilian, E.Z.; Beverley, P.C.; Salguero, F.J.; Xing, Z.; Vordermeier, H.M.; Villarreal-Ramos, B. Protection induced by simultaneous subcutaneous and endobronchial vaccination with BCG/BCG and BCG/adenovirus expressing antigen 85a against *Mycobacterium bovis* in cattle. *PLoS ONE* **2015**, *10*, e0142270. [CrossRef] [PubMed]
32. Taylor, G.; Thom, M.; Capone, S.; Pierantoni, A.; Guzman, E.; Herbert, R.; Scarselli, E.; Napolitano, F.; Giuliani, A.; Folgori, A.; et al. Efficacy of a virus-vectored vaccine against human and bovine respiratory syncytial virus infections. *Sci. Transl. Med.* **2015**, *7*, 300ra127. [CrossRef] [PubMed]
33. Binjawadagi, B.; Dwivedi, V.; Manickam, C.; Ouyang, K.; Torrelles, J.B.; Renukaradhya, G.J. An innovative approach to induce cross-protective immunity against porcine reproductive and respiratory syndrome virus in the lungs of pigs through adjuvanted nanotechnology-based vaccination. *Int. J. Nanomed.* **2014**, *9*, 1519–1535.
34. Bourdin, A.; Gras, D.; Vachier, I.; Chanez, P. Upper airway x 1: Allergic rhinitis and asthma: United disease through epithelial cells. *Thorax* **2009**, *64*, 999–1004. [CrossRef] [PubMed]
35. Hurst, J.R. Upper airway. 3: Sinonasal involvement in chronic obstructive pulmonary disease. *Thorax* **2010**, *65*, 85–90. [CrossRef] [PubMed]
36. Minne, A.; Louahed, J.; Mehauden, S.; Baras, B.; Renauld, J.C.; Vanbever, R. The delivery site of a monovalent influenza vaccine within the respiratory tract impacts on the immune response. *Immunology* **2007**, *122*, 316–325. [CrossRef] [PubMed]
37. Song, K.; Bolton, D.L.; Wei, C.J.; Wilson, R.L.; Camp, J.V.; Bao, S.; Mattapallil, J.J.; Herzenberg, L.A.; Herzenberg, L.A.; Andrews, C.A.; et al. Genetic immunization in the lung induces potent local and systemic immune responses. *Proc. Natl. Acad. Sci. USA* **2010**, *107*, 22213–22218. [CrossRef] [PubMed]
38. Powell, T.J.; Silk, J.D.; Sharps, J.; Fodor, E.; Townsend, A.R. Pseudotyped influenza A virus as a vaccine for the induction of heterotypic immunity. *J. Virol.* **2012**, *86*, 13397–13406. [CrossRef] [PubMed]
39. Baz, M.; Boonnak, K.; Paskel, M.; Santos, C.; Powell, T.; Townsend, A.; Subbarao, K. Nonreplicating influenza a virus vaccines confer broad protection against lethal challenge. *MBio* **2015**, *6*, e01487–01415. [CrossRef] [PubMed]
40. Morgan, S.B.; Hemmink, J.D.; Porter, E.; Harley, H.; Holly, H.; Aramouni, M.; Everett, H.E.; Brookes, S.; Bailey, M.; Townsend, A.M.; et al. Aerosol delivery of a candidate universal influenza vaccine reduces viral load in pigs challenged with pandemic H1N1 virus. *J. Immunol.* **2016**, *196*, 5014–5023. [CrossRef] [PubMed]
41. Meyer, M.; Garron, T.; Lubaki, N.M.; Mire, C.E.; Fenton, K.A.; Klages, C.; Olinger, G.G.; Geisbert, T.W.; Collins, P.L.; Bukreyev, A. Aerosolized ebola vaccine protects primates and elicits lung-resident T cell responses. *J. Clin. Invest.* **2015**, *125*, 3241–3255. [CrossRef] [PubMed]
42. Hoft, D.F.; Lottenbach, K.R.; Blazevic, A.; Turan, A.; Blevins, T.P.; Pacatte, T.P.; Yu, Y.; Mitchell, M.C.; Hoft, S.G.; Belshe, R.B. Comparisons of the humoral and cellular immune responses induced by live attenuated influenza vaccine and inactivated influenza vaccine in adults. *Clin. Vaccine Immunol.* **2017**, *24*. [CrossRef] [PubMed]
43. Belshe, R.B.; Mendelman, P.M.; Treanor, J.; King, J.; Gruber, W.C.; Piedra, P.; Bernstein, D.I.; Hayden, F.G.; Kotloff, K.; Zangwill, K.; et al. The efficacy of live attenuated, cold-adapted, trivalent, intranasal influenzavirus vaccine in children. *N. Engl. J. Med.* **1998**, *338*, 1405–1412. [CrossRef] [PubMed]
44. Treanor, J.J. Clinical practice. Influenza vaccination. *N. Engl. J. Med.* **2016**, *375*, 1261–1268. [CrossRef] [PubMed]
45. Loving, C.L.; Lager, K.M.; Vincent, A.L.; Brockmeier, S.L.; Gauger, P.C.; Anderson, T.K.; Kitikoon, P.; Perez, D.R.; Kehrli, M.E. Efficacy in pigs of inactivated and live attenuated influenza virus vaccines against infection and transmission of an emerging H3N2 similar to the 2011–2012 H3N2v. *J. Virol.* **2013**, *87*, 9895–9903. [CrossRef] [PubMed]
46. Masic, A.; Lu, X.; Li, J.; Mutwiri, G.K.; Babiuk, L.A.; Brown, E.G.; Zhou, Y. Immunogenicity and protective efficacy of an elastase-dependent live attenuated swine influenza virus vaccine administered intranasally in pigs. *Vaccine* **2010**, *28*, 7098–7108. [CrossRef] [PubMed]
47. Pena, L.; Vincent, A.L.; Ye, J.; Ciacci-Zanella, J.R.; Angel, M.; Lorusso, A.; Gauger, P.C.; Janke, B.H.; Loving, C.L.; Perez, D.R. Modifications in the polymerase genes of a swine-like triple-reassortant influenza virus to generate live attenuated vaccines against 2009 pandemic H1N1 viruses. *J. Virol.* **2011**, *85*, 456–469. [CrossRef] [PubMed]

48. Vincent, A.L.; Ma, W.; Lager, K.M.; Janke, B.H.; Webby, R.J.; Garcia-Sastre, A.; Richt, J.A. Efficacy of intranasal administration of a truncated ns1 modified live influenza virus vaccine in swine. *Vaccine* **2007**, *25*, 7999–8009. [CrossRef] [PubMed]
49. Masic, A.; Pyo, H.M.; Babiuk, S.; Zhou, Y. An eight-segment swine influenza virus harboring h1 and h3 hemagglutinins is attenuated and protective against H1N1 and H3N2 subtypes in pigs. *J. Virol.* **2013**, *87*, 10114–10125. [CrossRef] [PubMed]
50. Masic, A.; Booth, J.S.; Mutwiri, G.K.; Babiuk, L.A.; Zhou, Y. Elastase-dependent live attenuated swine influenza A viruses are immunogenic and confer protection against swine influenza A virus infection in pigs. *J. Virol.* **2009**, *83*, 10198–10210. [CrossRef] [PubMed]
51. Babiuk, S.; Masic, A.; Graham, J.; Neufeld, J.; van der Loop, M.; Copps, J.; Berhane, Y.; Pasick, J.; Potter, A.; Babiuk, L.A.; et al. An elastase-dependent attenuated heterologous swine influenza virus protects against pandemic H1N1 2009 influenza challenge in swine. *Vaccine* **2011**, *29*, 3118–3123. [CrossRef] [PubMed]
52. Hemmink, J.D.; Morgan, S.B.; Aramouni, M.; Everett, H.; Salguero, F.J.; Canini, L.; Porter, E.; Chase-Topping, M.; Beck, K.; Loughlin, R.M.; et al. Distinct immune responses and virus shedding in pigs following aerosol, intra-nasal and contact infection with pandemic swine influenza a virus, a(H1N1)09. *Vet. Res.* **2016**, *47*, 103. [CrossRef] [PubMed]
53. Low, N.; Bavdekar, A.; Jeyaseelan, L.; Hirve, S.; Ramanathan, K.; Andrews, N.J.; Shaikh, N.; Jadi, R.S.; Rajagopal, A.; Brown, K.E.; et al. A randomized, controlled trial of an aerosolized vaccine against measles. *N. Engl. J. Med.* **2015**, *372*, 1519–1529. [CrossRef] [PubMed]
54. Tannock, G.A.; Paul, J.A.; Barry, R.D. Relative immunogenicity of the cold-adapted influenza virus a/ann arbor/6/60 (a/aa/6/60-ca), recombinants of a/aa/6/60-ca, and parental strains with similar surface antigens. *Infect. Immun.* **1984**, *43*, 457–462. [PubMed]
55. Ambrose, C.S.; Coelingh, K.L. Small-particle aerosolization of live attenuated influenza vaccine virus. *J. Infect. Dis.* **2012**, *205*, 348–349. [CrossRef] [PubMed]
56. Townsend, A.R.; Gotch, F.M.; Davey, J. Cytotoxic T cells recognize fragments of the influenza nucleoprotein. *Cell* **1985**, *42*, 457–467. [CrossRef]
57. Sarawar, S.; Hatta, Y.; Watanabe, S.; Dias, P.; Neumann, G.; Kawaoka, Y.; Bilsel, P. M2sr, a novel live single replication influenza virus vaccine, provides effective heterosubtypic protection in mice. *Vaccine* **2016**, *34*, 5090–5098. [CrossRef] [PubMed]
58. Lee, L.Y.; Ha do, L.A.; Simmons, C.; de Jong, M.D.; Chau, N.V.; Schumacher, R.; Peng, Y.C.; McMichael, A.J.; Farrar, J.J.; Smith, G.L.; et al. Memory t cells established by seasonal human influenza a infection cross-react with avian influenza A (H5N1) in healthy individuals. *J. Clin. Invest.* **2008**, *118*, 3478–3490. [CrossRef] [PubMed]
59. Wilkinson, T.M.; Li, C.K.; Chui, C.S.; Huang, A.K.; Perkins, M.; Liebner, J.C.; Lambkin-Williams, R.; Gilbert, A.; Oxford, J.; Nicholas, B.; et al. Preexisting influenza-specific CD4+ t cells correlate with disease protection against influenza challenge in humans. *Nat. Med.* **2012**, *18*, 274–280. [CrossRef] [PubMed]
60. Yap, K.L.; Ada, G.L. The recovery of mice from influenza virus infection: Adoptive transfer of immunity with immune T lymphocytes. *Scand. J. Immunol.* **1978**, *7*, 389–397. [CrossRef] [PubMed]
61. Taylor, P.M.; Askonas, B.A. Influenza nucleoprotein-specific cytotoxic t-cell clones are protective in vivo. *Immunology* **1986**, *58*, 417–420. [PubMed]
62. Sridhar, S.; Begom, S.; Bermingham, A.; Hoschler, K.; Adamson, W.; Carman, W.; Bean, T.; Barclay, W.; Deeks, J.J.; Lalvani, A. Cellular immune correlates of protection against symptomatic pandemic influenza. *Nat. Med.* **2013**, *19*, 1305–1312. [CrossRef] [PubMed]
63. Hayward, A.C.; Wang, L.; Goonetilleke, N.; Fragaszy, E.B.; Bermingham, A.; Copas, A.; Dukes, O.; Millett, E.R.; Nazareth, I.; Nguyen-Van-Tam, J.S.; et al. Natural t cell-mediated protection against seasonal and pandemic influenza. Results of the flu watch cohort study. *Am. J. Respir. Crit. Care Med.* **2015**, *191*, 1422–1431. [CrossRef] [PubMed]
64. McMichael, A.J.; Gotch, F.M.; Noble, G.R.; Beare, P.A. Cytotoxic t-cell immunity to influenza. *N. Engl. J. Med.* **1983**, *309*, 13–17. [CrossRef] [PubMed]
65. Mullarkey, C.E.; Boyd, A.; van Laarhoven, A.; Lefevre, E.A.; Veronica Carr, B.; Baratelli, M.; Molesti, E.; Temperton, N.J.; Butter, C.; Charleston, B.; et al. Improved adjuvanting of seasonal influenza vaccines: Preclinical studies of mva-np+m1 coadministration with inactivated influenza vaccine. *Eur. J. Immunol.* **2013**, *43*, 1940–1952. [CrossRef] [PubMed]

66. Woodworth, J.S.; Cohen, S.B.; Moguche, A.O.; Plumlee, C.R.; Agger, E.M.; Urdahl, K.B.; Andersen, P. Subunit vaccine h56/caf01 induces a population of circulating CD4 T cells that traffic into the mycobacterium tuberculosis-infected lung. *Mucosal. Immunol.* **2016**. [CrossRef] [PubMed]
67. Su, F.; Patel, G.B.; Hu, S.; Chen, W. Induction of mucosal immunity through systemic immunization: Phantom or reality? *Hum. Vaccin Immunother.* **2016**, *12*, 1070–1079. [CrossRef] [PubMed]
68. Ronan, E.O.; Lee, L.N.; Beverley, P.C.; Tchilian, E.Z. Immunization of mice with a recombinant adenovirus vaccine inhibits the early growth of *Mycobacterium tuberculosis* after infection. *PLoS ONE* **2009**, *4*, e8235. [CrossRef] [PubMed]
69. Verreck, F.A.W.; Tchilian, E.Z.; Vervenne, R.A.W.; Sombroek, C.C.; Kondova, I.; Eissen, O.A.; Sommandas, V.; van der Werff, N.M.; Verschoor, E.; Braskamp, G.; et al. Variable bcg efficacy in rhesus populations: Pulmonary bcg provides protection where standard intra-dermal vaccination fails. *Tuberculosis* **2017**, *104*, 46–57. [CrossRef] [PubMed]
70. Gutierrez, A.H.; Loving, C.; Moise, L.; Terry, F.E.; Brockmeier, S.L.; Hughes, H.R.; Martin, W.D.; De Groot, A.S. In vivo validation of predicted and conserved T cell epitopes in a swine influenza model. *PLoS ONE* **2016**, *11*, e0159237. [CrossRef] [PubMed]
71. Pedersen, L.E.; Breum, S.O.; Riber, U.; Larsen, L.E.; Jungersen, G. Identification of swine influenza virus epitopes and analysis of multiple specificities expressed by cytotoxic T cell subsets. *Virol. J.* **2014**, *11*, 163. [CrossRef] [PubMed]
72. Talker, S.C.; Koinig, H.C.; Stadler, M.; Graage, R.; Klingler, E.; Ladinig, A.; Mair, K.H.; Hammer, S.E.; Weissenböck, H.; Dürrwald, R.; et al. Magnitude and kinetics of multifunctional CD4+ and CD8β+ T cells in pigs infected with swine influenza A virus. *Vet. Res.* **2015**, *46*, 52–68. [CrossRef] [PubMed]
73. Talker, S.C.; Stadler, M.; Koinig, H.C.; Mair, K.H.; Rodriguez-Gomez, I.M.; Graage, R.; Zell, R.; Durrwald, R.; Starick, E.; Harder, T.; et al. Influenza A virus infection in pigs attracts multifunctional and cross-reactive t cells to the lung. *J. Virol.* **2016**, *90*, 9364–9382. [CrossRef] [PubMed]
74. Park, C.O.; Kupper, T.S. The emerging role of resident memory T cells in protective immunity and inflammatory disease. *Nat. Med.* **2015**, *21*, 688–697. [CrossRef] [PubMed]
75. Mueller, S.N.; Mackay, L.K. Tissue-resident memory t cells: Local specialists in immune defence. *Nat. Rev. Immunol.* **2016**, *16*, 79–89. [CrossRef] [PubMed]
76. Steinert, E.M.; Schenkel, J.M.; Fraser, K.A.; Beura, L.K.; Manlove, L.S.; Igyarto, B.Z.; Southern, P.J.; Masopust, D. Quantifying memory cd8 t cells reveals regionalization of immunosurveillance. *Cell* **2015**, *161*, 737–749. [CrossRef] [PubMed]
77. Wu, T.; Hu, Y.; Lee, Y.T.; Bouchard, K.R.; Benechet, A.; Khanna, K.; Cauley, L.S. Lung-resident memory CD8 t cells (trm) are indispensable for optimal cross-protection against pulmonary virus infection. *J. Leukoc. Biol.* **2014**, *95*, 215–224. [CrossRef] [PubMed]
78. Connor, L.M.; Harvie, M.C.; Rich, F.J.; Quinn, K.M.; Brinkmann, V.; Le Gros, G.; Kirman, J.R. A key role for lung-resident memory lymphocytes in protective immune responses after BCG vaccination. *Eur. J. Immunol.* **2010**, *40*, 2482–2492. [CrossRef] [PubMed]
79. Teijaro, J.R.; Turner, D.; Pham, Q.; Wherry, E.J.; Lefrancois, L.; Farber, D.L. Cutting edge: Tissue-retentive lung memory cd4 t cells mediate optimal protection to respiratory virus infection. *J. Immunol.* **2011**, *187*, 5510–5514. [CrossRef] [PubMed]
80. Turner, D.L.; Bickham, K.L.; Thome, J.J.; Kim, C.Y.; D'Ovidio, F.; Wherry, E.J.; Farber, D.L. Lung niches for the generation and maintenance of tissue-resident memory t cells. *Mucosal. Immunol.* **2014**, *7*, 501–510. [CrossRef] [PubMed]
81. de Bree, G.J.; van Leeuwen, E.M.; Out, T.A.; Jansen, H.M.; Jonkers, R.E.; van Lier, R.A. Selective accumulation of differentiated CD8+ T cells specific for respiratory viruses in the human lung. *J. Exp. Med.* **2005**, *202*, 1433–1442. [CrossRef] [PubMed]
82. Purwar, R.; Campbell, J.; Murphy, G.; Richards, W.G.; Clark, R.A.; Kupper, T.S. Resident memory T cells (t(rm)) are abundant in human lung: Diversity, function, and antigen specificity. *PLoS ONE* **2011**, *6*, e16245. [CrossRef] [PubMed]
83. Sathaliyawala, T.; Kubota, M.; Yudanin, N.; Turner, D.; Camp, P.; Thome, J.J.; Bickham, K.L.; Lerner, H.; Goldstein, M.; Sykes, M.; et al. Distribution and compartmentalization of human circulating and tissue-resident memory t cell subsets. *Immunity* **2013**, *38*, 187–197. [CrossRef] [PubMed]

84. Jozwik, A.; Habibi, M.S.; Paras, A.; Zhu, J.; Guvenel, A.; Dhariwal, J.; Almond, M.; Wong, E.H.; Sykes, A.; Maybeno, M.; et al. Rsv-specific airway resident memory cd8+ t cells and differential disease severity after experimental human infection. *Nat. Commun.* **2015**, *6*, 10224. [CrossRef] [PubMed]
85. Napier, R.J.; Adams, E.J.; Gold, M.C.; Lewinsohn, D.M. The role of mucosal associated invariant T cells in antimicrobial immunity. *Front. Immunol.* **2015**, *6*, 344. [CrossRef] [PubMed]
86. Ussher, J.E.; Klenerman, P.; Willberg, C.B. Mucosal-associated invariant t-cells: New players in anti-bacterial immunity. *Front. Immunol.* **2014**, *5*, 450. [CrossRef] [PubMed]
87. Wong, E.B.; Ndung'u, T.; Kasprowicz, V.O. The role of mucosal-associated invariant T cells in infectious diseases. *Immunology* **2017**, *150*, 45–54. [CrossRef] [PubMed]
88. van Wilgenburg, B.; Scherwitzl, I.; Hutchinson, E.C.; Leng, T.Q.; Kurioka, A.; Kulicke, C.; de Lara, C.; Cole, S.; Vasanawathana, S.; Limpitikul, W.; et al. Mait cells are activated during human viral infections. *Nat. Commun.* **2016**, *7*, 11. [CrossRef] [PubMed]
89. Loh, L.; Wang, Z.F.; Sant, S.; Koutsakos, M.; Jegaskanda, S.; Corbett, A.J.; Liu, L.G.; Fairlie, D.P.; Crowe, J.; Rossjohn, J.; et al. Human mucosal-associated invariant t cells contribute to antiviral influenza immunity via Il-18-dependent activation. *Proc. Natl. Acad. Sci. USA* **2016**, *113*, 10133–10138. [CrossRef] [PubMed]
90. Corti, D.; Suguitan, A.L., Jr.; Pinna, D.; Silacci, C.; Fernandez-Rodriguez, B.M.; Vanzetta, F.; Santos, C.; Luke, C.J.; Torres-Velez, F.J.; Temperton, N.J.; et al. Heterosubtypic neutralizing antibodies are produced by individuals immunized with a seasonal influenza vaccine. *J. Clin. Invest.* **2010**, *120*, 1663–1673. [CrossRef] [PubMed]
91. Sui, J.; Hwang, W.C.; Perez, S.; Wei, G.; Aird, D.; Chen, L.M.; Santelli, E.; Stec, B.; Cadwell, G.; Ali, M.; et al. Structural and functional bases for broad-spectrum neutralization of avian and human influenza a viruses. *Nat. Struct. Mol. Biol.* **2009**, *16*, 265–273. [CrossRef] [PubMed]
92. Throsby, M.; van den Brink, E.; Jongeneelen, M.; Poon, L.L.; Alard, P.; Cornelissen, L.; Bakker, A.; Cox, F.; van Deventer, E.; Guan, Y.; et al. Heterosubtypic neutralizing monoclonal antibodies cross-protective against h5n1 and H1N1 recovered from human igm+ memory b cells. *PLoS ONE* **2008**, *3*, e3942. [CrossRef] [PubMed]
93. Henry Dunand, C.J.; Leon, P.E.; Kaur, K.; Tan, G.S.; Zheng, N.Y.; Andrews, S.; Huang, M.; Qu, X.; Huang, Y.; Salgado-Ferrer, M.; et al. Preexisting human antibodies neutralize recently emerged H7N9 influenza strains. *J. Clin. Invest.* **2015**, *125*, 1255–1268. [CrossRef] [PubMed]
94. Ekiert, D.C.; Friesen, R.H.; Bhabha, G.; Kwaks, T.; Jongeneelen, M.; Yu, W.; Ophorst, C.; Cox, F.; Korse, H.J.; Brandenburg, B.; et al. A highly conserved neutralizing epitope on group 2 influenza a viruses. *Science* **2011**, *333*, 843–850. [CrossRef] [PubMed]
95. Friesen, R.H.; Lee, P.S.; Stoop, E.J.; Hoffman, R.M.; Ekiert, D.C.; Bhabha, G.; Yu, W.; Juraszek, J.; Koudstaal, W.; Jongeneelen, M.; et al. A common solution to group 2 influenza virus neutralization. *Proc. Natl. Acad. Sci. USA* **2014**, *111*, 445–450. [CrossRef] [PubMed]
96. Corti, D.; Voss, J.; Gamblin, S.J.; Codoni, G.; Macagno, A.; Jarrossay, D.; Vachieri, S.G.; Pinna, D.; Minola, A.; Vanzetta, F.; et al. A neutralizing antibody selected from plasma cells that binds to group 1 and group 2 influenza a hemagglutinins. *Science* **2011**, *333*, 850–856. [CrossRef] [PubMed]
97. Dreyfus, C.; Laursen, N.S.; Kwaks, T.; Zuijdgeest, D.; Khayat, R.; Ekiert, D.C.; Lee, J.H.; Metlagel, Z.; Bujny, M.V.; Jongeneelen, M.; et al. Highly conserved protective epitopes on influenza b viruses. *Science* **2012**, *337*, 1343–1348. [CrossRef] [PubMed]
98. Nakamura, G.; Chai, N.; Park, S.; Chiang, N.; Lin, Z.; Chiu, H.; Fong, R.; Yan, D.; Kim, J.; Zhang, J.; et al. An in vivo human-plasmablast enrichment technique allows rapid identification of therapeutic influenza A antibodies. *Cell Host Microbe* **2013**, *14*, 93–103. [CrossRef] [PubMed]
99. Wu, Y.; Cho, M.; Shore, D.; Song, M.; Choi, J.; Jiang, T.; Deng, Y.Q.; Bourgeois, M.; Almli, L.; Yang, H.; et al. A potent broad-spectrum protective human monoclonal antibody crosslinking two haemagglutinin monomers of influenza a virus. *Nat. Commun.* **2015**, *6*, 7708. [CrossRef] [PubMed]
100. Kallewaard, N.L.; Corti, D.; Collins, P.J.; Neu, U.; McAuliffe, J.M.; Benjamin, E.; Wachter-Rosati, L.; Palmer-Hill, F.J.; Yuan, A.Q.; Walker, P.A.; et al. Structure and function analysis of an antibody recognizing all influenza a subtypes. *Cell* **2016**, *166*, 596–608. [CrossRef] [PubMed]
101. Cho, A.; Wrammert, J. Implications of broadly neutralizing antibodies in the development of a universal influenza vaccine. *Curr. Opin. Virol.* **2016**, *17*, 110–115. [CrossRef] [PubMed]
102. Krammer, F. Novel universal influenza virus vaccine approaches. *Curr. Opin. Virol.* **2016**, *17*, 95–103. [CrossRef] [PubMed]

103. Adachi, Y.; Onodera, T.; Yamada, Y.; Daio, R.; Tsuiji, M.; Inoue, T.; Kobayashi, K.; Kurosaki, T.; Ato, M.; Takahashi, Y. Distinct germinal center selection at local sites shapes memory b cell response to viral escape. *J. Exp. Med.* **2015**, *212*, 1709–1723. [CrossRef] [PubMed]
104. Renegar, K.B.; Small, P.A.; Boykins, L.G.; Wright, P.F. Role of iga versus igg in the control of influenza viral infection in the murine respiratory tract. *J. Immunol.* **2004**, *173*, 1978–1986. [CrossRef] [PubMed]
105. Taylor, H.P.; Dimmock, N.J. Mechanism of neutralization of influenza virus by secretory IGA is different from that of monomeric iga or igg. *J. Exp. Med.* **1985**, *161*, 198–209. [CrossRef] [PubMed]
106. Suzuki, T.; Kawaguchi, A.; Ainai, A.; Tamura, S.; Ito, R.; Multihartina, P.; Setiawaty, V.; Pangesti, K.N.; Odagiri, T.; Tashiro, M.; et al. Relationship of the quaternary structure of human secretory IGA to neutralization of influenza virus. *Proc. Natl. Acad. Sci. USA* **2015**, *112*, 7809–7814. [CrossRef] [PubMed]
107. Mazanec, M.B.; Coudret, C.L.; Fletcher, D.R. Intracellular neutralization of influenza virus by immunoglobulin a anti-hemagglutinin monoclonal antibodies. *J. Virol.* **1995**, *69*, 1339–1343. [PubMed]
108. Lee, B.W.; Bey, R.F.; Baarsch, M.J.; Larson, M.E. Class specific antibody response to influenza a H1N1 infection in swine. *Vet. Microbiol.* **1995**, *43*, 241–250. [CrossRef]
109. Larsen, D.L.; Karasin, A.; Zuckermann, F.; Olsen, C.W. Systemic and mucosal immune responses to H1N1 influenza virus infection in pigs. *Vet. Microbiol.* **2000**, *74*, 117–131. [CrossRef]
110. Jones, P.D.; Ada, G.L. Influenza-specific antibody-secreting cells and b cell memory in the murine lung after immunization with wild-type, cold-adapted variant and inactivated influenza viruses. *Vaccine* **1987**, *5*, 244–248. [CrossRef]
111. Nachbagauer, R.; Choi, A.; Hirsh, A.; Margine, I.; Iida, S.; Barrera, A.; Ferres, M.; Albrecht, R.A.; Garcia-Sastre, A.; Bouvier, N.M.; et al. Defining the antibody cross-reactome directed against the influenza virus surface glycoproteins. *Nat. Immunol.* **2017**, *18*, 464–473. [CrossRef] [PubMed]
112. Epstein, S.L. Prior H1N1 influenza infection and susceptibility of cleveland family study participants during the h2n2 pandemic of 1957: An experiment of nature. *J. Infect. Dis.* **2006**, *193*, 49–53. [CrossRef] [PubMed]
113. Gostic, K.M.; Ambrose, M.; Worobey, M.; Lloyd-Smith, J.O. Potent protection against H5N1 and H7N9 influenza via childhood hemagglutinin imprinting. *Science* **2016**, *354*, 722–726. [CrossRef] [PubMed]
114. Khurana, S.; Loving, C.L.; Manischewitz, J.; King, L.R.; Gauger, P.C.; Henningson, J.; Vincent, A.L.; Golding, H. Vaccine-induced anti-HA2 antibodies promote virus fusion and enhance influenza virus respiratory disease. *Sci. Transl. Med.* **2013**, *5*, 200ra114. [CrossRef] [PubMed]
115. Gauger, P.C.; Loving, C.L.; Khurana, S.; Lorusso, A.; Perez, D.R.; Kehrli, M.E.; Roth, J.A.; Golding, H.; Vincent, A.L. Live attenuated influenza a virus vaccine protects against a (H1N1) pdm09 heterologous challenge without vaccine associated enhanced respiratory disease. *Virology* **2014**, *471–473*, 93–104. [CrossRef] [PubMed]
116. Rajao, D.S.; Loving, C.L.; Gauger, P.C.; Kitikoon, P.; Vincent, A.L. Influenza a virus hemagglutinin protein subunit vaccine elicits vaccine-associated enhanced respiratory disease in pigs. *Vaccine* **2014**, *32*, 5170–5176. [CrossRef] [PubMed]
117. Rajao, D.S.; Chen, H.; Perez, D.R.; Sandbulte, M.R.; Gauger, P.C.; Loving, C.L.; Shanks, G.D.; Vincent, A. Vaccine-associated enhanced respiratory disease is influenced by haemagglutinin and neuraminidase in whole inactivated influenza virus vaccines. *J. Gen. Virol.* **2016**, *97*, 1489–1499. [PubMed]

© 2017 by the authors. Licensee MDPI, Basel, Switzerland. This article is an open access article distributed under the terms and conditions of the Creative Commons Attribution (CC BY) license (http://creativecommons.org/licenses/by/4.0/).

viruses

MDPI

Review

Porcine Rotaviruses: Epidemiology, Immune Responses and Control Strategies

Anastasia N. Vlasova [1,*], Joshua O. Amimo [2,3] and Linda J. Saif [1,*]

1 Food Animal Health Research Program, CFAES, Ohio Agricultural Research and Development Center, Department of Veterinary Preventive Medicine, The Ohio State University, Wooster, OH 44691, USA
2 Department of Animal Production, Faculty of Veterinary Medicine, University of Nairobi, Nairobi 30197, Kenya; jamimo@uonbi.ac.ke
3 Bioscience of Eastern and Central Africa, International Livestock Research Institute (BecA-ILRI) Hub, Nairobi 30709, Kenya
* Correspondence: vlasova.1@osu.edu (A.N.V.); saif.2@osu.edu (L.J.S.); Tel.: +1-330-263-3740 (A.N.V.); +1-330-263-3744 (L.J.S.)

Academic Editors: Simon Graham and Linda Dixon
Received: 20 February 2017; Accepted: 13 March 2017; Published: 18 March 2017

Abstract: Rotaviruses (RVs) are a major cause of acute viral gastroenteritis in young animals and children worldwide. Immunocompetent adults of different species become resistant to clinical disease due to post-infection immunity, immune system maturation and gut physiological changes. Of the 9 RV genogroups (A–I), RV A, B, and C (RVA, RVB, and RVC, respectively) are associated with diarrhea in piglets. Although discovered decades ago, porcine genogroup E RVs (RVE) are uncommon and their pathogenesis is not studied well. The presence of porcine RV H (RVH), a newly defined distinct genogroup, was recently confirmed in diarrheic pigs in Japan, Brazil, and the US. The complex epidemiology, pathogenicity and high genetic diversity of porcine RVAs are widely recognized and well-studied. More recent data show a significant genetic diversity based on the VP7 gene analysis of RVB and C strains in pigs. In this review, we will summarize previous and recent research to provide insights on historic and current prevalence and genetic diversity of porcine RVs in different geographic regions and production systems. We will also provide a brief overview of immune responses to porcine RVs, available control strategies and zoonotic potential of different RV genotypes. An improved understanding of the above parameters may lead to the development of more optimal strategies to manage RV diarrheal disease in swine and humans.

Keywords: Porcine rotavirus; group A, B, C, E and H rotaviruses; rotavirus vaccines; epidemiology; genetic variability; prevalence; active and passive immunity; swine; zoonotic potential

1. Introduction

Rotavirus (RV) is well established as a major cause of acute gastroenteritis in young children and animals, including nursing and weaned piglets [1]. The name "rotavirus" comes from the wheel-like virion appearance observed by electron microscopy. The virus is transmitted by the fecal–oral route and the infection results in destruction of mature small intestinal enterocytes [2]. RV-mediated damage is characterized by shortened villi with sparse, irregular microvilli and by mononuclear cell infiltration of the lamina propria [2]. Several mechanisms are suggested to contribute to the development of diarrhea including malabsorption due to the destruction of enterocytes, villus ischaemia, neuro-regulatory release of a vasoactive agent from infected epithelial cells. Also the RV non-structural protein 4 (NSP4) induces an age- and dose-dependent diarrheal response by acting as an enterotoxin and secretory agonist [2] (Figure 1) to: (i) stimulate Ca^{2+}-dependent cell permeability and (ii) alter the integrity of epithelial barrier.

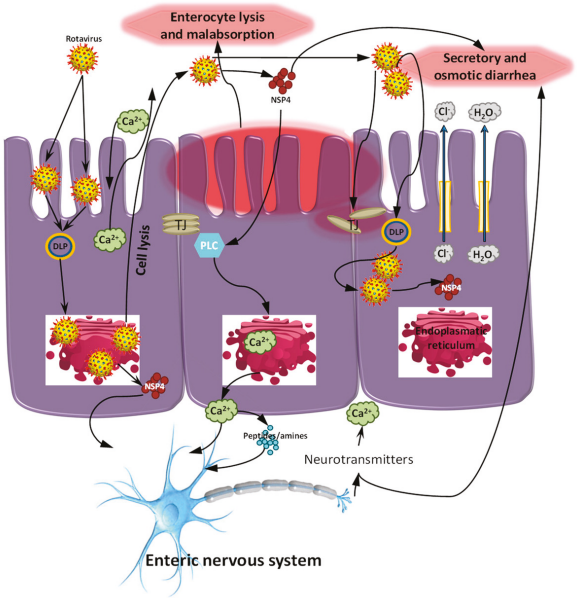

Figure 1. Potential mechanisms of rotavirus (RV) pathogenesis. RV replication inside enterocytes induces osmotic diarrhea. RV also increases the concentration of intracellular calcium (Ca^{2+}), disrupting the cytoskeleton and the tight junctions, increasing paracellular permeability. In addition, RV produces non-structural protein 4 (NSP4), an enterotoxin that induces Ca^{2+} efflux from endoplasmatic reticulum via the phospholipase C dependent (PLC) mechanism further contributing to electrolyte imbalance and secretory diarrhea. RV can also stimulate the enteric nervous system (ENS, via NSP4 dependent mechanism), further contributing to secretory diarrhea and increasing intestinal motility. Agents that can inhibit the ENS could be useful in alleviating RV diarrhea in children. Following, tryptic cleavage of viral protein 8 (VP8) from VP5, the VP8 fragment alters the localization of claudin-3, ZO-1 and occludin leading to the disruption of the barrier integrity of tight junctions (TJ) [3–6]. Late in the infectious process, RV destroys mature enterocytes, further contributing to malabsorptive or osmotic diarrhoea. RV antigens, genomic RNA and infectious particles have been found in the blood of children and blood and systemic organs in animals [7,8]. The role of systemic RV translocation in disease pathogenesis is currently unknown. DLP: double-layered particles.

RVs represent a genus in the *Reoviridae* family of double-stranded RNA (dsRNA) viruses, with a genome of 11 segments of dsRNA encoding six structural viral proteins (VP1–VP4, VP6 and VP7) and five nonstructural proteins (NSP1–NSP5/6). RVs are classified into 10 groups (A–J) based on antigenic relationships of their VP6 proteins, with provisional I and J species recently identified in sheltered dogs in Hungary and in bats in Serbia, respectively [9–12]. The outer capsid proteins, VP7 and VP4, induce neutralizing antibodies and form the basis for the G and P dual typing system [9]. The most common groups that infect humans and animals are groups A, B and C (RVA, RVB and RVC), with the highest prevalence of RVA strains that represent one of the most significant causes of acute dehydrating diarrhea from public health and veterinary health perspectives. To date, 27 different G- and 37 P-genotypes have been described in both humans and animals for RVAs [13,14]. For highly genetically diverse RVA strains, the dual (G/P) typing system was extended in 2008 to a full-genome sequence classification system, with nucleotide percent identity cut-off values established for all 11 gene segments, with the notations Gx-P[x]-Ix-Rx-Cx-Mx-Ax-Nx-Tx-Ex-Hx used for the VP7-VP4-VP6-VP1-VP2-VP3-NSP1-NSP2-NSP3-NSP4-NSP5/6 encoding genes, respectively [15].

Subsequently, a Rotavirus Classification Working Group (RCWG) was formed to set the RVA classification guidelines and maintain the proposed classification system [16] to facilitate complete classification of novel RVA strains. Currently, only RVA classification has been developed and is being maintained by the RCWG, while much less is known about the epidemiology and disease burden associated with infection by non-RVAs. However, RVB, RVC, RVE, RVH and RVI have been detected in sporadic, endemic or epidemic infections of various mammalian species, whereas RVD, RVF and RVG are found in poultry, such as chickens and turkeys [14,17–24]. RVs of groups A, B, C, E and H have been described in pigs [25–32].

In 1969, bovine RV was the first group A RV isolated in cell culture and confirmed as a cause of diarrhea in calves [33,34]. Human RV was discovered soon after, in 1973, by Bishop and colleagues [35]. Subsequent studies documented the widespread prevalence of RVA infections in young animals, including calves and pigs, and their association with diarrhea in animals <1 month of age [20,28,30,36,37]. Group C RVs were first isolated in piglets in 1980 [31] and were subsequently identified in other animals and humans [30,38–41]. Porcine RVB was first described as an RV-like agent identified in a diarrheic pig in the 1980s [29,42]. In addition to pigs, RVB strains have been also detected in cattle [43–46], lambs [47], and rats [48]. In contrast to human RVA and RVC that were described worldwide, human RVB strains have been described only in China [49–52], India [53,54], and Bangladesh [55–59]. An atypical group E porcine RV was only reported in UK swine, where a serological survey indicated a widespread distribution of antibodies to this virus in pigs older than 10 weeks [25,60]. Most recently, RVH strains were described in pigs in Japan, Brazil and in the US, where they were reportedly circulating since at least 2002 [27,61,62].

2. RV Genogroup/Genotype Classification and Prevalence in Swine

Infections by RVAs are confirmed in pigs worldwide with or without association with diarrhea [63–74]. RVA prevalence rates in pigs vary from 3.3% to 67.3% without evidence of seasonality, but with spatio-temporal fluctuations and re-emergence of certain genotypes, including G9 and G1 [67,71,75–87], with farm-level prevalence reaching 61%–74% [73,74]. Twelve G genotypes (G1 to G6, G8 to G12, and G26) and 16 P genotypes (P[1] to P[8], P[11], P[13], P[19], P[23], P[26], P[27], P[32], and P[34]) of RVA have been associated with pigs [65,67,70,72–74,84,88–91]. However, G3, G4, G5, G9 and G11 were historically considered the most common G genotypes in swine and were usually associated with P[5], P[6], P[7], P[13] and P[28] [16,89,92].

Similar to RVA, porcine RVCs are reported in most parts of the world [32,39]. Diarrhea outbreaks associated with RVCs have been documented in nursing, weaning and post-weaning pigs [31,32,93], either alone or in mixed infection with other enteric pathogens [1]. In addition, the antibody prevalence in pigs (58%–100%) shows that RVC infection may be very common and has circulated for many decades in swine herds in developed countries [32]. Recent studies on US and Canadian porcine samples demonstrated a 46% prevalence of RVC which was higher in very young (78%, $\leq$3 day old) and young (65%, 4–20 day old) piglets [94]. RVC genotypes G1 and G3 were initially assigned to the prototype porcine RVC Cowden and HF strains, respectively [95]. Further efforts to classify RVC strains into sequence-based genotypes resulted in identification of a total of nine G genotypes (G1–G9), seven P genotypes (P1–P7) and seven I genotypes (I1–I7) [94,96–100]. Additional attempts were made to extend RVC classification based on the sequencing of all 11 genes [101,102]; however, only limited genomic sequences are currently available. Porcine RVCs belong to G1, G3, G5–G9 genotypes and a newly described G10 genotype [103], while bovine and human RVCs are classified as G2 and G4 genotypes, respectively [94,96,97,104]. Additionally, two provisional G genotypes (G12 and G13 based on the 86% nucleotide identity cut-off value) are proposed by Niira et al. based on their recent results [105].

Rapid molecular characterization of RVB strains is hampered by the difficulty of adapting RVB strains to cell culture [32,58]. Additionally, limited and variable fecal shedding and instability in feces were shown for RVBs [44]. Complete genome sequences were obtained for several human RVB

strains from Southeast Asia [55,106–108] and partial genome sequencing was done for several rat and bovine RVB strains [43–46,48,53,57,109]. Kuga and colleagues analyzed sequences of the VP7 gene of 38 porcine RVB strains from Japan (2000–2007) and the five genotypes proposed were further divided into 12 clusters, using 67% and 76% nucleotide cut-off values (66% and 79% on the amino acid level, respectively) [110]. Recent results by Marthaler et al. suggested a broader diversity of porcine RVBs based on sequencing of the VP7 gene of 68 RVB strains (collected in 2009 from 14 US states and Japan) defining 20 G genotypes based on an 80% nucleotide identity cut-off value and providing the first evidence that porcine RVB genotypes may be host species- and region-specific [111]. Therefore, porcine RVB strains of genotypes G1, G2 and G3/G5 are only found in rats, humans and bovine species, respectively, while genotypes G4, G7, G9, G13, G15 and G19 are only confirmed in pigs in Japan, and a small number of porcine RVB strains of genotypes G10 and G17 are only found in the US. An additional G genotype, G21, was detected in pigs in India [112].

Three human RVH strains from Asia (ADRV-N, J19, B219) [113–116] and a porcine RVH strain (SKA-1) were identified during 1997–2002 [27]. In 2012, three more porcine RVH strains BR63, BR60, and BR59 from Brazil were identified [62]. Surprisingly high prevalence (15%) of porcine RVH strains was recently demonstrated by Marthaler and colleagues mostly in older (21–55 days old) piglets [18]. Their data suggested that porcine RVH strains circulated in the US herds since at least 2006 and that they are evolutionarily distinct from those of humans, as well as from porcine RVH strains in Brazil and Japan [18]. Complete genome analyses of a porcine RVH identified in South Africa showed that the novel RVH strain MRC-DPRU1575 clustered together with the SKA-1 strain and known porcine RVH strains from Brazil and the USA (only for available genome segments) [117]. However, it was only distantly related to human RVH strains from Asia and an RVH-like strain recently detected in bats from Cameroon [117].

Additional data is needed to evaluate the epidemiological importance of porcine RVE strains, because porcine RVE has only been identified in the UK approximately 3 decades ago and has not been reported to expand its geographic or host range since [25].

3. Porcine RV Distribution, Genotype Prevalence and Spatio-Temporal Variations in the Americas

3.1. North America

A high prevalence of porcine RV strains of groups A, B and C among samples from diarrheic piglets collected in 2009–2011 in the US, Canada and Mexico was reported by Marthaler et al. (2014) and Homwong et al. (2016) [69,71]. The highest overall prevalence of porcine RVs of 82.1% (90%–100% for UT, PA, VA and NC, and 5%–90% for the rest of the states) was observed in the US, and similar values of 79.7% and 73.3% are reported for Canada and Mexico, respectively. In the US, the highest proportion of RVA positive samples (70.1%) was in the Southeastern states, whereas the highest detection rate of RVB and RVC samples was found in the South-central states (34.2% and 62.2%, respectively); however no genotyping results were reported. The historic prevalence of porcine RVA, RVB and RVC strains in the US was reported as 67.8%, 10.0% and 11.1%, respectively [26]. A systematic review by Papp and colleagues [72] summarized genotype prevalence and distribution for porcine historic samples collected/analysed between 1976 and 2011 from both diarrheic and non-diarrheic animals. The most prevalent G type of porcine RVA in the Americas was G5 (71.4%), followed by G4 (8.2%), G3 (3.57%), G9 (2.31%) and G11 (1.9%) [68,72,82,118] (Figure 2). The frequencies of infections by other RVA genotypes found in pigs (G1, G2, G6, G8 and G10) were ~1% or less. P[7] genotype was the most common in the Americas (77.2%), while other P-types represented less than 1% of the identified RVA strains [72]. Finally, G5P[7] was the single most prevalent combination. In contrast, the analysis of more recent US RVA strains (2004–2012) conducted by Amimo and colleagues demonstrated that the dominant G-P combination was G9P[13] found in 60.9% of positive samples [from Ohio (OH) North Carolina (NC) and Michigan (MI)], followed by G9P[7] (8.7%), G4P[13] (8.7%), G11P[13] (4.3%), and G11P[7] (4.3%), while no G5 strains were detected [67]. Additionally, despite the relatively low overall prevalence of

porcine RVA strains in samples from US diarrheic and non-diarrheic animals of 9.4%, Amimo et al. reported that there was an increase in RVA detection from 5.9% in 2004 to 13.8% in 2012 [67], which may be due to the increase in the prevalence of novel or re-emerging genotypes (such as G9) because of lack of herd immunity against them.

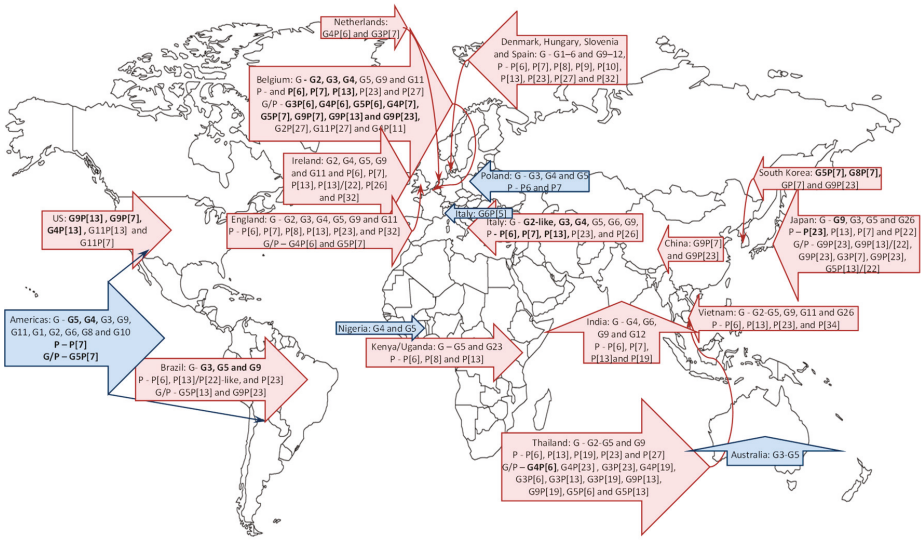

Figure 2. Global genotype distribution of porcine RVA strains reported in historic (1976–2011, blue figure arrows) and current (after 2000, pink figure arrows) studies. Porcine RVAs are also detected in Germany and Russia, but no genotyping data is available.

An earlier study by Kim et al. (1999) identified porcine RVC strains associated with diarrheal outbreaks in feeder pigs in the US [93]. Although the porcine RVC prevalence was not evaluated in this study, phylogenetic analysis demonstrated that the identified strains were more closely related to Cowden (G1) and more distant to HF (G3) strains. Recently, Amimo et al. reported a higher overall prevalence of porcine RVC strains compared to that of porcine RVA strains (19.5% versus 9.4%) in diarrheic and non-diarrheic piglets collected from several farms in the US (OH, NC and MI) in 2004–2012 [119]. In this study, the frequency of porcine RVC identification in the samples from diarrheic was higher than that in non-diarrheic piglets. The porcine RVC strains were confirmed as G3 and G6 in this study (Figure 3). Further, Marthaler analyzed 7520 porcine fecal samples (collected in 2009–2011 in the US and Canada) and identified RVC in 46% of the samples tested [94]. The porcine RVC prevalence was 16% in very young pigs (<3 days old), 21% in young pigs (4–20 days old), 42% in post-weaning pigs (21–55 days old), 13% in older pigs (455 days old), and 8% in pigs of unknown age. However, single porcine RVC infection prevalence was highest in very young (<3 days), and young pigs (4–22 days) in 78% and 65% of the RVC positive samples, respectively, whereas this percentage was much lower (6%–39%) in the older age groups. The most common VP7 genotype detected in this study was G6 (70%), followed by G5 (17%), G1 (12%), and G9 (1%); however, unlike in the study conducted by Amimo et al., no G3 strains were identified. These data suggest that despite the limited genotyping information available for porcine RVC strains, there was a possible shift in their prevalence from G1 and G3 genotypes associated with the prototype Cowden and HF strains to G6 and G5 genotypes.

The current knowledge of the genetic diversity of porcine RVB strains is mostly from two studies: Kuga et al. (2009) and Marthaler et al. (2012) from Japan and the US, respectively. They classified the existing porcine RVB strains into 20 G genotypes [110,111] (Figure 3). Due to the limited information

on porcine RVB epidemiology, it is hard to provide an accurate statistics on the temporal fluctuations in porcine RVB prevalence and porcine RVB genotype distribution in the North and South Americas. However, the new findings reported by Marthaler suggest an increased porcine RVB prevalence (46.8%) in the US that was previously observed by others elsewhere and in the US [67,104,110,112], and demonstrate that remarkably diverse porcine RVB genotypes (10 G genotypes: G6, G8, G10, G11, G12, G14, G16, G17, G18 and G20 associated with various I genotypes) are currently circulating in the US, with G8, G12, G16, G18 and G20 genotypes being most prevalent [111].

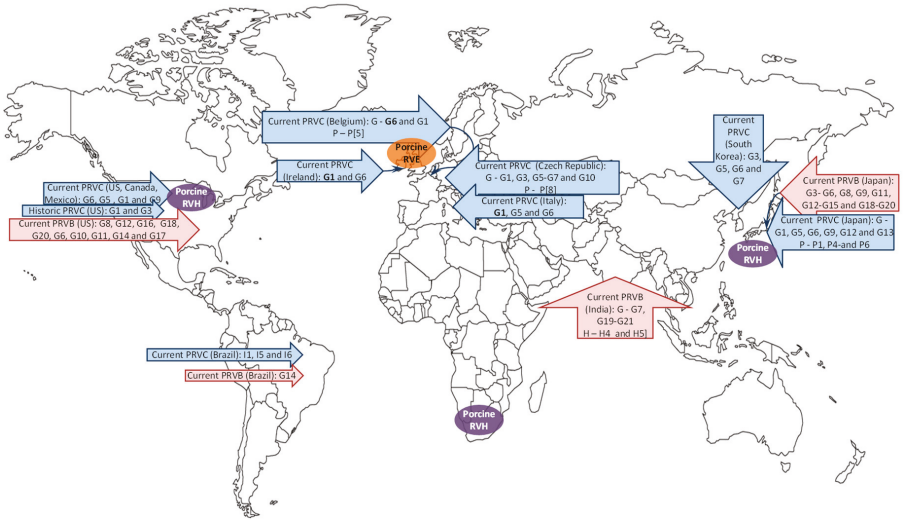

Figure 3. Global genotype distribution of porcine RVB (pink figure arrows) and RVC (blue figure arrows) strains and porcine RVE (bolded, orange circle)/RVH (bolded, purple circles) occurrence in different countries reported in historic (1976–2011) and current (after 2000) studies. Porcine RVCs are also detected in Germany and China, and porcine RVB is confirmed in Germany and Czech Republic, but no porcine RVC/RVB genotyping data is available for these countries.

3.2. South America

As reported for the US, G5, G4 and G9 genotypes of porcine RVA were most prevalent in Brazil and Argentina, with G5P[7] being the single most prevalent combination [68,72,82]. Similar to findings by Marthaler and Amimo, recent findings by Molinari (on samples collected from a single diarrheic outbreak in Brazil in a G5P[7] vaccinated herd in 2012) demonstrated that porcine RVC (78%) was the most prevalent group found in single (34%) and mixed (44%) infections, followed by porcine RVA (46%), RVB (32%), and RVH (18%) [112]. The porcine RVA genotypes detected were G5P[13] and G9P[23], that differed from the G5P[7] found in the vaccine. Another recent study from Brazil (2011–2012) demonstrated co-circulation of G3, G5, G9, and P[6], P[13]/P[22]-like, and P[23] genotypes [120], but with no indication of the historic G5P[7] genotype combination. These findings may indicate that application of the G5P[7] based porcine RVA vaccines in North and South America might have contributed to the previously reported increased prevalence of the G5P[7] strains, while subsequently developed herd immunity and selective pressure against the G5P[7] strains, resulted in their recent decline (or disappearance) and emergence of the G9 or reassortant variants. Similar to the findings by Marthaler [94], Molinari reported an increased prevalence of porcine RVC strains in Brazil in diarrheic piglets in a herd vaccinated with porcine RVA G5P[7] vaccine [112]. The VP6 gene sequence analysis demonstrated that the RVC strain possessed an I1 genotype like Cowden; however, G and P types

were not determined. Another study from Brazil, confirmed the presence of three I genotypes (I1, I5, and I6) in the samples from diarrheic piglets (2004–2010) suggesting that diverse porcine RVC strains circulate in different Brazilian states [98]. Additionally, Molinari et al. reported porcine RVB genotype G14 in diarrheic pigs in Brazil, as also reported by Kuga and Marthaler [110–112].

4. Global Porcine RV Distribution and Genotype Prevalence: Africa, Europe, Asia and Australia

4.1. Africa

The presence of group A, B, C and H porcine RVs has been confirmed in several African countries [65,117,121–123]. The prevalence of porcine RVA in Kenya and Uganda reported in the recent study by Amimo et al. of 26.2% [65] was higher compared to the prevalence rates of 6.5%–25.7% reported for samples collected in 2004–2011 in the USA [65], several European countries [75,84,85], Thailand [89], and India [124], but however, lower (32.7%–38.3%) to those observed in Vietnam [74], Brazil [80] and Korea [76]. It was lower than that reported for samples collected in the US in 2009–2011 [69], in asymptomatic pigs in Italy (71.5%) [70] or previously reported for South Africa (84.6%) [123]. This study provides the first evidence that porcine RVA infections are widespread and likely endemic in East African pig herds. The 18 characterized African porcine RVA strains were classified into three different P-types including P[6], P[8] and P[13] that were associated with G5 and G23 G-types [65] (Figure 2). An increased prevalence of porcine RVA strains in diarrheic and asymptomatic suckling and weaned piglets of 41.8% was also reported in Tanzania (2014), but the identified porcine RVA positive samples were not genotyped [125]. Interestingly, although previous attempts to characterize porcine RVA strains from piglets in Nigeria by classical serotyping methods demonstrated the presence of G4 and G5 types, substantial numbers of the strains from that study was non-typeable [122]. These findings indicate that phylogenetically distinct porcine RVA genotypes/strains may circulate in African countries together with the historically common (G4 and G5) genotypes and warrants further epidemiological investigation.

Apart from some data on porcine RVB and RVC prevalence in Africa reported by Geyer et al. nearly three decades ago [123], the absence of surveillance programs and adequate diagnostic facilities have resulted in a lack of data on porcine RVB and RVC prevalence and genetic composition [65]; however, recently Amimo and colleagues demonstrated 8.3% (37/446) prevalence of porcine RVC in swine populations in Kenya (8.8%) and Uganda (7.7%) (Amimo et al., 2014, unpublished data).

A recent discovery and characterization of a porcine RVH strain from diarrheic piglets in South Africa confirmed that it was closely related to Japanese, Brazilian and the US porcine RVH, but not human RVH or bat (RVH-like) strains [117,121].

4.2. Europe

Diarrhea associated with RVA, RVB and RVC infections in pigs is an important cause of increased mortality, growth impairment, and economic losses in Europe [73,85,126,127]. porcine RVA strains of G2, G3, G4, G5, G9 and G11 and P[6], P[7], P[13], P[23] and P[27] genotypes were isolated from feces of diarrheic and non-diarrheic Belgian piglets in 2012 [128] (Figure 2). A wide range of G/P genotype combinations including; G3P[6], G4P[6], G5P[6], G4P[7], G5P[7], G9P[7], G9P[13] and G9P[23] was commonly detected in stool samples of diarrheic and non-diarrheic pigs in Belgium. Additionally, uncommon genotypes/genotype combinations were reported; G2P[27], G11P[27] and G4P[11]. During a large surveillance study in Italy (2003–2004), a total of 751 fecal samples were collected from nursing and weaned pigs involved in outbreaks of diarrhea [70]. Porcine RVA prevalence of 16.1% was identified by electron microscopy or by a commercial immunoenzyme assay. Upon either PCR genotyping or sequencing, the porcine RVA strains displayed a broad spectrum of VP7 and VP4 types, including G2-like, G3, G4, G5, G6, G9, P[6], P[7], P[13], P[23], and P[26] [70,129,130]. However, an earlier study by Martella et al. (2001) demonstrated that porcine stool samples collected in Northern Italy during a massive diarrheal outbreak in 1983–1984 contained porcine RVA strains of

G6P[5] genotype combination [127]. Furthermore, Midgley et al. (2012) analyzed a total of 1101 fecal samples from pigs collected from 134 swine farms in four European countries (Denmark, Hungary, Slovenia and Spain) in 2003–2007 [85]. The results demonstrated that porcine RVA prevalence in Danish swine was only 10% although all samples were collected from diarrheic animals. In contrast, in Slovenia where the majority of swine were asymptomatic, the porcine RVA detection rate (20%) was significantly higher than that in swine with diarrhea in Denmark. This is consistent with the results by Amimo et al. [67] showing that unlike porcine RVC [119], there was no strong association between diarrhea and porcine RVA prevalence in nursing and suckling piglets in the US. However, in Spain, porcine RVA infections were significantly more frequent in animals with diarrhea (27%) than in asymptomatic animals (7%) [75]. Among these porcine RVA positive samples, ten different G types, G1–6 and G9–12, and nine different P types, P[6], P[7], P[8], P[9], P[10], P[13], P[23], P[27], P[32], were detected. No single G type was found to be dominant across the participating countries. In Slovenia G3, G4, and G5 were all common genotypes detected in 19%–30% of the samples. In Denmark, G4 was the most common genotype (44%). G9 was only detected in Spain, where it was the most prevalent genotype (33%). Among the various P types, only P[6] was detected in all four countries, which was the most common type in both Slovenia (41%) and in Denmark (56%). Otto et al. (2015) reported a porcine RVA prevalence of 51.2%, but no genotyping data was available from this study [126]. Finally, of the three positive porcine RVA samples identified in the Netherlands in 1999–2001, two were determined to possess G4P[6] and one G3P[7] genotype constellations [131]. Collins et al. tested 292 fecal samples collected from 4–5- to 8–9-week-old asymptomatic pigs in Ireland (2005–2007) and showed that 6.5% samples were positive for porcine RVA [84]. By sequence analysis of the VP7 and VP4 (VP8*) genes, the Irish porcine RVA strains were identified as G2, G4, G5, G9 and G11 and P[6], P[7], P[13], P[13]/[22], P[26] and P[32] genotypes, respectively [84]. The G5 and G11 strains were closely related to other human and porcine G11 strains, while the G2 and G9 strains resembled porcine G2 viruses detected recently in Europe and southern Asia. However, the G4 strains were only distantly related to other G4 human and animal strains, constituting a separate G4 VP7 lineage. Winiarczyk et al. (2002) identified G3, G4 and G5 types in combination with P6 and P7 types circulating in Poland [118]. Thus, in most European countries no dominant porcine RVA genotype/genotype constellations or temporal fluctuations in their prevalence was identified; however, the findings by Martella from different years suggest some epidemiological changes over time in Italy: disappearance of G6P[5] genotype constellation in more recent compared to historic studies [70,127]. A study conducted in England between 2010 and 2012 on samples from diarrheic pigs also revealed the presence of a wide range of porcine RVA genotypes: six G types: G2, G3, G4, G5, G9 and G11 and six P types: P[6], P[7], P[8], P[13], P[23], and P[32] [132]. G4 and G5 were the most common VP7 genotypes, accounting for 25% (16/64) and 36% (23/64) of the strains, respectively, while P[6] (33%, 21/64) and P[32] (27%, 17/64) were the most common VP4 genotypes, respectively. Overall, the most common genotype combinations were G4P[6] and G5P[7], similar to those detected in the historic US samples emphasizing the current unique epidemiology of porcine RVA in England compared to other European countries.

Porcine RVC strains have been detected in feces of asymptomatically infected 4–5 week old Irish pigs (in 2005–2007) and of diarrheic piglets from the Czech Republic at low rates of 4.4% (of 292 samples) and 4.6% (of 329 samples) [104,133]. In comparison 29% and 31% of diarrheic piglets in Belgium (2014) and Germany (1999–2011), respectively, were porcine RVC positive in recent studies [73,126]. All Belgian porcine RVC strains characterized in the study belonged to genotype G6, except for one strain possessing the G1 genotype, while the VP4 genes were genetically heterogeneous, but were classified in the genotype P5 [73] (Figure 3). The majority of the Irish porcine RVC strains were identified as G1 genotype, while only two strains belonged to the genotype G6 [104] and the German porcine RVC strains were not typed [126]. A higher genetic heterogeneity was reported among Czech porcine RVC strains that were grouped into six G genotypes (G1, G3, G5–G7, and a newly described G10 genotype) based on an 85% nucleotide identity cutoff value [103]. Analysis of the VP4 gene revealed low nucleotide sequence identities between two Czech strains and other porcine (72.2%–75.3%), bovine

(74.1%–74.6%), and human (69.1%–69.3%) RVCs and was tentatively classified as a novel RVC VP4 genotype, P8 [103]. Martella et al. (2007) characterized 20 porcine RVC strains collected from distinct diarrheal outbreaks in 2003–2005 in Northern and Central Italy [97]. They belonged to G1, G5 and G6 genotypes, similar to those identified in Ireland.

A very low prevalence rate of porcine RVB was reported in Germany in samples collected between 1999 and 2013, with no genotyping data available [126]. Additionally, Smitalova et al. (2009) reported that porcine RVB was detected in 0.6% of samples from diarrheic pigs in Czech Republic [133]; but they were not genotyped. Apart from the above information, no data for porcine RVB prevalence, pathogenic potential and genetic characteristics are available for Europe. Additionally, no reports of porcine RVH are available and only one historic study confirmed circulation of porcine RVE in England [25], requiring further evaluation and verification that pigs in fact serve as natural reservoir for porcine RVE strains.

4.3. Asia

Numerous prevalence studies conducted in Asian countries demonstrated the presence of uncommon RVA genotypes in humans suspected to originate from animal sources [134–137] and reassortants of human-animal origin [83,138] including the G9 strains emerging globally or regionally in pigs and humans and the need of careful monitoring of animal RVs. Teodoroff et al. (2005) reported that genotype G9 of porcine RVA was dominant in a survey among porcine RVA strains associated with outbreaks of diarrhea in young pigs in Japan between 2000 and 2002 [139] (Figure 2). Similarly, Miyazaki et al. (2011) demonstrated that G9P[23], G9P[13]/[22], G9P[23], G3P[7], G9P[23], G5P[13]/[22], and P[7] combined with an untypeable G genotype caused four different diarrheal outbreaks in Japan in 2009–2010 that affected almost all suckling pigs born to 20% to 30% of lactating sows [90]. Further, this study provided evidence that the untypeable G genotype was a novel porcine RVA G26 genotype [90], which was confirmed by the Rotavirus Classification Working Group. A large-scale surveillance study of smallholder pig farms in the Mekong Delta, Vietnam, was conducted in 2012 and demonstrated an overall animal-level and farm-level porcine RVA prevalence of 32.7% (239/730) and 74% (77/104), respectively; however, no significant association with clinical disease was observed [74]. The study also identified six different G types and four P types in various combinations (G2, G3, G4, G5, G9, G11 and P[6], P[13], P[23], and P[34]) [74]. Additionally, one G26 strain was detected. A novel genotype P[27] in combination with G2 was identified in Thailand in samples collected in 2000–2001 [140]. Saikruang et al. (2013) reported an overall prevalence of porcine RVA of 19.8% (of 207 samples) in diarrheic samples of piglets in Thailand (2009–2010) and identified a wider variety of G-P combinations [78]. In this study, G4P[6] was identified as the most prevalent genotype (39.0%), followed by G4P[23] (12.2%), G3P[23] (7.3%), G4P[19] (7.3%), G3P[6] (4.9%), G3P[13] (4.9%), G3P[19] (4.9%), G9P[13] (4.9%), G9P[19] (4.9%), G5P[6] and G5P[13] each of 2.4%. Furthermore, G5 and G9 in combinations with P-nontypeable strains were also found as 2.4% ($n = 1$) of the collection. Among the diverse porcine RVA strains, novel genotype combinations of G4P[19] and G9P[19] were detected for the first time. Further corroborating the emergence and widespread prevalence of non-classic G and P genotypes of porcine RVA in Asia, 92.9% of porcine RVA containing stool samples collected from piglets with diarrhea in northern Thailand (2006–2008) belonged to the rare P[23] genotype combination with G9 or G3 genotypes [89]. The G9P[23] combination was reported to circulate in pigs in China as well [141]. Porcine RVA strains of the G9 genotype in combination with the P[7] and P[23] genotypes were isolated and identified as the third most important genotype in the diarrheic pigs in South Korea, after G5P[7] and G8P[7] [93]. A review by Malik and colleagues summarized the results of various surveillance studies (using ELISA-, PAGE- and PCR-based typing) suggesting the presence of G4, G6, G9, G12 and P[6], P[7], P[13] and P[19] genotypes in different regions in India [124]. Although there are no documented large-scale surveillance programs in China, the presence of porcine RVA G9P[7] in piglets with diarrhea was confirmed in Jiangsu Province, China [142], suggesting that various G9 combinations circulate in most if not all Asian countries.

Despite somewhat scarce information on porcine RVC prevalence in Asian countries, there are several reports describing different porcine RVC genotypes circulating in Japan and South Korea [99,100,105]. The genotypes described in Japan include G1, G5, G6, G9, G12 and G13 G genotypes found in combination with P1, P4–P6 P genotypes, while G3, G5, G6 and G7 G genotypes were shown to circulate in South Korea [100,105] (Figure 3). There is also a report of porcine RVC circulation in China with a prevalence rate of 16.65% among diarrheic and asymptomatic piglets (2007–2008); however, no genotyping data is available [143].

Similar to porcine RVC data, very limited information on porcine RVB prevalence and dominant genotypes circulating in most Asian countries is available. A high prevalence of porcine RVB and porcine RVB specific antibodies in porcine fecal and serum samples, respectively, are reported in several studies in Japan [110,144]. Furthermore, at least G3–G6, G8, G9, G11, G12–G15 and G18–G20 genotypes with distinct sub-clusters within the genotypes were identified in porcine samples collected in Japan between 2000 and 2007 [71,110] (Figure 3). Additional evidence of remarkable porcine RVB diversity is highlighted in a report from India that demonstrates that at least G7, G19, G20 and tentative novel G21 genotypes (associated with H4 and H5 genotypes) circulate in the Northern and Western regions of India [145].

4.4. Australia

Apart from several reports on circulation of porcine RVA G3, G4 and G5 ~3 decades ago [146–148], there is no epidemiological data for porcine RVs in this region (Figure 2).

5. Zoonotic Potential of Porcine RV Strains

Historically, RVs were believed to be host-specific; however, recent and growing evidence challenges this postulation. Diverse animal reservoirs of zoonotic RVs are suggested to include at least porcine, bovine, ovine, pteropine, rodent, avian and insectivore species [17,85,149–151]. The widely documented zoonotic potential of RVA strains is best exemplified by globally emerging human RVs, such as G9 and G12, likely originating from porcine species by gene reassortment because similar G9 and G12 VP7 specificities are often observed in piglets [139,152–154]. Additionally, numerous reports have described interspecies transmission leading to sporadic cases of human disease with RVs from different animal species origin [72,155–158]. Table 1 summarizes common (G1–G4, P[6] and P[8]) and uncommon human RV G and P genotypes (suggestive of possible emergence via re-assortment) and G/P combinations (indicating possible direct transmission) that likely originated from swine. A total of 10 G genotypes (G1–5, G9–G12 and G26) and 7 P genotypes (P[4], P[6], P[8], P[13], P[14], P[19] and P[25]) of porcine origin have been identified in humans to date, with some genotypes including G10, G11, G12, G26, P[13], P[14], P[19] and P[25] displaying regional characteristics (found only in Asian or African countries), whereas the rest were found more commonly or emerging globally (Table 1). The recent discovery showing that different P-genotypes of RVA strains interact with distinct histo-blood group antigens (HBGA, ABOH, Lewis) and sialic acids via VP4 may provide insights into regional prevalence and increased zoonotic potential of some RVAs of swine origin [159–162]. While only a few animal RVs (of P[1], P[2], P[3], and P[7]) are sialidase sensitive, cellular attachment of human and the majority of animal RVs are sialic acid independent and use HBGAs as attachment factors or (co)receptors [161]. Further, RVs bearing different P-types recognize polymorphic HBGAs in a strain-specific manner, leading to variable host-specific susceptibility among different populations. Further, a stepwise-biosynthesis of HBGAs may represent one of the mechanisms regulating age-specific susceptibility to RV infection in early life [161]. Similar polymorphic HBGAs are also observed in many animals, including pigs (A and H antigens) [163]. The latter may provide an explanation why RVA strains of the P[6] genotype (that recognize H antigen) are commonly found in and transmitted between humans and pigs in different countries, while P[19] strains in humans of potential porcine origin appear to be restricted to India, Asian and African countries coinciding with distinct polymorphisms in Lewis antigens associated with Caucasian and other populations [164].

Table 1. Human RV genotypes of suspect or confirmed porcine origin via direct transmission or multiple re-assortment events.

Porcine RV Species	G and/or P Genotype	Geographic Region	Year Samples Collected	Epidemiological Status and Medical Relevance	Reference
A	**G1-G4, G9, G12 and P8**	Worldwide	2000s	Commonly seen in humans *	[152,153,165]
	G3–G5, G9 and G11, as well as P[6]	Denmark, France, Hungary, Italy, Slovenia	2003–2007	G3-G5—common in humans, G5—regional in humans, P6—rare in humans	[85]
	G1 and G4	Brazil	2007	Common	[166]
	G1P[8]	China; MD, USA	2004–2009	Common	[15,167,168]
	G1, G1P[6]	Japan	2001	Common	[169]
	G1P[6]	Japan	1997	Rare	[170]
	G1P[6], G4P[6] and G12P[6]	Democratic Republic of the Congo	2007–2010	Common	[171]
	G1P[19]	India	1992	Rare	[134]
	G2	Europe	1992	Uncommon	[130]
	G3P[6], G4P[6] and G4P[8]	China, Italy, Slovenia	2003–2013	Common	[172–174]
	G3P[25]	Taiwan	2009	Rare	[175]
	G4P[6] strains, one G5P[6]	Taiwan	2006–2012	Common	[176]
	G4P[6]	Hungary, China, Argentina, Madagascar	2006–2007 2008–2009	Sporadic identification in humans worldwide	[177–181]
	G5P[6]	Japan, Bulgaria	2011 2006	Rare	[182,183]
	G5P[8]	Brazil, Argentina, Paraguay, Cameroon, China, Thailand, and Vietnam	1986–2005	Common in Asian, African and South American countries	[184]
	G9	NE, USA; India	1980s, 1190s, 1997–2000	Uncommon, emerging worldwide	[153,185,186]
	G9P[6]	India	2007	Unusual	[187]
	G9P[19]	Thailand, India	2012–2013 1989–1990	Rare	[188,189]
	G9P[19] and G9P[13]	Taiwan	2014–2015	Rare	[190]
	G9P[19] and G10P[14]	Vietnam	2007–2008	Rare	[191]
	G11P[4], G11P[6], G11P[8] G11P[25]	Nepal, Bangladesh	2001–2004	Rare	[192]
	G11P[25]	India	2005–2009	Uncommon	[193,194]
	G12P[6] and G12P[8]	Kenya, Myanmar	2010, 2011	Common	[195,196]
	G26P[19]	Vietnam	2009–2010	Atypical in humans	[197]
B	**N/A**	Brazil	2000s	Regional significance	[198]
C	**N/A**	Japan, Brazil	1982–1986, 2000–2007	Regional significance	[100,199]

* G1P[8], G2P[4], G3P[8], G4P[8], and G9P[8]) were described in ~90% of samples from humans submitted to the EuroRotaNet database (that included data for 17 European countries: Belgium, Bulgaria, Denmark, Finland, France, Germany, Greece, Hungary, Italy, Lithuania, The Netherlands, Romania, Slovenia, Spain, Sweden, UK) between 2005 and 2009 from the 16 participating countries [200–202]. Letters of different colors represent different G-genotypes for easier distinction.

Unlike porcine RVA strains which are commonly demonstrated to possess zoonotic potential [17], there is currently little evidence in support of porcine RVC interspecies transmission. Identification of porcine RVC-derived genes in human and bovine RVC strains was reported in Brazil [199]. In addition to identification of bovine RVC strain WD534tc of likely porcine origin [203], whole genome analysis of porcine RVC strains from Japan has suggested a close phylogenetic relations between the human and some of these porcine RVC strains [100]. Additionally, a possible zoonotic role of animal RVCs has also been hypothesized based on increased seroprevalence rates to RVC in human populations [7] and the high prevalence of RVC infections in some geographic areas where they may cause <5% of gastroenteritis-associated hospitalizations in childhood [204]. However, it is important to note that the limited genetic variability of RVCs in humans contrasts with the high genetic diversity currently seen in pigs [97].

More recently, RVB strains were identified from sporadic cases of infantile diarrhea in Bangladesh as opposed to adult diarrhea cases associated with RVB in China and India. These recent strains differed genetically from the Chinese strain [53,55], suggesting that diverse RVB strains are circulating in humans. Limited evidence for the zoonotic potential of some porcine RVB strains was provided by Medici and colleagues demonstrated a high nucleotide identity between the NSP2 gene sequences of human and porcine strains [198].

Overall, these data indicate that frequent surveillance of porcine RVA and additional research on porcine RVB/RVC diversity in swine are needed to control their regional and global zoonotic spread.

6. Passive and Active Immunity

Immune responses and correlates of protection against RVs in humans and different animal species (mostly against RVA) are reviewed elsewhere [205,206]. Much of the knowledge of RV immune responses has been generated using a gnotobiotic (Gn) pig model and human RV infection/vaccines. In this review, we will briefly summarize passive and active immune responses in pigs induced by human RVA strains (Figure 4), since piglets can be infected with porcine and human RV strains, and develop clinical disease [206]. In terms of innate immunity, our recent studies have demonstrated that decreased severity of human RV clinical disease and infection was associated with enhanced function and frequencies of plasmacytoid dendritic cell (pDC) and natural killer (NK) cells evident systemically and locally and systemic IL-12 responses [207], similar to observations in humans and mice [208]. Although the role of interferon (IFN)-α in protection against homologous/heterologous RV infections is debated [209–211], earlier we demonstrated that an imbalanced IFN-α production coincided with increased human RV disease/infection severity [212]. Additionally, increased expression of toll-like receptor 3 (recognizes double-stranded RNA) was associated with improved protection against human RV infection and disease in Gn piglets, suggesting it could be an attractive target for therapeutic development [213]. Finally, reduced human RV replication in Gn piglets in our recent studies was associated with increased total Ig responses in systemic and local tissues [214].

The correlates of oral human RV vaccine induced protection against challenge with human RV (G1P[8]) were the presence and concentration of RV-specific IgA antibodies or antibody-secreting-cells (ASC) in serum or intestine, and frequencies of IFN-γ producing CD4+ T cells, but not the concentration of intestinal or systemic RV-neutralizing antibodies [215–217] or VP6-specific IgA antibodies [205,206,218] (Figure 4).

Priming orally with an attenuated human RV vaccine conferred protection in piglets that was augmented by a booster with VP 2/6 virus–like particles (VLPs) [218]. This protection was correlated with immune responses to VP4 and VP7 [206]. However, systemic and intestinal immune responses to human RV NSP4 alone did not correlate with protection of Gn piglets against human RV challenge [219]. While maternally derived circulating RV-specific antibodies mediated high levels of passive protection against human RV disease, active immune responses to replicating and non-replicating human RV vaccines were suppressed, as evident by reduced numbers of ASC in the intestine which decreased protection upon experimental challenge [220,221].

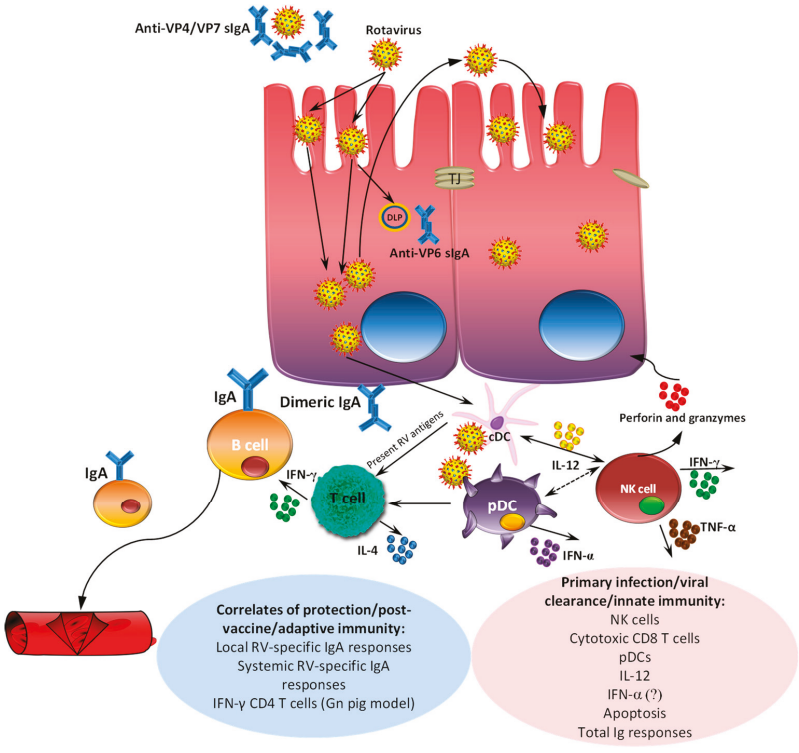

Figure 4. Immune responses to RV infection in pigs. Intestinal RV VP4/VP7 secretory immunoglobulin A (sIgA) neutralizing antibodies can prevent viral binding to enterocytes and penetration (early post-infection), while viral replication can be partially inhibited by anti-VP6 sIgA during transcytosis across enterocytes. In addition, a number of immune cells contribute to RV innate and adaptive immune responses: plasmacytoid dendritic cells (pDCs) produce antiviral (IFN-α) and pro-inflammatory (IL-12) cytokines which can inhibit RV replication or induce other immune cell subsets, including natural killer (NK) cells that produce granzymes, perforins and TNF-α and can lyse RV-infected cells. After antigen presentation by conventional dendritic cells (cDCs) to T cells, cytokine-secreting (IFN-γ in particular) RV-specific Th cells can also inhibit viral replication and activate IgA production by B cells. Additionally, RV-specific CD8 cytotoxic IFN-γ producing T cells contribute to the lysis of RV infected cells. RV induces apoptosis of intestinal epithelial (enterocytes) and immune cells; however, it is unclear whether this decreases (by eliminating infected cells) or promotes (via dissemination of the infectious particles) RV replication. Although high levels of systemic RV-neutralizing antibodies may coincide with improved protection against RV challenge, they are not correlated with protection in most studies. TJ: tight junctions. DLP: double-layered particles.

7. Porcine RVA Vaccines and Control Strategies: Potential Impact of Vaccines on Porcine RVA Genetic Diversity

Although following worldwide application of human RV vaccines, child mortality due to diarrhea declined, RV remains the most common cause of severe dehydrating diarrhea among children <5 years of age [222]. In livestock, vaccination strategies were focused on the induction of active or passive immunity, however, oral administration of attenuated RV vaccines to piglets and calves often lacked efficacy in the field [223]. The endemic porcine RV infections and the ubiquitous presence of porcine RV antibodies in swine revealed a need for strategies to boost lactogenic immunity in sows to provide

passive antibodies to the neonate with colostrum and milk. The variable success of maternal RV vaccines in the field is influenced by vaccine dose, strain, inactivating agent, adjuvant, route of administration, and porcine RV exposure levels. The use of genetically engineered VLP vaccines to boost antibodies in mammary secretions showed promise because they are replication independent allowing circumvention of maternal antibody interference. However, although the immunogenicity of such VLP vaccines was high, the protective efficacy they induced was insufficient demonstrating the need for priming with live attenuated RV vaccines [224]. Nevertheless, field application of ProSystem porcine RV vaccine (which contained modified live porcine RVA strains of G4P[6] and G5P[7] genotype combinations) or G5P[7] (porcine RVA OSU) based vaccines could have resulted in the widespread circulation of porcine RVA of these genotypes for several decades and their more recent substitution by G9 and G11 genotypes or reassortant G4 and G5 variants discussed in detail in Section 3 of this review. Alternatively, they could generate herd immunity gradually decreasing the prevalence of the historic G4/G5 porcine RVA genotypes and allowing for the spread of novel emerging porcine RVAs.

8. Concluding Remarks

The remarkable diversity and genetic plasticity of porcine RVs indicate a need for further research on molecular characterization and spatio-temporal prevalence and fluctuations of endemic and emerging porcine RVs. The recent emergence of unusual G and P genotypes of porcine RVA strains worldwide, the discovery of novel porcine RV groups in different geographic regions, as well as the growing evidence of increased porcine RV prevalence and genetic diversity compared to that previously estimated suggest that porcine RV epidemiology is very complex and highly dynamic. These observations lead to at least two conclusions: (i) molecular diagnostic and characterization toolkits should be frequently updated and expanded to include novel porcine RV variants to ensure accurate epidemiological monitoring (especially for the countries where such information is lacking: African countries, Russia, Australia, etc.); (ii) a better understanding of the molecular pathogenesis and immunity to porcine RV is needed to optimize and update classical vaccine approaches to control porcine RV infections and spread. Although not highly efficacious in the field, attenuated replicating porcine RVA vaccines may be contributing directly to the genetic diversity of porcine RVs (via reassortment of vaccine strains with wild type strains and their subsequent spread) and the emergence of novel genetic variants that can evade herd immunity against the vaccine strains, as observed with human RVA vaccines, RotaTeq and Rotarix, that generate within vaccine (RotaTeq) and vaccine-wild type strain re-assortants capable of further spread in susceptible populations [225]. Alternative or additional approaches (to live attenuated vaccine use) may include wide-scale probiotic use or therapeutic applications that target the virus replication cycle to enhance innate or anamnestic immune responses, to decrease RV shedding and environmental contamination, and to alleviate porcine RV-mediated intestinal damage. Finally, although not previously well recognized, the zoonotic potential of various porcine RV genogroups/genotypes should be carefully and extensively evaluated by conducting simultaneous epidemiological studies of human and porcine RVs in the same geographic regions. Additional studies to understand the higher propensity of some genogroups/genotypes to generate re-assorted variants and cross interspecies barriers are needed, including the potential interactions of different porcine RV genotypes with HBGAs as shown for human RV strains [159–162].

Acknowledgments: This work was supported by state and federal funds appropriated to the Ohio Agricultural Research and Development Center (OARDC) of the Ohio State University Grant support was from a Ohio State University SEED Grant—#2011-077 and a National Pork Board grant (NPB 12-094) for swine health.

Author Contributions: A.N.V. and L.J.S. conceived and designed the experiments described in this review; J.O.A. performed the experiments described in this review; A.N.V. and J.O.A. analyzed the data; A.N.V. wrote this review that was edited by L.J.S.

Conflicts of Interest: The authors declare no conflict of interest. The founding sponsors had no role in the design of the study; in the collection, analyses, or interpretation of data; in the writing of the manuscript, and in the decision to publish the results.

References

1. Chang, K.; Kim, Y.; Saif, L.J. Rotavirus and reovirus. In *Diseases of Swine*, 10 ed.; Zimmerman, J.J., Karriker, L.A., Ramirez, A., Schwartz, K.J., Stevenson, G.W., Eds.; Wiley-Blackwell: West Sussex, UK, 2012; pp. 621–634.
2. Estes, M.K.; Kang, G.; Zeng, C.Q.; Crawford, S.E.; Ciarlet, M. Pathogenesis of rotavirus gastroenteritis. *Novartis Found. Symp.* **2001**, *238*, 82–96. [PubMed]
3. Nava, P.; Lopez, S.; Arias, C.F.; Islas, S.; Gonzalez-Mariscal, L. The rotavirus surface protein VP8 modulates the gate and fence function of tight junctions in epithelial cells. *J. Cell Sci.* **2004**, *117 Pt 23*, 5509–5519. [CrossRef] [PubMed]
4. Obert, G.; Peiffer, I.; Servin, A.L. Rotavirus-induced structural and functional alterations in tight junctions of polarized intestinal Caco-2 cell monolayers. *J. Virol.* **2000**, *74*, 4645–4651. [CrossRef] [PubMed]
5. Dickman, K.G.; Hempson, S.J.; Anderson, J.; Lippe, S.; Zhao, L.; Burakoff, R.; Shaw, R.D. Rotavirus alters paracellular permeability and energy metabolism in Caco-2 cells. *Am. J. Physiol. Gastrointest. Liver Physiol.* **2000**, *279*, G757–G766. [PubMed]
6. Beau, I.; Cotte-Laffitte, J.; Amsellem, R.; Servin, A.L. A protein kinase A-dependent mechanism by which rotavirus affects the distribution and mRNA level of the functional tight junction-associated protein, occludin, in human differentiated intestinal Caco-2 cells. *J. Virol.* **2007**, *81*, 8579–8586. [CrossRef]
7. Iturriza-Gomara, M.; Clarke, I.; Desselberger, U.; Brown, D.; Thomas, D.; Gray, J. Seroepidemiology of group C rotavirus infection in England and Wales. *Eur. J. Epidemiol.* **2004**, *19*, 589–595. [CrossRef] [PubMed]
8. Blutt, S.E.; Conner, M.E. Rotavirus: to the gut and beyond! *Curr. Opin. Gastroenterol.* **2007**, *23*, 39–43. [CrossRef] [PubMed]
9. Estes, M.; Greenberg, H.B. Rotaviruses. In *Fields Virology*, 5 ed.; Knipe, D.M., Howley, P., Eds.; Wolters Kluwer Health/Lippincott Williams & Wilkins: Philadelphia, PA, USA, 2013; pp. 1347–1395.
10. Matthijnssens, J.; Otto, P.H.; Ciarlet, M.; Desselberger, U.; Van Ranst, M.; Johne, R. VP6-sequence-based cutoff values as a criterion for rotavirus species demarcation. *Arch. Virol.* **2012**, *157*, 1177–1182. [CrossRef]
11. Mihalov-Kovacs, E.; Gellert, A.; Marton, S.; Farkas, S.L.; Feher, E.; Oldal, M.; Jakab, F.; Martella, V.; Banyai, K. Candidate new rotavirus species in sheltered dogs, Hungary. *Emerg. Infect. Dis.* **2015**, *21*, 660–663. [CrossRef] [PubMed]
12. Banyai, K.; Kemenesi, G.; Budinski, I.; Foldes, F.; Zana, B.; Marton, S.; Varga-Kugler, R.; Oldal, M.; Kurucz, K.; Jakab, F. Candidate new rotavirus species in Schreiber's bats, Serbia. *Infect. Genet. Evol.* **2017**, *48*, 19–26. [CrossRef] [PubMed]
13. Matthijnssens, J.; Ciarlet, M.; McDonald, S.M.; Attoui, H.; Banyai, K.; Brister, J.R.; Buesa, J.; Esona, M.D.; Estes, M.K.; Gentsch, J.R.; et al. Uniformity of rotavirus strain nomenclature proposed by the Rotavirus Classification Working Group (RCWG). *Arch. Virol.* **2011**, *156*, 1397–1413. [CrossRef] [PubMed]
14. Trojnar, E.; Sachsenroder, J.; Twardziok, S.; Reetz, J.; Otto, P.H.; Johne, R. Identification of an avian group A rotavirus containing a novel VP4 gene with a close relationship to those of mammalian rotaviruses. *J. Gen. Virol.* **2013**, *94 Pt 1*, 136–142. [CrossRef] [PubMed]
15. Matthijnssens, J.; Ciarlet, M.; Heiman, E.; Arijs, I.; Delbeke, T.; McDonald, S.M.; Palombo, E.A.; Iturriza-Gomara, M.; Maes, P.; Patton, J.T.; et al. Full genome-based classification of rotaviruses reveals a common origin between human Wa-Like and porcine rotavirus strains and human DS-1-like and bovine rotavirus strains. *J. Virol.* **2008**, *82*, 3204–3219. [CrossRef] [PubMed]
16. Matthijnssens, J.; Ciarlet, M.; Rahman, M.; Attoui, H.; Banyai, K.; Estes, M.K.; Gentsch, J.R.; Iturriza-Gomara, M.; Kirkwood, C.D.; Martella, V.; et al. Recommendations for the classification of group A rotaviruses using all 11 genomic RNA segments. *Arch. Virol.* **2008**, *153*, 1621–1629. [CrossRef] [PubMed]
17. Martella, V.; Banyai, K.; Matthijnssens, J.; Buonavoglia, C.; Ciarlet, M. Zoonotic aspects of rotaviruses. *Vet. Microbiol.* **2010**, *140*, 246–255. [CrossRef] [PubMed]
18. Marthaler, D.; Suzuki, T.; Rossow, K.; Culhane, M.; Collins, J.; Goyal, S.; Tsunemitsu, H.; Ciarlet, M.; Matthijnssens, J. VP6 genetic diversity, reassortment, intragenic recombination and classification of rotavirus B in American and Japanese pigs. *Vet. Microbiol.* **2014**, *172*, 359–366. [CrossRef] [PubMed]
19. Matthijnssens, J.; Taraporewala, Z.F.; Yang, H.; Rao, S.; Yuan, L.; Cao, D.; Hoshino, Y.; Mertens, P.P.; Carner, G.R.; McNeal, M.; et al. Simian rotaviruses possess divergent gene constellations that originated from interspecies transmission and reassortment. *J. Virol.* **2010**, *84*, 2013–2026. [CrossRef] [PubMed]

20. McNulty, M.S. Rotaviruses. *J. Gen. Virol.* **1978**, *40*, 1–18. [CrossRef] [PubMed]
21. McNulty, M.S.; Allan, G.M.; Connor, T.J.; McFerran, J.B.; McCracken, R.M. An entero-like virus associated with the runting syndrome in broiler chickens. *Avian Pathol.* **1984**, *13*, 429–439. [CrossRef] [PubMed]
22. McNulty, M.S.; Allan, G.M.; McFerran, J.B. Prevalence of antibody to conventional and atypical rotaviruses in chickens. *Vet. Rec.* **1984**, *114*, 219. [CrossRef] [PubMed]
23. McNulty, M.S.; Todd, D.; Allan, G.M.; McFerran, J.B.; Greene, J.A. Epidemiology of rotavirus infection in broiler chickens: recognition of four serogroups. *Arch. Virol.* **1984**, *81*, 113–121. [CrossRef] [PubMed]
24. Otto, P.; Liebler-Tenorio, E.M.; Elschner, M.; Reetz, J.; Lohren, U.; Diller, R. Detection of rotaviruses and intestinal lesions in broiler chicks from flocks with runting and stunting syndrome (RSS). *Avian Dis.* **2006**, *50*, 411–418. [CrossRef] [PubMed]
25. Chasey, D.; Bridger, J.C.; McCrae, M.A. A new type of atypical rotavirus in pigs. *Arch. Virol.* **1986**, *89*, 235–243. [CrossRef] [PubMed]
26. Janke, B.H.; Nelson, J.K.; Benfield, D.A.; Nelson, E.A. Relative prevalence of typical and atypical strains among rotaviruses from diarrheic pigs in conventional swine herds. *J. Vet. Diagn. Investig.* **1990**, *2*, 308–311. [CrossRef] [PubMed]
27. Wakuda, M.; Ide, T.; Sasaki, J.; Komoto, S.; Ishii, J.; Sanekata, T.; Taniguchi, K. Porcine rotavirus closely related to novel group of human rotaviruses. *Emerg. Infect. Dis.* **2011**, *17*, 1491–1493. [CrossRef]
28. Bridger, J.C.; Woode, G.N. Neonatal calf diarrhoea: identification of a reovirus-like (rotavirus) agent in faeces by immunofluorescence and immune electron microscopy. *Br. Vet. J.* **1975**, *131*, 528–535. [PubMed]
29. Bridger, J.C.; Brown, J.F. Prevalence of antibody to typical and atypical rotaviruses in pigs. *Vet. Rec.* **1985**, *116*, 50. [CrossRef] [PubMed]
30. Saif, L.J.; Rosen, B.; Parwani, A. Animal rotaviruses. In *Virus Infections of the Gastrointestinal Tract*; Kapikian, A.Z., Ed.; Marcel-Dekker: New York, NY, USA, 1994; pp. 279–367.
31. Saif, L.J.; Bohl, E.H.; Theil, K.W.; Cross, R.F.; House, J.A. Rotavirus-like, calicivirus-like, and 23-nm virus-like particles associated with diarrhea in young pigs. *J. Clin. Microbiol.* **1980**, *12*, 105–111. [PubMed]
32. Saif, L.J.; Jiang, B. Nongroup A rotaviruses of humans and animals. *Curr. Top. Microbiol. Immunol.* **1994**, *185*, 339–371.
33. Mebus, C.A.; Underdahl, N.R.; Rhodes, M.B.; Twiehaus, M.J. Calf diarrhea (scours): Reproduced with a virus from field outbreak. *Neb. Agric. Exp. Stn. Res. Bull.* **1969**, *233*, 1–16.
34. Mebus, C.A.; Underdahl, N.R.; Rhodes, M.B.; Twiehaus, M.J. Further studies on neonatal calf diarrhea virus. *Proc. Annu. Meet. U. S. Anim. Health Assoc.* **1969**, *73*, 97–99. [PubMed]
35. Bishop, R.F.; Davidson, G.P.; Holmes, I.H.; Ruck, B.J. Virus particles in epithelial cells of duodenal mucosa from children with acute non-bacterial gastroenteritis. *Lancet* **1973**, *2*, 1281–1283. [CrossRef]
36. Theil, K.W. Group A rotaviruses. In *Viral Diarrheas of Man and Animals*; Saif, L.J., Theil, K.W., Eds.; CRC Press: Boca Raton, FL, USA, 1990; pp. 35–72.
37. Holmes, I.H. Rotaviruses. In *The Reoviridae*; Joklik, W.T., Ed.; Plenum Press: New York, NY, USA, 1983; pp. 359–423.
38. Rodger, S.M.; Bishop, R.F.; Holmes, I.H. Detection of a rotavirus-like agent associated with diarrhea in an infant. *J. Clin. Microbiol.* **1982**, *16*, 724–726. [PubMed]
39. Bridger, J.C.; Pedley, S.; McCrae, M.A. Group C rotaviruses in humans. *J. Clin. Microbiol.* **1986**, *23*, 760–763. [PubMed]
40. Torres-Medina, A. Isolation of an atypical rotavirus causing diarrhea in neonatal ferrets. *Lab. Anim. Sci.* **1987**, *37*, 167–171. [PubMed]
41. Tsunemitsu, H.; Saif, L.J.; Jiang, B.M.; Shimizu, M.; Hiro, M.; Yamaguchi, H.; Ishiyama, T.; Hirai, T. Isolation, characterization, and serial propagation of a bovine group C rotavirus in a monkey kidney cell line (MA104). *J. Clin. Microbiol.* **1991**, *29*, 2609–2613. [PubMed]
42. Theil, K.W.; Saif, L.J.; Moorhead, P.D.; Whitmoyer, R.E. Porcine rotavirus-like virus (group B rotavirus): characterization and pathogenicity for gnotobiotic pigs. *J. Clin. Microbiol.* **1985**, *21*, 340–345. [PubMed]
43. Barman, P.; Ghosh, S.; Das, S.; Varghese, V.; Chaudhuri, S.; Sarkar, S.; Krishnan, T.; Bhattacharya, S.K.; Chakrabarti, A.; Kobayashi, N.; et al. Sequencing and sequence analysis of VP7 and NSP5 genes reveal emergence of a new genotype of bovine group B rotaviruses in India. *J. Clin. Microbiol.* **2004**, *42*, 2816–2818. [CrossRef] [PubMed]

44. Chang, K.O.; Parwani, A.V.; Smith, D.; Saif, L.J. Detection of group B rotaviruses in fecal samples from diarrheic calves and adult cows and characterization of their VP7 genes. *J. Clin. Microbiol.* **1997**, *35*, 2107–2110. [PubMed]
45. Ghosh, S.; Varghese, V.; Sinha, M.; Kobayashi, N.; Naik, T.N. Evidence for interstate transmission and increase in prevalence of bovine group B rotavirus strains with a novel VP7 genotype among diarrhoeic calves in Eastern and Northern states of India. *Epidemiol. Infect.* **2007**, *135*, 1324–1330. [CrossRef] [PubMed]
46. Tsunemitsu, H.; Morita, D.; Takaku, H.; Nishimori, T.; Imai, K.; Saif, L.J. First detection of bovine group B rotavirus in Japan and sequence of its VP7 gene. *Arch. Virol.* **1999**, *144*, 805–815. [CrossRef] [PubMed]
47. Shen, S.; McKee, T.A.; Wang, Z.D.; Desselberger, U.; Liu, D.X. Sequence analysis and in vitro expression of genes 6 and 11 of an ovine group B rotavirus isolate, KB63: Evidence for a non-defective, C-terminally truncated NSP1 and a phosphorylated NSP5. *J. Gen. Virol.* **1999**, *80 Pt 8*, 2077–2085. [CrossRef]
48. Eiden, J.J.; Nataro, J.; Vonderfecht, S.; Petric, M. Molecular cloning, sequence analysis, in vitro expression, and immunoprecipitation of the major inner capsid protein of the IDIR strain of group B rotavirus (GBR). *Virology* **1992**, *188*, 580–589. [CrossRef]
49. Chen, G.M.; Hung, T.; Mackow, E.R. Identification of the gene encoding the group B rotavirus VP7 equivalent: primary characterization of the ADRV segment 9 RNA. *Virology* **1990**, *178*, 311–315. [CrossRef]
50. Dai, G.Z.; Sun, M.S.; Liu, S.Q.; Ding, X.F.; Chen, Y.D.; Wang, L.C.; Du, D.P.; Zhao, G.; Su, Y.; Li, J.; et al. First report of an epidemic of diarrhoea in human neonates involving the new rotavirus and biological characteristics of the epidemic virus strain (KMB/R85). *J. Med. Virol.* **1987**, *22*, 365–373. [PubMed]
51. Fang, Z.Y.; Ye, Q.; Ho, M.S.; Dong, H.; Qing, S.; Penaranda, M.E.; Hung, T.; Wen, L.; Glass, R.I. Investigation of an outbreak of adult diarrhea rotavirus in China. *J. Infect. Dis.* **1989**, *160*, 948–953. [CrossRef] [PubMed]
52. Hung, T.; Chen, G.M.; Wang, C.G.; Yao, H.L.; Fang, Z.Y.; Chao, T.X.; Chou, Z.Y.; Ye, W.; Chang, X.J.; Den, S.S.; et al. Waterborne outbreak of rotavirus diarrhoea in adults in China caused by a novel rotavirus. *Lancet* **1984**, *1*, 1139–1142.
53. Kelkar, S.D.; Zade, J.K. Group B rotaviruses similar to strain CAL-1, have been circulating in Western India since 1993. *Epidemiol. Infect.* **2004**, *132*, 745–749. [CrossRef] [PubMed]
54. Lahon, A.; Chitambar, S.D. Molecular characterization of VP4, VP6, VP7 and NSP4 genes of group B rotavirus strains from outbreaks of gastroenteritis. *Asian Pac. J. Trop. Med.* **2011**, *4*, 846–849. [CrossRef]
55. Ahmed, M.U.; Kobayashi, N.; Wakuda, M.; Sanekata, T.; Taniguchi, K.; Kader, A.; Naik, T.N.; Ishino, M.; Alam, M.M.; Kojima, K.; et al. Genetic analysis of group B human rotaviruses detected in Bangladesh in 2000 and 2001. *J. Med. Virol.* **2004**, *72*, 149–155. [CrossRef] [PubMed]
56. Saiada, F.; Rahman, H.N.; Moni, S.; Karim, M.M.; Pourkarim, M.R.; Azim, T.; Rahman, M. Clinical presentation and molecular characterization of group B rotaviruses in diarrhoea patients in Bangladesh. *J. Med. Microbiol.* **2011**, *60 Pt 4*, 529–536. [CrossRef] [PubMed]
57. Rahman, M.; Hassan, Z.M.; Zafrul, H.; Saiada, F.; Banik, S.; Faruque, A.S.; Delbeke, T.; Matthijnssens, J.; Van Ranst, M.; Azim, T. Sequence analysis and evolution of group B rotaviruses. *Virus Res.* **2007**, *125*, 219–225. [CrossRef] [PubMed]
58. Sanekata, T.; Ahmed, M.U.; Kader, A.; Taniguchi, K.; Kobayashi, N. Human group B rotavirus infections cause severe diarrhea in children and adults in Bangladesh. *J. Clin. Microbiol.* **2003**, *41*, 2187–2190. [CrossRef] [PubMed]
59. Aung, T.S.; Kobayashi, N.; Nagashima, S.; Ghosh, S.; Aung, M.S.; Oo, K.Y.; Win, N. Detection of group B rotavirus in an adult with acute gastroenteritis in Yangon, Myanmar. *J. Med. Virol.* **2009**, *81*, 1968–1974. [CrossRef] [PubMed]
60. Chasey, D.; Davies, P. Atypical rotaviruses in pigs and cattle. *Vet. Rec.* **1984**, *114*, 16–17. [CrossRef] [PubMed]
61. Marthaler, D.; Rossow, K.; Culhane, M.; Goyal, S.; Collins, J.; Matthijnssens, J.; Nelson, M.; Ciarlet, M. Widespread rotavirus H in commercially raised pigs, United States. *Emerg. Infect. Dis.* **2014**, *20*, 1195–1198. [CrossRef] [PubMed]
62. Molinari, B.L.; Lorenzetti, E.; Otonel, R.A.; Alfieri, A.F.; Alfieri, A.A. Species H rotavirus detected in piglets with diarrhea, Brazil, 2012. *Emerg. Infect. Dis.* **2014**, *20*, 1019–1022. [CrossRef] [PubMed]
63. Chinivasagam, H.N.; Thomas, R.J.; Casey, K.; McGahan, E.; Gardner, E.A.; Rafiee, M.; Blackall, P.J. Microbiological status of piggery effluent from 13 piggeries in the south east Queensland region of Australia. *J. Appl. Microbiol.* **2004**, *97*, 883–891. [CrossRef] [PubMed]

64. Amimo, J.O.; El Zowalaty, M.E.; Githae, D.; Wamalwa, M.; Djikeng, A.; Nasrallah, G.K. Metagenomic analysis demonstrates the diversity of the fecal virome in asymptomatic pigs in East Africa. *Arch. Virol.* **2016**, *161*, 887–897. [CrossRef] [PubMed]
65. Amimo, J.O.; Junga, J.O.; Ogara, W.O.; Vlasova, A.N.; Njahira, M.N.; Maina, S.; Okoth, E.A.; Bishop, R.P.; Saif, L.J.; Djikeng, A. Detection and genetic characterization of porcine group A rotaviruses in asymptomatic pigs in smallholder farms in East Africa: Predominance of P[8] genotype resembling human strains. *Vet. Microbiol.* **2015**, *175*, 195–210. [CrossRef] [PubMed]
66. Amimo, J.O.; Otieno, T.F.; Okoth, E.; Onono, J.O.; Bett, B. Risk factors for rotavirus infection in pigs in Busia and Teso subcounties, Western Kenya. *Trop. Anim. Health Prod.* **2017**, *49*, 105–112. [CrossRef] [PubMed]
67. Amimo, J.O.; Vlasova, A.N.; Saif, L.J. Detection and genetic diversity of porcine group A rotaviruses in historic (2004) and recent (2011 and 2012) swine fecal samples in Ohio: predominance of the G9P[13] genotype in nursing piglets. *J. Clin. Microbiol.* **2013**, *51*, 1142–1151. [CrossRef] [PubMed]
68. Da Silva, M.F.; Tort, L.F.; Gomez, M.M.; Assis, R.M.; de Mendonca, M.C.; Volotao Ede, M.; Leite, J.P. Phylogenetic analysis of VP1, VP2, and VP3 gene segments of genotype G5 group A rotavirus strains circulating in Brazil between 1986 and 2005. *Virus Res.* **2011**, *160*, 381–388. [CrossRef] [PubMed]
69. Homwong, N.; Diaz, A.; Rossow, S.; Ciarlet, M.; Marthaler, D. Three-Level Mixed-Effects Logistic Regression Analysis Reveals Complex Epidemiology of Swine Rotaviruses in Diagnostic Samples from North America. *PLoS ONE* **2016**, *11*, e0154734.
70. Martella, V.; Ciarlet, M.; Banyai, K.; Lorusso, E.; Arista, S.; Lavazza, A.; Pezzotti, G.; Decaro, N.; Cavalli, A.; Lucente, M.S.; et al. Identification of group A porcine rotavirus strains bearing a novel VP4 (P) Genotype in Italian swine herds. *J. Clin. Microbiol.* **2007**, *45*, 577–580. [CrossRef] [PubMed]
71. Marthaler, D.; Homwong, N.; Rossow, K.; Culhane, M.; Goyal, S.; Collins, J.; Matthijnssens, J.; Ciarlet, M. Rapid detection and high occurrence of porcine rotavirus A, B, and C by RT-qPCR in diagnostic samples. *J. Virol. Methods* **2014**, *209*, 30–34. [CrossRef] [PubMed]
72. Papp, H.; Matthijnssens, J.; Martella, V.; Ciarlet, M.; Banyai, K. Global distribution of group A rotavirus strains in horses: a systematic review. *Vaccine* **2013**, *31*, 5627–5633. [CrossRef] [PubMed]
73. Theuns, S.; Vyt, P.; Desmarets, L.M.; Roukaerts, I.D.; Heylen, E.; Zeller, M.; Matthijnssens, J.; Nauwynck, H.J. Presence and characterization of pig group A and C rotaviruses in feces of Belgian diarrheic suckling piglets. *Virus Res.* **2016**, *213*, 172–183. [CrossRef] [PubMed]
74. Pham, H.A.; Carrique-Mas, J.J.; Nguyen, V.C.; Ngo, T.H.; Nguyet, L.A.; Do, T.D.; Vo, B.H.; Phan, V.T.; Rabaa, M.A.; Farrar, J.; et al. The prevalence and genetic diversity of group A rotaviruses on pig farms in the Mekong Delta region of Vietnam. *Vet. Microbiol.* **2014**, *170*, 258–265. [PubMed]
75. Halaihel, N.; Masia, R.M.; Fernandez-Jimenez, M.; Ribes, J.M.; Montava, R.; De Blas, I.; Girones, O.; Alonso, J.L.; Buesa, J. Enteric calicivirus and rotavirus infections in domestic pigs. *Epidemiol. Infect.* **2010**, *138*, 542–548. [CrossRef] [PubMed]
76. Kim, H.J.; Park, S.I.; Ha, T.P.; Jeong, Y.J.; Kim, H.H.; Kwon, H.J.; Kang, M.I.; Cho, K.O.; Park, S.J. Detection and genotyping of Korean porcine rotaviruses. *Vet. Microbiol.* **2010**, *144*, 274–286. [CrossRef] [PubMed]
77. Katsuda, K.; Kohmoto, M.; Kawashima, K.; Tsunemitsu, H. Frequency of enteropathogen detection in suckling and weaned pigs with diarrhea in Japan. *J. Vet. Diagn. Investig.* **2006**, *18*, 350–354. [CrossRef] [PubMed]
78. Saikruang, W.; Khamrin, P.; Chaimongkol, N.; Suantai, B.; Kongkaew, A.; Kongkaew, S.; Ushijima, H.; Maneekarn, N. Genetic diversity and novel combinations of G4P[19] and G9P[19] porcine rotavirus strains in Thailand. *Vet. Microbiol.* **2013**, *161*, 255–262. [CrossRef] [PubMed]
79. Lamhoujeb, S.; Cook, A.; Pollari, F.; Bidawid, S.; Farber, J.; Mattison, K. Rotaviruses from Canadian farm samples. *Arch. Virol.* **2010**, *155*, 1127–1137. [CrossRef] [PubMed]
80. Racz, M.L.; Kroeff, S.S.; Munford, V.; Caruzo, T.A.; Durigon, E.L.; Hayashi, Y.; Gouvea, V.; Palombo, E.A. Molecular characterization of porcine rotaviruses from the southern region of Brazil: characterization of an atypical genotype G[9] strain. *J. Clin. Microbiol.* **2000**, *38*, 2443–2446. [PubMed]
81. Kusumakar, A.L.; Savita; Malik, Y.S.; Minakshi; Prasad, G. Genomic diversity among group A rotaviruses from diarrheic children, piglets, buffalo and cow calves of Madhya Pradesh. *Indian J. Microbiol.* **2010**, *50*, 83–88. [CrossRef] [PubMed]

82. Parra, G.I.; Vidales, G.; Gomez, J.A.; Fernandez, F.M.; Parreno, V.; Bok, K. Phylogenetic analysis of porcine rotavirus in Argentina: increasing diversity of G4 strains and evidence of interspecies transmission. *Vet. Microbiol.* **2008**, *126*, 243–250. [CrossRef] [PubMed]
83. Wieler, L.H.; Ilieff, A.; Herbst, W.; Bauer, C.; Vieler, E.; Bauerfeind, R.; Failing, K.; Klos, H.; Wengert, D.; Baljer, G.; et al. Prevalence of enteropathogens in suckling and weaned piglets with diarrhoea in southern Germany. *J. Vet. Med. B Infect. Dis. Vet. Public Health* **2001**, *48*, 151–159. [CrossRef] [PubMed]
84. Collins, P.J.; Martella, V.; Sleator, R.D.; Fanning, S.; O'Shea, H. Detection and characterisation of group A rotavirus in asymptomatic piglets in southern Ireland. *Arch. Virol.* **2010**, *155*, 1247–1259. [CrossRef] [PubMed]
85. Midgley, S.E.; Banyai, K.; Buesa, J.; Halaihel, N.; Hjulsager, C.K.; Jakab, F.; Kaplon, J.; Larsen, L.E.; Monini, M.; Poljsak-Prijatelj, M.; et al. Diversity and zoonotic potential of rotaviruses in swine and cattle across Europe. *Vet. Microbiol.* **2012**, *156*, 238–245. [CrossRef] [PubMed]
86. Morin, M.; Turgeon, D.; Jolette, J.; Robinson, Y.; Phaneuf, J.B.; Sauvageau, R.; Beauregard, M.; Teuscher, E.; Higgins, R.; Lariviere, S. Neonatal diarrhea of pigs in Quebec: Infectious causes of significant outbreaks. *Can. J. Comp. Med.* **1983**, *47*, 11–17. [PubMed]
87. Khamrin, P.; Peerakome, S.; Tonusin, S.; Malasao, R.; Okitsu, S.; Mizuguchi, M.; Ushijima, H.; Maneekarn, N. Changing pattern of rotavirus G genotype distribution in Chiang Mai, Thailand from 2002 to 2004: Decline of G9 and reemergence of G1 and G2. *J. Med. Virol.* **2007**, *79*, 1775–1782. [CrossRef] [PubMed]
88. Okitsu, S.; Khamrin, P.; Thongprachum, A.; Kongkaew, A.; Maneekarn, N.; Mizuguchi, M.; Hayakawa, S.; Ushijima, H. Whole-genomic analysis of G3P[23], G9P[23] and G3P[13] rotavirus strains isolated from piglets with diarrhea in Thailand, 2006–2008. *Infect. Genet. Evol.* **2013**, *18*, 74–86. [CrossRef] [PubMed]
89. Okitsu, S.; Khamrin, P.; Thongprachum, A.; Maneekarn, N.; Mizuguchi, M.; Ushijima, H. Predominance of porcine P[23] genotype rotaviruses in piglets with diarrhea in northern Thailand. *J. Clin. Microbiol.* **2011**, *49*, 442–445. [CrossRef] [PubMed]
90. Miyazaki, A.; Kuga, K.; Suzuki, T.; Kohmoto, M.; Katsuda, K.; Tsunemitsu, H. Genetic diversity of group A rotaviruses associated with repeated outbreaks of diarrhea in a farrow-to-finish farm: identification of a porcine rotavirus strain bearing a novel VP7 genotype, G26. *Vet. Res.* **2011**, *42*, 112. [CrossRef] [PubMed]
91. Collins, P.J.; Martella, V.; Buonavoglia, C.; O'Shea, H. Identification of a G2-like porcine rotavirus bearing a novel VP4 type, P[32]. *Vet. Res.* **2010**, *41*, 73. [CrossRef] [PubMed]
92. Wang, Y.H.; Kobayashi, N.; Nagashima, S.; Zhou, X.; Ghosh, S.; Peng, J.S.; Hu, Q.; Zhou, D.J.; Yang, Z.Q. Full genomic analysis of a porcine-bovine reassortant G4P[6] rotavirus strain R479 isolated from an infant in China. *J. Med. Virol.* **2010**, *82*, 1094–1102. [CrossRef] [PubMed]
93. Kim, Y.; Chang, K.O.; Straw, B.; Saif, L.J. Characterization of group C rotaviruses associated with diarrhea outbreaks in feeder pigs. *J. Clin. Microbiol.* **1999**, *37*, 1484–1488. [PubMed]
94. Marthaler, D.; Rossow, K.; Culhane, M.; Collins, J.; Goyal, S.; Ciarlet, M.; Matthijnssens, J. Identification, phylogenetic analysis and classification of porcine group C rotavirus VP7 sequences from the United States and Canada. *Virology* **2013**, *446*, 189–198. [CrossRef] [PubMed]
95. Tsunemitsu, H.; Jiang, B.; Saif, L.J. Sequence comparison of the VP7 gene encoding the outer capsid glycoprotein among animal and human group C rotaviruses. *Arch. Virol.* **1996**, *141*, 705–713. [CrossRef] [PubMed]
96. Rahman, M.; Banik, S.; Faruque, A.S.; Taniguchi, K.; Sack, D.A.; van Ranst, M.; Azim, T. Detection and characterization of human group C rotaviruses in Bangladesh. *J. Clin. Microbiol.* **2005**, *43*, 4460–4465. [CrossRef] [PubMed]
97. Martella, V.; Banyai, K.; Lorusso, E.; Decaro, N.; Bellacicco, A.; Desario, C.; Corrente, M.; Greco, G.; Moschidou, P.; Tempesta, M.; et al. Genetic heterogeneity in the VP7 of group C rotaviruses. *Virology* **2007**, *367*, 358–366. [CrossRef] [PubMed]
98. Stipp, D.T.; Alfieri, A.F.; Lorenzetti, E.; da Silva Medeiros, T.N.; Possatti, F.; Alfieri, A.A. VP6 gene diversity in 11 Brazilian strains of porcine group C rotavirus. *Virus Genes* **2015**, *50*, 142–146. [CrossRef] [PubMed]
99. Suzuki, T.; Hasebe, A.; Miyazaki, A.; Tsunemitsu, H. Phylogenetic characterization of VP6 gene (inner capsid) of porcine rotavirus C collected in Japan. *Infect. Genet. Evol.* **2014**, *26*, 223–227. [CrossRef] [PubMed]
100. Suzuki, T.; Hasebe, A.; Miyazaki, A.; Tsunemitsu, H. Analysis of genetic divergence among strains of porcine rotavirus C, with focus on VP4 and VP7 genotypes in Japan. *Virus Res.* **2015**, *197*, 26–34. [CrossRef] [PubMed]

101. Soma, J.; Tsunemitsu, H.; Miyamoto, T.; Suzuki, G.; Sasaki, T.; Suzuki, T. Whole-genome analysis of two bovine rotavirus C strains: Shintoku and Toyama. *J. Gen. Virol.* **2013**, *94 Pt 1*, 128–135. [CrossRef] [PubMed]
102. Yamamoto, D.; Ghosh, S.; Kuzuya, M.; Wang, Y.H.; Zhou, X.; Chawla-Sarkar, M.; Paul, S.K.; Ishino, M.; Kobayashi, N. Whole-genome characterization of human group C rotaviruses: identification of two lineages in the VP3 gene. *J. Gen. Virol.* **2011**, *92 Pt 2*, 361–369. [CrossRef] [PubMed]
103. Moutelikova, R.; Prodelalova, J.; Dufkova, L. Diversity of VP7, VP4, VP6, NSP2, NSP4, and NSP5 genes of porcine rotavirus C: phylogenetic analysis and description of potential new VP7, VP4, VP6, and NSP4 genotypes. *Arch. Virol.* **2015**, *160*, 1715–1727. [CrossRef] [PubMed]
104. Collins, P.J.; Martella, V.; O'Shea, H. Detection and characterization of group C rotaviruses in asymptomatic piglets in Ireland. *J. Clin. Microbiol.* **2008**, *46*, 2973–2979. [CrossRef] [PubMed]
105. Niira, K.; Ito, M.; Masuda, T.; Saitou, T.; Abe, T.; Komoto, S.; Sato, M.; Yamasato, H.; Kishimoto, M.; Naoi, Y.; et al. Whole genome sequences of Japanese porcine species C rotaviruses reveal a high diversity of genotypes of individual genes and will contribute to a comprehensive, generally accepted classification system. *Infect. Genet. Evol.* **2016**, *44*, 106–113. [CrossRef]
106. Kobayashi, N.; Naik, T.N.; Kusuhara, Y.; Krishnan, T.; Sen, A.; Bhattacharya, S.K.; Taniguchi, K.; Alam, M.M.; Urasawa, T.; Urasawa, S. Sequence analysis of genes encoding structural and nonstructural proteins of a human group B rotavirus detected in Calcutta, India. *J. Med. Virol.* **2001**, *64*, 583–588. [CrossRef] [PubMed]
107. Yamamoto, D.; Ghosh, S.; Ganesh, B.; Krishnan, T.; Chawla-Sarkar, M.; Alam, M.M.; Aung, T.S.; Kobayashi, N. Analysis of genetic diversity and molecular evolution of human group B rotaviruses based on whole genome segments. *J. Gen. Virol.* **2010**, *91 Pt 7*, 1772–1781. [CrossRef] [PubMed]
108. Yang, J.H.; Kobayashi, N.; Wang, Y.H.; Zhou, X.; Li, Y.; Zhou, D.J.; Hu, Z.H.; Ishino, M.; Alam, M.M.; Naik, T.N.; et al. Phylogenetic analysis of a human group B rotavirus WH-1 detected in China in 2002. *J. Med. Virol.* **2004**, *74*, 662–667. [CrossRef] [PubMed]
109. Petric, M.; Mayur, K.; Vonderfecht, S.; Eiden, J.J. Comparison of group B rotavirus genes 9 and 11. *J. Gen. Virol.* **1991**, *72 Pt 11*, 2801–2804. [CrossRef] [PubMed]
110. Kuga, K.; Miyazaki, A.; Suzuki, T.; Takagi, M.; Hattori, N.; Katsuda, K.; Mase, M.; Sugiyama, M.; Tsunemitsu, H. Genetic diversity and classification of the outer capsid glycoprotein VP7 of porcine group B rotaviruses. *Arch. Virol.* **2009**, *154*, 1785–1795. [CrossRef] [PubMed]
111. Marthaler, D.; Rossow, K.; Gramer, M.; Collins, J.; Goyal, S.; Tsunemitsu, H.; Kuga, K.; Suzuki, T.; Ciarlet, M.; Matthijnssens, J. Detection of substantial porcine group B rotavirus genetic diversity in the United States, resulting in a modified classification proposal for G genotypes. *Virology* **2012**, *433*, 85–96. [CrossRef] [PubMed]
112. Molinari, B.L.; Possatti, F.; Lorenzetti, E.; Alfieri, A.F.; Alfieri, A.A. Unusual outbreak of post-weaning porcine diarrhea caused by single and mixed infections of rotavirus groups A, B, C, and H. *Vet. Microbiol.* **2016**, *193*, 125–132. [CrossRef] [PubMed]
113. Yang, H.; Makeyev, E.V.; Kang, Z.; Ji, S.; Bamford, D.H.; van Dijk, A.A. Cloning and sequence analysis of dsRNA segments 5, 6 and 7 of a novel non-group A, B, C adult rotavirus that caused an outbreak of gastroenteritis in China. *Virus Res.* **2004**, *106*, 15–26. [CrossRef] [PubMed]
114. Alam, M.M.; Kobayashi, N.; Ishino, M.; Ahmed, M.S.; Ahmed, M.U.; Paul, S.K.; Muzumdar, B.K.; Hussain, Z.; Wang, Y.H.; Naik, T.N. Genetic analysis of an ADRV-N-like novel rotavirus strain B219 detected in a sporadic case of adult diarrhea in Bangladesh. *Arch. Virol.* **2007**, *152*, 199–208. [CrossRef] [PubMed]
115. Jiang, S.; Ji, S.; Tang, Q.; Cui, X.; Yang, H.; Kan, B.; Gao, S. Molecular characterization of a novel adult diarrhoea rotavirus strain J19 isolated in China and its significance for the evolution and origin of group B rotaviruses. *J. Gen. Virol.* **2008**, *89 Pt 10*, 2622–2629. [CrossRef] [PubMed]
116. Nagashima, S.; Kobayashi, N.; Ishino, M.; Alam, M.M.; Ahmed, M.U.; Paul, S.K.; Ganesh, B.; Chawla-Sarkar, M.; Krishnan, T.; Naik, T.N.; et al. Whole genomic characterization of a human rotavirus strain B219 belonging to a novel group of the genus Rotavirus. *J. Med. Virol.* **2008**, *80*, 2023–2033. [CrossRef] [PubMed]
117. Nyaga, M.M.; Peenze, I.; Potgieter, C.A.; Seheri, L.M.; Page, N.A.; Yinda, C.K.; Steele, A.D.; Matthijnssens, J.; Mphahlele, M.J. Complete genome analyses of the first porcine rotavirus group H identified from a South African pig does not provide evidence for recent interspecies transmission events. *Infect. Genet. Evol.* **2016**, *38*, 1–7. [CrossRef] [PubMed]

118. Winiarczyk, S.; Paul, P.S.; Mummidi, S.; Panek, R.; Gradzki, Z. Survey of porcine rotavirus G and P genotype in Poland and the United States using RT-PCR. *J. Vet. Med. B Infect. Dis. Vet. Public Health* **2002**, *49*, 373–378. [CrossRef] [PubMed]
119. Amimo, J.O.; Vlasova, A.N.; Saif, L.J. Prevalence and genetic heterogeneity of porcine group C rotaviruses in nursing and weaned piglets in Ohio, USA and identification of a potential new VP4 genotype. *Vet. Microbiol.* **2013**, *164*, 27–38. [PubMed]
120. Tonietti, P.O.; Hora, A.S.; Silva, F.D.; Ruiz, V.L.; Gregori, F. Phylogenetic analyses of the VP4 and VP7 genes of porcine group A rotaviruses in Sao Paulo State, Brazil: First identification of G5P[23] in piglets. *J. Clin. Microbiol.* **2013**, *51*, 2750–2753. [CrossRef] [PubMed]
121. Nyaga, M.M.; Jere, K.C.; Esona, M.D.; Seheri, M.L.; Stucker, K.M.; Halpin, R.A.; Akopov, A.; Stockwell, T.B.; Peenze, I.; Diop, A.; et al. Whole genome detection of rotavirus mixed infections in human, porcine and bovine samples co-infected with various rotavirus strains collected from sub-Saharan Africa. *Infect. Genet. Evol.* **2015**, *31*, 321–334. [CrossRef] [PubMed]
122. Atii, D.J.; Ojeh, C.K. Subgroup determination of group A rotaviruses recovered from piglets in Nigeria. *Viral Immunol.* **1995**, *8*, 151–157. [CrossRef] [PubMed]
123. Geyer, A.; Sebata, T.; Peenze, I.; Steele, A.D. Group B and C porcine rotaviruses identified for the first time in South Africa. *J. S. Afr. Vet. Assoc.* **1996**, *67*, 115–116. [PubMed]
124. Malik, Y.S.; Kumar, N.; Sharma, K.; Sircar, S.; Dhama, K.; Bora, D.P.; Dutta, T.; Prasad, M.; Tiwari, A.K. Rotavirus diarrhea in piglets: A review on epidemiology, genetic diversity and zoonotic risks. *Indian J. Anim. Sci.* **2014**, *84*, 1035–1042.
125. Gachanja, E.; Buza, J.; Petrucka, P. Prevalence of group A rotavirus in piglets in a periurban setting of Arusha, Tanzania. *J. Biosci. Med.* **2016**, *4*, 37–44.
126. Otto, P.H.; Rosenhain, S.; Elschner, M.C.; Hotzel, H.; Machnowska, P.; Trojnar, E.; Hoffmann, K.; Johne, R. Detection of rotavirus species A, B and C in domestic mammalian animals with diarrhoea and genotyping of bovine species A rotavirus strains. *Vet. Microbiol.* **2015**, *179*, 168–176. [CrossRef] [PubMed]
127. Martella, V.; Pratelli, A.; Greco, G.; Tempesta, M.; Ferrari, M.; Losio, M.N.; Buonavoglia, C. Genomic characterization of porcine rotaviruses in Italy. *Clin. Diagn. Lab. Immunol.* **2001**, *8*, 129–132. [CrossRef]
128. Theuns, S.; Desmarets, L.M.; Heylen, E.; Zeller, M.; Dedeurwaerder, A.; Roukaerts, I.D.; Van Ranst, M.; Matthijnssens, J.; Nauwynck, H.J. Porcine group A rotaviruses with heterogeneous VP7 and VP4 genotype combinations can be found together with enteric bacteria on Belgian swine farms. *Vet. Microbiol.* **2014**, *172*, 23–34. [CrossRef] [PubMed]
129. Martella, V.; Ciarlet, M.; Banyai, K.; Lorusso, E.; Cavalli, A.; Corrente, M.; Elia, G.; Arista, S.; Camero, M.; Desario, C.; et al. Identification of a novel VP4 genotype carried by a serotype G5 porcine rotavirus strain. *Virology* **2006**, *346*, 301–311. [CrossRef] [PubMed]
130. Martella, V.; Ciarlet, M.; Baselga, R.; Arista, S.; Elia, G.; Lorusso, E.; Banyai, K.; Terio, V.; Madio, A.; Ruggeri, F.M.; et al. Sequence analysis of the VP7 and VP4 genes identifies a novel VP7 gene allele of porcine rotaviruses, sharing a common evolutionary origin with human G2 rotaviruses. *Virology* **2005**, *337*, 111–123. [CrossRef] [PubMed]
131. Van der Heide, R.; Koopmans, M.P.; Shekary, N.; Houwers, D.J.; van Duynhoven, Y.T.; van der Poel, W.H. Molecular characterizations of human and animal group a rotaviruses in the Netherlands. *J. Clin. Microbiol.* **2005**, *43*, 669–675. [CrossRef] [PubMed]
132. Chandler-Bostock, R.; Hancox, L.R.; Nawaz, S.; Watts, O.; Iturriza-Gomara, M.; Mellits, K.H. Genetic diversity of porcine group A rotavirus strains in the UK. *Vet. Microbiol.* **2014**, *173*, 27–37. [CrossRef] [PubMed]
133. Smitalova, R.; Rodak, L.; Smid, B.; Psikal, I. Detection of nongroup A rotaviruses in faecal samples of pigs in the Czech Republic. *Vet. Med.* **2009**, *54*, 1–18.
134. Chitambar, S.D.; Arora, R.; Chhabra, P. Molecular characterization of a rare G1P[19] rotavirus strain from India: evidence of reassortment between human and porcine rotavirus strains. *J. Med. Microbiol.* **2009**, *58 Pt 12*, 1611–1615. [CrossRef] [PubMed]
135. Nguyen, T.A.; Khamrin, P.; Trinh, Q.D.; Phan, T.G.; Pham le, D.; Hoang le, P.; Hoang, K.T.; Yagyu, F.; Okitsu, S.; Ushijima, H. Sequence analysis of Vietnamese P[6] rotavirus strains suggests evidence of interspecies transmission. *J. Med. Virol.* **2007**, *79*, 1959–1965. [CrossRef] [PubMed]

136. Duan, Z.J.; Li, D.D.; Zhang, Q.; Liu, N.; Huang, C.P.; Jiang, X.; Jiang, B.; Glass, R.; Steele, D.; Tang, J.Y.; et al. Novel human rotavirus of genotype G5P[6] identified in a stool specimen from a Chinese girl with diarrhea. *J. Clin. Microbiol.* **2007**, *45*, 1614–1617. [PubMed]
137. Matsushima, Y.; Nakajima, E.; Nguyen, T.A.; Shimizu, H.; Kano, A.; Ishimaru, Y.; Phan, T.G.; Ushijima, H. Genome sequence of an unusual human G10P[8] rotavirus detected in Vietnam. *J. Virol.* **2012**, *86*, 10236–10237. [CrossRef] [PubMed]
138. Park, S.I.; Matthijnssens, J.; Saif, L.J.; Kim, H.J.; Park, J.G.; Alfajaro, M.M.; Kim, D.S.; Son, K.Y.; Yang, D.K.; Hyun, B.H.; et al. Reassortment among bovine, porcine and human rotavirus strains results in G8P[7] and G6P[7] strains isolated from cattle in South Korea. *Vet. Microbiol.* **2011**, *152*, 55–66. [CrossRef] [PubMed]
139. Teodoroff, T.A.; Tsunemitsu, H.; Okamoto, K.; Katsuda, K.; Kohmoto, M.; Kawashima, K.; Nakagomi, T.; Nakagomi, O. Predominance of porcine rotavirus G9 in Japanese piglets with diarrhea: close relationship of their VP7 genes with those of recent human G9 strains. *J. Clin. Microbiol.* **2005**, *43*, 1377–1384. [CrossRef] [PubMed]
140. Khamrin, P.; Maneekarn, N.; Peerakome, S.; Chan-it, W.; Yagyu, F.; Okitsu, S.; Ushijima, H. Novel porcine rotavirus of genotype P[27] shares new phylogenetic lineage with G2 porcine rotavirus strain. *Virology* **2007**, *361*, 243–252. [CrossRef] [PubMed]
141. Shi, H.; Chen, J.; Li, H.; Sun, D.; Wang, C.; Feng, L. Molecular characterization of a rare G9P[23] porcine rotavirus isolate from China. *Arch. Virol.* **2012**, *157*, 1897–1903. [CrossRef] [PubMed]
142. Zhang, H.; Zhang, Z.; Wang, Y.; Wang, X.; Xia, M.; Wu, H. Isolation, molecular characterization and evaluation of the pathogenicity of a porcine rotavirus isolated from Jiangsu Province, China. *Arch. Virol.* **2015**, *160*, 1333–1338. [CrossRef] [PubMed]
143. Peng, R.; Li, D.D.; Cai, K.; Qin, J.J.; Wang, Y.X.; Lin, Q.; Guo, Y.Q.; Zhao, C.Y.; Duan, Z.J. The epidemiological characteristics of group C rotavirus in Lulong area and the analysis of diversity of VP6 gene. *Zhonghua Shi Yan He Lin Chuang Bing Du Xue Za Zhi* **2013**, *27*, 164–166. [PubMed]
144. Suzuki, T.; Soma, J.; Miyazaki, A.; Tsunemitsu, H. Phylogenetic analysis of nonstructural protein 5 (NSP5) gene sequences in porcine rotavirus B strains. *Infect. Genet. Evol.* **2012**, *12*, 1661–1668. [CrossRef] [PubMed]
145. Lahon, A.; Ingle, V.C.; Birade, H.S.; Raut, C.G.; Chitambar, S.D. Molecular characterization of group B rotavirus circulating in pigs from India: identification of a strain bearing a novel VP7 genotype, G21. *Vet. Microbiol.* **2014**, *174*, 342–352. [CrossRef] [PubMed]
146. Huang, J.; Nagesha, H.S.; Dyall-Smith, M.L.; Holmes, I.H. Comparative sequence analysis of VP7 genes from five Australian porcine rotaviruses. *Arch. Virol.* **1989**, *109*, 173–183. [CrossRef] [PubMed]
147. Huang, J.A.; Nagesha, H.S.; Holmes, I.H. Comparative sequence analysis of VP4s from five Australian porcine rotaviruses: implication of an apparent new P type. *Virology* **1993**, *196*, 319–327. [CrossRef] [PubMed]
148. Nagesha, H.S.; Huang, J.; Holmes, I.H. A variant serotype G3 rotavirus isolated from an unusually severe outbreak of diarrhoea in piglets. *J. Med. Virol.* **1992**, *38*, 79–85. [CrossRef] [PubMed]
149. Khamrin, P.; Maneekarn, N.; Peerakome, S.; Yagyu, F.; Okitsu, S.; Ushijima, H. Molecular characterization of a rare G3P[3] human rotavirus reassortant strain reveals evidence for multiple human-animal interspecies transmissions. *J. Med. Virol.* **2006**, *78*, 986–994. [CrossRef] [PubMed]
150. Marton, S.; Doro, R.; Feher, E.; Forro, B.; Ihasz, K.; Varga-Kugler, R.; Farkas, S.L.; Banyai, K. Whole genome sequencing of a rare rotavirus from archived stool sample demonstrates independent zoonotic origin of human G8P[14] strains in Hungary. *Virus Res.* **2017**, *227*, 96–103. [CrossRef] [PubMed]
151. Li, K.; Lin, X.D.; Huang, K.Y.; Zhang, B.; Shi, M.; Guo, W.P.; Wang, M.R.; Wang, W.; Xing, J.G.; Li, M.H.; et al. Identification of novel and diverse rotaviruses in rodents and insectivores, and evidence of cross-species transmission into humans. *Virology* **2016**, *494*, 168–177. [CrossRef] [PubMed]
152. Ghosh, S.; Varghese, V.; Samajdar, S.; Bhattacharya, S.K.; Kobayashi, N.; Naik, T.N. Molecular characterization of a porcine Group A rotavirus strain with G12 genotype specificity. *Arch. Virol.* **2006**, *151*, 1329–1344. [CrossRef] [PubMed]
153. Hoshino, Y.; Honma, S.; Jones, R.W.; Ross, J.; Santos, N.; Gentsch, J.R.; Kapikian, A.Z.; Hesse, R.A. A porcine G9 rotavirus strain shares neutralization and VP7 phylogenetic sequence lineage 3 characteristics with contemporary human G9 rotavirus strains. *Virology* **2005**, *332*, 177–188. [CrossRef] [PubMed]
154. Rahman, M.; Matthijnssens, J.; Yang, X.; Delbeke, T.; Arijs, I.; Taniguchi, K.; Iturriza-Gomara, M.; Iftekharuddin, N.; Azim, T.; Van Ranst, M. Evolutionary history and global spread of the emerging g12 human rotaviruses. *J. Virol.* **2007**, *81*, 2382–2390. [CrossRef] [PubMed]

155. Mukherjee, A.; Mullick, S.; Deb, A.K.; Panda, S.; Chawla-Sarkar, M. First report of human rotavirus G8P[4] gastroenteritis in India: evidence of ruminants-to-human zoonotic transmission. *J. Med. Virol.* **2013**, *85*, 537–545. [CrossRef] [PubMed]
156. Doan, Y.H.; Nakagomi, T.; Aboudy, Y.; Silberstein, I.; Behar-Novat, E.; Nakagomi, O.; Shulman, L.M. Identification by full-genome analysis of a bovine rotavirus transmitted directly to and causing diarrhea in a human child. *J. Clin. Microbiol.* **2013**, *51*, 182–189. [CrossRef] [PubMed]
157. Luchs, A.; Cilli, A.; Morillo, S.G.; Carmona Rde, C.; Timenetsky Mdo, C. Rare G3P[3] rotavirus strain detected in Brazil: possible human-canine interspecies transmission. *J. Clin. Virol.* **2012**, *54*, 89–92. [CrossRef] [PubMed]
158. Ben Hadj Fredj, M.; Heylen, E.; Zeller, M.; Fodha, I.; Benhamida-Rebai, M.; Van Ranst, M.; Matthijnssens, J.; Trabelsi, A. Feline origin of rotavirus strain, Tunisia, 2008. *Emerg. Infect. Dis.* **2013**, *19*, 630–634. [CrossRef] [PubMed]
159. Liu, Y.; Huang, P.; Tan, M.; Liu, Y.; Biesiada, J.; Meller, J.; Castello, A.A.; Jiang, B.; Jiang, X. Rotavirus VP8*: phylogeny, host range, and interaction with histo-blood group antigens. *J. Virol.* **2012**, *86*, 9899–9910. [CrossRef] [PubMed]
160. Liu, Y.; Ramelot, T.A.; Huang, P.; Liu, Y.; Li, Z.; Feizi, T.; Zhong, W.; Wu, F.T.; Tan, M.; Kennedy, M.A.; et al. Glycan Specificity of P[19] Rotavirus and Comparison with Those of Related P Genotypes. *J. Virol.* **2016**, *90*, 9983–9996. [CrossRef]
161. Huang, P.; Xia, M.; Tan, M.; Zhong, W.; Wei, C.; Wang, L.; Morrow, A.; Jiang, X. Spike protein VP8* of human rotavirus recognizes histo-blood group antigens in a type-specific manner. *J. Virol.* **2012**, *86*, 4833–4843. [CrossRef] [PubMed]
162. Van Trang, N.; Vu, H.T.; Le, N.T.; Huang, P.; Jiang, X.; Anh, D.D. Association between norovirus and rotavirus infection and histo-blood group antigen types in Vietnamese children. *J. Clin. Microbiol.* **2014**, *52*, 1366–1374. [CrossRef] [PubMed]
163. Yamamoto, F.; Yamamoto, M. Molecular genetic basis of porcine histo-blood group AO system. *Blood* **2001**, *97*, 3308–3310. [CrossRef] [PubMed]
164. Cooling, L. Blood Groups in Infection and Host Susceptibility. *Clin. Microbiol. Rev.* **2015**, *28*, 801–870. [CrossRef] [PubMed]
165. Martella, V.; Banyai, K.; Ciarlet, M.; Iturriza-Gomara, M.; Lorusso, E.; De Grazia, S.; Arista, S.; Decaro, N.; Elia, G.; Cavalli, A.; et al. Relationships among porcine and human P[6] rotaviruses: evidence that the different human P[6] lineages have originated from multiple interspecies transmission events. *Virology* **2006**, *344*, 509–519. [CrossRef] [PubMed]
166. Mascarenhas, J.D.; Leite, J.P.; Lima, J.C.; Heinemann, M.B.; Oliveira, D.S.; Araujo, I.T.; Soares, L.S.; Gusmao, R.H.; Gabbay, Y.B.; Linhares, A.C. Detection of a neonatal human rotavirus strain with VP4 and NSP4 genes of porcine origin. *J. Med. Microbiol.* **2007**, *56 Pt 4*, 524–532. [CrossRef] [PubMed]
167. Shintani, T.; Ghosh, S.; Wang, Y.H.; Zhou, X.; Zhou, D.J.; Kobayashi, N. Whole genomic analysis of human G1P[8] rotavirus strains from different age groups in China. *Viruses* **2012**, *4*, 1289–1304. [CrossRef] [PubMed]
168. Wyatt, R.G.; James, W.D.; Bohl, E.H.; Theil, K.W.; Saif, L.J.; Kalica, A.R.; Greenberg, H.B.; Kapikian, A.Z.; Chanock, R.M. Human rotavirus type 2: Cultivation in vitro. *Science* **1980**, *207*, 189–191. [CrossRef] [PubMed]
169. Do, L.P.; Nakagomi, T.; Otaki, H.; Agbemabiese, C.A.; Nakagomi, O.; Tsunemitsu, H. Phylogenetic inference of the porcine Rotavirus A origin of the human G1 VP7 gene. *Infect. Genet. Evol.* **2016**, *40*, 205–213. [CrossRef] [PubMed]
170. Do, L.P.; Nakagomi, T.; Nakagomi, O. A rare G1P[6] super-short human rotavirus strain carrying an H2 genotype on the genetic background of a porcine rotavirus. *Infect. Genet. Evol.* **2014**, *21*, 334–350. [CrossRef] [PubMed]
171. Heylen, E.; Batoko Likele, B.; Zeller, M.; Stevens, S.; De Coster, S.; Conceicao-Neto, N.; Van Geet, C.; Jacobs, J.; Ngbonda, D.; Van Ranst, M.; et al. Rotavirus surveillance in Kisangani, the Democratic Republic of the Congo, reveals a high number of unusual genotypes and gene segments of animal origin in non-vaccinated symptomatic children. *PLoS ONE* **2014**, *9*, e100953. [CrossRef] [PubMed]
172. Zhou, X.; Wang, Y.H.; Ghosh, S.; Tang, W.F.; Pang, B.B.; Liu, M.Q.; Peng, J.S.; Zhou, D.J.; Kobayashi, N. Genomic characterization of G3P[6], G4P[6] and G4P[8] human rotaviruses from Wuhan, China: Evidence for interspecies transmission and reassortment events. *Infect. Genet. Evol.* **2015**, *33*, 55–71. [CrossRef] [PubMed]

173. Martella, V.; Colombrita, D.; Lorusso, E.; Draghin, E.; Fiorentini, S.; De Grazia, S.; Banyai, K.; Ciarlet, M.; Caruso, A.; Buonavoglia, C. Detection of a porcine-like rotavirus in a child with enteritis in Italy. *J. Clin. Microbiol.* **2008**, *46*, 3501–3507. [CrossRef] [PubMed]
174. Steyer, A.; Poljsak-Prijatelj, M.; Barlic-Maganja, D.; Marin, J. Human, porcine and bovine rotaviruses in Slovenia: evidence of interspecies transmission and genome reassortment. *J. Gen. Virol.* **2008**, *89 Pt 7*, 1690–1698. [CrossRef] [PubMed]
175. Wu, F.T.; Banyai, K.; Huang, J.C.; Wu, H.S.; Chang, F.Y.; Hsiung, C.A.; Huang, Y.C.; Lin, J.S.; Hwang, K.P.; Jiang, B.; et al. Human infection with novel G3P[25] rotavirus strain in Taiwan. *Clin. Microbiol. Infec.* **2011**, *17*, 1570–1573. [CrossRef] [PubMed]
176. Hwang, K.P.; Wu, F.T.; Banyai, K.; Wu, H.S.; Yang, D.C.; Huang, Y.C.; Lin, J.S.; Hsiung, C.A.; Huang, J.C.; Jiang, B.; et al. Identification of porcine rotavirus-like genotype P[6] strains in Taiwanese children. *J. Med. Microbiol.* **2012**, *61 Pt 7*, 990–997. [CrossRef] [PubMed]
177. Papp, H.; Borzak, R.; Farkas, S.; Kisfali, P.; Lengyel, G.; Molnar, P.; Melegh, B.; Matthijnssens, J.; Jakab, F.; Martella, V.; et al. Zoonotic transmission of reassortant porcine G4P[6] rotaviruses in Hungarian pediatric patients identified sporadically over a 15 year period. *Infect. Genet. Evol.* **2013**, *19*, 71–80. [CrossRef] [PubMed]
178. Dong, H.J.; Qian, Y.; Huang, T.; Zhu, R.N.; Zhao, L.Q.; Zhang, Y.; Li, R.C.; Li, Y.P. Identification of circulating porcine-human reassortant G4P[6] rotavirus from children with acute diarrhea in China by whole genome analyses. *Infect. Genet. Evol.* **2013**, *20*, 155–162. [CrossRef] [PubMed]
179. Degiuseppe, J.I.; Beltramino, J.C.; Millan, A.; Stupka, J.A.; Parra, G.I. Complete genome analyses of G4P[6] rotavirus detected in Argentinean children with diarrhoea provides evidence of interspecies transmission from swine. *Clin. Microbiol. Infec.* **2013**, *19*, E367–E371. [CrossRef]
180. Stupka, J.A.; Carvalho, P.; Amarilla, A.A.; Massana, M.; Parra, G.I.; Argentinean National Surveillance Network for Diarrheas. National Rotavirus Surveillance in Argentina: High incidence of G9P[8] strains and detection of G4P[6] strains with porcine characteristics. *Infect. Genet. Evol.* **2009**, *9*, 1225–1231. [CrossRef] [PubMed]
181. Razafindratsimandresy, R.; Heraud, J.M.; Ramarokoto, C.E.; Rabemanantsoa, S.; Randremanana, R.; Andriamamonjy, N.S.; Richard, V.; Reynes, J.M. Rotavirus genotypes in children in the community with diarrhea in Madagascar. *J. Med. Virol.* **2013**, *85*, 1652–1660. [CrossRef] [PubMed]
182. Komoto, S.; Maeno, Y.; Tomita, M.; Matsuoka, T.; Ohfu, M.; Yodoshi, T.; Akeda, H.; Taniguchi, K. Whole genomic analysis of a porcine-like human G5P[6] rotavirus strain isolated from a child with diarrhoea and encephalopathy in Japan. *J. Gen. Virol.* **2013**, *94 Pt 7*, 1568–1575. [PubMed]
183. Mladenova, Z.; Papp, H.; Lengyel, G.; Kisfali, P.; Steyer, A.; Steyer, A.F.; Esona, M.D.; Iturriza-Gomara, M.; Banyai, K. Detection of rare reassortant G5P[6] rotavirus, Bulgaria. *Infect. Genet. Evol.* **2012**, *12*, 1676–1684. [CrossRef] [PubMed]
184. Da Silva, M.F.; Tort, L.F.; Gomez, M.M.; Assis, R.M.; Volotao Ede, M.; de Mendonca, M.C.; Bello, G.; Leite, J.P. VP7 Gene of human rotavirus A genotype G5: Phylogenetic analysis reveals the existence of three different lineages worldwide. *J. Med. Virol.* **2011**, *83*, 357–366. [CrossRef] [PubMed]
185. Mijatovic-Rustempasic, S.; Banyai, K.; Esona, M.D.; Foytich, K.; Bowen, M.D.; Gentsch, J.R. Genome sequence based molecular epidemiology of unusual US Rotavirus A G9 strains isolated from Omaha, USA between 1997 and 2000. *Infect. Genet. Evol.* **2011**, *11*, 522–527. [CrossRef] [PubMed]
186. Martinez-Laso, J.; Roman, A.; Head, J.; Cervera, I.; Rodriguez, M.; Rodriguez-Avial, I.; Picazo, J.J. Phylogeny of G9 rotavirus genotype: a possible explanation of its origin and evolution. *J. Clin. Virol.* **2009**, *44*, 52–57. [CrossRef] [PubMed]
187. Mukherjee, A.; Dutta, D.; Ghosh, S.; Bagchi, P.; Chattopadhyay, S.; Nagashima, S.; Kobayashi, N.; Dutta, P.; Krishnan, T.; Naik, T.N.; et al. Full genomic analysis of a human group A rotavirus G9P[6] strain from Eastern India provides evidence for porcine-to-human interspecies transmission. *Arch. Virol.* **2009**, *154*, 733–746. [CrossRef] [PubMed]
188. Yodmeeklin, A.; Khamrin, P.; Chuchaona, W.; Kumthip, K.; Kongkaew, A.; Vachirachewin, R.; Okitsu, S.; Ushijima, H.; Maneekarn, N. Analysis of complete genome sequences of G9P[19] rotavirus strains from human and piglet with diarrhea provides evidence for whole-genome interspecies transmission of nonreassorted porcine rotavirus. *Infect. Genet. Evol.* **2017**, *47*, 99–108. [CrossRef] [PubMed]

189. Ghosh, S.; Urushibara, N.; Taniguchi, K.; Kobayashi, N. Whole genomic analysis reveals the porcine origin of human G9P[19] rotavirus strains Mc323 and Mc345. *Infect. Genet. Evol.* **2012**, *12*, 471–477. [CrossRef] [PubMed]
190. Wu, F.T.; Banyai, K.; Jiang, B.; Liu, L.T.; Marton, S.; Huang, Y.C.; Huang, L.M.; Liao, M.H.; Hsiung, C.A. Novel G9 rotavirus strains co-circulate in children and pigs, Taiwan. *Sci. Rep.* **2017**, *7*, 40731. [CrossRef] [PubMed]
191. Do, L.P.; Kaneko, M.; Nakagomi, T.; Gauchan, P.; Agbemabiese, C.A.; Dang, A.D.; Nakagomi, O. Molecular epidemiology of Rotavirus A, causing acute gastroenteritis hospitalizations among children in Nha Trang, Vietnam, 2007–2008: Identification of rare G9P[19] and G10P[14] strains. *J. Med. Virol.* **2017**, *89*, 621–631. [CrossRef] [PubMed]
192. Matthijnssens, J.; Rahman, M.; Ciarlet, M.; Zeller, M.; Heylen, E.; Nakagomi, T.; Uchida, R.; Hassan, Z.; Azim, T.; Nakagomi, O.; et al. Reassortment of human rotavirus gene segments into G11 rotavirus strains. *Emerg. Infect. Dis.* **2010**, *16*, 625–630. [CrossRef] [PubMed]
193. Shetty, S.A.; Mathur, M.; Deshpande, J.M. Complete genome analysis of a rare group A rotavirus, G11P[25], isolated from a child in Mumbai, India, reveals interspecies transmission and reassortment with human rotavirus strains. *J. Med. Microbiol.* **2014**, *63 Pt 9*, 1220–1227. [CrossRef] [PubMed]
194. Mullick, S.; Mukherjee, A.; Ghosh, S.; Pazhani, G.P.; Sur, D.; Manna, B.; Nataro, J.P.; Levine, M.M.; Ramamurthy, T.; Chawla-Sarkar, M. Genomic analysis of human rotavirus strains G6P[14] and G11P[25] isolated from Kolkata in 2009 reveals interspecies transmission and complex reassortment events. *Infect. Genet. Evol.* **2013**, *14*, 15–21. [CrossRef] [PubMed]
195. Komoto, S.; Wandera Apondi, E.; Shah, M.; Odoyo, E.; Nyangao, J.; Tomita, M.; Wakuda, M.; Maeno, Y.; Shirato, H.; Tsuji, T.; et al. Whole genomic analysis of human G12P[6] and G12P[8] rotavirus strains that have emerged in Kenya: identification of porcine-like NSP4 genes. *Infect. Genet. Evol.* **2014**, *27*, 277–293. [CrossRef] [PubMed]
196. Ide, T.; Komoto, S.; Higo-Moriguchi, K.; Htun, K.W.; Myint, Y.Y.; Myat, T.W.; Thant, K.Z.; Thu, H.M.; Win, M.M.; Oo, H.N.; et al. Whole Genomic Analysis of Human G12P[6] and G12P[8] Rotavirus Strains that Have Emerged in Myanmar. *PLoS ONE* **2015**, *10*, e0124965. [CrossRef] [PubMed]
197. My, P.V.; Rabaa, M.A.; Donato, C.; Cowley, D.; Phat, V.V.; Dung, T.T.; Anh, P.H.; Vinh, H.; Bryant, J.E.; Kellam, P.; et al. Novel porcine-like human G26P[19] rotavirus identified in hospitalized paediatric diarrhoea patients in Ho Chi Minh City, Vietnam. *J. Gen. Virol.* **2014**, *95 Pt 12*, 2727–2733. [CrossRef] [PubMed]
198. Medici, K.C.; Barry, A.F.; Alfieri, A.F.; Alfieri, A.A. Genetic analysis of the porcine group B rotavirus NSP2 gene from wild-type Brazilian strains. *Braz. J. Med. Biol. Res.* **2010**, *43*, 13–16. [CrossRef] [PubMed]
199. Gabbay, Y.B.; Borges, A.A.; Oliveira, D.S.; Linhares, A.C.; Mascarenhas, J.D.; Barardi, C.R.; Simoes, C.M.; Wang, Y.; Glass, R.I.; Jiang, B. Evidence for zoonotic transmission of group C rotaviruses among children in Belem, Brazil. *J. Med. Virol.* **2008**, *80*, 1666–1674. [CrossRef] [PubMed]
200. Iturriza-Gomara, M.; Dallman, T.; Banyai, K.; Bottiger, B.; Buesa, J.; Diedrich, S.; Fiore, L.; Johansen, K.; Koopmans, M.; Korsun, N.; et al. Rotavirus genotypes co-circulating in Europe between 2006 and 2009 as determined by EuroRotaNet, a pan-European collaborative strain surveillance network. *Epidemiol. Infect.* **2011**, *139*, 895–909. [CrossRef] [PubMed]
201. Iturriza-Gomara, M.; Dallman, T.; Banyai, K.; Bottiger, B.; Buesa, J.; Diedrich, S.; Fiore, L.; Johansen, K.; Korsun, N.; Kroneman, A.; et al. Rotavirus surveillance in europe, 2005–2008: web-enabled reporting and real-time analysis of genotyping and epidemiological data. *J. Infect. Dis.* **2009**, *200* (Suppl. S1), S215–S221. [CrossRef] [PubMed]
202. Iturriza-Gomara, M.; Green, J.; Brown, D.W.; Ramsay, M.; Desselberger, U.; Gray, J.J. Molecular epidemiology of human group A rotavirus infections in the United Kingdom between 1995 and 1998. *J. Clin. Microbiol.* **2000**, *38*, 4394–4401. [PubMed]
203. Chang, K.O.; Nielsen, P.R.; Ward, L.A.; Saif, L.J. Dual infection of gnotobiotic calves with bovine strains of group A and porcine-like group C rotaviruses influences pathogenesis of the group C rotavirus. *J. Virol.* **1999**, *73*, 9284–9293. [PubMed]
204. Banyai, K.; Jiang, B.; Bogdan, A.; Horvath, B.; Jakab, F.; Meleg, E.; Martella, V.; Magyari, L.; Melegh, B.; Szucs, G. Prevalence and molecular characterization of human group C rotaviruses in Hungary. *J. Clin. Virol.* **2006**, *37*, 317–322. [CrossRef] [PubMed]

205. Desselberger, U.; Huppertz, H.I. Immune responses to rotavirus infection and vaccination and associated correlates of protection. *J. Infect. Dis.* **2011**, *203*, 188–195. [CrossRef] [PubMed]
206. Saif, L.J.; Ward, L.A.; Yuan, L.; Rosen, B.I.; To, T.L. The gnotobiotic piglet as a model for studies of disease pathogenesis and immunity to human rotaviruses. *Arch. Virol. Suppl.* **1996**, *12*, 153–161. [PubMed]
207. Vlasova, A.N.; Shao, L.; Kandasamy, S.; Fischer, D.D.; Rauf, A.; Langel, S.N.; Chattha, K.S.; Kumar, A.; Huang, H.C.; Rajashekara, G.; et al. Escherichia coli Nissle 1917 protects gnotobiotic pigs against human rotavirus by modulating pDC and NK-cell responses. *Eur. J. Immunol.* **2016**, *46*, 2426–2437. [CrossRef] [PubMed]
208. Narvaez, C.F.; Angel, J.; Franco, M.A. Interaction of rotavirus with human myeloid dendritic cells. *J. Virol.* **2005**, *79*, 14526–14535. [CrossRef] [PubMed]
209. Feng, N.; Kim, B.; Fenaux, M.; Nguyen, H.; Vo, P.; Omary, M.B.; Greenberg, H.B. Role of interferon in homologous and heterologous rotavirus infection in the intestines and extraintestinal organs of suckling mice. *J. Virol.* **2008**, *82*, 7578–7590. [CrossRef] [PubMed]
210. Angel, J.; Franco, M.A.; Greenberg, H.B.; Bass, D. Lack of a role for type I and type II interferons in the resolution of rotavirus-induced diarrhea and infection in mice. *J. Interferon Cytokine Res.* **1999**, *19*, 655–659. [CrossRef] [PubMed]
211. Vancott, J.L.; McNeal, M.M.; Choi, A.H.; Ward, R.L. The role of interferons in rotavirus infections and protection. *J. Interferon Cytokine Res.* **2003**, *23*, 163–170. [CrossRef] [PubMed]
212. Vlasova, A.N.; Chattha, K.S.; Kandasamy, S.; Siegismund, C.S.; Saif, L.J. Prenatally acquired vitamin A deficiency alters innate immune responses to human rotavirus in a gnotobiotic pig model. *J. Immunol.* **2013**, *190*, 4742–4753. [CrossRef] [PubMed]
213. Vlasova, A.N.; Chattha, K.S.; Kandasamy, S.; Liu, Z.; Esseili, M.; Shao, L.; Rajashekara, G.; Saif, L.J. Lactobacilli and bifidobacteria promote immune homeostasis by modulating innate immune responses to human rotavirus in neonatal gnotobiotic pigs. *PLoS ONE* **2013**, *8*, e76962. [CrossRef] [PubMed]
214. Kandasamy, S.; Vlasova, A.N.; Fischer, D.; Kumar, A.; Chattha, K.S.; Rauf, A.; Shao, L.; Langel, S.N.; Rajashekara, G.; Saif, L.J. Differential Effects of Escherichia coli Nissle and Lactobacillus rhamnosus Strain GG on Human Rotavirus Binding, Infection, and B Cell Immunity. *J. Immunol.* **2016**, *196*, 1780–1789. [CrossRef] [PubMed]
215. Azevedo, M.S.; Yuan, L.; Iosef, C.; Chang, K.O.; Kim, Y.; Nguyen, T.V.; Saif, L.J. Magnitude of serum and intestinal antibody responses induced by sequential replicating and nonreplicating rotavirus vaccines in gnotobiotic pigs and correlation with protection. *Clin. Diagn. Lab. Immunol.* **2004**, *11*, 12–20. [CrossRef] [PubMed]
216. Yuan, L.; Kang, S.Y.; Ward, L.A.; To, T.L.; Saif, L.J. Antibody-secreting cell responses and protective immunity assessed in gnotobiotic pigs inoculated orally or intramuscularly with inactivated human rotavirus. *J. Virol.* **1998**, *72*, 330–338. [PubMed]
217. Yuan, L.; Wen, K.; Azevedo, M.S.; Gonzalez, A.M.; Zhang, W.; Saif, L.J. Virus-specific intestinal IFN-gamma producing T cell responses induced by human rotavirus infection and vaccines are correlated with protection against rotavirus diarrhea in gnotobiotic pigs. *Vaccine* **2008**, *26*, 3322–3331. [CrossRef] [PubMed]
218. Yuan, L.; Iosef, C.; Azevedo, M.S.; Kim, Y.; Qian, Y.; Geyer, A.; Nguyen, T.V.; Chang, K.O.; Saif, L.J. Protective immunity and antibody-secreting cell responses elicited by combined oral attenuated Wa human rotavirus and intranasal Wa 2/6-VLPs with mutant Escherichia coli heat-labile toxin in gnotobiotic pigs. *J. Virol.* **2001**, *75*, 9229–9238. [CrossRef] [PubMed]
219. Iosef, C.; Chang, K.O.; Azevedo, M.S.; Saif, L.J. Systemic and intestinal antibody responses to NSP4 enterotoxin of Wa human rotavirus in a gnotobiotic pig model of human rotavirus disease. *J. Med. Virol.* **2002**, *68*, 119–128. [CrossRef] [PubMed]
220. Hodgins, D.C.; Kang, S.Y.; deArriba, L.; Parreno, V.; Ward, L.A.; Yuan, L.; To, T.; Saif, L.J. Effects of maternal antibodies on protection and development of antibody responses to human rotavirus in gnotobiotic pigs. *J. Virol.* **1999**, *73*, 186–197. [PubMed]
221. Nguyen, T.V.; Yuan, L.; Azevedo, M.S.; Jeong, K.I.; Gonzalez, A.M.; Iosef, C.; Lovgren-Bengtsson, K.; Morein, B.; Lewis, P.; Saif, L.J. High titers of circulating maternal antibodies suppress effector and memory B-cell responses induced by an attenuated rotavirus priming and rotavirus-like particle-immunostimulating complex boosting vaccine regimen. *Clin. Vaccine Immunol. CVI* **2006**, *13*, 475–485. [CrossRef] [PubMed]

222. Tate, J.E.; Parashar, U.D. Rotavirus vaccines in routine use. *Clin. Infect. Dis.* **2014**, *59*, 1291–1301. [CrossRef] [PubMed]
223. Saif, L.J.; Fernandez, F.M. Group A rotavirus veterinary vaccines. *J. Infect. Dis.* **1996**, *174* (Suppl. S1), S98–S106. [CrossRef] [PubMed]
224. Azevedo, M.P.; Vlasova, A.N.; Saif, L.J. Human rotavirus virus-like particle vaccines evaluated in a neonatal gnotobiotic pig model of human rotavirus disease. *Expert Rev. Vaccines* **2013**, *12*, 169–181. [CrossRef] [PubMed]
225. Gautam, R.; Mijatovic-Rustempasic, S.; Esona, M.D.; Tam, K.I.; Quaye, O.; Bowen, M.D. One-step multiplex real-time RT-PCR assay for detecting and genotyping wild-type group A rotavirus strains and vaccine strains (Rotarix(R) and RotaTeq(R)) in stool samples. *PeerJ* **2016**, *4*, e1560. [CrossRef] [PubMed]

© 2017 by the authors. Licensee MDPI, Basel, Switzerland. This article is an open access article distributed under the terms and conditions of the Creative Commons Attribution (CC BY) license (http://creativecommons.org/licenses/by/4.0/).

viruses

MDPI

Article

Evaluation and Comparison of the Pathogenicity and Host Immune Responses Induced by a G2b Taiwan Porcine Epidemic Diarrhea Virus (Strain Pintung 52) and Its Highly Cell-Culture Passaged Strain in Conventional 5-Week-Old Pigs

Yen-Chen Chang [1,†], Chi-Fei Kao [1,†], Chia-Yu Chang [1], Chian-Ren Jeng [1,2], Pei-Shiue Tsai [2], Victor Fei Pang [1,2], Hue-Ying Chiou [3], Ju-Yi Peng [1], Ivan-Chen Cheng [1] and Hui-Wen Chang [1,2,*]

1 Graduate Institute of Molecular and Comparative Pathobiology, School of Veterinary Medicine, National Taiwan University, No. 1, Section 4, Roosevelt Rd., Taipei 10617, Taiwan; chyenjean@hotmail.com (Y.-C.C.); fei81005@gmail.com (C.-F.K.); f04644007@ntu.edu.tw (C.-Y.C.); crjeng@ntu.edu.tw (C.-R.J.); pang@ntu.edu.tw (V.F.P.); rudy4122@gmail.com (J.-Y.P.); Ivancheng@ntu.edu.tw (I.-C.C.)

2 School of Veterinary Medicine, National Taiwan University, No. 1, Section 4, Roosevelt Rd., Taipei 10617, Taiwan; psjasontsai@ntu.edu.tw

3 Graduate Institute of Veterinary Pathobiology, College of Veterinary Medicine, National Chung Hsing University, 250 Kuo Kuang Rd., Taichung 402, Taiwan; hic01.chiou@gmail.com

* Correspondence: huiwenchang@ntu.edu.tw; Tel.: +886-2-3366-1296; Fax: +886-2-2762-1965

† Y.-C. Chang and C.-F. Kao are co-first authors.

Academic Editors: Linda Dixon and Simon Graham
Received: 25 January 2017; Accepted: 15 May 2017; Published: 19 May 2017

Abstract: A genogroup 2b (G2b) porcine epidemic diarrhea virus (PEDV) Taiwan Pintung 52 (PEDVPT) strain was isolated in 2014. The pathogenicity and host antibody responses elicited by low-passage (passage 5; PEDVPT-P5) and high-passage (passage 96; PEDVPT-P96) PEDVPT strains were compared in post-weaning PEDV-seronegative pigs by oral inoculation. PEDVPT-P5-inoculation induced typical diarrhea during 1–9 days post inoculation with fecal viral shedding persisting for 26 days. Compared to PEDVPT-P5, PEDVPT-P96 inoculation induced none-to-mild diarrhea and lower, delayed fecal viral shedding. Although PEDVPT-P96 elicited slightly lower neutralizing antibodies and PEDV-specific immunoglobulin G (IgG) and immunoglobulin A (IgA) titers, a reduction in pathogenicity and viral shedding of the subsequent challenge with PEDVPT-P5 were noted in both PEDVPT-P5- and PEDVPT-P96-inoculated pigs. Alignment and comparison of full-length sequences of PEDVPT-P5 and PEDVPT-P96 revealed 23 nucleotide changes and resultant 19 amino acid substitutions in non-structure proteins 2, 3, 4, 9, 14, 15, spike, open reading frame 3 (ORF3), and membrane proteins with no detectable deletion or insertion. The present study confirmed the pathogenicity of the PEDVPT isolate in conventional post-weaning pigs. Moreover, data regarding viral attenuation and potency of induced antibodies against PEDVPT-P5 identified PEDVPT-P96 as a potential live-attenuated vaccine candidate.

Keywords: cell culture-adapted virus; conventional pig; neutralizing antibody; porcine epidemic diarrhea virus; viral shedding

1. Introduction

Porcine epidemic diarrhea (PED) is caused by the PED virus (PEDV), which belongs to the *Alphacoronavirus* genus of the family *Coronaviridae*. PEDV contains a positive-sense, single-stranded RNA genome of approximately 28 kb in size, which encodes four structural proteins, namely, spike (S),

envelope (E), membrane (M), and nucleocapsid (N) proteins as well as three non-structural proteins (NSP), namely, replicases 1a and 1b and open reading frame 3 (ORF3). The first outbreak of PED was recognized in England in 1971. During the 1980s and 1990s, PED caused severe economic losses in the swine industry in Europe and Asia, but it later turned into a sporadic disease [1]. However, since late 2010, devastating outbreaks of PED that affect all pigs, regardless of their age, with a mortality rate of up to 95% among suckling pigs, regardless of their vaccination status, have been reported in China [2]. The disease has rapidly spread to Asia and, subsequently, to North America, and has resulted in the death of millions of pigs, and has severely affected the swine industry [3,4].

Compared to traditional and CV777-based vaccine strains, the high genetic diversity of the genogroup 2b (G2b) PEDV suggests that PEDV CV777- or DR13-based attenuated vaccines may not completely protect pigs against the infection or control the disease progression [2,5]. Therefore, a new generation of PEDV vaccine against G2b PEDV is urgently required. In the past, successful attenuation of traditional PEDV strains such as SM98 [6], 83P-5 [3], KPED-9 [7], and DR13 [8] by in vitro serial passages in Vero cells has been achieved [9]. It has been demonstrated that conventional 11-day-old pigs orally inoculated with 2.55×10^5 fluorescent focus forming units of the highly-passaged cell culture strain CV777 presents transient or no fecal viral shedding without clinical symptoms [10]. In addition, sows intramuscularly immunized with 10^7 50% tissue culture infective dose ($TCID_{50}$)/mL of the highly cell culture-adapted CV777 strain twice every two weeks induces serum and colostrum antibody titers and reduces the mortality rate from 100 to 20% in neonatal piglets born to these vaccinated sows challenged with 10 50% lethal dose (LD_{50}) of wild PEDV compared with those born to unvaccinated sows [7]. By using the cell culture passage strategy, evident attenuations of a high-passage PEDV YN Chinese strain (passage 144; YN-144) in 10-day-old conventional pigs [11] or highly-passaged PC21A-derived strains (passage 120 and passage 160) in 4-day-old, caesarian-derived, colostrum-deprived (CD/CD) or conventional suckling piglets [12] have been established. However, the detailed immune responses or the efficacy of cross-protection induced by these attenuated G2b PEDV strains against the parental virus or heterologous viruses are either unknown or only partially effective [12].

In Taiwan, new strains of PEDV have been detected since late 2013. Phylogenetic analysis of these field strains indicate that their *S* gene sequences are highly identical to each other and are closely related to those of G2b PEDV strains [5,13]. In the present study, a Taiwan PEDV Pingtung 52 (PEDVPT) strain was successfully isolated from a suckling pig during a farm outbreak in 2014 and serially passaged in Vero cells. To evaluate and compare the pathogenicity of the G2b Taiwan PEDVPT field isolate with its cell culture-adapted strain, we orally inoculated 5-week-old, PEDV-seronegative conventional pigs with a low-passage (passage 5; PEDVPT-P5) or high-passage (passage 96; PEDVPT-P96) PEDV strain. After confirming complete viral clearance in feces, these pigs were then challenged or re-challenged with PEDVPT-P5 to compare the efficacy of immune protection between the groups previously inoculated with PEDVPT-P5 or PEDVPT-P96.

2. Materials and Methods

2.1. Virus Isolation and Serial Passage of PEDVPT Strain

The parental PEDVPT strain (GenBank Accession No. KP276252) was isolated in early 2014 from the intestinal homogenate of a 7-day-old suckling pig in Taiwan and adapted to Vero cells as previously described [7,14]. Viral infection and propagation were confirmed by daily observation of cytopathic effects (CPE), real-time reverse transcription quantitative PCR (RT-qPCR), immunofluorescence assay (IFA), and immunocytochemistry (ICC) staining. In brief, Vero C1008 cells (American Type Culture Collection (ATCC) No. CRL-1586) were cultured overnight (O/N) to 80% confluence and were washed twice with modified post-inoculation medium (PI medium) containing Dulbecco's modified Eagle's medium (DMEM, Gibco, Grand Island, NY, USA) supplemented with tryptose phosphate broth (0.3%), yeast extract (0.02%), and 10 μg/mL of trypsin. After two blind passages, PEDV-inoculated Vero

cells showing CPE, characterized by cell fusion, syncytial cell formation, and cell detachment, were subjected to three rounds of plaque purification. PEDV-infected Vero cells showing more than 90% CPE were subjected to one freeze-and-thaw cycle, and the supernatants were harvested. Viral stocks of the low-passage PEDV (passage 5; PEDVPT-P5) strain and the high-passage PEDV (passage 96; PEDVPT-P96) strain were prepared by serial passaging of the culture supernatants in Vero cells. The virus stocks were titrated by performing a 10-fold serial dilution of the supernatants in 96-well plates in triplicates for each dilution. The viral titers of the PEDVPT-P5 and PEDVPT-P96 stocks were 10^5 and 10^6 $TCID_{50}$/mL, respectively.

2.2. Detection of PEDV Antigens by IFA and ICC

Supernatants of the virus-inoculated Vero cells showing typical CPE were eluted, 200 μL of 80% ice-cold acetone (Sigma-Aldrich, St. Louis, MO, USA) was added to each well, and the cells were fixed at −20 °C for 10 min. After fixation, acetone was removed, and the plate was air dried at room temperature for 30 min. The air-dried cells were then incubated with an in-house anti-PEDV N protein monoclonal antibody diluted 1000-fold (for ICC stain) or with PEDV hyperimmune pig serum diluted 200-fold (for IFA) and incubated at room temperature for 1 h. After incubation, the wells were washed three times with phosphate-buffered saline (PBS). For IFA, 100 μL of fluorescein isothiocyanate (FITC)-labeled goat anti-mouse immunoglobulin G (IgG) (Bethyl Laboratories, Montgomery, TX, USA) diluted to 200-fold in PBS was added to each well and incubated in dark at room temperature for 1 h. For ICC, a polyclonal anti-rabbit/mouse immunoglobulin EnVision-DAB+ system (Dako, Carpinteria, CA, USA) was used according to the manufacturer's protocol. After incubation with the secondary antibody, each well was washed three times with PBS. For ICC staining, the labeled cells were exposed to 3,3′-diaminobenzidine (DAB) chromogen using a peroxidase DAB substrate kit (Dako, Carpinteria, CA, USA), according to the manufacturer's instructions. For IFA, the labeled cells in the 96-well plate were mounted with 1% glycerol (Sigma-Aldrich) in PBS. The stained cells were detected using an inverted light/fluorescence microscope.

2.3. Comparative Pathogenicity and Assessment of Immunogenicity in PEDVPT-P5 and PEDVPT-P96-Inoculated 5-Week-Old Conventional Pigs

Eighteen 5-week-old, PEDV-seronegative, PEDV-fecal RNA-negative, Large White × Duroc crossbred pigs were selected from a conventional pig farm. Selected pigs were negative for porcine circovirus type II, porcine respiratory and reproductive virus, porcine rotavirus, transmissible gastroenteritis virus, porcine respiratory coronavirus, and porcine deltacoronavirus as tested by routine conventional or real-time PCR detection. These pigs were randomly assigned to four groups, viz., the mock-inoculated group with PEDVPT-P5 challenge (pigs A1 to A3; $n = 3$), mock-inoculated group without PEDVPT-P5 challenge (pigs A4 to A6; $n = 3$), the PEDVPT-P5-inoculated group with PEDVPT-P5 challenge (pigs B1 to B6; $n = 6$), and the PEDVPT-P96-inoculated group with PEDVPT-P5 challenge (pigs C1 to C6; $n = 6$). All pigs were labeled with ear tags. Three pigs of the same group were housed in a separate room. Each pig in the PEDVPT-P5- and PEDVPT-P96-inoculated groups was orally inoculated with 5 mL of 10^5 $TCID_{50}$/mL of the respective virus diluted in PI medium. Each pig in the mock-inoculated group received 5 mL of PI medium orally. Rectal swabs were collected every day to monitor the duration of viral shedding, and clinical signs were recorded and scored daily. To monitor seroconversion and mucosal immunity, 10 mL of ethylenediaminetetraacetic acid (EDTA)-anticoagulated blood and fecal swabs were collected from inoculated pigs every two weeks for detecting PEDV-specific plasma IgG and mucosal IgA, respectively. All experiments procedures performed on the animals were reviewed and approved by the Institutional Animal Care and Use Committee of National Taiwan University (Taipei, Taiwan, NTU105-EL-00087).

2.4. Re-Challenging with PEDVPT-P5 to Assess the Protection in PEDVPT-P5- and PEDVPT-P96-Inoculated Pigs

After confirming that all PEDVPT-P5- and PEDVPT-P96-inoculated pigs were seroconverted and negative for fecal virus shedding by RT-qPCR, all pigs were orally inoculated with 5 mL of 10^5 $TCID_{50}$/mL of PEDVPT-P5 to evaluate immune protection. At this time point, all pigs were 9-weeks old.

2.5. Scoring for Clinical Signs of Infection

After each inoculation, animals were monitored daily for clinical signs of infection until the end of the experiment. PEDV-associated diarrhea was scored based on the fecal consistency as follows: 0, normal; 1, loose; 2, semi-fluid; and 3, watery [15]. The weight of individual pigs in each group was monitored and recorded weekly.

2.6. RNA Extraction, cDNA Synthesis, and SYBR Green-Based Quantitative Real-Time PCR

Fecal swabs were diluted with 700 μL of PBS, and RNA was extracted using a QIAamp Viral RNA Mini Kit (Qiagen, Chatsworth, CA, USA), according to the manufacturer's instructions. The total amount of feces contained in each fecal swab ranged from 0.25 to 0.35 g [15,16]. Complementary DNA (cDNA) synthesis was performed by reverse transcription using the QuantiTect Reverse Transcription Kit (Qiagen), according to the manufacturer's instructions. The synthetized cDNA was amplified by real-time qPCR using SYBR Advantage qPCR Premix (Clontech, Palo Alto, CA, USA) under the following conditions: 45 cycles of 95 °C for 5 s, followed by 60 °C for 30 s. The primers used for detection of PEDV in the fecal samples have been previously published [17]. All real-time qPCR reactions were performed in duplicates, and the results were expressed as genomic equivalents (GE), as previously stated [17]. Ten-fold serial dilutions of a known amount of plasmid (pCR-XL-TOPO DNA; Thermo Fisher Scientific, Waltham, MA, USA) containing the PEDV *N* gene was used as the positive control to generate a standard curve. According to this standard curve, the detection limit of RT-qPCR was approximately 60 GE of DNA (data not shown). The amplification product for each reaction was also confirmed by performing the melting curve assay. Samples with a melting temperature of 84.7–86.1 °C were considered PEDV positive. The efficiency of the qPCR ranged from 90.42 to 96.92%.

2.7. Antibody Responses

For concentration and purification of PEDV virions, the cell component of the supernatants collected from PEDV-infected Vero cells was first freeze–thawed three times, and the cell debris was eluted by centrifugation at 6000× *g* for 30 min. To concentrate the virions, viral supernatants were pelleted by centrifugation at 75,000× *g* for 2.5 h using an Avanti J-25 centrifuge (Beckman, Fullerton, CA, USA) and were resuspended in PBS. Viral protein concentrations were determined using a Pierce BCA (bicinchoninic acid) Protein Assay Kit (Thermo Fisher Scientific Inc.). Ninety-six-well, flat-bottom plates (Corning Life Sciences, Corning, NY, USA) were coated O/N with 2 μg/well of concentrated PEDV virions. The PEDV-coated plates were washed six times with 100 mL of PBST (PBS containing 0.05% Tween 20), and wells were incubated for 1 h at room temperature with plasma samples diluted to 20-fold in PBS or with syringe-filtered (0.22 μm pore size) fecal samples, which was diluted two-fold in PBS; each fecal swab was diluted in 700 μL PBS. Each sample was added to the plate in duplicates. After incubation with samples, the wells were washed six times with PBST, and antibodies were detected using horseradish peroxidase (HRP) conjugated goat anti-pig IgG (Kirkegaard & Perry Laboratories, Gaithersburg, MD, USA) diluted to 1:1000 or goat-anti-pig IgA (Abcam, Cambridge, UK) diluted to 1:5000. After washing six times with PBST, 100 μL of tetramethylbenzidine (TMB) substrate solution (Kirkegaard & Perry Laboratories) was added to each well and incubated at room temperature for 20 min. The reaction was stopped using TMB stop solution (Kirkegaard & Perry Laboratories), and the optical density (OD) at 405 nm was recorded on an enzyme-linked immunosorbent assay (ELISA)

reader. Antibody titers were expressed as sample-to-positive control ratio (S/P ratio) values. Using a panel of positive and negative controls, the cutoff values of plasma IgG and fecal IgA detection were 0.1 (95% confidence level) and 0.3 (95% confidence level), respectively.

2.8. Neutralizing Antibody Assay

For neutralization assay, 100 μL of Vero cell suspension at a density of 3×10^5/mL were seeded onto 96-well culture plates (Corning Life Sciences) and incubated at 37 °C, 5% CO_2 overnight to reach 70% confluence. Prior to performing neutralizing antibody assay, plasma samples were heated in water bath at 56 °C for 30 min to inactivate the complement and diluted at 1:10, 1:20, 1:40, 1:80, and 1:160 in PI medium. Fifty microliters of diluted plasma samples were admixed and incubated with 200 $TCID_{50}$/mL PEDVPT-P5 at 37 °C and 5% CO_2 for 1 h. After removing the medium from the 70% confluent Vero cells and washing the cells twice with PI medium, mixtures containing PEDVPT-P5 and different diluted plasma were added to Vero cells in duplicates and were incubated at 37 °C, 5% CO_2 for 1 h. After 1 h of incubation, the supernatants were replaced by fresh PI medium. The cells were maintained at 37 °C and 5% CO_2, and the CPE were monitored for the next three days. The neutralizing titer was determined as the last dilution without CPE.

2.9. Complete Viral Genome Sequencing and Full-Length Sequence Analysis

Viral RNA extraction and subsequent reverse transcription of both PEDVPT-P5 and PEDVPT-P96 were performed as previously described [5] using sequence-specific reverse primers (see Supplementary Table S1). The complete genomes of both viruses were obtained by using seven pairs of oligonucleotide primers that flank different regions of the novel strains of PEDV genome with at least 200-base pair overhangs (see Supplementary Table S1). The PCR amplicons of each fragment were gel-purified, cloned into plasmid vector (pJET1.2; Thermo Fisher Scientific), and subjected for sequencing after plasmid isolation. To acquire sequences of the extreme 3′ and 5′ ends, SMART RACE cDNA Amplification Kit was used according to the manufacture's instruction (Clontech, Tokyo, Japan). Sequence assembly and comparison of complete genomes of both PEDVPT-P5 and PEDVPT-P96 were performed by using Lasergene 7.1 (DNASTAR, Madison, WI, USA) and MEGA7 [18] , respectively.

2.10. Statistical Analysis

The results of body weights, antibody titers, and fecal viral shedding were analyzed statistically using SAS 9.4 (Statistical Analysis System, SAS Institute Inc., Cary, NC, USA). The variables among groups were compared using one way analysis of variance (ANOVA) combined with Scheffe's method. A p-value of <0.05 was interpreted as statistically significant.

3. Results

3.1. Viral Isolation of the PEDVPT Strain

After two blind passages in Vero cells, the intestinal homogenate of inoculated cells at passage three showed typical PEDV-associated CPE [19] characterized by enlarged cells, cell fusion, and syncytial cell formation (Figure 1A). Positive, PEDV-specific cytoplasmic signals in cytopathic syncytial cells were detected by IFA using pig hyperimmune serum (Figure 1B) and by ICC using a monoclonal anti-PEDV N antibody (Figure 1C). No CPE and positive PEDV antigen signals were detected in Vero cells not inoculated with media containing PEDVPT (Figure 1D).

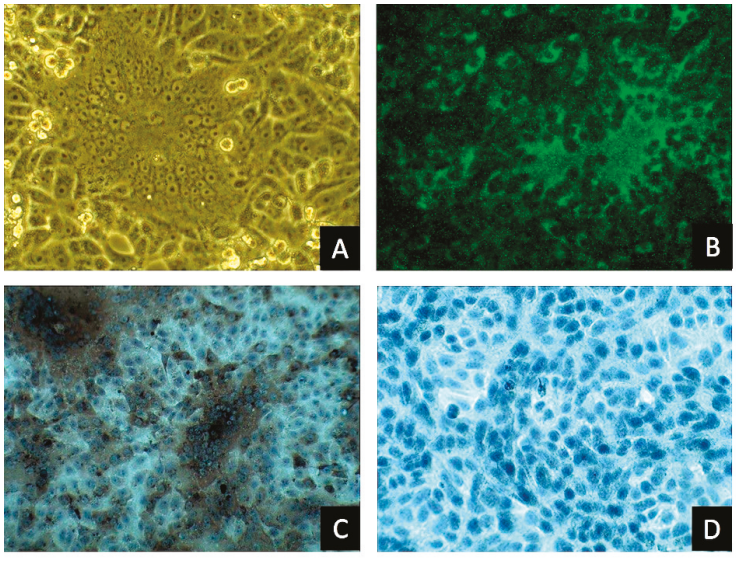

Figure 1. Detection of porcine epidemic diarrhea virus strain Pintung 52 (PEDVPT) infection in Vero cells. Typical PEDV-induced cytopathic effects (CPE) characterized by enlarged cells, cell fusion, and syncytia formation was present in cultures of PEDVPT passage 3-inoculated Vero cells (**A**). Positive signals located in the cytoplasm of typical syncytial cells were detected by immunofluorescence assay using PEDV hyperimmune pig serum (**B**) or by immunocytochemistry (ICC) using an anti-PEDV N protein monoclonal antibody (**C**). Non-PEDV infected Vero cells stained by ICC as negative control (**D**).

3.2. Pathogenicity of PEDVPT-P5 and PEDVPT-P96 in Conventional Pigs

The results of clinical scoring for all pigs are shown in Table 1. In the PEDVPT-P5-inoculated group, all pigs (6/6) presented with typical PEDV-associated, loose-to-watery diarrhea. With the exception of two pigs, most pigs in this group presented with loose diarrhea (score = 1) at 2–3 days post-inoculation (DPI) that worsened to watery diarrhea (score = 3) at 3–7 DPI and eventually ameliorated to loose diarrhea (score = 1) again at 6–9 DPI. Pig B5 exhibited only mild loose feces (score = 1) for three days during the study. Moreover, pig B6 presented with severe watery diarrhea (score = 3), severe dehydration, and electrolyte imbalance at 1 DPI. The animal was diagnosed with a poor prognosis and was immediately euthanized according to the guidelines of Institutional Animal Care and Use Committee of National Taiwan University (Taiwan, Republic of China). Most pigs in the PEDVPT-P96-inoculated group showed no obvious clinical signs of infection with the exception of two pigs (C3 and C4), which presented with transient loose feces (score = 1) at a few time points during the experiment. In the mock-infected groups, no clinical signs of infection were observed before challenge with PEDVPT-P5.

To evaluate the clinical effects of PEDV-associated diarrhea in post-weaning pigs, the mean value of the body weight in each group was also calculated (Figure 2). Although PEDVPT-P5-inoculated pigs showed a relative decrease in body weight gain compared to the other groups in the first two weeks post-inoculation, no significant differences in weight gain were observed among all groups in the study.

Table 1. Clinical scoring of fecal consistency.

Age (Weeks)	5					6							7					8	9							10
DPI	1	2	3	4	5	6	7	8	9	10	11	12	13	14	15	16	17–21	22–27								
DPC																		0	1	2	3	4	5	6	7	8–11
Mock group																										
A1	0	0	0	0	0	0	0	0	0	0	0	0	0	0	0	0	0	0	0	1	3	3	3	2	1	0
A2	0	0	0	0	0	0	0	0	0	0	0	0	0	0	0	0	0	0	0	0	0	1	3	0	0	0
A3	0	0	0	0	0	0	0	0	0	0	0	0	0	0	0	0	0	0	0	0	2	3	0	0	0	0
A4	0	0	0	0	0	0	0	0	0	0	0	0	0	0	0	0	0	0	0	0	0	0	0	0	0	0
A5	0	0	0	0	0	0	0	0	0	0	0	0	0	0	0	0	0	0	0	0	0	0	0	0	0	0
A6	0	0	0	0	0	0	0	0	0	0	0	0	0	0	0	0	0	0	0	0	0	0	0	0	0	0
PEDVPT-P5 group																										
B1	0	1	1	2	3	3	1	0	0	0	0	0	0	0	0	0	0	0	0	0	0	0	0	0	0	0
B2	0	2	3	3	2	3	2	0	0	0	0	0	0	2	1	0	0	0	0	0	0	0	0	0	0	0
B3	0	0	2	3	3	3	2	0	0	0	0	0	0	0	0	0	0	0	0	0	0	0	0	0	0	0
B4	0	0	2	2	2	3	3	2	1	0	1	0	0	0	0	0	0	0	0	0	0	0	0	0	0	0
B5	0	0	1	1	0	1	0	0	0	0	0	0	0	0	0	0	0	0	0	0	0	0	0	0	0	0
B6	2 †																									
PEDVPT-P96 group																										
C1	0	0	0	0	0	0	0	0	0	0	0	0	0	0	0	0	0	0	0	0	0	0	0	0	0	0
C2	0	0	0	0	0	0	0	0	0	0	0	0	0	0	0	0	0	0	0	0	0	0	0	0	0	0
C3	0	0	0	0	0	0	1	0	1	0	0	0	0	0	0	0	0	0	0	0	0	0	0	0	0	0
C4	0	0	0	0	0	0	0	0	0	0	0	0	0	0	0	1	0	0	0	1	0	0	0	0	0	0
C5	0	0	0	0	0	0	0	0	0	0	0	0	0	0	0	0	0	0	0	0	0	1	0	0	0	0
C6	0	0	0	0	0	0	0	0	0	0	0	0	0	0	0	0	0	0	0	0	0	1	0	0	0	0

The scores were graded as follows: 0, normal; 1, loose diarrhea; 2, semi-fluid diarrhea; and 3, watery diarrhea. Pigs of each group were orally inoculated with post-inoculation (PI) medium, porcine epidemic diarrhea virus strain Pintung 52 (PEDVPT)-P5, or PEDVPT-P96 at 5-weeks old and later re-challenged or challenged with PEDVPT-P5 at 9-weeks old (27 days after the first inoculation). DPI: days post-inoculation; DPC: days post-challenge; PEDVPT-P5: low passage PEDV strain; PEDVPT-P96: high passage PEDV; mock: PI medium control. † Euthanized due to severe clinical signs and poor prognosis.

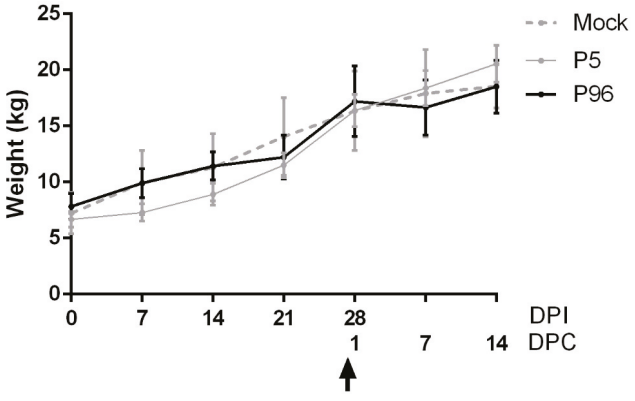

Figure 2. Weekly change in the body weight of 5-week-old pigs after porcine epidemic diarrhea virus strain Pintung 52 (PEDVPT)-P5 or PT-P96 inoculation. The weekly differences in mean body weight for each group are shown as mean ± standard error of the mean (SEM). The black, gray, and dashed lines illustrate the values obtained for the PEDVPT-P96-inoculated group, PEDVPT-P5-inoculated group, and mock-infected group, respectively. The arrow indicates the time point when the pigs were challenged with the low passage PEDVPT-P5 (27 DPI or 0 DPC) strain. P5: low passage virus, PEDVPT-P5; P96: high passage virus, PEDVPT-P96; mock: PI medium control; DPC: days post-challenge.

3.3. Fecal Viral Shedding in PEDVPT-P5- and PEDVPT-P96-Inoculated Pigs

The changes and the length of fecal viral shedding in PEDVPT-P5- and PEDVPT-P96-inoculated pigs were determined using RT-qPCR and are presented as mean values in Figure 3. In the

PEDVPT-P5-inoculated group (gray line in Figure 3), viral shedding was detected starting at 1 DPI, and it reached the peak viral load (6.73 $\log_{10}$ GE) at 4 DPI and was continuously detected until 17 DPI, after which intermittent low levels (1.93–2.07 $\log_{10}$ GE) were detected during 18–24 DPI. Fecal shedding in this group terminated at 26 DPI. The fecal viral shedding increased significantly ($p < 0.05$) in the PEDVPT-P5-inoculated group during the initial five DPI compared to the mock and the PEDVPT-P96-inoculated groups. Pigs in the PEDVPT-P96-inoculated group exhibited a delayed shedding pattern and lower peak viral loads compared to the PEDVPTP5-inoculated group. The average viral shedding in the PEDVPT-P96-inoculated group started at 4 DPI, exhibited a lower peak viral load (4.57 $\log_{10}$ GE) that was continuously detected until 21 DPI, after which intermittent viral shedding was observed until 22–23 DPI. Except the time point of 8 DPI, no significant difference was noted in fecal viral shedding between the mock and the PEDVPT-P96-inoculated groups during the study. No viral shedding in the mock-inoculated group was detected before challenged with PEDVPT-P5.

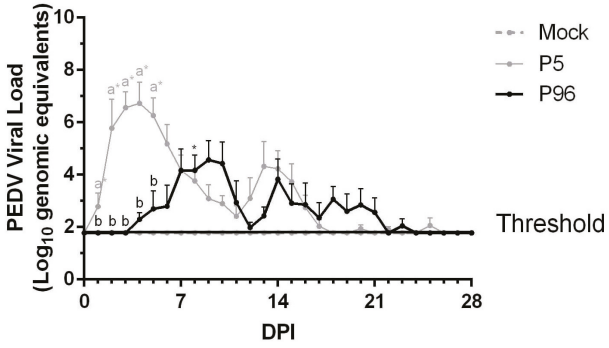

Figure 3. Fecal shedding of PEDV in 5-week-old pigs after porcine epidemic diarrhea virus strain Pintung 52 (PEDVPT)-P5 or PEDVPT-P96 inoculation. Changes in the mean values of genomic equivalents (GE)/mL are shown as $\log_{10}$ values ± SEM. The threshold indicates the limitation of detection for the SYBR Green-based real-time PCR (RT-PCR). The black, gray, and dashed lines illustrate the results obtained for the PEDVPT-P96-inoculated group, PEDVPT-P5-inoculated group, and mock-infected group, respectively. *: significant difference with the mock group ($p < 0.05$); a, b: significant difference between groups labeled with different alphabets ($p < 0.05$).

3.4. Antibody Responses Induced in Pigs after Inoculation with PEDVPT-P5 or PEDVPT-P96

To evaluate the plasma IgG and fecal IgA antibody responses induced by PEDVPT-P5 and PEDVPT-P96 inoculations in conventional pigs, a whole PEDV particle-based ELISA was performed. The levels of plasma IgG (Figure 4) and fecal IgA (Figure 5) were measured in pigs at 0, 14, and 28 DPI. Elevated PEDV-specific IgG level was detected in all PEDVPT-P5- and PEDVPT-P96-inoculated pigs at 14 DPI, which reached a plateau at 28 DPI. In the PEDVPT-P96-inoculated group, PEDV-specific plasma IgG mean values (reported as the S/P ratio) ranged from 0.41 to 0.60. These values were significantly lower than those of the PEDVPT-P5-inoculated pigs, which ranged from 0.88 to 0.91 at 14–28 DPI, and were significantly higher than those of the mock-inoculated groups at 28 DPI. As for mock-infected pigs, no seroconversion was detected before the challenge with PEDVPT-P5 at 28 DPI (Figure 4). For the induction of mucosal IgA (Figure 5), a weak but detectable elevation of the mean S/P ratios for PEDV-specific IgA (0.31) was observed in both PEDVPT-P5 and PEDVPT-P96-inoculated pigs as early as at 14 DPI. No detectable mucosal IgA was noted in the mock-infected group during the study.

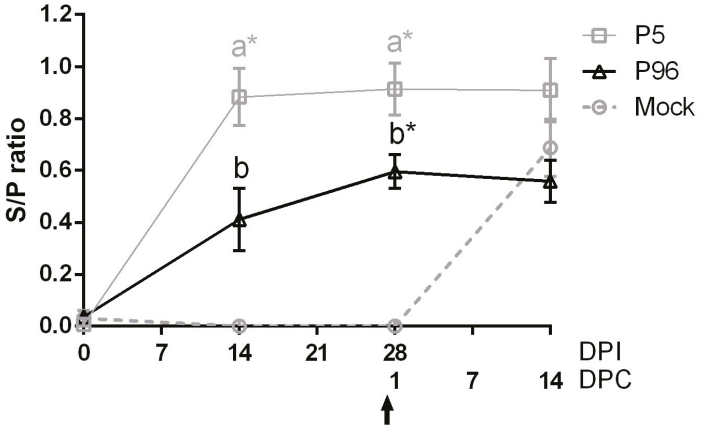

Figure 4. Changes in PEDV-specific immunoglobulin G (IgG) levels in plasma after PEDV strain Pintung 52 (PEDVPT)-P5 or PEDVPT-P96 inoculation and after PEDVPT-P5 challenge in all pigs. Plasma samples from ethylenediaminetetraacetic acid (EDTA)-anticoagulated blood were collected biweekly and diluted 20-fold. The levels of PEDV-specific IgG were detected by ELISA with PEDV particles as coating antigen and expressed as sample-to-positive control ratios (S/P ratio). S/P ratios were defined as the difference between the optical density (OD) values of sample and negative control divided by the difference between OD values of positive and negative controls. PEDV-specific plasma IgG levels are represented as mean ± SEM. The arrow indicates the time point when pigs were challenged with the low passage PEDVPT-P5 (27 DPI or 0 DPC) strain. The black, gray, and dashed lines illustrate the results for the PEDVPT-P96-inoculated group, PEDVPT-P5-inoculated group, and mock-infected group, respectively. *: significant difference with the mock group ($p < 0.05$); a, b: significant difference between groups labeled with different alphabets ($p < 0.05$).

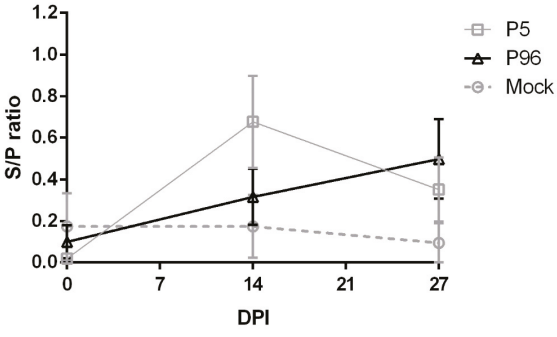

Figure 5. Changes in PEDV-specific mucosal IgA levels obtained from fecal swabs after PEDV strain Pintung 52 (PEDVPT)-P5 or PEDVPT-P96 inoculation of pigs. Each fecal swab was diluted with 700 μL PBS and filtered; the supernatants were diluted two-fold, and the levels of PEDV-specific IgA were detected by ELISA with PEDV virions as the coating antigen. The results obtained were expressed as sample-to-positive ratios (S/P ratio), which were defined as the difference between the OD values of sample and negative control divided by the difference between the OD values of positive and negative control, with SEM. The black, gray, and dashed lines illustrate the results of the PEDVPT-P96-inoculated group, PEDVPT-P5-inoculated group, and mock-infected group, respectively.

3.5. Neutralizing Antibodies Detection

To evaluate the neutralizing antibody titer, PEDVPT-P5 was used as the challenging virus for the neutralization assay. The mean values of PEDV-specific neutralizing antibody titers in PEDVPT-P5- and PEDVPT-P96-inoculated pigs at 0 and 27 DPI are presented in Figure 6. The neutralizing antibody titer in all animals harbored a background titer of <20-fold at 0 DPI. Elevations in the mean value of neutralizing antibody titers in PEDVPT-P5- and PEDVPT-P96-inoculated pigs at 27 DPI ranged from 24- to 58-fold and from 18.3- to 58.3-fold, respectively, and were relatively higher (although not statistically significant) than those of mock-inoculated pigs, which ranged from 17.5 to 7.5-fold.

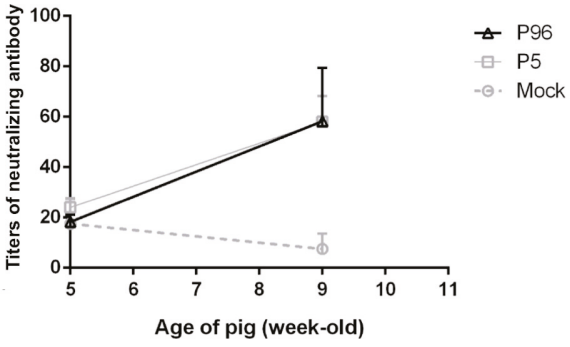

Figure 6. Changes in plasma PEDV neutralizing antibody levels after inoculation with PEDV strain Pintung 52 (PEDVPT)-P5 or PEDVPT-P96. The plasma samples were collected from 5- and 9-week-old (0 and 27 DPI) pigs, and neutralizing antibody assay was performed. Values are represented as mean ± SEM. The black, gray, and dashed lines illustrate the results of the PEDVPT-P96-inoculated group, PEDVPT-P5-inoculated group, and mock-infected group, respectively.

3.6. Immune Protective Efficacy Induced in Pigs after PEDVPT-P5 or PEDVPT-P96 Inoculation

To evaluate whether PEDVPT-P5 and PEDVPT-P96 inoculation induced immune protection against PEDVPT-P5, three pigs (A1–A3) in the mock-infected group and all pigs in both PEDVPT-P5- and PEDVPT-P96-inoculated groups were challenged with 5 mL of 10^5 $TCID_{50}$/mL of PEDVPT-P5 at 27 DPI. The three pigs in the mock group (A1–A3) challenged with PEDVPT-P5 started to develop loose diarrhea at 2 DPC that worsened to watery diarrhea at 3–5 DPC and terminated or ameliorated to loose diarrhea at 5–7 DPC (Table 1). Fecal viral shedding (Figure 7) was detected in these pigs starting at 1 DPC with a mean peak value of 7.56 $\log_{10}$ GE at 4 DPC and was continuously detected until 9 DPC. Furthermore, an elevated level of PEDV-specific plasma IgG (mean S/P ratio = 0.69) was detected in all three pigs (A1–A3) at 14 DPC (Figure 4). The clinical signs of infection, fecal viral shedding, and plasma IgG values of the other three pigs in mock group (A4–A6) not challenged remained undetectable during the experiment.

In PEDVPT-P5-inoculated pigs, no diarrhea was observed after the subsequent PEDVPT-P5 challenge, but a single time point of low-level of fecal viral shedding was detected at 9 DPC. In the PEDVPT-P96-inoculated group, three out of six pigs showed clinical loose feces (score = 1) at one time point and a transient detectable fecal viral shedding of 1.83–2.67 $\log_{10}$ GE during 1–4 DPC, whereas the other three pigs in the group showed no clinical signs of infection during 11 days of monitoring after PEDVPT-P5 challenge (Table 1). In all PEDVPT-P96- and PEDVPT-P5-inoculated pigs, no detectable increases in the mean values for plasma PEDV-specific IgG S/P ratios were noted after the challenge.

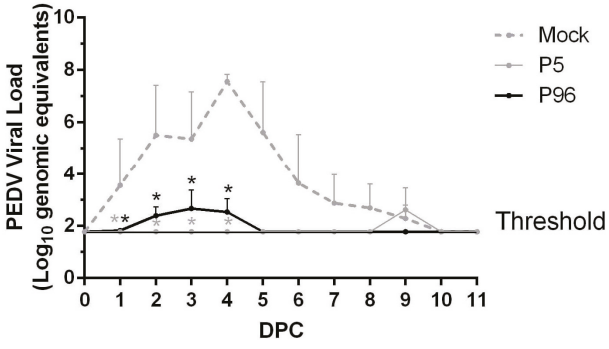

Figure 7. Fecal shedding of porcine epidemic diarrhea virus (PEDV) in PEDV strain Pintung 52 (PEDVPT)-P5- or PEDVPT-P96-inoculated pigs following PEDVPT-P5 challenge. Changes in the mean values GE/mL are shown as $\log_{10}$ values ± SEM. The threshold indicates the limitation of detection by the SYBR Green-based RT-PCR. The black, gray, and dashed lines illustrate the results for the PEDVPT-P96-inoculated group, PEDVPT-P5-inoculated group, and mock-infected group, respectively. *: significant difference in the mock group ($p < 0.05$).

3.7. Sequence Comparison of PEDVPT-P5 and PEDVPT-P96 Strains

To gain a deeper understanding of the potential molecular mechanisms of viral attenuation of the high passage PEDVPT-P96 strain, we performed full-length sequencing of both PEDVPT-P5 and PEDVPT-P96 strains, and the sequence data were deposited in GenBank under accession Nos. KY929405 and KY929406, respectively. The complete genome sequence of both PEDVPT-P5 and PEDVPT-P96 were 28,038 nucleotides (nt) in length, excluding the 3′ poly(A) tail. After sequence alignment, no deletion or insertion was detected on comparing PEDVPT-P5 with PEDVPT-P96. In total, 23 nucleotide changes and the resultant 19 amino acid (aa) substitutions were revealed (Table 2). The *S* and *M* genes appeared to be the most variable, and each contained nine (T144I, F554S, S887R, S968A, I1021S, R1026K, L1252R, C1354F, C1358F) and three (I12V, S79A, F145L) aa changes, respectively. In the *S* gene, most mutations (7/9) were located in the S2 region. Moreover, many mutations were notably found in the functional regions, viz., the F554S in the CO–26K equivalent neutralizing epitope (COE) and C1354F as well as C1358F in the transmembrane domain. Among other genes encoding structural proteins, both the *E* and *N* genes were highly conserved and they retained 100% amino acid homology between these two viruses. For NSP, nine nucleotide changes were found in the *ORF1a/b* gene, but only five of these mutations resulted in aa substitutions, located at *NSP2* (K159N and T510I), *NSP3* (F669S), *NSP4* (E421A), and *NSP15* (M252I) genes. The *ORF3* gene also harbored one aa substitution (Y170H).

Table 2. Changes in nucleotides and amino acid between PEDVPT-P5 and PEDVPT-P96.

Gene	Nucleotide Change			Amino Acid Substitution
	Position	PEDVPT-P5	PEDVPT-P96	
NSP2	1099	G	T	K159N
NSP2	2151	C	T	T510I
NSP3	3172	T	C	—
NSP3	4983	T	C	F669S
NSP4	8518	T	C	—
NSP4	9102	A	C	E421A
NSP9	11951	C	T	—
NSP14	17065	T	A	—
NSP15	19471	G	T	M252I

Table 2. *Cont.*

Gene	Nucleotide Change			Amino Acid Substitution
	Position	PEDVPT-P5	PEDVPT-P96	
S	21064	C	T	T144I
S	22294	T	C	F554S
S	23292	A	C	S887R
S	23535	T	G	S968A
S	23695	T	G	I2021S
S	23710	A	G	R1026K
S	24388	T	G	L1252R
S	24694	G	T	C1354F
S	24706	G	T	C1358F
ORF3	25301	T	C	Y170H
E	25517	C	T	—
M	25720	A	G	I12V
M	25921	T	G	S79A
M	26119	T	C	F145L

—: silent mutation.

4. Discussion

In the present study, we successfully isolated and characterized the pathogenicity of a new Taiwan PEDVPT strain, PEDVPT-P5. We have demonstrated that this G2b PEDVPT-P5 strain can induce typical watery diarrhea in 5-week-old pigs but milder symptoms and a shorter viral shedding period in 9-week-old pigs. By serial passaging of PEDVPT in Vero cells, a PEDVPT-P96 viral stock was also prepared. Compared to PEDVPT-P5-inoculated pigs, PEDVPT-P96-inoculated pigs showed a delayed, mild, and transient diarrhea, or in some cases undetectable, providing evidence of viral attenuation. Of importance, inoculation of both PEDVPT-P5 and PEDVPT-P96 induced PEDV-specific plasma IgG, mucosal IgA, and neutralizing antibodies and elicited protection against a subsequent challenge with the low passage PEDVPT-P5 strain. This study provides valuable information regarding the viral shedding period, immunogenicity, and pathogenicity of different passaged PEDV in conventional post-weaning pigs. Moreover, the evidence of viral attenuation and the efficacy of protection induced by PEDVPT-P96 in conventional pigs highlights PEDVPT-P96 as a potential, live-attenuated PEDV vaccine candidate.

It has been shown that PEDV can infect seronegative pigs of all ages. However, the susceptibility to PEDV infection is age-dependent and is significantly higher in neonatal pigs than in weaning pigs [20]. In the present study, we demonstrated that compared to 5-week-old pigs, which exhibited PEDV-associated clinical signs for 7–9 days and long viral shedding period of 26 days, older 9-week-old pigs exhibited milder clinical symptoms for a shorter period lasting of 4–7 days and viral shedding lasting for only nine days. Furthermore, we demonstrated that even without displaying clinical signs, the viral shedding periods could be longer than three weeks in PEDV-infected post-weaning pigs. It has been reported that oral fluid samples are suitable for screening PEDV in commercial growing pig herds [21]. These findings suggest that routine screening for oral and fecal PEDV shedding in clinically healthy pigs when purchasing feeder pigs from swine producers is necessary to reduce the risk of disease transmission from farm to farm.

In the present study, we demonstrated that 5-week-old conventional pigs inoculated with the PEDVPT-P5 strain exhibited fecal viral shedding, peaked at 2–4 DPI, and persisted for 26 days. An increase in PEDV-specific IgG titer in these pigs started at 14 DPI and reached a plateau at 21 DPI. The result is similar to a previous finding in 4-week-old conventional pigs challenged with 1.42×10^5 $TCID_{50}$ of a USA/KS/2013 PEDV isolate. In this study, USA/KS/2013 isolate-inoculated pigs displayed fecal viral shedding primarily during the first two weeks with a peak at 5–6 DPI and fecal swabs that were positive for PEDV nucleic acid at 21 and 28 DPI in some pigs. Seroconversion was also noted at 14 DPI and reached a peak level at 21 DPI [22]. When the spike sequence of the USA/KS/2013 isolate

was compared to the Taiwan PEDVPT isolate, we found that these two viruses share high sequence identity (99%).

In Asia, the attenuated CV777-based and DR13-based PEDV vaccines have been used for decades and, as a consequence, PED in Asia has been generally under control with low prevalence and mortality rates in the past [9]. These live-attenuated vaccines are derived from cell culture-adapted PEDV strains and have proven to be effective in controlling PED by reducing the severity and duration of diarrhea, shortening the period of viral shedding, stimulating the immune response of sows, and protecting the delivered piglets through elevated maternal antibodies [7,23,24]. Unfortunately, the exposure to traditional PEDV strains or the above-mentioned live-attenuated vaccine strains provide limited cross-protection against the epidemics of the novel virulent PEDV strains [15]. Therefore, a novel vaccine against these new strains is urgently needed. In the present study, we have developed a high passage PEDVPT-P96 viral stock by serial passaging in Vero cells and have provided evidence of its viral attenuation. In addition, PEDVPT-P96 inoculation of pigs induced plasma IgG, mucosal IgA, and neutralizing antibodies and provided complete immunization against a subsequent low passage PEDVPT-P5 challenge, suggesting that PEDVPT-P96 may serve as a potential live-attenuated vaccine candidate.

By comparing the sequences of the parental virulent PEDVPT-P5 and attenuated PEDVPT-P96 strains to identify potential genetic determinants for viral attenuation, we demonstrated that most non-silent mutations are located in the *S* gene. On comparing the result of sequence analysis with other previous studies, two mutations (S887R and C1354F) identified in the attenuated late passages of YN1 strain were also identified in our PEDVPT-P96 strain. However, the deletion at the position of aa 144 of the *S* gene, suggested by the same study as a potential attenuation marker for PEDV [10] was not found in PEDVPT-P96; alternatively, an aa substitution (T144I) occurred in this particular region. The clinical significance of these mutations requires further elucidation. Of note, one unique aa substitution (F554S) was observed in the COE neutralizing domain in PEDVPT-P96, but the mechanism of how it interferes with antibody recognition remains to be elucidated. However, the results of in vivo animal challenge performed in this study suggest that this mutation does not result in the loss of the cross-protection against the parental PEDVPT-P5 strain. In the present study, aa substitutions of F669S in the *NSP3* gene and M252I in the *NSP15* gene were identified in PEDVPT-P96. The NSP of coronaviruses are well known to be responsible for viral replication, and many of them are reported to be interferon (IFN) antagonists. In PEDV, NSP1, NSP3, NSP7, NSP14, NSP15, and NSP16 have been demonstrated to suppress the IFN-β and IRF3 promoter activities [23]. The effects of mutations in *NSP3* and *NSP15* genes of PEDVPT-P96 on immune modulation need further investigation. Unlike other reports wherein the *NSP3* and *ORF3* genes tend to comprise more mutations through PEDV attenuation, only one non-silent mutation was observed in each gene in the present study. To date, many studies have been conducted aiming to map attenuating mutation(s) [10,11,24]; however, there is little consistency among different studies, indicating that different strains may harbor different mutation patterns, thereby suggesting that the attenuation may be multifactorial and introduction of attenuating mutation(s) may have implications in generating a safe live attenuated vaccine. This information is invaluable for further quick and rational development of effective and genetically stable vaccines via reverse genetics.

It has been reported that the gut–mammary secretory IgA axis is the most promising and effective pathway against enteric diseases, including PED. For PEDV vaccine development, it is crucial for neonatal piglets to receive sufficient maternal antibodies against PEDV via colostrum or milk from previously immunized sows [8,25]. Furthermore, the amount and the duration of maternal antibodies is closely related to the antibody titers of the immunized sows [9]. Immune protection against PEDV infection, including pathogenicity, immunogenicity, and fecal viral shedding, in nursing pigs born to PEDVPT-P96-inoculated sows as well as the potential for reversal of virulence of the PEDVPT-P96 strain by serial animal passages will be further evaluated.

5. Conclusions

In conclusion, our study describes a PEDV challenge model using conventional post-weaning pigs to simulate the actual immune situation in the field and provides a model for the preclinical evaluation of vaccines and other interventions aiming to prevent PEDV infection. A high passage PEDVPT-P96 strain has also been demonstrated as a potential live-attenuated PEDV vaccine candidate. The present study provides insights into the pathogenicity, length of viral shedding, and immunogenicity of different passages of cell-adapted PEDV in conventional pigs.

Supplementary Materials: The following are available online at www.mdpi.com/1999-4915/9/5/121/s1, Table S1: List of sequencing primers.

Acknowledgments: This work was supported by the Ministry of Science and Technology (MOST), Taiwan, R.O.C. (MOST 103-2321-B-002-077-MY3 and MOST 105-2622-B-002-014-CC2).

Author Contributions: All authors have contributed to the manuscript. Y.-C. Chang performed the animal study, data analysis, and wrote the manuscript. C.-F. Kao performed full-length genome sequencing, data analysis, and wrote the manuscript. C.-Y. Chang, H.-Y. Chiou, C.-F. Kao, and J.-Y. Peng performed the analysis and the animal study. P.-S. Tsai, V.F. Pang, C.-R. Jeng, and H.-W. Chang designed the study and developed the methodology. I.-C. Cheng contributed reagents. H.-W. Chang performed analysis of the study and final approval of the version to be published.

Conflicts of Interest: The authors declare no conflict of interest with respect to the research, authorship, and/or the publication of the article.

References

1. Pensaert, M.B.; de Bouck, P. A new coronavirus-like particle associated with diarrhea in swine. *Arch. Virol.* **1978**, *58*, 243–247. [CrossRef] [PubMed]
2. Li, W.; Li, H.; Liu, Y.; Pan, Y.; Deng, F.; Song, Y.; Tang, X.; He, Q. New variants of porcine epidemic diarrhea virus, China, 2011. *Emerg. Infect. Dis.* **2012**, *18*, 1350–1353. [CrossRef] [PubMed]
3. Jung, K.; Saif, L.J. Porcine epidemic diarrhea virus infection: Etiology, epidemiology, pathogenesis and immunoprophylaxis. *Vet. J.* **2015**, *204*, 134–143. [CrossRef] [PubMed]
4. Jarvis, M.C.; Lam, H.C.; Zhang, Y.; Wang, L.; Hesse, R.A.; Hause, B.M.; Vlasova, A.; Wang, Q.; Zhang, J.; Nelson, M.I.; et al. Genomic and evolutionary inferences between American and global strains of porcine epidemic diarrhea virus. *Prev. Vet. Med.* **2016**, *123*, 175–184. [CrossRef] [PubMed]
5. Chiou, H.Y.; Huang, Y.L.; Deng, M.C.; Chang, C.Y.; Jeng, C.R.; Tsai, P.S.; Yang, C.; Pang, V.F.; Chang, H.W. Phylogenetic Analysis of the Spike (S) Gene of the New Variants of Porcine Epidemic Diarrhoea Virus in Taiwan. *Transbound. Emerg. Dis.* **2017**, *64*, 157–166. [CrossRef] [PubMed]
6. Kim, S.H.; Lee, J.M.; Jung, J.; Kim, I.J.; Hyun, B.H.; Kim, H.I.; Park, C.K.; Oem, J.K.; Kim, Y.H.; Lee, M.H.; et al. Genetic characterization of porcine epidemic diarrhea virus in Korea from 1998 to 2013. *Arch. Virol.* **2015**, *160*, 1055–1064. [CrossRef] [PubMed]
7. Kweon, C.H.; Kwon, B.J.; Lee, J.G.; Kwon, G.O.; Kang, Y.B. Derivation of attenuated porcine epidemic diarrhea virus (PEDV) as vaccine candidate. *Vaccine* **1999**, *17*, 2546–2553. [CrossRef]
8. Song, D.; Moon, H.; Kang, B. Porcine epidemic diarrhea: A review of current epidemiology and available vaccines. *Clin. Exp. Vaccine Res.* **2015**, *4*, 166–176. [CrossRef] [PubMed]
9. Song, D.; Park, B. Porcine epidemic diarrhoea virus: A comprehensive review of molecular epidemiology, diagnosis, and vaccines. *Virus Genes* **2012**, *44*, 167–175. [CrossRef] [PubMed]
10. De Arriba, M.L.; Carvajal, A.; Pozo, J.; Rubio, P. Mucosal and systemic isotype-specific antibody responses and protection in conventional pigs exposed to virulent or attenuated porcine epidemic diarrhoea virus. *Vet. Immunol. Immunopathol.* **2002**, *85*, 85–97. [CrossRef]
11. Chen, F.; Zhu, Y.; Wu, M.; Ku, X.; Ye, S.; Li, Z.; Guo, X.; He, Q. Comparative Genomic Analysis of Classical and Variant Virulent Parental/Attenuated Strains of Porcine Epidemic Diarrhea Virus. *Viruses* **2015**, *7*, 5525–5538. [CrossRef] [PubMed]
12. Lin, C.M.; Hou, Y.; Marthaler, D.G.; Gao, X.; Liu, X.; Zheng, L.; Saif, L.J.; Wang, Q. Attenuation of an original US porcine epidemic diarrhea virus strain PC22A via serial cell culture passage. *Vet. Microbiol.* **2017**, *201*, 62–71. [CrossRef] [PubMed]

13. Lin, C.N.; Chung, W.B.; Chang, S.W.; Wen, C.C.; Liu, H.; Chien, C.H.; Chiou, M.T. US-like strain of porcine epidemic diarrhea virus outbreaks in Taiwan, 2013–2014. *J. Vet. Med. Sci.* **2014**, *76*, 1297–1299. [CrossRef] [PubMed]
14. Hofmann, M.; Wyler, R. Propagation of the virus of porcine epidemic diarrhea in cell culture. *J. Clin. Microbiol.* **1988**, *26*, 2235–2239. [PubMed]
15. Jung, K.; Annamalai, T.; Lu, Z.; Saif, L.J. Comparative pathogenesis of US porcine epidemic diarrhea virus (PEDV) strain PC21A in conventional 9-day-old nursing piglets vs. 26-day-old weaned pigs. *Vet. Microbiol.* **2015**, *178*, 31–40. [CrossRef] [PubMed]
16. Lin, C.-M.; Annamalai, T.; Liu, X.; Gao, X.; Lu, Z.; El-Tholoth, M.; Hu, H.; Saif, L.J.; Wang, Q. Experimental infection of a US spike-insertion deletion porcine epidemic diarrhea virus in conventional nursing piglets and cross-protection to the original US PEDV infection. *Vet. Res.* **2015**, *46*, 134. [CrossRef] [PubMed]
17. Jung, K.; Wang, Q.; Scheuer, K.A.; Lu, Z.; Zhang, Y.; Saif, L.J. Pathology of US porcine epidemic diarrhea virus strain PC21A in gnotobiotic pigs. *Emerg. Infect. Dis.* **2014**, *20*, 662–665. [CrossRef] [PubMed]
18. Kumar, S.; Stecher, G.; Tamura, K. MEGA7: Molecular Evolutionary Genetics Analysis Version 7.0 for Bigger Datasets. *Mol. Biol. Evol.* **2016**, *33*, 1870–1874. [CrossRef] [PubMed]
19. Chen, Q.; Li, G.; Stasko, J.; Thomas, J.T.; Stensland, W.R.; Pillatzki, A.E.; Gauger, P.C.; Schwartz, K.J.; Madson, D.; Yoon, K.J.; et al. Isolation and characterization of porcine epidemic diarrhea viruses associated with the 2013 disease outbreak among swine in the United States. *J. Clin. Microbiol.* **2014**, *52*, 234–243. [CrossRef] [PubMed]
20. Thomas, J.T.; Chen, Q.; Gauger, P.C.; Gimenez-Lirola, L.G.; Sinha, A.; Harmon, K.M.; Madson, D.M.; Burrough, E.R.; Magstadt, D.R.; Salzbrenner, H.M.; et al. Effect of Porcine Epidemic Diarrhea Virus Infectious Doses on Infection Outcomes in Naive Conventional Neonatal and Weaned Pigs. *PLoS ONE* **2015**, *10*, e0139266. [CrossRef] [PubMed]
21. Bjustrom-Kraft, J.; Woodard, K.; Gimenez-Lirola, L.; Rotolo, M.; Wang, C.; Sun, Y.; Lasley, P.; Zhang, J.; Baum, D.; Gauger, P.; et al. Porcine epidemic diarrhea virus (PEDV) detection and antibody response in commercial growing pigs. *BMC Vet. Res.* **2016**, *12*, 99. [CrossRef] [PubMed]
22. Niederwerder, M.C.; Nietfeld, J.C.; Bai, J.; Peddireddi, L.; Breazeale, B.; Anderson, J.; Kerrigan, M.A.; An, B.; Oberst, R.D.; Crawford, K.; et al. Tissue localization, shedding, virus carriage, antibody response, and aerosol transmission of Porcine epidemic diarrhea virus following inoculation of 4-week-old feeder pigs. *J. Vet. Diagn. Investig.* **2016**, *28*, 671–678. [CrossRef] [PubMed]
23. De Arriba, M.; Carvajal, A.; Pozo, J.; Rubio, P. Lymphoproliferative responses and protection in conventional piglets inoculated orally with virulent or attenuated porcine epidemic diarrhoea virus. *J. Virol. Methods* **2002**, *105*, 37–47. [CrossRef]
24. Song, D.; Oh, J.; Kang, B.; Yang, J.; Song, J.; Moon, H.; Kim, T.; Yoo, H.; Jang, Y.; Park, B. Fecal shedding of a highly cell-culture-adapted porcine epidemic diarrhea virus after oral inoculation in pigs. *J. Swine Health Prod.* **2005**, *13*, 269.
25. Langel, S.N.; Paim, F.C.; Lager, K.M.; Vlasova, A.N.; Saif, L.J. Lactogenic immunity and vaccines for porcine epidemic diarrhea virus (PEDV): Historical and current concepts. *Virus Res.* **2016**, *226*, 93–107. [CrossRef] [PubMed]

© 2017 by the authors. Licensee MDPI, Basel, Switzerland. This article is an open access article distributed under the terms and conditions of the Creative Commons Attribution (CC BY) license (http://creativecommons.org/licenses/by/4.0/).

viruses

MDPI

Article

Redistribution of Endosomal Membranes to the African Swine Fever Virus Replication Site

Miguel Ángel Cuesta-Geijo [1,2], Lucía Barrado-Gil [1], Inmaculada Galindo [1], Raquel Muñoz-Moreno [3] and Covadonga Alonso [1,*]

[1] Department of Biotechnology, Instituto Nacional de Investigación y Tecnología Agraria y Alimentaria, INIA, Ctra. de la Coruña Km 7.5, 28040 Madrid, Spain; mangelcuestageijo@gmail.com (M.Á.C.-G.); barrado.lucia@inia.es (L.B.-G.); galindo@inia.es (I.G.)

[2] Department of Infectious Diseases, King's College London School of Medicine, Guy's Hospital, London SE1 9RT, UK

[3] Department of Microbiology and Global Health and Emerging Pathogens Institute, Icahn School of Medicine at Mount Sinai, New York, NY 10029, USA; raquel.munoz@mssm.edu

* Correspondence: calonso@inia.es; Tel.: +34-91-347-3793

Academic Editors: Linda Dixon and Simon Graham
Received: 4 April 2017; Accepted: 25 May 2017; Published: 1 June 2017

Abstract: African swine fever virus (ASFV) infection causes endosomal reorganization. Here, we show that the virus causes endosomal congregation close to the nucleus as the infection progresses, which is necessary to build a compact viral replication organelle. ASFV enters the cell by the endosomal pathway and reaches multivesicular late endosomes. Upon uncoating and fusion, the virus should exit to the cytosol to start replication. ASFV remodels endosomal traffic and redistributes endosomal membranes to the viral replication site. Virus replication also depends on endosomal membrane phosphoinositides (PtdIns) synthesized by PIKfyve. Endosomes could act as platforms providing membranes and PtdIns, necessary for ASFV replication. Our study has revealed that ASFV reorganizes endosome dynamics, in order to ensure a productive infection.

Keywords: african swine fever virus (ASFV); ASF viral factory; endosomes; endosomal pathway; phosphoinositides; phosphatidylinositol kinases; microtubules

1. Introduction

Endocytosis is a common entry pathway for nutrients, receptors and pathogens to get into cells that converges on early endosomes (EE). From EE, cargo can be sorted back to the plasma membrane (PM) through the recycling pathway. Alternatively, it can be directed to the trans-Golgi network or to late endosomes (LE), and finally targeted to lysosomes for degradation [1]. LE is a major cargo-sorting compartment. In contrast, lysosomes are the end-point of the degradative pathway. Endosomal maturation from EE to LE is a dynamic process. Starting on the cytosolic face of the EE, invaginations of the limiting membrane into the lumen of the endosome give rise to the intraluminal vesicles (ILV). Then, EE matures into multivesicular bodies (MVB), and as the pH decreases more ILV are generated [2]. The systematic maturation of this pathway depends on endosomal membrane signaling that is tightly regulated by both proteins and lipids [3]. In fact, the heterogeneity of lipid distribution in endosomal membranes is an organizing principle for the distribution of membrane-associated proteins. Sequential transport from EE to LE involves the switch of GTPase Rab5 to Rab7. Rab proteins and their effectors are recruited by phosphoinositides by specific lipid-binding domains. Short-lived phosphatidylinositol-3-phosphate (PtdIns3P) synthesized by PI3K controls EE functions and is a substrate for the generation of PtdIns(3,5)P_2 at the LE membrane by the

kinase PIKfyve. Other PtdIns, and their respective converting enzymes, are molecular signatures of the PM and the recycling and secretory pathways.

The endocytic pathway ensures a highly dynamic and controlled sorting of cargoes, discriminating the ones that are targeted for degradation from those destined to other cellular locations and functions. Indeed, endocytosis can be exploited by many viruses to infect mammalian cells [4–6] and they have adapted to this precise molecular machinery to complete their viral replication cycle successfully.

African swine fever virus (ASFV) is a double-stranded DNA (dsDNA) virus that kills wild and domestic pigs [7,8]. There is currently no effective vaccine, but new experimental approaches to elicit protection have been found [9,10]. From the economic perspective, ASFV is an important pathogen, as it has spread from Africa into east Europe, and currently there is an epidemic outbreak in the Caucasus and eastern European countries [8,11]. African swine fever virus enters the host cells by a complex process involving dynamin and clathrin-mediated and cholesterol-dependent endocytosis [12,13] and macropinocytosis [14,15]. These entry mechanisms, either acting independently or combined, lead the virus to traffic through the endosomal pathway [16]. Endosomal intraluminal acidification [16] and the activity of the GTPase dynamin are the most consistent pre-requisites for ASFV infectivity [13]. Within a few minutes of infection, ASFV is found in LE compartments [16]. Viral decapsidation is the first step of the uncoating process and occurs in the acidic pH of LE. Rab7 is essential for ASFV infection to progress [16]. Then, the cholesterol efflux from endosomes, which is regulated by lipid transporter proteins, is required for further fusion and endosomal exit [17].

Once the uncoated virions are in the cytosol, ASFV replication starts at a single site called viral factory (VF) or viral replication organelle [18] where DNA and proteins accumulate in a microtubule dependent manner. Microtubules (MTs) are cytoskeleton components that are important for ASFV transport [19]. Our group previously reported that ASFV virions interact with dynein motor proteins that move along MTs towards the MT organizing center (MTOC) [19]. Interestingly, the staining pattern of ASFV structural proteins, such as p72 and p54, typically has very strong signals coincident with the virus factory [20]. Additionally, some viral membranes found in VFs can be identified as endoplasmic reticulum (ER) components [20–22] and other components such as endosomes and endosomal lipids can also be found in these replication sites. Furthermore, newly-synthesized virions associate with kinesin that drives movement of virions from the VFs to the cell periphery [23,24]. Once there, the new viral progeny is released by budding. Importantly, it has been shown that treatment of cells with MTs depolimerization drugs such as nocodazole, result in the dispersal of ASFV VFs, preventing their correct localization at perinuclear sites [19,25,26]. These facts highlight the dependence of an intact MT network for a successful ASFV infection [19,27].

Since its introduction in Europe through the Caucasus in 2007, African swine fever (ASF) has spread to other neighboring countries, thus threatening porcine production worldwide. Due to the lack of an effective vaccine, ASF control relies on early diagnosis and massive culling of animals. In our aim to discover how ASFV surpasses host cell defenses and reorganizes cellular structures to initiate replication, we started looking for targets occurring at the early stages of infection. ASFV enters host cells by endocytosis, and within a few minutes after infection, viral decapsidation takes place at the acid pH of late endosomes. Then, ASFV exits endosomes to start viral replication and reorganizes endosomal traffic to the perinuclear replication site where VFs are built. Given this, endosomes and endosomal lipid signaling might be adapted by ASFV entering the endosomal pathway to promote replication.

In this work, we have examined the distribution of endosomes, upon ASFV infection, to the viral replication site. These results add to a growing body of evidence pointing out the endosomal membrane and its components as crucial elements at the start of viral replication in several virus models.

2. Materials and Methods

2.1. Cells, Virus and Infections

Vero cells were purchased from American Type Culture Collection (ATCC) and grown at 37 °C in a 5% CO_2 atmosphere in Dulbecco's Modified Eagle's Medium (DMEM), supplemented with 5% fetal bovine serum (FBS), or 2% for viral infections, containing penicillin/streptomycin (P/S) and Glutamax (G; Gibco, Gaithersburg, MD, USA). Cells were grown on chamber slides (Lab-Tek; Nunc, Roskilde, Denmark), approximately 1.5×10^4 cells/chamber and mock-infected or infected with ASFV-Ba71V isolate [28,29] recombinant ASFV expressing green fluorescent protein (GFP; B54GFP), or cherry fluorescent protein (ChFP; B54ChFP) [21], at a multiplicity of infection (moi) of 1. Both recombinant viruses showed accumulation of the fluorescent GFP or ChFP, expressed as a fusion protein of the viral p54 in the VF, at late times after infection (9–24 h post-infection; hpi). African swine fever virus stocks from culture supernatants were clarified and semi-purified from vesicles by ultracentrifugation at 40,000$\times$ *g* through a 40% (*w*/*v*) sucrose cushion in phosphate-buffered saline (PBS) for 1 h at 4 °C. Purified ASFV stocks were sonicated on ice once for 1 min and stored at −80 °C. When synchronization of infection was required, cells were chilled at 4 °C for 20 min, and then, the virus was added. Virus adsorption was performed for 90 min at 4 °C, and after cold PBS washing to remove unbound virus, cells were rapidly shifted to 37 °C with fresh pre-warmed media. YM201636 (YM; Symansis, Cell Signaling Science, Auckland, NZ) was used at 1 μM as a cell permeable inhibitor of the enzyme PIKfyve and was added from 2 h before to 4 h after infection as below described.

2.2. ASFV Titration

Viral stocks, or infective ASFV yields from infected samples, were titrated by plaque assay in Vero cells, as previously described [28]. Briefly, preconfluent monolayers of Vero cells in 12-well plates were inoculated with 10-fold sample serial dilutions from samples for 90 min at 37 °C. The inoculum was then removed and 3 mL of semisolid medium was added (1:1 low-melting-point agarose; Gibco), as well as 2$\times$ minimal essential medium (MEM; Gibco). Plaque development was visualized after 10–12 days post-infection (dpi), after staining with crystal violet 1% (*w*/*v*) (Sigma-Aldrich, St. Louis, MI, USA).

2.3. Detection and Quantitation of the ASFV Genome

The quantitation of the number of copies of ASFV genome was achieved by quantitative real-time PCR (qPCR). The qPCR assay used fluorescent hybridization probes to amplify a region of the p72 viral gene, as described previously described [30]. DNA from cells mock-infected or infected with ASFV Ba71V at an moi of 1 pfu/cell was extracted at 16 hpi and purified with a DNAeasy blood and tissue kit (Qiagen, Hilden, Germany). DNA concentration was measured with Nanodrop. The amplification mixture was prepared on ice as follows: 250 ng template DNA to a final reaction mixture of 20 μL, containing 50 pmol sense and anti-sense oligonucleotides, 5 pmol TaqMan probe and 10 μL PCR Premix Ex Taq (2$\times$; Takara Bio, Clontech, Mountain view, CA, USA) [30]. Positive amplification controls were DNA purified from ASFV virions at different concentrations, as standards. Negative amplification controls consisted of DNA extracted from mock-infected cells. Each sample was included in triplicates, and values were normalized to standard positive controls. Reactions were performed using the ABI 7500 Fast Real-Time PCR System (Life Technologies, Thermo Fisher Scientific, Applied Biosystems, Waltham, MA, USA) with the following parameters: 1 cycle at 94 °C for 10 min, 45 cycles at 94 °C for 15 s and 45 cycles at 58 °C for 1 min.

2.4. Proteins Detection by Western Blot

Protein extracts from Vero cells were separated by electrophoresis in 12% acrylamide–bisacrylamide gels, or 7% to detect PIKfyve. Separated proteins were transferred to nitrocellulose membranes, and proteins were detected with specific antibodies in each case. As a secondary antibody, anti-mouse

IgG (GE Healthcare, Little Chalfont, UK) or anti-rabbit IgG (Bio-Rad, Oslo, Norway) conjugated to horseradish peroxidase, were used at a 1:5000 dilution. Precision Protein StrepTactin-HRP Conjugate (Bio-Rad) was used to reveal the ladder Precision Plus Protein WesternC (Bio-Rad). As a load control in WB analysis, an anti-mouse antibody against β-tubulin (Sigma) 1:2000 was used. Finally, bands obtained after development with ECL reagent were detected on the Molecular Imager Chemidoc XRSplus Imaging System (Bio-Rad, Hercules, CA, USA). Bands were quantified by densitometry, and data were normalized to control values using Image system software.

2.5. Antibodies

Monoclonal antibodies against the virus major capsid protein p72 (Ingenasa, Madrid, Spain) were used at a working dilution of 1:1000 and anti-p30 antibody at 1:100 dilution [31]. African swine fever virus p30 protein is expressed since the initial phases of the infection [32], and p72 and p54 protein are late proteins expressed after viral replication [20]. Both p54 and p72 viral proteins are very abundant in infection and accumulated in the viral replication organelle or VF.

Early endosomes were labeled with anti-mouse EEA1 antibody (BD Biosciences Pharmingen, San Diego, CA, USA), EEA1 being a Rab5 GTPase effector, and anti-rabbit Rab7 (Cell Signaling Technologies, Danvers, MA, USA) was used to label LE both at 1:50 dilution. Multivesicular endosomes (MVE, were labeled with anti-CD63 (Developmental Studies Hybridoma Bank, University of Iowa, clone H5C6), a tetraspanin characteristic of this compartment, at a 1:200 dilution. LY were labeled with anti-Lamp1 (Abcam, Cambridge, UK) at 1:50 dilution. Anti-PIKfyve polyclonal antibody (1:500) was obtained from Abnova (Taoyuan City, Taiwan). The secondary antibodies used were anti-mouse immunoglobulin G (IgG) antibody conjugated to Alexa Fluor 594 and anti-rabbit IgG antibody conjugated to Alexa Fluor 488. Secondary antibodies were purchased from Molecular Probes (Eugene, OR, USA) and diluted 1:200. The specificity of labeling and the absence of signal crossover were determined by examination of single labeled control samples.

2.6. Flow Cytometry

At 6 hpi, cells were washed with PBS and harvested by trypsinization. After washing with fluorescence-activated cell sorter (FACS) buffer (PBS, 0.01% sodium azide and 0.1% bovine serum albumin (BSA), cells were fixed and permeabilized with Perm2 (BD Sciences, San Jose, CA, USA) for 10 min at room temperature (RT). Infected cells were detected after incubation with anti-p30 monoclonal antibody (diluted 1:100 in FACS buffer) for 30 min at 4 °C, followed by incubation with phycoerythrin (PE)-conjugated anti-mouse immunoglobulins (1:50, diluted in FACS buffer (Dako, Agilent Tech. Santa Clara, CA, USA) for 30 min at 4 °C. After extensive washing, 10,000 cells per tube in triplicates were scored and analyzed in a FACSCalibur flow cytometer (BD Sciences) to determine the percentage of infected cells under these conditions. The obtained infection rates were normalized to the corresponding control.

2.7. Indirect Immunofluorescence, Conventional and Confocal Microscopy

Cells were grown on glass coverslips and fixed in PBS 4% paraformaldehyde (PFA) for 15 min and permeabilized with PBS-0.1% Triton X-100 or saponin (Sigma) for 10 min. Following cell fixation, aldehyde fluorescence was quenched by incubation of cells with 50 mM NH_4Cl in PBS for 10 min. After blocking with BSA (Sigma) or normal goat serum (Sigma), cells were incubated with corresponding antibodies and nucleus and were stained with Topro3 (Molecular Probes) before mounting.

Confocal microscopy was carried out in a Leica TCS SPE confocal microscope, using a 63× immersion oil objective. Conventional fluorescence microscopy to analyze Filipin staining was performed in a Leica DM RB microscope, through a 63× immersion oil objective. Image analyses were performed with Leica Application Suite advanced fluorescence (LAS AF Lite) and Image J software version 1.47v for Windows.

2.8. Measurement of Rab7 Endosomal Aggregates

The distance of the Rab7 signal to the cellular nucleus in mock- or ASFV-infected cells was carried out with the Image J plug-in "Distance measure", kindly provided by Dr. Esteban Veiga and Giulia Morlino (Institute for Health Research "Hospital Universitario La Princesa", CNB, Madrid, Spain).

To measure the distance between two three-dimensional fluorescence distributions in independent channels, we binarized both grey-scale stacks (the plug-in was designed to select two thresholds, thus the region of interest is isolated in both channels). Then, the Euclidean distance between every possible pair of voxels was computed (one in Distribution A and the other in Distribution B). This yields the exact distribution of pairwise distances. Note that the calculation is fully computed in three-dimensions; therefore, it calculates the actual distance between the two regions of interest. Finally, the mean distance was computed after discarding the 5% lower and upper values. This mean is known to be a robust estimate of the distribution mean.

2.9. Measurement of Viral Factories and Endosomal Aggregates

The area occupied by VF or endosomal aggregates was measured from immunofluorescence representative images by drawing regions of interest in each picture. It was performed using LAS AF confocal software. Finally, the mean $\pm$ *SD* (standard deviation) was calculated from these regions at several time points.

2.10. Nocodazole Treatment

Nocodazole was used as a MT depolymerizing drug. Vero cells were seeded and infected at an moi of 1 pfu/cell and treated with 10 μM nocodazole in DMSO 1 hour prior to infection (−1 h), at the time of infection (0 hpi), or 2 and 4 hpi (+2 and +4 hpi). To address the effect of nocodazole in endosome movement in this cell line, we detected acidic endosomes using lysotracker (75 nM), a pH-sensitive dye, for 30 min at 37 °C. Then, confocal images were taken before and after nocodazole treatment and after washing the drug and adding fresh media. Time-lapse microscopy was carried out using a Leica TCS SPE confocal microscope that included a humidified incubation chamber, a CO_2 controller and a heating unit. Selected stacks were recorded every 10 s using the Leica Microsystems LAS AF program, and the movies were displayed at 1–5 frames per second. Then, 10 μM nocodazole stopped vesicular traffic, and movement was recovered after washing, as it is a reversible drug (data not shown).

2.11. Statistical Analysis

Differences between groups were analyzed by the Bonferroni test with GraphPad Prism 6 and Instat 3.05 software for Windows. All experiments were performed in triplicates, and data are presented as mean $\pm$ SD of independent experiments. Metrics were normalized to control values and represented in graphics. Asterisks denote statistically-significant differences (*** $p < 0.001$, ** $p < 0.01$ and * $p < 0.05$).

3. Results

3.1. ASFV Remodels Endosomes

Immunofluorescence analysis of the endosomal distribution in ASFV-infected cells showed that ASFV induces a profound change in the vesicular pattern at late time points (10–24 hpi). For this analysis, we used the early endosome marker EEA1, the MVB marker CD63, the LE marker Rab7 and lysosomal marker Lamp1 (Figure 1A), and Vero cells were infected with recombinant ASFV engineered to express GFPs or ChFPs as fusion proteins of p54, as previously described [27], or non-infected.

Between 8 and 16 hpi, the virus establishes its site of replication or VF, which is recognized by confocal fluorescent microscopy as recombinant fluorescent virus accumulated in the perinuclear region. In contrast to non-infected controls, endosomes repositioned around the perinuclear VF in

approximately 90% of the VFs in infected cells (Figure 1B). Considerably large areas of aggregated endosomes and VF are depicted in the graphs at 16 and 24 hpi (Figure 1C). Distances to the nucleus of Rab7-expressing vesicles were measured in the x, y and z planes to show that the LE were closer to the nucleus in ASFV-infected cells compared to mock-infected controls (** $p < 0.01$; Figure 1D). Cells with similar sizes were analyzed, and this was obtained when culture conditions were kept constant, and cells were plated at 80% confluence and analyzed at the same time point.

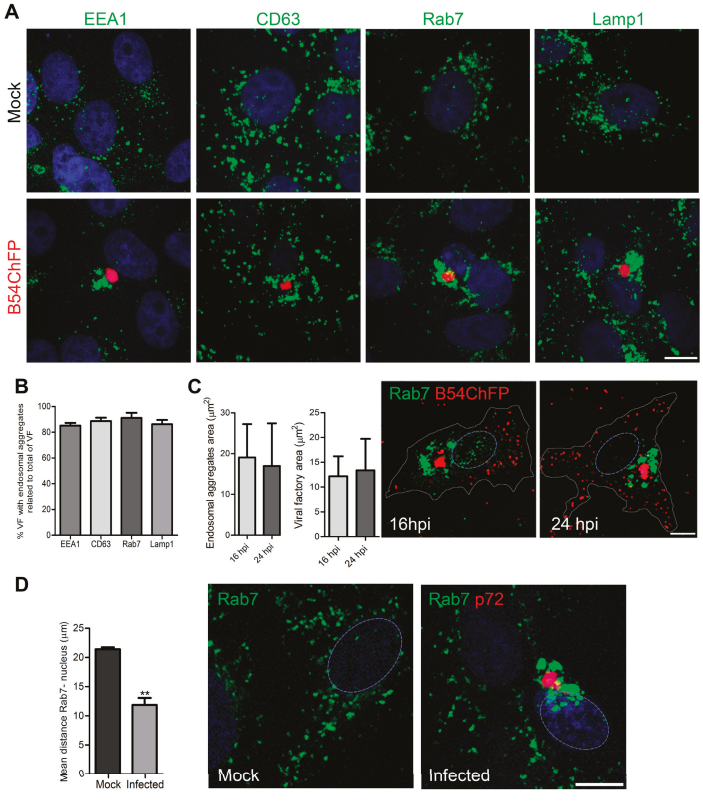

Figure 1. African swine fever virus (ASFV) remodels endosomes. (**A**) Endosome recruitment around the ASFV viral factory (VF) in Vero cells infected with recombinant fluorescent B54ChFP (red) at 16 hpi. Endosome markers are shown in green, on early endosomes (EE; EEA1), multivesicular bodies (MVB; CD63), late endosomes (LE; Rab7) and lysosomes (LY; Lamp1). Above, the typical diffuse cytoplasmic distribution of endosomes in mock-infected cells. Bar 10 µm. (**B**) Percentages of VF with endosome aggregation relative to the total number of VF. (**C**) Cytoplasmic areas occupied by endosomal aggregates or VF at 16 and 24 hpi. Mean ± *SD* from two independent experiments. Bar 10 µm. (**D**) Three-dimensional distances from LE endosomes to the nucleus in control and infected cells at 16 hpi. Mean ± *SD*; $n = 10$ cells in duplicates; significant differences are marked with asterisks (** $p < 0.01$). Bar 10 µm.

The VF that ASFV builds between 8 and 16 hpi consists of a single large cytoplasmic structure with no surrounding membrane located at the perinuclear area where viral replication and morphogenesis occur [7]. We found that the VF was formed in close relationship or interspersed with endosomal membranes (Figure 2A). Endosome clustering occurred in close relationship to the VF as shown in the zoom images (Figure 2B) or sequential optical planes by confocal microscopy (Figure 2C).

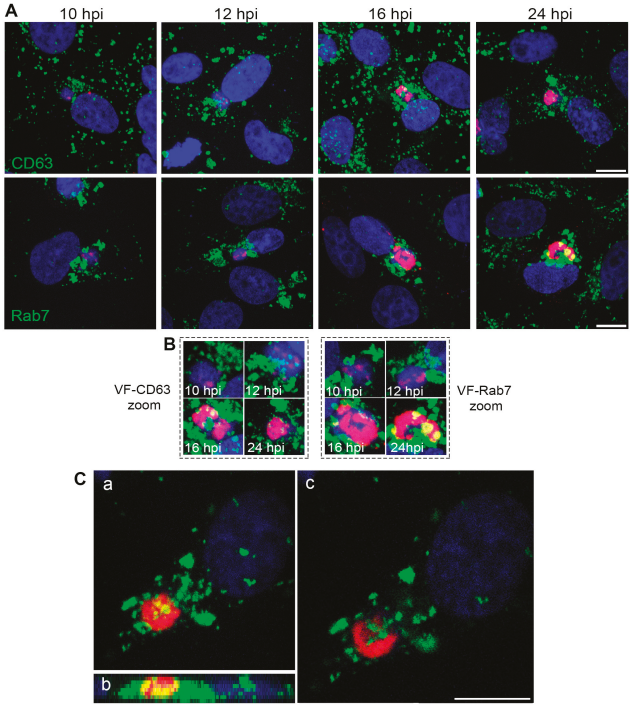

Figure 2. Endosomal membranes participate in the formation of the viral replication organelle. (**A**) VF formation at sequential time points (red; 10–24 hpi). Endosomes are labeled in green (CD63, Rab7), and DNA was stained with Topro3 (blue). Viral DNA and endosomes were first accumulated at the perinuclear area (microtubule (MT) organizing center; MTOC), then dispersed foci of viral proteins appeared intermingled with endosomal membranes colocalizing with viral DNA (pink) or endosomes (yellow). (**B**) Detail of VF is shown in zoom areas for CD63 and Rab7. (**C**) Endosomal membranes arrange together with viral DNA and proteins at the VF. Maximum (a), lateral projections (b), and individual sequential optical planes (c) of ASFV VF, are shown at 16 hpi (B54ChFP; red and Rab7; green). Bars: 10 μm.

3.2. Endosomal Recruitment Relies on Viral Infection Progression

Given the changes in vesicular distribution, we examined the impact of depolymerizing MT on ASFV endosome repositioning and virus infectivity. Treatment of Vero cells with MT-depolymerizing drug nocodazole effectively inhibited cytoplasmic vesicular traffic labelled with lysotracker. Removal of this drug by adding fresh media restored movement (data not shown). MT depolymerization abolished both VF formation and endosome recruitment when the drug was added at −1 hpi (Figure 3A). Additionally, it inhibited infectivity (*** $p < 0.001$; Figure 3B), expression of viral p30 at 6 hpi (*** $p < 0.001$; Figure 3C,D) and viral replication at 16 hpi (** $p < 0.01$; Figure 3E). This effect was noticeable in cells in which the drug treatment started at 1 h prior to infection. However, when nocodazole was added at infection or at 2 hpi, VF formation (Figure 3B) and viral replication (Figure 3E) were altered, but not p30 expression (Figure 3D).

In the few cells that did become infected under MT depolymerization-initiated post-infection, the viral replication organelle appeared disaggregated (Figure 3A). African swine fever virus VF formation was MT-dependent regardless of the time of nocodazole addition. In contrast, MT depolymerization only affected early p30 protein expression when nocodazole was added before

or at the time of infection (Figure 3D). These data suggest that endosomal membrane recruitment occurs after virion transport to the perinuclear area and once early protein expression has taken place, when viral replication starts. Therefore, endosomal recruitment was infection progression dependent.

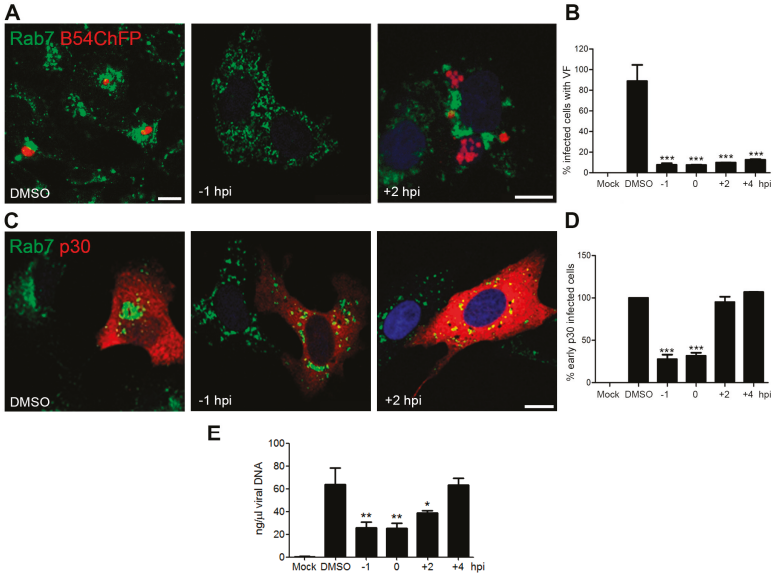

Figure 3. (**A**) The MT cytoskeleton was required for VF formation. MT depolymerization impaired viral replication and endosomal recruitment when nocodazole was added before infection. MT depolymerization later at infection (+2 hpi) reduced the number of cells with VF, and the few visible VF lacked cohesion with smaller endosomal aggregates at 16 hpi. B54ChFP (red) and Rab7 (green). Control cells conserved the characteristic single VF morphology surrounded by aggregated endosomes. Bar: 10 µm. (**B**) Under MT-depolymerizing drug nocodazole treatment, the number of infected cells with VF decreased over 80% as evaluated by fluorescence-activated cell sorter (FACS) analysis at 16 hpi (*** $p < 0.001$). (**C**) Endosome dispersal and early protein p30 expression in cells left untreated, pre-treated with nocodazole or treated after 2 hpi analyzed by confocal microscopy at 16 hpi, using a monoclonal antibody against p30 (red) and an anti-Rab7 (green). (**D**) Pretreatment with nocodazole before infection decreased viral protein p30 expression by FACS analysis at 6 hpi (*** $p < 0.001$). Protein expression was not affected when treatment was started after 2 hpi. (**E**) Viral replication by qPCR in cells left untreated, treated with DMSO, pretreated with nocodazole or treated after 2 and 4 hpi (** $p < 0.01$; * $p < 0.05$).

3.3. Endosome Membrane Lipids Are Essential for a Successful ASFV Infection

The dynamic properties of the endosomal membrane are provided by its changing phospholipid composition. PtdIns3P is a substrate for the generation of PtdIns(3,5)P_2 by the action of the kinase PIKfyve (see the schematics in Figure 4A). Inhibition of PtdIns-converting enzyme PIKfyve with the drug YM (1 µM) from 2 h before infection to 4 hpi as described in Materials and Methods resulted in a significant decrease in viral replication (Figure 4B). Furthermore, PIKfyve enzyme expression increased upon ASFV infection at the time of viral replication (*** $p < 0.001$; Figure 4C).

Inhibition of PtdIns-converting enzyme PIKfyve with the drug YM201636 (1 µM) from 1 h before infection to 4 hpi resulted in a significant decrease in viral replication (Figure 4B). Furthermore, PIKfyve enzyme expression increased upon ASFV infection at the time of viral replication upon ASFV infection (*** $p < 0.001$; Figure 4C).

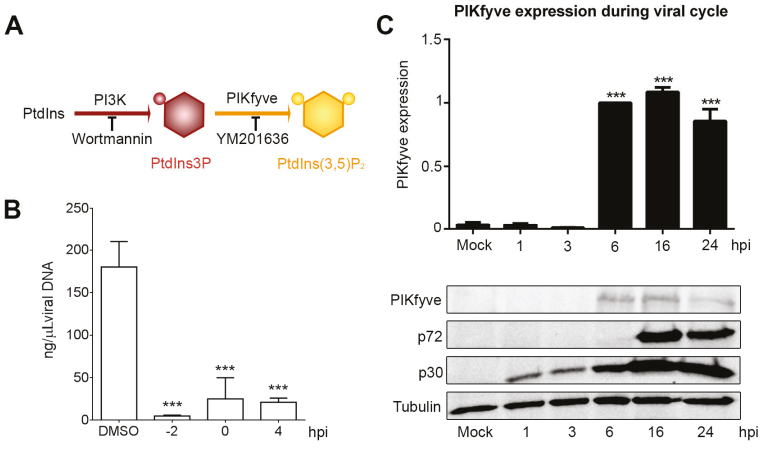

Figure 4. Phosphoinositide interconversion is relevant for ASFV infection. (**A**) Schematics of phosphatidylinositol 3-phosphate (PtdIns3P) and 3,5-biphosphate (PtdIns(3,5)P_2) interconversions mediated by kinases PI3K and PIKfyve at the endolysosomal membranes. (**B**) Inhibition of PIKfyve converting enzyme activity with YM severely impaired viral DNA replication as shown by qPCR (*** $p < 0.001$). (**C**) PIKfyve expression was upregulated after ASFV infection at the time of viral replication (6–24 hpi). Metrics show the mean ± *SD* in duplicates of WB densitometry related to load control compared to mock-infected cells. Significant differences are marked with asterisks (*** $p < 0.001$).

4. Discussion

Our observations demonstrate that ASFV is able to reorganize endosomal traffic to ensure a successful replication. ASFV replication organelle or viral factory (VF) is a single structure lacking an outer limiting membrane in a cytoplasmic location near the nucleus at the MTOC [7]. Fully-formed ASFV VF is surrounded by mitochondria [33,34] and a vimentin cage [35]. We have now described endosomal aggregation at the ASFV replication site. Endosomal membranes are part of early VFs and are found interspersed with the accumulation of newly-synthesized viral DNA and proteins.

It was previously described that membranes used for ASF virion assembly are originated at the ER [22] and membranes close to ASFV particles labelled with antibodies against viral and ER proteins [21,22]. Immunofluorescence analysis shows areas of apparent exclusion of resident ER proteins relative to the rest of the cytoplasm [21,34] where endosomal membranes are accumulated. However, both ER and endosomal membranes could be coincident at the inner part of the VFs in direct contact of areas of viral morphogenesis, which seems possible, but should be considered for further studies.

Viruses hijack several host cell membranes for an efficient replication. Most of these membranes are building elements originated from the secretory pathway, namely ER, Golgi and trans-Golgi [36,37]. However, the presence of endosomal components in a DNA virus assembly site is less frequent. An exception to this is the case of cytomegalovirus (CMV), given that EE markers were found as CMV VF components [38,39]. In the case of RNA virus, endosomes and lysosomes are considered the origin of the cytopathic vacuoles (CPVs) in the *Togaviridae* family (Rubella virus and Semiliki Forest virus). Cytopathic vacuoles are multiple and independent cytoplasmic structures of endo-lysosomal origin entailing a double membrane bilayer containing nascent RNA and viral proteins. Hence, replication and assembly in *Togaviruses* takes place within these modified endo-lysosomes [37]. In contrast, ASFV exits endosomes to complete its replication cycle.

MT-dependence for ASFV infection was previously thought to represent the first transport step of the viral particles to the nucleus [19] and the transport of virions to exit the cell [23,24]. However, our data suggest that intact MTs are also required for viral replication and the VF formation. The absence of MTs resulted in the lack of aggregation of the ASFV VF. Moreover, it impaired endosomal recruitment. Early protein expression only occurred when nocodazole was added before or at the time of infection, but not when it was added at a post-entry stage, suggesting that MTs are also required after virion transport to the perinuclear area. Furthermore, the disaggregation found in VFs under MT depolymerization has been previously reported [19,25,26]. This indicates a crucial role of MTs in the cohesion of the viral replication site.

ASFV reorganizes endosomes to the VFs. Recruitment of endosomes to VFs was dependent on infection progression. MT depolymerization affected endosome recruitment when nocodazole was added before infection, but at late postinfection times (2 hpi) MT depolymerization was unable to inhibit endosomal recruitment completely. ASFV infection progression correlates with endosomal recruitment probably to ensure a successful replication. Whether these events are sequential or simultaneous is still intriguing as the VF is built and therefore should be the subject of further studies.

Endosomal membranes could be a source of lipids that are substrates for replication. We have previously shown that inhibition of PtdIns biosynthesis by PI3K or PIKfyve reduces ASFV production [16]. Now, we found that reduction in viral production by the PIKfyve inhibitor was due to the abolition of ASFV replication. Our results provide further insights in the field of ASFV by demonstrating that the activity of PtdIns-converting kinases is essential for some intracellular pathogens to build their replication sites/niches [40,41]. PI4KIII-converting enzyme that synthesizes PtdIns4P is essential to build the enterovirus replication site and to form the hepatitis C virus membranous web, in both cases by reorganization of the secretory pathway [42,43]. This was shown by detecting modifications of the activity of this enzyme throughout the infective cycle. Furthermore, PIKfyve, responsible for PtdIns(3,5)P2 generation at the LE, participates in the replication of poxvirus [44] as well as in the formation of the replicative vacuole of the intracellular bacteria *Salmonella* [40].

In this study, we found that the inhibition of PIKfyve greatly reduces ASFV replication, and its expression is enhanced upon ASFV replication. In ASFV infection, PIKfyve could exert a similar function as observed in the case of *Salmonella* infection, which also strongly relies on the LE [16]. In conclusion, our results suggest that ASFV replication requires endosomal membranes and PIKfyve enzyme activity.

Acknowledgments: This work was supported by AGL2012-34533 and AGL2015-69598-R from the Ministerio de Economía, Industria y Competitividad of Spain. The Distance measure software plug-inn of Image J was kindly provided by Dr. Esteban Veiga and Giulia Morlino from Institute for Health Research "Hospital Universitario La Princesa", Centro Nacional de Biotecnología, Madrid, Spain.

Author Contributions: C.A., M.A.C.-G. and I.G. conceived and designed the experiments; L.B.-G., M.A.C.-G. and R.M.M. performed the experiments; I.G., R.M.M., L.B.-G., M.A.C.-G. and C.A. analyzed the data; L.B.-G., M.A.C.-G. and R.M.M. contributed reagents and analysis tools; M.A.C.-G. and C.A. wrote the paper.

Conflicts of Interest: The authors declare no conflict of interest. The founding sponsors had no role in the design of the study; in the collection, analyses, or interpretation of data; in the writing of the manuscript, and in the decision to publish the results.

References

1. Huotari, J.; Helenius, A. Endosome maturation. *Embo. J.* **2011**, *30*, 3481–3500. [CrossRef] [PubMed]
2. Gruenberg, J. The endocytic pathway: A mosaic of domains. *Nat. Rev. Mol. Cell. Biol.* **2001**, *2*, 721–730. [CrossRef] [PubMed]
3. Bissig, C.; Lenoir, M.; Velluz, M.C.; Kufareva, I.; Abagyan, R.; Overduin, M.; Gruenberg, J. Viral infection controlled by a calcium-dependent lipid-binding module in alix. *Dev. Cell* **2013**, *25*, 364–373. [CrossRef] [PubMed]
4. Greber, U.F. Signalling in viral entry. *Cell. Mol. Life Sci.* **2002**, *59*, 608–626. [CrossRef] [PubMed]

5. Marsh, M.; Helenius, A. Virus entry: Open sesame. *Cell* **2006**, *124*, 729–740. [CrossRef] [PubMed]
6. Mercer, J.; Schelhaas, M.; Helenius, A. Virus entry by endocytosis. *Annu. Rev. Biochem.* **2010**, *79*, 803–833. [CrossRef] [PubMed]
7. Alonso, C.; Galindo, I.; Cuesta-Geijo, M.A.; Cabezas, M.; Hernaez, B.; Munoz-Moreno, R. African swine fever virus-cell interactions: From virus entry to cell survival. *Virus Res.* **2013**, *173*, 42–57. [CrossRef] [PubMed]
8. Callaway, E. Pig fever sweeps across Russia. *Nature* **2012**, *488*, 565–566. [CrossRef] [PubMed]
9. Zakaryan, H.; Revilla, Y. African swine fever virus: Current state and future perspectives in vaccine and antiviral research. *Vet. Microbiol.* **2016**, *185*, 15–19. [CrossRef] [PubMed]
10. O'Donnell, V.; Holinka, L.G.; Krug, P.W.; Gladue, D.P.; Carlson, J.; Sanford, B.; Alfano, M.; Kramer, E.; Lu, Z.; Arzt, J.; et al. African swine fever virus Georgia 2007 with a deletion of virulence-associated gene *9GL* (b119l), when administered at low doses, leads to virus attenuation in swine and induces an effective protection against homologous challenge. *J. Virol.* **2015**, *89*, 8556–8566. [CrossRef] [PubMed]
11. Pejsak, Z.; Truszczynski, M.; Niemczuk, K.; Kozak, E.; Markowska-Daniel, I. Epidemiology of african swine fever in poland since the detection of the first case. *Pol. J. Vet. Sci.* **2014**, *17*, 665–672. [CrossRef] [PubMed]
12. Galindo, I.; Cuesta-Geijo, M.A.; Hlavova, K.; Munoz-Moreno, R.; Barrado-Gil, L.; Dominguez, J.; Alonso, C. African swine fever virus infects macrophages, the natural host cells, via clathrin- and cholesterol-dependent endocytosis. *Virus Res.* **2015**, *200*, 45–55. [CrossRef] [PubMed]
13. Hernaez, B.; Alonso, C. Dynamin- and clathrin-dependent endocytosis in african swine fever virus entry. *J. Virol.* **2010**, *84*, 2100–2109. [CrossRef] [PubMed]
14. Sanchez, E.G.; Quintas, A.; Perez-Nunez, D.; Nogal, M.; Barroso, S.; Carrascosa, A.L.; Revilla, Y. African swine fever virus uses macropinocytosis to enter host cells. *PLoS Pathog.* **2012**, *8*, e1002754. [CrossRef] [PubMed]
15. Hernaez, B.; Guerra, M.; Salas, M.L.; Andres, G. African swine fever virus undergoes outer envelope disruption, capsid disassembly and inner envelope fusion before core release from multivesicular endosomes. *PLoS Pathog.* **2016**, *12*, e1005595. [CrossRef] [PubMed]
16. Cuesta-Geijo, M.A.; Galindo, I.; Hernaez, B.; Quetglas, J.I.; Dalmau-Mena, I.; Alonso, C. Endosomal maturation, RAB7 GTPase and phosphoinositides in african swine fever virus entry. *PLoS ONE* **2012**, *7*, e48853. [CrossRef] [PubMed]
17. Cuesta-Geijo, M.A.; Chiappi, M.; Galindo, I.; Barrado-Gil, L.; Munoz-Moreno, R.; Carrascosa, J.L.; Alonso, C. Cholesterol flux is required for endosomal progression of African swine fever virions during the initial establishment of infection. *J. Virol.* **2015**, *90*, 1534–1543. [CrossRef] [PubMed]
18. Netherton, C.L.; Wileman, T.E. African swine fever virus organelle rearrangements. *Virus Res.* **2013**, *173*, 76–86. [CrossRef] [PubMed]
19. Alonso, C.; Miskin, J.; Hernaez, B.; Fernandez-Zapatero, P.; Soto, L.; Canto, C.; Rodriguez-Crespo, I.; Dixon, L.; Escribano, J.M. African swine fever virus protein p54 interacts with the microtubular motor complex through direct binding to light-chain dynein. *J. Virol.* **2001**, *75*, 9819–9827. [CrossRef] [PubMed]
20. Cobbold, C.; Whittle, J.T.; Wileman, T. Involvement of the endoplasmic reticulum in the assembly and envelopment of African swine fever virus. *J. Virol.* **1996**, *70*, 8382–8390. [PubMed]
21. Andres, G.; Garcia-Escudero, R.; Simon-Mateo, C.; Vinuela, E. African swine fever virus is enveloped by a two-membraned collapsed cisterna derived from the endoplasmic reticulum. *J. Virol.* **1998**, *72*, 8988–9001. [PubMed]
22. Rouiller, I.; Brookes, S.M.; Hyatt, A.D.; Windsor, M.; Wileman, T. African swine fever virus is wrapped by the endoplasmic reticulum. *J. Virol.* **1998**, *72*, 2373–2387. [PubMed]
23. Andres, G.; Garcia-Escudero, R.; Vinuela, E.; Salas, M.L.; Rodriguez, J.M. African swine fever virus structural protein pR120R is essential for virus transport from assembly sites to plasma membrane but not for infectivity. *J. Virol.* **2001**, *75*, 6758–6768. [CrossRef] [PubMed]
24. Jouvenet, N.; Monaghan, P.; Way, M.; Wileman, T. Transport of African swine fever virus from assembly sites to the plasma membrane is dependent on microtubules and conventional kinesin. *J. Virol.* **2004**, *78*, 7990–8001. [CrossRef] [PubMed]
25. Carvalho, Z.G.; de Matos, A.P.; Rodrigues-Pousada, C. Association of African swine fever virus with the cytoskeleton. *Virus Res.* **1988**, *11*, 175–192. [CrossRef]
26. De Matos, A.P.; Carvalho, Z.G. African swine fever virus interaction with microtubules. *Biol. Cell* **1993**, *78*, 229–234. [CrossRef]

27. Hernaez, B.; Escribano, J.M.; Alonso, C. Visualization of the African swine fever virus infection in living cells by incorporation into the virus particle of green fluorescent protein-p54 membrane protein chimera. *Virology* **2006**, *350*, 1–14. [CrossRef] [PubMed]
28. Enjuanes, L.; Carrascosa, A.L.; Moreno, M.A.; Vinuela, E. Titration of African swine fever (ASF) virus. *J. Gen. Virol.* **1976**, *32*, 471–477. [CrossRef] [PubMed]
29. Yanez, R.J.; Rodriguez, J.M.; Nogal, M.L.; Yuste, L.; Enriquez, C.; Rodriguez, J.F.; Vinuela, E. Analysis of the complete nucleotide sequence of African swine fever virus. *Virology* **1995**, *208*, 249–278. [CrossRef] [PubMed]
30. King, D.P.; Reid, S.M.; Hutchings, G.H.; Grierson, S.S.; Wilkinson, P.J.; Dixon, L.K.; Bastos, A.D.; Drew, T.W. Development of a TaqMan PCR assay with internal amplification control for the detection of African swine fever virus. *J. Virol Methods* **2003**, *107*, 53–61. [CrossRef]
31. Hernaez, B.; Escribano, J.M.; Alonso, C. African swine fever virus protein p30 interaction with heterogeneous nuclear ribonucleoprotein k (HNRNP-K) during infection. *FEBS Lett.* **2008**, *582*, 3275–3280. [CrossRef] [PubMed]
32. Afonso, C.L.; Alcaraz, C.; Brun, A.; Sussman, M.D.; Onisk, D.V.; Escribano, J.M.; Rock, D.L. Characterization of p30, a highly antigenic membrane and secreted protein of African swine fever virus. *Virology* **1992**, *189*, 368–373. [CrossRef]
33. Rojo, G.; Chamorro, M.; Salas, M.L.; Vinuela, E.; Cuezva, J.M.; Salas, J. Migration of mitochondria to viral assembly sites in African swine fever virus-infected cells. *J. Virol.* **1998**, *72*, 7583–7588. [PubMed]
34. Netherton, C.L.; McCrossan, M.C.; Denyer, M.; Ponnambalam, S.; Armstrong, J.; Takamatsu, H.H.; Wileman, T.E. African swine fever virus causes microtubule-dependent dispersal of the trans-golgi network and slows delivery of membrane protein to the plasma membrane. *J. Virol.* **2006**, *80*, 11385–11392. [CrossRef] [PubMed]
35. Stefanovic, S.; Windsor, M.; Nagata, K.I.; Inagaki, M.; Wileman, T. Vimentin rearrangement during African swine fever virus infection involves retrograde transport along microtubules and phosphorylation of vimentin by calcium calmodulin kinase II. *J. Virol.* **2005**, *79*, 11766–11775. [CrossRef] [PubMed]
36. Novoa, R.R.; Calderita, G.; Arranz, R.; Fontana, J.; Granzow, H.; Risco, C. Virus factories: Associations of cell organelles for viral replication and morphogenesis. *Biol. Cell* **2005**, *97*, 147–172. [CrossRef] [PubMed]
37. Miller, S.; Krijnse-Locker, J. Modification of intracellular membrane structures for virus replication. *Nat. Rev. Microbiol.* **2008**, *6*, 363–374. [CrossRef] [PubMed]
38. Das, S.; Vasanji, A.; Pellett, P.E. Three-dimensional structure of the human cytomegalovirus cytoplasmic virion assembly complex includes a reoriented secretory apparatus. *J. Virol.* **2007**, *81*, 11861–11869. [CrossRef] [PubMed]
39. Alwine, J.C. The human cytomegalovirus assembly compartment: A masterpiece of viral manipulation of cellular processes that facilitates assembly and egress. *PLoS Pathog.* **2012**, *8*, e1002878. [CrossRef] [PubMed]
40. Kerr, M.C.; Wang, J.T.; Castro, N.A.; Hamilton, N.A.; Town, L.; Brown, D.L.; Meunier, F.A.; Brown, N.F.; Stow, J.L.; Teasdale, R.D. Inhibition of the PtdIns(5) kinase PIKfyve disrupts intracellular replication of Salmonella. *EMBO J.* **2010**, *29*, 1331–1347. [CrossRef] [PubMed]
41. Weber, S.S.; Ragaz, C.; Reus, K.; Nyfeler, Y.; Hilbi, H. *Legionella pneumophila* exploits PI(4)P to anchor secreted effector proteins to the replicative vacuole. *PLoS Pathog.* **2006**, *2*, e46. [CrossRef] [PubMed]
42. Hsu, N.Y.; Ilnytska, O.; Belov, G.; Santiana, M.; Chen, Y.H.; Takvorian, P.M.; Pau, C.; van der Schaar, H.; Kaushik-Basu, N.; Balla, T.; et al. Viral reorganization of the secretory pathway generates distinct organelles for RNA replication. *Cell* **2010**, *141*, 799–811. [CrossRef] [PubMed]
43. Tait, S.W.; Reid, E.B.; Greaves, D.R.; Wileman, T.E.; Powell, P.P. Mechanism of inactivation of NF-κb by a viral homologue of i kappa b alpha. Signal-induced release of i kappa b alpha results in binding of the viral homologue to NF-κb. *J. Biol. Chem.* **2000**, *275*, 34656–34664. [CrossRef] [PubMed]
44. Rizopoulos, Z.; Balistreri, G.; Kilcher, S.; Martin, C.K.; Syedbasha, M.; Helenius, A.; Mercer, J. Vaccinia virus infection requires maturation of macropinosomes. *Traffic* **2015**, *16*, 814–831. [CrossRef] [PubMed]

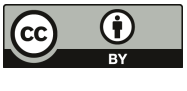

© 2017 by the authors. Licensee MDPI, Basel, Switzerland. This article is an open access article distributed under the terms and conditions of the Creative Commons Attribution (CC BY) license (http://creativecommons.org/licenses/by/4.0/).

viruses

MDPI

Review

Porcine Circoviruses and Xenotransplantation

Joachim Denner * and Annette Mankertz

Robert Koch Institute, Nordufer 20, 13353 Berlin, Germany; MankertzA@rki.de
* Correspondence: DennerJ@rki.de; Tel.: +49-30-18754-2800

Academic Editors: Linda Dixon and Simon Graham
Received: 1 March 2017; Accepted: 12 April 2017; Published: 20 April 2017

Abstract: Allotransplantation and xenotransplantation may be associated with the transmission of pathogens from the donor to the recipient. Whereas in the case of allotransplantation the transmitted microorganisms and their pathogenic effect are well characterized, the possible influence of porcine microorganisms on humans is mostly unknown. Porcine circoviruses (PCVs) are common in pig breeds and they belong to porcine microorganisms that still have not been fully addressed in terms of evaluating the potential risk of xenotransplantation using pig cells, tissues, and organs. Two types of PCVs are known: porcine circovirus (PCV) 1 and PCV2. Whereas PCV1 is apathogenic in pigs, PCV2 may induce severe pig diseases. Although most pigs are subclinically infected, we do not know whether this infection impairs pig transplant functionality, particularly because PCV2 is immunosuppressive. In addition, vaccination against PCV2 is able to prevent diseases, but in most cases not transmission of the virus. Therefore, PCV2 has to be eliminated to obtain xenotransplants from uninfected healthy animals. Although there is evidence that PCV2 does not infect—at least immunocompetent—humans, animals should be screened using sensitive methods to ensure virus elimination by selection, Cesarean delivery, vaccination, or embryo transfer.

Keywords: porcine circoviruses; transspecies transmission of viruses; xenotransplantation; virus safety of xenotransplantation

1. Introduction

Allotransplantation can be associated with transmission of microorganisms which induce severe diseases in the recipient [1,2]. Among the transmitted microorganisms are bacteria [3] and viruses such as the human immunodeficiency virus-1 [4], rabies virus [5–7], and human cytomegalovirus (HCMV) [8]. Infection with HCMV is a common complication after transplantation of different organs and contributes significantly to morbidity and mortality, both by direct and indirect mechanisms [9]. Therefore, HCMV status has to be determined and transplantations from HCMV-positive individuals to HCMV-negative individuals are generally avoided (for review see [8,9]). If necessary, an antiviral treatment is available and new antiviral drugs are under development [10]. Xenotransplantation using pig cells, tissues, and organs may also be associated with transmission of microorganisms, including bacteria, viruses, and others from the donor pig [11]. Transmission of porcine cytomegalovirus (PCMV) with the transplant and its increased replication, also called reactivation, on the background of the absence of the pig immune system and of the applied immunosuppression in the non-human primate recipient, was observed after pig kidney transplantations into baboons [12] or cynomolgus monkeys [13]. Transmission of PCMV was also observed after pig heart transplantations into baboons [14]. Although the virus titre in the recipients increases, it is unclear whether PCMV is able to infect cells of the recipient or is replicating only in the cells of the transplant.

There are obvious differences between the transmission inside the human species during allotransplantation and transspecies transmission into a new species during xenotransplantation. Human microorganisms are adapted to humans and can be easily transmitted [1–4,8,9]. The porcine

microorganisms are not adapted to humans, and it is clear that many of them cannot infect human cells due to the absence of a receptor or due to cellular factors restricting replication in human cells. In contrast to human pathogens, sensitive detection methods for porcine microorganisms were developed only in a few specialized laboratories, and it is unclear whether commercial test laboratories can detect low virus load infections, as shown in one case of PCMV infection [15]. Sending identical virus dilutions to different laboratories worldwide for testing, so called round robin tests, may answer this question. The results of the testing will indicate the sensitivity of their methods. In this context, in a recent round robin or ring test including 11 North American laboratories, the most sensitive assay detected DNA levels of a porcine virus about 100,000 times lower than the least sensitive assay [16]. This study demonstrated that the polymerase chain reaction (PCR) assays available in these diagnostic labs vary considerably in their detection limits and quantification.

Even if porcine microorganisms can infect humans and replicate, it is still unclear whether they are pathogenic. For example, hepatitis E virus (HEV) genotype 3 coming from pigs mostly induces diseases in chronically ill and immunosuppressed humans, but not in healthy individuals [17], although the influence of the subclinical infection on the health of the infected person is still unknown.

The porcine circoviruses (PCVs) belong to the genus *Circovirus* of the family *Circoviridae* [18]. Porcine circovirus 1 (PCV1) was first described at the Robert Koch Institute, Berlin [19]. Other members of this family are PCV2, several avian circoviruses [18], and recently new circoviruses have been isolated from mammals: bat [20,21], dogs [22–25], mink [26,27], and others. Circoviruses are non-enveloped spherical (16–18 nm) particles (Figure 1) with a single-stranded and circular small DNA genome. PCVs are the smallest viruses found to be replicating in mammalian cells. PCVs are quite stable, the effectiveness of disinfectants for reducing PCV2 in vitro is variable and PCV2 is very stable in the pig environment. The virus is very resistant under high temperatures and a wide range of pH conditions (for review see [28]). Two major open reading frames (*orfs*) have been recognized. Orf1 encodes the two replicases indispensable for viral replication (Rep and Rep'), and *orf*2 encodes the capsid protein Cap, which is the major structural protein [29]. Three other genes, *orf*3, *orf*4, and *orf*5 encode proteins not essential for virus replication, but involved in the virulence and spread of the virus [30,31]. Cells of the monocyte and macrophage lineage have consistently been shown to be targets for porcine circovirus replication in vivo, and appear to be important in the pathogenesis of the postweaning multisystemic wasting syndrome (PMWS) [32–34]. Additionally, a variety of other cell types, including hepatocytes, enterocytes, renal and alveolar epithelial cells, vascular endothelial cells, pancreatic acinar and ductular cells, lymphocytes, smooth muscle cells, and fibroblasts, have also been shown to contain PCV2 antigens and/or nucleic acid [35]. It was shown that heparin, heparan sulphate, and chondroitin sulphate are attachment factors for PCV2 [36], whereas the main receptor is still unknown [37].

PCV1 is apathogenic in pigs, but PCV2 is associated with severe diseases, among them PMWS, which is considered the most significant PCV2-related disease (PCVD) (see Section 3). PCV2 is an immunosuppressive virus, targeting the lymphoid tissues, which leads to lymphoid depletion and immunosuppression in pigs. The virus resides in immune cells, such as macrophage and dendritic cells, and modulates their functions. Upregulation of interleukin (IL)-10 and proinflammatory cytokines in infected pigs may contribute to pathogenesis and co-infection with other pathogens. PCV2 DNA and proteins interact with various cellular genes that control immune responses [38–40]. Although numerous reviews summarise the impact of PCV2 on pig production and give detailed descriptions of the pathogenesis of PCV2-induced diseases in pigs [40–43], this review is the first to analyse the potential impact of PCV2 on xenotransplantation, and to analyse whether PCV2 may represent a risk for xenotransplantation. PCV2 induces severe diseases in pigs, but it remains unclear whether subclinical infections may reduce the quality of the pig transplants, particularly because the virus is immunosuppressive. Vaccination against PCV2 is able to prevent diseases, but in most cases is unable to prevent the transmission of the virus (for details see Section 6). Using sensitive methods will increase the probability of detecting the virus. However, it remains unclear how sensitive these

methods should be. At the very least, in order to prevent transmission during xenotransplantation, the sensitivity of the detection methods should allow for the detection of the virus below the load which is able to be transmitted and to induce zoonosis [44]. We also indicate different strategies to eliminate the viruses from the donor pig herd in order to prevent transmission to human recipients.

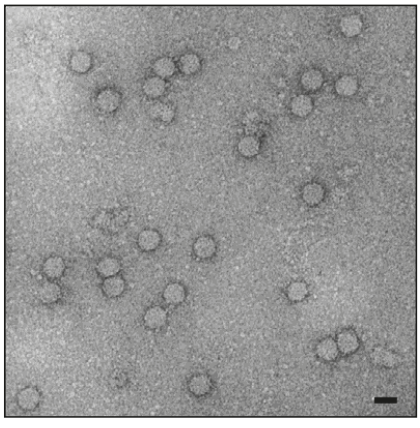

Figure 1. Electron microscopy of porcine circovirus (PCV), negative staining with uranyl acetate. The scale bar corresponds to 20 nm. Hans Gelderblom, Michael Laue, Robert Koch-Institute.

2. Diagnosis and Transmission

PCR is a sensitive method of choice to detect a circovirus infection in viremic animals and different PCR assays, including real-time PCR or quantitative PCR (qPCR) and digital droplet PCR (ddPCR) using specific primers for PCV1 and PCV2 have been developed and applied [45–50]. In some cases, PCVs were detected simultaneously with other porcine viruses using multiplex PCR [51,52]. Other detection methods are antibody-based methods such as enzyme-linked immunosorbent assay (ELISA), Western blot analysis, and immunofluorescence [53–58]. The use of saliva for antibody detection gained popularity because of the ease of use and associated cost-saving [59]. Serum antibodies to PCV1 and PCV2 have been demonstrated in a large percentage of pigs in different countries at a time when vaccination had not yet been introduced [60]. PCR screening in the year 2000 of randomly collected 109 organ samples from German pigs not affected with PCVD revealed a rate of infection with PCV1 of 5% and with PCV2 of 26.8% [46]. Seroconversion usually occurs by two to four months of age irrespective of whether clinical signs of PCVD are observed. PCV2 is shed for a long time by different routes, both after natural as well as experimental infection [61,62]. Therefore, it easily spreads within the population, mainly by direct contact with contaminated respiratory, digestive, and urinary secretions. Although PCV2 has been identified in the semen of acutely affected boars, transmission of the virus via this route has not been documented in a field setting [63,64].

Based on phylogenetic analysis, PCV2 is divided into different genotypes (PCV2a, PCV2b, PVC2c, PCV2d, PCV2e, PCV2f) [65]. The first three variants show 97%–100% nucleotide identity in the *rep* gene and 91%–96% in the *cap* gene [66]. They are believed to have evolved from a common ancestor 100 years ago [67]. In recent years, evidence has accumulated for a global shift of the main PCV2 genotypes in different countries from PCV2a to PCV2b, which is generally associated with more severe disease symptoms [68,69]. PCV2d was initially identified in Switzerland, now it appears to be widespread in China and North America. During 2012–2013, 37% of all investigated PCV2 sequences from U.S. pigs were classified as PCV2d, and overall data analysis suggests an ongoing genotype shift from PCV2b towards PCV2d [70]. Recombinations and mutations have been often observed and may result in altered fitness or phenotypic properties [71–73].

Since changes in the nucleotide sequence of genomic regions used as targets for PCR-detection of PCV may result in false-negative findings, the primers must be checked routinely by a Basic Local Alignment Search Tool (BLAST) search of GenBank for their fitness to detect new variants. If no highly conserved regions can be identified and problems related to genomic variation are anticipated, multiplex PCRs for different viral variants using more than one primer pair or next generation sequencing can be employed.

Recently, a new virus, PCV3, with significant differences in the sequence when compared with PCV1 and PCV2, but more related to a bat-faeces associated circovirus, was described in pigs with cardiac and multi-organ inflammation [74]. Since the pigs were co-infected with other porcine viruses, the pathogenicity of PCV3 warrants further investigations. PCV3 was found to be associated with porcine dermatitis and nephropathy syndrome (PDNS), reproductive failure, and multisystemic inflammation in China [75,76] and in the USA [77]. Sequence analysis showed that the Chinese isolates are the result of a recombination between bat circoviruses [76], and the closest relative of the U.S.A. isolate is a canine circovirus [77].

3. PCV2-Related Diseases in Pigs

PCVD was first detected in the early 1990s and has since then emerged as an economically important pig disease worldwide [61]. The main disease induced by PCV2 is PMWS [41,42]. However, PCV2 induces an entire complex of diseases now called PCVD in Europe or PCV-associated disease (PCVAD) in North America [33]. PCVD can be subdivided into PCV2-systemic disease (PCV2-SD, directly replacing PMWS), PCV2-subclinical infection (PCV2-SI), PCV2-reproductive disease (PCV2-RD), and PDNS. PCV2 is necessary but not sufficient for the induction of PCVD. Some purported risk factors include coinfection with other viruses. Porcine reproductive and respiratory syndrome virus (PRRSV) is one of these viruses, it causes the porcine reproductive and respiratory syndrome associated with reproductive failure in breeding stocks and respiratory tract illness in young pigs. Co-infection with porcine parvovirus may also contribute to PCVD as well as nonspecific immune stimulation (e.g., by vaccination).

Clinical signs of the disease include gradual wasting, fever, rough hair coat, dyspnea, pallor, diarrhea, and occasionally icterus. PCVD is characterized by lymphoid depletion, immunosuppression, and inflammation in affected organs. Morbidity varies from 2%–30%, but case fatality is high, approaching 80%. Occasionally, pigs may develop purple skin lesions and nephropathy, likely as an immune mediated sequel to viral infection, termed PDNS [78,79]. Occasionally reproductive failure is observed as abortions, stillbirths, and mummification (PCV2-RD) [62,80,81].

4. PCV Does Not Infect Immunocompetent Humans

When trying to infect human cell lines with PCV1 and PCV2, PCV1 persisted in most cell lines without causing any visible changes, while PCV2-transfected cells showed a cytopathogenic effect [82]. Most importantly, in both cases the infection was non-productive [82,83]. Infection with PCV1 was observed in human 293, HeLa, and Chang liver cells, whereas PCV2 infected only human Rd cells [82]. Although it is well known that, in addition to PCV2, outbreaks of PCVD in pigs require cofactors (e.g., PRRSV), co-infecting human cells with PCV2 and PRRSV was not yet performed. In addition to cell lines, primary human leukocytes could also be infected with PCV1, inducing severe morphological alterations in the infected cells [84], indicating that PCV1 may also be pathogenic.

When humans were screened for antibodies against PCV, in an early study, antibodies to PCV were found in 30% of samples from hospitalized patients with fever of unknown etiology [85]. These results are in striking contrast to those from another group that did not detect antibodies in serum samples from the general population and from veterinarians working with PCVD affected animals [61]. Additional studies are necessary to confirm the latter negative results.

A large "experiment" testing the susceptibility of the human population to PCV was involuntary conducted when two vaccines against rotaviral gastroenteritis from two different manufacturers

were found to be contaminated with PCV1 and PCV2 [86–88]. Both contaminated vaccines had been used world-wide for a number of years, preventing disease and saving millions of children's lives [89,90]. Over 10^5 or 10^6 particle-associated full-length PCV1 genomes were present in each dose of the contaminated vaccine [83,87–89], and cell culture assays in swine testis and PCV-free porcine kidney (PK-15) cells confirmed that PCV1 sequences in this vaccine represented infectious virus [86–88,91]. Another rotavirus vaccine contained only subgenomic PCV1 and PCV2 fragments, but no full-length PCV genomes, and cell culture assays did not amplify PCV from this vaccine [88]. When stool samples from children vaccinated with Rotarix, an oral live attenuated vaccine based on the human rotavirus RIX4414 produced by GlaxoSmithKline (London, UK), were analyzed, in 4 of 40 samples PCV1 DNA was detected [83]. PCV1 DNA was detected only soon after vaccination, indicating that viral replication did not occur in the gastrointestinal tract. Antibodies were not detected in the sera of vaccinated children, confirming that no replication of the virus had taken place. The pattern of adverse events reported in vaccinated infants with PCV1 in their stool did not differ from that observed in placebo recipients [83]. This correlated with the reports that the Rotarix vaccine in general had nearly no adverse events [89,90].

However—and this is the main question in the context of xenotransplantation—up until now it is still unknown whether PCV is zoonotic in severely immunosuppressed humans.

5. PCV2 and First Preclinical and Clinical Xenotransplantations

In all of the clinical xenotransplantation trials documented in Paradise et al. [92], no screening for PCV was performed in the Large White donor pigs and human recipients. Auckland Island pigs were used as source for the first clinical pig islet cell transplantation to human diabetic patients in New Zealand and Argentina [93–96]. These donor animals were free of PCV1 and PCV2, and therefore could not transmit circoviruses [94]. The sensitivity of the PCR used to detect PCV in Auckland Island pigs was estimated to be 10^6 mg of DNA per reaction [97]. Islet cells from Auckland Island pigs were also used in a prospective pig-to-primate islet xenotransplantation study, and as expected, no PCV was transmitted [98]. In most of the reported pig-to-non-human primate transplantations, no screening for PCV was performed, with the exception of a the just mentioned trial transplanting islet cells from Auckland Island pigs into cynomolgus monkeys [98]. In addition, pig donors for islet cell transplantation into mice had also been found to be PCV-negative [99]. Recently, islet cells from Large White/Yorkshire landrace F1 pigs were transplanted into non-immunosuppressed cynomolgus monkeys, and no PCV was detected in the recipients [100]. Testing was performed based on the presence of PCV in the source herd, although the donor pigs had been vaccinated with CircoFLEX (Table 1). PCV was not tested in the monthly herd screening and in the sentinel and pancreas donor post-mortem screening, the islet cells had been encapsulated in macrobeads.

Table 1. Protective vaccines against PCV2 [101,102].

Vaccine	Producer	Vaccine Based on
Circumvent PCV, Porcilis PCV, Circumvent G2 PCV	MSD/Merck Animal Health (Madison, New Jersey, United States)	PCV2a Cap protein expressed by baculovirus
Ingelvac CircoFLEX	Boehringer-Ingelheim (St. Joseph, Missouri, United States)	PCV2a Cap protein expressed by baculovirus
Fostera PCV, Suvaxyn PCV	Zoetis (Parsippany, New Jersey, United States)	Inactivated recombinant PCV1 expressing the PCV2a Cap protein (ORF2 from PCV2)
Circovac	Merial (Lyon France)	Inactivated whole PCV2a

ORF: Open reading frame.

In future preclinical, as well as clinical trials, donor pigs—and, if necessary, also recipients—should be screened for the presence of circoviruses. When PCV is not found in the donor pig, no screening of the recipients needs to be performed.

6. Treatment and Vaccination

There is no specific treatment for pigs with PCVD. Anti-inflammatory agents and antimicrobials may help to suppress co-factors and secondary diseases associated with PCVD. All in/all out pig flow, thorough cleaning, and rigid disinfection between batches of pigs are measures that can help control the disease [103]. In the case that the donor animal is PCV-infected, it may be considered to analyze whether the xenotransplantation product (e.g., isolated islet cells) is still negative. Since PCV2 is infecting macrophages, certainly all organs are infected and it will be safer to use only negative animals, especially since no effective antiviral treatment is available. PCV2 infection is associated with an immune response including neutralising antibodies, and these coincide with a decrease in serum virus load. Cell-mediated immunity has also been shown to be necessary to control PCV2 infection (for review see [102]). PCV2 vaccines became commercially available in the summer of 2006 (Table 1) [103]. The vaccines reduced the severity and incidence rate of PCVD on many farms. Vaccination against PCV2 did not only imply a direct beneficial effect on pig productivity, but also contributed to reduction of antimicrobial use [104]. PCV2 vaccines effectively increased average daily weight gain (ADWG) and prevented diseases with a positive result for meat production. In all vaccination trials a lower virus load was registered in the vaccinated animals, however, it remains unclear whether the virus load is reduced to zero. In most reported cases, virus transmission took place despite vaccination [102,105–107]. In a study vaccinating 28 pigs, the virus load was not reduced to zero in any of the animals [108]. In another study, 17 of 32 vaccinated animals still showed PCV in the serum, as measured by PCR [90]. PCV2 vaccination of sows was associated with high antibody responses, but did not prevent fetal infections *in utero* or soon after birth by infectious colostrum in 29 of 100 cases [107]. When comparing four different vaccines, use of the inactivated chimeric vaccines (Fostera PCV and Circovax) resulted in significantly lower viremia compared with use of the subunit vaccines (Circoflex, Porcilis PCV), however, histopathological lesions and PCV antigens were still detected in all 80 immunized animals [109]. Successful vaccination is mainly associated with induction of neutralizing antibodies, but T cell-mediated immunity also plays a role in the reduction of the virus load and prevention of diseases as mentioned above [102,110].

Since new PCV2 variants have emerged, the question of whether or not current vaccines can protect against new PCV2 variants that may be more virulent for pigs becomes a serious concern. Although it is still unclear whether the global switch from PCV2a to PCV2b and PCV2d was associated with higher fitness of PCV2, as reported [68,69], rather than vaccine induced selection pressure, the emergence and rapid spread of new PCV2 variants provide evidence that current vaccines need to be updated.

7. How to Eliminate PCV

For a safe xenotransplantation, elimination programs have been proposed for porcine viruses such as HEV [17], PCMV [111], porcine lymphotropic herpesviruses, and others [112], by isolation of virus-free animals, treatment, and vaccination. Elimination programs in the case of circoviruses should be based on (i) selection of animals found non-infected using highly sensitive detection methods to avoid false-negative testing; (ii) vaccination or other strategies (see below), since treatment is not available; and (iii) isolation of virus-negative animals to prevent de novo infection. Elimination means elimination from the herd, elimination from a single individual is impossible, since there is no treatment presently available. The efficacy of the vaccines should be improved and new vaccines against emerging variant virus strains should be developed. Since PCV2 is easily transmitted through the placenta and since colostrum was shown to be infectious, Cesarean section, and colostrum derivation are two promising strategies to eliminate PCV [80,106,107,113]. Recent findings of PCV2 in Göttingen

Minipigs [114], which were introduced into the facility by Cesarean delivery and are produced under specified pathogen-free breeding conditions that are very similar to designated pathogen-free breeding conditions [115], confirm transmission through the placenta and indicate that selection of PCV2-free animals may be difficult. However, when 384 embryos recovered from PCV2 infected pigs 10 days after inoculation were transferred to seronegative donors, no infection of the recipient pig and the piglets was observed, indicating that embryo transfer can be successfully used for the elimination of PCV2 [116].

8. Summary

PCV2 is a very small virus, it is stable and resistant to some disinfectants, pH, and heat, and it induces severe diseases in infected pigs. PCV2 is an immunosuppressive virus and it is still unclear whether subclinical infections of pigs may decrease the functionality of the organs required for transplantation. Vaccination against PCV2 is able to prevent diseases, but in most cases is unable to prevent the transmission of the virus. Although PCV2 infects human cells and induces a cytopathic effect in vitro, no pathogenic effects were observed when PCV was transmitted by contaminated vaccines to children. It remains unknown whether PCV may infect severely immunosuppressed individuals. In conclusion, for all of these reasons, sensitive detection methods should be used to screen for the virus and improved vaccination, Cesarean delivery, colostrum deprivation, and embryo transfer should be used to prevent transmission of the virus.

Acknowledgments: This study was supported in part by a grant from the German Research Foundation (Deutsche Forschungsgemeinschaft), TRR 127, to J.D.

Author Contributions: Both of the authors reviewed the literature and wrote the manuscript.

Conflicts of Interest: The authors declare no conflict of interest.

References

1. Fishman, J.A. Infection in solid-organ transplant recipients. *N. Engl. J. Med.* **2007**, *357*, 2601–2614. [CrossRef] [PubMed]
2. Romero, F.A.; Razonable, R.R. Infections in liver transplant recipients. *World J. Hepatol.* **2011**, *3*, 83–92. [CrossRef] [PubMed]
3. Kim, S. Bacterial infection after liver transplantation. *World J. Gastroenterol.* **2014**, *20*, 6211–6220. [CrossRef] [PubMed]
4. Petrosillo, N.; Puro, V.; D'Anna, C.; Marquez, J.R.; Ippolito, G. HIV infection after kidney transplantation. *Nephron* **1996**, *72*, 124. [CrossRef] [PubMed]
5. Vora, N.M.; Basavaraju, S.V.; Feldman, K.A.; Paddock, C.D.; Orciari, L.; Gitterman, S.; Griese, S.; Wallace, R.M.; Said, M.; Blau, D.M.; et al. Raccoon rabies virus variant transmission through solid organ transplantation. *JAMA* **2013**, *310*, 398–407. [CrossRef] [PubMed]
6. Maier, T.; Schwarting, A.; Mauer, D.; Ross, R.S.; Martens, A.; Kliem, V.; Wahl, J.; Panning, M.; Baumgarte, S.; Müller, T.; et al. Management and outcomes after multiple corneal and solid organ transplantations from a donor infected with rabies virus. *Clin. Infect. Dis.* **2010**, *50*, 1112–1119. [CrossRef] [PubMed]
7. Srinivasan, A.; Burton, E.C.; Kuehnert, M.J.; Rupprecht, C.; Sutker, W.L.; Ksiazek, T.G.; Paddock, C.D.; Guarner, J.; Shieh, W.J.; Goldsmith, C.; et al. Transmission of rabies virus from an organ donor to four transplant recipients. *N. Engl. J. Med.* **2005**, *352*, 1103–1111. [CrossRef] [PubMed]
8. Ramanan, P.; Razonable, R.R. Cytomegalovirus infections in solid organ transplantation: A review. *Infect. Chemother.* **2013**, *45*, 260–271. [CrossRef] [PubMed]
9. Razonable, R.R. Cytomegalovirus infection after liver transplantation: Current concepts and challenges. *World J. Gastroenterol.* **2008**, *14*, 4849–4860. [CrossRef] [PubMed]
10. Lischka, P.; Zimmermann, H. Antiviral strategies to combat cytomegalovirus infections in transplant recipients. *Curr. Opin. Pharmacol.* **2008**, *8*, 541–548. [CrossRef] [PubMed]
11. Fishman, J.A. Assessment of infectious risk in clinical xenotransplantation: The lessons for clinical allotransplantation. *Xenotransplantation* **2014**, *21*, 307–308. [CrossRef] [PubMed]

12. Yamada, K.; Tasaki, M.; Sekijima, M.; Wilkinson, R.A.; Villani, V.; Morgan, S.G.; Cormack, T.A.; Hanekamp, I.M.; Hawley, R.J.; Arn, J.S.; et al. Porcine cytomegalovirus infection is associated with early rejection of kidney grafts in a pig to baboon xenotransplantation model. *Transplantation* **2014**, *98*, 411–418. [CrossRef] [PubMed]
13. Sekijima, M.; Waki, S.; Sahara, H.; Tasaki, M.; Wilkinson, R.A.; Villani, V.; Shimatsu, Y.; Nakano, K.; Matsunari, H.; Nagashima, H.; et al. Result of life-supporting galactosyltransferase knockout swine. *Transplantation* **2014**, *98*, 419–426. [CrossRef] [PubMed]
14. Morozov, V.A.; Abicht, J.M.; Reichart, B.; Mayr, T.; Guethoff, S.; Denner, J. Active replication of porcine cytomegalovirus (PSMV) following transplantation of a pig heart into a baboon despite undetected virus in the donor pig. *Ann. Virol. Res.* **2016**, *2*, 1018.
15. Morozov, V.A.; Plotzki, E.; Rotem, A.; Barkai, U.; Denner, J. Extended microbiologicial characterization of Göttingen minipigs: Porcine cytomegalovirus and other viruses. *Xenotransplantation* **2016**, *24*, 34–40.
16. Harding, J.C.; Baker, C.; Rhodes, C.; McIntosh, K.A.; Bonneau, M. Ring tests to evaluate the performance of porcine circovirus-2 (PCV-2) polymerase chain reaction (PCR) assays used in North American diagnostic laboratories. *Can. J. Vet. Res.* **2009**, *73*, 7–14. [PubMed]
17. Denner, J. Xenotransplantation and hepatitis E virus. *Xenotransplantation* **2015**, *22*, 167–173. [CrossRef] [PubMed]
18. Finsterbusch, T.; Mankertz, A. Porcine circoviruses—Small but powerful. *Virus Res.* **2009**, *143*, 177–183. [CrossRef] [PubMed]
19. Tischer, I.; Rasch, R.; Tochtermann, G. Characterization of papovavirus-and picornavirus-like particles in permanent pig kidney cell lines. *Zentralbl. Bakteriol. Orig. A.* **1974**, *226*, 153–167. [PubMed]
20. Lima, F.E.; Cibulski, S.P.; Dall Bello, A.G.; Mayer, F.Q.; Witt, A.A.; Roehe, P.M.; d'Azevedo, P.A. A novel chiropteran circovirus genome recovered from a Brazilian insectivorous bat species. *Genome Announc.* **2015**, *3*, e01393-15. [CrossRef] [PubMed]
21. Han, H.J.; Wen, H.L.; Zhao, L..; Liu, J.W.; Luo, L.M.; Zhou, C.M.; Qin, X.R.; Zhu, Y.L.; Liu, M.M.; Qi, R.; et al. Novel coronaviruses; astroviruses; adenoviruses and circoviruses in insectivorous bats from northern China. *Zoonoses Public Health* **2017**. [CrossRef]
22. Kapoor, A.; Dubovi, E.J.; Henriquez-Rivera, J.A.; Lipkin, W.I. Complete genome sequence of the first canine circovirus. *J. Virol.* **2012**, *86*, 7018. [CrossRef] [PubMed]
23. Zaccaria, G.; Malatesta, D.; Scipioni, G.; Di Felice, E.; Campolo, M.; Casaccia, C.; Savini, G.; Di Sabatino, D.; Lorusso, A. Circovirus in domestic and wild carnivores: An important opportunistic agent? *Virology* **2016**, *490*, 69–74. [CrossRef] [PubMed]
24. Thaiwong, T.; Wise, A.G.; Maes, R.K.; Mullaney, T.; Kiupel, M. Canine circovirus 1 (CaCV-1) and canine parvovirus 2 (CPV-2): Recurrent dual Infections in a Papillon breeding colony. *Vet. Pathol.* **2016**, *53*, 1204–1209. [CrossRef] [PubMed]
25. Anderson, A.; Hartmann, K.; Leutenegger, C.M.; Proksch, A.L.; Mueller, R.S.; Unterer, S. Role of canine circovirus in dogs with acute haemorrhagic diarrhoea. *Vet. Rec.* **2017**. [CrossRef] [PubMed]
26. Lian, H.; Liu, Y.; Li, N.; Wang, Y.; Zhang, S.; Hu, R. Novel circovirus from mink; China. *Emerg. Infect. Dis.* **2014**, *20*, 1548–1550. [CrossRef] [PubMed]
27. Wang, G.S.; Sun, N.; Tian, F.L.; Wen, Y.J.; Xu, C.; Li, J.; Chen, Q.; Wang, J.B. Genetic analysis of porcine circovirus type 2 from dead minks. *J. Gen. Virol.* **2016**, *97*, 2316–2322. [CrossRef] [PubMed]
28. Patterson, A.R.; Opriessnig, T. Epidemiology and horizontal transmission of porcine circovirus type 2 (PCV2). *Anim. Health Res. Rev.* **2010**, *11*, 217–234. [CrossRef] [PubMed]
29. Finsterbusch, T.; Steinfeldt, T.; Doberstein, K.; Rödner, C.; Mankertz, A. Interaction of the replication proteins and the capsid protein of porcine circovirus type 1 and 2 with host proteins. *Virology* **2009**, *386*, 122–131. [CrossRef] [PubMed]
30. Lv, Q.; Guo, K.; Wang, T.; Zhang, C.; Zhang, Y. Porcine circovirus type 2 ORF4 protein binds heavy chain ferritin. *J. Biosci.* **2015**, *40*, 477–485. [CrossRef] [PubMed]
31. Lv, Q.; Guo, K.; Xu, H.; Wang, T.; Zhang, Y. Identification of putative ORF5 protein of porcine circovirus type 2 and functional analysis of GFP-fused ORF5 protein. *PLoS ONE* **2015**, *10*, e0127859.
32. Allan, G.M.; McNeilly, F.; Foster, J.C.; Adair, B.M. Infection of leucocyte cell cultures derived from different species with pig circovirus. *Vet. Microbiol.* **1994**, *41*, 267–279. [CrossRef]

33. Sanchez, R.E., Jr.; Meerts, P.; Nauwynck, H.J.; Pensaert, M.B. Change of porcine circovirus 2 target cells in pigs during development from fetal to early postnatal life. *Vet. Microbiol.* **2003**, *95*, 15–25. [CrossRef]
34. Meerts, P.; Misinzo, G.; McNeilly, F.; Nauwynck, H.J. Replication kinetics of different porcine circovirus 2 strains in PK-15 cells, fetal cardiomyocytes and macrophages. *Arch. Virol.* **2005**, *150*, 427–441. [CrossRef] [PubMed]
35. Darwich, L.; Segales, J.; Mateu, E. Pathogenesis of postweaning multisystemic wasting syndrome caused by porcine circovirus 2: An immune riddle. *Arch. Virol.* **2004**, *149*, 857–874. [CrossRef] [PubMed]
36. Jolly, C.L.; Sattentau, Q.J. Attachment factors. *Adv. Exp. Med. Biol.* **2013**, *790*, 1–23. [PubMed]
37. Misinzo, G.; Delputte, P.L.; Meerts, P.; Lefebvre, D.J.; Nauwynck, H.J. Porcine circovirus 2 uses heparan sulfate and chondroitin sulfate B glycosaminoglycans as receptors for its attachment to host cells. *J. Virol.* **2006**, *80*, 3487–3494. [CrossRef] [PubMed]
38. Meng, X.-J. Porcine circovirus type 2 (PCV2): Pathogenesis and interaction with the immune system. *Annu. Rev. Anim. Biosci.* **2013**, *1*, 43–64. [CrossRef] [PubMed]
39. Segalés, J.; Mateu, E. Immunosuppression as a feature of postweaning multisystemic wasting syndrome. *Vet. J.* **2006**, *171*, 396–397. [CrossRef] [PubMed]
40. Gillespie, J.; Opriessnig, T.; Meng, X.J.; Pelzer, K.; Buechner-Maxwell, V. Porcine circovirus type 2 and porcine circovirus-associated disease. *J. Vet. Intern. Med.* **2009**, *23*, 1151–1163. [CrossRef] [PubMed]
41. Segalés, J.; Allan, G.M.; Domingo, M. Porcine circovirus diseases. *Anim. Health Res. Rev.* **2005**, *6*, 119–142. [CrossRef] [PubMed]
42. Opriessnig, T.; Langohr, I. Current state of knowledge on porcine circovirus type 2-associated lesions. *Vet. Pathol.* **2013**, *50*, 23–38. [CrossRef] [PubMed]
43. Opriessnig, T.; Meng, X.J.; Halbur, P.G. Porcine circovirus type 2 associated disease: Update on current terminology, clinical manifestations, pathogenesis, diagnosis, and intervention strategies. *J. Vet. Diagn. Investig.* **2007**, *19*, 591–615. [CrossRef] [PubMed]
44. Denner, J. Sensitive methods and improved screening strategies are needed for the detection of pig viruses. *Xenotransplantation*. in press.
45. Quintana, J.; Segalés, J.; Calsamiglia, M.; Domingo, M. Detection of porcine circovirus type 1 in commercial pig vaccines using polymerase chain reaction. *Vet. J.* **2006**, *171*, 570–573. [CrossRef] [PubMed]
46. Segalés, J.; Calsamiglia, M.; Olvera, A.; Sibila, M.; Badiella, L.; Domingo, M. Quantification of porcine circovirus type 2 (PCV2) DNA in serum and tonsillar, nasal, tracheo-bronchial, urinary and faecal swabs of pigs with and without postweaning multisystemic wasting syndrome (PMWS). *Vet. Microbiol.* **2005**, *111*, 223–229. [CrossRef] [PubMed]
47. Mankertz, A.; Domingo, M.; Folch, J.M.; LeCann, P.; Jestin, A.; Segalés, J.; Chmielewicz, B.; Plana-Durán, J.; Soike, D. Characterisation of PCV-2 isolates from Spain, Germany and France. *Virus Res.* **2000**, *66*, 65–77. [CrossRef]
48. Wang, J.; Wang, J.; Liu, L.; Li, R.; Yuan, W. Rapid detection of Porcine circovirus 2 by recombinase polymerase amplification. *J. Vet. Diagn. Investig.* **2016**, *28*, 574–578. [CrossRef] [PubMed]
49. Zhao, S.; Lin, H.; Chen, S.; Yang, M.; Yan, Q.; Wen, C.; Hao, Z.; Yan, Y.; Sun, Y.; Hu, J.; et al. Sensitive detection of Porcine circovirus-2 by droplet digital polymerase chain reaction. *J. Vet. Diagn. Investig.* **2015**, *27*, 784–788. [CrossRef] [PubMed]
50. Wang, C.; Pang, V.F.; Lee, F.; Liao, P.C.; Huang, Y.L.; Lin, Y.L.; Lai, S.S.; Jeng, C.R. Development and evaluation of a loop-mediated isothermal amplification method for rapid detection and differentiation of two genotypes of porcine circovirus type 2. *J. Microbiol. Immunol. Infect.* **2014**, *47*, 363–370. [CrossRef] [PubMed]
51. Pérez, L.J.; Perera, C.L.; Frías, M.T.; Núñez, J.I.; Ganges, L.; de Arce, H.D. A multiple SYBR Green I-based real-time PCR system for the simultaneous detection of porcine circovirus type 2; porcine parvovirus; pseudorabies virus and Torque teno sus virus 1 and 2 in pigs. *J. Virol. Methods.* **2012**, *179*, 233–241. [CrossRef] [PubMed]
52. Blomström, A.L.; Belák, S.; Fossum, C.; Fuxler, L.; Wallgren, P.; Berg, M. Studies of porcine circovirus type 2; porcine boca-like virus and torque teno virus indicate the presence of multiple viral infections in postweaning multisystemic wasting syndrome pigs. *Virus Res.* **2010**, *152*, 59–64. [CrossRef] [PubMed]
53. Blanchard, P.; Mahé, D.; Cariolet, R.; Truong, C.; Le Dimna, M.; Arnauld, C.; Rose, N.; Eveno, E.; Albina, E.; Madec, F.; et al. An ORF2 protein-based ELISA for porcine circovirus type 2 antibodies in post-weaning multisystemic wasting syndrome. *Vet. Microbiol.* **2003**, *94*, 183–194. [CrossRef]

54. Liu, Q.; Wang, L.; Willson, P.; O'Connor, B.; Keenliside, J.; Chirino-Trejo, M.; Babiuk, L. Seroprevalence of porcine circovirus type 2 in swine populations in Canada and Costa Rica. *Can. J. Vet. Res.* **2002**, *66*, 225–231. [PubMed]
55. Patterson, A.R.; Johnson, J.; Ramamoorthy, S.; Ramamoorthy, S.; Meng, X.J.; Halbur, P.G.; Opriessnig, T. Comparison of three enzyme-linked immunosorbent assays to detect porcine circovirus-2 (PCV-2)-specific antibodies after vaccination or inoculation of pigs with distinct PCV-1 or PCV-2 isolates. *J. Vet. Diagn. Investig.* **2008**, *20*, 744–751. [CrossRef] [PubMed]
56. Mahé, D.; Blanchard, P.; Truong, C.; Arnauld, C.; Le Cann, P.; Cariolet, R.; Madec, F.; Albina, E.; Jestin, A. Differential recognition of ORF2 protein from type 1 and type 2 porcine circoviruses and identification of immunorelevant epitopes. *J. Gen. Virol.* **2000**, *81*, 1815–1824. [CrossRef] [PubMed]
57. Nawagitgul, P.; Harms, P.A.; Morozov, I.; Thacker, B.J.; Sorden, S.D.; Lekcharoensuk, C.; Paul, P.S. Modified indirect porcine circovirus (PCV) type 2-based and recombinant capsid protein (ORF2)-based enzyme-linked immunosorbent assays for detection of antibodies to PCV. *Clin. Diagn. Lab. Immunol.* **2002**, *9*, 33–40. [CrossRef] [PubMed]
58. Patterson, A.R.; Johnson, J.K.; Ramamoorthy, S.; Patterson, A.R.; Johnson, J.K.; Ramamoorthy, S.; Hesse, R.A.; Murtaugh, M.P.; Puvanendiran, S.; Meng, X.J. Interlaboratory comparison of porcine circovirus-2 indirect immunofluorescent antibody test and enzyme-linked immunosorbent assay results on experimentally infected pigs. *J. Vet. Diagn. Investig.* **2011**, *23*, 206–212. [CrossRef] [PubMed]
59. Ramirez, A.; Wang, C.; Prickett, J.R.; Pogranichniy, R.; Yoon, K.J.; Main, R.; Kurtz, A. Efficient surveillance of pig populations using oral fluids. *Prev. Vet. Med.* **2012**, *104*, 292–300. [CrossRef] [PubMed]
60. Allan, G.M.; Ellis, J.A. Porcine circoviruses: A review. *J. Vet. Diagn. Investig.* **2000**, *12*, 3–14. [CrossRef] [PubMed]
61. Patterson, A.R.; Madson, D.M.; Halbur, P.G.; Opriessnig, T. Shedding and infection dynamics of porcine circovirus type 2 (PCV2) after natural exposure. *Vet. Microbiol.* **2011**, *149*, 225–229. [CrossRef] [PubMed]
62. Patterson, A.R.; Ramamoorthy, S.; Madson, D.M.; Meng, X.J.; Halbur, P.G.; Opriessnig, T. Shedding and infection dynamics of porcine circovirus type 2 (PCV2) after experimental infection. *Vet. Microbiol.* **2011**, *149*, 91–98. [CrossRef] [PubMed]
63. Lang, Ch.; Griessler, A.; Pirker, E.; Söllner, H.; Segalés, J.; Kekarainen, T.; Ritzmann, M. Detection of porcine circovirus type 2 and Torque-teno-sus-virus 1 and 2 in semen samples of boars from an Austrian artificial insemination centre. *Tierarztl. Prax. Ausg. G. Grosstiere Nutztiere* **2011**, *39*, 201–204. [PubMed]
64. Grasland, B.; Blanchard, P.; Kéranflech, A.; Bigault, L.; Oger, A.; Rose, N.; Madec, F.; Jestin, A.; Cariolet, R. Evaluation of the transmission of porcine circovirus type 2 (PCV-2) genogroups a and b with semen from infected specific-pathogen-free boars. *Vet. Microbiol.* **2013**, *162*, 381–387. [CrossRef] [PubMed]
65. Zhai, S.L.; Chen, S.N.; Zhang, J.W.; Wei, Z.Z.; Long, J.X.; Yuan, S.S.; Wei, W.K.; Chen, Q.L.; Wu, H.X.; Wu, D.C. Dissection of the possible routes on porcine circoviruses infecting human. *J. Anim. Veterin. Adv.* **2012**, *11*, 1281–1286.
66. Larochelle, R.; Magar, S.; D'Allaire, S. Genetic characterization and phylogenetic analysis of porcine circovirus type 2 (PCV2) strains from cases presenting various clinical conditions. *Virus Res.* **2002**, *90*, 101–112. [CrossRef]
67. Firth, C.; Charleston, M.A.; Duffy, S.; Shapiro, B.; Holmes, E.C. Insights into the evolutionary history of an emerging livestock pathogen: Porcine circovirus 2. *J. Virol.* **2009**, *83*, 12813–12821. [CrossRef] [PubMed]
68. Segalés, J.; Olvera, A.; Grau-Roma, L.; Charreyre, C.; Nauwynck, H.; Larsen, L.; Dupont, K.; McCullough, K.; Ellis, J.; Krakowka, S.; et al. PCV-2 genotype definition and nomenclature. *Vet. Rec.* **2008**, *162*, 867–868. [CrossRef] [PubMed]
69. Rose, N.; Opriessnig, T.; Grasland, B.; Jestin, A. Epidemiology and transmission of porcine circovirus type 2 (PCV2). *Virus Res.* **2012**, *164*, 78–89. [CrossRef] [PubMed]
70. Xiao, C.T.; Halbur, P.G.; Opriessnig, T. Global molecular genetic analysis of porcine circovirus type 2 (PCV2) sequences confirms the presence of four main PCV2 genotypes and reveals a rapid increase of PCV2d. *J. Gen. Virol.* **2015**, *96*, 1830–1841. [CrossRef] [PubMed]
71. Ssemadaali, M.A.; Ilha, M.; Ramamoorthy, S. Genetic diversity of porcine circovirus type 2 and implications for detection and control. *Res. Vet. Sci.* **2015**, *103*, 179–186. [CrossRef] [PubMed]

72. Hu, J.; Zhai, S.L.; Zeng, S.Y.; Sun, B.B.; Deng, S.F.; Chen, H.L.; Zheng, Y.; Wang, H.X.; Li, X.P.; Liu, J.K.; et al. Identification of natural recombinants derived from PCV2a and PCV2b. *Genet. Mol. Res.* **2015**, *14*, 11780–11790. [CrossRef] [PubMed]
73. Gagnon, C.A.; Music, N.; Fontaine, G.; Tremblay, D.; Harel, J. Emergence of a new type of porcine circovirus in swine (PCV): A type 1 and type 2 PCV recombinant. *Vet. Microbiol.* **2010**, *144*, 18–23. [CrossRef] [PubMed]
74. Phan, G.T.; Giannitti, F.; Rossow, S.; Marthaler, D.; Knutson, T.; Linlin, L.; Deng, X.; Resende, T.; Vannucci, F.; Delwart, E. Detection of a novel circovirus PCV3 in pigs with cardiac and multi-systemic inflammation. *Virol. J.* **2016**, *13*, 184. [CrossRef] [PubMed]
75. Shen, H.; Liu, X.; Zhang, P.; Wang, L.; Liu, Y.; Zhang, L.; Liang, P.; Song, C. Genome characterization of a porcine circovirus type 3 in South China. *Transbound. Emerg. Dis.* **2017**. [CrossRef] [PubMed]
76. Ku, X.; Chen, F.; Li, P.; Wang, Y.; Yu, X.; Fan, S.; Qian, P.; Wu, M.; He, Q. Identification and genetic characterization of porcine circovirus type 3 in China. *Transbound. Emerg. Dis.* **2017**. [CrossRef] [PubMed]
77. Palinski, R.; Piñeyro, P.; Shang, P.; Yuan, F.; Guo, R.; Fang, Y.; Byers, E.; Hause, B.M. A Novel porcine circovirus distantly related to known circoviruses is associated with porcine dermatitis and nephropathy syndrome and reproductive failure. *J. Virol.* **2016**, *91*, e01879-16. [CrossRef] [PubMed]
78. Meehan, B.M.; McNeilly, F.; McNair, I.; Walker, I.; Ellis, J.A.; Krakowka, S.; Allan, G.M. Isolation and characterization of porcine circovirus 2 from cases of sow abortion and porcine dermatitis and nephropathy syndrome. *Arch. Virol.* **2001**, *146*, 835–842. [CrossRef] [PubMed]
79. Rosell, C.; Segalés, J.; Ramos-Vara, J.A.; Folch, J.M.; Rodríguez-Arrioja, G.M.; Duran, C.O.; Balasch, M.; Plana-Durán, J.; Domingo, M. Identification of porcine circovirus in tissues of pigs with porcine dermatitis and nephropathy syndrome. *Vet. Rec.* **2000**, *146*, 40–43. [CrossRef] [PubMed]
80. Ladekjaer-Mikkelsen, A.S.; Nielsen, J.; Storgaard, T.; Bøtner, A.; Allan, G.; McNeilly, F. Transplacental infection with PCV-2 associated with reproductive failure in a gilt. *Vet. Rec.* **2001**, *148*, 759–760. [PubMed]
81. West, K.H.; Bystrom, J.M.; Wojnarowicz, C.; Bøtner, A.; Allan, G.; McNeilly, F. Myocarditis and abortion associated with intrauterine infection of sows with porcine circovirus 2. *J. Vet. Diagn. Investig.* **1999**, *11*, 530–532. [CrossRef] [PubMed]
82. Hattermann, K.; Roedner, C.; Schmitt, C.; Finsterbusch, T.; Steinfeldt, T.; Mankertz, A. Infection studies on human cell lines with porcine circovirus type 1 and porcine circovirus type 2. *Xenotransplantation* **2004**, *11*, 284–294. [CrossRef] [PubMed]
83. Dubin, G.; Toussaint, J.F.; Cassart, J.P.; Howe, B.; Boyce, D.; Friedland, L.; Abu-Elyazeed, R.; Poncelet, S.; Han, H.H.; Debrus, S. Investigation of a regulatory agency enquiry into potential porcine circovirus type 1 contamination of the human rotavirus vaccine, Rotarix: Approach and outcome. *Hum. Vaccin Immunother.* **2013**, *9*, 2398–2408. [CrossRef] [PubMed]
84. Arteaga-Troncoso, G.; Guerra-Infante, F.; Rosales-Montano, L.M.; Diaz-Garcia, F.J.; Flores-Medina, S. Ultrastructural alterations in human blood leukocytes induced by porcine circovirus type 1 infection. *Xenotransplantation* **2005**, *12*, 465–472. [CrossRef] [PubMed]
85. Tischer, I.; Bode, L.; Apodaca, J.; Timm, H.; Peters, D.; Rasch, R.; Pociuli, S.; Gerike, E. Presence of antibodies reacting with porcine circovirus in sera of humans, mice, and cattle. *Arch. Virol.* **1995**, *140*, 1427–1439. [CrossRef] [PubMed]
86. Victoria, J.G.; Wang, C.; Jones, M.S.; Victoria, J.G.; Wang, C.; Jones, M.S.; Jaing, C.; McLoughlin, K.; Gardner, S.; Delwart, E.L. Viral nucleic acids in live-attenuated vaccines: Detection of minority variants and an adventitious virus. *J. Virol.* **2010**, *84*, 6033–6040. [CrossRef] [PubMed]
87. Gilliland, S.M.; Forrest, L.; Carre, H.; Jenkins, A.; Berry, N.; Martin, J.; Minor, P.; Schepelmann, S. Investigation of porcine circovirus contamination in human vaccines. *Biologicals* **2012**, *40*, 270–277. [CrossRef] [PubMed]
88. McClenahan, S.D.; Krause, P.R.; Uhlenhaut, C. Molecular and infectivity studies of porcine circovirus in vaccines. *Vaccine* **2011**, *29*, 4745–4753. [CrossRef] [PubMed]
89. Ruiz-Palacios, G.M.; Pérez-Schael, I.; Velázquez, F.R.; Abate, H.; Breuer, T.; Clemens, S.C.; Cheuvart, B.; Espinoza, F.; Gillard, P.; Innis, B.L.; et al. Human Rotavirus Vaccine Study Group. Safety and efficacy of an attenuated vaccine against severe rotavirus gastroenteritis. *N. Engl. J. Med.* **2006**, *354*, 11–22. [CrossRef] [PubMed]

90. Vesikari, T.; Clark, H.F.; Offit, P.A.; Dallas, M.J.; DiStefano, D.J.; Goveia, M.G.; Ward, R.L.; Schödel, F.; Karvonen, A.; Drummond, J.E.; et al. Effects of the potency and composition of the multivalent human-bovine (WC3) reassortant rotavirus vaccine on efficacy, safety and immunogenicity in healthy infants. *Vaccine* **2006**, *24*, 4821–4829. [CrossRef] [PubMed]
91. Baylis, S.A.; Finsterbusch, T.; Bannert, N.; Blümel, J.; Mankertz, A. Analysis of porcine circovirus type 1 detected in Rotarix vaccine. *Vaccine* **2011**, *29*, 690–697. [CrossRef] [PubMed]
92. Paradis, K.; Langford, G.; Long, Z.; Heneine, W.; Sandstrom, P.; Switzer, W.M.; Chapman, L.E.; Lockey, C.; Onions, D. Otto ESearch for cross-species transmission of porcine endogenous retrovirus in patients treated with living pig tissue. The XEN 111 Study Group. *Science* **1999**, *285*, 1236–1241. [CrossRef] [PubMed]
93. Matsumoto, S.; Abalovich, A.; Wechsler, C.J.; Wynyard, S.; Elliott, R.B. Clinical Benefit of Islet Xenotransplantation for the Treatment of Type 1. *EBio Med.* **2016**, *12*, 255–262. [CrossRef] [PubMed]
94. Wynyard, S.; Nathu, D.; Garkavenko, O.; Denner, J.; Elliott, R.B. Microbiological safety of the first clinical pig islet xenotransplantation trial in New Zealand. *Xenotransplantation* **2014**, *21*, 309–323. [CrossRef] [PubMed]
95. Cooper, D.K.; Matsumoto, S.; Abalovich, A.; Itoh, T.; Mourad, N.I.; Gianello, P.R.; Wolf, E.; Cozzi, E. Progress in clinical encapsulated islet xenotransplantation. *Transplantation* **2016**, *100*, 2301–2308. [CrossRef] [PubMed]
96. Morozov, A.V.; Wynyard, S.; Matsumoto, S.; Abalovich, A.; Denner, J.; Elliott, R.B. No PERV transmission during a clinical trial of pig islet cell transplantation. *Virus Res.* **2016**, *227*, 34–40. [CrossRef] [PubMed]
97. Muzina, M.; Muzina, Z.; Powels, K.; Elliot, R.B.; Croxson, M.C. Monitoring for potentially xenozoonotic virus in New Zealand pigs. *J. Med. Virol.* **2004**, *72*, 338–344.
98. Garkavenko, O.; Dieckhoff, B.; Wynyard, S.; Denner, J.; Elliot, R.B.; Tan, P.L.; Croxson, M.C. Absence of transmission of potentially xenotic viruses in a prospective pig to primate islet xenotransplantation study. *J. Med. Virol.* **2008**, *80*, 2046–2052. [CrossRef] [PubMed]
99. Jin, S.M.; Shin, J.S.; Kim, K.S.; Gong, C.H.; Park, S.K.; Kim, J.S.; Yeom, S.C.; Hwang, E.S.; Lee, C.T.; Kim, S.J.; et al. Islet isolation from adult designated pathogen-free pigs: Use of the newer bovine nervous tissue-free enzymes and a revised donor selection strategy would improve the islet graft function. *Xenotransplantation* **2011**, *18*, 369–379. [CrossRef] [PubMed]
100. Gazda, L.S.; Collins, J.; Lovatt, A.; Holdcraft, R.W.; Morin, M.J.; Galbraith, D.; Graham, M.; Laramore, M.A.; Maclean, C.; Black, J.; et al. A comprehensive microbiological safety approach for agarose encapsulated porcine islets intended for clinical trials. *Xenotransplantation* **2016**, *23*, 444–463. [CrossRef] [PubMed]
101. Beach, N.M.; Meng, X.J. Efficacy and future prospects of commercially available and experimental vaccines against porcine circovirus type 2 (PCV2). *Virus Res.* **2012**, *164*, 33–42. [CrossRef] [PubMed]
102. Segalés, J. Best practice and future challenges for vaccination against porcine circovirus type 2. *Expert Rev. Vaccines* **2015**, *14*, 473–487. [CrossRef] [PubMed]
103. Madec, F.; Rose, N.; Grasland, B.; Cariolet, R.; Jestin, A. Post-weaning multisystemic wasting syndrome and other PCV2-related problems in pigs: A 12-year experience. *Transbound Emerg. Dis.* **2008**, *55*, 273–283. [CrossRef] [PubMed]
104. Glass, F. PCV2 vaccination changing the pig industry. Part 3. Reduced antibiotic usage and improved performance go together. *Pig Progr.* **2010**, *26*, 28–30.
105. Fort, M.; Sibila, M.; Allepuz, A.; Mateu, E.; Roerink, F.; Segalés, J. Porcine circovirus type 2 (PCV2) vaccination of conventional pigs prevents viremia against PCV2 isolates of different genotypes and geographic origins. *Vaccine* **2008**, *26*, 1063–1071. [CrossRef] [PubMed]
106. Madson, D.M.; Patterson, A.R.; Ramamoorthy, S.; Pal, N.; Meng, X.J.; Opriessnig, T. Effect of porcine circovirus type 2 (PCV2) vaccination of the dam on PCV2 replication in utero. *Clin. Vaccine Immunol.* **2009**, *16*, 830–834. [CrossRef] [PubMed]
107. Gerber, P.F.; Garrocho, F.M.; Lana, A.M.Q.; Lobato, Z.I.P. Fetal infections and antibody profiles in pigs naturally infected with porcine circovirus type 2 (PCV2). *Can. J. Vet. Res.* **2012**, *76*, 38–44. [PubMed]
108. O'Neill, K.C.; Shen, H.G.; Lin, K.; Hemann, M.; Beach, N.M.; Meng, X.J.; Halbur, PG.; Opriessnig, T. Studies on porcine circovirus type 2 vaccination of 5-day-old piglets. *Clin. Vaccine Immunol.* **2011**, *18*, 1865–1871. [CrossRef] [PubMed]
109. Seo, H.W.; Han, K.; Park, C.; Chae, C. Clinical, virological, immunological and pathological evaluation of four porcine circovirus type 2 vaccines. *Vet. J.* **2014**, *200*, 65–70. [CrossRef] [PubMed]
110. Afghah, Z.; Webb, B.; Meng, X.J.; Ramamoorthy, S. Ten years of PCV2 vaccines and vaccination: Is eradication a possibility. *Vet. Mic.* **2016**. [CrossRef] [PubMed]

111. Denner, J. Xenotransplantation and porcine cytomegalovirus (PCMV). *Xenotransplantation* **2015**, *22*, 329–335. [CrossRef] [PubMed]
112. Denner, J.; Mueller, N.J. Preventing transfer of infectious agents. *Int. J. Surg.* **2015**, *23*, 306–311. [CrossRef] [PubMed]
113. Park, J.S.; Kim, J.; Ha, Y.; Jung, K.; Choi, C.; Lim, J.K.; Kim, S.H.; Chae, C. Birth abnormalities in pregnant sows infected intranasally with porcine circovirus 2. *J. Com. Pathol.* **2005**, *132*, 139–144. [CrossRef] [PubMed]
114. Heinze, J.; Plotzki, E.; Denner, J. Virus safety of xenotranplantation: Prevalence of porcine circovirus 2 (PCV2) in pigs. *Ann. Virol. Res.* **2016**, *2*, 1023.
115. Schuurman, H.J. Microbiological Denner, J. safety of clinical xenotransplantation products: Monitoring strategies and regulatory aspects. A commentary. *Xenotransplantation* **2016**, *23*, 440–443. [CrossRef] [PubMed]
116. Bielanski, A.; Algire, J.; Lalonde, A.; Garceac, A.; Pollard, J.W.; Plante, C. Nontransmission of porcine circovirus 2 (PCV2) by embryo transfer. *Theriogenology* **2013**, *80*, 77–83. [CrossRef] [PubMed]

© 2017 by the authors. Licensee MDPI, Basel, Switzerland. This article is an open access article distributed under the terms and conditions of the Creative Commons Attribution (CC BY) license (http://creativecommons.org/licenses/by/4.0/).

viruses

MDPI

Article

Characterization of an Immunodominant Epitope in the Endodomain of the Coronavirus Membrane Protein

Hui Dong [1,2,†], Xin Zhang [1,†], Hongyan Shi [1], Jianfei Chen [1], Da Shi [1], Yunnuan Zhu [1] and Li Feng [1,*]

1 State Key Laboratory of Veterinary Biotechnology, Division of Swine Infectious Diseases, Harbin Veterinary Research Institute, Chinese Academy of Agricultural Sciences, Harbin 150001, China; donghui_12215084@126.com (H.D.); zhangxin2410@163.com (X.Z.); shy2005y@163.com (H.S.); chenjianfei@126.com (J.C.); dashi198566@163.com (D.S.); zyn18345038162@163.com (Y.Z.)

2 Molecular Biology (Gembloux Agro-Bio Tech), University of Liège (ULg), Liège 4000, Belgium

* Correspondence: fl@hvri.ac.cn; Tel.: +86-451-5105-1667

† These authors contributed equally to this work.

Academic Editors: Linda Dixon and Simon Graham

Received: 24 October 2016; Accepted: 6 December 2016; Published: 10 December 2016

Abstract: The coronavirus membrane (M) protein acts as a dominant immunogen and is a major player in virus assembly. In this study, we prepared two monoclonal antibodies (mAbs; 1C3 and 4C7) directed against the transmissible gastroenteritis virus (TGEV) M protein. The 1C3 and 4C7 mAbs both reacted with the native TGEV M protein in western blotting and immunofluorescence (IFA) assays. Two linear epitopes, 243YSTEART249 (1C3) and 243YSTEARTDNLSEQEKLLHMV262 (4C7), were identified in the endodomain of the TGEV M protein. The 1C3 mAb can be used for the detection of the TGEV M protein in different assays. An IFA method for the detection of TGEV M protein was optimized using mAb 1C3. Furthermore, the ability of the epitope identified in this study to stimulate antibody production was also evaluated. An immunodominant epitope in the TGEV membrane protein endodomain was identified. The results of this study have implications for further research on TGEV replication.

Keywords: immunodominant epitope; coronavirus; membrane protein; endodomain

1. Introduction

Coronaviruses (CoVs) are clustered in the *Coronavirinae* subfamily and are divided into four genera (alpha-, beta-, gamma-, and deltacoronavirus) [1,2]. CoVs are enveloped, single-stranded, positive-sense RNA viruses [3–5]. The CoV genomes range from 26.2 kb to 31.7 kb in size. Four structural proteins are encoded by the CoV genomes: spike (S), membrane (M), envelope (E), and nucleocapsid (N).

Transmissible gastroenteritis virus (TGEV) is an excellent model of CoV biology [6–12]. The M protein is the viral assembly scaffold and the most abundant protein in the viral envelope [13]. The avian infectious bronchitis virus (IBV) M protein contains Golgi-targeting information in its first transmembrane domain [14], whereas the transmembrane domains and the cytoplasmic tail domain of the mouse hepatitis virus (MHV) M protein play important roles in Golgi targeting [15,16]. The M protein interacts with the E, S, and N proteins and plays an essential role in virus assembly [17–19]. M is a necessary component of virus-like particles (VLP) during viral assembly [18,20–22]. The M proteins interact other M proteins to form homo-oligomers [23]. In MHV, the M protein interacts with S, and deletion of the cytoplasmic tail of the M protein abolishes the effective interaction between the two proteins [24,25]. Interactions between the M and S proteins have also been identified in IBV [26], bovine coronavirus [27], and severe acute respiratory syndrome (SARS)-CoV [17,21].

The CoV M protein plays an important role in virion morphogenesis [28]. The M protein is composed of the following three regions: a small extracellular domain (ectodomain), a transmembrane domain (Tm), and a large carboxyl terminal domain (endodomain) [29]. The signal peptide of the M protein is located at amino acids (aa) 1–16 [30]. A single tyrosine in the M protein cytoplasmic tail is important for efficient interaction with the S protein of SARS-CoV [13]. The M protein of SARS CoV is localized in the endoplasmic reticulum (ER), Golgi, and ER Golgi intermediate compartment (ERGIC) [31,32]. The cytoplasmic tail of the CoV M protein is essential for its retention in the Golgi [16]. Current diagnostic tools for TGEV detection usually rely on PCR, and a specific method of indirect immunofluorescence assay (IFA) for TGEV detection is needed. TGEV M protein epitopes have been reported previously [28,33], but few functional studies have examined the cytoplasmic terminal domain (endodomain) of the CoV M protein. Monoclonal antibodies (mAbs) to the M protein are needed to dissect the function of the CoV M protein cytoplasmic tail.

In this study, the 1C3 and 4C7 mAbs against the TGEV M protein cytoplasmic tail are described. Two linear epitopes, 243YSTEART249 (1C3) and 243YSTEARTDNLSEQEKLLHMV262 (4C7), were identified in the M protein endodomain. An immunodominant epitope (aa 243–262) in the TGEV membrane protein endodomain was identified. The results of this study have implications for further research on TGEV replication.

2. Materials and Methods

2.1. Cells, Antibodies, and Virus

Porcine kidney 15 (PK-15) cells and Vero E6 cells were grown in DMEM medium supplemented with 10% fetal calf serum (5% CO_2 and 37 °C). TGEV infectious strain H (Accession No. FJ755618) was propagated on PK-15 cells. Porcine epidemic diarrhea virus (PEDV) strain CV777 (Accession No. AF353511), the mAb against N protein of PEDV, and the mAb against N protein of TGEV were maintained in our lab. PEDV strain CV777 was propagated on Vero E6 cells.

2.2. Recombinant Plasmid Construction and Recombinant Protein Expression

The pCold-TGEV-M plasmid was constructed using the F-GST-M and R-GST-M primers (tab:viruses-08-00327-t001). Seven partial TGEV M genes corresponding to M protein amino acids (aa) 17–76 (nt 49–228), aa 67–126 (nt 199–378), aa 117–176 (nt 349–528), aa 167–226 (nt 499–678), aa 217–262 (nt 649–789), aa 217–246 (nt 649–738), and aa 234–262 (nt 700–789) were amplified with the primers shown in tab:viruses-08-00327-t001, which contained the *Bam* HI and *Xho* I restriction enzyme sites. The PCR products were cloned into the prokaryotic expression plasmid pGEX-6p-1. The recombinant plasmids were named pGEX GST-M1 (aa 17–76), pGEX GST-M2 (aa 67–126), pGEX GST-M3 (aa 117–176), pGEX GST-M4 (aa 167–226), pGEX GST-M5 (aa 217–262), pGEX GST-M6 (aa 217–246), and pGEX GST-M7 (aa 234–262).

Table 1. Primers used in this study.

Name	Sequence	Enzyme
F-GST-M	CCGCTCGAGGAACGCTATTGTGC	*Xho* I
R-GST-M	CGGAATTCTTATACCATATGTA	*Eco* RI
F-M (49–228)-6p	GTGGATCCGAACGCTATTGTGCTATGAA	*Bam* HI
R-M (49–228)-6p	GACTCGAGGAATTGAGGTCTTCCATATT	*Xho* I
F-M (199–378)-6p	GTGGATCC ACTGTGCTACAATATGGAAG	*Bam* HI
R-M (199–378)-6p	GACTCGAGAAATGTAACAATTGCACCTG	*Xho* I
F-M (349–528)-6p	GTGGATCCTTTAGTATTGCAGGTGCAAT	*Bam* HI
R-M (349–528)-6p	GACTCGAGACCAGTTGGCACACCTTCGA	*Xho* I
F-M (499–678)-6p	GTGGATCCGTGCTTCCTCTCGAAGGTGT	*Bam* HI
R-M (499–678)-6p	GACTCGAGTGCTTTCAACTTCTTGCCAA	*Xho* I
F-M (649–789)-6p	GTGGATCCTACACACTTGTTGGCAAGAA	*Bam* HI
R-M (649–789)-6p	GACTCGAGTTATACCATATGTAATAATT	*Xho* I
F-M (649–738)-6p	GTGGATCCTACACACTTGTTGGCAAGAA	*Bam* HI
R-M (649–738)-6p	GACTCGAGCTCTGTTGAGTAATCACCAG	*Xho* I
F-M (700–789)-6p	GTGGATCCTACTATGTAAAATCTAAAGC	*Bam* HI
R-M (700–789)-6p	GACTCGAGTTATACCATATGTAATAATT	*Xho* I

2.3. Preparation of mAbs Targeting the M Protein

Proteins were expressed in *E. coli* BL21 (DE3) using previously described methods [34]. The GST-M fusion protein was purified using Glutathione Sepharose 4B (GE Healthcare, Amersham, UK) according to the manufacturer's protocol. The mAbs against the M protein were prepared as previously described [35]. The SBA Clonotyping System-Horseradish Peroxidase (HRP) kit (Southern Biotechnology Associates, Inc., Birmingham, AL, USA) was used to determine the IgG subtype of the mAbs.

2.4. Immunofluorescence Assay (IFA)

PK-15 cells were infected with the TGEV H strain at a multiplicity of infection (MOI) of 0.1 and cultured for 36 h. The cells were fixed for 30 min with paraformaldehyde (4%) at 4 °C. The fixed cells were blocked with 5% skimmed milk and then incubated with the 1C3 or 4C7 mAb for 60 min at 37 °C. The cells were incubated with the anti-mouse IgG (whole molecule) Atto 488 antibody (1:1000, Sigma, St. Louis, MO, USA) after washing three times with 0.05% Tween 20 in PBS (PBST). Nuclear staining was performed with 4′,6-diamidino-2-phenylindole (DAPI, Sigma) [36]. The cells were washed three times with PBST and examined using a Leica TCS SP5 laser confocal microscope.

2.5. Immunoperoxidase Monolayer Assay (IPMA)

PK-15 cells were infected with the TGEV H strain and then fixed and blocked as described above. Then, the cells were incubated with the 1C3 or 4C7 mAb for 60 min at 37 °C. The cells were washed three times with PBST and incubated with HRP-labeled goat anti-mouse IgG (1:500, Sigma, USA) at 37 °C for 60 min. The cells were visualized with the 3-amino-9-ethylcarbazole (AEC) substrate and examined by microscopy.

2.6. Immunoprecipitation of the TGEV M Protein

Immunoprecipitation was performed as previously described [34]. The lysate from TGEV-infected or mock-infected PK-15 cells was incubated with 1 μg of the 1C3 or 4C7 mAbs at 4 °C. Protein A/G PLUS-Agarose was used according to the manufacturer's instructions, and 60 μg of cell lysates was loaded in the gels. The immunoprecipitated proteins were analyzed by western blotting using the 1C3 or 4C7 mAbs as described previously [34].

2.7. Polypeptide Design and Coupling

Ten peptides spanning aa 217–262 of the TGEV M protein were synthesized by GL Biotech (Shanghai, China) (tab:viruses-08-00327-t002). Additionally, 4 mg of the RS-15 (RGDYSTEARTGGGGS), YT-16 (YSTEARTGGYSTEART), and YV-20 (YSTEARTDNLSEQEKLLHMV) peptides coupled with KLH (RS-15-KLH, YT-16-KLH, and YV-20-KLH) or BSA (RS-15-BSA, YT-16-BSA, and YV-20-BSA) were synthesized by GL Biotech.

Table 2. Synthesized polypeptides based on the M protein of the transmissible gastroenteritis virus (TGEV).

Residues	Amino Acid Sequence	Residues	Amino Acid Sequence
217–236	YTLVGKKLKASSATGWAYYV	230–249	TGWAYYVKSKAGDYSTEART
243–262	YSTEARTDNLSEQEKLLHMV	234–248	YYVKSKAGDYSTEAR
243–257	YSTEARTDNLSEQEK	244–258	STEARTDNLSEQEKL
245–259	TEARTDNLSEQEKLL	246–260	EARTDNLSEQEKLLH
247–261	ARTDNLSEQEKLLHM	248–262	RTDNLSEQEKLLHMV
RS-15	RGDYSTEARTGGGGS	YT-16	YSTEARTGGYSTEART
YV-20	YSTEARTDNLSEQEKLLHMV		

2.8. Animal Immunization with RS-15-KLH, YT-16-KLH, and YV-20-KLH

Four BALB/c mice were immunized subcutaneously (s.c.) with RS-15-KLH, YT-16-KLH, or YV-20-KLH (100 μg per mouse) emulsified in complete Freund's adjuvant (Sigma). The mice were immunized four times at two-week intervals. The sera were evaluated using ELISA plates coated with RS-15-BSA, YT-16-BSA, or YV-20-BSA (2 μg/well).

2.9. Peptide ELISA

ELISA plates were coated with the synthesized RS-15-BSA, YT-16-BSA, or YV-20-BSA peptide (2 μg/well) overnight at 4 °C and then blocked with 5% skimmed milk for 2 h at 37 °C. The plates were incubated with sera from mice immunized with RS-15-KLH, YT-16-KLH, or YV-20-KLH for 1 h at 37 °C. HRP-labeled goat anti-mouse IgG (1:2000, Sigma) was added and incubated for 1 h at 37 °C. The reaction was stopped with 2M H_2SO_4.

2.10. Immunohistochemistry (IHC)

The IHC assay was performed as previously described [37]. Slides were incubated with the 1C3 or 4C7 mAb (1:100) overnight at 4 °C, followed by incubation with HRP-labeled goat anti-mouse IgG (1:2000, Sigma) for 1 h at 37 °C. The reactions were detected with 3,3′-diaminobenzidine tetrahydrochloride (DAB) substrate.

2.11. 3D Epitope Modelling

The spatial distribution of the identified epitopes in the TGEV M protein were analyzed using PyMOL software with the SWISS-MODEL server [38].

2.12. Animal Ethics

This study was approved by Harbin Veterinary Research Institute and was performed in accordance with animal ethics guidelines and approved protocols. The animal Ethics Committee approval number is Heilongjiang-SYXK-2006-032.

3. Results

3.1. Expression and Purification of the GST-M Protein

For prokaryotic expression of the M protein, the signal peptide (aa 1–16) was removed, and the M gene was cloned into the prokaryotic expression vector pCold GST DNA. The recombinant proteins were expressed by induction with 1 mM IPTG in pCold-TGEV-M-transformed cells. The size of the recombinant GST-M protein was approximately 54 kDa. The purified GST-M protein reacted with the anti-GST mAb in the western blotting experiment (Figure 1a).

3.2. Preparation of mAbs against the TGEV M Protein

Two mAbs against the TGEV M protein (1C3 and 4C7) were prepared using the purified GST-M protein. The 1C3 and 3D7 mAbs belonged to the IgG2b isotype. As shown in Figure 1b, the 1C3 and 4C7 mAbs specifically reacted with both the GST-M protein and the native M protein in TGEV-infected PK-15 cells but not with GST and mock-infected PK-15 cells.

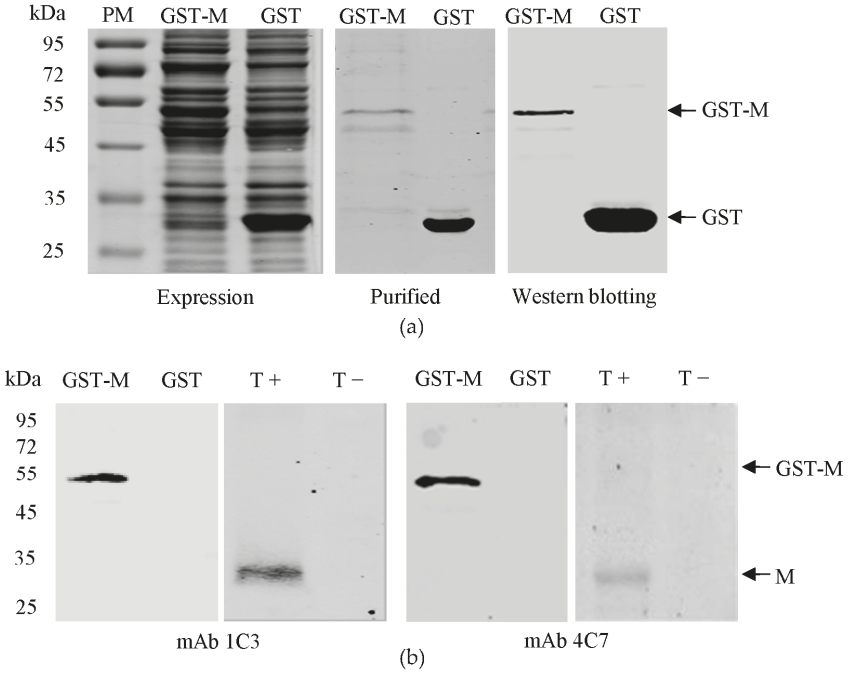

Figure 1. Preparation of monoclonal antibodies (mAbs) against the M protein of TGEV. (**a**) Expression and purification of GST-M protein. The proteins were detected after western blotting with a GST mAb; (**b**) Reactivity of the 1C3 and 4C7 mAbs with the GST-M protein and the TGEV M protein. PM represents protein marker. T+ represents the cell lysates of TGEV-infected porcine kidney 15 (PK-15) cells. T− represents the cell lysates of mock infected PK-15 cells.

3.3. Determination of the 1C3 and 4C7 mAb Epitopes

To identify the 1C3 and 4C7 mAb epitopes, five truncated M proteins (GST-M1, GST-M2, GST-M3, GST-M4 and GST-M5) were expressed (Figure 2a). Figure 2b shows that 1C3 and 4C7 were reactive with GST-M5. Subsequently, two truncated M proteins that covered aa 217–262 were expressed.

The western blotting results demonstrated that both 1C3 and 4C7 reacted against GST-M7 aa 234–262 (Figure 2c).

To further define the 1C3 and 4C7 mAb epitopes, ten overlapping polypeptides were synthesized (tab:viruses-08-00327-t002). The epitope ELISA results showed that 243YSTEART249 were the core amino acids of the 1C3 epitope, whereas 243YSTEARTDNLSEQEKLLHMV262 were the core amino acids of the 4C7 epitope (Figure 2d).

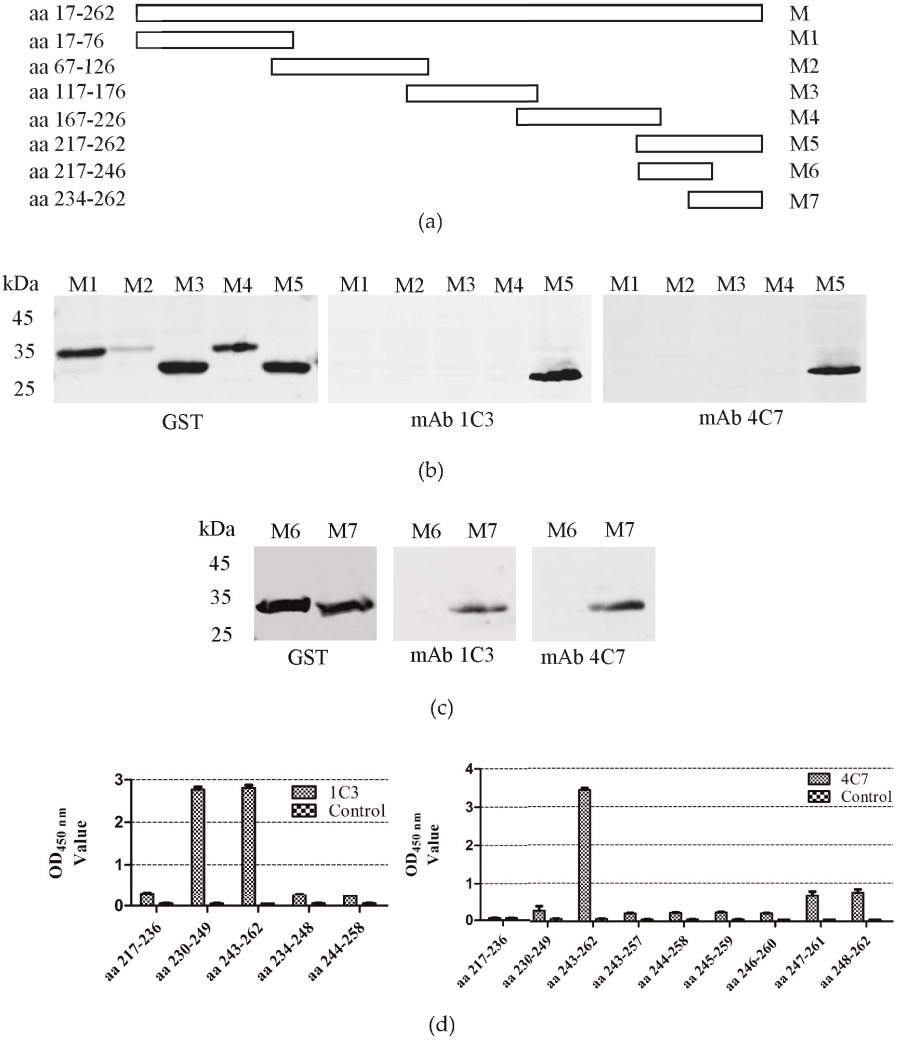

Figure 2. Identification of the epitopes of the 1C3 and 4C7 mAbs. (**a**) Scheme of the M protein and M fragments; (**b**) Western blotting analysis of the GST-M1, GST-M2, GST-M3, GST-M4, and GST-M5 proteins using the 1C3 and 4C7 mAbs; (**c**) Western blotting analysis of the GST-M6 and GST-M7 proteins using the 1C3 and 4C7 mAbs; (**d**) Five peptides were reacted with the mAb 1C3 and nine peptides with 4C7 by peptide ELISA. aa represents amino acids. PM represents protein marker.

3.4. 3D Epitope Mapping

The TGEV M protein sequence was compared against the SWISS-MODEL template library. The solution structure of ADP-ribosyl cyclase (SMTL id 1r15.1) [39] was selected for model building. The identified epitope recognized by mAb 1C3 (YSTEART) formed an alpha spiral structure (Figure 3a). Furthermore, the conservation of the M epitopes (YSTEART) in TGEV, PEDV, and porcine deltacoronavirus (PDCoV) was compared. As shown in the sequence alignment in Figure 3b, the epitope (YSTEART) is well conserved among TGEV, but differs greatly from the sequence in PEDV and PDCoV.

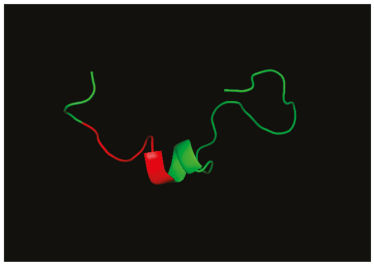

(a)

Viruses (GenBank accession number)	^{239}KAGDYSTEARTDNLS^{253}
TGEV attenuated H (EU074218)	• • • • • • • • • • • • • • •
TGEV H16 (FJ755618)	• • • • • • • • • • • • • • •
TGEV Miller M6 (DQ811785)	• • • • • • • • • • • • • • •
TGEV Miller M60 (DQ811786)	• • • • • • • • • • • • • • •
TGEV Purdue P115 (DQ811788)	• • • • • • • • • • • • • • •
TGEV virulent Purdue (DQ811789)	• • • • • • • • • • • • • • •
TGEV SC-Y (DQ443743)	• • • • • • • • • • • • • • •
TGEV TS (DQ201447)	• • • • • • • • • • • • • • •
TGEV WH-1 (HQ462571)	• • • • • • • • • • • • • • •
PEDV CH/FJND-3/2011 (JQ282909)	• H • • • • AVSNPSSVL
PEDV USA/Ohio249/2014 (KR265840)	• H • • • • AVSNPSSVL
PEDV USA/IL20697/2014 (KT860508)	• H • • • • AVSNPSSVL
PEDV CV777 (AF353511)	• H • • • • AVSNPSSVL
PDCoV NH (KU981062)	YQ • • RASNAGLHTIT
PDCoV SA/Iowa136/2015 (KX022602)	YQ • • RASNAGLHTIT

(b)

Figure 3. Location of the identified epitope in the predicted structure of the TGEV M protein. (**a**) The location of the epitope (shown in red) for mAb 1C3 (YSTEART) in the TGEV M protein is highlighted; (**b**) Conservation of the M epitopes (YSTEART) in TGEV, porcine epidemic diarrhea virus (PEDV) and porcine deltacoronavirus (PDCoV). Dots indicate identical residues.

3.5. Reactivity of 1C3 and 4C7 with the TGEV M Protein in IFA and IPMA

IFA and IPMA were used to verify the reactivity of mAbs 1C3 and 4C7 with the M protein in TGEV-infected PK-15 cells. The 1C3 and 4C7 mAbs showed reactivity with the M protein in TGEV-infected PK-15 cells in the IFA (Figure 4a) and IPMA (Figure 4b). The TGEV M protein was distributed in the cytoplasm of the PK-15 cells. The reaction ability of 1C3 was superior to 4C7 in the IFA and IPMA.

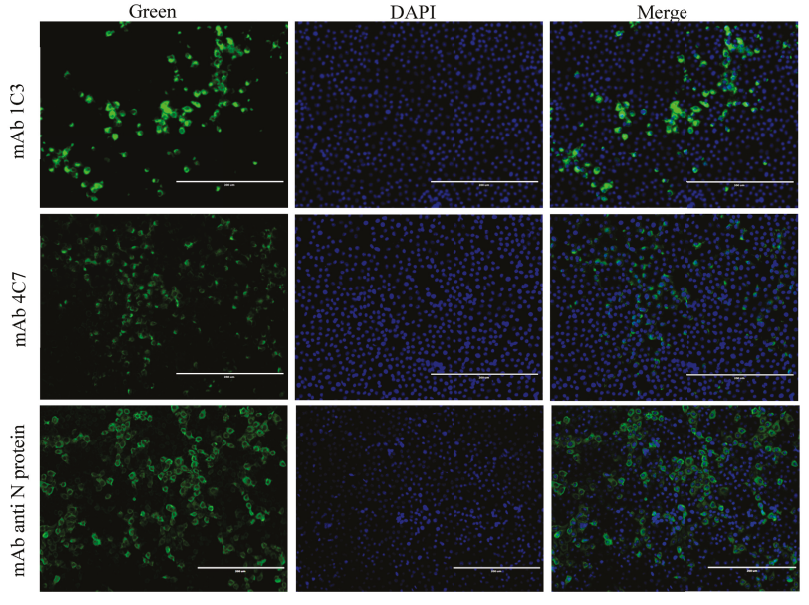

(a)

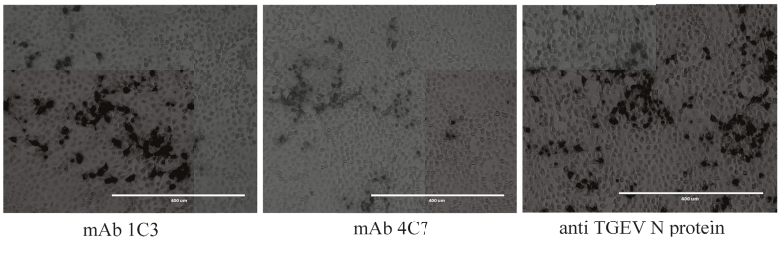

(b)

Figure 4. Application of the generated mAbs 1C3 and 4C7 in immunofluorescence assay (IFA) and immunoperoxidase monolayer assay (IPMA). (**a**) IFA analysis of the M protein in TGEV-infected PK-15 cells using 1C3 and 4C7 mAbs; (**b**) IPMA assay of the M protein in TGEV-infected PK-15 cells using 1C3 and 4C7 mAbs. The mAb against the N protein of TGEV was used as a positive control.

3.6. Immunoprecipitation of 1C3 and 4C7 with the TGEV M Protein

To elucidate whether the TGEV M protein could be precipitated with the 1C3 or 4C7 mAb, an immunoprecipitation assay was performed in the TGEV-infected PK-15 cells. As shown in Figure 5a, the TGEV M protein was precipitated from the TGEV-infected PK-15 cells by mAb 1C3 but not 4C7.

3.7. mAb 1C3 Reacted with the M Protein in the Small Intestine

The IHC assay was utilized to elucidate whether mAb 1C3 could recognize the M protein in the small intestines of animals inoculated with TGEV. As shown in Figure 5b, the TGEV M protein was recognized by mAb 1C3 but not 4C7 in TGEV-inoculated animal small intestines.

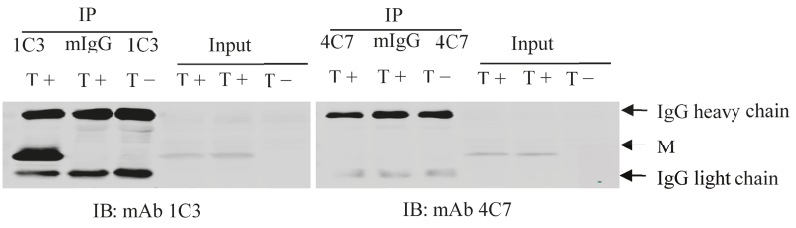

(a)

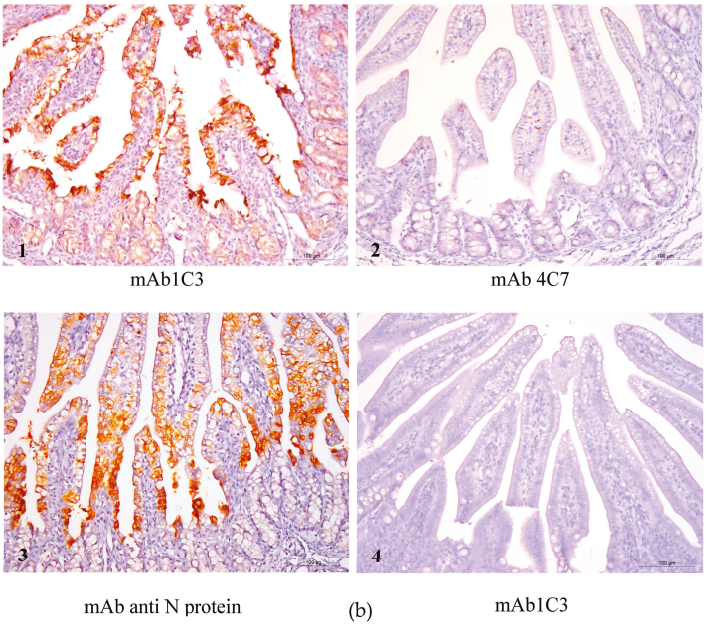

(b)

Figure 5. Application of the generated mAbs 1C3 and 4C7 in IP and immunohistochemistry (IHC). (**a**) Immunoprecipitation analysis of the M protein in TGEV-infected PK-15 cells using 1C3 and 4C7 mAbs. T+ represents the cell lysates of TGEV-infected PK-15 cells. T− represents the cell lysates of mock-infected PK-15 cells. The mIgG represents mouse control IgG; (**b**) IHC analysis of the M protein in the small intestines of TGEV-inoculated animals using 1C3 (1) and 4C7 (2) mAbs and an N-protein mAb (3) as a positive control. Staining of the small intestines of mock-inoculated animals with 1C3 mAb is shown as a negative control (4).

3.8. Optimizing of the IFA Method for the Detection of the M Protein

The IgG of mAb 1C3 was purified using HiTrapTM protein G HP (Figure 6a). The IFA method was optimized for the detection of the TGEV M protein. At 36 h, TGEV-infected PK-15 cells (10^3 $TCID_{50}$) were fixed with paraformaldehyde (4%) for 30 min at 4 °C. Then, the cells were blocked with 5% skimmed milk at 37 °C for 1 h. The optimum concentration of the primary antibody (purified 1C3 IgG) was 1 ng/μL, and the dilution of the secondary antibody was 1:500. The IFA detected green fluorescence in the TGEV-infected PK-15 cells (Figure 6b). To further validate whether 1C3 react with PEDV, IFA was used. As shown in Figure 6b, 1C3 did not react with the PEDV.

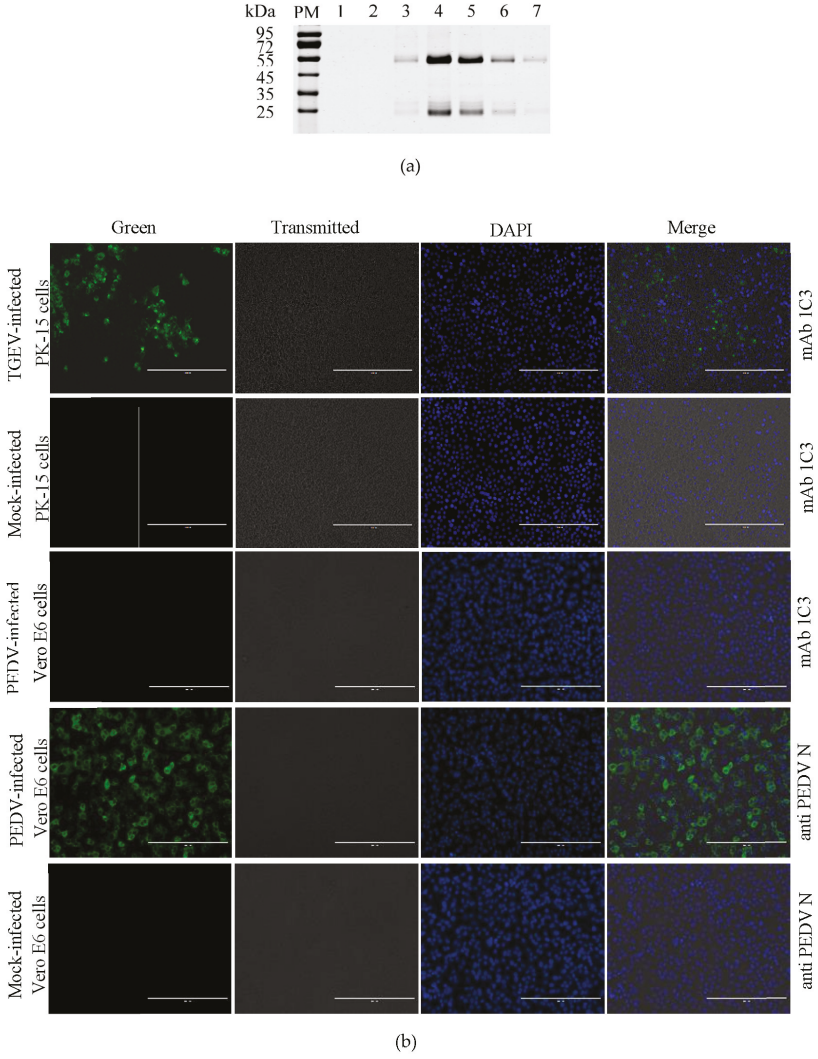

Figure 6. Optimization of the IFA method using mAb 1C3 for the M protein. (**a**) Purification of mAb 1C3 IgG. Lanes 1–7: purified IgG; (**b**) Optimization of the IFA method for M protein detection using the purified mAb 1C3 IgG in PK-15 cells. PM represents protein marker.

3.9. Antibody Responses to the Identified Epitopes

To examine the ability of the two epitopes identified in this study to induce antibody responses, arginine-glycine-aspartate [40] was added on the N-terminal side of peptide aa 243–249 (RS-15), and an overlay of peptide aa 243–249 (YT-16) and peptide aa 243–262 (YV-20) were used to immunize mice. The epitopes were coupled with KLH and named RS-15-KLH, YT-16-KLH, and YV-20-KLH, respectively. BALB/c mice were immunized once every two weeks using RS-15-KLH, YT-16-KLH, or YV-20-KLH. Sera were collected at 0, 2, 4, 6 and 8 weeks. The antibodies elicited by RS-15-KLH, YT-16-KLH, and YV-20-KLH were detected using an indirect peptide ELISA with RS-15-BSA, YT-16-BSA, and YV-20-BSA as the antigen, respectively. At 4 weeks, the sera collected from the three immunized

groups showed a detectable antibody response. In contrast, the control group inoculated with PBS did not show any significant immunity (Figure 7a). The antibody level increased with the number of immunizations. At 8 weeks, the antibody levels of all three immunized groups reached the highest values. Next, we examined whether the antibody was able to react with the native M protein in TGEV-infected PK-15 cells. Figure 7b shows that only the antibody elicited by the YV-20-KLH epitope reacted with the M protein, whereas no reaction was detected for RS-15-KLH or YT-16-KLH.

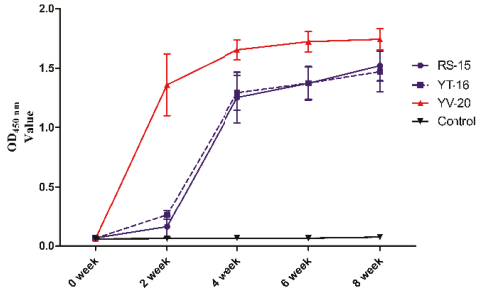

(a)

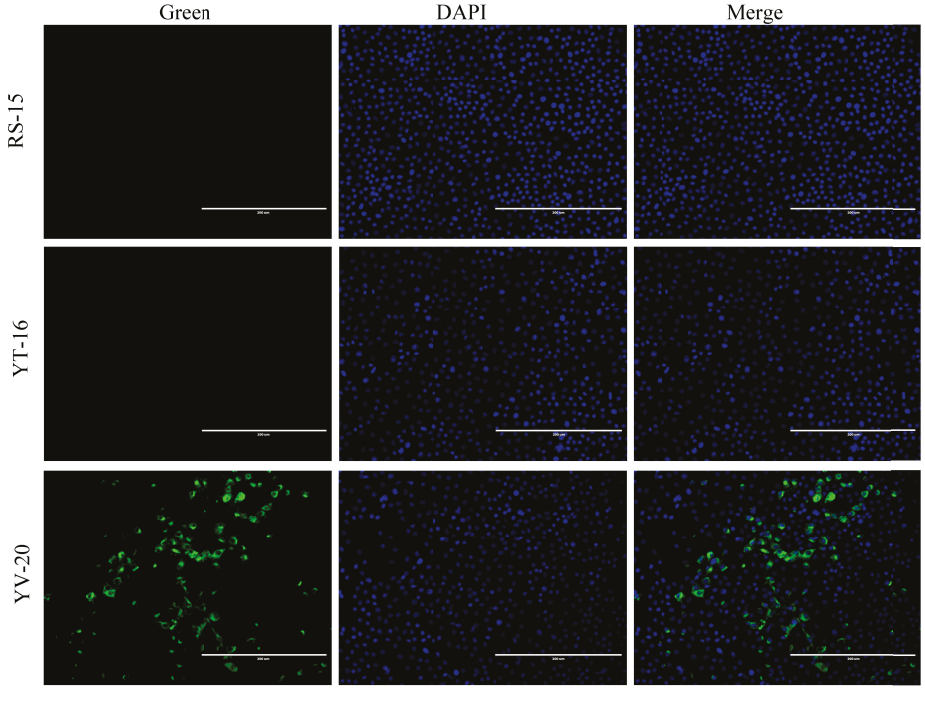

(b)

Figure 7. Antibody responses to the identified epitopes. (**a**) Humoral responses elicited by the aa 243-249 and aa 243–262 epitopes; (**b**) Reaction of antibodies elicited by epitopes with the TGEV virus in PK-15 cells.

4. Discussion

The mapping of CoV viral protein epitopes can promote our understanding of the structure and function of the antigen. The CoV M protein is a major player in virus assembly [41], although its biology has not been fully elucidated. Monoclonal antibodies against the M protein are necessary to elucidate its various functions and mechanisms in viral replication. Some immunodominant epitopes have been identified on the M proteins (aa 193–200) of the porcine epidemic diarrhoea virus (PEDV) [42], IBV (aa 199–206) [43] and SARS-CoV (aa 1–31 and aa 132–161) [44]. Additionally, a few studies have reported monoclonal antibodies against the TGEV M protein [45–47]. However, no study has reported the TGEV M protein epitopes. In this study, two mAbs against the TGEV M protein (1C3 and 4C7) were prepared. Two epitopes recognized by mAbs 1C3 and 4C7 corresponding to 243YSTEART249 and 243YSTEARTDNLSEQEKLLHMV262 in the TGEV M protein were identified for the first time through a combination of experiments with truncated M proteins (M1–M7) and the peptide scanning technique. These results may indicate that the major immunodominant domain is located in the M protein endodomain.

Based on the peptide ELISA results, mAb 1C3 did not react with aa 244–258 and aa 234–248, indicating that Y243 and T249 were key residues for the activity of 243YSTEART249. The mAb 4C7 did not react with aa 243–257, aa 244–258, aa 245–259 or aa 246–260, which indicated that R248 and M261 were key residues for the activity of 243YSTEARTDNLSEQEKLLHMV262. Furthermore, by comparing aa 247–261 and 248–262 with aa 243–262, we found that the reactive activity of aa 243–262 was significantly higher than the reactive activity of the other amino acids (Figure 2d).

The CoVs M protein is a transmembrane protein with three domains: a small extracellular domain (ectodomain), a transmembrane domain (Tm), and a large carboxyl terminal domain (endodomain) [29,41,48]. M protein self-interactions occur among the transmembrane domains [49,50]. The ectodomain of the CoV M protein plays an important role in interactions with other viral proteins, such as the N protein of MHV [51–53], SARS-CoV [54–56], and TGEV [28] and the S protein of MHV [25] and SARS-CoV [13]. TGEV M aa 233–257 (AYYVKSKAAGDYSTEARTDNLSEQEK), which contains the epitopes recognized by the mAbs 1C3 and 4C7 (underlined), is involved in M-N binding to allow virion morphogenesis [28]. The fact might be a problem for mAbs (1C3 and 4C7) performance in a diagnostic test. In this study, the identified linear epitopes of mAbs 1C3 and 4C7 were located in the TGEV M protein endodomain. Thus, this information could be widely used in future research on the function of this domain in TGEV.

The IFA method we established has some advantages, including simple operation and easy evaluation of the results. A specific IFA method for the detection of the TGEV M protein is still needed. In this study, an IFA method for the detection of the M protein of TGEV was optimized. Optimization of this IFA method will be helpful for future studies of the function of the M protein in the process of TGEV replication. In general, coronavirus diagnostics is based on the N protein, because it is the most abundant protein, is produced early during infection, and is highly immunogenic. For detection of the TGEV virus, the established assay has no advantage over other N protein-based assays. Further research is needed to establish an IFA method for the detection of TGEV based on the N protein.

CoV structural protein can induce virus-specific antibodies [57]. The CoV S protein is a class I fusion protein involved in attachment of the CoV surface to the host aminopeptidase N [2,58]. The S protein is presented as a trimer and mediates receptor binding, membrane fusion, and virus entry [59–61]. The S protein is the major target for neutralizing antibodies [62,63]. The M protein can induce neutralizing antibodies, but these antibodies are weaker than those induced by the S protein. The TGEV M protein endodomain is also exposed on the virion surface [33] and some mAbs directed against the TGEV M endodomain are weakly neutralizing [64]. Further study is needed to evaluate the neutralizing activity of the prepared antibodies (1C3 and 4C7). An antibody against the M protein was induced and used to detect CoV [47,65]. In this study, mice were immunized with RS-15, YT-16, and YV-20. The antibody induced by aa 243–262 exhibited higher activity than the antibodies induced by RS-15 and YT-16 (Figure 7a). Furthermore, the antibody to YV-20 reacted with the TGEV M protein

in TGEV-infected PK-15 cells in the IFA assay. However, the antibody to RS-15 and YT-16 did not react with the M protein in TGEV-infected PK-15 cells (Figure 7b). These results indicate that the YV-20 epitope has potential for the development of a TGEV vaccine.

5. Conclusions

Two specific mAbs against the TGEV M protein (1C3 and 4C7) were prepared in this study, and two linear B cell epitopes located in the M protein endodomain were successfully identified. The 1C3 mAb was used to immunoprecipitate the M protein from TGEV-infected PK-15 cell lysates. The 1C3 mAb is a useful tool for investigations of the antigenic properties of the M protein. These antibodies are relevant to furthering our understanding of the mechanism of the M protein in TGEV replication. Furthermore, an immunodominant epitope (aa 243–262) in the TGEV membrane protein endodomain was identified.

Acknowledgments: This work was supported by the National Key Technology Support Program (grant numbers 2015BAD12B02); the National Natural Science Foundation of China (grant number 31572541, and 31502092).

Author Contributions: Li Feng conceived and designed the experiments; Hui Dong and Xin Zhang performed the experiments; Hongyan Shi and Jianfei Chen analyzed the data; Da Shi and Yunnuan Zhu contributed reagents/materials/analysis tools; Xin Zhang and Li Feng wrote the paper.

Conflicts of Interest: The authors declare no conflict of interest.

References

1. De Groot, R.J.; Baker, S.G.; Baric, R.S.; Enjuanes, L.; Gorbalenya, A.E. Coronaviridae. In *Virus Taxonomy: Ninth Report of the International Committee on Taxonomy of Viruses*; King, A.M.Q., Adams, M.J., Carstens, E.B., Lefkowitz, E.J., Eds.; Elsevier Academic Press: San Diego, CA, USA, 2011; pp. 774–796.
2. Reguera, J.; Santiago, C.; Mudgal, G.; Ordono, D.; Enjuanes, L.; Casasnovas, J.M. Structural bases of coronavirus attachment to host aminopeptidase N and its inhibition by neutralizing antibodies. *PLoS Pathog.* **2012**, *8*, e1002859. [CrossRef] [PubMed]
3. Perlman, S.; Netland, J. Coronaviruses post-SARS: Update on replication and pathogenesis. *Nat. Rev. Microbiol.* **2009**, *7*, 439–450. [CrossRef] [PubMed]
4. Lai, M.M.; Cavanagh, D. The molecular biology of coronaviruses. *Adv. Virus Res.* **1997**, *48*, 1–100. [PubMed]
5. Yang, D.; Leibowitz, J.L. The structure and functions of coronavirus genomic 3′ and 5′ ends. *Virus Res.* **2015**, *206*, 120–133. [CrossRef] [PubMed]
6. Jenwitheesuk, E.; Samudrala, R. Identifying inhibitors of the SARS coronavirus proteinase. *Bioorg. Med. Chem. Lett.* **2003**, *13*, 3989–3992. [CrossRef] [PubMed]
7. Anand, K.; Ziebuhr, J.; Wadhwani, P.; Mesters, J.R.; Hilgenfeld, R. Coronavirus main proteinase (3CLpro) structure: Basis for design of anti-SARS drugs. *Science* **2003**, *300*, 1763–1767. [CrossRef] [PubMed]
8. Yount, B.; Curtis, K.M.; Baric, R.S. Strategy for systematic assembly of large RNA and DNA genomes: Transmissible gastroenteritis virus model. *J. Virol.* **2000**, *74*, 10600–10611. [PubMed]
9. Sola, I.; Almazan, F.; Zuniga, S.; Enjuanes, L. Continuous and discontinuous RNA synthesis in coronaviruses. *Annu. Rev. Virol.* **2015**, *2*, 265–288. [CrossRef] [PubMed]
10. Cruz, J.L.; Sola, I.; Becares, M.; Alberca, B.; Plana, J.; Enjuanes, L.; Zuñiga, S. Coronavirus gene 7 counteracts host defenses and modulates virus virulence. *PLoS Pathog.* **2011**, *7*, e1002090. [CrossRef] [PubMed]
11. Zuniga, S.; Sola, I.; Moreno, J.L.; Sabella, P.; Plana-Duran, J.; Enjuanes, L. Coronavirus nucleocapsid protein is an RNA chaperone. *Virology* **2007**, *357*, 215–227. [CrossRef] [PubMed]
12. Almazan, F.; Gonzalez, J.M.; Penzes, Z.; Izeta, A.; Calvo, E.; Plana-Duran, J.; Enjuanes, L. Engineering the largest RNA virus genome as an infectious bacterial artificial chromosome. *Proc. Natl. Acad. Sci. USA* **2000**, *97*, 5516–5521. [CrossRef] [PubMed]
13. McBride, C.E.; Machamer, C.E. A single tyrosine in the severe acute respiratory syndrome coronavirus membrane protein cytoplasmic tail is important for efficient interaction with spike protein. *J. Virol.* **2010**, *84*, 1891–1901. [CrossRef] [PubMed]
14. Swift, A.M.; Machamer, C.E. A Golgi retention signal in a membrane-spanning domain of coronavirus E1 protein. *J. Cell Biol.* **1991**, *115*, 19–30. [CrossRef] [PubMed]

15. Armstrong, J.; Patel, S.; Riddle, P. Lysosomal sorting mutants of coronavirus E1 protein, a Golgi membrane protein. *J. Cell Sci.* **1990**, *95*, 191–197. [PubMed]
16. Locker, J.K.; Klumperman, J.; Oorschot, V.; Horzinek, M.C.; Geuze, H.J.; Rottier, P.J. The cytoplasmic tail of mouse hepatitis virus M protein is essential but not sufficient for its retention in the Golgi complex. *J. Biol. Chem.* **1994**, *269*, 28263–28269. [PubMed]
17. Hsieh, Y.C.; Li, H.C.; Chen, S.C.; Lo, S.Y. Interactions between M protein and other structural proteins of severe, acute respiratory syndrome-associated coronavirus. *J. Biomed. Sci.* **2008**, *15*, 707–717. [CrossRef] [PubMed]
18. Siu, Y.L.; Teoh, K.T.; Lo, J.; Chan, C.M.; Kien, F.; Escriou, N.; Tsao, S.W.; Nicholls, J.M.; Altmeyer, R.; Peiris, J.S. The M, E, and N structural proteins of the severe acute respiratory syndrome coronavirus are required for efficient assembly, trafficking, and release of virus-like particles. *J. Virol.* **2008**, *82*, 11318–11330. [CrossRef] [PubMed]
19. Tseng, Y.T.; Wang, S.M.; Huang, K.J.; Lee, A.I.; Chiang, C.C.; Wang, C.T. Self-assembly of severe acute respiratory syndrome coronavirus membrane protein. *J. Biol. Chem.* **2010**, *285*, 12862–12872. [CrossRef] [PubMed]
20. Baudoux, P.; Carrat, C.; Besnardeau, L.; Charley, B.; Laude, H. Coronavirus pseudoparticles formed with recombinant M and E proteins induce alpha interferon synthesis by leukocytes. *J. Virol.* **1998**, *72*, 8636–8643. [PubMed]
21. Huang, Y.; Yang, Z.Y.; Kong, W.P.; Nabel, G.J. Generation of synthetic severe acute respiratory syndrome coronavirus pseudoparticles: Implications for assembly and vaccine production. *J. Virol.* **2004**, *78*, 12557–12565. [CrossRef] [PubMed]
22. Mortola, E.; Roy, P. Efficient assembly and release of SARS coronavirus-like particles by a heterologous expression system. *FEBS Lett.* **2004**, *576*, 174–178. [CrossRef] [PubMed]
23. De Haan, C.A.; Vennema, H.; Rottier, P.J. Assembly of the coronavirus envelope: Homotypic interactions between the M proteins. *J. Virol.* **2000**, *74*, 4967–4978. [CrossRef] [PubMed]
24. Opstelten, D.J.; Raamsman, M.J.; Wolfs, K.; Horzinek, M.C.; Rottier, P.J. Envelope glycoprotein interactions in coronavirus assembly. *J. Cell Biol.* **1995**, *131*, 339–349. [CrossRef] [PubMed]
25. De Haan, C.A.; Smeets, M.; Vernooij, F.; Vennema, H.; Rottier, P.J. Mapping of the coronavirus membrane protein domains involved in interaction with the spike protein. *J. Virol.* **1999**, *73*, 7441–7452. [PubMed]
26. Youn, S.; Collisson, E.W.; Machamer, C.E. Contribution of trafficking signals in the cytoplasmic tail of the infectious bronchitis virus spike protein to virus infection. *J. Virol.* **2005**, *79*, 13209–13217. [CrossRef] [PubMed]
27. Nguyen, V.P.; Hogue, B.G. Protein interactions during coronavirus assembly. *J. Virol.* **1997**, *71*, 9278–9284. [PubMed]
28. Escors, D.; Ortego, J.; Laude, H.; Enjuanes, L. The membrane M protein carboxy terminus binds to transmissible gastroenteritis coronavirus core and contributes to core stability. *J. Virol.* **2001**, *75*, 1312–1324. [CrossRef] [PubMed]
29. Rottier, P.; Brandenburg, D.; Armstrong, J.; van der Zeijst, B.; Warren, G. Assembly in vitro of a spanning membrane protein of the endoplasmic reticulum: The E1 glycoprotein of coronavirus mouse hepatitis virus A59. *Proc. Natl. Acad. Sci. USA* **1984**, *81*, 1421–1425. [CrossRef] [PubMed]
30. Kapke, P.A.; Tung, F.Y.; Hogue, B.G.; Brian, D.A.; Woods, R.D.; Wesley, R. The amino-terminal signal peptide on the porcine transmissible gastroenteritis coronavirus matrix protein is not an absolute requirement for membrane translocation and glycosylation. *Virology* **1988**, *165*, 367–376. [CrossRef]
31. Lopez, L.A.; Jones, A.; Arndt, W.D.; Hogue, B.G. Subcellular localization of SARS-CoV structural proteins. *Adv. Exp. Med. Biol.* **2006**, *581*, 297–300. [PubMed]
32. Nal, B.; Chan, C.; Kien, F.; Siu, L.; Tse, J.; Chu, K.; Kam, J.; Staropoli, I.; Crescenzo-Chaigne, B.; Escriou, N.; et al. Differential maturation and subcellular localization of severe acute respiratory syndrome coronavirus surface proteins S, M and E. *J. Gen. Virol.* **2005**, *86*, 1423–1434. [CrossRef] [PubMed]
33. Escors, D.; Camafeita, E.; Ortego, J.; Laude, H.; Enjuanes, L. Organization of two transmissible gastroenteritis coronavirus membrane protein topologies within the virion and core. *J. Virol.* **2001**, *75*, 12228–12240. [CrossRef] [PubMed]

34. Zhang, X.; Shi, H.; Chen, J.; Shi, D.; Li, C.; Feng, L. EF1A interacting with nucleocapsid protein of transmissible gastroenteritis coronavirus and plays a role in virus replication. *Vet. Microbiol.* **2014**, *172*, 443–448. [CrossRef] [PubMed]
35. Kohler, G.; Milstein, C. Continuous cultures of fused cells secreting antibody of predefined specificity. *Nature* **1975**, *256*, 495–497. [CrossRef] [PubMed]
36. Jungmann, A.; Nieper, H.; Muller, H. Apoptosis is induced by infectious bursal disease virus replication in productively infected cells as well as in antigen-negative cells in their vicinity. *J. Gen. Virol.* **2001**, *82*, 1107–1115. [CrossRef] [PubMed]
37. Wang, X.; Qiu, H.; Zhang, M.; Cai, X.; Qu, Y.; Hu, D.; Zhao, X.; Zhou, E.; Liu, S.; Xiao, Y. Distribution of highly pathogenic porcine reproductive and respiratory syndrome virus (HP-PRRSV) in different stages of gestation sows: HP-PRRSV distribution in gestation sows. *Vet. Immunol. Immunopathol.* **2015**, *166*, 88–94. [CrossRef] [PubMed]
38. Biasini, M.; Bienert, S.; Waterhouse, A.; Arnold, K.; Studer, G.; Schmidt, T.; Kiefer, F.; Gallo Cassarino, T.; Bertoni, M.; Bordoli, L. SWISS-MODEL: Modelling protein tertiary and quaternary structure using evolutionary information. *Nucleic Acids Res.* **2014**, *42*, 252–258. [CrossRef] [PubMed]
39. Love, M.L.; Szebenyi, D.M.; Kriksunov, I.A.; Thiel, D.J.; Munshi, C.; Graeff, R.; Lee, H.C.; Hao, Q. ADP-ribosyl cyclase; crystal structures reveal a covalent intermediate. *Structure* **2004**, *12*, 477–486. [CrossRef] [PubMed]
40. Yano, A.; Miwa, Y.; Kanazawa, Y.; Ito, K.; Makino, M.; Imai, S.; Hanada, N.; Nisizawa, T. A novel method for enhancement of peptide vaccination utilizing T-cell epitopes from conventional vaccines. *Vaccine* **2013**, *31*, 1510–1515. [CrossRef] [PubMed]
41. Kuo, L.; Hurst-Hess, K.R.; Koetzner, C.A.; Masters, P.S. Analyses of coronavirus assembly interactions with interspecies membrane and nucleocapsid protein chimeras. *J. Virol.* **2016**, *90*, 4357–4368. [CrossRef] [PubMed]
42. Zhang, Z.; Chen, J.; Shi, H.; Chen, X.; Shi, D.; Feng, L.; Yang, B. Identification of a conserved linear B-cell epitope in the M protein of porcine epidemic diarrhea virus. *Virol. J.* **2012**, *9*. [CrossRef] [PubMed]
43. Xing, J.; Liu, S.; Han, Z.; Shao, Y.; Li, H.; Kong, X. Identification of a novel linear B-cell epitope in the M protein of avian infectious bronchitis coronaviruses. *J. Microbiol.* **2009**, *47*, 589–599. [CrossRef] [PubMed]
44. He, Y.; Zhou, Y.; Siddiqui, P.; Niu, J.; Jiang, S. Identification of immunodominant epitopes on the membrane protein of the severe acute respiratory syndrome-associated coronavirus. *J. Clin. Microbiol.* **2005**, *43*, 3718–3726. [CrossRef] [PubMed]
45. Laviada, M.D.; Videgain, S.P.; Moreno, L.; Alonso, F.; Enjuanes, L.; Escribano, J.M. Expression of swine transmissible gastroenteritis virus envelope antigens on the surface of infected cells: Epitopes externally exposed. *Virus Res.* **1990**, *16*, 247–254. [CrossRef]
46. De Diego, M.; Laviada, M.D.; Enjuanes, L.; Escribano, J.M. Epitope specificity of protective lactogenic immunity against swine transmissible gastroenteritis virus. *J. Virol.* **1992**, *66*, 6502–6508. [PubMed]
47. Rodak, L.; Smid, B.; Nevorankova, Z.; Valicek, L.; Smitalova, R. Use of monoclonal antibodies in blocking ELISA detection of transmissible gastroenteritis virus in faeces of piglets. *J. Vet. Med. B Infect. Dis. Vet. Public Health* **2005**, *52*, 105–111. [CrossRef] [PubMed]
48. Rottier, P.J.; Welling, G.W.; Welling-Wester, S.; Niesters, H.G.; Lenstra, J.A.; van der Zeijst, B.A. Predicted membrane topology of the coronavirus protein E1. *Biochemistry* **1986**, *25*, 1335–1339. [CrossRef] [PubMed]
49. Neuman, B.W.; Kiss, G.; Kunding, A.H.; Bhella, D.; Baksh, M.F.; Connelly, S.; Droese, B.; Klaus, J.P.; Makino, S.; Sawicki, S.G. A structural analysis of M protein in coronavirus assembly and morphology. *J. Struct. Biol.* **2011**, *174*, 11–22. [CrossRef] [PubMed]
50. Kuo, L.; Masters, P.S. Evolved variants of the membrane protein can partially replace the envelope protein in murine coronavirus assembly. *J. Virol.* **2010**, *84*, 12872–12885. [CrossRef] [PubMed]
51. Kuo, L.; Masters, P.S. Genetic evidence for a structural interaction between the carboxy termini of the membrane and nucleocapsid proteins of mouse hepatitis virus. *J. Virol.* **2002**, *76*, 4987–4999. [CrossRef] [PubMed]
52. Hurst, K.R.; Kuo, L.; Koetzner, C.A.; Ye, R.; Hsue, B.; Masters, P.S. A major determinant for membrane protein interaction localizes to the carboxy-terminal domain of the mouse coronavirus nucleocapsid protein. *J. Virol.* **2005**, *79*, 13285–13297. [CrossRef] [PubMed]
53. Verma, S.; Lopez, L.A.; Bednar, V.; Hogue, B.G. Importance of the penultimate positive charge in mouse hepatitis coronavirus A59 membrane protein. *J. Virol.* **2007**, *81*, 5339–5348. [CrossRef] [PubMed]

54. Luo, H.; Wu, D.; Shen, C.; Chen, K.; Shen, X.; Jiang, H. Severe acute respiratory syndrome coronavirus membrane protein interacts with nucleocapsid protein mostly through their carboxyl termini by electrostatic attraction. *Int. J. Biochem. Cell Biol.* **2006**, *38*, 589–599. [CrossRef] [PubMed]
55. He, R.; Leeson, A.; Ballantine, M.; Andonov, A.; Baker, L.; Dobie, F.; Li, Y.; Bastien, N.; Feldmann, H.; Strocher, U. Characterization of protein-protein interactions between the nucleocapsid protein and membrane protein of the SARS coronavirus. *Virus Res.* **2004**, *105*, 121–125. [CrossRef] [PubMed]
56. Fang, X.; Ye, L.; Timani, K.A.; Li, S.; Zen, Y.; Zhao, M.; Zheng, H.; Wu, Z. Peptide domain involved in the interaction between membrane protein and nucleocapsid protein of SARS-associated coronavirus. *J. Biochem. Mol. Biol.* **2005**, *38*, 381–385. [CrossRef] [PubMed]
57. Anton, I.M.; Gonzalez, S.; Bullido, M.J.; Corsin, M.; Risco, C.; Langeveld, J.P.; Enjuanes, L. Cooperation between transmissible gastroenteritis coronavirus (TGEV) structural proteins in the in vitro induction of virus-specific antibodies. *Virus Res.* **1996**, *46*, 111–124. [CrossRef]
58. Kirchdoerfer, R.N.; Cottrell, C.A.; Wang, N.; Pallesen, J.; Yassine, H.M.; Turner, H.L.; Corbett, K.S.; Graham, B.S.; McLellan, J.S.; Ward, A.B. Pre-fusion structure of a human coronavirus spike protein. *Nature* **2016**, *531*, 118–121. [CrossRef] [PubMed]
59. Belouzard, S.; Millet, J.K.; Licitra, B.N.; Whittaker, G.R. Mechanisms of coronavirus cell entry mediated by the viral spike protein. *Viruses* **2012**, *4*, 1011–1033. [CrossRef] [PubMed]
60. Gao, J.; Lu, G.; Qi, J.; Li, Y.; Wu, Y.; Deng, Y.; Geng, H.; Li, H.; Wang, Q.; Xiao, H. Structure of the fusion core and inhibition of fusion by a heptad repeat peptide derived from the S protein of Middle East respiratory syndrome coronavirus. *J. Virol.* **2013**, *87*, 13134–13140. [CrossRef] [PubMed]
61. Wicht, O.; Burkard, C.; de Haan, C.A.; van Kuppeveld, F.J.; Rottier, P.J.; Bosch, B.J. Identification and characterization of a proteolytically primed form of the murine coronavirus spike proteins after fusion with the target cell. *J. Virol.* **2014**, *88*, 4943–4952. [CrossRef] [PubMed]
62. Hofmann, H.; Hattermann, K.; Marzi, A.; Gramberg, T.; Geier, M.; Krumbiegel, M.; Kuate, S.; Uberla, K.; Niedrig, M.; Pohlmann, S. S protein of severe acute respiratory syndrome-associated coronavirus mediates entry into hepatoma cell lines and is targeted by neutralizing antibodies in infected patients. *J. Virol.* **2004**, *78*, 6134–6142. [CrossRef] [PubMed]
63. Chen, Z.; Zhang, L.; Qin, C.; Ba, L.; Yi, C.E.; Zhang, F.; Wei, Q.; He, T.; Yu, W.; Yu, J. Recombinant modified vaccinia virus Ankara expressing the spike glycoprotein of severe acute respiratory syndrome coronavirus induces protective neutralizing antibodies primarily targeting the receptor binding region. *J. Virol.* **2005**, *79*, 2678–2688. [CrossRef] [PubMed]
64. Risco, C.; Anton, I.M.; Sune, C.; Pedregosa, A.M.; Martín-Alonso, J.M.; Parra, F.; Carrascosa, J.L.; Enjuanes, L. Membrane protein molecules of transmissible gastroenteritis coronavirus also expose the carboxy-terminal region on the external surface of the virion. *J. Virol.* **1995**, *69*, 5269–5277. [PubMed]
65. Fan, J.H.; Zuo, Y.Z.; Shen, X.Q.; Gu, W.Y.; Di, J.M. Development of an enzyme-linked immunosorbent assay for the monitoring and surveillance of antibodies to porcine epidemic diarrhea virus based on a recombinant membrane protein. *J. Virol. Methods* **2015**, *225*, 90–94. [CrossRef] [PubMed]

© 2016 by the authors. Licensee MDPI, Basel, Switzerland. This article is an open access article distributed under the terms and conditions of the Creative Commons Attribution (CC BY) license (http://creativecommons.org/licenses/by/4.0/).

viruses

MDPI

Article

Antigenic and Biological Characterization of ORF2–6 Variants at Early Times Following PRRSV Infection

Alyssa B. Evans [1], Hyelee Loyd [1], Jenelle R. Dunkelberger [1], Sarah van Tol [1], Marcus J. Bolton [1], Karin S. Dorman [2], Jack C. M. Dekkers [1] and Susan Carpenter [1,*]

[1] Department of Animal Science, Iowa State University, Ames, IA 50011, USA; alyssa.ben.evans@gmail.com (A.B.E.); heri1008@iastate.edu (H.L.); jenelled@iastate.edu (J.R.D.); savantol@utmb.edu (S.v.T.); mjohnbolton@gmail.com (M.J.B.); jdekkers@iastate.edu (J.C.M.D.)

[2] Departments of Statistics and Genetics, Development and Cell Biology, Iowa State University, Ames, IA 50011, USA; kdorman@iastate.edu

* Correspondence: scarp@iastate.edu; Tel.: +1-515-294-5694

Academic Editors: Linda Dixon and Simon Graham
Received: 8 March 2017; Accepted: 24 April 2017; Published: 16 May 2017

Abstract: Genetic diversity of porcine reproductive and respiratory syndrome virus (PRRSV) challenges efforts to develop effective and broadly acting vaccines. Although genetic variation in PRRSV has been extensively documented, the effects of this variation on virus phenotype are less well understood. In the present study, PRRSV open reading frame (ORF)2–6 variants predominant during the first six weeks following experimental infection were characterized for antigenic and replication phenotype. There was limited genetic variation during these early times after infection; however, distinct ORF2–6 haplotypes that differed from the NVSL97-7895 inoculum were identified in each of the five pigs examined. Chimeric viruses containing all or part of predominant ORF2–6 haplotypes were constructed and tested in virus neutralization and in vitro replication assays. In two pigs, genetic variation in ORF2–6 resulted in increased resistance to neutralization by autologous sera. Mapping studies indicated that variation in either ORF2–4 or ORF5–6 could confer increased neutralization resistance, but there was no single amino acid substitution that was predictive of neutralization phenotype. Detailed analyses of the early steps in PRRSV replication in the presence and absence of neutralizing antibody revealed both significant inhibition of virion attachment and, independently, a significant delay in the appearance of newly synthesized viral RNA. In all pigs, genetic variation in ORF2–6 also resulted in significant reduction in infectivity on MARC-145 cells, suggesting variation in ORF2–6 may also be important for virus replication in vivo. Together, these data reveal that variation appearing early after infection, though limited, alters important virus phenotypes and contributes to antigenic and biologic diversity of PRRSV.

Keywords: PRRSV; genetic diversity; antigenic variation; replication phenotype; neutralization

1. Introduction

Porcine reproductive and respiratory syndrome virus (PRRSV) is a 15-kb positive-stranded RNA virus belonging to the family *Arteriviridae*, which emerged simultaneously in the United States and Europe in the late 1980s [1,2]. PRRSV is currently classified into two major genotypes that share clinical disease features but differ genetically and antigenically. Type I genotypes are mainly European strains, while Type II genotypes are found primarily in North America and Asia. PRRSV causes respiratory signs in growing pigs and spontaneous abortions in pregnant sows [3], with annual economic losses estimated to be $664 million in the United States alone [4]. Several vaccines have been developed against PRRSV; however, their effectiveness is limited by genetic heterogeneity among field isolates as well as by the continual emergence of antigenic and phenotypic variants [5].

Genetic variation can alter susceptibility to neutralizing antibody through antigenic variation in neutralizing epitopes and/or changes in *N*-linked glycosylation sites that mask, or shield, neutralizing epitopes [6–9]. Neutralizing epitopes have been identified in the major and minor PRRSV envelope proteins, which are encoded by open reading frame (ORF)2–6 [10,11]. ORF5 and ORF6 encode the major envelope proteins GP5 and M, respectively, which interact to form a heterodimer on the virion surface [11] that is believed to be important for attachment [12–15]. GP5 is highly variable and has long been thought to be the major target of neutralizing antibody [16–20]. Two regions of GP5 have been found to be important for neutralization [16,18,21], and recent studies suggest the neutralization epitope(s) is conformational, rather than linear [20,22,23]. A single tyrosine residue in the highly-conserved M protein was shown to mediate resistance to broadly neutralizing antibody [24]. ORF2–4 encode the minor envelope glycoproteins GP2, GP3, and GP4, respectively, which form an oligomer on the virion surface that interacts with the CD163 receptor [25–29]. Neutralizing antibodies are reported to target GP3 and M in Type II isolates, and GP3, GP4 and M in Type I isolates [8,30–32]. Nested within ORF2 and ORF5 are ORF2b and ORF5a, which encode the E and the 5a proteins, respectively [33,34]. Both proteins are minor components of the virion, but are not thought to be targets of neutralizing antibody [34,35].

Although neutralizing antibody has been shown to be important for PRRSV clearance [23,36–38], the mechanism(s) by which neutralizing antibody acts to inhibit productive virus replication is not known. PRRSV appears to utilize a variety of host cell receptors and viral glycoproteins for attachment, entry, and uncoating [15,39]. The primary site of PRRSV replication in vivo is differentiated porcine alveolar macrophages (PAM), although the virus can be propagated in vitro in the monkey kidney cell line MARC-145. Infection is initiated by low-affinity attachment to heparan sulfate, which is on the surface of both PAM and MARC-145. This interaction, which is mediated by the M protein in the GP5-M heterodimer [12,14], is neither sufficient nor necessary for productive infection. CD169, also referred to as sialoadhesion, facilitates internalization of the virus in PAM, but not in MARC-145 cells, which lack CD169 [14,40,41]. PRRSV is able to establish a productive infection in CD169-knockout pigs [42], demonstrating that CD169 is also not required for virus replication in vivo. In contrast, the scavenger receptor CD163 is absolutely required for PRRSV replication in vitro and in vivo [42,43], and is now recognized as the primary PRRSV receptor. CD163 is expressed in both the endosome and on the cell surface [44], interacts with GP2 and GP4 [28], and is thought to play an essential role in the process of uncoating [45,46]. Most recently, non-muscle myosin heavy chain protein 9 (MYH9) was reported to interact with GP5 and play an essential role at an early step in PRRSV entry [47]. The variety of viral glycoproteins reported to play key roles during the initial stages of PRRSV suggests that, similar to flaviviruses [48], neutralizing antibody may target multiple viral glycoproteins and act at multiple steps during the early stages of PRRSV replication.

Genetic variation in PRRSV can also lead to changes in biological phenotypes associated with replication and/or virulence, but few studies directly link genotype and phenotype. Genetic variation in both structural and non-structural proteins occurs during sequential passage of PRRSV in vitro, with resultant changes in virulence, immunogenicity, and rate of replication in vivo [49,50]. Increased knowledge as to how specific genetic changes alter virus phenotype can lead to a better understanding of the factors that shape variant selection in vivo. Towards that end, sera samples from five experimentally infected pigs collected at early times after infection were used to characterize ORF2–6 variation and determine the effects of variation on the antigenic and replication phenotype of PRRSV. Limited genetic variation was observed during the first six weeks after infection. However, predominant ORF2–6 haplotypes were identified in each pig which, using reverse genetics, were found to vary in antigenic and/or replication phenotype. These studies indicate that genetic variation arises early after infection and, though limited, alters important virus phenotypes that contribute to antigenic and biologic diversity of PRRSV.

2. Materials and Methods

2.1. Cells, Virus, and Pigs

MARC-145 cells used for virus passage and infection assays were maintained in high glucose (4500 mg/L) Dulbecco's Modified Eagle's Medium (DMEM) (Sigma-Aldrich Co., LLC., St. Louis, MO, USA) supplemented with 10% FBS, 100 U/mL penicillin, 100 μg/mL streptomycin, and 2 mM L-glutamine. MARC-145 cells used for electroporation were grown in low glucose (1000 mg/L) DMEM (Thermo Fisher Scientific, Waltham, MA, USA) supplemented with 10% FBS, 700 mg/L sodium bicarbonate, 100 U/mL penicillin, and 100 μg/mL streptomycin.

The inoculum virus, NVSL97-7895 (GenBank accession AY545985), was kindly provided by the PRRS Host Genetics Consortium (PHGC). Chimeric viruses were generated in the pFL12 infectious molecular clone backbone, which contains the genome consensus of the NVSL97-7895 inoculum virus [51]. The experimental infections and virus load data were previously described [52,53]. Sera samples from five pigs experimentally infected with NVSL97-7895 were obtained from the PHGC. Two of the pigs had maintained high levels of viremia throughout 35 days post-infection (dpi) (Figure 1A), and three pigs initially cleared the virus, but experienced a rebound in viremia by 42 dpi (Figure 1B).

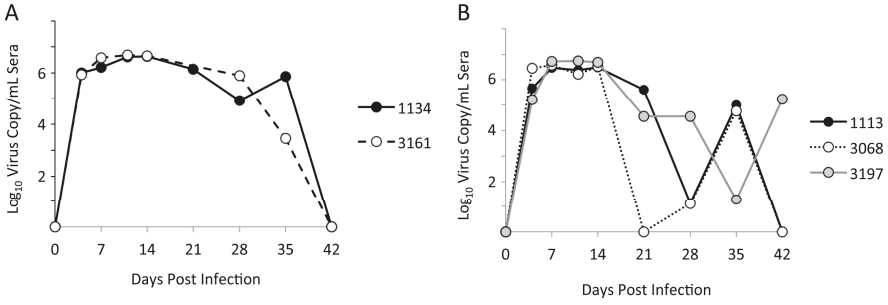

Figure 1. Viremia profiles in porcine reproductive and respiratory syndrome virus (PRRSV)-infected pigs: (**A**) Two pigs with prolonged viremia, as indicated by sustained virus loads $>10^3$ copies/mL sera through 35 days post-infection (dpi). (**B**) Three pigs with rebound viremia, indicated by an initial reduction of viremia, followed by greater than 100-fold increase in viremia.

2.2. Cloning and Sequencing PRRSV Variants

Viral RNA was isolated from the NVSL97-7895 inoculum and sera collected from experimentally infected pigs at seven dpi and at a high-viremic late dpi (Table 1) using the QIAamp Viral RNA Mini Kit according to manufacturer's instructions (Qiagen, Hilden, Germany). Viral RNA was converted to cDNA via random hexamer primers using the Superscript III first strand synthesis kit according to manufacturer's protocol (Invitrogen, Carlsbad, CA, USA). Approximately 3 kb from PRRSV ORF2–6 was amplified using PRRSV specific primers and high fidelity platinum Taq polymerase (Invitrogen). ORF2–6 was amplified with forward primer 5′ACCAGGTACCGGCCTGAATTGAAATGAAA and reverse primer 5′GGTTGAATTCGGTCAAGCATCTCCCCAAC. Four separate polymerase chain reactions (PCR) from each sample were pooled, purified, TA-cloned into pGEM-T Easy vectors (Promega, Madison, WI, USA) and transformed in Stbl2 *Escherichia coli* cells. Individual colonies were screened for the correct insert size, and positive clones were Sanger sequenced at the Iowa State University DNA Facility (Ames, IA, USA). The sequences were assembled using Phred and Phrap algorithms in MacVector. ORF2–6 was then separated into the individual genes (E, GP2, GP3, GP4, GP5, ORF5a, and M), and each gene was translated to the amino acid sequence. The nucleotide sequences

were compared via multiple sequence alignment (ClustalW, MacVector) to determine average pairwise identity and generate consensus sequences.

To visualize the variation in the sequences, we used the phyclust package (http://cran.r-project.org/web/packages/phyclust/, version 0.1-15) function plotdots, grouping sequences by pig and dpi. Nucleotide changes at each position relative to the consensus nucleotide in the inoculum are shown as colored dots, making it easy to visually identify both single nucleotide variants (SNVs) that appeared with high frequency as well as coordinated changes in variant distributions across multiple pigs.

Table 1. Summary of sequenced clones and ORF2–6 (open reading frame) variation.

Sample ID	Viremia Classification	Day Post Inoculation	Number Clones Sequenced [a]	Pairwise Identity [b]
Inoculum	N/A	0	25	99.71
1134	Prolonged	7	8	99.76
		28	21	99.63
3161	Prolonged	7	9	99.71
		28	28	99.72
1113	Rebound	7	9	99.71
		35	26	99.62
3068	Rebound	7	9	99.40
		35	31	99.78
3197	Rebound	7	10	99.49
		41	26	99.76
	Combined		202	99.57 [c]

[a] Number of individual clones sequenced from each sample. [b] Average nucleotide pairwise identity across all clones from a sample. [c] Average nucleotide pairwise identity across all clones sequenced from each gene region.

2.3. Identification of Viral Haplotypes

Multiple sequence alignments of the late dpi sample from each individual pig were used to construct viral haplotypes based on the late day virus of each pig. Due to the high mutation rate of the virus, unique single nucleotide changes occurred within most virus clones. Therefore, each haplotype included sites with a minor variant frequency of $\geq$25% as well as consensus changes from the inoculum that were shared between haplotypes within each individual pig. Each unique combination of nucleotides across the variable sites within a single pig's virus sample was designated a haplotype. The number of clones within a pig containing each unique haplotype was used to calculate the frequency of that haplotype. The haplotype within each pig present at the highest frequency was designated Haplotype A, and the haplotype present at the second highest frequency was designated Haplotype B. In the case where there was only a single, consensus haplotype, that haplotype is designated Haplotype C.

2.4. Construction of Chimeric Virus

Chimeric viruses containing the predominant ORF2–6 haplotypes were generated in the backbone of the infectious molecular clone pFL12 [51] using shuttle plasmids to facilitate swapping regions of pFL12 and the ORF2–6 haplotypes. The ORF2–6 sequences were selected from haplotypes existing in our library or synthesized (GeneArt, Thermo Fisher Scientific), inserted into the pFL12 backbone and transformed in DH5α *E. coli* cells. Chimeric viruses (designated with a "v" prior to the haplotype name, e.g., v3197A) were generated from the chimeric infectious clones via in vitro transcription and electroporation into MARC-145 cells, as described in [51]. Briefly, plasmid DNA was linearized by digestion with AclI and viral RNA was synthesized using the T7 Ultra mMESSAGE mMACHINE in vitro transcription kit (Ambion, Life Technologies, Carlsbad, CA, USA). Five μg of in vitro transcripts and 5 μg naïve MARC-145 cellular RNA were added to 2×10^6 MARC-145 cells in 400 μL DMEM containing 1.25% DMSO and electroporated at 250 V and 950 uF (GenePulser Xcell, Bio-Rad, Hercules, CA, USA). Electroporated cells were plated in a single well of a 6-well plate in 5 mL DMEM

supplemented with 10% fetal bovine serum (FBS), antibiotics, and 1.25% dimethyl sulfoxide (DMSO). At 18 h post transfection (hpt), media was replaced with 5 mL DMEM supplemented with 5% FBS and antibiotics. At 96 hpt, supernatants were harvested and cells were stained by immunocytochemistry to verify virus replication. Supernatants were passaged two to three times in MARC-145 cells to produce high titer chimeric virus stocks. All stocks were sequenced through ORF2–6 to confirm the correct haplotype sequence.

2.5. Virus Neutralization Assays

Neutralizing antibody assays were performed using a focus-reduction assay adapted from Wu et al. [54]. Briefly, sera was heat-inactivated, diluted, incubated for 1 h at 37 °C with 200 focus-forming units (FFU) of virus, and inoculated in duplicate or triplicate onto MARC-145 cells seeded the previous day in a 12-well plate at 3×10^5 cells/well. Cells and virus were incubated an additional 24 h at 37 °C in 5% CO_2, then the cells were fixed in ice-cold acetone:methanol and stained for PRRSV N protein by immunocytochemistry using the monoclonal antibody SDOW17 (RTI, LLC, Brookings, SD, USA) as the primary antibody and sheep anti-mouse IgG conjugated horse radish peroxidase (HRP) (Jackson ImmunoResearch, West Grove, PA, USA) as the secondary antibody. Following addition of the HRP substrate, cells were rinsed with distilled water, air-dried, and foci of infected cells enumerated by light microscopy. The percent reduction in FFU compared to a virus-only control was calculated as the percent neutralization. Assays were done in duplicate and repeated at least twice.

Autologous sera samples from PHGC pigs were kindly provided by Drs. J.K. Lunney and R.R.R. Rowland and Type II PRRSV broadly neutralizing antiserum was a gift from Harrisvaccines, Ames, IA, USA.

2.6. PRRSV Binding and Entry Assays

To assess binding/attachment of PRRSV to MARC-145 cells, vFL12 was incubated in the presence or absence of neutralizing antibody for 1 h at 37 °C. The antibody source was a 1:2 dilution of pooled sera collected at 42 dpi from ~200 pigs experimentally infected with NVSL97-7895. The pooled sera sample was found to neutralize 86% of vFL12 at 1:8 dilution. The samples were chilled on ice and inoculated onto MARC-145 cells at a multiplicity of infection (MOI) of 1, and cells were incubated at 4 °C for one hour to facilitate virion attachment, but not uptake into the cells. Following incubation, media was removed, cells were washed six times with media and bound virus was eluted by incubating cells in 300 µL trypsin-ethylenediaminetetraacetic acid (EDTA) (1X solution, Sigma Scientific) for 10 min at room temperature. Following the addition of 50 µL FBS, cells and supernatant were collected and separated by centrifugation. Virion RNA was isolated from the supernatant fraction using the QIAamp Viral RNA Mini kit (Qiagen) and RNA was quantified by reverse transcriptase quantitative PCR (RT-qPCR) using primers specific for PRRSV ORF7 RNA.

For entry and replication assays, PRRSV was incubated in the presence or absence of antisera and inoculated onto MARC-145 cells at 4 °C as described above. Following washing to remove unattached virions, fresh media was added and the cells were shifted to 37 °C, designated as time 0 h. At 1, 4, 8, 12, or 24 h, cells were treated with trypsin and pelleted by centrifugation as described above, and total RNA was isolated from the cell fraction with the RNeasy mini kit (Qiagen) and quantified by RT-qPCR as above. All assays were done in duplicate and repeated 2–3 times and results are reported as mean copy number of viral RNA/well.

2.7. Virus Replication Assays

Stocks of vFL12 and chimeric viruses were generated from p2 stocks by inoculation onto MARC-145 cells at an MOI of 0.001. Cells and virus were incubated 1 h at 37 °C at which time the inoculum was aspirated, cells washed two times and fresh media was added. Cells were washed again at 24 h post-infection, and p3 supernatant collected at 72 h post-infection was aliquoted and assayed for virus titer and virion copy number. Ten-fold serial dilutions of p3 stocks were inoculated

onto MARC-145 cells that had been seeded the previous day at 3×10^5 cells per well in 12-well plates. Following incubation at 37 °C for 24 h, cells were fixed in 50% acetone:50% methanol and foci of PRRSV infected cells were detected by immunocytochemistry as described above. Each FFU corresponds to a single infectious unit, and virus titer was calculated as FFU/mL of p3 stock. To determine virion copy number, RNA was isolated from p3 stocks using the QIAamp Viral RNA Mini Kit (Qiagen) and viral RNA was quantified using the VetMAX NA and EU PRRSV ORF7-specific RT-qPCR kit (Applied Biosystems, Thermo Fisher Scientific). Infectivity of each p3 stock is reported as the particle:infectivity ratio, calculated by dividing the least square mean for virus copy number by its corresponding least square mean for virus titer.

2.8. Statistical Analyses

A student's *t*-test was used to compare percent neutralization of vFL12 to each chimeric virus and to analyze viral copy number at each time point in the presence or absence of neutralizing antibody. Replication phenotypes were analyzed using SAS 9.4 (Statistical Analysis System Institute Inc., Cary, NC, USA). Virus copy number was analyzed using a mixed model with the fixed class effects of virus, dilution (3 levels: 1:10, 1:50, or 1:100), and their interaction. Experiment (four levels) was fitted as a random effect to account for experimental variation. Virus titer was analyzed using a mixed model with the fixed class effects of virus and technician (two levels) and experiment (eight levels) fitted as a random effect. For each virus, infectivity was calculated as the ratio of virus copy number to viral titer using least square means obtained from analysis of each trait separately. The standard error of infectivity was calculated as the standard deviation of copy number to viral titer divided by the square root of the number of samples collected on each virus. Pairwise comparisons between all viruses, and comparisons of vFL12 with each chimeric virus, were then assessed using a student's *t*-test.

For all analyses presented, a threshold of $p = 0.05$ was used to determine statistical significance.

2.9. Nucleotide Sequence Accession Numbers

The GenBank Accession numbers for the nucleotide sequences are KX286534-KX286735.

3. Results

3.1. Limited Genetic Variation at Early Times after Experimental PRRSV Infection

Sera samples from five pigs with detectable viremia at 5–6 weeks following experimental infection with NVSL97-7895 were used to analyze genetic variation in ORF2–6 at early times after infection. Viral RNA was isolated from the NVSL97-7895 inoculum and from sera samples collected at 7 dpi and at a late viremic day from each pig. Approximately 3 kb of ORF2–6 were amplified, TA-cloned, and up to 31 clones from each sample were sequenced. Multiple sequence alignments of all nucleotide sequences were generated by ClustalW to determine the amount of ORF2–6 variation in vivo (Table 1). In all pigs, the average pairwise identity within each sample was greater than 99%, similar to that observed in the starting inoculum. This high level of genetic identity revealed that very little genetic variation occurred in vivo during the six weeks following experimental PRRSV infection.

3.2. Location and Patterns of Genetic Variation in ORF2–6 at Early Times after Infection

Due to the sequential sampling times within pigs, we were able to observe changes in the frequency of single nucleotide variants (SNVs) across sampling days. To visualize variation, the ORF2–6 sequences from the NVSL97-7895 inoculum and each pig sample were aligned relative to the consensus sequence of the inoculum (Figure 2A). Variation was observed in all open reading frames and, with the exception of two changes that were observed in all pigs (Figure 2A, solid arrows), the sites of variation differed across pigs. Within each individual pig, we identified variable sites with dominant changes present in all clones in a given sample (Figure 2A, dashed arrows). Interestingly, several sites of variation within a given sample appeared to be linked (Figure 2A, arrowheads), raising

the possibility that effects of variation on viral phenotype may be influenced by epistatic interactions between/among different viral envelope proteins. In addition to changes at highly variable sites, there were numerous SNVs that were observed only in single clones, likely reflecting random variation. The most striking observations from these analyses was that virus variation was largely pig-specific and no single variant, or pattern of variation, clearly distinguished virus isolated from pigs with rebound viremia (1113, 3068, 3197) and virus from pigs with prolonged viremia (1134, 3161).

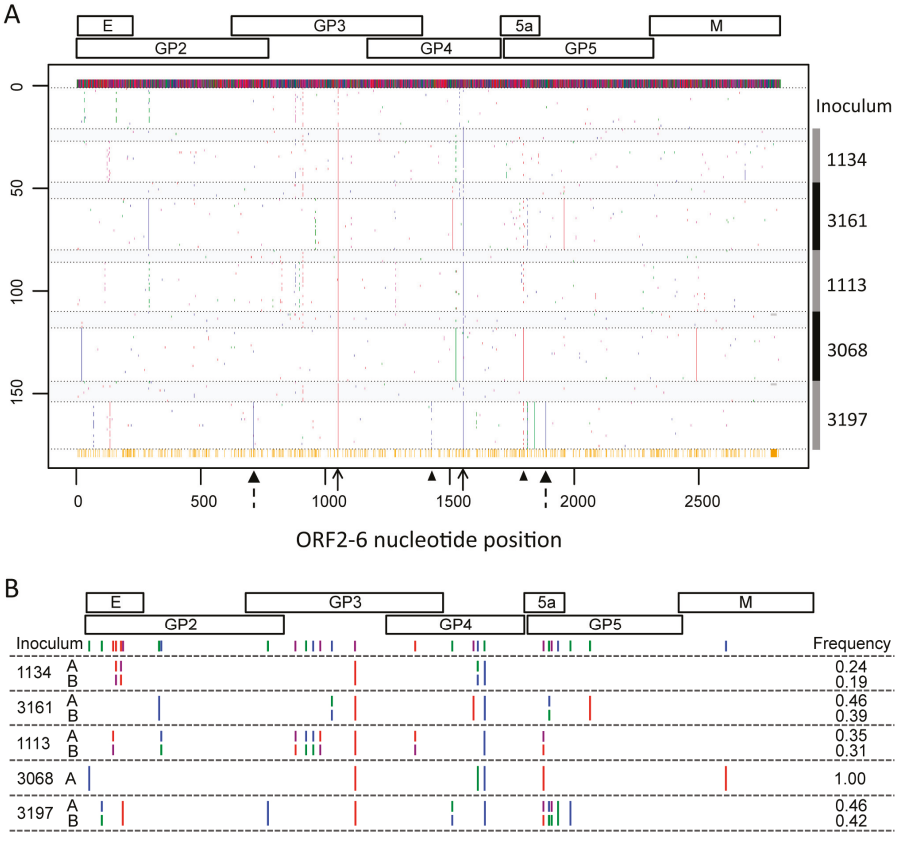

Figure 2. Variation in PRRSV open reading frame (ORF)2–6 following experimental infection. (**A**) ORF2–6 sequences are aligned to the consensus sequence of the inoculum (top line), with sites of variation from the inoculum consensus indicated by a colored dots. Sequences of individual clones are arranged vertically by inoculum and by pig (legend on the right). The dpi within a pig is separated by dotted horizontal lines, with seven dpi sequences shaded in gray. Numbers on the left denote the number of sequences aligned. Colors in the plot indicate nucleotide: A = green, G = blue, C = purple, T = red, and deletion = gray. Orange ticks at the bottom of the alignment indicate sites with at least one mutation across all clone sequences from all pigs, including possible deletions. Solid arrows denote sites of variation common across the majority of dpi and pigs. Dashed arrows indicate sites of variation within all clones in the late day sample from pig 3197. Arrowheads indicate linked sites of variation in late day sample from pig 3197. (**B**) Schematic of predominant ORF2–6 haplotypes constructed from the late day virus within each pig. Small colored ticks indicate sites where haplotypes differ from each other. Longer ticks indicate sites where haplotypes differ from the inoculum, but not from each other. Nucleotide colors are consistent with (A). The frequency of each haplotype is shown.

3.3. Identification of Pig-Specific ORF2–6 Haplotypes within Late Day Virus Populations

The major and minor PRRSV envelope proteins interact to form oligomeric complexes on the virion surface, and it is possible that variation at a particular site in one envelope protein may affect or constrain variation at a second site in the same or different envelope protein. Because we utilized single clone sequencing, where each clone represents a single viral genome, it was possible to identify linked sites of variation across ORF2–6 (Figure 2A). Based on these linked sites, we identified unique viral haplotypes, where a haplotype refers to the set of SNVs on an individual genome (Figure 2B). In four of the five pigs, two predominant haplotypes co-existed at relatively similar frequencies (Figure 2B), while a single haplotype representing the consensus sequence was found in pig 3068. In addition to the predominant haplotypes shown in Figure 2B, all samples contained minor haplotypes that were present at lower frequencies, and that often comprised combinations of the predominant haplotypes (not shown). Additional SNVs and haplotypes are present in the population, but were not detected using our sequencing strategy.

The non-synonymous SNVs and associated amino acid sequences for the predominant ORF2–6 haplotypes are shown in Tables S1 and S2 and in Figure 3. While some ORF2–6 SNVs were shared across virus samples in different pigs, the predominant haplotypes were pig-specific. Some haplotypes included SNVs that were detected in the inoculum and/or seven dpi samples, while other SNVs were present in only the late dpi sample (Tables S1 and S2). It is not known if the SNVs appearing only in late dpi samples arose de novo during the course of infection, or were present at low frequency in the inoculum. Importantly, none of the predominant haplotypes detected in late day viremic periods were observed in any of the inoculum clones. The fact that late day virus populations were characterized by the predominance of distinct haplotypes suggests that, although there was limited variation overall, the changes that did occur may be biologically important for virus replication at early times after infection.

3.4. Variation in ORF2–6 Increases Resistance to Neutralizing Antibody in Some, but Not All, Pigs

To investigate the possibility that limited genetic variation may nonetheless alter important virus phenotypes, the predominant ORF2–6 haplotypes from each of the five experimentally infected pigs were used to generate ORF2–6 chimeric viruses in the background of vFL12, which was derived from the NVSL97-7895 inoculum (Figure 4A, Table S3). Chimeric viruses were tested for effects of variation on antigenic and replication phenotypes that might contribute to virus replication in vivo. To ascertain if genetic variation altered susceptibility to virus neutralizing antibody, we first determined if any of the five experimentally infected pigs had developed detectable neutralizing antibody to the inoculum virus, NVSL97-7895, by 42 dpi (Figure 4B). Although no sera was able to neutralize 100% of the inoculum virus, three pigs (1113, 3068, and 3197) were able to neutralize over 75% of inoculum virus at a 1:8 serum dilution. In contrast, pigs 1134 and 3161 had no detectable neutralizing activity against the inoculum virus, even though they were both cleared of virus by 42 dpi. Of note, the pigs with detectable neutralizing activity were those three that experienced a rebound in viremia, raising the possibility that ORF2–6 haplotypes associated with rebound viremia could be immune escape variants. To explore this, chimeric viruses containing predominant ORF2–6 haplotypes from the three pigs with detectable neutralizing antibody to the inoculum virus were tested for sensitivity to neutralization by autologous serum collected the same day that rebound viremia was detected (Figure 4C). The pFL12 infectious molecular clone represents the consensus sequence of the inoculum virus, NVSL97-7895 [51], and neutralization of vFL12 was used as a reference in all neutralization assays. Due to the limited amount of pig sera available, all assays were done using a 1:4 or 1:8 dilution of autologous sera, which neutralized ~50% of vFL12.

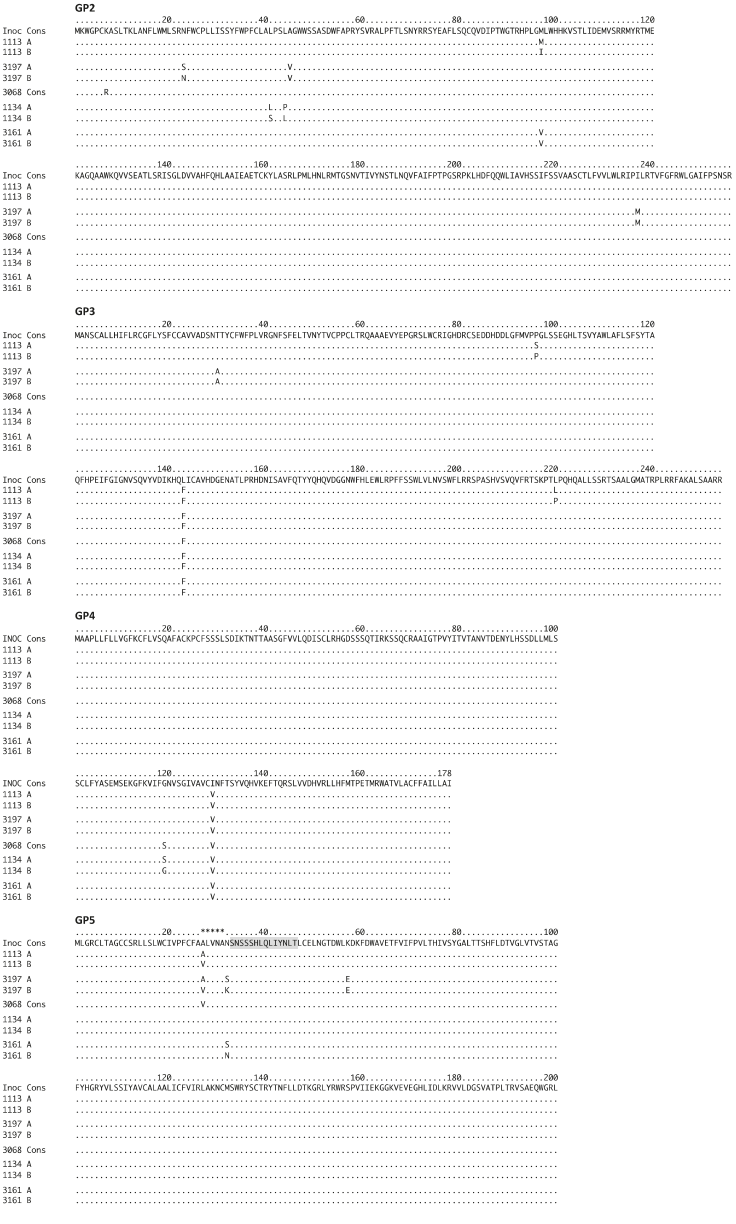

Figure 3. Amino acid sequence variation in the major and minor glycoproteins encoded by ORF2–6. The amino acid sequences of predominant haplotypes in the five experimentally-infected pigs are aligned to the consensus sequence of the inoculum. The amino acid is shown for sites where the haplotype differs from the inoculum and/or from each other. Dots (.) indicate an identical amino acid to the reference sequence in both haplotypes. Shaded area denotes location of reported neutralizing epitope in GP5 [16,18]. Asterisks in GP5 indicate location of the decoy epitope [36]. Numbering at the top of the alignment is based on translational start site of each glycoprotein.

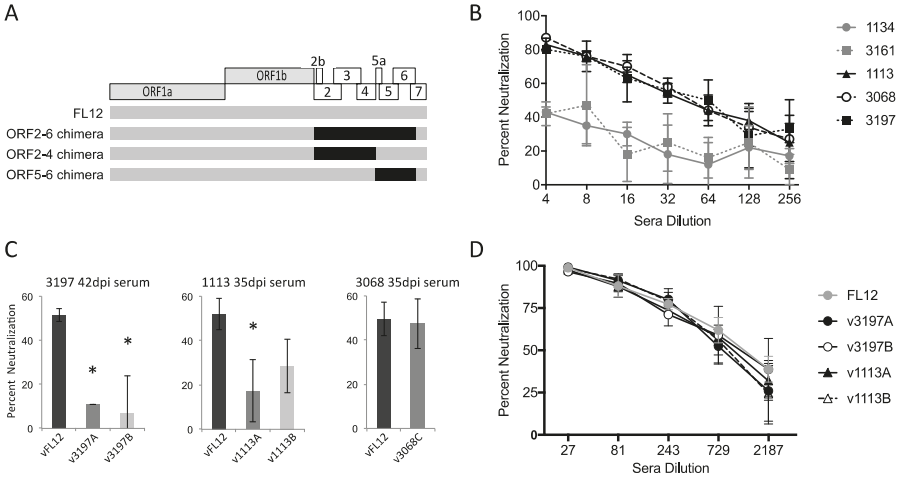

Figure 4. Neutralization phenotype of ORF2–6 haplotypes: (**A**) Schematic of chimeric viruses containing rebound haplotypes. (**B**) Virus neutralizing activity of 42 dpi pig sera from each of the five pigs against the inoculum virus. (**C**) Susceptibility of vFL12 and ORF2–6 chimeric viruses to neutralization by autologous sera diluted 1:4 (1113 and 3068) or 1:8 (3197). Asterisks indicate significant difference ($p < 0.05$) in neutralization compared to vFL12. (**D**) Susceptibility of vFL12 and ORF2–6 haplotype to neutralization by broadly neutralizing PRRSV anti-sera. Results denote the mean percent neutralization ± SD compared to a no-serum control.

In two of the three pigs with neutralizing antibody to the inoculum virus, predominant ORF2–6 haplotypes from rebound viremia were found to confer increased resistance to neutralization by autologous sera (Figure 4C). Chimeric viruses containing either haplotype A or haplotype B from pig 3197, designated v3197A or v3197B, were significantly more resistant to neutralization by autologous sera than was vFL12, with average neutralization of 11% ($p = 0.0002$) and 7% ($p \leq 0.001$), respectively. Chimeric virus containing haplotype A from pig 1113, v1113A, was also significantly more resistant to neutralization than vFL12 (average neutralizations of 18%, $p = 0.009$). Chimeric virus containing haplotype B from pig 1113, v1113B, showed increased resistance to neutralization, however this difference was only close to being significant (average neutralization of 29%, $p = 0.059$). In contrast, chimeric virus containing the single dominant ORF2–6 haplotype from pig 3068 (v3068C) was neutralized at levels similar to vFL12 (48%, $p = 0.8$). Each of the four chimeric viruses with increased resistance to autologous sera was also tested for sensitivity to neutralization using sera with broadly neutralizing activity against Type II PRRSV (Figure 4D). All were highly susceptible to broadly neutralizing sera, as was vFL12. Together, these results indicate that detectable neutralizing antibody is not required for control of viremia in PRRSV-infected pigs. However, in some, but not all pigs with neutralizing antibody to the inoculum virus, genetic changes in ORF2–6 can alter sensitivity to autologous, type-specific neutralizing antibody.

3.5. Variation in Either Major or Minor Envelope Glycoproteins Can Mediate Escape from Autologous Neutralizing Antibody

To identify the envelope protein(s) that contributed to increased resistance to neutralization by autologous sera, we generated a set of chimeric viruses in which the predominant haplotypes from pigs 3197 and 1113 were separated into their oligomeric units (Figure 4A, Table S3). None of these haplotypes contained amino acid changes in M (Table S1), so the chimeric virus designations include either 2–4 or 5 (Figure 5). As before, each of the chimeric viruses was tested for sensitivity to

neutralization by autologous sera, using vFL12 as a reference in all neutralization assays. In pig 3197, both v3197A-5 and v3197B-5 viruses were significantly more resistant to neutralization by autologous sera than vFL12, with average neutralizations of 29 and 6% (p = 0.035 and <0.001), respectively (Figure 5A). In contrast, chimeric viruses containing the ORF2–4 region (v3197A-2-4 and v3197B-2-4) were neutralized at levels similar to vFL12. Thus, increased resistance to neutralization in both v3197A and v3197B mapped to ORF5. There are three sites in GP5 at which the 3197A and/or 3197B haplotypes differ from vFL12: amino acid positions 27, 32, and 57 (Figure 3). An alanine is found at position 27 in vFL12 and in the 3197A haplotype, while 3197B contains a valine at this position. A K57E change is found in both 3197A and 3197B, and each haplotype differs from vFL12 at GP5 residue 32: 3197A contains an N32S mutation, while 3197B contains an N32K mutation. The N32K mutation is coincident with a Q36K change in protein 5a, which overlaps GP5 (Table S1). Protein 5a is a very minor component of the virion and previous studies found that immunization with 5a does not elicit neutralizing antibodies [34,35].

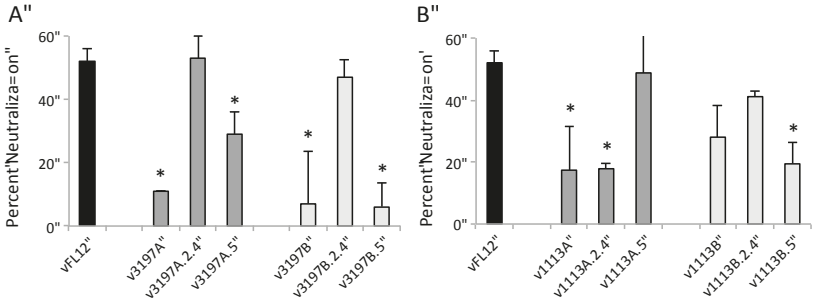

Figure 5. Mapping regions of ORF2–6 that confer resistance to autologous neutralizing antibody in (**A**) pig 3197 and (**B**) pig 1113. Two hundred focus-forming units (FFU) of vFL12 or chimeric viruses containing either ORF2–4 of ORF5 haplotypes were tested in neutralization assays using autologous sera. Results denote the mean percent neutralization ± standard deviation (SD) compared to a no-serum control. Asterisks (*) indicate significant reduction (p < 0.05) in percent neutralization as compared to vFL12.

In pig 1113, haplotypes A and B differed in respect to the region that mediated increased resistance to neutralization (Figure 5B). Chimeric virus v1113A-2-4 was neutralized at 18%, (p = 0.016) whereas v1113A-5 was neutralized at levels similar to vFL12, indicating that resistance to neutralization in the 1113A haplotype mapped to ORF2–4. In contrast, increased resistance of v1113B was mediated through ORF5: v1113B2-4 chimeric virus was neutralized at similar levels as vFL12 (41%, p = 0.2), but v1113-B-5 chimeric virus was significantly more resistant to neutralization (19%, p = 0.025) (Figure 5B). There are three sites in ORF2–4 where the 1113A haplotype differs from vFL12: P96S and L143F in GP3 and I129V in GP4. Two of these changes, GP3 L143F and GP4 I129V, were found in all pigs, whereas the GP3 P96S change was unique to the 1113A haplotype. The only amino acid difference between v1113B-5 and vFL12 is the A27V substitution in GP5 (Figure 3), indicating that a single point mutation can increase resistance to autologous neutralizing antibody.

Because of the limited variation in ORF2–6, it was of interest to determine if other single amino acid changes conferred resistance to autologous neutralizing antibody. Viruses were generated that contained unique amino acid changes found only in neutralization resistant haplotypes: GP3 P96S, GP5 N32K, or GP5 K57E. Individually, none of these single amino acid changes resulted in increased resistance to autologous neutralizing antibody (not shown). The GP5 A27V substitution was found in predominant genotypes from all three pigs that had neutralizing antibody to the inoculum virus (1113, 3197, 3068) (Figure 3). As noted above, the GP5 A27V substitution alone was sufficient to confer resistance to neutralization by pig 1113 autologous sera (Figure 5B); however, this was not true for

3197 autologous sera (data not shown). In addition, the presence of GP5 A27V in the 3068C haplotype did not confer resistance to 3068 neutralizing sera (Figure 4C). In most cases, therefore, resistance or sensitivity to neutralization depended on a combination of amino acid changes that were unique to each haplotype, and to each pig. Importantly, there was no single amino acid change that was predictive of neutralization phenotype.

Overall, results of these mapping studies revealed that variation in ORF2–4 or ORF5 could, independently, confer increased resistance to neutralization. Because the minor and major glycoproteins are believed to play different and/or distinct roles during early stages of virus replication [15,45,55], these findings raise the possibility that PRRSV is susceptible to neutralization at multiple steps in the virus replication cycle.

3.6. The Effects of Neutralizing Antibody at Early Steps in the PRRSV Replication Cycle

Mapping studies indicated that targets of virus-neutralizing antibody include both the major and minor glycoprotein complexes. To better understand how variation in PRRSV glycoproteins contributes to increased resistance to neutralization, we quantified the effects of neutralizing antibody at early steps in PRRSV replication (Figure 6). For these assays, we used pooled sera collected at 42 dpi from ~200 pigs experimentally infected with NVSL 97-7895. This sera is expected to have broad specificity, and was found to neutralize all chimeric viruses at similar titers (data not shown). Binding/attachment of PRRSV to MARC-145 cells was significantly reduced in the presence of virus-neutralizing antibody ($p < 0.05$) (Figure 6A). Following entry, detectable virus RNA decreased in both treatment groups from 1–4 h post-entry, indicative of the eclipse phase of virus replication. In the absence of antibody, production of new virion RNA occurred between 4 and 8 h post-entry and rapidly increased through 24 h post-entry. In the presence of neutralizing antibody, however, newly synthesized viral RNA was not detected until after 8 h post-entry, after which time the rate of increase in viral RNA was similar to that seen in the absence of antibody. The delayed appearance of newly synthesized RNA was not merely a consequence of reduced virion attachment, as the cells that were infected at different MOIs showed similar kinetics during the eclipse phase, and synthesis of viral RNA was always initiated between 4 and 8 h post-entry (Figure 6B). In addition to blocking attachment, therefore, neutralizing antibody also targets a post-entry step in virus replication that occurs between 4 and 8 h post-entry. It is not clear from these data which of the viral proteins are targeted at the attachment and/or post-entry steps in virus replication. Nonetheless, these data provide support for the mapping results indicating that virus-neutralizing antibody may target both the major and minor glycoproteins to inhibit multiple steps during early stages of PRRSV infection.

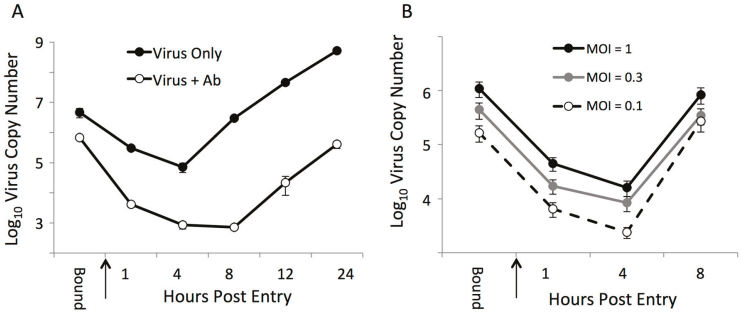

Figure 6. The effect of neutralizing antibody at early stages of PRRSV replication. Quantitation of PRRSV vFL12 binding and entry: (**A**) in the presence and absence of neutralizing antibody; and (**B**) in cells inoculated at varying multiplicity of infection (MOI). Bound represents the RNA copy number present in attached virions after incubation at 4 °C, and the arrow indicates time 0, when cells were shifted to 37 °C. Results denote the mean virus copy number per well ± standard error of the mean (SEM).

3.7. The Effect of ORF2–6 Variation on PRRSV Replication Phenotype

The result of our immunological analyses indicated that variation in ORF2–6 can result in antigenic variation and increased resistance to neutralization by autologous sera. However, this was not the case in three of the five pigs, two of which (1134 and 3161) had no detectable neutralizing antibody to the inoculum virus. Variation in ORF2–6 has been shown to occur during sequential in vitro passage and attenuation of PRRSV [49,50], and it is possible that some of the observed variation in ORF2–6 altered virus replication phenotype. To explore this, stocks of chimeric viruses were assayed for virus titer and virion copy number (Figure S1) and the particle: infectivity ratio was calculated for each of the chimeric viruses (Figure 7). Genetic variation in ORF2–6 resulted in significant differences in infectivity on MARC-145 cells (Figure S1). Most notably, vFL12 was significantly more infectious for MARC-145 cells than all of the chimeric viruses that contained ORF2–6 ($p < 0.0005$), ORF2–4 ($p < 0.05$) and two of the viruses that contained ORF5–6 (1113B-5 and 3068C-5, $p < 0.05$) haplotypes from experimentally infected pigs. Within each haplotype, the least infectious viruses were usually those that contained the complete ORF2–6 haplotype (Figure 7A). It is likely, therefore, that ORF2–6 variation early after experimental infection includes changes that increased adaptation to replication in vivo at a cost for replication in cell lines such as MARC-145. In support of this, the two amino acid changes shared by all predominant haplotypes, GP3 L143F and GP4 I129V (Figure 3), occurred at sites previously reported to vary during serial in vitro passage and/or attenuation of PRRSV field strains [49].

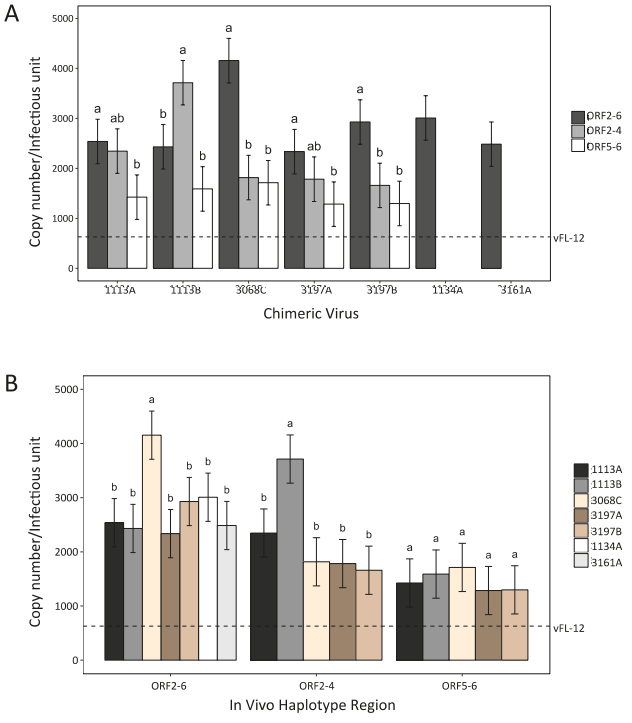

Figure 7. Infectivity of ORF2–6 chimeric viruses on MARC-145 cells: (**A**) The effect of ORF2–6 regions from different haplotypes on infectivity of MARC-145 cells. Within a haplotype, different letter assignments significantly differ at $p < 0.05$. (**B**) Comparison of infectivity on MARC-145 cells among chimeric viruses containing different ORF2–6 haplotypes, or regions within the ORF2–6 haplotypes. Within each group (ORF2–6, ORF2-4, and ORF5-6), viruses with different letter assignments significantly differ at $p < 0.05$. Dotted line indicates the infectivity of vFL12.

Few significant differences in infectivity were observed across the different haplotypes (Figure 7B). Haplotypes that were predominant in pigs with rebound viremia (1113, 3068, 3197) had similar infectivity as haplotypes from pigs with prolonged viremia (1134, 3161). The A and B haplotypes that were predominant in pigs 1113 and 3197 showed no differences in infectivity, and differences in infectivity among chimeric viruses were not associated with differences in the neutralization phenotype of the virus.

4. Discussion

Genetic diversity of porcine reproductive and respiratory syndrome virus (PRRSV) confounds efforts to develop effective and broadly acting vaccines. Genetic variation may lead to changes in virus phenotypes that are important in replication, immune evasion, host cell tropism and/or transmissibility; however, few studies directly link PRRSV genotype and phenotype. Here, sera samples from five experimentally infected pigs collected at early times after infection were used to characterize ORF2–6 variation and determine the effects of variation on the antigenic and replication phenotype of PRRSV. Limited genetic variation was observed during the first six weeks after infection. However, predominant ORF2–6 haplotypes were identified in each pig which, using reverse genetics, were found to vary in antigenic and/or replication phenotype. In some but not all pigs, genetic changes in ORF2–4 and/or ORF5 resulted in increased resistance to autologous, type-specific neutralizing antibody. Resistance or sensitivity to neutralization depended on a combination of amino acid changes that were unique to each pig, and there was no single amino acid change that was predictive of neutralization phenotype. Rather, results suggest that virus-neutralizing antibody may target both the major and minor glycoproteins to inhibit multiple steps at early stages of PRRSV replication. In all five pigs, genetic variation in ORF2–6 resulted in significant reduction in infectivity on MARC-145 cells, suggesting variation in ORF2–6 may also be important for virus replication in vivo. Together, these data reveal that variation appearing early after infection alters important virus phenotypes and contributes to antigenic and biologic diversity of PRRSV.

In two of the five pigs, chimeric viruses that contained ORF2–6 haplotypes that were predominant during a period of rebound viremia conferred increased resistance to neutralization by autologous sera that neutralized the inoculum virus. These findings provide experimental evidence that immune pressure by neutralizing antibody can alter the neutralization phenotype of PRRSV in vivo. Immune escape from neutralizing antibody has been previously associated with genetic changes in GP4 and GP5 of Type I and Type II PRRSV, respectively [9,56,57]. Costers et al. [9,56] identified amino acid substitutions in the GP4 neutralizing epitope of Type I strains that arose during immune selection in vitro or in vivo, and resulted in immune escape. Type II strains do not contain an analogous GP4 neutralizing epitope, but a neutralizing epitope has been identified in the GP5 ectodomain of Type II stains [16,18]. However, strong evidence that amino acid substitutions in this epitope give rise to immune escape variants in vivo is lacking [58]. Amino acid substitutions at positions 102 and 105 in the C-terminal region of GP5 occur following immune selection in vivo [21,57], and it was suggested that the GP5 neutralizing epitope may be conformational, rather than linear [23,57]. In the present study, changes within neutralization epitopes did not always lead to increased resistance to neutralization, and occurred in pigs that lacked detectable neutralizing antibody (i.e., pig 3161). In the three pigs with neutralizing antibody, amino acid substitutions were found at A27 and/or N32 in GP5. These sites are located in the GP5 ectodomain, and variation at these positions can alter GP5 peptide signal processing or *N*-linked glycosylation [6,7,16,59]. In addition, a recent study identified these positions as sites of diversifying selection early after PRRSV infection [60], suggesting these sites may be targets of immune selection. However, amino acid substitutions A27 and/or N32 in GP5 were present in both neutralization-resistant and neutralization-sensitive ORF2–6 haplotypes (Figure 3), indicating that variation at these sites was not predictive of neutralization phenotype. A single A27V substitution in GP5 led to increased neutralization resistance in the v1113B haplotype, but this was not the case with other ORF2–6 haplotypes. Indeed, with the exception of GP5 A27V in 1113B, no single amino acid

change analyzed was sufficient to confer increased neutralization resistance. Therefore, sensitivity or resistance to neutralization appeared to depend on the repertoire of amino acid substitutions, rather than the presence of a single amino acid substitution. Importantly, the repertoire and pattern of amino acid substitutions in ORF2–6 was different in each of the five pigs and was independent of the presence or absence of neutralizing antibody. A consequence of the unique, pig-specific patterns of neutralization resistance is a lack of robustness. All ORF2–6 haplotypes that increased resistance to concomitant autologous sera were easily neutralized by broadly neutralizing sera (Figure 4D), pooled sera, or by autologous sera collected later in infection (not shown). The presence of high-titered, cross-reacting neutralizing antibody in commercial sows [61] suggests that, over time, exposure to increasingly diverse virus populations in vivo can result in a stronger, broader, and more effective host immune response to PRRSV.

Models of the early steps of PPRSV replication were originally developed by analysis of virus replication in macrophages in vitro [15]. In these models, the initial steps of attachment and internalization are mediated by interactions between the GP5/M heterodimer and attachment factors on the cell surface, including heparan sulfate and CD169. The initial interactions are thought to enhance binding of the GP 2/3/4 trimer to the primary PRRSV receptor, CD163, which is located on both the cell surface and in the endosome. Based on these models, neutralizing antibody targeted to GP5 would be predicted to inhibit attachment and entry, whereas antibody targeted to GP2/3/4 would inhibit later steps in replication, including fusion and/or uncoating. In our studies, comparison of PRRSV replication in the presence and absence of neutralizing antibody revealed a modest but significant block in attachment. In addition, there was a delay in the appearance of newly synthesized viral RNA, with significantly reduced levels of virus RNA through 24 h post-entry. The delay in synthesis of viral RNA was not due to lower levels of attachment, indicating that neutralizing antibody can also inhibit a second, post-entry step in PRRSV replication. The antisera used in these assays was pooled sera collected from ~200 pigs at 42 days after infection with NVSL97-7895, the same inoculum used in the five pigs analyzed in this study. It is expected that the targets of neutralizing antibody in this pool would be similar to what we observed in pigs 1113 and 3197, and include both the major and minor envelope glycoproteins. Based on models of PRRSV entry cited above, it is tempting to speculate that antibody targeted to GP5 inhibited attachment, while the post-entry inhibition was due to antibody targeted to GP2/3/4. A caveat to this interpretation is that MARC-145 cells do not express CD169, and CD169 was recently shown to be dispensable for PRRSV replication in vivo [42]. It is possible that antibody targeted to GP5 blocks interaction with another cellular protein important in virus replication. For example, a recent study reported that MYH9 interacts with GP5 and is an essential factor in PRRSV replication [47]. Due to the limited amount of available sera, we are unable to explore these possibilities using our panel of chimeric viruses and autologous sera. The finding that PRRSV-infected pigs generate a neutralizing antibody response that targets both GP5 and GP2/3/4, and one that inhibits multiple stages in early virus replication, may motivate additional studies to delineate mechanism(s) by which neutralizing antibody inhibits PRRSV replication.

In vivo fitness of PRRSV within an individual host, or herd, depends on a number of interacting factors, including replication fitness, immune evasion, cell tropism, and transmissibility. Experimental analyses of replication fitness can be measured in vivo, but most studies rely on in vitro surrogates, such as replicative capacity and/or infectivity in cell culture. An added complication is the limited cell tropism of PRRSV. Replication of PRRSV in vitro is limited to differentiated macrophages such as porcine alveolar macrophages (PAM) or MARC-145 and other MA104-derived monkey kidney cell lines. Primary PAM cultures can be established in vitro, but the cultures are short lived and there is great heterogeneity within and between different PAMs that confounds reproducibility of experimental results. These difficulties have contributed to our limited knowledge regarding the link between PRRSV genotype and replication phenotype. Some insight has been gained by characterizing viral populations during sequential passage of field isolates in vitro. Sequence analysis of viral population at different passage levels, as well as comparisons among different attenuated vaccine viruses with

their parental strains, has revealed common sites of amino acid variation that arose during in vitro selection [49,50]. Based on these analyses, it is likely that at least some of the ORF2–6 variation observed in this study reflects selection for replication in vivo. Two amino acid substitutions in ORF2–6 were observed in all five of the experimentally infected pigs: GP3 L143F and GP4 I129V. In both cases, the change resulted in reversion to an amino acid found in field strains PRRSV [49]. Moreover, chimeric viruses containing ORF2–6 haplotypes from each of the five pigs were found to be significantly less infectious for MARC-145 cells than vFL12, and mapping studies revealed that changes in either or both major and minor glycoproteins contributed to replication phenotype in MARC-145 cells. It is not clear how the specific substitutions in GP3 and GP4 affect PRRSV replication phenotype, or what other changes observed in ORF2–6 might contribute to virus replication in vivo. It is possible that one selective factor is cell tropism [62]. As noted above, MARC-145 cells lack the CD169 receptor found in PAM, and in vitro passage selects for viruses able to replicate in the absence of CD169. Although CD169 is not required for PRRSV replication in vivo, the presence of both receptors enhances in vitro replication of Type I PRRSV strains [45]. Some of the observed variation in ORF2–6 may reflect genetic adaptations to virus replication in the presence or absence of CD169.

Genetic diversity is a hallmark of PRRSV infection in vivo, and it was not surprising to find SNVs in all proteins encoded by ORF2–6. For the most part, sites of variation differed across pigs; however, within individual pigs, we observed highly variable sites in all, or nearly all, sequenced clones. In four of the five pigs analyzed, predominant haplotypes co-existed, indicative of the quasispecies population structure of PRRSV in vivo. Within a quasispecies, interactions between or within variant genomes collectively contribute to the overall characteristics that impact virus evolution and pathogenesis. In an effort to capture potential interactions within/between PRRSV ORF2–6 genotypes, we chose to clone and sequence individual viral genomes, rather than use high-throughput sequencing platforms that yield shorter read lengths. An advantage of our approach was the ability to discern distinct viral haplotypes that co-existed within an individual pig. Moreover, using reverse genetics, we demonstrated that individual haplotypes could have different, and potentially complementary, phenotypes predicted to enhance virus replication in vivo. It is not practical to phenotype each individual genotype within a viral quasispecies, and we recognize the limitations of sampling and characterizing only the predominant genotypes. It is hoped that continued progress in defining links between PRRSV genotype and biologically significant phenotypes, together with rapid advances in high-throughput sequencing technologies and computational tools, will increase our understanding of genetic and phenotypic diversity in PRRSV and aid efforts to control this significant swine pathogen.

Supplementary Materials: The following are available online at www.mdpi.com/1999-4915/9/5/113/s1. Figure S1: Replication phenotype of chimeric virus containing predominant ORF2–6 haplotypes. Table S1: Amino Acid changes in ORF2–6 haplotypes from late day samples from pigs with rebound viremia. Table S2: Amino acid changes in ORF2–6 haplotypes predominant in late day samples from pigs with prolonged viremia. Table S3: List of chimeric viruses assayed for neutralization and/or replication phenotype.

Acknowledgments: This work was partially supported by National Pork Board project 12-173 and 14-222. A.B.E. was supported by USDA, NIFA, HEP, 2011-38420-20050. The authors thank the following for generously providing samples and reagents: Raymond R. R. Rowland and Joan Lunney for providing the NVSL 97-7895 inoculum virus and sera samples from PHGC trials; Mark Mogler and Harrisvaccines for the PRRSV Type II broadly neutralizing antisera; Fernando A. Osorio and Asit K. Pattnaik for pFL12 clone. We also thank Byung Kwon for advice in construction of chimeric infectious clones and Miranda Kapfer for assistance in preparing the manuscript.

Author Contributions: A.B.E. and S.C. conceived and designed the study, analyzed data, and wrote and revised the article and approved the final version. A.B.E. also designed and executed experimental procedures. H.L. contributed to experimental design, collected and analyzed data, edited the article and approved the final version. J.R.D. and K.S.D. contributed to analysis of data, edited the article and approved the final version. S.V.T. and M.J.B. performed laboratory work, edited the article and approved the final version. J.C.M.D. contributed to study design, revised and edited the article, and approved the final version. S.C. and A.B.E. are responsible for the integrity of the work as a whole.

Conflicts of Interest: The authors declare no conflict of interest.

References

1. Wensvoort, G.; Terpstra, C.; Pol, J.M.A.; ter Laak, E.A.; Bloemraad, M.; de Kluyver, E.P.; Kragten, C.; van Buiten, L.; den Besten, A.; Wagenaar, F.; et al. Mystery swine disease in The Netherlands: The isolation of Lelystad virus. *Vet. Q.* **1991**, *13*, 121–130. [CrossRef] [PubMed]
2. Loula, T. Mystery Pig-Disease. *Agri-Practice* **1991**, *12*, 23–34.
3. Collins, J.E.; Benfield, D.A.; Christianson, W.T.; Harris, L.; Hennings, J.C.; Shaw, D.P.; Goyal, S.M.; McCullough, S.; Morrison, R.B.; Joo, H.S.; et al. Isolation of swine infertility and respiratory syndrome virus (Isolate ATCC VR-2332) in North America and experimental reproduction of the disease in gnotobiotic pigs. *J. Vet. Diagn. Investig.* **1992**, *4*, 117–126. [CrossRef] [PubMed]
4. Holtkamp, D.J.; Kliebenstein, J.B.; Zimmerman, J.J.; Neumann, E.; Rotto, H.; Yoder, T.K.; Wang, C.; Yeske, P.; Mowrer, C.L.; Haley, C. *Economic Impact of Porcine Reproductive and Respiratory Syndrome Virus on U.S. Pork Producers*; Animal Industry Report 2012; AS 658; Iowa State University: Ames, IA, USA, 2012.
5. Kimman, T.G.; Cornelissen, L.A.; Moormann, R.J.; Rebel, J.M.; Stockhofe-Zurwieden, N. Challenges for porcine reproductive and respiratory syndrome virus (PRRSV) vaccinology. *Vaccine* **2009**, *27*, 3704–3718. [CrossRef] [PubMed]
6. Ansari, I.H.; Kwon, B.; Osorio, F.A.; Pattnaik, A.K. Influence of *N*-linked glycosylation of porcine reproductive and respiratory syndrome virus GP5 on virus infectivity, antigenicity, and ability to induce neutralizing antibodies. *J. Virol.* **2006**, *80*, 3994–4004. [CrossRef] [PubMed]
7. Faaberg, K.S.; Hocker, J.D.; Erdman, M.M.; Harris, D.L.; Nelson, E.A.; Torremorell, M.; Plagemann, P.G. Neutralizing antibody responses of pigs infected with natural GP5 *N*-glycan mutants of porcine reproductive and respiratory syndrome virus. *Viral Immunol.* **2006**, *19*, 294–304. [CrossRef] [PubMed]
8. Kim, W.I.; Yoon, K.J. Molecular assessment of the role of envelope-associated structural proteins in cross neutralization among different PRRS viruses. *Virus Genes* **2008**, *37*, 380–391. [CrossRef] [PubMed]
9. Costers, S.; Lefebvre, D.J.; Van Doorsselaere, J.; Vanhee, M.; Delputte, P.L.; Nauwynck, H.J. GP4 of porcine reproductive and respiratory syndrome virus contains a neutralizing epitope that is susceptible to immunoselection in vitro. *Arch. Virol.* **2010**, *155*, 371–378. [CrossRef] [PubMed]
10. Meulenberg, J.J.; Petersen-den Besten, A.; De Kluyver, E.P.; Moormann, R.J.; Schaaper, W.M.; Wensvoort, G. Characterization of proteins encoded by ORFs 2 to 7 of Lelystad virus. *Virology* **1995**, *206*, 155–163. [CrossRef]
11. Mardassi, H.; Massie, B.; Dea, S. Intracellular synthesis, processing, and transport of proteins encoded by ORFs 5 to 7 of porcine reproductive and respiratory syndrome virus. *Virology* **1996**, *221*, 98–112. [CrossRef] [PubMed]
12. Delputte, P.L.; Vanderheijden, N.; Nauwynck, H.J.; Pensaert, M.B. Involvement of the matrix protein in attachment of porcine reproductive and respiratory syndrome virus to a heparinlike receptor on porcine alveolar macrophages. *J. Virol.* **2002**, *76*, 4312–4320. [CrossRef] [PubMed]
13. Snijder, E.J.; Dobbe, J.C.; Spaan, W.J.M. Heterodimerization of the two major envelope proteins is essential for arterivirus infectivity. *J. Virol.* **2003**, *77*, 97–104. [CrossRef] [PubMed]
14. Delputte, P.L.; Costers, S.; Nauwynck, H.J. Analysis of porcine reproductive and respiratory syndrome virus attachment and internalization: Distinctive roles for heparan sulphate and sialoadhesin. *J. Gen. Virol.* **2005**, *86*, 1441–1445. [CrossRef] [PubMed]
15. Van Breedam, W.; Delputte, P.L.; Van Gorp, H.; Misinzo, G.; Vanderheijden, N.; Duan, X.; Nauwynck, H.J. Porcine reproductive and respiratory syndrome virus entry into the porcine macrophage. *J. Gen. Virol.* **2010**, *91*, 1659–1667. [CrossRef] [PubMed]
16. Ostrowski, M.; Galeota, J.A.; Jar, A.M.; Platt, K.B.; Osorio, F.A.; Lopez, O.J. Identification of neutralizing and nonneutralizing epitopes in the porcine reproductive and respiratory syndrome virus GP5 ectodomain. *J. Virol.* **2002**, *76*, 4241–4250. [CrossRef] [PubMed]
17. Wissink, E.H.J. The major envelope protein, GP5, of a European porcine reproductive and respiratory syndrome virus contains a neutralization epitope in its *N*-terminal ectodomain. *J. Gen. Virol.* **2003**, *84*, 1535–1543. [CrossRef] [PubMed]
18. Plagemann, P.G.; Rowland, R.R.; Faaberg, K.S. The primary neutralization epitope of porcine respiratory and reproductive syndrome virus strain VR-2332 is located in the middle of the GP5 ectodomain. *Arch. Virol.* **2002**, *147*, 2327–2347. [CrossRef] [PubMed]

19. Plagemann, P.G. Neutralizing antibody formation in swine infected with seven strains of porcine reproductive and respiratory syndrome virus as measured by indirect ELISA with peptides containing the GP5 neutralization epitope. *Viral Immunol.* **2006**, *19*, 285–293. [CrossRef] [PubMed]
20. Li, J.; Murtaugh, M.P. Dissociation of porcine reproductive and respiratory syndrome virus neutralization from antibodies specific to major envelope protein surface epitopes. *Virology* **2012**, *433*, 367–376. [CrossRef] [PubMed]
21. Delisle, B.; Gagnon, C.A.; Lambert, M.E.; D'Allaire, S. Porcine reproductive and respiratory syndrome virus diversity of Eastern Canada swine herds in a large sequence dataset reveals two hypervariable regions under positive selection. *Infect. Genet. Evol.* **2012**, *12*, 1111–1119. [CrossRef] [PubMed]
22. Vanhee, M.; Van Breedam, W.; Costers, S.; Geldhof, M.; Noppe, Y.; Nauwynck, H. Characterization of antigenic regions in the porcine reproductive and respiratory syndrome virus by the use of peptide-specific serum antibodies. *Vaccine* **2011**, *29*, 4794–4804. [CrossRef] [PubMed]
23. Loving, C.L.; Osorio, F.A.; Murtaugh, M.P.; Zuckermann, F.A. Innate and adaptive immunity against porcine reproductive and respiratory syndrome virus. *Vet. Immunol. Immunopathol.* **2015**, *167*, 1–14. [CrossRef] [PubMed]
24. Trible, B.R.; Popescu, L.N.; Monday, N.; Calvert, J.G.; Rowland, R.R. A single amino acid deletion in the matrix protein of porcine reproductive and respiratory syndrome virus confers resistance to a polyclonal swine antibody with broadly neutralizing activity. *J. Virol.* **2015**, *89*, 6515–6520. [CrossRef] [PubMed]
25. Van Nieuwstadt, A.P.; Meulenberg, J.J.; van Essen-Zanbergen, A.; Petersen-den Besten, A.; Bende, R.J.; Moormann, R.J.; Wensvoort, G. Proteins encoded by open reading frames 3 and 4 of the genome of Lelystad virus (Arteriviridae) are structural proteins of the virion. *J. Virol.* **1996**, *70*, 4767–4772. [PubMed]
26. Wissink, E.H.; Kroese, M.V.; van Wijk, H.A.; Rijsewijk, F.A.; Meulenberg, J.J.; Rottier, P.J. Envelope protein requirements for the assembly of infectious virions of porcine reproductive and respiratory syndrome virus. *J. Virol.* **2005**, *79*, 12495–12506. [CrossRef] [PubMed]
27. De Lima, M.; Ansari, I.H.; Das, P.B.; Ku, B.J.; Martinez-Lobo, F.J.; Pattnaik, A.K.; Osorio, F.A. GP3 is a structural component of the PRRSV type II (US) virion. *Virology* **2009**, *390*, 31–36. [CrossRef] [PubMed]
28. Das, P.B.; Dinh, P.X.; Ansari, I.H.; de Lima, M.; Osorio, F.A.; Pattnaik, A.K. The minor envelope glycoproteins GP2a and GP4 of porcine reproductive and respiratory syndrome virus interact with the receptor CD163. *J. Virol.* **2010**, *84*, 1731–1740. [CrossRef] [PubMed]
29. Whitworth, K.M.; Rowland, R.R.; Ewen, C.L.; Trible, B.R.; Kerrigan, M.A.; Cino-Ozuna, A.G.; Samuel, M.S.; Lightner, J.E.; McLaren, D.G.; Mileham, A.J.; et al. Gene-edited pigs are protected from porcine reproductive and respiratory syndrome virus. *Nat. Biotechnol.* **2016**, *34*, 20–22. [CrossRef] [PubMed]
30. Vu, H.L.; Kwon, B.; Yoon, K.J.; Laegreid, W.W.; Pattnaik, A.K.; Osorio, F.A. Immune evasion of porcine reproductive and respiratory syndrome virus through glycan shielding involves both glycoprotein 5 as well as glycoprotein 3. *J. Virol.* **2011**, *85*, 5555–5564. [CrossRef] [PubMed]
31. Cancel-Tirado, S.M.; Evans, R.B.; Yoon, K.J. Monoclonal antibody analysis of porcine reproductive and respiratory syndrome virus epitopes associated with antibody-dependent enhancement and neutralization of virus infection. *Vet. Immunol. Immunopathol.* **2004**, *102*, 249–262. [CrossRef] [PubMed]
32. Meulenberg, J.J.; van Nieuwstadt, A.P.; van Essen-Zandbergen, A.; Langeveld, J.P. Posttranslational processing and identification of a neutralization domain of the GP4 protein encoded by ORF4 of Lelystad virus. *J. Virol.* **1997**, *71*, 6061–6067. [PubMed]
33. Wu, W.H.; Fang, Y.; Farwell, R.; Steffen-Bien, M.; Rowland, R.R.; Christopher-Hennings, J.; Nelson, E.A. A 10-kDa structural protein of porcine reproductive and respiratory syndrome virus encoded by ORF2b. *Virology* **2001**, *287*, 183–191. [CrossRef] [PubMed]
34. Johnson, C.R.; Griggs, T.F.; Gnanandarajah, J.; Murtaugh, M.P. Novel structural protein in porcine reproductive and respiratory syndrome virus encoded by an alternative ORF5 present in all arteriviruses. *J. Gen. Virol.* **2011**, *92*, 1107–1116. [CrossRef] [PubMed]
35. Robinson, S.R.; Figueiredo, M.C.; Abrahante, J.E.; Murtaugh, M.P. Immune response to ORF5a protein immunization is not protective against porcine reproductive and respiratory syndrome virus infection. *Vet. Microbiol.* **2013**, *164*, 281–285. [CrossRef] [PubMed]
36. Lopez, O.J.; Osorio, F.A. Role of neutralizing antibodies in PRRSV protective immunity. *Vet. Immunol. Immunopathol.* **2004**, *102*, 155–163. [CrossRef] [PubMed]

37. Osorio, F.A.; Galeota, J.A.; Nelson, E.; Brodersen, B.; Doster, A.; Wills, R.; Zuckermann, F.; Laegreid, W.W. Passive transfer of virus-specific antibodies confers protection against reproductive failure induced by a virulent strain of porcine reproductive and respiratory syndrome virus and establishes sterilizing immunity. *Virology* **2002**, *302*, 9–20. [CrossRef] [PubMed]
38. Murtaugh, M.P.; Xiao, Z.; Zuckermann, F. Immunological responses of swine to porcine reproductive and respiratory syndrome virus infection. *Viral Immunol.* **2002**, *15*, 533–547. [CrossRef] [PubMed]
39. Welch, S.K.W.; Calvert, J.G. A brief review of CD163 and its role in PRRSV infection. *Virus Res.* **2010**, *154*, 98–103. [CrossRef] [PubMed]
40. Duan, X.; Nauwynck, H.J.; Favoreel, H.; Pensaert, M.B. Porcine reproductive and respiratory syndrome virus infection of alveolar macrophages can be blocked by monoclonal antibodies against cell surface antigens. *Adv. Exp. Med. Biol.* **1998**, *440*, 81–88. [PubMed]
41. Vanderheijden, N.; Delputte, P.L.; Favoreel, H.W.; Vandekerckhove, J.; Van Damme, J.; van Woensel, P.A.; Nauwynck, H.J. Involvement of sialoadhesin in entry of porcine reproductive and respiratory syndrome virus into porcine alveolar macrophages. *J. Virol.* **2003**, *77*, 8207–8215. [CrossRef] [PubMed]
42. Prather, R.S.; Rowland, R.R.; Ewen, C.; Trible, B.; Kerrigan, M.; Bawa, B.; Teson, J.M.; Mao, J.; Lee, K.; Samuel, M.S. An intact sialoadhesin (Sn/SIGLEC1/CD169) is not required for attachment/internalization of the porcine reproductive and respiratory syndrome virus. *J. Virol.* **2013**, *87*, 9538–9546. [CrossRef] [PubMed]
43. Calvert, J.G.; Slade, D.E.; Shields, S.L.; Jolie, R.; Mannan, R.M.; Ankenbauer, R.G.; Welch, S.K. CD163 expression confers susceptibility to porcine reproductive and respiratory syndrome viruses. *J. Virol.* **2007**, *81*, 7371–7379. [CrossRef] [PubMed]
44. Schaer, D.J.; Schaer, C.A.; Buehler, P.W.; Boykins, R.A.; Schoedon, G.; Alayash, A.I.; Schaffner, A. CD163 is the macrophage scavenger receptor for native and chemically modified hemoglobins in the absence of haptoglobin. *Blood* **2006**, *107*, 373–380. [CrossRef] [PubMed]
45. Van Gorp, H.; Van Breedam, W.; Delputte, P.L.; Nauwynck, H.J. Sialoadhesin and CD163 join forces during entry of the porcine reproductive and respiratory syndrome virus. *J. Gen. Virol.* **2008**, *89*, 2943–2953. [CrossRef] [PubMed]
46. Dokland, T. The structural biology of PRRSV. *Virus Res.* **2010**, *154*, 86–97. [CrossRef] [PubMed]
47. Gao, J.M.; Xiao, S.Q.; Xiao, Y.H.; Wang, X.P.; Zhang, C.; Zhao, Q.; Nan, Y.C.; Huang, B.C.; Liu, H.L.; Liu, N.N.; et al. MYH9 is an essential factor for porcine reproductive and respiratory syndrome virus infection. *Sci. Rep.* **2016**, *6*, 25120. [CrossRef] [PubMed]
48. Pierson, T.C.; Fremont, D.H.; Kuhn, R.J.; Diamond, M.S. Structural insights into the mechanisms of antibody-mediated neutralization of flavivirus infection: Implications for vaccine development. *Cell Host Microbe* **2008**, *4*, 229–238. [CrossRef] [PubMed]
49. Chen, Y.; He, S.; Sun, L.; Luo, Y.; Sun, Y.; Xie, J.; Zhou, P.; Su, S.; Zhang, G. Genetic variation, pathogenicity, and immunogenicity of highly pathogenic porcine reproductive and respiratory syndrome virus strain XH-GD at different passage levels. *Arch. Virol.* **2016**, *161*, 77–86. [CrossRef] [PubMed]
50. Yu, X.; Chen, N.; Deng, X.; Cao, Z.; Han, W.; Hu, D.; Wu, J.; Zhang, S.; Wang, B.; Gu, X; et al. Genomic sequencing reveals mutations potentially related to the overattenuation of a highly pathogenic porcine reproductive and respiratory syndrome virus. *Clin. Vaccine Immunol.* **2013**, *20*, 613–619. [CrossRef] [PubMed]
51. Truong, H.M.; Lu, Z.; Kutish, G.F.; Galeota, J.; Osorio, F.A.; Pattnaik, A.K. A highly pathogenic porcine reproductive and respiratory syndrome virus generated from an infectious cDNA clone retains the in vivo virulence and transmissibility properties of the parental virus. *Virology* **2004**, *325*, 308–319. [CrossRef] [PubMed]
52. Lunney, J.K.; Steibel, J.P.; Reecy, J.M.; Fritz, E.; Rothschild, M.F.; Kerrigan, M.; Trible, B.; Rowland, R.R. Probing genetic control of swine responses to PRRSV infection: Current progress of the PRRS host genetics consortium. *BMC Proc.* **2011**, *5* (Suppl. 4), S30. [CrossRef] [PubMed]
53. Boddicker, N.; Waide, E.H.; Rowland, R.R.; Lunney, J.K.; Garrick, D.J.; Reecy, J.M.; Dekkers, J.C. Evidence for a major QTL associated with host response to porcine reproductive and respiratory syndrome virus challenge. *J. Anim. Sci.* **2012**, *90*, 1733–1746. [CrossRef] [PubMed]
54. Wu, W.; Blythe, D.C.; Loyd, H.; Mealey, R.H.; Tallmadge, R.L.; Dorman, K.S.; Carpenter, S. Decreased infectivity of a neutralization-resistant equine infectious anemia virus variant can be overcome by efficient cell-to-cell spread. *J. Virol.* **2011**, *85*, 10421–10424. [CrossRef] [PubMed]

55. Van Gorp, H.; Van Breedam, W.; Delputte, P.L.; Nauwynck, H.J. The porcine reproductive and respiratory syndrome virus requires trafficking through CD163-positive early endosomes, but not late endosomes, for productive infection. *Arch. Virol.* **2009**, *154*, 1939–1943. [CrossRef] [PubMed]
56. Costers, S.; Vanhee, M.; Van Breedam, W.; Van Doorsselaere, J.; Geldhof, M.; Nauwynck, H.J. GP4-specific neutralizing antibodies might be a driving force in PRRSV evolution. *Virus Res.* **2010**, *154*, 104–113. [CrossRef] [PubMed]
57. Fan, B.; Liu, X.; Bai, J.; Zhang, T.; Zhang, Q.; Jiang, P. The amino acid residues at 102 and 104 in GP5 of porcine reproductive and respiratory syndrome virus regulate viral neutralization susceptibility to the porcine serum neutralizing antibody. *Virus Res.* **2015**, *204*, 21–30. [CrossRef] [PubMed]
58. Murtaugh, M.P.; Stadejek, T.; Abrahante, J.E.; Lam, T.T.; Leung, F.C. The ever-expanding diversity of porcine reproductive and respiratory syndrome virus. *Virus Res.* **2010**, *154*, 18–30. [CrossRef] [PubMed]
59. Thaa, B.; Sinhadri, B.C.; Tielesch, C.; Krause, E.; Veit, M. Signal peptide cleavage from GP5 of PRRSV: A minor fraction of molecules retains the decoy epitope, a presumed molecular cause for viral persistence. *PLoS ONE* **2013**, *8*, e65548. [CrossRef] [PubMed]
60. Chen, N.; Trible, B.R.; Kerrigan, M.A.; Tian, K.; Rowland, R.R. ORF5 of porcine reproductive and respiratory syndrome virus (PRRSV) is a target of diversifying selection as infection progresses from acute infection to virus rebound. *Infect. Genet. Evol.* **2016**, *40*, 167–175. [CrossRef] [PubMed]
61. Robinson, S.R.; Li, J.; Nelson, E.A.; Murtaugh, M.P. Broadly neutralizing antibodies against the rapidly evolving porcine reproductive and respiratory syndrome virus. *Virus Res.* **2015**, *203*, 56–65. [CrossRef] [PubMed]
62. Tian, D.; Wei, Z.; Zevenhoven-Dobbe, J.C.; Liu, R.; Tong, G.; Snijder, E.J.; Yuan, S. Arterivirus minor envelope proteins are a major determinant of viral tropism in cell culture. *J. Virol.* **2012**, *86*, 3701–3712. [CrossRef] [PubMed]

© 2017 by the authors. Licensee MDPI, Basel, Switzerland. This article is an open access article distributed under the terms and conditions of the Creative Commons Attribution (CC BY) license (http://creativecommons.org/licenses/by/4.0/).

viruses

MDPI

Article

Porcine Epidemic Diarrhea Virus Induces Autophagy to Benefit Its Replication

Xiaozhen Guo [1,2], Mengjia Zhang [1,2], Xiaoqian Zhang [1,2], Xin Tan [1,2], Hengke Guo [1,2], Wei Zeng [1,2], Guokai Yan [2,3], Atta Muhammad Memon [1,2], Zhonghua Li [1,2], Yinxing Zhu [1,2], Bingzhou Zhang [1,2], Xugang Ku [1,2], Meizhou Wu [1,2], Shengxian Fan [1,2,*] and Qigai He [1,2,*]

1 State Key Laboratory of Agricultural Microbiology, College of Veterinary Medicine, Huazhong Agricultural University, Wuhan 430070, China; guoxiaozhen@webmail.hzau.edu.cn (X.G.); zhangmengjia@webmail.hzau.edu.cn (M.Z.); 632071039@webmail.hzau.edu.cn (X.Z.); wstx1992@163.com (X.T.); 15071194245@163.com (H.G.); aiyouwei0620@163.com (W.Z.); Memonatta80@webmail.hzau.edu.cn (A.M.M.); lzh1990@webmail.hzau.edu.cn (Z.L.); yingzizhu10@163.com (Y.Z.); abing0313@webmail.hzau.edu.cn (B.Z.); kuxugang84@163.com (X.K.); wumeizhou@mail.hzau.edu.cn (M.W.)

2 The Cooperative Innovation Center for Sustainable Pig Production, Wuhan 430070, China; gkyangk@163.com

3 College of Animal Sciences and Technology, Huazhong Agricultural University, Wuhan 430070, China

* Correspondence: fanshengxian@mail.hzau.edu.cn (S.F.); he628@mail.hzau.edu.cn (Q.H.); Tel.:+86-27-8728-3005 (S.F.); +86-27-8728-6974 (Q.H.)

Academic Editors: Linda Dixon and Simon Graham
Received: 28 December 2016; Accepted: 15 March 2017; Published: 19 March 2017

Abstract: The new porcine epidemic diarrhea (PED) has caused devastating economic losses to the swine industry worldwide. Despite extensive research on the relationship between autophagy and virus infection, the concrete role of autophagy in porcine epidemic diarrhea virus (PEDV) infection has not been reported. In this study, autophagy was demonstrated to be triggered by the effective replication of PEDV through transmission electron microscopy, confocal microscopy, and Western blot analysis. Moreover, autophagy was confirmed to benefit PEDV replication by using autophagy regulators and RNA interference. Furthermore, autophagy might be associated with the expression of inflammatory cytokines and have a positive feedback loop with the NF-κB signaling pathway during PEDV infection. This work is the first attempt to explore the complex interplay between autophagy and PEDV infection. Our findings might accelerate our understanding of the pathogenesis of PEDV infection and provide new insights into the development of effective therapeutic strategies.

Keywords: autophagy machinery; PEDV replication; inflammatory responses; apoptosis

1. Introduction

The new porcine epidemic diarrhea (PED) outbreaks caused by porcine epidemic diarrhea virus (PEDV) variant has been documented in China since late 2010 and is now distributed all over the world. PED is characterized by acute enteric infection and high mortality in sucking piglets, causing enormous economic losses to the swine industry [1–4]. PEDV is an enveloped, single-stranded positive-sense RNA virus of the Coronaviridae family. The viral genome is approximately 28 kb, arranged with at least seven open reading frames (ORFs), ORF1a, ORF1b, S, ORF3, E, M, and N. ORF1a and ORF1b are further processed into 16 nonstructural proteins, nsp1 to nsp16. The S, E, M, and N genes encode four structural proteins, whereas ORF3 encodes an accessory protein [5–7]. Despite the elucidation of PEDV pathogenesis in some aspects, the underlying mechanism of PEDV replication is still largely unknown.

Autophagy is an evolutionarily highly conserved intracellular degradation process in which double-membrane vesicles (termed autophagosomes) are generated, and the long-lived proteins and

damaged organelles are delivered to lysosomes for degradation and recycling [8,9]. Autophagy can be induced by diverse intracellular and extracellular stimuli, such as nutrient starvation, endoplasmic reticulum (ER) stress, pathogen-associated molecular patterns (PAMPs), and virus infection [10]. Increasing evidence indicates that autophagy plays both anti-viral and pro-viral roles in the life cycles and pathogenesis of a broad range of viruses [11]. Specifically, autophagy is an intrinsic host defense mechanism that inhibits viral replication or eliminates viruses by delivering them to the lysosomal compartment for degradation. Meanwhile, viruses develop many mechanisms to block autophagy or even hijack it for their own benefit, such as human cytomegalovirus (HCMV) and herpes simplex virus type 1 (HSV-1) [9,12–14]. However, autophagy is also believed to serve as a platform for viral replication, especially for RNA viruses, such as classical swine fever virus (CSFV), porcine reproductive and respiratory syndrome virus (PRRSV), and rotavirus (RV), utilizing the membranes of the autophagosome-like vesicles for their replication [15–17]. These polar characteristics reveal the complicated relationship between autophagy and viral infection.

A previous proteomic study indicated that more differentially expressed proteins were mapped to the autophagy pathway, and the microtubule-associated protein 1B, a useful biomarker protein for autophagy was up-regulated in PEDV-infected Vero cells [18]. In addition, our previous study demonstrated that mTOR (the mammalian target of rapamycin) pathway, which was closely associated with cellular autophagy, was down-regulated, and that the autophagy associated protein ATG5 was up-regulated during PEDV infection [19]. These studies indicated that autophagy might participate in PEDV infection, but the specific function of autophagy in the process of PEDV infection has not been elucidated. In the present study, we demonstrated for the first time that autophagy was triggered in Vero cells during PEDV infection to promote its replication. Moreover, autophagy might mediate the inflammatory responses induced by PEDV infection and have a positive correlation with the NF-κB signaling pathway.

2. Materials and Methods

2.1. Cells and Viruses

African green monkey kidney cell lines, Vero-E6 cells, were cultured in Dulbecco's modified Eagle's medium (DMEM), supplemented with 10% fetal bovine serum (Invitrogen, Carlsbad, CA, USA) at 37 °C with 5% CO_2. The PEDV variant strain CH/YNKM-8/2013 (Accession no. KF761675) was isolated from a sucking piglet with acute diarrhea. To obtain replication-incompetent PEDV, virus suspension was irradiated with UV light for 1 h. The absence of virus infectivity was confirmed by $TCID_{50}$ and real-time PCR [16].

2.2. Virus Infection

For autophagy induction and inhibition experiments, Vero cells were pretreated with rapamycin (1 μg/mL, Santa Cruz, CA, USA), 3-methyladenine (3-MA, 5 μm, Sigma, St. Louis, USA), Chloroquine (CQ, 50 μm, Sigma), and BAY 11-7082 (10 μm, Sigma) for the indicated time, and were then infected with PEDV at a MOI (multiplicity of infection) of 0.1. After 1 h incubation at 37 °C, unbound viruses were removed by washing three times with PBS, followed by incubation with serum-free DMEM with 8 μg/mL trypsin (Invitrogen) containing varying concentrations of rapamycin, 3-MA, CQ, BAY 11-7082, or DMSO.

2.3. Quantitative Real-Time PCR

Total RNA was extracted from Vero cells using the TRIzol reagent (Invitrogen) according to the manufacturer's protocol, and was then reverse-transcribed into cDNA using oligo (dT) as the primer (Invitrogen). Relative and absolute quantitative real-time PCR were performed in an Applied Biosystems ViiA 7 real-time PCR system as previously described [19]. The primers and probe used are listed in Table 1.

Table 1. Primers used for real-time real time PCR.

Primer	Sequence (5′–3′)
PEDV-F	CGTACAGGTAAGTCAATTAC
PEDV-R	GATGAAGCATTGACTGAA
PEDV-probe-M	TTCGTCACAGTCGCCAAGG
ATG5-F	TTCACGCTATATCAGGAT
ATG5-R	ATCTCACTAATGTCTTCTTG
Beclin1-F	TGGCACAATCAATAACTTC
Beclin1-R	CAAGCAGCATTAATCTCAT
IL-6-F	TGTGAAAGCAGCAAAGAG
IL-6-R	AGTGTCCTCATTGAATCCA
IL-1β-F	GCGGCAACGAGGATGACTT
IL-1β-R	TGGCTACAACAACTGACACGG
IL-8-F	GGAACCATCTCGCTCTGTGTAA
IL-8-R	GGTCCACTCTCAATCACTCTCAG
CCL5-F	ACGCCTCGCTGTCATCCT
CCL5-R	GCACTTGCCACTGGTGTAGAA
TNF-α-F	CACCACGCTCTTCTGTCT
TNF-α-R	AGATGATCTGACTGCCTGAG
MCP-1-F	CTTCTGTGCCTGCTGCTCATA
MCP-1-R	ACTTGCTGCTGGTGATTCTTCT
GAPDH-F	ACATCATCCCTGCCTCTACTG
GAPDH-R	CCTGCTTCACCACCTTCTTG
β-actin-F	TTAGTTGCGTTACACCCTTTC
β-actin-R	ACCTTCACCGTTCCAGTT

2.4. Transmission Electron Microscopy

Vero cells were mock infected or infected with PEDV at 0.1 MOI and collected at 24 h post-infection (hpi) for ultrastructural analysis. Ultra-thin sections were viewed on a Hitachi H-7650 transmission electron microscope (Hitachi Ltd., Tokyo, Japan). Autophagosome-like vesicles were defined as double- or single-membrane vesicles measuring 0.3 to 2.0 μm in diameter with clearly recognizable cytoplasmic contents.

2.5. Confocal Fluorescence Microscopy

Vero cells were seeded on coverslips and transfected with GFP-LC3 or mRFP-GFP-LC3. After transfection for 24 h, the cells were infected with PEDV and fixed with cold 4% paraformaldehyde. After permeabilization and blocking, the cells were then incubated with mouse monoclonal antibody directed against the PEDV S protein (made in our laboratory), and were then inoculated with Alexa Fluor 594 Donkey Anti Mouse IgG (H+L) antibody (Ant Gene). Cell nuclei were counterstained with 0.01% 4′,6-diamidino-2-phenylindole (DAPI, Invitrogen). The fluorescent images were examined under a confocal laser scanning microscope (LSM 510 Meta, Carl Zeiss, Munich, Germany).

2.6. Western Blot Analysis

Vero cells were lysed in lysis buffer containing 50 mM Tris-HCl (pH 6.8), 10% glycerol, and 2% SDS [20]. The protein concentration was quantified by the BCA protein assay kit and equal amounts of protein samples were mixed with 5× sample loading buffer and boiled for 10 min, and then separated by 12% sodium dodecyl sulfate polyacrylamide gel electrophoresis (SDS-PAGE). The proteins were electro-transferred to 0.45 μm PVDF membranes (Millipore, Mississauga, ON, Canada). Membranes were blocked with 5% (w/v) skim milk-TBST at room temperature for 2 h and then incubated overnight at 4 °C with primary antibodies. The blots were then incubated with corresponding horseradish peroxidase (HRP) conjugated secondary antibodies (ABclonal, Wuhan, China). The protein bands were visualized using the Clarity™ Western ECL Blotting Substrate (Bio-Rad, Hercules, CA, USA). The protein blots were quantified by Image J software (National Institutes of Health, Bethesda, MD, USA).

2.7. RNA Interference

Vero cells grown to 60% confluence were transfected separately with Beclin1 or ATG5 and the corresponding scrambled siRNA with Lipofectamine 2000 (Invitrogen) according to the manufacturer's guidelines. The silencing efficiency was determined by Western blot and real-time PCR. Twenty-four hours after transfection, the cells were infected with PEDV as described above.

The siRNA was designed by and obtained from GenePharma (Shanghai, China). *Beclin1* siRNA sequence: 5′-CCCAGUGUUCCCGUAGAAUTTAUUCUACGGGAACACUGGGTT-3′; *ATG5* siRNA sequence: 5′-GCAACUCUGGAUGGGAUUATTUAAUCCCAUCCAGAGUUGCTT-3′.

2.8. Cell Viability Assay

The cytotoxic effects of reagents on Vero cells were determined using the MTT (3-[4, 5-dimethylthiazol-2-yl]-2, 5-diphenyl-2H-tetra-zolium bromide) assay as previously described [21]. Briefly, Vero cells were inoculated in a 96-well plate and treated with different concentrations of pharmacological drugs. Then, the cells were inoculated with MTT and the resulting formazan crystals were dissolved in dimethyl sulfoxide (DMSO). The absorbance was measured by a microplate spectrophotometer at a wavelength of 490 nm.

2.9. Statistical Analysis

All experiments were performed independently three times, and variables are expressed as the means with SEM. Statistical analyses were performed using student's *t*-test. A p-value < 0.05 was considered as statistically significant.

3. Results

3.1. PEDV Infection Increases the Levels of Autophagy in Vero Cells

Whether PEDV infection can activate the autophagy machinery was investigated by examining the formation of autophagosome-like vesicles in Vero cells at 24 h post PEDV infection through transmission electron microscopy (TEM). A large number of double- or single-membrane vesicles were observed in PEDV-infected cells, which contained cytosolic components or sequestered organelles. However, autophagosome-like vesicles were rarely observed in the mock-infected cells (Figure 1A). It is well known that coronavirus infection can induce a large number of double-membrane vesicles (DMVs), and the functional link between autophagic DMVs and coronavirus-induced replication-associated DMVs remains controversial [22–24]. In this study, these two different DMVs might co-exist in PEDV-infected cells [25].

In addition, the GFP-LC3 tandem plasmid was transfected into Vero cells to verify the response of cellular autophagy to PEDV infection. As is well-known, the LC3, a protein, is selectively recruited to autophagic vesicles, which can be considered as its redistribution from a diffuse cytoplasmic localization to a distinctive punctate cytoplasmic pattern during autophagy [16]. GFP-LC3 positive cells treated with rapamycin showed high punctate LC3 accumulation. Additionally, large amounts of punctate GFP-LC3 proteins were observed in PEDV-infected cells at 18 hpi, while GFP-LC3 was detected as a diffuse distribution in mock-infected cells (Figure 1B), indicating that the accumulation of GFP-LC3 dots was induced by PEDV infection. The quantitative analysis of the percentage of punctate GFP-LC3 cells in the total GFP-positive cells was performed and 100 GFP-positive cells were detected in each sample. The percentage of punctate GFP-LC3 cells in PEDV infected cells was nearly 70%, which was obviously higher than that in the mock-treated cells (Figure 1C).

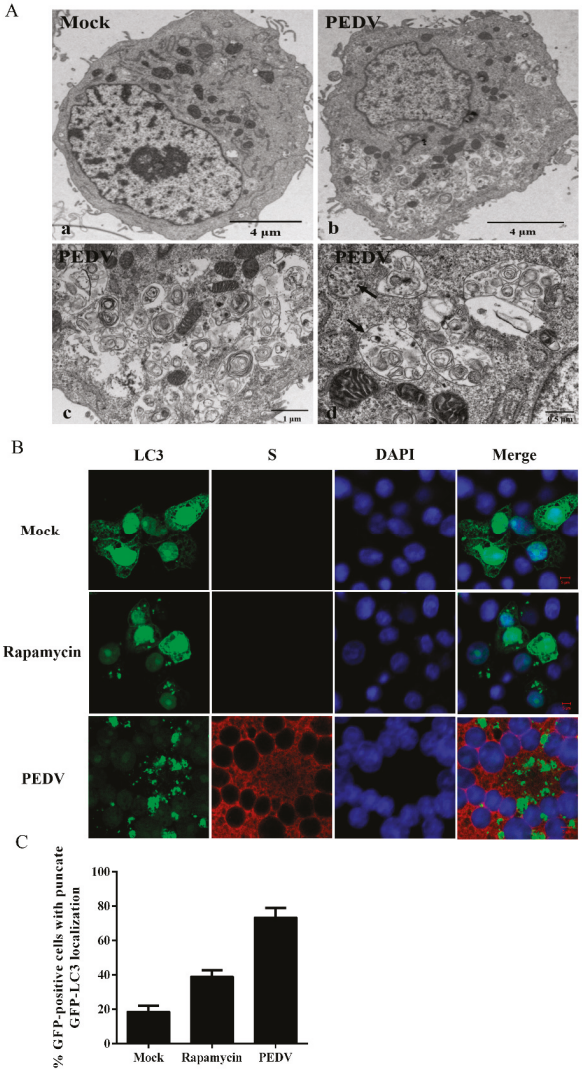

Figure 1. Porcine epidemic diarrhea virus (PEDV) infection increases the formation of autophagosome-like vesicles. (**A**) TEM observation. Vero cells were mock-treated (**a**) or infected with PEDV at 0.1 MOI for 24 h (**b**). Scale bar, 4 μm (**a**,**b**). (**c**) higher-magnification views of (**b**). Scale bar, 1 μm. (**d**) enlargement of the autophagosome-like structure. Scale bar, 0.5 μm. (**B**) Confocal microscope. The redistribution of GFP-LC3 was induced by PEDV infection. Vero cells were transfected with the plasmid GFP-LC3. Twenty-four hours later, the transfected cells were infected or mock-infected with PEDV at 0.1 MOI for 18 h. Meanwhile, cells pretreated with rapamycin for 4 h served as a positive control. PEDV infection was detected with the monoclonal antibody against PEDV S and cell nuclei were counterstained with 4',6-diamidino-2-phenylindole (DAPI). Scale bar, 5 μm. (**C**) The relative number of cells with punctate GFP-LC3 locations relative to all green fluorescent protein-positive cells. The data were presented as mean ± SEM of three independent experiments.

To further analyze whether autophagy was induced by PEDV infection, we examined the level of autophagy marker proteins in PEDV-infected cells by using immunoblotting. The conversion from LC3-I to LC3-II was monitored at 6, 12, 18, 24, and 30 h post PEDV infection. As shown in Figure 2A,B, a significant conversion of LC3-I to LC3-II was observed during the progression of PEDV infection, which was tracked by the PEDV N protein. Meanwhile, PEDV infection increased the expression of ATG5 and beclin1 in Vero cells relative to the mock-infected cells (Figure 2C). The results further supported that autophagy was induced by the PEDV infection.

Whether viral replication was required in PEDV-induced autophagy was confirmed by an experiment with ultraviolet (UV)-inactivated PEDV. The results demonstrated that no obvious detectable conversion from LC3-I to LC3-II was observed at 24 hpi, while autophagy was triggered normally by native PEDV (Figure 2D). The results indicated that viral replication was required for PEDV-induced autophagy.

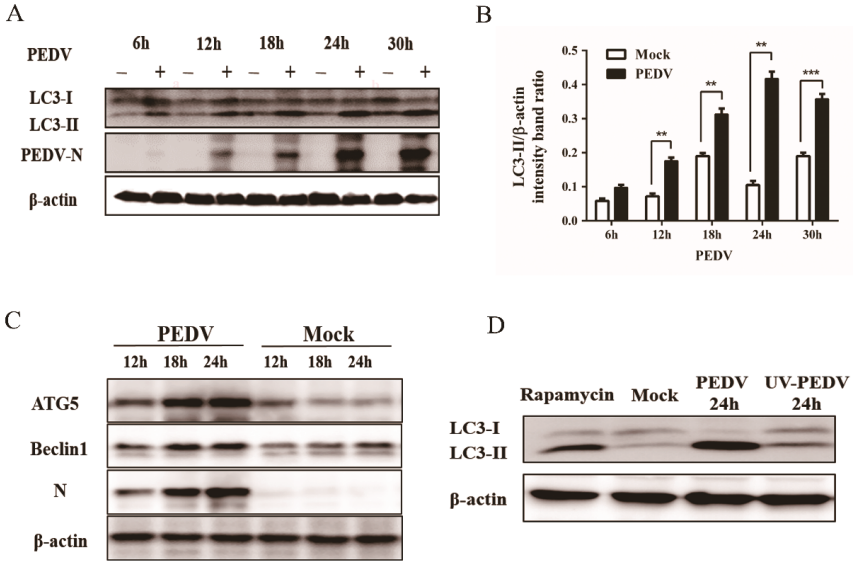

Figure 2. Expression of autophagy marker proteins in PEDV infected Vero cells. (**A**) Western blot analysis of the turnover of LC3-I to LC3-II in Vero cells at the indicated time points post PEDV infection using a polyclonal antibody against LC3 or a monoclonal antibody against PEDV N. β-actin expression was used as a protein loading control. (**B**) The intensity band ratio of LC3-II to β-actin was analyzed by using ImageJ software. The data were presented as mean ± SEM of three independent experiments (*t*-test, * $p < 0.05$, ** $p < 0.01$, *** $p < 0.001$). (**C**) Western blot analysis of the level of ATG5 and Beclin1 in Vero cells at 12, 18, and 24 hpi. β-actin expression was used as a protein loading control. (**D**) The turnovers of LC3-I to LC3-II were detected for mock-treated, rapamycin-treated, native PEDV, and UV-inactivated PEDV (MOI = 0.1) infection.

3.2. PEDV Infection Can Enhance Autophagy Flux

The degradation of SQSTM1 (p62) was recognized as an indicator for assessing autophagy flux. Whether a complete autophagic process was triggered by the PEDV infection was first determined by the degradation of p62 through immunoblotting analysis. As shown in Figure 3A,B, p62 was slightly accumulated during the early life cycle of PEDV infection, but degraded at the later stages. Meanwhile, p62 showed no obvious change from 6 to 30 h in the mock-infected cells.

The autophagy flux upon PEDV infection was further verified by measuring the levels of LC3-II and p62 through the treatment with chloroquine (CQ), which can inhibit the fusion of the autophagosome with lysosome. As shown in Figure 3C, CQ elevated the levels of LC3-II and p62 markedly at 24 h post PEDV infection, compared to the mock-treated cells.

Furthermore, the PEDV-induced autophagy flux was also confirmed using a tandem-reporter construct, GFP-mRFP-LC3. GFP is sensitive to lysosomal proteolysis and may diminish quickly in acidic pH, whereas RFP (red fluorescent protein) retains its fluorescence even at acidic pH. Our results showed that PEDV infection resulted in a partially red fluorescence at 24 hpi (Figure 3D), indicating the elevated level of autophagic flux. Taken together, this substantial evidence suggests that PEDV infection can enhance autophagy flux in Vero cells.

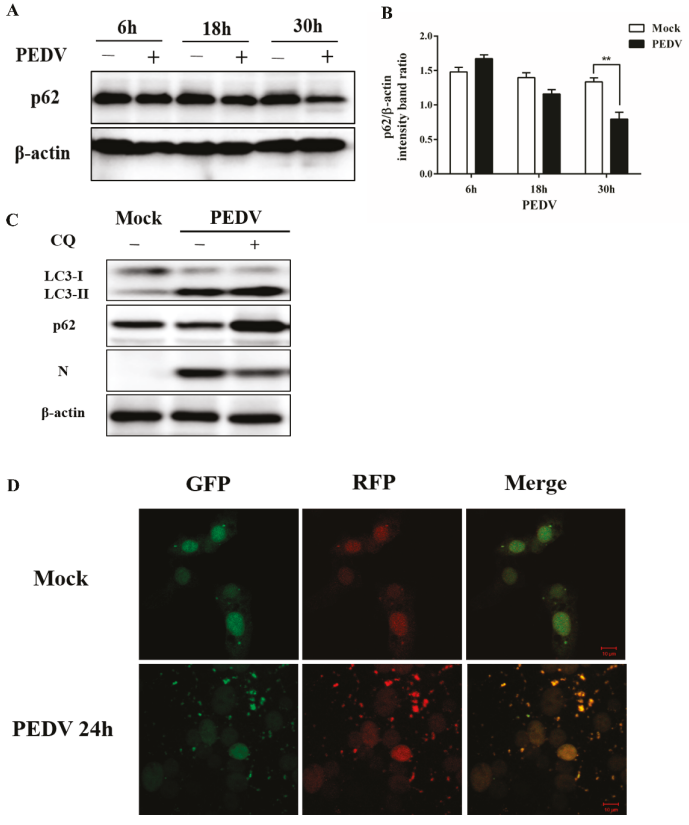

Figure 3. PEDV infection enhances autophagy flux. (**A**) Vero cells were mock-infected or infected with PEDV (0.1 MOI) for 6, 18, and 30 h. The cells were then analyzed by Western blot with antibodies against p62 and β-actin, separately. (**B**) The intensity band ratio of p62 to β-actin was analyzed by using ImageJ software. The data were presented as mean ± SEM of three independent experiments (*t*-test, * $p < 0.05$, ** $p < 0.01$, *** $p < 0.001$). (**C**) Vero cells were pretreated with CQ (50 μm) for 4 h, prior to PEDV (0.1 MOI) infection. After PEDV adsorption for 1 h, the cells were further cultured in fresh medium in the absence or presence of CQ. At 24 hpi, cell samples were detected by Western blot with antibodies against LC3, p62, N, and β-actin. (**D**) Vero cells were transfected with mRFP-GFP-LC3. Twenty-four hours later, the cells were mock-infected or infected with PEDV (0.1 MOI), then collected and visualized at 24 hpi, respectively. Scale bar, 10 μm.

3.3. Pharmacological Inhibition of Autophagy Decreases Viral Yield

The specific role of autophagy machinery on PEDV replication was explored by exposing Vero cells to 3-MA, which can inhibit autophagy at the early stage by suppressing the formation of autophagosomes [26]. As shown in Figure 4A,C,E, when compared to the mock-treated cells, 3-MA treatment not only reduced the level of LC3-II, but also significantly decreased the virus titer at different time points. In addition, CQ treatment (described above) reduced the expression of N protein, although it elevated the level of LC3-II (Figure 3C). These data indicated that autophagy inhibition could block PEDV infection. Similar results were also found in PEDV-infected ST cells.

Meanwhile, the role of autophagy machinery on PEDV replication was confirmed by rapamycin treatment, an inducer of autophagy through inhibition of the mTOR signaling pathway [8,17]. As shown in Figure 4B,D,F, induction of autophagy with rapamycin increased the LC3-II level and elevated the virus titer, compared to the mock-treated cells. The results suggested that autophagy induction could facilitate PEDV replication.

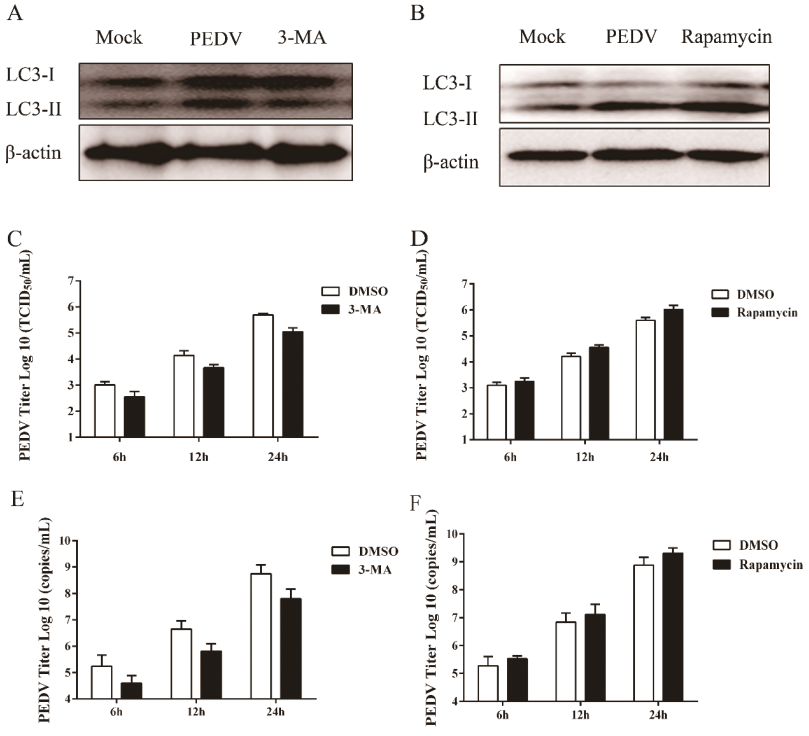

Figure 4. Pharmacological inhibition of autophagy decreases viral yield. (**A**,**B**) Vero cells were pretreated separately with 3-MA (5 mM) (**A**) or rapamycin (1 μg/mL) (**C**) for 4 h prior to PEDV (0.1 MOI) infection. After PEDV adsorption for 1 h, the cells were further cultured in fresh medium in the absence or presence of 3-MA or rapamycin. DMSO was used as a control. At 24 hpi, cell samples were detected by Western blot with antibodies against LC3 and β-actin. (**C**,**D**) The cells were collected separately at 6, 12, and 24 hpi to determine the viral titer. The data were presented as mean ± SEM of three independent experiments. (**E**,**F**) The cells were collected separately at 6, 12, and 24 hpi. The virus copy number was determined by real time PCR. The data were presented as mean ± SEM of three independent experiments.

3.4. Silencing Endogenous Beclin1 or ATG5 Gene Reduces the PEDV Titer

The relationship between autophagy and PEDV replication was further confirmed through gene-silencing experiments, with the endogenous *Beclin1* or *ATG5* gene specifically silenced, which was verified at both the transcriptional and translational levels (Figure 5A,B). Data from Figure 5C,D demonstrated that suppression of Beclin1 or ATG5 expression obviously decreased the viral titer and virus copy number compared to the control group. All the aforementioned data indicated that the autophagy mechanism was triggered by PEDV infection to facilitate its replication.

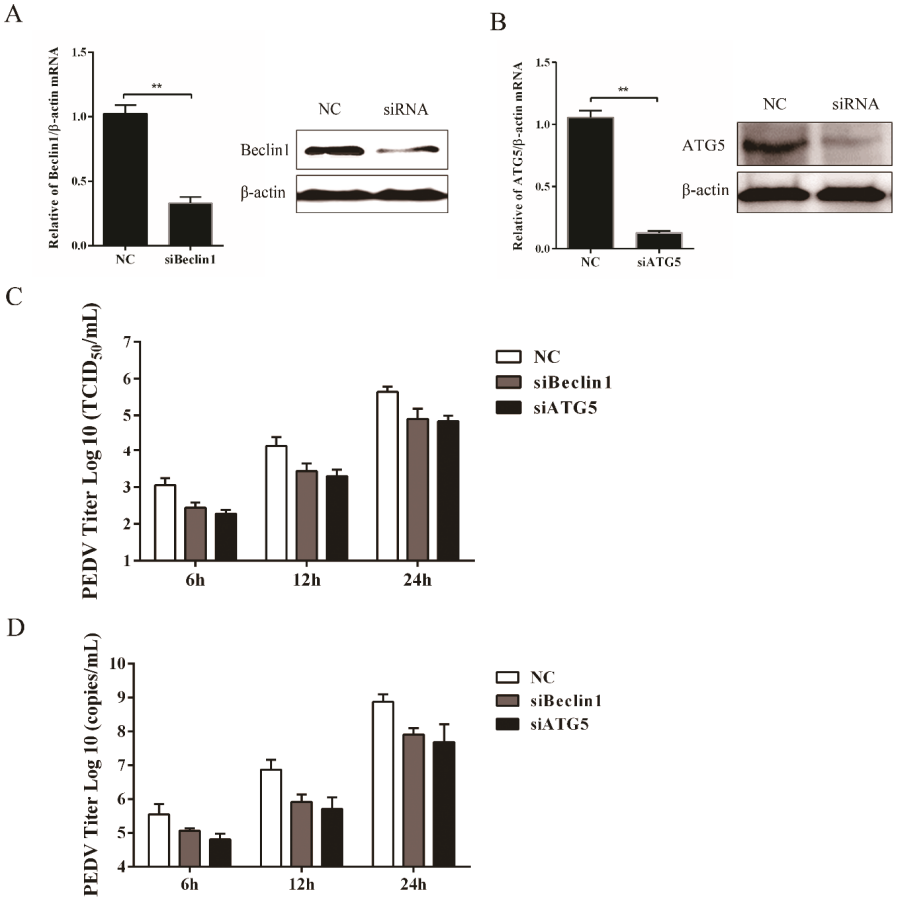

Figure 5. Inhibition of autophagy with specific siRNA targeting *Beclin1* or *ATG5* reduces PEDV replication. (**A**,**B**) Vero cells were transfected with siRNA targeting *Beclin1*, *ATG5*, or negative control (NC) for 48 h. The silencing efficiency was determined separately by quantitative real-time PCR and Western blot. (**C**) At 24 h post-transfection, cells were mock-infected or infected with PEDV for another 6, 12, and 24 h. The virus titer was determined by $TCID_{50}$. The data were presented as mean ± SEM of three independent experiments. (**D**) The cells were treated as described in (**C**) and collected separately at 6, 12, and 24 hpi, respectively. The virus copy number was determined by qRT-PCR. The data were presented as mean ± SEM of three independent experiments.

3.5. Autophagy Has a Positive Correlation with NF-κB Signaling Pathway

Accumulating data revealed a strong association between autophagy and the host immune response in the progression of virus infection [27,28]. Thus, the role of autophagy in PEDV induced inflammatory responses was investigated first by measuring the level of inflammatory cytokines under the circumstances when autophagy was suppressed by silencing the expression of Beclin1 and ATG5 proteins. Data showed that the inflammatory cytokines (such as IL-1β, IL-6, IL-8, CCL5, TNF-α, and MCP-1) were significantly down-regulated at 24 hpi when autophagy was inhibited in PEDV infected cells (Figure 6A,B), suggesting the potential involvement of autophagy in PEDV induced inflammation. It is well-known that the NF-κB signaling pathway plays a pivotal role in PEDV induced inflammatory response and Vero cells are interferon deficient [19,29]. Therefore, the influence of autophagy on the NF-κB pathway was determined under the deficient expression of Beclin1 and ATG5 at 24 h upon PEDV infection by immunoblotting analysis. The level of LC3-II decreased, and the phosphorylation of p65 was also down-regulated at the same time (Figure 6C). The results indicated that autophagy might participate in PEDV induced inflammation through the NF-κB pathway.

To further explore the relationship between autophagy and the NF-κB pathway mediated inflammatory response, the NF-κB pathway was attenuated by administrating BAY 11-7082, an NF-κB inhibitor. As shown in Figure 6D,E, the administration of BAY 11-7082 abolished the elevated level of LC3-II at 16, 20, and 24 h post PEDV infection, which was especially significantly at 24 hpi. These data indicated that a potential positive feedback loop between autophagy and the NF-κB signaling pathway might exist during PEDV infection.

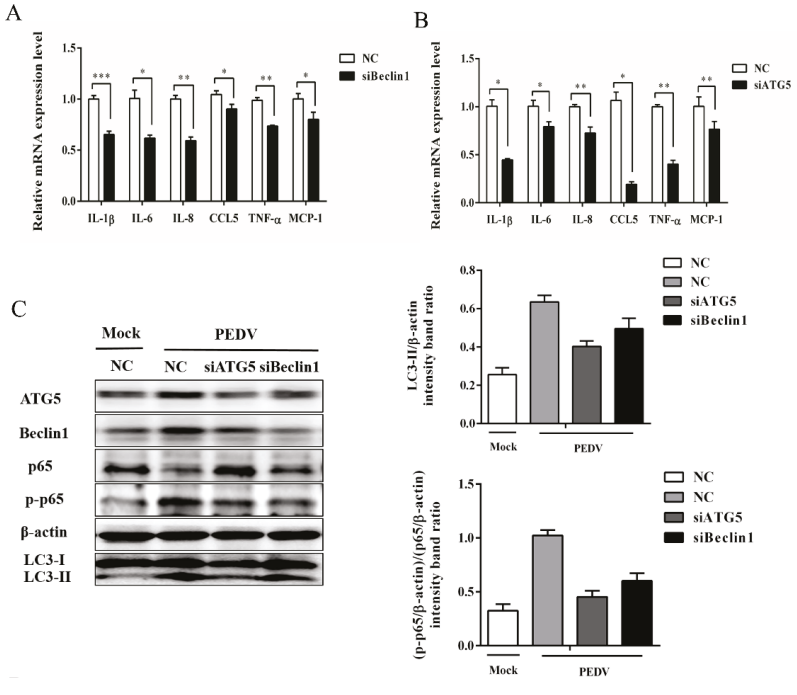

Figure 6. *Cont.*

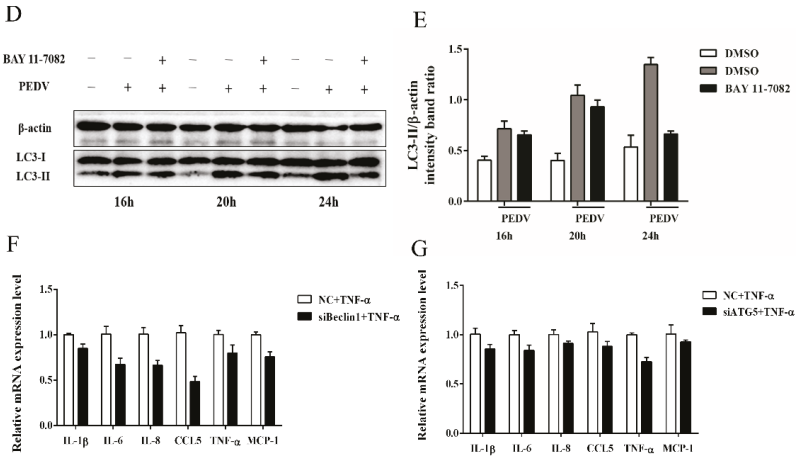

Figure 6. Autophagy mediates the production of inflammatory cytokines and correlates with the NF-κB signaling pathway in PEDV infected Vero cells. (**A**,**B**) The expression of inflammatory cytokines. Vero cells were transfected with siRNA targeting *Beclin1*, *ATG5*, or negative control (NC) for 24 h, followed by PEDV infection (0.1 MOI). The mRNA levels of cytokines were determined at 24 hpi by quantitative real-time PCR. (**C**) The level of LC3-II, p65, or phospho-p65 was also examined separately at 24 hpi with the corresponding antibodies by Western blot. The intensity band ratios of LC3-II to β-actin and p-p65 to p65 were analyzed by using ImageJ software. (**D**) Vero cells were pretreated with 10 μm BAY11-7082 for 12 h, then followed by PEDV infection for 16, 20, and 24 h, separately. The cell samples were collected for LC3-II detection by Western blot. (E) The intensity band ratio of LC3-II to β-actin was analyzed by using ImageJ software. All data were presented as mean ± SEM of three independent experiments. (**F**,**G**) Vero cells were transfected with siATG5, siBeclin1, or negative control. Twenty-four hours post-transfection, the cells were treated with TNF-α for 4 h, and then the expression of inflammatory cytokines were determined by qRT-PCR. The data were presented as mean ± SEM of three independent experiments.

Considering that autophagy inhibition can block PEDV replication, a TNF-α induction of inflammatory cytokines experiment in autophagy-deficiency cells was carried out to exclude the effect of PEDV replication on cytokine production. From Figure 6F,G, it can be seen that the expression of inflammatory cytokines induced by TNF-α in ATG5-or Beclin1-deficient cells was significantly down-regulated, when compared to the transfected cells of the negative control. These results also supported the potential positive relationship between autophagy and the NF-κB signaling pathway induced by PEDV infection.

3.6. Pharmacological Regulation of Autophagy Does Not Affect Cell Viability

The effect of the autophagy regulators on the capability of PEDV replication by changing the cell viability was tested by the MTT assay. No significant effects on cell viability were observed from the treatment with CQ, 3-MA, rapamycin, or BAY11-7082, respectively ($p > 0.05$) (Figure 7), indicating that pharmacological regulation of autophagy does not affect the cell viability.

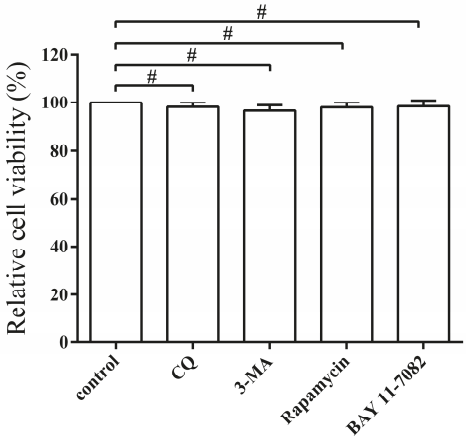

Figure 7. Pharmacological regulation of autophagy does not affect cell viability. The cell viability was determined by MTT assay after treatment with CQ (50 μm), 3-MA (5 μm), rapamycin (1 μg/mL), and BAY 11-7082 (10 μm) for 48 h, respectively. The data represent the mean ± SEM of three independent experiments. (*t*-test, $^{\#}$ $p > 0.05$).

4. Discussion

In recent years, autophagy has been widely investigated due to its important role in the pathogenesis of many diseases [9,30]. The relationship between autophagy and viral infection, including coronavirus, has attracted the attention of an increasing number of researchers [11,31,32]. For instance, the formation of double membrane-bound MHV replication complexes was found essential for the autophagy induced by mouse hepatitis virus (MHV) infection [33]. A further study revealed that the autophagy-like process induced by infectious bronchitis virus (IBV) infection might not be important for virus replication [34]. In addition, autophagy was confirmed to negatively regulate transmissible gastroenteritis virus (TGEV) replication [35]. However, the specific role of autophagy on PEDV infection has not been reported until now. In this study, we provide the first strong evidence that PEDV infection can trigger autophagy to facilitate its replication.

In the present study, we firstly found that PEDV infection promoted the formation of DMVs by TEM, which is a hallmark of coronavirus replication and might potentially provide a platform for viral RNA synthesis [23,36]. In coronavirus infection, the formation of DMVs is usually believed to be associated with the autophagy pathway. This observation was further supported by the accumulation of GFP-LC3 dots in virus induced syncytia and the increased expression of autophagic marker proteins from the immunoblotting analysis. These data indicated that autophagy activity might be triggered by PEDV infection [37]. In addition, autophagy was documented to play a role in syncytia formation, which could further increase autophagy in multinucleated cells as well. Therefore, we inferred that autophagy might closely associate with the syncytia formation in Vero cells during PEDV infection [38,39]. Moreover, the UV inactivation test implied that the effective replication of PEDV was required for autophagy induction. Previous reports indicated that autophagosome accumulation might be attributed to their de novo formation or a block in trafficking to lysosomes for maturation. The cellular state of autophagy can be measured by detecting the degradation of SQSTM1 (p62), using a lysosome inhibitor, or a tandem reporter construct mRFP-GFP-LC3 [40]. Our results from these tests indicated that a complete autophagy process might be triggered to modulate PEDV infection in Vero cells.

Recent studies have demonstrated that the replication mechanisms may vary among different members of the *Coronaviridae* family. For example, TGEV infection induces autophagy to negatively

regulate its replication [35]. IBV can induce autophagy but does not require autophagy for its replication [34]. The specific effect of autophagy induction on MHV infection is controversial. Prentice et al. reported that MHV utilized the autophagy process to form DMVs to enhance its replication [33]. However, another study showed that autophagy was not important for MHV replication [41]. In the present study, the concrete effect of autophagy upon PEDV infection was examined by administrating pharmacological regulators. The yield of PEDV was found to be suppressed whenever the autophagy process was inhibited by 3-MA at the early stage, or by CQ at the late stage. Additionally, the induction of autophagy by rapamycin also enhanced the viral titer. The effect of autophagy modulation on PEDV replication was further evaluated by silencing the two essential endogenous components *Beclin1* and *ATG5* [26,42]. Beclin1 (ATG6), a critical component in the class III PI3 kinase complex (PI3KC3), is involved in the initial step of autophagosome formation, while the ATG12-ATG5 conjugate, a key regulator, participates in autophagosome maturation [43]. The abolishment of their expression reduced the PEDV titer. These results suggested that autophagy induction might benefit PEDV replication. Autophagy has also been documented to have a complex interaction with apoptosis during viral infection [44–46]. For instance, influenza A virus was documented to induce apoptosis in autophagy protein deficient cells [47]. Autophagy was also reported to postpone apoptotic cell death during porcine reproductive and respiratory syndrome virus (PRRSV) infection through Bad-Beclin1 interaction [48,49]. The interplay of autophagy and apoptosis during PEDV infection needs to be further elucidated for a better understanding of the autophagy mechanism by which PEDV benefits its infection.

Recently, autophagy has been identified as an important component of the immune system, functioning from the elimination of infectious agents to the modulation of inflammatory responses [50,51]. The crosstalk between autophagy and inflammation has drawn much attention from researchers in recent years, while the relationship between autophagy and PEDV induced inflammatory responses is largely unclear. In the present study, we showed the expression of inflammatory cytokines and the activation of the NF-κB signaling pathway were both restrained in PEDV infected autophagy deficient cells, implying that autophagy might participate in PEDV induced inflammatory responses, especially for the NF-κB signaling pathway. Meanwhile, Vero cells with a NF-κB pathway deficiency exhibited a decreased level of LC3-II after PEDV infection, suggesting that the NF-κB signaling pathway might also have a positive role in autophagy induction. It was worth mentioning that the PEDV yield was reduced in both autophagy deficient or NF-κB pathway deficient cells. The decreased expression of inflammatory cytokines induced by TNF-α in autophagy deficient cells might provide new clues for deciphering the complex relationship between autophagy and inflammation. The cause-and-effect relationship between the restriction of PEDV yield reduction on the expression of inflammatory cytokines and the restraint of inflammation inhibition on PEDV replication in autophagy deficient cells needs further elucidation. A previous study reported that the positive feedback loop between autophagy and the NF-κB signaling cascade might exacerbate the inflammation induced by H5N1 pseudotyped viral particles [28]. The inhibition of NF-κB was also documented to induce autophagy suppression, leading to apoptosis in pancreatic ductal adenocarcinoma cells [52]. We speculate that autophagy and inflammatory cascade reactions might be positively regulated by PEDV infection to exacerbate inflammation. Furthermore, apoptosis might play a pivotal role in the complex relationship between autophagy and inflammation.

In summary, this is the first report concerning the potential induction of autophagy in PEDV infected Vero cells to facilitate its replication. Autophagy induction might be manipulated by PEDV to mediate the inflammatory cascade responses, and have a positive feedback loop with the NF-κB signaling pathway. Our knowledge regarding the interplay between PEDV infection and autophagy is still insufficient. The integrated data facilitate our understanding of the pathogenesis of PEDV infection and provide novel insights into the development of effective therapeutic strategies. Further research can focus on the complex relationship between autophagy modulation and immune responses, as well as apoptosis.

Acknowledgments: This work was supported by grants from the National Key Research and Development Program of China (2016YFD0500702) and the China Agricultural Research System (CARS-36). We thank prof. Xiang Mao from the Shanghai Veterinary Research Institute, for providing the GFP-mRFP-LC3 tandem reporter construct.

Author Contributions: Xiaozhen Guo had full access to all of the data in the study and takes responsibility for the integrity of the data and the accuracy of the data analysis; Study conception and design: Xiaozhen Guo, Mengjia Zhang, Xiaoqian Zhang, Zhonghua Li, Meizhou Wu, Atta Muhan mMad Memon, and Qigai He; Acquisition of data: Xiaozhen Guo, Xin Tan, Hengke Guo, Wei Zeng, Guokai Yan; Analysis and interpretation of data: Xiaozhen Guo, Yinxing Zhu, Bingzhou Zhang, Xugang Ku, Shengxian Fan.

Conflicts of Interest: The authors declare no conflict of interest.

References

1. Li, W.; Li, H.; Liu, Y.; Pan, Y.; Deng, F.; Song, Y.; Tang, X.; He, Q. New variants of porcine epidemic diarrhea virus, China, 2011. *Emerg. Infect. Dis.* **2012**, *18*, 1350–1353. [CrossRef] [PubMed]
2. Crawford, K.; Lager, K.M.; Kulshreshtha, V.; Miller, L.C.; Faaberg, K.S. Status of vaccines for porcine epidemic diarrhea virus in the United States and Canada. *Virus Res.* **2016**, *226*, 108–116. [CrossRef] [PubMed]
3. Islam, M.T.; Kubota, T.; Ujike, M.; Yahara, Y.; Taguchi, F. Phylogenetic and antigenic characterization of newly isolated porcine epidemic diarrhea viruses in Japan. *Virus Res.* **2016**, *222*, 113–119. [CrossRef] [PubMed]
4. Dastjerdi, A.; Carr, J.; Ellis, R.J.; Steinbach, F.; Williamson, S. Porcine epidemic diarrhea virus among farmed pigs, ukraine. *Emerg. Infect. Dis.* **2015**, *21*, 2235–2237. [CrossRef] [PubMed]
5. Duarte, M.; Gelfi, J.; Lambert, P.; Rasschaert, D.; Laude, H. Genome organization of porcine epidemic diarrhoea virus. *Adv. Exp. Med. Biol.* **1993**, *342*, 55–60. [PubMed]
6. Song, D.; Park, B. Porcine epidemic diarrhoea virus: A comprehensive review of molecular epidemiology, diagnosis, and vaccines. *Virus Genes* **2012**, *44*, 167–175. [CrossRef] [PubMed]
7. Zhang, Q.; Shi, K.; Yoo, D. Suppression of type I interferon production by porcine epidemic diarrhea virus and degradation of creb-binding protein by NSP1. *Virology* **2016**, *489*, 252–268. [CrossRef] [PubMed]
8. Kim, H.J.; Lee, S.; Jung, J.U. When autophagy meets viruses: A double-edged sword with functions in defense and offense. *Semin. Munopathol.* **2010**, *32*, 323–341. [CrossRef] [PubMed]
9. Sun, Y.; Yu, S.; Ding, N.; Meng, C.; Meng, S.; Zhang, S.; Zhan, Y.; Qiu, X.; Tan, L.; Chen, H.; et al. Autophagy benefits the replication of newcastle disease virus in chicken cells and tissues. *J. Virol.* **2014**, *88*, 525–537. [CrossRef] [PubMed]
10. Kroemer, G.; Marino, G.; Levine, B. Autophagy and the integrated stress response. *Mol. Cell* **2010**, *40*, 280–293. [CrossRef] [PubMed]
11. Kudchodkar, S.B.; Levine, B. Viruses and autophagy. *Rev. Med. Virol.* **2009**, *19*, 359–378. [CrossRef] [PubMed]
12. Dreux, M.; Chisari, F.V. Viruses and the autophagy machinery. *Cell Cycle* **2010**, *9*, 1295–1307. [CrossRef] [PubMed]
13. Chaumorcel, M.; Souquere, S.; Pierron, G.; Codogno, P.; Esclatine, A. Human cytomegalovirus controls a new autophagy-dependent cellular antiviral defense mechanism. *Autophagy* **2008**, *4*, 46–53. [CrossRef] [PubMed]
14. Talloczy, Z.; Jiang, W.; Virgin, H.W.T.; Leib, D.A.; Scheuner, D.; Kaufman, R.J.; Eskelinen, E.L.; Levine, B. Regulation of starvation- and virus-induced autophagy by the eIF2alpha kinase signaling pathway. *Proc. Natl. Acad. Sci. USA* **2002**, *99*, 190–195. [CrossRef] [PubMed]
15. Pei, J.; Zhao, M.; Ye, Z.; Gou, H.; Wang, J.; Yi, L.; Dong, X.; Liu, W.; Luo, Y.; Liao, M.; et al. Autophagy enhances the replication of classical swine fever virus in vitro. *Autophagy* **2014**, *10*, 93–110. [CrossRef] [PubMed]
16. Sun, M.X.; Huang, L.; Wang, R.; Yu, Y.L.; Li, C.; Li, P.P.; Hu, X.C.; Hao, H.P.; Ishag, H.A.; Mao, X. Porcine reproductive and respiratory syndrome virus induces autophagy to promote virus replication. *Autophagy* **2012**, *8*, 1434–1447. [CrossRef] [PubMed]
17. Berkova, Z.; Crawford, S.E.; Trugnan, G.; Yoshimori, T.; Morris, A.P.; Estes, M.K. Rotavirus nsp4 induces a novel vesicular compartment regulated by calcium and associated with viroplasms. *J. Virol.* **2006**, *80*, 6061–6071. [CrossRef] [PubMed]
18. Sun, D.; Shi, H.; Guo, D.; Chen, J.; Shi, D.; Zhu, Q.; Zhang, X.; Feng, L. Analysis of protein expression changes of the vero E6 cells infected with classic pedv strain CV777 by using quantitative proteomic technique. *J. Virol. Methods* **2015**, *218*, 27–39. [CrossRef] [PubMed]

19. Guo, X.; Hu, H.; Chen, F.; Li, Z.; Ye, S.; Cheng, S.; Zhang, M.; He, Q. Itraq-based comparative proteomic analysis of vero cells infected with virulent and CV777 vaccine strain-like strains of porcine epidemic diarrhea virus. *J. Proteom.* **2016**, *130*, 65–75. [CrossRef] [PubMed]
20. Cheng, S.; Yan, W.; Gu, W.; He, Q. The ubiquitin-proteasome system is required for the early stages of porcine circovirus type 2 replication. *Virology* **2014**, *456–457*, 198–204. [CrossRef] [PubMed]
21. Kim, Y.; Lee, C. Porcine epidemic diarrhea virus induces caspase-independent apoptosis through activation of mitochondrial apoptosis-inducing factor. *Virology* **2014**, *460–461*, 180–193. [CrossRef] [PubMed]
22. Reggiori, F.; Monastyrska, I.; Verheije, M.H.; Cali, T.; Ulasli, M.; Bianchi, S.; Bernasconi, R.; de Haan, C.A.; Molinari, M. Coronaviruses hijack the LC3-I-positive EDEmosomes, ER-derived vesicles exporting short-lived ERAD regulators, for replication. *Cell Host Microbe* **2010**, *7*, 500–508. [CrossRef] [PubMed]
23. Knoops, K.; Kikkert, M.; Worm, S.H.; Zevenhoven-Dobbe, J.C.; van der Meer, Y.; Koster, A.J.; Mo mMaas, A.M.; Snijder, E.J. Sars-coronavirus replication is supported by a reticulovesicular network of modified endoplasmic reticulum. *PLoS Biol.* **2008**, *6*, e226. [CrossRef] [PubMed]
24. Cottam, E.M.; Maier, H.J.; Manifava, M.; Vaux, L.C.; Chandra-Schoenfelder, P.; Gerner, W.; Britton, P.; Ktistakis, N.T.; Wileman, T. Coronavirus NSP6 proteins generate autophagosomes from the endoplasmic reticulum via an omegasome intermediate. *Autophagy* **2011**, *7*, 1335–1347. [CrossRef] [PubMed]
25. Chen, Q.; Fang, L.; Wang, D.; Wang, S.; Li, P.; Li, M.; Luo, R.; Chen, H.; Xiao, S. Induction of autophagy enhances porcine reproductive and respiratory syndrome virus replication. *Virus Res.* **2012**, *163*, 650–655. [CrossRef] [PubMed]
26. Seglen, P.O.; Gordon, P.B. 3-methyladenine: Specific inhibitor of autophagic/lysosomal protein degradation in isolated rat hepatocytes. *Proc. Natl. Acad. Sci. USA* **1982**, *79*, 1889–1892. [CrossRef] [PubMed]
27. Shrivastava, S.; Raychoudhuri, A.; Steele, R.; Ray, R.; Ray, R.B. Knockdown of autophagy enhances the innate i mMune response in hepatitis C virus-infected hepatocytes. *Hepatology* **2011**, *53*, 406–414. [CrossRef] [PubMed]
28. Pan, H.; Zhang, Y.; Luo, Z.; Li, P.; Liu, L.; Wang, C.; Wang, H.; Li, H.; Ma, Y. Autophagy mediates avian influenza H5N1 pseudotyped particle-induced lung infla mMation through NF-kappab and p38 MAPK signaling pathways. *Am. J. Physiol. Lung Cell. Mol. Physiol.* **2014**, *306*, L183–L195. [CrossRef] [PubMed]
29. Cao, L.; Ge, X.; Gao, Y.; Ren, Y.; Ren, X.; Li, G. Porcine epidemic diarrhea virus infection induces NF-kappab activation through the TLR2, TLR3 and TLR9 pathways in porcine intestinal epithelial cells. *J. Gen. Virol.* **2015**, *96*, 1757–1767. [CrossRef] [PubMed]
30. Ke, P.Y.; Chen, S.S. Autophagy in hepatitis C virus-host interactions: Potential roles and therapeutic targets for liver-associated diseases. *World J. Gastroenterol.* **2014**, *20*, 5773–5793. [CrossRef] [PubMed]
31. Dreux, M.; Gastaminza, P.; Wieland, S.F.; Chisari, F.V. The autophagy machinery is required to initiate hepatitis c virus replication. *Proc. Natl. Acad. Sci. USA* **2009**, *106*, 14046–14051. [CrossRef] [PubMed]
32. Orvedahl, A.; Alexander, D.; Talloczy, Z.; Sun, Q.; Wei, Y.; Zhang, W.; Burns, D.; Leib, D.A.; Levine, B. HSV-1 ICP34.5 confers neurovirulence by targeting the beclin 1 autophagy protein. *Cell Host Microbe* **2007**, *1*, 23–35. [CrossRef] [PubMed]
33. Prentice, E.; Jerome, W.G.; Yoshimori, T.; Mizushima, N.; Denison, M.R. Coronavirus replication complex formation utilizes components of cellular autophagy. *J. Biol. Chem.* **2004**, *279*, 10136–10141. [CrossRef] [PubMed]
34. Maier, H.J.; Cottam, E.M.; Stevenson-Leggett, P.; Wilkinson, J.A.; Harte, C.J.; Wileman, T.; Britton, P. Visualizing the autophagy pathway in avian cells and its application to studying infectious bronchitis virus. *Autophagy* **2013**, *9*, 496–509. [CrossRef] [PubMed]
35. Klionsky, D.J.; Abdelmohsen, K.; Abe, A.; Abedin, M.J.; Abeliovich, H.; Acevedo Arozena, A.; Adachi, H.; Adams, C.M.; Adams, P.D.; Adeli, K.; et al. Guidelines for the use and interpretation of assays for monitoring autophagy (3rd edition). *Autophagy* **2016**, *12*, 1–222. [CrossRef] [PubMed]
36. Ulasli, M.; Verheije, M.H.; de Haan, C.A.; Reggiori, F. Qualitative and quantitative ultrastructural analysis of the membrane rearrangements induced by coronavirus. *Cell Microbiol.* **2010**, *12*, 844–861. [CrossRef] [PubMed]
37. Mizushima, N.; Yoshimori, T.; Levine, B. Methods in ma mMalian autophagy research. *Cell* **2010**, *140*, 313–326. [CrossRef] [PubMed]

38. Richetta, C.; Gregoire, I.P.; Verlhac, P.; Azocar, O.; Baguet, J.; Flacher, M.; Tangy, F.; Rabourdin-Combe, C.; Faure, M. Sustained autophagy contributes to measles virus infectivity. *PLoS Pathogens* **2013**, *9*, e1003599. [CrossRef] [PubMed]
39. Buckingham, E.M.; Carpenter, J.E.; Jackson, W.; Grose, C. Autophagy and the effects of its inhibition on varicella-zoster virus glycoprotein biosynthesis and infectivity. *J. Virol.* **2014**, *88*, 890–902. [CrossRef] [PubMed]
40. Klionsky, D.J.; Abdalla, F.C.; Abeliovich, H.; Abraham, R.T.; Acevedo-Arozena, A.; Adeli, K.; Agholme, L.; Agnello, M.; Agostinis, P.; Aguirre-Ghiso, J.A.; et al. Guidelines for the use and interpretation of assays for monitoring autophagy. *Autophagy* **2012**, *8*, 445–544. [CrossRef] [PubMed]
41. Zhao, Z.; Thackray, L.B.; Miller, B.C.; Lynn, T.M.; Becker, M.M.; Ward, E.; Mizushima, N.N.; Denison, M.R.; Virgin, H.W.T. Coronavirus replication does not require the autophagy gene ATG5. *Autophagy* **2007**, *3*, 581–585. [CrossRef] [PubMed]
42. Petiot, A.; Ogier-Denis, E.; Blo mMaart, E.F.; Meijer, A.J.; Codogno, P. Distinct classes of phosphatidylinositol 3′-kinases are involved in signaling pathways that control macroautophagy in HT-29 cells. *J. Biol. Chem.* **2000**, *275*, 992–998. [CrossRef] [PubMed]
43. Wang, J. Beclin 1 bridges autophagy, apoptosis and differentiation. *Autophagy* **2008**, *4*, 947–948. [CrossRef] [PubMed]
44. Wang, K. Autophagy and apoptosis in liver injury. *Cell Cycle* **2015**, *14*, 1631–1642. [CrossRef] [PubMed]
45. Gougeon, M.L.; Piacentini, M. New insights on the role of apoptosis and autophagy in hiv pathogenesis. *Apoptosis* **2009**, *14*, 501–508. [CrossRef] [PubMed]
46. Xin, L.; Xiao, Z.; Ma, X.; He, F.; Yao, H.; Liu, Z. Coxsackievirus b3 induces crosstalk between autophagy and apoptosis to benefit its release after replicating in autophagosomes through a mechanism involving caspase cleavage of autophagy-related proteins. *Infect. Genet. Evol.* **2014**, *26*, 95–102. [CrossRef] [PubMed]
47. Gannage, M.; Dormann, D.; Albrecht, R.; Dengjel, J.; Torossi, T.; Ramer, P.C.; Lee, M.; Strowig, T.; Arrey, F.; Conenello, G.; et al. Matrix protein 2 of influenza a virus blocks autophagosome fusion with lysosomes. *Cell Host Microbe* **2009**, *6*, 367–380. [CrossRef] [PubMed]
48. Zhou, A.; Li, S.; Khan, F.A.; Zhang, S. Autophagy postpones apoptotic cell death in prrsv infection through bad-beclin1 interaction. *Virulence* **2016**, *7*, 98–109. [CrossRef] [PubMed]
49. Li, S.; Zhou, A.; Wang, J.; Zhang, S. Interplay of autophagy and apoptosis during prrsv infection of marc145 cell. *Infect. Genet. Evol.* **2016**, *39*, 51–54. [CrossRef] [PubMed]
50. Valdor, R.; Macian, F. Autophagy and the regulation of the I mMune response. *Pharmacol. Res.* **2012**, *66*, 475–483. [CrossRef] [PubMed]
51. Levine, B.; Mizushima, N.; Virgin, H.W. Autophagy in I mMunity and infla mMation. *Nature* **2011**, *469*, 323–335. [CrossRef] [PubMed]
52. Papademetrio, D.L.; Lompardia, S.L.; Simunovich, T.; Costantino, S.; Mihalez, C.Y.; Cavaliere, V.; Alvarez, E. Inhibition of survival pathways MAPK and NF-kb triggers apoptosis in pancreatic ductal adenocarcinoma cells via suppression of autophagy. *Target Oncol.* **2016**, *11*, 183–195. [CrossRef] [PubMed]

© 2017 by the authors. Licensee MDPI, Basel, Switzerland. This article is an open access article distributed under the terms and conditions of the Creative Commons Attribution (CC BY) license (http://creativecommons.org/licenses/by/4.0/).

viruses

MDPI

Review

Update on Senecavirus Infection in Pigs

Raquel A. Leme [1,2], Alice F. Alfieri [1,2] and Amauri A. Alfieri [1,2,*]

[1] Laboratory of Animal Virology, Department of Veterinary Preventive Medicine, Universidade Estadual de Londrina, P.O. Box 10011, Paraná 86057-970, Brazil; raquelarrudaleme@gmail.com (R.A.L.); aalfieri@uel.br (A.F.A.)

[2] Multi-User Animal Health Laboratory, Molecular Biology Unit, Department of Veterinary Preventive Medicine, Universidade Estadual de Londrina, P.O. Box 10011, Paraná 86057-970, Brazil

* Correspondence: alfieri@uel.br; Tel.: +55-43-33715876; Fax: +55-43-33714485

Academic Editors: Linda Dixon and Simon Graham
Received: 26 April 2017; Accepted: 28 June 2017; Published: 3 July 2017

Abstract: *Senecavirus A* (SVA) is a positive-sense single-stranded RNA virus that belongs to the *Senecavirus* genus within the *Picornaviridae* family. The virus has been silently circulating in pig herds of the USA since 1988. However, cases of senecavirus-associated vesicular disease were reported in Canada in 2007 and in the USA in 2012. Since late 2014 and early 2015, an increasing number of senecavirus outbreaks have been reported in pigs in different producing categories, with this virus being detected in Brazil, China, and Thailand. Considering the novel available data on senecavirus infection and disease, 2015 may be a divisor in the epidemiology of the virus. Among the aspects that reinforce this hypothesis are the geographical distribution of the virus, the affected pig-producing categories, clinical signs associated with the infection, and disease severity. This review presents the current knowledge regarding the senecavirus infection and disease, especially in the last two years. Senecavirus epidemiology, pathogenic potential, host immunological response, diagnosis, and prophylaxis and control measures are addressed. Perspectives are focused on the need for complete evolutionary, epidemiological and pathogenic data and the capability for an immediate diagnosis of senecavirus infection. The health risks inherent in the swine industry cannot be neglected.

Keywords: swine; picornavirus; Seneca Valley virus; emergent disease; vesicular disease; neonatal mortality

1. Introduction

A new virus named Seneca Valley virus was identified in 2002, and classified as the only representative strain of the *Senecavirus A* species in the new genus *Senecavirus*. Since then, until the end of 2014, little progress has been made regarding the virus features and infection in swine, including its epidemiology, transmission, pathogenesis, pathology, clinical signs, and diagnosis. The disease was considered exotic and limited in terms of geographic distribution. Senecavirus infection in swine has not been extensively studied by North American researchers or by worldwide research groups, even though it is a vesicular disease, likely due to the low frequency of infection, with the only reported cases being in North American countries.

In early 2015, different isolates of senecavirus were first reported in vesicular disease outbreaks outside of North America in Brazil, China, and Thailand. In the same year, the virus infection was associated with novel clinical manifestations in newborn pigs. Simultaneously, new cases occurred in the USA. These events were responsible for an increase in the number and the diversity of research approaches based on the senecavirus infection.

More knowledge has been accumulated and more unknown points have been clarified on the etiological agent and the virus infection, in approximately the last 24 months, than have been in all

of the previous years. The scientific community was able to comply promptly with the demand for objective and clear answers to issues raised by pig producers and consultant veterinarians in private and public sectors who suddenly faced outbreaks of a completely unknown vesicular infectious disease.

The currently available data were generated in a short timeframe, which is rarely seen in similar cases of viral diseases in animals without a public health impact. The goal of this review is to present the step-by-step evolution of senecavirus-based studies, particularly in the last two years, and to describe the features of the etiological agent and infection in pigs.

2. History, Classification, and Molecular Features

Seneca Valley virus was incidentally isolated in Gaithersburg, Maryland, USA in 2002 from the PER.C6 (transformed fetal retinoblast) cell line. The virus had evidently been introduced into the cell culture through the use of contaminated fetal bovine serum or porcine trypsin [1]. The virus was discovered in the laboratories of Neotropix, Inc., located near Seneca Creek State Park, Gaithersburg, MA, USA, which explains the name of the virus [2].

Until 2014, only three complete genomic sequences of Seneca Valley virus were available in public databases (GenBank accession numbers NC_011349, DQ641257, KC667560). Therefore, few studies were based on the complete genome of the virus, with the predominant prototype being SVV-001 (GenBank accession number DQ641257) [3–5]. These studies led to the definitive classification of Seneca Valley virus as the single representative strain of the species *Senecavirus A* (SVA), genus *Senecavirus* within *Picornaviridae* family [6].

SVV-001 has the typical genome of other picornaviruses, with the standard L-4-3-4, layout, namely Leader—4 polypeptides of the P1—3 polypeptides of P2—and 4 polypeptides of P3. The SVV genomic RNA consists of approximately 7200 nucleotides (nt), with additional 666 nt in the 5′UTR portion and 71 nt in the 3′UTR portion and a poly(A) tail. The virus genome has a single open reading frame (ORF) that encodes a polyprotein of approximately 2180 amino acids (aa) [3].

An analysis of the nt sequence within 5′UTR of the SVV-001 prototype revealed high levels of secondary structures [3]. The 5′UTR region of the SVA genome has an internal ribosome entry site (IRES), the function of which is to allow independent translation of the viral RNA by inhibiting the translation of cellular RNA. The 406–625 nt sequence is 57.3% identical to the Hepatitis C virus (*Flaviviridae* family), suggesting that the IRES of senecaviruses is type IV [5]. This finding corroborates previous results, in which several secondary structures from flaviviruses and picornaviruses were identified [7–9].

The genomic characteristics of SVA are very similar to the members of *Cardiovirus* genus, especially in relation to the polypeptides P1, 2C, 3C, and 3D. However, SVV-001 differs from cardiovirus in polypeptides 2B and 3A and the IRES type. Genomic regions 2A, 2B, 3A, and 3B of SVV-001 differ considerably from those of all other picornaviruses [3].

Initially, senecaviruses were not associated with any specific pathology. However, many studies have focused on the potential oncolytic activity of senecavirus in human cancer therapy [3,10]. The first evidence that senecaviruses could be associated with porcine vesicular disease was obtained in Canada (2008) and the USA (2012), where symptomatic pigs were detected with the viral RNA by reverse transcription (RT)-PCR assay [11,12]. In both cases, the clinical signs were indistinguishable from vesicular foreign animal diseases, such as foot-and-mouth disease (FMD), swine vesicular disease (SVD), vesicular stomatitis (VS), and vesicular exanthema of swine (VES). These findings prompted the North American animal health authorities to adopt surveillance measures immediately and invest in new studies [13].

3. Senecavirus Infection in Swine Until 2014

Cases of vesicular diseases of unknown etiologies were reported in pigs in New Zealand [14,15], Australia [16], and the USA [17] in the 1980s. In Europe, reports were performed in the UK in 2007 [18] and Italy in 2010 [19]. In the cases reported in New Zealand and Australia, the occurrence of vesicular

lesions in pigs were associated with contact with a green vegetable material infected with the fungus *Sclerotinia sclerotiorum* [14,15] and the feeding of marine products [16]. In the cases that occurred in the USA, the United Kingdom, and Italy, the diagnostic results were negative for the vesicular foreign animal diseases, and the possible cause(s) of the vesicular disease outbreaks in those animals remained unknown.

Senecavirus was not investigated in any of these cases. In New Zealand, Australia, and the USA, the cases of senecavirus infection were not investigated due to the event dates, since the virus was not known at that time. However, the reasons that the virus was not investigated in the United Kingdom and Italy cannot be ascertained due to the limited data available on the outbreaks in these countries [20].

In 2004, outbreaks of vesicular disease were reported in pigs of different production categories in Indiana, USA. Clinical manifestations resembled those of vesicular foreign animal diseases, which were investigated and not detected [21]. Since the etiology of the clinical signs could not be determined, the syndrome was named Porcine Idiopathic Vesicular Disease (PIVD) [21].

Pasma, Davidson, and Shaw [11] in 2007 reported that approximately 80% of 187 pigs that were being transported from Canada to the USA presented vesicular lesions that were indistinguishable of those of vesicular foreign animal diseases. FMD, SVD, VS, and VES viruses tested negative in those symptomatic animals. However, senecavirus RNA was detected in the biological samples and was proposed as the etiological agent of the vesicular disease in those pigs [11]. The second detection of senecavirus occurred in 2012 in Indiana, USA, in a single 6-month-old animal with vesicular lesions. This finding reinforced the possible association of senecavirus infection with vesicular disease [12].

Although only two reports of senecavirus detection in symptomatic animals were available, a 20-year (1988–2008) retrospective serological study conducted with serum samples of asymptomatic pigs from different states in the USA showed the wide temporal and geographical distribution of senecavirus [3], revealing the silent circulation of the virus throughout the country over the years.

Considering these studies and the indistinguishable feature of the vesicular lesions associated to senecavirus infection with those caused by the vesicular foreign animal diseases, especially FMD, the United States Animal Health Association elaborated a resolution in which senecaviruses and PIVD are the main subjects, with the aim of developing and implementing plans to minimize the consequences of vesicular lesions not associated with foreign animal diseases found in pigs of that country [13], reinforcing the health and economic importance of these emerging pathogens and disease in swine [20].

4. Senecavirus Infection in Swine during/after 2015

At the end of 2014 and the beginning of 2015, outbreaks of vesicular disease in weaned and adult pigs were reported in different geographical regions of Brazil. Simultaneously, increasing mortality rates of newborn pigs at 1 to 4 days of age were recorded in the main Brazilian pig-producing regions. The reported clinical signs in affected piglets included lethargy, cutaneous hyperemia, diarrhea, neurological signs, and/or sudden death [22–25]. The Animal Health Department of the Brazilian Ministry of Agriculture, Livestock, and Food Supply (MAPA) provided official tests to screen for foreign animal diseases, specifically FMD, classical swine fever (CSF), and porcine epidemic diarrhea virus (PEDV), but negative results were observed [20,26]. However, other study groups detected senecavirus in pigs with vesicular lesions of different states in the country [20,22,25,27] (Figure 1A), and the virus was considered to be the etiological agent of the reported vesicular disease outbreaks. Additionally, piglets that spontaneously died were submitted to diagnostic investigations and tested negative for different infectious agents that could be associated with one or more of the reported clinical signs, including diarrhea. Since most of the cases were from pig herds with a clinical history of vesicular disease, senecavirus was investigated in piglet biological samples, with positive results being observed in feces, serum, and diverse organ/tissue samples [22–25] (Figure 1B).

Figure 1. Lesions associated with senecavirus infection. (**A**) Fluid-filled vesicles on the snouts of senecavirus-positive sows. (**B**) Ulcerative lesions on the foot of a three-day-old piglet (**left**) and diphteric gengivitis in a one-day-old piglet (**right**), both positive for senecavirus.

These reports were the first describing senecavirus outside of North American countries. Whether the virus was circulating in Brazil before this period was unknown. However, a 10-year (2007–2016) retrospective serological study conducted in Brazil from serum samples of pigs at different ages suggested that senecavirus was not circulating in the country before 2014, the same year in which senecavirus-associated vesicular disease outbreaks were first reported in the country [28].

Senecavirus was first reported outside of the American continent in China in 2015 [29,30]. Pigs in herds located in Guangdong province presented vesicular lesions, and sudden death was observed in newborn piglets. The samples derived from these outbreaks were negative for classic vesicular diseases, but they presented positive results for senecavirus [29,30]. Later, senecavirus infection was reported in symptomatic piglets in other Chinese provinces [31].

Since July 2015, an increased number of senecavirus-vesicular disease outbreaks was reported in the USA [32]; but for the first time in that country, the virus infection was also associated with pig neonatal mortality, especially in pig herds with vesicular disease-affected sows [33,34]. In 2016, pig herds from Canada and Thailand were also affected by senecavirus infection [35,36] (Figure 2).

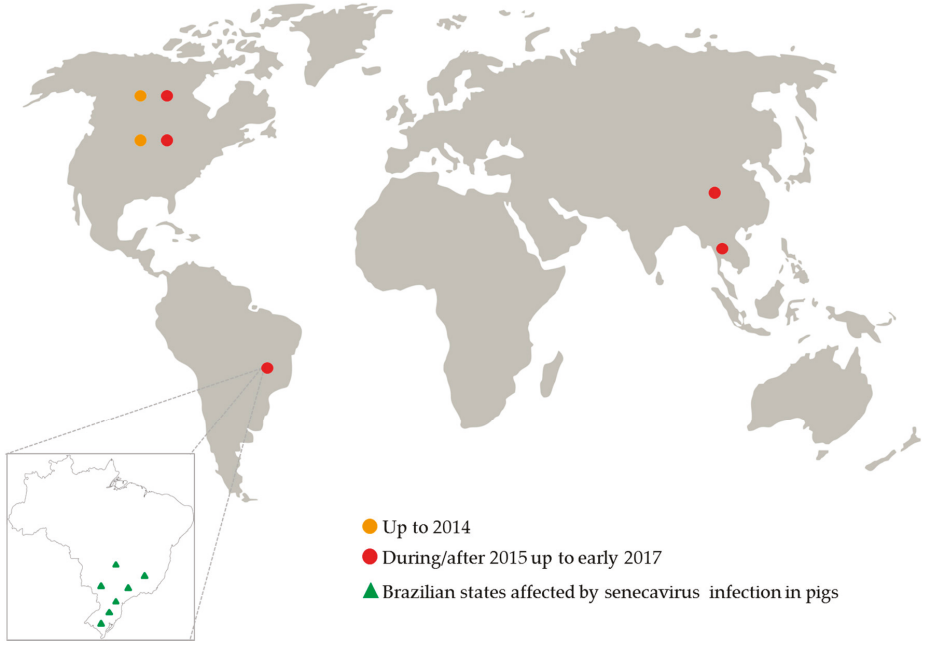

Figure 2. Senecavirus global distribution from 1988 up to early 2017.

4.1. Epidemiology of Senecavirus Infection

Based on all of these events, 2015 can be considered a turning point for the epidemiology of the senecavirus infection, with many important features of senecaviruses being identified. Until that year, only two cases of senecavirus-induced vesicular disease were reported with a limited number of affected pigs [11,12]. However, during/after 2015 the number of senecavirus infection reports significantly increased and also the morbidity and mortality rates associated with the infection. The morbidity and mortality rates of senecavirus-induced disease vary according to the affected pig category. In a herd that is affected for the first time, the morbidity rates range from 4 to 70% depending on the clinical signs and the pig age groups [20,23,33,34,37]. Senecavirus outbreaks presented morbidity rates of 0.5 to 5% in weaned pigs and 5 to 30% in finishing pigs and breeders [2,20,34], which varied according to the geographical region and the herd origin. Remarkably higher morbidity rates in sows were reported, reaching 70 to 90% [37]. However, the mortality in these categories is very low (≈0.2%), with pigs recovering soon after the remission of clinical signs that last for 10 to 15 days.

In newborn pigs, morbidity and mortality rates are considerably higher, especially in one- to four-day-old piglets, with morbidity rates that can reach 70%, but the mortality rates vary from 15 to 30% [2,23,24,33,34,37]. However, the clinical manifestations and the high mortality rates in piglets last for approximately 2 to 3 weeks in the affected herd.

To the authors' knowledge, no re-breaks were reported in previously affected herds, but this is not a permanent condition. The infection likely becomes endemic when most of the animals present asymptomatically and/or with subclinical infection and when clinical manifestations occur in pigs that have not been previously infected, are seronegative, or have low titers of senecavirus-specific antibodies. Furthermore, the declining immunity or the introduction of naive gilts in affected herds and the persistence of the virus in the animal and in the environment may trigger a new outbreak in previously affected herds [2].

After many outbreaks of senecavirus infection were reported in 2015 in the USA, an investigation of 2033 oral fluid samples of asymptomatic pigs from herds located in 25 states of that country revealed that only 1.2% of the samples were RT-PCR-positive for the virus RNA [38]. In contrast, senecavirus RNA was amplified from different biological samples of finishing pigs with vesicular disease. Vesicular fluid and/or the lesions of naturally infected pigs presented high virus loads (2×10^7 to 1.2×10^{11} genomic copies/mL) [39], suggesting that direct contact between animals with fluid-filled and/or recently ruptured vesicles and susceptible individuals likely represents one of the most important transmission routes of the virus.

Senecavirus shedding was demonstrated in fecal samples from piglets that presented multisystemic clinical signs, including diarrhea [23,24], and from finishing pigs that were naturally infected with the virus and presented vesicular lesions [39]. Additionally, immunohistochemical and RT-PCR assays revealed the senecavirus presence in the urinary epithelium of clinically affected piglets, suggesting that urine may represent a senecavirus dissemination route and a possible contamination source in affected pig herds [23,24].

Senecavirus RNA and viable infective virus particles were isolated in cell cultures from fecal and small intestine samples of mice from clinically affected pig herds in the USA. Houseflies collected from both affected and non-affected herds tested positive for the virus [40]. The detection of the virus genome and/or the isolation of infective senecavirus particles in houseflies and mice suggest that these species may play a role in the epidemiology of the infection [40]. The movement of people, primarily on-farm employee entry, and vehicles, especially those used for the disposal of dead animals and feed delivery, farm tools and equipment, including those used for carcass removal, were also implicated as possible means of introduction and indirect transmission routes of senecaviruses in different pig breeding herds in the USA [37,40].

The possibility that senecavirus can be vertically transmitted was raised after the virus was detected by both RT-PCR and immunohistochemical assays from different tissue/organ samples of piglets aged one to two days old [24]. However, further studies are needed to confirm this route of viral transmission.

After the occurrence and/or the increasing incidence of senecavirus-associated vesicular disease in Brazil, China, the USA, Canada, and Thailand [22,29,30,39,41–43] complete (n = 42) and partial (n = 15) (These numbers were determined based on the complete and partial senecavirus genomic sequences available in GenBank during/after 2015 (Genbank accesses date: 8 June 2017)) genomic sequences were established from senecavirus strains in most of these countries. Therefore, advances were also possible in terms of the molecular epidemiology of the virus. The 42 complete genomic sequences of senecaviruses from 2015 to 2016 showed high nt (95.8 to 99.9%) similarities among each other and lower nt (93.8 to 94.6%) identities with the prototype strain SVV-001. The exception was the Canadian 11-55910-3 strain (GenBank accession number KC667560), which shares 95% and 96–98.2% nt similarities with the prototype SVV-001 and contemporary senecavirus strains, respectively. The grouping of senecavirus strains into three temporal clades was also observed [2,40]. Clade I includes the initially identified senecavirus strains, including SVV-001, clade II includes the USA senecavirus strains identified between 1988 and 1997, and clade III contains the senecavirus strains from Brazil, Canada, China, Thailand, and the USA identified between 2001 and 2016. A phylogenetic tree constructed with all of the currently available nt sequences of the VP1 region of senecaviruses showed a geographical grouping within clade III, with the senecavirus strains clustering according to the country of origin (Figure 3). Despite the divergence between historical and contemporary senecavirus strains, whether genetic changes in the senecavirus genome have led to different biological behaviors of the virus and/or contributed to the emergence of senecavirus infections remains unknown [32,40].

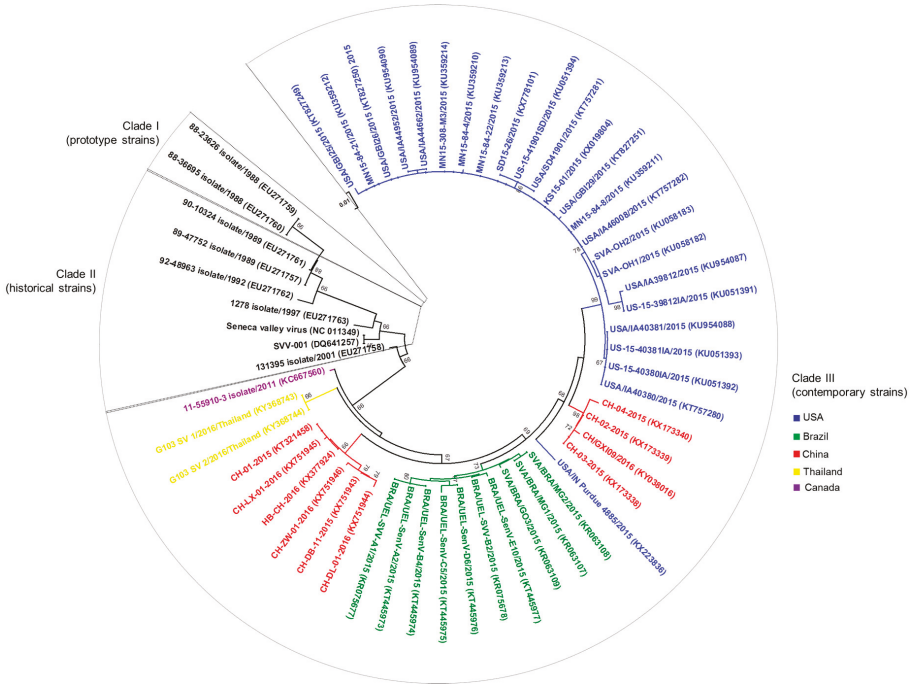

Figure 3. Evolutionary relationships of senecavirus strains identified in the USA, Canada, Brazil, China, and Thailand from 1988 to 2016. Phylogenetic tree constructed with 56 partial (541 bp) nucleotide sequences of the VP1 region of senecavirus genome. Year of sample collection and GenBank accession numbers for each senecavirus strain are presented within the tree. The evolutionary history was inferred using the Neighbor–Joining method [44]. The percentage of replicate trees in which the associated senecavirus strains clustered together in the bootstrap test (1000 replicates) are shown next to the branches [45]. The tree is drawn to scale, with branch lengths in the same units as those of the evolutionary distances used to infer the phylogenetic tree. The evolutionary distances were computed using the Maximum Composite Likelihood method [46] and are in the units of the number of base substitutions per site. Evolutionary analyses were conducted in MEGA7 [47].

4.2. Pathogenesis Evidence of Senecavirus

The definitive association of senecavirus with porcine vesicular disease was shown in experimental infections of 9-week- and 4-month-old pigs with contemporary senecavirus strains [32,48]. In both studies, the incubation period of senecavirus was of 4–5 days [32,48]. The tonsils were indicated as one of the primary sites of senecavirus replication during the acute stage of infection [32]. The viremia period was short, lasting approximately 7 days, and the peak of senecavirus genomic copies ($\approx 1 \times 10^{6.5}$/mL) was detected in serum on the third day post-inoculation (dpi) with a subsequent progressive reduction up to the 10th dpi from when the virus was no longer detected [32].

Senecaviruses induce an acute, self-limiting vesicular disease in pigs [32]. Inoculated pigs developed vesicular lesions on the snout, lips, and/or hooves [32,48], specifically on the coronary bands and/or the interdigital space [48]. Other clinical manifestations reported in senecavirus experimental infections include lethargy, lameness, and anorexia [32]. Multifocal deep ulcers and skin erosions/abrasions that evolved to crusted lesions were observed during the infection progress [32,48].

Tissue microscopic alterations in experimentally infected pigs were restricted to the tonsils, the spleen, lymph nodes, and the lungs and consisted of mild to moderate lymphoid hyperplasia in the

lymphoid tissue and multifocal mild atelectasis and occasionally diffuse congestion with multifocal mild perivascular accumulation of lymphocytes, plasma cells, and macrophages in the lungs [32]. A wide senecavirus tissue distribution was shown, with the presence of virus RNA and infectious particles in the lungs, the mediastinal and mesenteric lymph nodes, the liver, the spleen, the small and large intestines, and the tonsils during the acute phase of the disease. Convalescent pigs were positive for senecavirus RNA in different organs, except for the lungs, the heart, and the liver, but viable virus particles were not isolated from these tissues at a later infection period [32].

According to the experimental studies, senecavirus shedding lasts up to 28 days. The virus can be shed by oral and nasal secretions and feces. The virus excretion peak occurs between 1 and 5 dpi, especially in oral secretions, which presented higher virus loads relative to the nasal secretions and feces [32]. Additionally, senecavirus infectious particles were successfully isolated from oral secretions up to 21 dpi, feces up to 10 dpi, and nasal secretions up to 7 dpi [32]. The combined findings from natural and experimental senecavirus infection suggest that the oral/nasal secretions, feces, and likely urine [23,24] excretions of pigs infected with senecavirus may contribute to the dissemination of the virus both directly, through contact between the animals in the same facility, and indirectly, with the viral agent contaminating the environment. However, further studies are required to confirm the role of these secretions/excretions in senecavirus transmission in field conditions.

4.3. Immunological Response against Senecavirus

Currently there are only a few studies that have evaluated the host immunological response against senecavirus infection. These studies indicate that the senecavirus infection induces early immunological response in clinically affected and non-affected sows under field conditions [34] and in experimentally challenged finishing pigs [32,48]. Seroconvertion to the senecavirus occurs approximately 5 days after the infection, regardless of the clinical manifestations of the disease [32,34,49]. The increasing neutralizing antibody titers occurs simultaneously with decreasing disease severity, viral load in tissues, viremia, and virus shedding, suggesting that antibody responses lead to the progressive clearance of senecavirus from the circulation and most organs, excretions, and secretions [32,34].

The maximum concentration of senecavirus-specific immunoglobulin (Ig) M antibodies lasts for approximately 10 days (from 5 to 15 dpi) followed by a decreasing serological IgM concentration to undetectable titers by 21 dpi [49]. In contrast, the senecavirus-specific IgG response develops later [32,49], with a strong positive response after 21 dpi [49].

Different senecavirus antibody titers have been reported in naturally infected pigs and may vary from 160 to 2880 by indirect fluorescent antibody (IFA) or virus neutralization (VN) test [39,50]; but higher titers ($\geq$4096) were detected by the VN test from clinically affected animals in Brazil [28].

4.4. Senecavirus Diagnosis

Many diagnostic tests are currently available for the detection of senecavirus infection and/or its association with lesions and disease. Conventional [20,27,40,42] and quantitative RT-PCR (qRT-PCR) [27,33,34,38–40,51–53] molecular assays are the most used tests in addition to next-generation sequencing (NGS) technology [22,41,51,53]. Molecular assays, especially qRT-PCR, are the gold standards for any vesicular disease, since they are rapid, sensitive, and specific methods that enable the fast and accurate diagnosis of vesicular diseases, including senecavirus genome detection from different biological samples. A disadvantage of senecavirus diagnosis by molecular assay may be the inconsistent detection due to the progression of senecavirus infection, with variations in the viral shedding and/or load in different biological samples [34]. Therefore, a variety of specimens including serum, tonsils, feces, and oral and vesicular fluids, should be collected for senecavirus screening by molecular assays [54].

The other diagnostic tools currently available include immunohistochemical and in situ hybridization, which are assays that identify specific virus antigens and nucleic acid in tissue samples, respectively. Both of these techniques have been successfully used by different study groups for

senecavirus-associated disease diagnosis [23–25,32,55]. Although histopathological evaluation alone is not conclusive for senecavirus infection diagnosis, findings from this technique may guide the selection of tissue/organ samples for the immunohistochemical and in situ hybridization analyses.

The antibody detection methods available for senecavirus screening in pigs are indirect [34,49,56] and competitive [49,50] enzyme-linked immunosorbent assay (ELISA), IFA, and VN tests [28,50]. The main advantage of the antibody detection assays is the capability for processing large numbers of samples in epidemiological studies, mass diagnostic programs, and/or in epidemiological surveillance [57], indicating previous virus exposure and/or presence in a herd [56].

Regardless of the diagnostic method, senecavirus-associated disease in pigs is clinically indistinguishable from classical viral vesicular infections, especially FMD. The clinical history and/or the presence of lesions that indicate the possibility of vesicular disease should always lead to a complete vesicular foreign animal disease investigation, primarily in the major pig-producing countries, since the emergence of senecavirus infections could adversely affect the prompt reporting of FMD in swine [53].

4.5. Prophylaxis and Control Management

Currently, no vaccines or specific treatments are available for senecavirus infections. Therefore, sanitary practices should include prophylactic and control measures that include the herd, the animals, and the environment. Measures should be taken to avoid the introduction of the etiological agent into the pig herds and in those where the infection is established to avoid virus dissemination among the animals of the different pig-producing categories present in the same herd.

The introduction of senecavirus and other infectious agents can be prevented by adopting strict biosecurity measures. The entry of vehicles, equipment, people, animals, and food into the pig production unit must be strictly controlled [37,40,58]. Livestock trailers and carcass removal equipment were subjectively assessed as the most likely routes of senecavirus introduction in a risk-assessment study [37]. Therefore, the area of vehicle circulation, generally around the farm, should be limited to areas away from the premises where the animals are housed. Preferably, pig transportation should be performed by the same vehicle or livestock trailer, which should not have been in contact with vehicles, personnel, or animals from senecavirus-positive herds [37].

Biosecurity measures for people movement events should also be addressed. On-farm employees should shower-in or shower-out of the facility, change clothing and boots prior to entry, and observe a period of downtime after contacting other swine [37]. In the case of animal replacement, pigs should be purchased from farms that are free of the infectious agents of importance in pig health and kept in quarantine before incorporation into the herd. Additional measures include the control of mice and houseflies and the restriction of non-swine domestic animals' access to the premises within a herd.

In senecavirus-positive farms, in addition to the measures previously mentioned, strict cleaning and disinfection of the facilities and the equipment, an in-pen downtime period, and the all in-all out system have to be adopted. The effectiveness of disinfectants against senecavirus is not yet well-known. Since the clinical signs caused by the senecavirus infection are very similar to those caused by the FMD virus, control measures should be adopted that consider the possibility of FMD virus circulation, including disinfection protocols. This includes the use of sodium hydroxide (2%), sodium carbonate (4%), citric acid (0.2%), acetic acid (2%), sodium hypochlorite (3%), potassium peroxymonosulfate/sodium chloride (1%), and chlorine dioxide [59]. Three disinfectants based on household bleach (Sodium hypochlorite (5.25%)), phenolic derivatives (*p*-tertiary-amilphenol (4%); *o*-benzyl-p-chlorophenol (10%); *o*-phenylphenol (12%)), and quaternary ammonium-aldehyde compounds (alkyl dimethyl benzyl ammonium chloride (26%); Glutaraldehyde (7%)) that have been used against senecavirus were evaluated at different temperatures (4 °C and ≈25 °C) on five different surfaces including cement, rubber, plastic, stainless steel, and aluminum. The results showed that 1:20 diluted household bleach was the most effective disinfectant for the inactivation of the virus at any temperature and on any of the five surfaces evaluated. The disinfectant based on phenolic derivatives was not effective against the virus at any temperature, and the results obtained from the disinfectant

based on quaternary ammonia and aldehyde were between those of sodium hypochlorite and phenolic derivatives [60].

Accelerated hydrogen peroxide (AHP) is another chemical compound that has been tested as a broad-spectrum disinfectant against bacteria, fungi, and viruses. Disinfectants containing AHP showed virucide activity against some human and animal viruses, such as bovine viral diarrhea virus (BVDV), feline calicivirus, and poliovirus, which also belongs to the Picornaviridae family. In 2016 AHP was shown to be an effective disinfectant against FMD virus, SVD virus, and senecavirus; but its efficacy is dependent on the dilution (1:20) and the contact period (10 min), which are greater than the manufacturer's recommendations [61].

Monitoring of the senecavirus circulation should be performed by means of periodical diagnostic examinations conducted on biological samples of symptomatic and asymptomatic pigs from different sites of the production unit. In addition to serological tests, molecular, immunohistochemical, and/or in situ hybridization tests can be performed. Depending on the laboratory methodology to be used, a variety of biological samples such as vesicular and oral fluids and organ/tissue fragments of pigs at different ages, especially tonsils, lymph nodes, spleen, heart, lungs, liver, kidneys, and urinary vesicles, can be analyzed [20,24,32]. The introduction of susceptible pigs in the farm as sentinel animals can also be adopted with great discretion. Suckling animals, especially piglets up to one week of age, should consume adequate quantities of high-quality colostrum and be kept in an appropriate environment that provides comfort and welfare to newborns and sows.

Importantly, the adoption of these measures does not rule out the officially recommended procedures. In 2016, the United States Department of Agriculture (USDA) released a list of recommendations, procedures, and responsibilities for the management of diagnosed or suspected cases of animal vesicular diseases to ensure that investigations into exotic animal diseases occur properly, such that precautions can be taken to prevent the spread of communicable diseases [62]. In Brazil in July 2015, the Department of Animal Health (DSA) of the MAPA published the resolution 018/2015/CGI/DIPOA/SDA with guidelines for procedures to be adopted in the case of clinical signs of vesicular lesions in pigs. The document also guides the veterinarians of the Federal Inspection Departments on how to proceed in the slaughter of pigs that display suspected lesions [63]. However, in order to avoid misinterpretations regarding the conduct to be adopted, the standardization of procedures within and between the pig-producing units is essential [58].

5. Conclusions and Perspectives

The studies focusing on the etiological agent and viral infection have considerably expanded the knowledge related to senecavirus and its associated vesicular disease in a short period of time. New study methodologies and tools, particularly the molecular techniques that are notable for the speed, specificity, and sensitivity of their results, have been quickly developed and evaluated. In these studies, some features of senecavirus infection were elucidated in adult animals, and infection in neonates was also described, providing important information on the epidemiology of senecavirus infection, the likely forms of transmission, the pathogenesis, clinical signs, anatomopathological changes, immunity, and a number of suggestions for prophylaxis and control strategies. However, many questions remain to be answered regarding the (i) specific features of the virus, including its biological and molecular evolution, pH stability, receptors and co-receptors, cellular macromolecules, replication cycle, environmental survival; (ii) senecavirus epidemiology, such as how the virus has been disseminated to other countries, non-swine species reservoirs and/or vectors, likely through vertical transmission; (iii) pathogenicity in piglets; and (iv) host immunological response, including the protective antibody titers in colostrum.

Currently, the swine industry, specifically the pig farming sector, is increasingly challenged in terms of animal health and biosecurity. Emerging viral diseases in swine have significantly increased in the past two decades in the global swine population and pose risks to animal health and, consequently, to the production chain [64]. Good examples of economically significant viral agents are porcine

reproductive and respiratory syndrome (PRRSV), porcine circovirus type-2 (PCV-2), PEDV, swine influenza virus, and transboundary infectious animal diseases, such as FMD, CSF, and African swine fever [65]. Regarding senecavirus, the available data indicate that the infection is currently limited to the USA, Canada, Brazil, China, and Thailand. The description of the infection in Asia suggests that the senecavirus is not only restricted to a certain geographic region and that senecavirus may well be distributed on a global scale in the future. Therefore, epidemiological investigations should be conducted in countries where the virus has never been reported, especially in those with extensive pig production, where senecavirus infection may have more economic relevance.

Equally important is the capability of the country to detect and diagnose the disease. The rapid establishment of the etiological agent of a disease enables the rapid adoption of control measures, mitigating and/or preventing the local, regional, and/or international dissemination of the infectious agent. Despite the technological advances in the diagnostic field, weaknesses in the veterinary infrastructure of many countries make disease control even more difficult [66].

Acknowledgments: The authors thank the following Brazilian Institutes for financial support: the National Council of Scientific and Technological Development (CNPq), the Brazilian Federal Agency for Support and Evaluation of Graduate Education (CAPES), Financing of Studies and Projects (FINEP), and the Araucária Foundation (FAP/PR). Amauri A. Alfieri, Alice F. Alfieri and Raquel A. Leme are recipients of CNPq fellowships.

Author Contributions: Amauri A. Alfieri provided the conception of the article; Alice F. Alfieri and Raquel A. Leme designed and drafted the article; and Amauri A. Alfieri made critical revisions related to important intellectual content of the manuscript and approved the final version of the article to be published.

Conflicts of Interest: The authors declared no potential conflicts of interest with respect to the research, authorship, and/or publication of this article.

References

1. Knowles, N.J.; Hallenbeck, P.L. A new picornavirus is most closely related to cardioviruses. In Proceedings of the EUROPIC 2005: XIIIth Meeting of the European Study Group on the Molecular Biology of Picornaviruses, Lunteren, The Netherlands, 23–29 May 2005; p. A14.
2. Segales, J.; Barcellos, D.; Alfieri, A.; Burrough, E.; Marthaler, D. *Senecavirus A*: An Emerging Pathogen Causing Vesicular Disease and Mortality in Pigs? *Vet. Pathol.* **2017**, *54*, 11–21. [CrossRef] [PubMed]
3. Hales, L.M.; Knowles, N.J.; Reddy, P.S.; Xu, L.; Hay, C.; Hallenbeck, P.L. Complete genome sequence analysis of Seneca Valley virus-001, a novel oncolytic picornavirus. *J. Gen. Virol.* **2008**, *89*, 1265–1275. [CrossRef] [PubMed]
4. Venkataraman, S.; Reddy, S.P.; Loo, J.; Idamakanti, N.; Hallenbeck, P.L.; Reddy, V.S. Structure of Seneca Valley virus-001: An oncolytic picornavirus representing a new genus. *Structure* **2008**, *16*, 1555–1561. [CrossRef] [PubMed]
5. Willcocks, M.M.; Locker, N.; Gomwalk, Z.; Royall, E.; Bakhshesh, M.; Belsham, G.J.; Idamakanti, N.; Burroughs, K.D.; Reddy, P.S.; Hallenbeck, P.L.; et al. Structural features of the Seneca Valley virus internal ribosome entry site (IRES) element: A picornavirus with a pestivirus-like IRES. *J. Virol.* **2011**, *85*, 4452–4461. [CrossRef] [PubMed]
6. International Committee on Taxonomy of Viruses. Virus Taxonomy: 2015 Release. Available online: http://www.ictvonline.org/virustaxonomy.asp (accessed on 10 January 2017).
7. Flather, D.; Semler, B.L. Picornaviruses and nuclear functions: Targeting a cellular compartment distinct from the replication site of a positive-strand RNA virus. *Front. Microbiol.* **2015**, *6*, 594. [CrossRef] [PubMed]
8. Hellen, C.U.; de Breyne, S. A distinct group of hepacivirus/pestivirus-like internal ribosomal entry sites in members of diverse picornavirus genera: Evidence for modular exchange of functional noncoding RNA elements by recombination. *J. Virol.* **2007**, *81*, 5850–5863. [CrossRef] [PubMed]
9. Martinez-Salas, E.; Francisco-Velilla, R.; Fernandez-Chamorro, J.; Lozano, G.; Diaz-Toledano, R. Picornavirus IRES elements: RNA structure and host protein interactions. *Virus Res.* **2015**, *206*, 62–73. [CrossRef] [PubMed]
10. Reddy, P.S.; Burroughs, K.D.; Hales, L.M.; Ganesh, S.; Jones, B.H.; Idamakanti, N.; Hay, C.; Li, S.S.; Skele, K.L.; Vasko, A.J.; et al. Seneca Valley virus, a systemically deliverable oncolytic picornavirus, and the treatment of neuroendocrine cancers. *J. Natl. Cancer Inst.* **2007**, *99*, 1623–1633. [CrossRef] [PubMed]

11. Pasma, T.; Davidson, S.; Shaw, S.L. Idiopathic vesicular disease in swine in Manitoba. *Can. Vet. J.* **2008**, *49*, 84–85. [PubMed]
12. Singh, K.; Corner, S.; Clark, S.G.; Scherba, G.; Fredrickson, R. Seneca Valley virus and vesicular lesions in a pig with idiopathic vesicular disease. *J. Vet. Sci. Technol.* **2012**, *3*, 1–3.
13. United States Animal Health Association. Committee on Transmissible Diseases of Swine—Research on Seneca Valley Virus. Available online: http://www.usaha.org/Portals/6/Resolutions/2012/resolution14-2012.pdf (accessed on 21 March 2015).
14. Montgomery, J.F.; Oliver, R.E.; Poole, W.S. A vesiculo-bullous disease in pigs resembling foot and mouth disease. I. Field cases. *N. Z. Vet. J.* **1987**, *35*, 21–26. [CrossRef] [PubMed]
15. Montgomery, J.F.; Oliver, R.E.; Poole, W.S.; Julian, A.F. A vesiculo-bullous disease in pigs resembling foot and mouth disease. II. Experimental reproduction of the lesion. *N. Z. Vet. J.* **1987**, *35*, 27–30. [CrossRef] [PubMed]
16. Munday, B.L.; Ryan, F.B. Vesicular lesions in swine—Possible association with the feeding of marine products. *Aust. Vet. J.* **1982**, *59*, 193. [CrossRef] [PubMed]
17. Gibbs, E.P.J.; Stoddard, H.L.; Yedloutchnig, R.J.; House, J.A.; Legge, M. A vesicular disease of pigs in Florida of unknown etiology. *Fla. Vet. J.* **1983**, *12*, 25–27.
18. International Society for Infectious Diseases. Vesicular Disease, Porcine UK (N. Ireland): Not FMD, SVD. ProMED-Mail Archive Number: 20070110.0099. Available online: http://www.promedmail.org/direct.php?id=6471 (accessed on 8 February 2015).
19. Sensi, M.; Catalano, A.; Tinaro, M.; Mariotti, C.; Panzieri, C.; Marchi, S.; Costarelli, S. Idiopathic vesicular disease (IVD): A case report in the centre of Italy. In Proceedings of the 21st International Pig Veterinary Society (IPVS) Congress, Vancouver, BC, Canada, 18–21 July 2010; p. 46.
20. Leme, R.A.; Zotti, E.; Alcantara, B.K.; Oliveira, M.V.; Freitas, L.A.; Alfieri, A.F.; Alfieri, A.A. *Senecavirus A*: An emerging vesicular infection in Brazilian pig herds. *Transbound. Emerg. Dis.* **2015**, *62*, 603–611. [CrossRef] [PubMed]
21. Amass, S.F.; Schneider, J.L.; Miller, C.A.; Shawky, S.A.; Stevenson, G.W.; Woodruff, M.E. Idiopathic vesicular disease in a swine herd in Indiana. *J. Swine Health Prod.* **2004**, *12*, 192–196.
22. Vannucci, F.A.; Linhares, D.C.; Barcellos, D.E.; Lam, H.C.; Collins, J.; Marthaler, D. Identification and complete genome of Seneca Valley virus in vesicular fluid and sera of pigs affected with idiopathic vesicular disease, Brazil. *Transbound. Emerg. Dis.* **2015**, *62*, 589–593. [CrossRef] [PubMed]
23. Leme, R.A.; Oliveira, T.E.S.; Alcântara, B.K.; Headley, S.A.; Alfieri, A.F.; Yang, M.; Alfieri, A.A. Clinical manifestations of *Senecavirus A* infection in neonatal pigs, Brazil, 2015. *Emerg. Infect. Dis.* **2016**, *22*, 1238–1241. [CrossRef] [PubMed]
24. Leme, R.A.; Oliveira, T.E.; Alfieri, A.F.; Headley, S.A.; Alfieri, A.A. Pathological, immunohistochemical and molecular findings associated with *Senecavirus A*-induced lesions in neonatal piglets. *J. Comp. Pathol.* **2016**, *155*, 145–155. [CrossRef] [PubMed]
25. Leme, R.A.; Headley, S.A.; Oliveira, T.E.; Yang, M.; Gomes, R.; Feronato, C.; Alfieri, A.F.; Alfieri, A.A. Molecular, pathological, and immunohistochemical evidence of *Senecavirus A*-induced infections in pigs of different age groups with vesicular disease from Brazil. In Proceedings of the Allen D. Leman Swine Conference, Saint Paul, MN, USA, 19–22 September 2015; p. 26.
26. Ministry of Agriculture, Livestock, and Food Supply. Circular n°12/2015, in 13 February 2015. Ocurrence of Pig Mortality. Available online: http://www.agricultura.gov.br/assuntos/inspecao/produtos-animal/arquivos-publicacoes-dipoa/relatorio-de-gestao-dipoa-atualizado.pdf (accessed on 14 July 2015).
27. Laguardia-Nascimento, M.; Gasparini, M.R.; Sales, E.B.; Rivetti, A.V., Jr.; Sousa, N.M.; Oliveira, A.M.; Camargos, M.F.; Pinheiro de Oliveira, T.F.; Goncalves, J.P.; Madureira, M.C.; et al. Molecular epidemiology of *Senecavirus A* associated with vesicular disease in pigs in Brazil. *Vet. J.* **2016**, *216*, 207–209. [CrossRef] [PubMed]
28. Saporiti, V.; Fritzen, J.T.T.; Feronato, C.; Leme, R.A.; Alfieri, A.F.; Alfieri, A.A. A ten years (2007–2016) retrospective serological survey for *Senecavirus A* infection in Brazilian pig herds. *Vet. Res. Commun.* Under review.
29. Wu, Q.; Zhao, X.; Chen, Y.; He, X.; Zhang, G.; Ma, J. Complete genome sequence of Seneca Valley virus CH-01-2015 identified in China. *Genome Announc.* **2016**, *4*. [CrossRef] [PubMed]

30. Wu, Q.; Zhao, X.; Bai, Y.; Sun, B.; Xie, Q.; Ma, J. The first identification and complete genome of *Senecavirus A* affecting pig with Idiopathic Vesicular Disease in China. *Transbound. Emerg. Dis.* **2016**. [CrossRef] [PubMed]
31. Qian, S.; Fan, W.; Qian, P.; Chen, H.; Li, X. Isolation and full-genome sequencing of Seneca Valley virus in piglets from China, 2016. *Virol. J.* **2016**, *13*, 173. [CrossRef] [PubMed]
32. Joshi, L.R.; Fernandes, M.H.; Clement, T.; Lawson, S.; Pillatzki, A.; Resende, T.P.; Vannucci, F.A.; Kutish, G.F.; Nelson, E.A.; Diel, D.G. Pathogenesis of *Senecavirus A* infection in finishing pigs. *J. Gen. Virol.* **2016**, *97*, 3267–3279. [CrossRef] [PubMed]
33. Canning, P.; Canon, A.; Bates, J.L.; Gerardy, K.; Linhares, D.C.; Pineyro, P.E.; Schwartz, K.J.; Yoon, K.J.; Rademacher, C.J.; Holtkamp, D.; et al. Neonatal mortality, vesicular lesions and lameness associated with *Senecavirus A* in a U.S. sow farm. *Transbound. Emerg. Dis.* **2016**, *63*, 373–378. [CrossRef] [PubMed]
34. Gimenez-Lirola, L.G.; Rademacher, C.; Linhares, D.; Harmon, K.; Rotolo, M.; Sun, Y.; Baum, D.H.; Zimmerman, J.; Pineyro, P. Serological and molecular detection of *Senecavirus A* associated with an outbreak of swine idiopathic vesicular disease and neonatal mortality. *J. Clin. Microbiol.* **2016**, *54*, 2082–2089. [CrossRef] [PubMed]
35. International Society for Infectious Diseases. *Senecavirus A* Canada: (Ontario) Swine, 2016. ProMED-Mail Archive Number: 20161009.4546471. Available online: http://www.promedmail.org/direct.php?id=20161009.4546471 (accessed on 28 December 2016).
36. Saeng-Chuto, K.; Rodtian, P.; Temeeyasen, G.; Wegner, M.; Nilubol, D. The first detection of *Senecavirus A* in pigs in Thailand, 2016. *Transbound. Emerg. Dis.* **2017**. [CrossRef] [PubMed]
37. Baker, K.L.; Mowrer, C.; Canon, A.; Linhares, D.C.; Rademacher, C.; Karriker, L.A.; Holtkamp, D.J. Systematic epidemiological investigations of cases of *Senecavirus A* in US swine breeding herds. *Transbound. Emerg. Dis.* **2017**, *64*, 11–18. [CrossRef] [PubMed]
38. Hause, B.M.; Myers, O.; Duff, J.; Hesse, R.A. *Senecavirus A* in Pigs, United States, 2015. *Emerg. Infect. Dis.* **2016**, *22*, 1323–1325. [CrossRef] [PubMed]
39. Guo, B.; Pineyro, P.E.; Rademacher, C.J.; Zheng, Y.; Li, G.; Yuan, J.; Hoang, H.; Gauger, P.C.; Madson, D.M.; Schwartz, K.J.; et al. Novel *Senecavirus A* in swine with vesicular disease, United States, July 2015. *Emerg. Infect. Dis.* **2016**, *22*, 1325–1327. [CrossRef] [PubMed]
40. Joshi, L.R.; Mohr, K.A.; Clement, T.; Hain, K.S.; Myers, B.; Yaros, J.; Nelson, E.A.; Christopher-Hennings, J.; Gava, D.; Schaefer, R.; et al. Detection of the emerging picornavirus *Senecavirus A* in pigs, mice, and houseflies. *J. Clin. Microbiol.* **2016**, *54*, 1536–1545. [CrossRef] [PubMed]
41. Zhang, J.; Pineyro, P.; Chen, Q.; Zheng, Y.; Li, G.; Rademacher, C.; Derscheid, R.; Guo, B.; Yoon, K.J.; Madson, D.; et al. Full-length genome sequences of *Senecavirus A* from recent idiopathic vesicular disease outbreaks in U.S. swine. *Genome Announc.* **2015**, *3*. [CrossRef] [PubMed]
42. Wang, L.; Prarat, M.; Hayes, J.; Zhang, Y. Detection and genomic characterization of *Senecavirus A*, Ohio, USA, 2015. *Emerg. Infect. Dis.* **2016**, *22*, 1321–1323. [CrossRef] [PubMed]
43. Zhao, X.; Wu, Q.; Bai, Y.; Chen, G.; Zhou, L.; Wu, Z.; Li, Y.; Zhou, W.; Yang, H.; Ma, J. Phylogenetic and genome analysis of seven *Senecavirus A* isolates in China. *Transbound. Emerg. Dis.* **2017**. [CrossRef] [PubMed]
44. Saitou, N.; Nei, M. The neighbor-joining method: A new method for reconstructing phylogenetic trees. *Mol. Biol. Evol.* **1987**, *4*, 406–425. [CrossRef] [PubMed]
45. Felsenstein, J. Confidence limits on phylogenies: An approach using the bootstrap. *Evolution* **1985**, *39*, 783–791. [CrossRef] [PubMed]
46. Tamura, K.; Nei, M.; Kumar, S. Prospects for inferring very large phylogenies by using the neighbor-joining method. *Proc. Natl. Acad. Sci. USA* **2004**, *101*, 11030–11035. [CrossRef] [PubMed]
47. Kumar, S.; Stecher, G.; Tamura, K. MEGA7: Molecular evolutionary genetics analysis version 7.0 for bigger datasets. *Mol. Biol. Evol.* **2016**, *33*, 1870–1874. [CrossRef] [PubMed]
48. Montiel, N.; Buckley, A.; Guo, B.; Kulshreshtha, V.; VanGeelen, A.; Hoang, H.; Rademacher, C.; Yoon, K.J.; Lager, K. Vesicular disease in 9-week-old pigs experimentally infected with *Senecavirus A*. *Emerg. Infect. Dis.* **2016**, *22*, 1246–1248. [CrossRef] [PubMed]
49. Yang, M.; van Bruggen, R.; Xu, W. Generation and diagnostic application of monoclonal antibodies against Seneca Valley virus. *J. Vet. Diagn. Investig.* **2012**, *24*, 42–50. [CrossRef] [PubMed]
50. Bracht, A.J.; O'Hearn, E.S.; Fabian, A.W.; Barrette, R.W.; Sayed, A. Real-Time reverse transcription PCR assay for detection of *Senecavirus A* in swine vesicular diagnostic specimens. *PLoS ONE* **2016**, *11*, e0146211. [CrossRef] [PubMed]

51. Dall Agnol, A.M.; Otonel, R.A.; Leme, R.A.; Alfieri, A.A.; Alfieri, A.F. A TaqMan-based qRT-PCR assay for *Senecavirus A* detection in tissue samples of neonatal piglets. *Mol. Cell. Probes* **2017**. [CrossRef] [PubMed]
52. Fowler, V.L.; Ransburgh, R.H.; Poulsen, E.G.; Wadsworth, J.; King, D.P.; Mioulet, V.; Knowles, N.J.; Williamson, S.; Liu, X.; Anderson, G.A.; et al. Development of a novel real-time RT-PCR assay to detect Seneca Valley virus-1 associated with emerging cases of vesicular disease in pigs. *J. Virol. Methods* **2017**, *239*, 34–37. [CrossRef] [PubMed]
53. Piñeyro, P.; Rademacher, C.; Derscheid, R.J.; Guo, B.; Yoon, K.J.; Zhang, J.; Harmon, K.M.; Magstadt, D.R.; Gauger, P.C.; Chen, Q.; et al. *Senecavirus A* vesicular disease outbreak in Midwest show and commercial pigs. In Proceedings of the 58th Annual Conference of the American Association of Veterinary Laboratory Diagnosticians, Providence, RI, USA, 22–28 October 2015.
54. Resende, T.P.; Marthaler, D.G.; Vannucci, F.A. A novel RNA-based in situ hybridization to detect Seneca Valley virus in neonatal piglets and sows affected with vesicular disease. *PLoS ONE* **2017**, *12*, e0173190. [CrossRef] [PubMed]
55. World Organization for Animal Health. Development and Otimisation of Antibody Detection Assays. Available online: http://www.oie.int/fileadmin/Home/eng/Health_standards/tahm/3.6.01_ANTIBODY_DETECT.pdf (accessed on 10 April 2017).
56. Dvorak, C.M.; Akkutay-Yoldar, Z.; Stone, S.R.; Tousignant, S.J.; Vannucci, F.A.; Murtaugh, M.P. An indirect enzyme-linked immunosorbent assay for the identification of antibodies to *Senecavirus A* in swine. *BMC Vet. Res.* **2017**, *13*, 50. [CrossRef] [PubMed]
57. Goolia, M.; Vannucci, F.; Yang, M.; Patnayak, D.; Babiuk, S.; Nfon, C.K. Validation of a competitive ELISA and a virus neutralization test for the detection and confirmation of antibodies to *Senecavirus A* in swine sera. *J. Vet. Diagn. Investig.* **2017**. [CrossRef] [PubMed]
58. Zanella, J.R.C.; Morés, N. Epidemic Transient Neonatal Losses and Vesicular Disease Associated with Seneca Valley Virus (*Senecavirus A*) Infection. Available online: http://www.infoteca.cnptia.embrapa.br/handle/doc/1040626 (accessed on 9 July 2016).
59. World Organisation for Animal Health. Technical Disease Card: Foot-and-Mouth Disease. Available online: http://www.oie.int/animal-health-in-the-world/technical-disease-cards/ (accessed on 10 January 2017).
60. Singh, A.; Mor, S.K.; Aboubakr, H.; Vannucci, F.; Patnayak, D.P.; Goyal, S.M. Efficacy of three disinfectants against *Senecavirus A* on five surfaces and at two temperatures. *J. Swine Health Prod.* **2017**, *25*, 64–68.
61. Hole, K.; Ahmadpour, F.; Krishnan, J.; Stansfield, C.; Copps, J.; Nfon, C. Efficacy of accelerated hydrogen peroxide disinfectant on foot-and-mouth disease virus, swine vesicular disease virus and *Senecavirus A*. *J. Appl. Microbiol.* **2017**, *122*, 634–639. [CrossRef] [PubMed]
62. United States Department of Agriculture. Veterinary Service Guidance (7406.2)—Recommendations for Swine with Potential Vesicular Disease. Available online: https://www.aasv.org/documents/VSG7406.2_SVA_Guidelines_4516.pdf (accessed on 25 June 2016).
63. Ministry of Agriculture, Livestock, and Food Supply. Circular n°18/2015/CGI/DIPOA/SDA, in 07 July 2015. Establish Guideline Procedures to Be Adopted in Cases of Vesicular Lesions in Swine. Available online: http://www.agricultura.gov.br/assuntos/inspecao/produtos-animal/arquivos-publicacoes-dipoa/relatorio-de-gestao-dipoa-atualizado.pdf (accessed on 7 December 2015).
64. Meng, X.J. Emerging and re-emerging swine viruses. *Transbound. Emerg. Dis.* **2012**, *59* (Suppl. 1), 85–102. [CrossRef] [PubMed]
65. Segales, J. Emerging swine diseases and infections: An increasing zoonotic threat. In Proceedings of the Safepork 2015 Conference, Porto, Portugal, 7–10 September 2015; pp. 97–100.
66. Morales, R.G.; Umandal, A.C.; Lantican, C.A. Emerging and Re-emerging diseases in Asia and the Pacific with special emphasis on porcine epidemic diarrhoea. In Proceedings of the 25th Conference of the OIE Regional Commission for Asia, the Far East and Oceania, Queenstown, New Zealand, 26–30 November 2007; pp. 185–189.

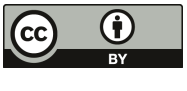

© 2017 by the authors. Licensee MDPI, Basel, Switzerland. This article is an open access article distributed under the terms and conditions of the Creative Commons Attribution (CC BY) license (http://creativecommons.org/licenses/by/4.0/).

viruses

MDPI

Review

Complex Virus–Host Interactions Involved in the Regulation of Classical Swine Fever Virus Replication: A Minireview

Su Li †, Jinghan Wang †, Qian Yang, Muhammad Naveed Anwar, Shaoxiong Yu and Hua-Ji Qiu *

State Key Laboratory of Veterinary Biotechnology, Harbin Veterinary Research Institute, Chinese Academy of Agricultural Sciences, 678 Haping Road, Harbin 150069, China; lisu@hvri.ac.cn (S.L.); wangjinghan1278@163.com (J.W.); yangqian@hvri.ac.cn (Q.Y.); dr.naveed903@gmail.com (M.N.A.); yushaoxiong1987@hotmail.com (S.Y.)

* Correspondence: huajiqiu@hvri.ac.cn; Tel.: +86-451-5105-1708

† S.L. and J.W. contributed equally to this article.

Academic Editors: Linda Dixon and Simon Graham

Received: 24 April 2017; Accepted: 27 June 2017; Published: 5 July 2017

Abstract: Classical swine fever (CSF), caused by classical swine fever virus (CSFV), is one of the most devastating epizootic diseases of pigs in many countries. Viruses are small intracellular parasites and thus rely on the cellular factors for replication. Fundamental aspects of CSFV–host interactions have been well described, such as factors contributing to viral attachment, modulation of genomic replication and translation, antagonism of innate immunity, and inhibition of cell apoptosis. However, those host factors that participate in the viral entry, assembly, and release largely remain to be elucidated. In this review, we summarize recent progress in the virus–host interactions involved in the life cycle of CSFV and analyze the potential mechanisms of viral entry, assembly, and release. We conclude with future perspectives and highlight areas that require further understanding.

Keywords: classical swine fever virus; virus–cell interactions; attachment; entry; cell apoptosis; virus life cycle

1. Introduction

Classical swine fever (CSF), which is caused by classical swine fever virus (CSFV), is a severe and highly contagious disease in pigs that is listed by the World Organization for Animal Health (OIE). The disease is distributed in many countries and areas including Asia, Eastern Europe, Russia, and South America [1]. Currently, CSF is prevented by stamping-out (non-vaccination) and systemic prophylactic (vaccination) policies [2]. In China, vaccines based on C-strain, a lapinized live attenuated vaccine strain, have been widely used to control CSFV infections in the pig population. Therefore, large-scale outbreaks have been rarely observed in the field during the past decades. However, annual sporadic epizootics or endemics in some regions are continuously being observed. A mild, atypical form of the disease with a long duration, atypical clinical signs, and relatively low morbidity and mortality has been observed constantly, even in a proportion of vaccinated pigs [3]. Based on the phylogenetic analysis of nucleotide sequences, there are three genotypes of CSFV isolates, which can be further divided into 11 subgenotypes. So far, there is no clear correlation between specific sequence motifs and the virulence of the different field strains [4,5].

CSFV is an enveloped, positive-sense, single-stranded RNA virus, which belongs to the *Pestivirus* genus of the *Flaviviridae* family [6]. The genome of CSFV contains a 5′-noncoding region (5′-NCR), a large open reading frame (ORF), and a 3′-NCR. The ORF is translated into a precursor polyprotein of 3898 amino acids (aa), which is cleaved into four structural proteins (C, E^{rns}, E1, and E2) and eight

non-structural proteins (N^{pro}, p7, NS2, NS3, NS4A, NS4B, NS5A, and NS5B) (Figure 1) [7]. CSFV enters the host through the mucous membranes of the oral and nasal cavities, and initially infects cells of the tonsil, then spreads around the body via the blood and lymph circulation. CSFV has a distinct tropism for cells of the immune system, which causes severe leukopenia that is associated with apoptosis of leukocytes in the thymus, spleen, lymph nodes, and bone marrow of infected pigs [8,9]. The eventual outcomes of virus infection are generally associated with complex and multifaceted host responses to the virus.

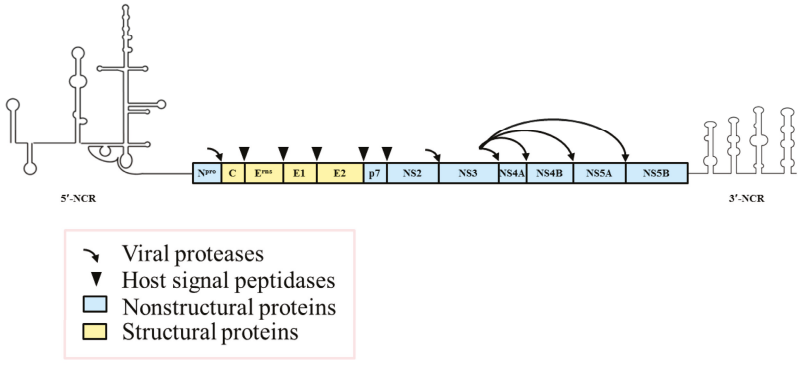

Figure 1. The organization of the classical swine fever virus (CSFV) genome and the encoding proteins. The positive-sense, single-stranded RNA genome of 12.3 kb contains 5′- and 3′-noncoding regions (NCRs) important for viral RNA replication and/or protein translation and a large open reading frame (ORF) that encodes a large polyprotein. The polyprotein is processed into four structural proteins and eight nonstructural proteins by a combination of viral and cellular proteases.

This review aims to summarize recent progress in the virus biology and virus–host interactions at the interface of virus replication, and highlight potential mechanisms in the CSFV life cycle. The review concludes with future perspectives and highlights areas that require further understanding.

2. The CSFV Envelope Proteins Mediate Virus Attachment and Entry

The structural components of the CSFV virions include a capsid protein (C) and three envelope glycoproteins (E^{rns}, E1, and E2). The glycoproteins are processed from the precursor E^{rns}-E1-E2 by the host signal peptidase. The E^{rns} protein consists of 227 aa with a molecular weight of around 48 kDa, which is glycosylated with carbohydrate moieties at seven glycosylation sites [10]. Due to the unusual C terminus, the protein is loosely associated with mature virions and is also secreted into the medium of cultured infected cells. In general, E^{rns} is present as a homodimer (with a molecular mass of about 100 kDa) [11] and a heterodimer with E2 [12] on the virion. The ectodomain of E^{rns} contains five α helices and seven β strands with a concave and a convex face and is stabilized by four intramolecular disulfide bonds [13]. In addition, structural analyses of the C-terminus of E^{rns} show that the amphipathic α-helix is inserted slightly tilted into the membrane [14]. E^{rns} possesses ribonuclease activity, induces lymphocytes apoptosis, and antagonizes the response of type I interferon (IFN) signaling. In addition, the interaction between E^{rns} and membrane-associated heparan sulfate (HS) [15] or laminin receptor (LamR) [16] mediates virus attachment. CSFV cultured in swine kidney cells (SK6 cells) selects a virus variant (with S476R mutation) of E^{rns} that attaches to the surface of cells by interacting with HS [15].

The E1 glycoprotein consists of 195 aa with an apparent molecular mass of 33 kDa, which contains three *N*-linked putative glycosylation sites and six cysteine residues. E1 is a type I transmembrane protein with an N-terminal ectodomain and a C-terminal hydrophobic anchor that attaches E1 to the envelope of the virus [11]. E1 and E2 form heterodimers via disulfide bridges between cysteine

residues that are present in the CSFV virions. The formed heterodimers then mediate the process of viral entry [17,18].

The E2 protein is a 55-kDa glycoprotein that consists of 373 aa, and contains six N-linked and one O-linked putative glycosylation sites. E2 possesses an N-terminal signal peptide and a C-terminal transmembrane domain that anchors E2 to the viral envelope. The CSFV E2 protein forms disulfide-linked homodimers with molecular weights of 100 kDa. E2 is the most immunogenic of the CSFV glycoproteins, in terms of inducing neutralizing antibodies and protection against lethal virus challenge [19–22]. Removal of the glycosylation sites of E2 can significantly reduce the immunogenicity of the protein [23]. Antigenic mapping of E2 has been determined that attributes to domains A to D using a panel of monoclonal antibodies (MAbs) [24]. The antigenic epitopes of domains D/A, but not the domains B/C, are the most conserved epitopes. A highly conserved neutralizing linear epitope in the domain A, 829TAVSPTTLR837, which is recognized by the MAb WH303, has been identified [25]. The epitope is widely used to develop marker vaccines [26–28] and diagnostic assays [27,29]. However, the crystal structure of the CSFV E2 protein has not been resolved so far, which renders it difficult to map conformational epitopes on the protein. The CSFV E2 protein shares a sequence identity of 65% with the bovine virus diarrhea virus (BVDV) E2 protein. Recently, the crystal structure of the BVDV E2 has been resolved, which can be divided into three domains (I to III) [30]. Comparative analysis of the E2 proteins revealed that domains I and II of BVDV correspond to CSFV antigenic domains B/C and D/A, respectively. E2 is characterized as a class II fusion protein that harbors two fusion peptides, ^{818}CPIGWTGVIEC^{828} and ^{869}CKWGGNWTCV^{878} (Figure 2). Interestingly, the peptides exert membrane fusion activity and play critical roles in viral replication and virulence [31,32]. The mechanism of the fusion process of pestiviruses has not been fully elucidated. Based on the crystal structure of the BVDV E2 protein, Li and his colleagues presumed three potential fusion mechanisms for pestiviruses: (a) the aromatic residues in domain IIIc of E2 function as a fusion motif, (b) domain I of E2 contains a fusion motif, and (c) E1 contains the fusion motif and E2 functions as a coeffector [30]. Another study has also resolved the structure of the BVDV E2 protein and presumed that E2 becomes disordered at low pH and exposes the fusion loop of E1, thus mediating the fusion between viral envelope and endosome membrane [18]. In addition, several host cellular factors have been shown to be associated with E2 and are involved in the CSFV life cycle, e.g., CD46 has been identified as a receptor for BVDV using an anti-E2 idiotypic antibody [33], which also functions as an important factor for the attachment of CSFV [34]. Host factors that mediate viral attachment have been defined, but the functional receptor(s) of CSFV has not been determined, and the process of fusion should be focused on future studies.

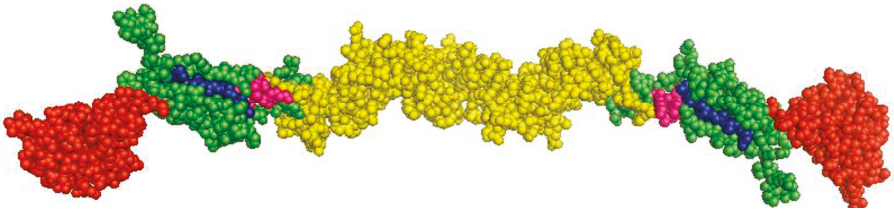

Figure 2. Predicted three-dimensional structure of the CSFV E2 protein. Homology modeling analysis of the CSFV E2 protein was performed using the software PyMOL 1.7 according to the structure of the BVDV E2 protein. Domains B/C are shown in red, domains D/A in green, the other region in yellow, and the fusion peptides (FP1 and FP2) of E2 in blue or purple.

3. Modulation of Viral Genomic Replication and Translation by NCRs and Nonstructural Proteins (NSPs)

The 5′- and 3′-NCRs of CSFV, approximately 373 and 228 nucleotides (nt) in length, respectively, form stem-loops at the N- and C-termini of the genome [7]. The 5′-NCR does not contain the cap

structure, but harbors an internal ribosome entry site (IRES) to initiate cap-independent translation. The 3′-NCR, lacks a poly(A) tail but contains a variable AU-rich region and a conserved region, is involved in the initiation of viral genome replication [35]. The NSPs of CSFV consist of N^{pro}, NS2, NS3, NS4A, NS4B, NS5A, and NS5B. N^{pro}, NS2, NS3, and NS4A have been shown to be involved in the cleavage of the NSPs. A previous study has shown that NS3, NS4A, NS4B, NS5A, and NS5B are required for CSFV replication [36]. NS2, a transmembrane protein, harbors an auto-protease activity that is responsible for *cis*-cleavage of NS2-3 [37]. Previous studies have shown that the uncleaved NS2-3 is crucial for the generation of infectious viral particles for CSFV or BVDV [38,39]. However, additional evidence suggests that the uncleaved NS2-3 is not required for the virion morphogenesis of pestiviruses [40]. As a multifunctional protein, NS3 acts as serine protease, helicase, and nucleoside triphosphatase (NTPase) [41–43]. NS3 and its cofactor, NS4A, process all downstream cleavage sites of viral NSPs [44]. The structure of the NS3-NS4A complex reveals surface interactions between the NS3 protease domain and NS4A-kink region that is required for RNA replication and replicase assembly [45]. NS4B contains two conserved domains, Walkers A (aa 209–216) and B (aa 335–342). Walker A exhibits NTPase activity and is essential for RNA replication [46]. Analysis of simple modular architecture research tool (SMART) has revealed that NS4B contains a Toll/interleukin-1 receptor (TIR)-like domain, and mutations in the TIR-like domain of NS4B significantly attenuate the virulence of CSFV in pigs [47]. The CSFV NS5A contains the conserved sequence C^{2717}-C^{2740}-C^{2742}-C^{2767}, which forms the zinc-binding motif that is required for viral RNA synthesis and viral growth. The NS5A protein of BVDV or hepatitis C virus (HCV) is a highly-phosphorylated protein [48]. Similarly, several potential phosphorylated sites of the CSFV NS5A can also be found using the bioinformatic analysis (NetPhos 3.1 Server). It has been reported that NS5A can induce the autophagy pathway of host cells and enhance viral replication [49]. A recent study shows that the inhibition of autophagy promotes apoptosis in CSFV-infected cells via the reactive oxygen species (ROS)-dependent retinoic acid inducible gene I (RIG-I)-like receptor signaling pathway [50]. NS5B is an RNA-dependent RNA polymerase (RdRp) that harbors a conserved motif GDD, which is in charge of RNA replication [51]. The structure of pestiviral NS5B proteins resembles a right hand with fingers, palm, and thumb domains, thus exhibiting the typical general fold of RdRp [52]. It has been shown that NS3, NS4A, NS4B, NS5A, and NS5B are sufficient for the genome replication [36]. The interactions between NSPs and NCRs have been determined to be involved in modulation of RNA replication and translation [53–55].

The CSFV genome can be transcribed into negative-strand RNA that can be used as the template to produce the positive-strand RNA. During this process, NS5B binds to the negative-strand RNA to produce more positive-strand RNA copies [44]. Moreover, NS3 interacts with NS5B and enhances the NS5B RdRp activity through its N-terminal protease domain. NS5A regulates viral RNA synthesis through interacting with NS5B and 3′-NCR [56]. When NS5A is present at a lower expression level in the cells, it preferably interacts with NS5B and enhances viral RNA replication. But oversaturated NS5A will interact with 3′-NCR and thus inhibit viral RNA replication [56]. It is likely that CSFV modulates RNA replication via the regulation of NS5A expression.

Unlike cellular mRNA, the CSFV genome lacks 5′-terminal cap structure, and the IRES located in the 5′-NCR can be recognized by the ribosome to initiate translation [57]. NS3 can bind to IRES and promote IRES-mediated translation [54]. In comparison with NS3, NS5A inhibits the IRES-mediated translation, whereas NS5B can suppress the effect of NS5A on the IRES [55]. In addition, NS5B can stimulate NS3 to increase the efficiency of viral genome translation [54].

4. Interactions between CSFV and Host Cellular Proteins Are Necessary for the CSFV Life Cycle

During CSFV infection, interactions between the virus and HS/LamR mediate virus attachment [15,16]. Subsequently, virus entry is a dynamin-, and cholesterol-dependent, and clathrin-mediated endocytosis that requires Ras-related in brain (Rab) 5 and Rab7 [58]. The fusion between cellular membrane and viral envelope is pH-dependent and is triggered by the acidification of the endosome. Another pestivirus, BVDV entry also requires clathrin-mediated endocytosis and low endosomal pH [59].

Similarly, Rab5 and Rab7 are involved in the life cycles of HCV [60], dengue virus (DENV) [61], and West Nile virus [62] that belong to the family *Flaviviridae*. It has been demonstrated that the peptides ^{129}CPIGWTGVIEC^{139} and ^{180}CKWGGNWTCV^{189} of the CSFV E2 protein mediate fusion between viral envelope and cellular membrane [31,32] (Figure 2). After uncoating, the viral genome is released and translated into the viral proteins, followed by the cleavage of the cellular and viral proteases. In addition, the viral genome can be transcribed into negative-strand RNA, which is used as a template to produce progeny positive-sense RNA. Virion morphogenesis is mediated by NS2-3 and NS4A [38]. Then, the virion is released from the host cells (Figure 3). Host cellular factors also participate in various steps of the life cycle of CSFV.

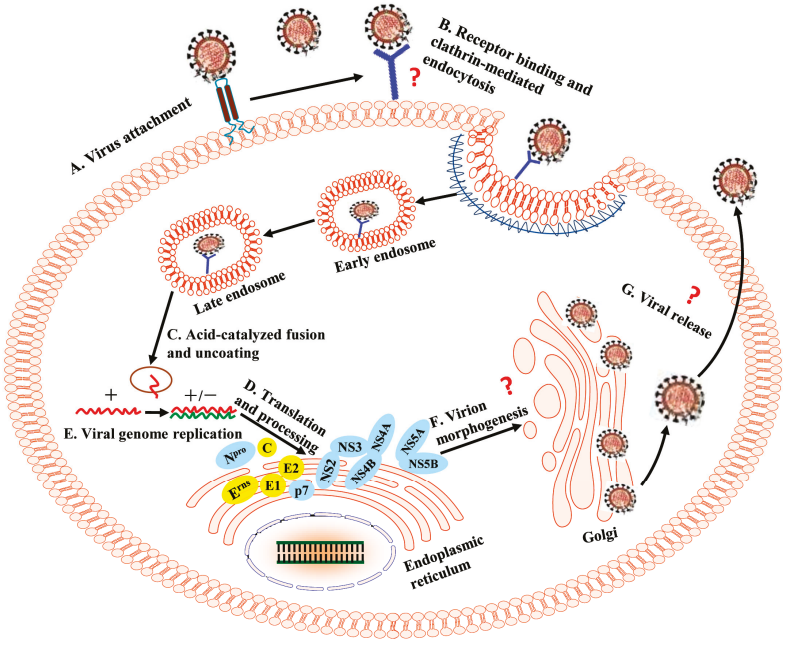

Figure 3. Schematic diagram of the CSFV life cycle. (**A**) Interactions between E^{rns} and host cellular heparan sulfate (HS) and/or laminin receptor (LamR) mediate virus attachment. (**B**) Virus binds to an unknown entry receptor(s) and triggers clathrin-mediated endocytosis. (**C**) Low pH facilitates viral envelope and membrane fusion. (**D**) Translation and processing of viral proteins. (**E**) Viral genome replication. (**F**) Virion morphogenesis harbors an unknown strategy. (**G**) Mature virions are released from the cell via an unknown secretory pathway. +, positive-strand genomic RNA; +/−, positive- and negative-strand replicative intermediate.

4.1. Host Factors Modulate the Production of Progeny Virus

The interactions between flaviviruses and cytoskeleton are involved in the entry, transport, assembly, and egress processes [63]. The cellular β-actin interacts with the E2 protein and affects the early stage of the replication cycle of CSFV [64], which is most likely related to the interaction affects intracellular transport process of CSFV or E2 protein in the cell at the post-entry step. Annexin A2 (Anx2) is a lipid raft-associated scaffold protein that functions in membrane trafficking, aggregation of vesicles, and endosome formation. Anx2 is involved in the regulation of the life cycles of many viruses, such as cytomegalovirus [65], human immunodeficiency virus type 1 [66], influenza virus [67], and HCV [68]. Anx2 interacts with E2 and promotes CSFV production [69], and treatment of PK-15 cells with Anx2-specific polyclonal antibody significantly inhibited CSFV growth, thus we presume

that Anx2 likely participates in the virus attachment or entry. In addition, interaction between Anx2 and NS5A enhances the virus assembly rather than in genome replication and virion release [70]. It is possible that Anx2 participates in the multiple steps of the CSFV life cycles. The interaction between C and osteosarcoma amplified protein 9 (OS9) inhibits the virus replication in the cell culture [71]. Host factors also affect NS5A-regualted viral genome synthesis and translation, e.g., heat shock protein 70 (HSP70) interacts with NS5A and promotes viral RNA replication [72]. Furthermore, eukaryotic elongation factor 1A (eEF1A) has been shown to interact with NS5A of CSFV and inhibit IRES-mediated translation efficiency [73] (Table 1). eEF1A also binds to the NS5A protein of BVDV. However, the effect of eEF1A on the BVDV replication remains unclear [74]. It is plausible to speculate that eEF1A is a broad host factor that interacts with the pestiviral NS5A protein.

Table 1. Interactions between classical swine fever virus (CSFV) and host cellular proteins and replication cycle-contributing factors.

Viral Proteins	Interacting Partners or Replication Cycle-Contributing Factors	Functions	Ref.
5′- and 3′-NCRs	RHA	Modulation of RNA synthesis, replication and translation of CSFV	[75]
N^{pro}	IRF-3	Blockage of IFN-β production	[76]
	IRF-7	Blockage of IFN-α production	[77]
	PCBP1	Blockage of IFN-β production	[78]
	IκBα	—	[79]
	HAX-1	Cellular resistance to apoptosis	[80]
C	OS9	Regulation of virus replication	[71]
	HB	Blockage of IFN-β production	[81]
	UBC9	Involvement of viral virulence	[82]
	SUMO-1	Involvement of viral virulence	[82]
	IQGAP1	Involvement of viral virulence	[83]
E^{rns}	HS	Attachment receptor	[15]
	LamR	Attachment receptor	[16]
E2	β-Actin	Regulation of virus replication	[64]
	Anx2	Regulation of virus growth	[69]
	Trx2	Inhibition of the NF-κB signaling	[84]
	MEK2	Inhibition of the JAK-STAT signaling	[85]
NS5A	Anx2	Regulation of viral assembly	[70]
	HSP70	Regulation of virus replication	[72]
	eEF1A	Inhibition of IRES-mediated translation efficiency	[73]
	GBP1	Regulation of virus replication	[86]
–	CD46	Involvement of virus attachment	[34]
–	Clathrin	Involvement of virus internalization	[58]
–	Cholesterol	Involvement of virus internalization	[58]
–	Dynamin	Involvement of virus internalization	[58]
–	Rab5	Involvement of virus internalization	[58]
–	Rab7	Involvement of virus internalization	[58]
–	HO-1	Regulation of virus replication	[87]

NCR: noncoding region; RHA: RNA helicase A; IRF: interferon regulatory factor; IκBα: inhibitor of kappa B; HAX-1: HS-1-associated protein X 1; PCBP1: Poly(C)-binding protein 1; IFN: interferon; SUMO-1: small ubiquitin-like modifier 1; UBC9: SUMO-1-conjugating enzyme 9; IQGAP1: Ras GTPase-activating-like protein 1; HB: hemoglobin subunit beta; OS9: osteosarcoma amplified protein 9; HS: heparan sulfate; LamR: laminin receptor; Trx2: thioredoxin 2; NF-κB: nuclear factor kappa-light-chain-enhancer of activated B cells; JAK-STAT: Janus kinase/signal transducers and activators of transcription; Anx2: annexin A2; MEK2: mitogen-activated protein kinase kinase 2; eEF1A: eukaryotic elongation factor 1-alpha 1; HSP70: heat shock protein 70; GBP1: guanylate-binding protein 1; CD46: cluster of differentiation 46; Rab: Ras-related in brain; HO-1: heme oxygenase 1.

4.2. Viral Proteins Block the Host Innate Immunity

Viruses have evolutionary evolved strategies to evade host innate immune responses for successful virus replication. To facilitate virus infection, CSFV N^{pro} interacts with IFN regulatory factor-3 (IRF-3) or IRF-7 and blocks type I IFN induction [76,77]. The structure of BVDV N^{pro} has been resolved, and the interaction domain harbors a TRASH motif to recognize the immune factors [88]. The host poly(C)-binding protein 1 (PCBP1) negatively regulates the type I IFN pathway and enhances CSFV growth [78]. Hemoglobin subunit beta (HB) interacts with the C protein and antagonizes CSFV replication via the RIG-I-mediated IFN signaling, whereas CSFV inhibits expression of HB to block the pathway [81]. Our recent study has shown that thioredoxin 2 (Trx2) interacts with E2 and negatively regulates CSFV replication via nuclear factor kappa-light-chain-enhancer of activated B cells (NF-κB) signaling, whereas CSFV inhibits protein expression of Trx2 to antagonize the antiviral effects [84]. Another study shows that mitogen-activated protein kinase kinase 2 (MEK2) interacts with the E2 protein and promotes CSFV replication via attenuation of the Janus kinase/signal transducers and activators of transcription (JAK-STAT) signaling pathway [85]. Recently, host guanylate-binding protein 1 (GBP1) has been shown to inhibit CSFV replication depending on its GTPase activity. As an antagonism, CSFV blocks the antiviral activities of GBP1 via inhibition of GBP1 expression [86]. Furthermore, the interaction between N^{pro} and IκBα (the inhibitor of NF-κB) may be involved in the modulation of the NF-κB signaling pathway [79] (Figure 4).

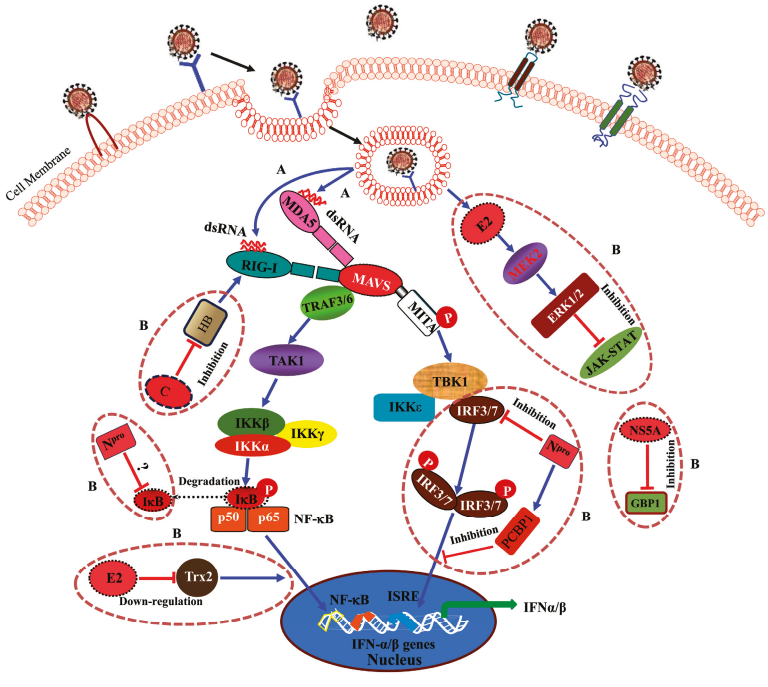

Figure 4. Activation and blockage of the intracellular signaling pathways of innate immunity during CSFV infection. (**A**) CSFV RNA is sensed by melanoma differentiation-associated protein 5 (MDA-5) and retinoic acid inducible gene I (RIG-I). (**B**) CSFV blocks the host innate immunity through multiple steps.

4.3. Disruption of Some Virus-Host Interactions Affects the Viral Virulence in Pigs

SUMOylation is a post-translational modification involved in various cellular processes, such as transport, transcriptional regulation, protein stability, cell apoptosis, stress response, and progression of the cell cycle. Viruses have evolved various strategies to evade the host immune response through interacting the cellular SUMOylation pathway [89–91], thus destruction of the interaction between virus and host usually attenuates viral virulence [92]. It has been demonstrated that the C protein of CSFV interacts with SUMO-1 (small ubiquitin-like modifier 1) and UBC9 (SUMO-1-conjugating enzyme 9) of the SUMOylation pathway [82]. Intriguingly, the virulence of mutant viruses, which are defective in binding to components of the SUMOylation pathway, is completely attenuated in pigs [82]. The cytoskeleton is required for the life cycle of flaviviruses [63]. As a major cytoskeleton regulator, Ras GTPase-activating-like protein 1 (IQGAP1) interacts with the C protein, and a disruption of such interaction also results in the attenuation of viral virulence [83] (Table 1).

5. Changes of Cell Apoptosis and Cell Cycle Induced by CSFV Infection

Acute CSF is associated with high fever, leukopenia, thrombocytopenia, and hemorrhages observed in various organs. During the processes of acute CSF, the virus induces aberrant levels of type I IFN and pro-inflammatory mediators causing a so-called cytokine storm [93,94]. It has been shown that lymphocyte depletion is associated with the strong IFN-α response [94]. In addition, interleukin (IL)-1α, IL-6, and tumor necrosis factor (TNF)-α appeared to be the major cytokines involved in lymphocytopenia [95]. Another study has shown that CSFV infection induces the expression of apoptotic genes, such as CD49d, major histocompatibility complex (MHC) class II, and Fas [8]. Virus components can induce or inhibit apoptosis. Previous studies indicated that E^{rns}, 5′- or 3′-NCR of CSFV can induce lymphocyte apoptosis in vivo [96,97]. However, some of the viral proteins, such as N^{pro} and NS2, can inhibit cell apoptosis in vitro [98,99]. As a multi-functional protein, N^{pro} can antagonize the double-stranded RNA-mediated apoptosis [98], whereas, it cannot suppress the apoptosis induced by the NCRs of CSFV [97]. In addition, N^{pro} binds to HS-1-associated protein X 1 (HAX-1, an anti-apoptotic protein) and leads to a redistribution of HAX-1 from the mitochondria to the endoplasmic reticulum (ER), which might increase cellular resistance to apoptosis [80]. The NS2 protein can inhibit MG132-induced apoptosis, and the expression of NS2 results in the cell cycle arrest at S-phase and the induction of ER stress in the swine umbilical vein endothelial cells [99,100]. It is possible that the apoptosis induced by CSFV infection in vivo is associated with the magnitude of cytokine production.

6. Concluding Remarks and Prospects

The eventual outcome of viral infection usually relies on the host response to the virus. The virus life cycle consists of attachment, entry, uncoating, biosynthesis, assembly, and release. Attachment factors serve to bind the virion and thus help to concentrate viruses on the cell surface. These factors include HS and other carbohydrate structures on the cell surface. However, the factors usually cannot activate the downstream signals of the host to mediate virus entry. The entry receptor(s) can trigger conformational changes of the virion, activate host signaling pathways, and promote endocytic internalization. The attachment of CSFV is mediated by the host cellular HS or/and LamR [15,16]. As HS or LamR cannot mediate virus internalization, the virus maybe bind to an unknown entry receptor and trigger signaling pathways, such as clathrin-mediated endocytic pathway. CSFV can be internalized by clathrin-mediated endocytosis [58]. Entry of BVDV into Madin–Darby bovine kidney (MDBK) cells also requires active clathrin-dependent endocytosis [59]. However, viruses have evolved divergent strategies to invade host cells, e.g., the entry of influenza virus into simian kidney epithelial cells shows that almost 60% of the particles enter via clathrin-coated pits, whereas 40% use a clathrin-independent pathway [101]. Chlorpromazine, an inhibitor of clathrin lattice polymerization, cannot abrogate the CSFV infection [58], thus we presume that CSFV can be internalized via the

clathrin-independent pathway. Furthermore, the low pH facilitates virus membrane fusion [17,58], indicating that the fusion step occurs in the endosome but not the cellular membrane. However, the entry receptors have not been defined, and the detailed entry and fusion mechanisms of CSFV remain to be revealed. Host factors also participate in viral genome replication and translation. Cytoplasmic RNA helicase A (RHA) participates in the modulation of RNA synthesis, replication, and translation of CSFV through binding 5′- and 3′-NCRs [75]. Anx2 has been shown to interact with E2 and NS5A, enhancing viral growth and assembly [69,70]. Thus, we speculate that Anx2 plays critical roles in the multiple phases of the virus life cycle. Furthermore, host heme oxygenase 1 (HO-1) positively regulates CSFV replication [87]. In addition, eEF1A has been demonstrated to modulate viral genome translation through binding to the viral IRES [73]. During virus infection, the cytoskeletal proteins play an essential role in the viral transport and egress processes. The interaction between β-actin and E2 proteins affects the early stage of the replication [64], indicating that β-actin may participate in the transport process of the virus at the post-entry step of the virus life cycle. The process of virus assembly usually involves protein–protein interactions between viral structural proteins and NSPs and the coordinated action of host factors. HCV, DENV, and Japanese encephalitis virus are assembled at ER-derived membranes and exit the cell through the secretory pathway. Host factors, such as Anx2, endosomal sorting complexes required for sorting (ESCRT) components, and Rab18 promote virus assembly, ER budding, and maturation [102]. Anx2 has been shown to interact with NS5A to enhance CSFV assembly [70]. However, detailed dissection of CSFV assembly and release remains to be demonstrated. Taken together, future studies should be focused on the mechanisms of the virus entry, assembly, and release.

Virus infection can trigger a series of signaling cascades in host cells. To establish and maintain persistent infection, the CSFV N^{pro} targets IRF3 and IRF7 to block type I IFN production [76,77], NS5A antagonizes the antiviral activity of GBP1 [86], and C inhibits the RIG-I-mediated IFN-β signaling pathway through interacting with HB [81]. Thus, it seems that CSFV antagonizes the host innate immunity through multiple mechanisms. Novel insights into the mutual antagonism of the virus and host innate immunity will be beneficial for providing valuable targets for virus attenuation. It has been demonstrated that CSFV replicates poorly in cells from MxA-transgenic pigs [103]. More recently, it was reported that the monocytes and macrophages from the genome-edited pigs lacking the scavenger receptor cysteine-rich domain 5 (SRCR5) of CD163 are completely resistant to porcine reproductive and respiratory syndrome virus infection [104]. Dissection of the interplay between CSFV and the host will undoubtedly enrich the understanding of CSFV pathogenesis and facilitate the development of novel strategies for the control and eradication of CSF, such as development of novel antiviral agents, construction of quickly attenuated, efficacious, and highly productive vaccine strains, and generation of CSF-resistant transgenic pigs.

Acknowledgments: This work was supported by the Natural Science Foundation of China (grants 31630080, 31672537, and 31572540).

Author Contributions: All the authors reviewed the literature and wrote the manuscript.

Conflicts of Interest: The authors declare no conflict of interest.

References

1. Ji, W.; Guo, Z.; Ding, N.Z.; He, C.Q. Studying classical swine fever virus: Making the best of a bad virus. *Virus Res.* **2015**, *197*, 35–47. [CrossRef] [PubMed]
2. Tu, C.; Lu, Z.; Li, H.; Yu, X.; Liu, X.; Li, Y.; Zhang, H.; Yin, Z. Phylogenetic comparison of classical swine fever virus in China. *Virus Res.* **2001**, *81*, 29–37. [CrossRef]
3. Luo, Y.; Ji, S.; Liu, Y.; Lei, J.L.; Xia, S.L.; Wang, Y.; Du, M.L.; Shao, L.; Meng, X.Y.; Zhou, M.; et al. Isolation and characterization of a moderately virulent classical swine fever virus emerging in China. *Transbound. Emerg. Dis.* **2016**. [CrossRef] [PubMed]

4. Tu, C. Classical swine fever: International trend, Chinese status and control measures. *Sci. Agri. Sin.* **2003**, *36*, 955–960.
5. Zhu, Y.; Shi, Z.; Drew, T.W.; Wang, Q.; Qiu, H.; Guo, H.; Tu, C. Antigenic differentiation of classical swine fever viruses in China by monoclonal antibodies. *Virus Res.* **2009**, *142*, 169–174. [CrossRef] [PubMed]
6. Pletnev, A.; Gould, E.; Heinz, F.X.; Meyers, G.; Thiel, H.J.; Bukh, J.; Stiasny, K.; Collett, M.S.; Becher, P.; Simmonds, P.; et al. Flaviviridae. In *Virus Taxonomy: Classification and Nomenclature of Viruses. Ninth Report of the International Committee on Taxonomy of Viruses*; King, A.M.Q., Adams, M.J., Carstens, E.B., Lefkowitz, E.J., Eds.; Academic Press: London, UK, 2011; pp. 1003–1020.
7. Lindenbach, B.D.; Murray, C.L.; Thiel, H.J. Flaviviridae. In *Fields Virology*, 6th ed.; Knipe, D.M., Howley, P.M., Cohen, J.I., Griffin, D.E., Lamb, R.A., Martin, M.A., Racaniello, V.R., Roizman, B., Eds.; Lippincott Williams & Wilkins: Philadelphia, PA, USA, 2013; Volume 2, pp. 712–746.
8. Summerfield, A.; Knötig, S.M.; McCullough, K.C. Lymphocyte apoptosis during classical swine fever: Implication of activation-induced cell death. *J. Virol.* **1998**, *72*, 1853–1861. [PubMed]
9. Summerfield, A.; Knötig, S.M.; Tschudin, R.; McCullough, K.C. Pathogenesis of granulocytopenia and bone marrow atrophy during classical swine fever involves apoptosis and necrosis of uninfected cells. *Virology* **2000**, *272*, 50–60. [CrossRef] [PubMed]
10. Branza-Nichita, N.; Lazar, C.; Dwek, R.A.; Zitzmann, N. Role of *N*-glycan trimming in the folding and secretion of the pestivirus protein E^{rns}. *Biochem. Biophys. Res. Commun.* **2004**, *319*, 655–662. [CrossRef] [PubMed]
11. Thiel, H.J.; Stark, R.; Weiland, E.; Rümenapf, T.; Meyers, G. Hog cholera virus: Molecular composition of virions from a pestivirus. *J. Virol.* **1991**, *65*, 4705–4712. [PubMed]
12. Lazar, C.; Zitzmann, N.; Dwek, R.A.; Branza-Nichita, N. The pestivirus E^{rns} glycoprotein interacts with E2 in both infected cells and mature virions. *Virology* **2003**, *2*, 696–705. [CrossRef]
13. Krey, T.; Bontems, F.; Vonrhein, C.; Vaney, M.C.; Bricogne, G.; Rümenapf, T.; Rey, F.A. Crystal structure of the pestivirus envelope glycoprotein E^{rns} and mechanistic analysis of its ribonuclease activity. *Structure* **2012**, *20*, 862–873. [CrossRef] [PubMed]
14. Aberle, D.; Muhle-Goll, C.; Bürck, J.; Wolf, M.; Reißer, S.; Luy, B.; Wenzel, W.; Ulrich, A.S.; Meyers, G. Structure of the membrane anchor of pestivirus glycoprotein E^{rns}, a long tilted amphipathic helix. *PLoS Pathog.* **2014**, *10*, e1003973. [CrossRef] [PubMed]
15. Hulst, M.M.; van Gennip, H.G.; Moormann, R.J. Passage of classical swine fever virus in cultured swine kidney cells selects virus variants that bind to heparan sulfate due to a single amino acid change in envelope protein E^{rns}. *J. Virol.* **2000**, *74*, 9553–9561. [CrossRef] [PubMed]
16. Chen, J.; He, W.R.; Shen, L.; Dong, H.; Yu, J.; Wang, X.; Yu, S.; Li, Y.; Li, S.; Luo, Y.; et al. The laminin receptor is a cellular attachment receptor for classical swine fever virus. *J. Virol.* **2015**, *89*, 4894–4906. [CrossRef] [PubMed]
17. Wang, Z.; Nie, Y.; Wang, P.; Ding, M.; Deng, H. Characterization of classical swine fever virus entry by using pseudotyped viruses: E1 and E2 are sufficient to mediate viral entry. *Virology* **2004**, *330*, 332–341. [CrossRef] [PubMed]
18. El Omari, K.; Iourin, O.; Harlos, K.; Grimes, J.M.; Stuart, D.I. Structure of a pestivirus envelope glycoprotein E2 clarifies its role in cell entry. *Cell Rep.* **2013**, *3*, 30–35. [CrossRef] [PubMed]
19. König, M.; Lengsfeld, T.; Pauly, T.; Stark, R.; Thiel, H.J. Classical swine fever virus: Independent induction of protective immunity by two structural glycoproteins. *J. Virol.* **1995**, *69*, 6479–6486. [PubMed]
20. Yu, X.; Tu, C.; Li, H.; Hu, R.; Chen, C.; Li, Z.; Zhang, M.; Yin, Z. DNA-mediated protection against classical swine fever virus. *Vaccine* **2001**, *19*, 1520–1525. [CrossRef]
21. Li, N.; Qiu, H.J.; Zhao, J.J.; Li, Y.; Wang, M.J.; Lu, B.W.; Han, C.G.; Hou, Q.; Wang, Z.H.; Gao, H.; et al. A Semliki forest virus replicon vectored DNA vaccine expressing the E2 glycoprotein of classical swine fever virus protects pigs from lethal challenge. *Vaccine* **2007**, *25*, 2907–2912. [CrossRef] [PubMed]
22. Sun, Y.; Li, H.Y.; Tian, D.Y.; Han, Q.Y.; Zhang, X.; Li, N.; Qiu, H.J. A novel alphavirus replicon-vectored vaccine delivered by adenovirus induces sterile immunity against classical swine fever. *Vaccine* **2011**, *29*, 8364–8372. [CrossRef] [PubMed]
23. Gavrilov, B.K.; Rogers, K.; Fernández-Sainz, I.J.; Holinka, L.G.; Borca, M.V.; Risatti, G.R. Effects of glycosylation on antigenicity and immunogenicity of classical swine fever virus envelope proteins. *Virology* **2011**, *420*, 135–145. [CrossRef] [PubMed]

24. Wensvoort, G. Topographical and functional mapping of epitopes on hog cholera virus with monoclonal antibodies. *J. Gen. Virol.* **1989**, *70*, 2865–2876. [CrossRef] [PubMed]
25. Lin, M.; Lin, F.; Mallory, M.; Clavijo, A. Deletions of structural glycoprotein E2 of classical swine fever virus strain Alfort/187 resolve a linear epitope of monoclonal antibody WH303 and the minimal N-terminal domain essential for binding immunoglobulin G antibodies of a pig hyperimmune serum. *J. Virol.* **2000**, *24*, 11619–11625. [CrossRef]
26. Liu, S.; Yu, X.; Wang, C.; Wu, J.; Kong, X.; Tu, C. Quadruple antigenic epitope peptide producing immune protection against classical swine fever virus. *Vaccine* **2006**, *24*, 7175–7180. [CrossRef] [PubMed]
27. Qi, Y.; Zhang, B.Q.; Shen, Z.; Chen, Y.H. Antigens containing TAVSPTTLR tandem repeats could be used in assaying antibodies to classical swine fever virus. *Acta Virol.* **2009**, *53*, 241–246. [CrossRef] [PubMed]
28. Li, G.X.; Zhou, Y.J.; Yu, H.; Li, L.; Wang, Y.X.; Tong, W.; Hou, J.W.; Xu, Y.Z.; Zhu, J.P.; Xu, A.T.; et al. A novel dendrimeric peptide induces high level neutralizing antibodies against classical swine fever virus in rabbits. *Vet. Microbiol.* **2012**, *156*, 200–204. [CrossRef] [PubMed]
29. Van der Wal, F.J.; Jelsma, T.; Fijten, H.; Achterberg, R.P.; Loeffen, W.L. Towards a peptide-based suspension array for the detection of pestivirus antibodies in swine. *J. Virol. Methods* **2016**, *235*, 15–20. [CrossRef] [PubMed]
30. Li, Y.; Wang, J.; Kanai, R.; Modis, Y. Crystal structure of glycoprotein E2 from bovine viral diarrhea virus. *Proc. Natl. Acad. Sci. USA* **2013**, *110*, 6805–6810. [CrossRef] [PubMed]
31. Fernández-Sainz, I.J.; Largo, E.; Gladue, D.P.; Fletcher, P.; O'Donnell, V.; Holinka, L.G.; Carey, L.B.; Lu, X.; Nieva, J.L.; Borca, M.V. Effect of specific amino acid substitutions in the putative fusion peptide of structural glycoprotein E2 on classical swine fever virus replication. *Virology* **2014**, *456–457*, 121–130. [CrossRef] [PubMed]
32. Holinka, L.G.; Largo, E.; Gladue, D.P.; O'Donnell, V.; Risatti, G.R.; Nieva, J.L.; Borca, M.V. Alteration of a second putative fusion peptide of structural glycoprotein E2 of classical swine fever virus alters virus replication and virulence in swine. *J. Virol.* **2016**, *90*, 10299–10308. [CrossRef] [PubMed]
33. Maurer, K.; Krey, T.; Moennig, V.; Thiel, H.J.; Rümenapf, T. CD46 is a cellular receptor for bovine viral diarrhea virus. *J. Virol.* **2004**, *78*, 1792–1799. [CrossRef] [PubMed]
34. Dräger, C.; Beer, M.; Blome, S. Porcine complement regulatory protein CD46 and heparan sulfates are the major factors for classical swine fever virus attachment in vitro. *Arch. Virol.* **2015**, *160*, 739–746. [CrossRef] [PubMed]
35. Björklund, H.; Stadejek, T.; Belák, S. Molecular characterization of the 3′ non-coding region of classical swine fever virus vaccine strains. *Virus Genes* **1998**, *16*, 307–312. [CrossRef] [PubMed]
36. Risager, P.C.; Fahnøe, U.; Gullberg, M.; Rasmussen, T.B.; Belsham, G.J. Analysis of classical swine fever virus RNA replication determinants using replicons. *J. Gen. Virol.* **2013**, *94*, 1739–1748. [CrossRef] [PubMed]
37. Lackner, T.; Thiel, H.J.; Tautz, N. Dissection of a viral autoprotease elucidates a function of a cellular chaperone in proteolysis. *Proc. Natl. Acad. Sci. USA* **2006**, *103*, 1510–1515. [CrossRef] [PubMed]
38. Moulin, H.R.; Seuberlich, T.; Bauhofer, O.; Bennett, L.C.; Tratschin, J.D.; Hofmann, M.A.; Ruggli, N. Nonstructural proteins NS2-3 and NS4A of classical swine fever virus: Essential features for infectious particle formation. *Virology* **2007**, *365*, 376–389. [CrossRef] [PubMed]
39. Agapov, E.V.; Murray, C.L.; Frolov, I.; Qu, L.; Myers, T.M.; Rice, C.M. Uncleaved NS2-3 is required for production of infectious bovine viral diarrhea virus. *J. Virol.* **2004**, *78*, 2414–2425. [CrossRef] [PubMed]
40. Klemens, O.; Dubrau, D.; Tautz, N. Characterization of the determinants of NS2-3-independent virion morphogenesis of *Pestiviruses*. *J. Virol.* **2015**, *89*, 11668–11680. [CrossRef] [PubMed]
41. Tamura, J.K.; Warrener, P.; Collett, M.S. RNA-stimulated NTPase activity associated with the p80 protein of the pestivirus bovine viral diarrhea virus. *Virology* **1993**, *193*, 1–10. [CrossRef] [PubMed]
42. Warrener, P.; Collett, M.S. Pestivirus NS3 (p80) protein possesses RNA helicase activity. *J. Virol.* **1995**, *69*, 1720–1726. [PubMed]
43. Wiskerchen, M.; Collett, M.S. Pestivirus gene expression: Protein p80 of bovine viral diarrhea virus is a proteinase involved in polyprotein processing. *Virology* **1991**, *184*, 341–350. [CrossRef]
44. Tautz, N.; Kaiser, A.; Thiel, H.J. NS3 serine protease of bovine viral diarrhea virus: Characterization of active site residues, NS4A cofactor domain, and protease-cofactor interactions. *Virology* **2000**, *273*, 351–363. [CrossRef] [PubMed]

45. Dubrau, D.; Tortorici, M.A.; Rey, F.A.; Tautz, N. A positive-strand RNA virus uses alternative protein-protein interactions within a viral protease/cofactor complex to switch between RNA replication and virion morphogenesis. *PLoS Pathog.* **2017**, *13*, e1006134. [CrossRef] [PubMed]
46. Gladue, D.; Gavrilov, B.K.; Holinka, L.G.; Fernández-Sainz, I.J.; Vepkhvadze, N.; Rogers, K.; O'Donnell, V.; Risatti, G.R.; Borca, M.V. Identification of an NTPase motif in classical swine fever virus NS4B protein. *Virology* **2011**, *411*, 41–49. [CrossRef] [PubMed]
47. Fernandez-Sáinz, I.; Gladue, D.P.; Holinka, L.G.; O'Donnell, V.; Gudmundsdottir, I.; Prarat, M.V.; Patch, J.R.; Golde, W.T.; Lu, Z.; Zhu, J.; et al. Mutations in classical swine fever virus NS4B affect virulence in swine. *J. Virol.* **2010**, *3*, 1536–1539. [CrossRef] [PubMed]
48. Reed, K.E.; Gorbalenya, A.E.; Rice, C.M. The NS5A/NS5 proteins of viruses from three genera of the family *Flaviviridae* are phosphorylated by associated serine/threonine kinases. *J. Virol.* **1998**, *72*, 6199–6206. [PubMed]
49. Pei, J.; Zhao, M.; Ye, Z.; Gou, H.; Wang, J.; Yi, L.; Dong, X.; Liu, W.; Luo, Y.; Liao, M.; et al. Autophagy enhances the replication of classical swine fever virus in vitro. *Autophagy* **2013**, *10*, 93–110. [CrossRef] [PubMed]
50. Pei, J.; Deng, J.; Ye, Z.; Wang, J.; Gou, H.; Liu, W.; Zhao, M.; Liao, M.; Yi, L.; Chen, J. Absence of autophagy promotes apoptosis by modulating the ROS-dependent RLR signaling pathway in classical swine fever virus-infected cells. *Autophagy* **2016**, *12*, 1738–1758. [CrossRef] [PubMed]
51. Wang, Y.; Xiao, M.; Chen, J.; Zhang, W.; Luo, J.; Bao, K.; Nie, M.; Chen, J.; Li, B. Mutational analysis of the GDD sequence motif of classical swine fever virus RNA-dependent RNA polymerases. *Virus Genes* **2007**, *34*, 63–65. [CrossRef]
52. Choi, K.H.; Gallei, A.; Becher, P.; Rossmann, M.G. The structure of bovine viral diarrhea virus RNA-dependent RNA polymerase and its amino-terminal domain. *Structure* **2006**, *14*, 1107–1113. [CrossRef] [PubMed]
53. Xiao, M.; Gao, J.; Wang, W.; Wang, Y.; Chen, J.; Chen, J.; Li, B. Specific interaction between the classical swine fever virus NS5B protein and the viral genome. *Eur. J. Biochem.* **2004**, *271*, 3888–3896. [CrossRef] [PubMed]
54. Xiao, M.; Bai, Y.; Xu, H.; Geng, X.; Chen, J.; Wang, Y.; Chen, J.; Li, B. Effect of NS3 and NS5B proteins on classical swine fever virus internal ribosome entry site-mediated translation and its host cellular translation. *J. Gen. Virol.* **2008**, *89*, 994–999. [CrossRef] [PubMed]
55. Sheng, C.; Chen, Y.; Xiao, J.; Xiao, J.; Wang, J.; Li, G.; Chen, J.; Xiao, M. Classical swine fever virus NS5A protein interacts with 3′-untranslated region and regulates viral RNA synthesis. *Virus Res.* **2012**, *3*, 636–643. [CrossRef] [PubMed]
56. Chen, Y.; Xiao, J.; Xiao, J.; Sheng, C.; Wang, J.; Jia, L.; Zhi, Y.; Li, G.; Chen, J.; Xiao, M. Classical swine fever virus NS5A regulates viral RNA replication through binding to NS5B and 3′-UTR. *Virology* **2012**, *432*, 376–388. [CrossRef] [PubMed]
57. Rijnbrand, R.; van der Straaten, T.; van Rijn, P.A.; Spaan, W.J.; Bredenbeek, P.J. Internal entry of ribosomes is directed by the 5′ noncoding region of classical swine fever virus and is dependent on the presence of an RNA pseudoknot upstream of the initiation codon. *J. Virol.* **1997**, *71*, 451–457. [PubMed]
58. Shi, B.J.; Liu, C.C.; Zhou, J.; Wang, S.Q.; Gao, Z.C.; Zhang, X.M.; Zhou, B.; Chen, P.Y. Entry of classical swine fever virus into PK-15 cells via a pH-, dynamin-, and cholesterol-dependent, clathrin-mediated endocytic pathway that requires Rab5 and Rab7. *J. Virol.* **2016**, *90*, 9194–9208. [CrossRef] [PubMed]
59. Lecot, S.; Belouzard, S.; Dubuisson, J.; Rouillé, Y. Bovine viral diarrhea virus entry is dependent on clathrin-mediated endocytosis. *J. Virol.* **2005**, *79*, 10826–10829. [CrossRef] [PubMed]
60. Manna, D.; Aligo, J.; Xu, C.; Park, W.S.; Koc, H.; Heo, W.D.; Konan, K.V. Endocytic Rab proteins are required for hepatitis C virus replication complex formation. *Virology* **2010**, *398*, 21–37. [CrossRef] [PubMed]
61. Van der Schaar, H.M.; Rust, M.J.; Chen, C.; van der Ende-Metselaar, H.; Wilschut, J.; Zhuang, X.; Smit, J.M. Dissecting the cell entry pathway of dengue virus by single-particle tracking in living cells. *PLoS Pathog.* **2008**, *12*, e1000244. [CrossRef] [PubMed]
62. Krishnan, M.N.; Sukumaran, B.; Pal, U.; Agaisse, H.; Murray, J.L.; Hodge, T.W.; Fikrig, E. Rab 5 is required for the cellular entry of dengue and West Nile viruses. *J. Virol.* **2007**, *81*, 4881–4885. [CrossRef] [PubMed]
63. Foo, K.Y.; Chee, H.Y. Interaction between *Flavivirus* and cytoskeleton during virus replication. *Biomed. Res. Int.* **2015**, *2015*, 427814. [CrossRef] [PubMed]

64. He, F.; Ling, L.; Liao, Y.; Li, S.; Han, W.; Zhao, B.; Sun, Y.; Qiu, H.J. Beta-actin interacts with the E2 protein and is involved in the early replication of classical swine fever virus. *Virus Res.* **2014**, *179*, 161–168. [CrossRef] [PubMed]
65. Wright, J.F.; Kurosky, A.; Pryzdial, E.L.; Wasi, S. Host cellular annexin II is associated with cytomegalovirus particles isolated from cultured human fibroblasts. *J. Virol.* **1995**, *69*, 4784–4791. [PubMed]
66. Ryzhova, E.V.; Vos, R.M.; Albright, A.V.; Harrist, A.V.; Harvey, T.; González-Scarano, F. Annexin 2: A novel human immunodeficiency virus type 1 Gag binding protein involved in replication in monocyte-derived macrophages. *J. Virol.* **2006**, *80*, 2694–2704. [CrossRef] [PubMed]
67. LeBouder, F.; Morello, E.; Rimmelzwaan, G.F.; Bosse, F.; Péchoux, C.; Delmas, B.; Riteau, B. Annexin II incorporated into influenza virus particles supports virus replication by converting plasminogen into plasmin. *J. Virol.* **2008**, *82*, 6820–6828. [CrossRef] [PubMed]
68. Backes, P.; Quinkert, D.; Reiss, S.; Binder, M.; Zayas, M.; Rescher, U.; Gerke, V.; Bartenschlager, R.; Lohmann, V. Role of annexin A2 in the production of infectious hepatitis C virus particles. *J. Virol.* **2010**, *84*, 5775–5789. [CrossRef] [PubMed]
69. Yang, Z.; Shi, Z.; Guo, H.; Qu, H.; Zhang, Y.; Tu, C. Annexin 2 is a host protein binding to classical swine fever virus E2 glycoprotein and promoting viral growth in PK-15 cells. *Virus Res.* **2015**, *201*, 16–23. [CrossRef] [PubMed]
70. Sheng, C.; Liu, X.; Jiang, Q.; Xu, B.; Zhou, C.; Wang, Y.; Chen, J.; Xiao, M. Annexin A2 is involved in the production of classical swine fever virus infectious particles. *J. Gen. Virol.* **2015**, *96*, 1027–1032. [CrossRef] [PubMed]
71. Gladue, D.; O'Donnell, V.; Fernández-Sainz, I.J.; Fletcher, P.; Baker-Branstetter, R.; Holinka, L.; Sanford, B.; Carlson, J.; Lu, Z.; Borca, M.V. Interaction of structural core protein of classical swine fever virus with endoplasmic reticulum-associated degradation pathway protein OS9. *Virology* **2014**, *460*, 173–179. [CrossRef] [PubMed]
72. Zhang, C.; Kang, K.; Ning, P.; Peng, Y.; Lin, Z.; Cui, H.; Cao, Z.; Wang, J.; Zhang, Y. Heat shock protein 70 is associated with CSFV NS5A protein and enhances viral RNA replication. *Virology* **2015**, *482*, 9–18. [CrossRef] [PubMed]
73. Li, S.; Feng, S.; Wang, J.H.; He, W.R.; Qin, H.Y.; Dong, H.; Li, L.F.; Yu, S.X.; Li, Y.; Qiu, H.J. eEF1A interacts with the NS5A protein and inhibits the growth of classical swine fever virus. *Viruses* **2015**, *7*, 4563–4581. [CrossRef] [PubMed]
74. Johnson, C.M.; Perez, D.R.; French, R.; Merrick, W.C.; Donis, R.O. The NS5A protein of bovine viral diarrhoea virus interacts with the alpha subunit of translation elongation factor-1. *J. Gen. Virol.* **2001**, *82*, 2935–2943. [CrossRef] [PubMed]
75. Sheng, C.; Yao, Y.; Chen, B.; Wang, Y.; Chen, J.; Xiao, M. RNA helicase is involved in the expression and replication of classical swine fever virus and interacts with untranslated region. *Virus Res.* **2013**, *171*, 257–261. [CrossRef] [PubMed]
76. Bauhofer, O.; Summerfield, A.; Sakoda, Y.; Tratschin, J.D.; Hofmann, M.A.; Ruggli, N. Classical swine fever virus N^{pro} interacts with interferon regulatory factor 3 and induces its proteasomal degradation. *J. Virol.* **2007**, *81*, 3087–3096. [CrossRef] [PubMed]
77. Fiebach, A.R.; Guzylack-Piriou, L.; Python, S.; Summerfield, A.; Ruggli, N. Classical swine fever virus N^{pro} limits type I interferon induction in plasmacytoid dendritic cells by interacting with interferon regulatory factor 7. *J. Virol.* **2011**, *85*, 8002–8011. [CrossRef] [PubMed]
78. Li, D.; Li, S.; Sun, Y.; Dong, H.; Li, Y.; Zhao, B.; Guo, D.; Weng, C.; Qiu, H.J. Poly(C)-binding protein 1, a novel N^{pro}-interacting protein involved in classical swine fever virus growth. *J. Virol.* **2013**, *87*, 2072–2080. [CrossRef] [PubMed]
79. Doceul, V.; Charleston, B.; Crooke, H.; Reid, E.; Powell, P.P.; Seago, J. The N^{pro} product of classical swine fever virus interacts with Ikappa B alpha, the NF-kappaB inhibitor. *J. Gen. Virol.* **2008**, *89*, 1881–1889. [CrossRef] [PubMed]
80. Johns, H.L.; Doceul, V.; Everett, H.; Crooke, H.; Charleston, B.; Seago, J. The classical swine fever virus N-terminal protease N^{pro} binds to cellular HAX-1. *J. Gen. Virol.* **2010**, *91*, 2677–2686. [CrossRef] [PubMed]
81. Li, D.; Dong, H.; Li, S.; Munir, M.; Chen, J.; Luo, Y.; Sun, Y.; Liu, L.; Qiu, H.J. Hemoglobin subunit beta interacts with the capsid protein and antagonizes the growth of classical swine fever virus. *J. Virol.* **2013**, *87*, 5707–5717. [CrossRef] [PubMed]

82. Gladue, D.; Holinka, L.; Fernández-Sainz, I.J.; Prarat, M.; O'Donell, V.; Vepkhvadze, N.; Lu, Z.; Rogers, K.; Risatti, G.; Borca, M.V. Effects of the interactions of classical swine fever virus Core protein with proteins of the SUMOylation pathway on virulence in swine. *Virology* **2010**, *407*, 129–136. [CrossRef] [PubMed]
83. Gladue, D.; Holinka, L.; Fernández-Sainz, I.J.; Prarat, M.; O'Donnell, V.; Vepkhvadze, N.; Lu, Z.; Risatti, G.; Borca, M.V. Interaction between Core protein of classical swine fever virus with cellular IQGAP1 protein appears essential for virulence in swine. *Virology* **2011**, *412*, 68–74. [CrossRef] [PubMed]
84. Li, S.; Wang, J.; He, W.R.; Feng, S.; Li, Y.; Wang, X.; Liao, Y.; Qin, H.Y.; Li, L.F.; Dong, H.; et al. Thioredoxin 2 is a novel E2-interacting protein that inhibits the replication of classical swine fever virus. *J. Virol.* **2015**, *89*, 8510–8524. [CrossRef] [PubMed]
85. Wang, J.; Chen, S.; Liao, Y.; Zhang, E.; Feng, S.; Yu, S.; Li, L.F.; He, W.R.; Li, Y.; Luo, Y.; et al. Mitogen-activated protein kinase kinase 2, a novel E2-interacting protein, promotes the growth of classical swine fever virus via attenuation of the JAK-STAT signaling pathway. *J. Virol.* **2016**, *90*, 10271–10283. [CrossRef] [PubMed]
86. Li, L.F.; Yu, J.H.; Li, Y.; Wang, J.; Li, S.; Zhang, L.K.; Xia, S.L.; Yang, Q.; Wang, X.; Yu, S.; et al. Guanylate-binding protein 1, an interferon-induced GTPase, exerts an antiviral activity against classical swine fever virus depending on its GTPase activity. *J. Virol.* **2016**, *90*, 4412–4426. [CrossRef] [PubMed]
87. Shi, Z.; Sun, J.; Guo, H.; Yang, Z.; Ma, Z.; Tu, C. Down-regulation of cellular protein heme oxygenase 1 inhibits proliferation of classical swine fever virus in PK-15 cells. *Virus Res.* **2013**, *173*, 315–320. [CrossRef] [PubMed]
88. Zögg, T.; Sponring, M.; Schindler, S.; Koll, M.; Schneider, R.; Brandstetter, H.; Auer, B. Crystal structures of the viral protease N^{pro} imply distinct roles for the catalytic water in catalysis. *Structure* **2013**, *21*, 929–938. [CrossRef] [PubMed]
89. Xu, K.; Klenk, C.; Liu, B.; Keiner, B.; Cheng, J.K.; Zheng, B.J.; Li, L.; Han, Q.L.; Wang, C.; Li, T.X.; et al. Modification of nonstructural protein 1 of influenza A virus by SUMO1. *J. Virol.* **2011**, *85*, 1086–1098. [CrossRef] [PubMed]
90. Han, Q.; Chang, C.; Li, L.; Klenk, C.; Cheng, J.; Chen, Y.; Xia, N.; Shu, Y.; Chen, Z.; Gabriel, G.; et al. SUMOylation of influenza A virus nucleoprotein is essential for intracellular trafficking and virus growth. *J. Virol.* **2014**, *88*, 9379–9390. [CrossRef] [PubMed]
91. Higginbotham, J.M.; O'Shea, C.C. Adenovirus E4-ORF3 targets PIAS3 and together with E1B-55K remodels SUMO interactions in the nucleus and at virus genome replication domains. *J. Virol.* **2015**, *89*, 10260–10272. [CrossRef] [PubMed]
92. Richt, J.A.; García-Sastre, A. Attenuated influenza virus vaccines with modified NS1 proteins. *Curr. Top. Microbiol. Immunol.* **2009**, *333*, 177–195. [PubMed]
93. Sanchez-Cordon, P.J.; Romanini, S.; Salguero, F.J.; Nunez, A.; Bautista, M.J.; Jover, A.; Gomez-Villamos, J.C. Apoptosis of thymocytes related to cytokine expression in experimental classical swine fever. *J. Comp. Pathol.* **2002**, *127*, 239–248. [CrossRef] [PubMed]
94. Summerfield, A.; Alves, M.; Ruggli, N.; de Bruin, M.G.; McCullough, K.C. High IFN-alpha responses associated with depletion of lymphocytes and natural IFN-producing cells during classical swine fever. *J. Interferon Cytokine Res.* **2006**, *26*, 248–255. [CrossRef] [PubMed]
95. Sánchez-Cordón, P.J.; Núñez, A.; Salguero, F.J.; Pedrera, M.; Fernández de Marco, M.; Gómez-Villamandos, J.C. Lymphocyte apoptosis and thrombocytopenia in spleen during classical swine fever: Role of macrophages and cytokines. *Vet. Pathol.* **2005**, *42*, 477–488. [CrossRef] [PubMed]
96. Bruschke, C.J.; Hulst, M.M.; Moormann, R.J.; van Rijn, P.A.; van Oirschot, J.T. Glycoprotein E^{rns} of pestiviruses induces apoptosis in lymphocytes of several species. *J. Virol.* **1997**, *71*, 6692–6696. [PubMed]
97. Hsu, W.L.; Chen, C.L.; Huang, S.W.; Wu, C.C.; Chen, I.H.; Nadar, M.; Su, Y.P.; Tsai, C.H. The untranslated regions of classic swine fever virus RNA trigger apoptosis. *PLoS ONE* **2014**, *9*, e88863. [CrossRef] [PubMed]
98. Ruggli, N.; Bird, B.H.; Liu, L.; Bauhofer, O.; Tratschin, J.D.; Hofmann, M.A. N^{pro} of classical swine fever virus is an antagonist of double-stranded RNA-mediated apoptosis and IFN-α/β induction. *Virology* **2005**, *340*, 265–276. [CrossRef] [PubMed]
99. Tang, Q.H.; Guo, K.; Kang, K.; Zhang, Y.; He, L.; Wang, J. Classical swine fever virus NS2 protein promotes interleukin-8 expression and inhibits MG132-induced apoptosis. *Virus Genes* **2011**, *42*, 355–362. [CrossRef] [PubMed]

100. Tang, Q.H.; Zhang, Y.M.; Fan, L.; Tong, G.; He, L.; Dai, C. Classic swine fever virus NS2 protein leads to the induction of cell cycle arrest at S-phase and endoplasmic reticulum stress. *Virol. J.* **2010**, *7*, 4. [CrossRef] [PubMed]
101. Rust, M.J.; Lakadamyali, M.; Zhang, F.; Zhuang, X. Assembly of endocytic machinery around individual influenza viruses during viral entry. *Nat. Struct. Mol. Biol.* **2004**, *11*, 567–573. [CrossRef] [PubMed]
102. Gerold, G.; Bruening, J.; Weigel, B.; Pietschmann, T. Protein interactions during the *Flavivirus* and *Hepacivirus* life cycle. *Mol. Cell. Proteom.* **2017**, *16*, 75–91. [CrossRef] [PubMed]
103. Zhao, Y.; Wang, T.; Yao, L.; Liu, B.; Teng, C.; Ouyang, H.S. Classical swine fever virus replicated poorly in cells from MxA transgenic pigs. *BMC Vet. Res.* **2016**, *12*, 169. [CrossRef] [PubMed]
104. Burkard, C.; Lillico, S.G.; Reid, E.; Jackson, B.; Mileham, A.J.; Ait-Ali, T.; Whitelaw, C.B.; Archibald, A.L. Precision engineering for PRRSV resistance in pigs: Macrophages from genome edited pigs lacking CD163 SRCR5 domain are fully resistant to both PRRSV genotypes while maintaining biological function. *PLoS Pathog.* **2017**, *13*, e1006206. [CrossRef] [PubMed]

© 2017 by the authors. Licensee MDPI, Basel, Switzerland. This article is an open access article distributed under the terms and conditions of the Creative Commons Attribution (CC BY) license (http://creativecommons.org/licenses/by/4.0/).

viruses

MDPI

Article

Effective Detection of Porcine Cytomegalovirus Using Non-Invasively Taken Samples from Piglets

Vladimir A. Morozov [1,*], Gerd Heinrichs [2] and Joachim Denner [1,*]

1 Robert Koch Institute, 13353 Berlin, Germany
2 Aachen Minipigs, 52525 Heinsberg, Germany; heinrichs.karken@web.de
* Correspondence: MorozovV@rki.de (V.A.M.); DennerJ@rki.de (J.D.);
Tel.: +49-30-18754-2913 (V.A.M.); +49-30-18754-2800 (J.D.)

Academic Editors: Linda Dixon and Simon Graham
Received: 20 October 2016; Accepted: 3 January 2017; Published: 12 January 2017

Abstract: Shortage of human organs forced the development of xenotransplantation using cells, tissues, and organs from pigs. Xenotransplantation may be associated with the transmission of porcine zoonotic microorganisms, among them the porcine cytomegalovirus (PCMV). To prevent virus transmission, pigs have to be screened using sensitive methods. In order to perform regular follow-ups and further breeding of the animals, samples for testing should be collected by low-invasive or non-invasive methods. Sera, ear biopsies, as well as oral and anal swabs were collected from ten 10-day-old Aachen minipigs (AaMP) and tested for PCMV using sensitive nested polymerase chain reaction (PCR) as well as uniplex and duplex real-time PCR. Porcine cytomegalovirus DNA was detected most frequently in oral and anal swabs. Comparison of duplex and uniplex real-time PCR systems for PCMV detection demonstrated a lower sensitivity of duplex real-time PCR when the copy numbers of the target genes were low (less 200). Therefore, to increase the efficacy of PCMV detection in piglets, early testing of oral and anal swabs by uniplex real-time PCR is recommended.

Keywords: Aachen minipigs (AaMP); non-invasive sampling; porcine cytomegalovirus (PCMV); infection; detection; sensitivity; nested PCR; real-time PCR

1. Introduction

Xenotransplantation using pig cells, tissues, or organs made enormous progress in recent years as an alternative for allotransplantation [1]. However, xenotransplantation may be associated with the transmission of porcine zoonotic microorganisms, including the porcine cytomegalovirus (PCMV).

Cells, organs, and tissues of pigs have been used in first preclinical and clinical xenotransplantation trials (for review see [2]) and it was clearly shown that in pig to non-human primate transplantation trials using transplants from PCMV-infected animals, replication of PCMV took place in the recipient [3,4]. In another case, despite the fact that PCMV was undetectable in a donor animal, the virus was transmitted with the heart transplant and actively replicated later in the non-human primate recipient [5]. In all cases, it remained unclear whether PCMV infected cells of the recipient. However, PCMV transmission reduced nearly three times the survival time of the transplant as demonstrated in two kidney xenotransplantation trials using organs from α-1,3-galactosytransferase knockout (GalT-KO) pigs into baboons [6] or cynomolgus monkeys [7]. Based on these and some earlier data, PCMV is considered a potential zoonotic pathogen [8–11].

PCMV is an enveloped virus with a double stranded DNA genome. It belongs to the *Herpesviridae* family, subfamily *Betaherpesvirinae*, genus *Roseolavirus*. The PCMV genome contains 128,367 nucleotide pairs, 79 open reading frames (ORFs), and 73 of those have promotors and eight genes coding for putative proteins with unique sequences and yet unknown functions [12]. The diversity of

PCMV on a full genome level was not well investigated, since only one virus isolate from pulmonary alveolar macrophages was completely sequenced [12]. Porcine cytomegalovirus is genetically more closely related to human herpesviruses 6A and 6B (HHV-6A, B) and 7 (HHV-7), than to human cytomegalovirus (HCMV, HHV-5).

Porcine cytomegalovirus infection of pigs is endemic [13–16]. Virus transmission occurs horizontally through nasal and ocular secretions, milk, and urine. Data on transplacental infections are controversial [15,17–19]. In newborn and young piglets, the virus may cause inclusion body rhinitis and generalized infection. However, in adult animals PCMV is latent and the virus titer in body fluids and organs is very low or undetectable [15]. The low virus titer in the blood is a principal obstacle in PCMV diagnostic by PCR. Furthermore, at present it is still unknown whether PCMV infects human cells. Results of in vitro infection studies using co-cultivation of infected porcine cells with two established human cell lines [8] and primary fibroblasts [20] were controversial.

Pig blood and sera were most frequently used for routine PCMV testing. However, it was shown that in terms of PCMV, blood is not the most representative biological material [15]. Testing of organs for PCMV could be more informative, but the results are limited to the tested animals and do not provide a full-scale picture of virus spread in the herd. To improve systematic testing of pigs, there are several possibilities: early testing using non-invasive sampling methods, optimized DNA extraction for selected material, and highly sensitive methods of virus diagnostic. However, it was unknown what might be the best diagnostic sample material to be collected by non-invasive methods.

Previously, extensive screenings for the PCMV genome were performed in a variety of tissues and body fluids from farm animals of different ages using real-time polymerase chain reaction (PCR) [15,21]. These studies demonstrated that, in adult animals, the virus was not detected in blood, urine, feces, nasal, and oral swabs, but it was present in low copy number in the spleen and in peripheral blood mononuclear cells (PMBC). In contrast, PCMV was found in all examined organs in three out of four, three to five-week-old piglets, and in nasal and saliva swabs of one piglet, however the feces of all piglets were PCMV DNA negative [15]. When three week-old piglets were tested, a high virus load ($>4 \times 10^7$ copies/mg) was detected in the thymus [22]. However, other organs were not analyzed.

Here a comparative study of PCMV detection in selected biological sample material collected by low-invasive and non-invasive methods was performed with the goal to select negative animals for further breeding. A cohort of 10-day-old Aachen minipigs (AaMP) was analyzed by different PCR approaches using sera, ear biopsies and oral and anal swabs. Sensitive nested PCR and real-time PCR systems in uniplex and duplex versions were used for PCMV DNA detection and the sensitivity of the methods was compared. In addition, PCMV amplicones were sequenced in order to confirm that it was PCMV, to investigate putative viral variability and to exclude that there was contamination during PCR handling.

2. Materials and Methods

2.1. Animals and Examined Samples

Aachen minipigs are new minipig breeds produced in Aachen (Germany) for medical and pharmaceutical research. Production of animals is registered under protocol no. 27605370/0120349 (Veterinär- und Lebensmittelüberwachungsamt, Kreis Heinsberg, Germany).

Pregnant sows were kept separately in special bays. After birth, the piglets stayed with the mother for six weeks for breast feeding. Then, the animals were weaned and different litters were mixed to form groups of 20 animals. Testing at this time point is relevant to segregation strategies for animals destined for research purposes. The first microbiological characterization of randomly selected AaMP was performed recently [23].

In this study, a cohort of 10-day-old AaMP from five litters born from five parent pairs (five sows and four boars) was examined. Oral and anal swabs were collected using sterile cotton buds and

shipped cooled together with blood and ear biopsies (about 3 mm^2), and processed immediately after delivery.

2.2. DNA Extraction

To obtain comparable results, all DNA extraction procedures were performed using the Quick-DNA Universal kit (Zymo Research, The Epigenetics Company, Irvine, CA, USA). Material from cotton swabs were eluted in 200 µL of phosphate buffered saline (PBS) and 100 µL were used for DNA extraction that was repeated twice. To reduce the amount of PCR inhibitors, DNA samples from anal swabs were additionally purified using One Step PCR Inhibitor Removing kit (Zymo Research). DNA from ear biopsies was extracted from 10 to 15 mg of the tissue. For complete sample digestion, proteinase K treatment was extended to 18 h. DNA extraction from sera was performed two times, using each time 100 µL and the DNA was eluted in a final volume of 35 µL. The DNA specimens were quantified on NanoDrop spectrophotometer ND-1000 (Thermo Fisher Scientific, Inc., Worcester, MA, USA).

2.3. Conventional Polymerase Chain Reaction and Nested Polymerase Chain Reaction

Primers and probes for PCR systems (Table 1) were synthesized by Sigma-Aldrich (Munich, Germany). The Gibbs free energy change (ΔG) and melting temperature (T_m) for oligonucleotides hair pins were estimated using Oligo Analyzer 3.1 (Integrated DNA technologies, Coralville, IA, USA; Table 1). Estimation of the PCR sensitivity was reported earlier [24].

The nested PCR was performed with the GoTaq Green master mix according to the protocol of the supplier (Promega, Madison, WI, USA) using primers F1 and R1. After initial denaturation at 95 °C for 2 min 40 cycles of denaturation at 94 °C for 30 s, annealing at 58 °C for 30 s and extension at 70 °C for 40 s were performed. The length of the amplicon after the first-round PCR was 350 bp. Using one microliter from the first reaction the second PCR round of 35 cycles was performed with primers F2 and R2 (annealing temperature 54 °C) and extension was reduced to 30 s. The length of the amplicon after the second-round PCR was 206 bp.

2.4. Cloning and Sequence Analysis of the Amplicons

Polymerase chain reaction amplicons were ligated into the pCR2.1-TOPO vector according to the protocol of the supplier (Invitrogen Life Technologies, Carlsbad CA, USA). Mix & Go competent cells (Zymo Research, The Epigenetics Company, Irvine, CA, USA) were transformed with the constructs and plated on lysogeny broth (LB) agar/ampicillin dishes for 18 h at 37 °C. Colonies were collected and amplified in LB/ampicillin medium overnight at 37 °C. Plasmids were isolated using PureYield plasmid miniprep system (Promega, Madison, WI, USA) and sequenced in both directions using primers from the cloning kit and BigDye terminator v.3.1 cycle sequencing kit (Applied Biosystems, Darmstadt, Germany).

Table 1. Primers and probes.

Primers (nt)	Sequence (5′-3′)	T_m (°C)	Oligonucleotide Length	Homo-Dimers. ΔG below −7 kcal/mol	T_m Hairpin (°C)
Conventional Polymerase Chain Reaction (PCR)					
F1 (63–81) *	ACGGGGATCGACGAGAAAG	66.4	19	none	49
R1 (412–390) *	CTAGACGAGAGGACATTGTTGAT	61.1	23	none	29
F2 (182–201) *	GAAGAGAAAGGAAGTGAAGG	57.1	20	none	None
R2 (386–368) *	GTCACTCGTCTGCCTAAGC	60.2	19	none	30
Real-time PCR					
Fr-t (279–299) *	AATGCGTTTTACAACTTCACG	61.5	21	none	29
Rr-t (373–354) *	CTGAGCATGTCCCGCCCTAT	67.4	20	none	19
Probe (331–350) *	6FAM-CTCTAGCGGCGTCCATCACC-BHQ	69.2	20	none	17
F cyclophilin A (174–196) **	TGCTTTCACAGAATAATTCCAGGATTTA	59.1	28	none	23
R cyclophilin A (250–230) **	GACTTGCCACCAGTGCCATTA	61.7	21	none	22
Probe cyclophilin A (205–228) **	Cy5-TGCCAGGGTGGTGACTTCACACGCC-BHQ	67.1	25	none	44

* Nucleotide position of primers and probe for porcine cytomegalovirus (PCMV) amplification (GenBank accession no: AJ222640) [24]; ** Nucleotide position of primers and probe for cyclophilin A amplification (GenBank accession no: FN401368) [24]; T_m: melting temperature; 6FAM: 6-carboxyfluorescein; BHQ: black hole quencher; Cy5: cyanine 5.

2.5. Real-Time Polymerase Chain Reaction

DNA (200 ng) was extracted from ears, oral and anal swabs, and 50 ng of DNA was extracted from sera and used for testing. The real-time PCR was performed using SensiFast probe no ROX kit according to supplier recommendations (Bioline GmbH, Luckenwalde, Germany). Primers and probes are listed in Table 1. The reaction was performed in 20 µL. The PCR conditions were as follows: enzyme activation for 5 min at 95 °C was followed by 45 cycles of denaturation at 95 °C for 10 s, annealing at 59 °C for 20 s, and extension at 62 °C for 30 s. Design of the reference plasmid was described previously [24]. For the target quantification experiments were accompanied by a serial 10-fold dilution ($1x10^5$, $1x10^4$, $1x10^3$, $1x10^2$, $1x10^1$ and two or one copy) of the reference plasmid, example is shown (Figure 1). The sensitivity of the uniplex real-time PCR system was 1–2 copies per reaction and the estimated efficiency of the real-time PCR was between 0.98 and 1.02. The real-time PCR was performed as uniplex or as duplex PCR, using the porcine *cyclophilin A* gene as a housekeeping control with primers and probe described previously [25]. Reaction was performed in a Stratagene MX3005P system (Agilent Technologies, Santa Clara, CA, USA). Each sample was tested in duplicates, once using uniplex real-time PCR and once using duplex real-time PCR. In addition for confirmation, oral samples were tested using two uniplex real-time PCRs and one duplex real-time PCR. Serum samples were tested using two uniplex real-time PCRs and one duplex real-time PCR. Anal swabs were tested using three uniplex real-time PCRs. Ear biopsies were tested using two uniplex real-time PCRs and one duplex real-time PCR.

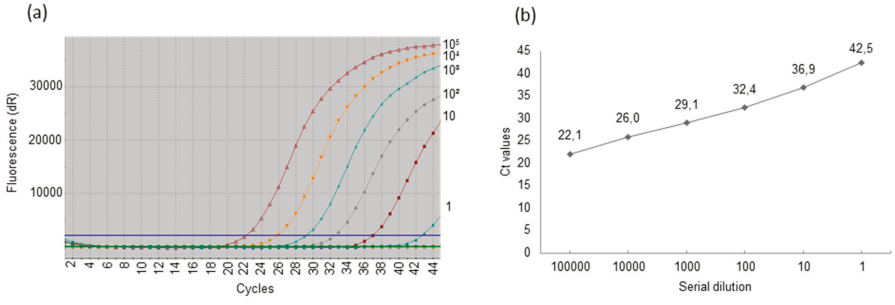

Figure 1. Estimation of the sensitivity of the real-time polymerase chain reaction (PCR)—a representative result. Serial 10-fold dilutions of the reference plasmid containing the PCMV *DNA polymerase* (*DNApol*) gene were used for quantification. (**a**) Amplification plots. dR: reporter signal normalized to the fluorescent signal of the fluorophore ROX (Rn) minus the base line; (**b**) Standard curve. The reference plasmid was diluted in nuclease-free H_2O containing 100 ng/µL of salmon sperm DNA. Cycle threshold (Ct) is inversely proportional to the amounts of target in the reaction.

2.6. Software

The Basic Local Alignment Search Tool (BLAST) program from the National Center for Biotechnology Information (NCBI) [26], was used for search. Oligo analyzer 3.1 (Integrated DNA technologies, Coralville, IA, USA) was used to estimate parameters of the oligonucleotides. The sequence alignments were performed using software package Lasergene Version 10 (DNASTAR, Inc., Madison, WI, USA).

3. Results

3.1. Characterization of DNA from Samples Collected by Non-Invasive and Low-Invasive Methods

To analyze the PCMV virus load, samples collected by non-invasive or low-invasive methods from 10-day-old AaMP were analyzed. DNA was extracted from all samples and tested by PCR

specific for the PCMV *DNA polymerase* (*DNApol*) gene. Two forms of viral DNA might be expected in these samples, DNA-associated with virus particles, and viral DNA from the nucleus and cytoplasm of the infected cells. Since swabs contain both viral DNA from infected cells and cell-free viral DNA from saliva or anal mucosal fluid, a comparison of delta cycle threshold-ΔCt (Ct of the detected target minus Ct of the housekeeping gene), that are frequently used in real-time PCR for quantification, is not applicable. It should be emphasized, that the anal swabs contained only traces (if any) of stool. To eliminate possible PCR inhibitors, the DNA underwent additional purification steps as described in Material and Methods section.

An equal amount (200 ng) of DNA from ear biopsies and oral and anal swabs was tested in each reaction. Since the amount of cellular DNA in sera was low, only 50 ng of DNA were tested in every experiment. The presence and integrity of cellular DNA was estimated by uniplex real-time PCR using the porcine *cyclophilin A* gene (Table 2). Tests were performed in duplicates. Since the external ear contains predominantly cartilaginous tissues (ear chondrocytes were the most abundant cells, representing 10% of the total ear mass), the amount of extracted DNA was relatively low compared to the amount of DNA that might be extracted using the same amount of material from other organs. However, among all samples examined, the highest amount of cellular DNA was extracted from the ear biopsies and the lowest, as expected, from sera. Mean values for the extracted DNA were the following: ear biopsies - 95 ng/μL; oral swabs - 57 ng/μL, anal swabs - 66 ng/μL and sera - 12 ng/μL.

Table 2. Comparison of host DNA load in samples from piglets using real-time PCR using *cyclophilin A* as housekeeping gene. Samples were tested in duplicates. Mean Ct values are given.

Piglet #/Material	Sera	Anal Swabs	Ears Biopsies	Oral Swabs
1	29.7	22.2	22.3	26.1
2	29.6	23.4	24.6	24.3
3	27.8	21.5	23.0	25.5
4	26.8	21.8	22.0	25.5
5	27.7	21.6	20.5	28.5
6	27.8	21.7	20.7	26.4
7	28.3	21.9	21.3	28.5
8	28.3	22.3	23.5	28.0
9	28.2	25.6	21.6	26.7
10	27.1	23.6	21.0	25.9
Mean values:	28.13	22.56	22.05	26.54
Copies/reaction:	6×10^3	5×10^6	5×10^6	2×10^4
Copy/μg:	1.2×10^5	2.5×10^7	2.5×10^7	1×10^5

The amount of saliva in oral swabs was not possible to estimate, explaining the high Ct values (Table 2) of a housekeeping gene despite relatively high amounts of DNA. It is known, that cellular DNA undergoes fragmentation in saliva because of nuclease activity [27]. As a result, a significant amount of short oligonucleotides are present in oral swab samples. These oligonucleotides can increase the overall optical density reading, but because of their size they cannot be detected by real-time PCR targeting a house-keeping gene. Most likely that was the reason why the Ct values of a house-keeping gene, when testing the DNA from oral swabs, were relatively high. The mean Ct values of *cyclophilin A* in sera and oral swabs were close, and those of the anal swabs and ear biopsies were nearly identical (Table 2), therefore they were adequate to make a judgement.

3.2. Comparative Analysis of DNA Samples from Aachen Minipigs by Nested Polymerase Chain Reaction

DNA extracted from all biological samples was initially tested using conventional nested PCR using primers targeting the PCMV *DNApol* gene. Positive samples were revealed in all types of specimens, but the number of positive samples differed significantly (Figure 2). Samples from piglet #4 were all positive and three out of four samples from piglet #3 were positive too. Most frequently,

PCMV DNA was detected in oral swabs. All 10 DNA samples from oral swabs were positive in the first PCR round, indicating that the initially present target load was above 100 gene equivalent (g.e.)/reaction [24]. The high PCMV load in oral swabs was further confirmed by real-time PCR (see Section 3.4). Among DNA samples, 4 out of 10 ear biopsies were also tested positive. Finally, when sera was tested, only 1 out of 10 samples was found positive, indicating that the PCMV DNA load in sera is lower compared to other specimens. Some extra bands were detected above the expected amplicon after nested PCR (Figure 2B,C). These amplicons were sequenced, but they were all not virus-specific.

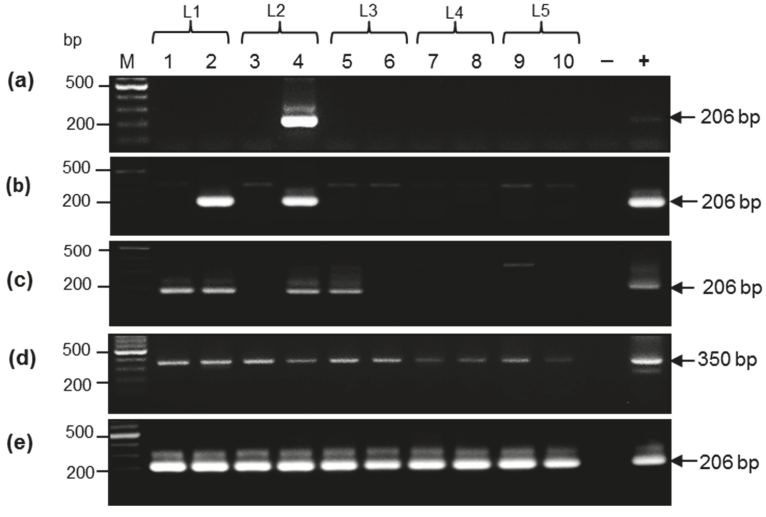

Figure 2. Detection of PCMV *DNApol* gene by nested PCR in different biological samples from Aachen minipig (AaMP) piglets. Animals from five litters (L) were examined. Brackets mark animals from the same litter. (**a**) DNA from sera; (**b**) DNA from anal swabs; (+) positive control 50 copies of a plasmid [23]; (**c**) DNA from ears; (**d**) DNA from oral swabs (first round PCR); (**e**) DNA from oral swabs (second round PCR). (+), positive control in (**b**–**e**) is DNA from a PCMV infected pig. (−), master mix without DNA. Positions of the amplicons are marked with arrow heads. Position of size markers (500 and 200 bp) are given on the left.

3.3. Porcine Cytomegalovirus Sequences Detected in Piglets

The 206 bp PCR amplicons from piglets #3 (anal swabs), #4 (serum and oral swabs), and #6 (oral swabs) were cloned and sequenced and after sequence edition, a 170 bp nucleotide fragment was aligned with a set of PCMV *DNApol* gene sequences from pigs of different geographical origin (United Kingdom, Spain, Germany, Japan, China, and Brazil) (Figure 3). All amplicons from serum and oral and anal swabs showed full identity in-between. Thus, it is very likely that the same virus is circulating in all examined animals. Compared to the reference plasmid, a single nucleotide mismatch (substitution C165T) was found, but does not induce an amino acid change. However, this indicates that the sequenced viruses do not represent a contamination and that the primers are still adequate.

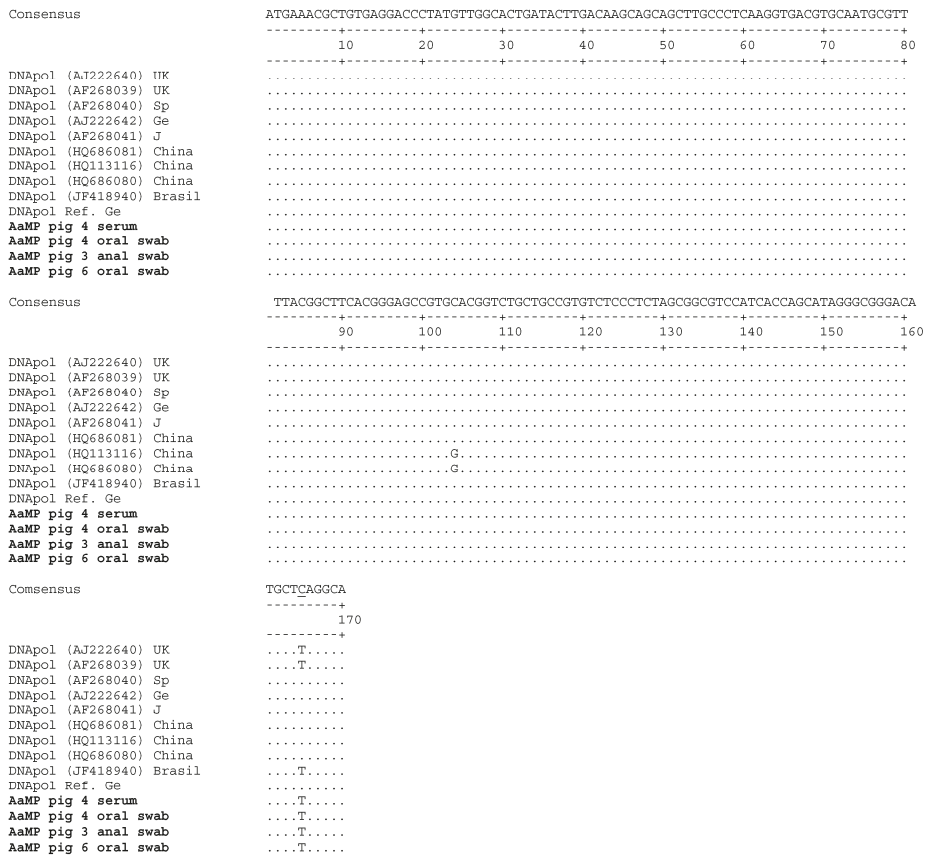

Figure 3. Alignment of the PCMV *DNApol* gene sequences amplified by nested PCR using DNA from serum and oral and anal swabs of three AaMP pigs. Each PCMV sequence detected in AaMP represented a consensus of five cloned sequences. "DNApol Ref. Ge" is a reference sequence amplified from a German landrace pig [23]. Genbank accession numbers are given in brackets. UK, United Kingdom; Sp, Spain; Ge, Germany; J, Japan. The substitution C165T is underlined.

3.4. Detection of Porcine Cytomegalovirus by Real-Time Polymerase Chain Reaction and Comparison of the Sensitivity of Uniplex and Duplex Systems

The efficiency of a duplex PCR specific for the PCMV *DNApol* gene and porcine cyclophilin A gene was compared with that of a uniplex PCR specific for the PCMV *DNApol* gene. Duplex PCR was previously successfully used to investigate multiple virus infections [28]. Equal amounts of the same biological samples from AaMP were analyzed using both uniplex and duplex PCR systems (Table 3).

More PCMV-positive samples were detected by real-time PCR. To simplify the quantification based on Ct counts, the positive samples were divided into five groups: very strong (Ct 29 or lower; above 1×10^3 g.e./reaction); strong (Ct 29–30; 1000–500 g.e./reaction); moderate (Ct 31–35; 250–50 g.e./reaction); weak (Ct 36–37; 25–10 g.e/reaction); and single copy positive (Ct 38–43 g.e./reaction; 5–1 g.e./reaction). In our hands, using SensiFast Probe No-Rox kit and a uniplex real-time PCR system, a single copy target was detectable in 3/5 tests at Ct 42–43. Note, that detection of single copies (<5) by real-time PCR is stochastic.

Table 3. Detection of PCMV in AaMP: comparative sensitivity of uniplex and duplex real-time PCR detection systems (mean Ct values are given, the samples were tested in duplicates).

Piglet #	Sera		Oral Swabs		Ears Biopsies		Anal Swabs	
	Uniplex	Duplex	Uniplex	Duplex	Uniplex	Duplex	Uniplex	Duplex
1	Neg.	Neg.	30.0	30.0	35.8	Neg.	Neg.	Neg.
2	Neg.	Neg.	27.5	28.2	30.9	31.8	39.7	Neg.
3	38.6	Neg.	29.2	30.9	Neg.	Neg.	Neg.	Neg.
4	36.6	Neg.	28.4	30.8	39.4	Neg.	37.0	Neg.
5	Neg.	Neg.	27.3	29.1	34.0	41.3	36.2	Neg.
6	37.1	Neg.	28.1	28.6	Neg.	Neg.	41.3	Neg.
7	Neg.	Neg.	30.1	31.1	Neg.	Neg.	Neg.	Neg.
8	40.1	Neg.	29.4	31.4	32.3	39.7	39.5	Neg.
9	35.2	Neg.	26.1	26.9	35.2	Neg.	42.0	Neg.
10	37.2	Neg.	30.6	Neg.	43.0	Neg.	40.4	Neg.

Neg.: negative result.

The positivity of all DNA samples from 10 oral swabs as detected by conventional PCR was further confirmed by uniplex real-time PCR (Tables 3 and 4). All samples were rated as 'very strong' positive. Nine samples were also positive and comparably strong when tested in duplex PCR. Eight anal swabs samples were positive too, but all positive reactions were rated from 'low' to 'single copy positive'. Of the sera samples, 6 of 10 were positive and rated as 'low positive' or 'single copy positive'. It should be emphasized that none of the anal swabs and sera samples were positive when tested in duplex real-time PCR. Interestingly, six ear biopsies were positive in uniplex real-time PCR and three of them were positive in duplex PCR while the virus loads were very diverse, ranging from 'strong' positive to a 'single-copy' positive.

Table 4. Virus load in examined samples and comparative sensitivity of nested and uniplex real-time PCR. Mean Ct values were given.

Piglet #	Sample	DNA Load (ng)	PCR	Nested PCR	Uniplex Real-Time PCR (Ct Values)	G.e./Reaction
1	Serum	50	Neg.	Neg.	Neg.	Neg.
	Anal swab	200	Neg.	Neg.	Neg.	Neg.
	Oral swab	200	+	+	30.0	~10^3
	Ear biopsies	200	Neg.	+	35.8	~40
2	Serum	50	Neg.	Neg.	Neg.	Neg.
	Anal swab	200	Neg.	+	39.7	~2–5
	Oral swab	200	+	+	27.5	10^4
	Ear biopsies	200	Neg.	+	30.9	~10^3
3	Serum	50	Neg.	Neg.	38.6	~10
	Anal swab	200	Neg.	Neg.	Neg.	Neg.
	Oral swab	200	+	+	29.2	~2×10^3
	Ear biopsies	200	Neg.	Neg.	Neg.	Neg.
4	Serum	50	+	+	36.6	~20
	Anal swab	200	Neg.	+	36.9	~20
	Oral swab	200	+	+	28.4	~7×10^3
	Ear biopsies	200	Neg.	+	39.4	~2–5
5	Serum	50	Neg.	Neg.	Neg.	Neg.
	Anal swab	200	Neg.	Neg.	36.2	~20
	Oral swab	200	+	+	27.3	~10^4
	Ear biopsies	200	Neg.	+	34.0	10e2
6	Serum	50	Neg.	Neg.	37.1	10
	Anal swab	200	Neg.	Neg.	41.3	~1–2
	Oral swab	200	+	+	28.1	~7×10^3
	Ear biopsies	200	Neg.	Neg.	Neg.	Neg.

Table 4. *Cont.*

Piglet #	Sample	DNA Load (ng)	PCR	Nested PCR	Uniplex Real-Time PCR (Ct Values)	G.e./Reaction
7	Serum	50	Neg.	Neg.	Neg.	Neg.
	Anal swab	200	Neg.	Neg.	Neg.	Neg.
	Oral swab	200	+	+	30.1	10^3
	Ear biopsies	200	Neg.	Neg.	Neg.	Neg.
8	Serum	50	Neg.	Neg.	40.1	~2
	Anal swab	200	Neg.	+(weak)	39.5	~2
	Oral swab	200	+	+	30.4	10^3
	Ear biopsies	200	Neg.	Neg.	40.1	~2
9	Serum	50	Neg.	Neg.	35.2	~30
	Anal swab	200	Neg.	Neg.	41.9	~1–2
	Oral swab	200	+	+	26.1	2×10^4
	Ear biopsies	200	Neg.	Neg.	35.2	~40
10	Serum	50	Neg.	Neg.	37.2	~10
	Anal swab	200	Neg.	Neg.	40.4	~2
	Oral swab	200	+	+	30.6	10^3
	Ear biopsies	200	Neg.	Neg.	38.1	~5

G.e.: genome equivalent.

The comparison of two real-time PCR systems demonstrated a lower sensitivity of the duplex real-time PCR system (Table 3). However, when the amount of the target was above 200 g.e./reaction, both systems were equally sensitive. The uniplex PCR demonstrated a superior sensitivity when the amount of target was less than 100–200 g.e./reaction (>Ct 34). Further on, when using the duplex real-time PCR system, the targets could not be detected if the amount is below 15 copies/reaction (>Ct 35 or 'low positive' samples). Thus, the duplex real-time PCR used in this study was successful when hundreds or more copies of the main target per reaction were present.

4. Discussion

Despite substantial progress in xenotransplantation [1] the microbiological safety remains a still unresolved problem. Whereas acute viral infection could be detected in the donor pigs by clinical manifestations, some infections including PCMV are symptomless and may become chronic and therefore difficult to detect. Porcine cytomegalovirus is easily transmitted horizontally, but vertical transmission might not be excluded [15,17,18]. Porcine cytomegalovirus infection is ubiquitous and generally causes mild disease in pigs younger than six weeks [13,18]. In contrast, in adult pig PCMV is latent and if using only blood for analysis it is difficult to detect. The virus reservoir during latency is not clearly defined, but it likely includes immune cells. Transmission and replication of PCMV was observed in several preclinical xenotransplantations with a serious impact on the recipient [4–7].

Previously, an extended screening for PCMV in farm animals was performed using sensitive nested PCR, real-time PCR and serologic tests. Analyses of organs, blood, urine, feces, and oral and nasal swabs of adult pigs revealed PCMV predominantly in the spleen and lungs, while in body fluids, and nasal and oral swabs the virus was not detected [15]. In three out of four, three to five-week-old piglets, the virus was detected in blood and in the majority of the tested organs, but in only one animal was it detected in nasal and oral eluates [15]. However, it should be emphasized that DNA was not extracted from nasal and saliva eluates, but the aliquots were directly used in the PCR reaction after sample boiling. Though, it cannot be excluded that protein aggregates interfered with the Taq polymerase and significantly (if not completely) inhibit the amplification. As a consequence, false-negative results might be expected. No virus was detected in feces from piglets, but the authors did not indicate whether DNA was purified from PCR inhibitors that are associated with this type of samples. Interestingly, the same group reported that all DNA samples of blood from 1 to 14-day-old

piglets were negative [15]. This result is close to what we observed analysing sera from 10-day-old AaMP. In the examined group, only 1 in 10 animals was found positive by nested PCR. In addition, evaluation of the prevalence of PCMV in farm animals older than six months in Brazil indicated that virus detection in the spleen was seven times more efficient than that in sera [29].

Sampling of blood and ear biopsies is a stressful procedure, especially for piglets. Nevertheless, blood and sera remained the most frequently used biological samples for PCMV testing in commercial farms and in facilities producing multitransgenic animals for xenotransplantation. Blood and ear biopsies were obtained by low-invasive methods, since the animals are not sacrificed. Here non-invasive samples such as oral and anal swabs have shown to be more favorable. Other samples such as urine, feces, and vaginal swabs have to be tested in future.

Early testing of piglets using oral swabs might represent the most efficient strategy to detect PCMV. Oral swabs may contain both DNA from virus particles and PCMV DNA from infected epithelial cells. However, low stability of free DNA in saliva means that mostly DNA from viral particles was detected in these samples. The viral DNA load in oral swabs was estimated as 5×10^3–1×10^5 g.e./μg and it was about two orders of magnitude higher than that detected in other samples (Table 5).

Table 5. Summary. PCMV detection by different PCR methods and estimation of viral DNA load by uniplex and duplex real-time PCR.

Samples/Methods	PCR (Positive/Total)	Nested PCR (Positive/Total)	Uniplex Real-Time PCR (Positive/Total)	Duplex Real-Time PCR (Positive/Total)	G.e., Detected
Sera	1/10	1/10	6/10	0/10	10–150/mL
Anal swabs	0/10	3/10	7/10	0/10	5–100/μg
Oral swabs	10/10	10/10	10/10	9/10	5×10^3–1×10^5/μg
Ear biopsies	0/10	1/10	7/10	3/10	25–5×10^3/μg
Total	11/40	15/40	30/40	12/40	

It should be emphasized that the oral swabs were obtained from suckling AaMP piglets and milk is considered to be a source of PCMV infection. Earlier, it has been shown that early weaning prevents virus transmission [4]. Thus, it cannot be excluded that cell-free PCMV or PCMV-infected epithelial cells from the milk contributed to the positive reaction observed with oral swabs. In this regard, it remains to be determined if PCMV from milk can infect and actively replicate in oral epithelial cells of piglets soon after birth. It is worth mentioning that analysis of porcine milk for PCMV infection has not been performed and, in this study, milk was not available for investigation. In this regard, it cannot be excluded that the efficacy of detecting PCMV positive oral swabs from fatteners or adult pigs might be lower.

Oral swabs from all piglets were PCMV DNA-positive; however, virus positivity in other samples varied. All samples from four animals (#4, #8, #9, and #19) were positive. Interestingly, the lowest frequency of PCMV detection was found for sera, a material that is frequently used for PCMV diagnostic. Analysis of ear biopsies showed a surprising result. A high number of positive animals was detected, including animals which serum DNA samples were PCMV DNA negative (#1, #2, and #5). Another unexpected result was a significant difference in PCMV DNA load (Table 4). For example, the highest PCMV DNA load was detected in piglet #2, it was 10–200 times above the level in the remaining six PCMV-positive animals. One explanation for the high virus load may be based on the aggressive behavior of the piglets within the first week of life, when a teat order and dominance hierarchy is established. Piglets may bite and chew ears of the others and contaminate the ears with saliva. In this regard, contaminated ear biopsies might demonstrate a significantly higher virus load in real-time PCR compared to the non-contaminated ones.

In this study, we compared duplex and uniplex real-time PCR as diagnostic tools for PCMV. This issue had been addressed earlier when analyzing conventional multiplex PCR systems for viral diagnostic [30]. In particular, problems with primer interference resulting in a reduction of the

sensitivity in multiplex versus uniplex PCR were discussed. Limitations of duplex real-time PCR methods in detection of low copies of target genes five to seven orders of magnitude lower than the housekeeping gene were reported [25].

Here we demonstrated that compared to the sensitivity of the uniplex real-time PCR that of the duplex real-time PCR was lower. For example, samples that when analyzed by uniplex real-time PCR contained below 15 g.e./reaction were found negative when tested by duplex real-time PCR. Since the amount of the housekeeping gene compared with that of the target viral gene may differ by more than five to six orders of magnitude, proportional decreasing the concentration of the primers targeting the housekeeping gene would not solve the problem. Thus, to avoid false-negative results in diagnostic testing, it is useful to perform separate PCR reactions: one for the detection of the target gene, and another for the control housekeeping gene. However, it cannot be excluded that other duplex real-time PCR systems might perform better and be more sensitive in simultaneous detection of the housekeeping gene and the main target gene present at very low copy numbers.

5. Conclusions

Porcine cytomegalovirus DNA was detected in all ten 10-day-old piglets. Most frequently PCMV DNA was found by real-time PCR in oral (10 of 10 animals) and anal swabs (7 of 10 animals). In comparison, only 6 of 10 serum samples were positive. Based on the results described, several proposals on how to improve screening of piglets for PCMV infection can be made. First, piglets should be tested as soon as possible after birth, since the virus titer might be high and easy to detect. Second, to avoid stress and allowing further breeding, sampling should be performed by non-invasive means, for instance using oral and anal swabs. Simultaneous testing of both oral and anal samples may be a diagnostic advantage. Third, DNA extraction procedure should be optimized and only highly sensitive diagnostic method should be used for virus detection. Non-infected animals should be kept separately to prevent de novo infection. Finally, pigs used for xenotransplantation should be tested immediately before the organ transplantation.

Acknowledgments: This study was supported in part by the German Research Foundation (Deutsche Forschungsgemeinschaft), TRR 127.

Author Contributions: V.A.M. and J.D. conceived the study; V.A.M. designed and performed the experiments, analyzed the data and, together with J.D., wrote the paper. G.H. produced the AaMP, performed sampling, and provided the biological material. All the authors read and approved the final manuscript.

Conflicts of Interest: G.H. produces and supplies the Aachen Minipigs. The other authors report no conflict of interests.

References

1. Denner, J. Recent Progress in Xenotransplantation, with Emphasis on Virological Safety. *Ann. Transplant.* **2016**, *21*, 717–727. [CrossRef]
2. Denner, J.; Tönjes, R.R. Infection barriers to successful xenotransplantation focusing on porcine endogenous retroviruses. *Clin. Microbiol. Rev.* **2012**, *25*, 318–343. [CrossRef] [PubMed]
3. Mueller, N.J.; Barth, R.N.; Yamamoto, S.; Kitamura, H.; Patience, C.; Yamada, K.; Cooper, D.K.; Sachs, D.H.; Kaur, A.; Fishman, J.A. Activation of cytomegalovirus in pig-to-primate organ xenotransplantation. *J. Virol.* **2002**, *76*, 4734–4764. [CrossRef] [PubMed]
4. Mueller, N.J.; Livingston, C.; Knosalla, C.; Barth, R.N.; Yamamoto, S.; Gollackner, B.; Dor, F.J.; Buhler, L.; Sachs, D.H.; Yamada, K.; et al. Activation of porcine cytomegalovirus, but not porcine lymphotropic herpesvirus, in pig-to baboon xenotransplantation. *J. Inf. Dis.* **2004**, *189*, 1628–1633. [CrossRef] [PubMed]
5. Morozov, V.A.; Abicht, J.M.; Reichart, B.; Mayr, T.; Guethoff, S.; Denner, J. Active replication of porcine cytomegalovirus (PCMV) following transplantation of a pig heart into a baboon despite undetected virus in the donor pig. *Ann. Virol. Res.* **2016**, *2*, 1018.

6. Yamada, K.; Tasaki, M.; Sekijima, M.; Wilkinson, R.A.; Villani, V.; Moran, S.G.; Cormac, T.A.; Hanekamp, I.M.; Arn, J.S.; Fishman, J.A.; et al. Porcine cytomegalovirus infection is associated with early rejection of kidney grafts in a pig to baboon xenotransplantation model. *Transplantation* **2014**, *98*, 411–417. [CrossRef] [PubMed]
7. Sekijima, M.; Waki, S.; Sahara, H.; Tasaki, M.; Wilkinson, R.A.; Villani, V.; Shimatsu, Y.; Nakano, K.; Matsunari, H.; Nagashima, H.; et al. Results of life-supporting galactosyltransferase knockout kidneys in cynomolgus monkeys using two different sources of galactosyltransferase knockout swine. *Transplantation* **2014**, *98*, 419–426. [CrossRef] [PubMed]
8. Tucker, A.W.; Galbraith, D.; McEwan, P.; Onions, D. Evaluation of porcine cytomegalovirus as a potential zoonotic agent in Xenotransplantation. *Transplant. Proc.* **1999**, *31*, 915. [CrossRef]
9. Fishman, J.A.; Patience, C. Xenotransplantation: Infectious risk revisited. *Am. J. Transplant.* **2004**, *4*, 1383–1390. [CrossRef] [PubMed]
10. Fishman, J.A.; Scobie, L.; Takeuchi, Y. Xenotransplantation-associated infectious risk: A WHO consultation. *Xenotransplantation* **2012**, *19*, 72–81. [CrossRef] [PubMed]
11. Denner, J. Xenotransplantation and porcine cytomegalovirus. *Xenotransplantation* **2015**, *22*, 329–335. [CrossRef] [PubMed]
12. Gu, W.; Zeng, N.; Zhou, L.; Ge, X.; Guo, X.; Yang, H. Genomic organization and molecular characterization of porcine cytomegalovirus. *Virology* **2014**, *460–461*, 165–172. [CrossRef] [PubMed]
13. Edington, N. Porcine cytomegalovirus. *Dis. Swine* **1986**, *138*, 330–336.
14. Goltz, M.; Widen, F.; Banks, M.; Belak, S.; Ehlers, B. Characterization of the DNA polymerase loci of porcine cytomegalovirus from diverse geographical origins. *Virus Genes* **2000**, *21*, 249–255. [CrossRef] [PubMed]
15. Clark, D.A.; Fryer, J.F.L.; Tucker, A.W.; McArdle, P.D.; Hughes, A.E.; Emery, V.C.; Griffiths, P.D. Porcine cytomegalovirus in pigs being bred for xenograft organs; progress towards control. *Xenotransplantation* **2003**, *10*, 142–148. [CrossRef] [PubMed]
16. Liu, X.; Liao, S.; Zhu, L.; Xu, Z.; Zhou, Y. Molecular epidemiology of porcine cytomegalovirus (PCMV) in Sichuan province, China: 2010–2013. *PLoS ONE* **2013**, *8*, e64648.
17. Edington, N.; Watt, R.G.; Plowright, W. Experimental transplacental transmission of porcine cytomegalovirus. *J. Hyg.* **1977**, *78*, 243–251. [CrossRef] [PubMed]
18. Edington, N.; Broad, S.; Wrathall, A.E.; Done, J.T. Superinfection with porcine cytomegalovirus initiate infection. *Vet. Microbiol.* **1988**, *16*, 189–193. [CrossRef]
19. Mueller, N.J.; Kuwaki, K.; Knosalla, C.; Dor, F.J.; Gollackner, B.; Wilkinson, R.A.; Arn, S.; Sachs, D.H.; Cooper, D.K.; Fishman, J.A. Early weaning of piglets fails to exclude porcine lymphotropic herpesvirus. *Xenotransplantation* **2005**, *12*, 59–62. [CrossRef] [PubMed]
20. Whitteker, J.L.; Dudani, A.K.; Tackaberry, E.S. Human fibroblasts are permissive for porcine cytomegalovirus in vitro. *Transplantation* **2008**, *86*, 155–162. [CrossRef] [PubMed]
21. Fryer, J.F.L.; Griffiths, P.D.; Fishman, J.A.; Emery, V.C.; Clark, D.A. Quantitation of porcine cytomegalovirus in pig tissues by PCR. *J. Clin. Microbiol.* **2001**, *39*, 1155–1156. [CrossRef] [PubMed]
22. Liu, X.; Xu, Z.; Zhu, L.; Liao, S.; Guo, W. Transcriptome analysis of porcine thymus following porcine cytomegalovirus infection. *PLos ONE* **2014**, *9*, e113921. [CrossRef] [PubMed]
23. Plotzki, E.; Heinrichs, G.; Kubicková, B.; Ulrich, R.G.; Denner, J. Microbiological characterization of a newly established pig breed, Aachen minipigs. *Xenotransplantation* **2016**, *23*, 159–167. [CrossRef] [PubMed]
24. Morozov, V.A.; Morozov, A.V.; Denner, J. New nested and real-time PCR systems for porcine cytomegalovirus (PCMV) detection and quantification. *Arch. Virol.* **2016**, *161*, 1159–1168. [CrossRef] [PubMed]
25. Duvigneau, J.C.; Hartl, R.T.; Groiss, S.; Gemeiner, M. Quantitative simultaneous multiplex real-time PCR for the detection of porcine cytokines. *J. Immunol. Methods* **2005**, *30*, 16–27. [CrossRef] [PubMed]
26. Basic Local Alignment Search Tool (BLAST). Available online: https://blast.ncbi.nlm.nih.gov/Blast.cgi (accessed on 11 January 2017).
27. Abraham, J.E.; Maranian, M.J.; Spiteri, I.; Russell, R.; Ingle, S.; Luccarini, C.; Earl, H.M.; Pharoah, P.P.; Dunning, A.M.; Caldas, C. Saliva samples are a viable alternative to blood samples as a source of DNA for high throughput genotyping. *BMC Med. Genom.* **2012**, *5*, 19. [CrossRef] [PubMed]
28. Lee, C.S.; Moon, H.J.; Yang, J.S.; Park, S.J.; Song, D.S.; Kang, B.K.; Park, B.K. Multiplex PCR for the simultaneous detection of pseudorabies virus, porcine cytomegalovirus, and porcine circovirus in pigs. *J. Virol. Methods* **2007**, *139*, 39–43. [CrossRef] [PubMed]

29. Cibulski, S.P.; Pasqualim, G.; Teixera, T.; Varela, A.P.M.; Dezen, D.; Holz, C.L.; Franco, A.C.; Roehe, P.M. Porcine cytomegalovirus infection is not associated to the occurrence of post-weaning multisystemic wasting syndrome. *Vet. Med. Sci.* **2016**, *1*, 23–29. [CrossRef]
30. Elnifro, E.M.; Ashshi, A.M.; Cooper, R.J.; Klapper, P.E. Multiplex PCR: Optimization and application in diagnostic virology. *Clin. Microbiol. Rev.* **2000**, *13*, 559–570. [CrossRef] [PubMed]

© 2017 by the authors. Licensee MDPI, Basel, Switzerland. This article is an open access article distributed under the terms and conditions of the Creative Commons Attribution (CC BY) license (http://creativecommons.org/licenses/by/4.0/).

viruses

MDPI

Article

Genetic Assessment of African Swine Fever Isolates Involved in Outbreaks in the Democratic Republic of Congo between 2005 and 2012 Reveals Co-Circulation of p72 Genotypes I, IX and XIV, Including 19 Variants

Leopold K. Mulumba–Mfumu [1,2], Jenna E. Achenbach [3,*], Matthew R. Mauldin [4,7], Linda K. Dixon [5], Curé Georges Tshilenge [1], Etienne Thiry [2], Noelia Moreno [6], Esther Blanco [6], Claude Saegerman [2], Charles E. Lamien [3] and Adama Diallo [3]

1 Central Veterinary Laboratory, Avenue Wangata, P.O. Box 8842, Kinshasa I, Democratic Republic of Congo; labovetkin@yahoo.fr (L.K.M.-M.); george.tshilenge@sacids.org (C.G.T.)
2 Research Unit of Epidemiology and Risk Analysis Applied to Veterinary (UREAR-Ulg), Fundamental and Applied Research for Animals & Health, Faculty of Veterinary Medicine, University of Liege, 4000 Liege, Belgium; etienne.thiry@ulg.ac.be (E.T.); claude.saegerman@ulg.ac.be (C.S.)
3 Animal Production and Health Laboratory, International Atomic Energy Agency, Wagramer Strasse 5, P.O. Box 100, A-1400 Vienna, Austria; c.lamien@iaea.org (C.E.L.); adama.diallo@cirad.fr (A.D.)
4 Centers for Disease Control and Prevention, Atlanta, GA 30333, USA; MMauldin@cdc.gov
5 Pirbright Institute, Ash Road, Pirbright, Woking, Surrey GU24 ONF, UK; linda.dixon@pirbright.ac.uk
6 Centro de Investigación en Sanidad Animal (CISA), INIA, Valdeolmos, 28130 Madrid, Spain; moreno.noelia@inia.es (N.M.); blanco@inia.es (E.B.)
7 Oak Ridge Institute for Science and Education (ORISE) CDC Fellowship Program, Oak Ridge, TN 37830, USA
* Correspondence: achenbach@battelle.org; Tel.: +1-434-951-2128

Academic Editor: Eric O. Freed
Received: 19 November 2016; Accepted: 10 February 2017; Published: 18 February 2017

Abstract: African swine fever (ASF) is a devastating disease of domestic pigs. It is a socioeconomically important disease, initially described from Kenya, but subsequently reported in most Sub-Saharan countries. ASF spread to Europe, South America and the Caribbean through multiple introductions which were initially eradicated—except for Sardinia—followed by re-introduction into Europe in 2007. In this study of ASF within the Democratic Republic of the Congo, 62 domestic pig samples, collected between 2005–2012, were examined for viral DNA and sequencing at multiple loci: C-terminus of the *B646L* gene (p72 protein), central hypervariable region (CVR) of the *B602L* gene, and the *E183L* gene (p54 protein). Phylogenetic analyses identified three circulating genotypes: I (64.5% of samples), IX (32.3%), and XIV (3.2%). This is the first evidence of genotypes IX and XIV within this country. Examination of the CVR revealed high levels of intra-genotypic variation, with 19 identified variants.

Keywords: African swine fever virus; outbreaks; Democratic Republic of Congo; swine; genotypes; molecular epidemiology; *p72* gene; *p54* gene; CVR

1. Introduction

African swine fever (ASF) is a complex and highly lethal haemorrhagic disease of domestic swine with mortality rates reaching 100%. ASF, which is threatening the world pig industry, is a notifiable disease by the World Organization for Animal Health (OIE) [1]. Since the recognition of ASF in Kenya in the 1920s [2], ASF has expanded to most sub-Saharan countries [3], and was exported outside Africa in 1957 to Portugal [4]. Subsequent exportations to Europe occurred in 1960 and 2007 [5,6].

Introduction of ASF has not been limited to Europe, as outbreaks with putative causal links to Spain have occurred in the Caribbean and South America [7].

Domestic pigs are most susceptible, with the disease course ranging from peracute, acute, subacute, chronic and unapparent and, mortality rates ranging from 100% to as little as 3% [8]. ASF is caused by African swine fever virus (ASFV), which is transmitted to swine through three main routes: (1) a sylvatic cycle involving wild swine and *Ornithodoros* ticks; (2) from the sylvatic cycle to domestic pigs; and (3) domestic pig cycle involving domesticated pig to pig transmission [3,9]. ASFV is a large arbovirus within the genus *Asfivirus* and is the sole member of the family *Asfarviridae* [10].

Due to the lack of treatment and vaccine, rapid and accurate diagnosis complemented by the genotyping of circulating ASFVs may contribute to timely improvement of prevention and control strategies. In order to identify and determine the heterogeneity of circulating ASFVs, a rapid method of polymerase chain reaction (PCR)-based sequencing of a 478 base pair (bp) fragment at the C-terminal end of the *p72* gene has been commonly used to differentiate the different genotypes of ASFV [11]. Given the low level of genetic variation detected at the *p72* locus among ASFVs recovered in domestic pig outbreaks, examination of more variable genomic regions such as the central hypervariable region (CVR) of the *B602L* gene [12] in combination with the *p54* and *p30* genes [13] were used to differentiate between isolates within a single outbreak.

Currently, there are 23 confirmed genotypes of ASFV based on the sequencing of the *p72* gene [11], not all of which are known to be currently circulating. The most recent, genotype XXIII, was discovered in Ethiopia [14]. In Africa, further diagnostic analysis of suspected outbreaks shows genotype I continuing to circulate in Western and Central Africa [15,16]. Countries with continued presence of genotypes IX and X include Uganda and Kenya [17–19]. Genotype II has maintained its presence in Tanzania, Mozambique, Madagascar and Zambia, and is what led to the introduction of genotype II into Georgia in the Caucasus region in 2007 [6,20]. Since that time, ASFV has spread from Georgia and the Caucasus to the Baltic states (Estonia, Latvia and Lithuania), the Russian Federation, Ukraine, and Poland [21–23].

The Democratic Republic of the Congo (DRC) is the second largest country in Africa, with the central and western portions of the country being dominated by the second largest block of rainforest in the world, whereas the southern and eastern regions are characterized by savannas. The 9000-km perimeter of the DRC contacts nine countries and includes a number of lakes (e.g., Edward, Albert, Kivu, Tanganyika) and rivers (e.g., the Congo, Ubangi, Kasai, Semliki). These geographic elements, as well the presence of many trans-frontier tribes that inhabit the DRC and surrounding countries contribute to the semi-porous nature of the DRC's political boundary.

In 2011, the DRC reported 84 outbreaks and a loss of 105,614 swine, leading African countries in both statistics [24]. Despite the prevalence of ASF in the DRC, the variety of genotypes reported in surrounding countries [9,19], and the large number of studies that have examined this disease, no in-depth study has focused on understanding the genetic diversity of ASFV within the DRC. The goal of this study was to improve the scientific community's understanding of ASFV strains circulating in the DRC. To achieve this goal, we collected samples from swine that exhibited ASF clinical signs and pathological findings over a broad geographic and temporal range. We utilized a multi-locus genotyping approach to categorize gene sequences into genotypes, and used this data to improve the understanding of the natural history as well as the links between outbreaks of ASFV in the DRC.

2. Materials and Methods

2.1. Study Area and Samples

A total of 62 tissue samples (spleen, lymph node, kidney, lung, liver, heart and stomach) of ASF suspected cases were collected between 2005 and 2012 from 57 domestic pig carcasses and from 25 locations. Of these carcasses, 54 were collected in outbreaks and three were slaughtered in urban

markets. Sampling localities were located in six provinces (Kinshasa, Equateur, Katanga, Orientale, Bas-Congo and Maniema) that contain the majority of the country's domestic pig population. Tissue samples were transported to the laboratory, homogenized and supernatants were stored at −80 °C until use. Samples, collection localities, and other details are provided in Table 1.

Table 1. Samples, details, and genotypes.

Virus	Outbreak Date	Location	GPS	Ecological Profile	Tissues	Farming System	Genotype
drc49/05/p1a	May 2005	Limete	4°18 S/15°22 E	City	Spl	Commercial	I
drc49/05p1b	May 2005	Limete	4°18 S/15°22 E	City	Ln	Commercial	I
drc49/05/P2a	May 2005	Limete	4°18 S/15°22 E	City	Spl	Commercial	I
drc70/05/1	2005	Limete	4°18 S/15°22 E	City	Spl	Commercial	I
drc75/05/1	2005	Maniema	2°93 S/25°86 E	City	Spl	Commercial	I
drc99/05/a	2005	Ngafula	4°21 S/15°14 E	Peri-urban	Spl	Commercial	I
drcKG28110805	Nov 2008	Ngaliema	4°21 S/15°21 E	City	Spl	Backyard	I
drcKG28040802	Apr 2008	Kasavubu	4°20 S/15°20 E	City	Spl	Backyard	I
drc74/09/2	2009	Nsele	4°24 S/15°30 E	Peri-urban	Kd	Commercial	I
drc74/09/3	2009	Nsele	4°24 S/15°30 E	Peri-urban	Lg	Commercial	I
drc74/09/4	2009	Nsele	4°24 S/15°30 E	Peri-urban	Lv	Commercial	I
drc74/09/6	2009	Nsele	4°24 S/15°30 E	Peri-urban	Hrt	Commercial	I
drc94/09/2	2009	Kintambo	4°20 S/15°18 E	City	Ln	Commercial	I
drc35/10/1	2010	Ngaliema	4°21 S/15°05 E	City	Spl	Backyard	I
drc35/10/5	2010	Ngaliema	4°21 S/15°05 E	City	Ln	Backyard	I
drc35/10/4	2010	Ngaliema	4°21 S/15°05 E	City	Ln	Backyard	I
drc51/10/23	2010	Ndjili	4°24 S/15°21 E	City	Spl	Commercial	I
drc73/10/2	2010	Ngaliema	4°21 S/15°05 E	City	Kn	Backyard	I
drc73/10/3	2010	Ngaliema	4°21 S/15°05 E	City	Lv	Backyard	I
drc73/10/4	2010	Ngaliema	4°21 S/15°05 E	City	Ln	Backyard	I
drc85/10/13	2010	Ngafula	4°21 S/15°14 E	Peri-urban	Spl	Commercial	I
drc85/10/12	2010	Ngafula	4°21 S/15°14 E	Peri-urban	Hrt	Commercial	I
drc85/10/11	2010	Ngafula	4°21 S/15°14 E	Peri-urban	Lg	Commercial	I
drc85/10/27	2010	Ngafula	4°21 S/15°14 E	Peri-urban	Hrt	Commercial	I
drc85/10/25	2010	Ngafula	4°21 S/15°14 E	Peri-urban	Lv	Commercial	I
drc86/10/1	2010	Ngafula	4°21 S/15°14 E	Peri-urban	Kd	Commercial	I
drc86/10/3	2010	Ngafula	4°21 S/15°14 E	Peri-urban	Lv	Commercial	I
drc108/10/3	2010	Ngafula	4°21 S/15°14 E	Peri-urban	Lv	Commercial	I
drc108/10/5	2010	Ngafula	4°21 S/15°14 E	Peri-urban	Spl	Commercial	I
drc27/11/1	2011	Ngafula	4°21 S/15°14 E	Peri-urban	Spl	Commercial	I
drc27/11/2	2011	Ngafula	4°21 S/15°14 E	Peri-urban	Ln	Commercial	I
drc27/11/3	2011	Ngafula	4°21 S/15°14 E	Peri-urban	Stm	Commercial	I
drc27/11/5	2011	Ngafula	4°21 S/15°14 E	Peri-urban	Lv	Commercial	I
drc65/11/2	2011	Nsele	4°24 S/15°30 E	Peri-urban	Kd	Commercial	I
drc65/11/3	2011	Nsele	4°24 S/15°30 E	Peri-urban	Spl	Commercial	I
drc65/11/4	2011	Nsele	4°24 S/15°30 E	Peri-urban	Lg	Commercial	I
drc96/12/1	2012	Mayanda	5°12 S/15°14 E	Rural	Lg	Village	I
drc96/12/2	2012	Mayanda	5°12 S/15°14 E	Rural	Spl	Village	I
drc96/12/3	2012	Mayanda	5°12 S/15°14 E	Rural	Hrt	Village	I
drc108/10/1	Dec 2010	Ngafula	4°21 S/15°14 E	Peri-urban	Lg	Commercial	I
drc46/11/2	Jun 2011	Kinshasa	4°20 S/15°18 E	City	Hrt	Backyard	I
drc20/07/19	Apr 2007	Mahagi *	2° S/31° E	Rift Valley	Kd	Backyard	IX
drc20/07/20	Apr 2007	Mahagi *	2° S/31° E	Rift Valley	Ln	Backyard	IX
drc25/08/3a	Mar 2008	Boende	0°15 S/21°01 E	Forest	Kd	Free range	IX
drc25/08/3	Mar 2008	Boende	0°15 S/21°01 E	Forest	Spl	Free range	IX
drc25/08/42	Mar 2008	Boende	0°15 S/21°01 E	Forest	Kd	Free range	IX
drc25/08/9	Mar 2008	Boende	0°15 S/21°01 E	Forest	Spl	Free range	IX
drc35/08/1	Apr 2008	Boende	0°15 S/21°01 E	Forest	Spl	Free range	IX
drc35/08/13	Apr 2008	Boende	0°15 S/21°01 E	Forest	Spl	Free range	IX
drc35/08/$P4_2$	Apr 2008	Boende	0°15 S/21°01 E	Forest	Spl	Free range	IX
drc35/08/15	Apr 2008	Boende	0°15 S/21°01 E	Forest	Spl	Free range	IX
drc35/08/18	Apr 2008	Boende	0°15 S/21°01 E	Forest	Kd	Free range	IX
drc35/08/20	Apr 2008	Boende	0°15 S/21°01 E	Forest	Spl	Free range	IX
drc35/08/3	Apr 2008	Boende	0°15 S/21°01 E	Forest	Spl	Free range	IX
drc66/07/43	Nov 2007	Yakoma	4° S/22° E	Forest	Lg	Free range	IX
drc66/07/48	Nov 2007	Yakoma	4° S/22° E	Forest	Spl	Free range	IX
drc66/07/49_1	Nov 2007	Yakoma	4° S/22° E	Forest	Spl	Free range	IX
drc66/07/49_2	Nov 2007	Yakoma	4° S/22° E	Forest	Ln	Free range	IX
drc66/07/50	Nov 2007	Yakoma	4° S/22° E	Forest	Spl	Free range	IX
drcKG31208/3	Dec 2008	Lingwala	4°20 S/15°19 E	City	Spl	Backyard	IX
drc35/10/3	Apr 2010	Ngaliema	4°21 S/15°05 E	City	Kd	Backyard	XIV
drc21/07/22	2007	Kipushi †	12° S/28° E	City	Spl	Backyard	XIV

drc, Democratic Republic of the Congo; Ln, lymph node; Hrt, heart; Spl, spleen; Kd, kidney; Lg, lung; Lv, liver; Stm, stomach; GPS, global positioning system; *, Uganda border; †, Zambia border.

2.2. African Swine Fever (ASFV) DNA by Polymerase Chain Reaction (PCR)

ASFV DNA was extracted from tissue samples using the QIAGEN blood and tissue extraction kit (Qiagen, Hilden, Germany) according to the manufacturers' protocol. Each sample of extracted DNA was then tested by real-time PCR (qPCR), as described by King et al. [25] to confirm the presence of viral DNA for ASFV using the primers King forward (5′-CTGCTCATGGTATC AATCTTATCGA-3′), King reverse (5′-GATACCACAAGATCRGCCGT-3′), and the King probe (5′-Fam-CCACGGGAGGAATACCAACCCAGTG-Tam-3′).

2.3. Generation of ASFV Sequence Data

Samples that were positive by qPCR had each target gene fragments amplified separately using the PCR protocols outlined below. The C terminal end of the *B646L* (*p72*) gene was amplified using primers p72U (5′-GGCACAAGTTCGGACATGT-3′) and p72D (5′-GTACTGTAACGCAGCACAG-3′) as recommended [11]. The CVR locus was amplified using primers, ORF9RLW_F (5′-AATGCGCTCAG GATCTGTTAAATCGG-3′) and ORF9RLW_R (5′-TCTTCATGCTCAAAGTGCGTATACCT-3′) as described [26], The full *E183L* (*p54*) gene was amplified using primers P54F (5′-GCCTGCGGA TTCTGAAGATA-3′), and P54R (5′-AGGACGCAATTGCTTAAACG-3′) using a touchdown PCR protocol as follows, 95 °C for 5 min, followed by 15 cycles of 95 °C, 30 s, 60 °C, 30 s, 72 °C, 1 min, then 25 cycles of 95 °C, 30 s, 58 °C, 30 s, 72 °C, 1 min, with a final extension or 72 °C for 5 min. PCR products were purified using Wizard SV Gel and PCR Clean Up kit, according to the manufacturers' protocol (Promega Corporation, Madison, WI, USA). Purified PCR products were submitted to LGC Genomics (Berlin, Germany) with amplification primers, for sequencing. Raw sequences were assembled and edited using Vector NTI 11.5 Software (Life Technologies, Carlsbad, CA, USA). Sequences were then aligned with GenBank reference sequences using MEGA (Version 6.0) or BioEdit (Version 7.2.3) using the ClustalW method. All nucleotide sequences were deposited in GenBank (Accession # KX121429-KX121600).

2.4. Molecular Characterization of ASFV

Multiple sequence alignments of both the *p54* and *p72* genes were generated in MEGA (Version 6.0) [27] using default values of the 'by codon' option with the ClustalW algorithm with additional manual editing as needed. The *p72* alignment was 404 bp in length and contained 120 sequences. Of these 120 sequences, 62 were generated for this study and 58 were reference sequences with at least one representing each of the known 23 genotypes. The *p54* alignment was 657 bp in length and included 84 sequences; 34 were generated for this study, and 50 were reference sequences for 20 of the 23 known *p72* genotypes. Published sequences for genotypes XI, XII, and XVIII were unavailable for examination. The most appropriate model of molecular evolution was determined by the corrected Akaike Information Criterion (AICc) using MEGA [27]. Maximum likelihood (ML) analyses with 1000 bootstrap replicates were performed using the program MEGA with the predetermined model of molecular evolution (GTR+I+G for the *p72* dataset and HKY+G for the *p54* dataset) using all sites. The intra-genotypic genetic distances for the *p72* and *p54* nucleotides sequences of DRC samples were calculated using MEGA [27].

2.5. Central Hypervariable Region (CVR) of B602L *Gene*

Grouping of amino acids into tetramers at this locus has been utilized by other researchers, therefore the coding of tetramers followed methods outlined previously [20,26,28–30]. The amino acid tetramer codes are provided in Table 2.

3. Results

3.1. Clinical Findings and African Swine Fever (ASF) Diagnosis

Field Identification and Description of Collecting Localities

Fifty-four out of the 57 sampled pigs exhibited many of the following signs or pathological findings: hemorrhagic edema; enlargement of spleen and some internal lymph nodes; hydropericardium and pericarditis; hydrothorax; ascites; as well as skin cyanosis and petechiae. The three remaining pigs sampled in the markets appeared superficially healthy, but presented with enlarged, congestive or hemorrhagic spleens and/or gastrohepatic lymph nodes. Massive mortality was documented in the 25 sampled localities. Four of the 25 sampling sites, including the cities of Yakoma, Boende, Mahagi and Kipushi, recorded indigenous pigs of local breeds, primarily free ranging to be the most commonly lost. The remaining 21 locations were commercial farms raising improved breeds of pigs in backyards or securely fenced areas, minimizing intermingling of wildlife and domestic swine.

3.2. Laboratory Diagnostics

Real time PCR identified 62 samples (100%) as positive for ASFV DNA and distributed per location as follows: Ngafula (n = 17) Boende (n = 11), Ngaliema (n = 8), Nsele (n = 7) Yakoma (n = 5) Limete (n = 4), Mayanda (n = 3), Mahagi (n = 2), Kasavubu (n = 1), Kintambo (n = 1), Kipushi (n = 1), Lingwala (n = 1), Maniema (n = 1) and Ndjili (n = 1). The *p72* gene was sequenced for all 62 positive samples and 55 positive samples were sequenced for the *p54* gene and 54 for the CVR (Table 1).

3.3. Molecular Characterization of ASFV

Phylogenetic analyses of the *p72* gene revealed that the newly sequenced ASFV strains which circulated in the DRC from 2005 to 2012 clustered into three *p72* genotypes: I, IX and XIV (Figure 1). Of the newly analyzed stains, 40 (64.5%) grouped with strains previously identified as belonging to genotype I, including three published strains from the DRC (Katanga63 (Genbank: AF301540) [11], Kat67 (Genbank: FJ174377) [13] and Zaire (Genbank: AY351515) [9]); 20 strains (32.3%) were recognized as genotype IX, and 2 (3.2%) belong to genotype XIV. This is the first report of genotypes IX and XIV circulating in the DRC. Although sequences generated herein grouped with high bootstrap support (>75%) with reference samples of their respective genotypes, support for both inter- and intra-genotypic relationships varied.

Phylogenetic analyses of the *p*54 gene recovered the same groupings of new sequences with respective genotypes as the *p72* analyses with high bootstrap support (>83%) (Figure 2). The arithmetic means of nucleotide substitutions per site between the DRC ASFVs of each of the three genotypes (within group mean distance) were estimated using MEGA version 6. The within group mean distance for the *p72* nucleotide sequences were 0.002 for genotype I and 0.0 for genotype IX and XIV. Likewise, for the *p54* nucleotide sequences, the within group mean distance was 0.02 for the genotype I members, and 0.0 for genotype IX members. Only one isolate of genotype XIV was successfully amplified and sequenced for this gene.

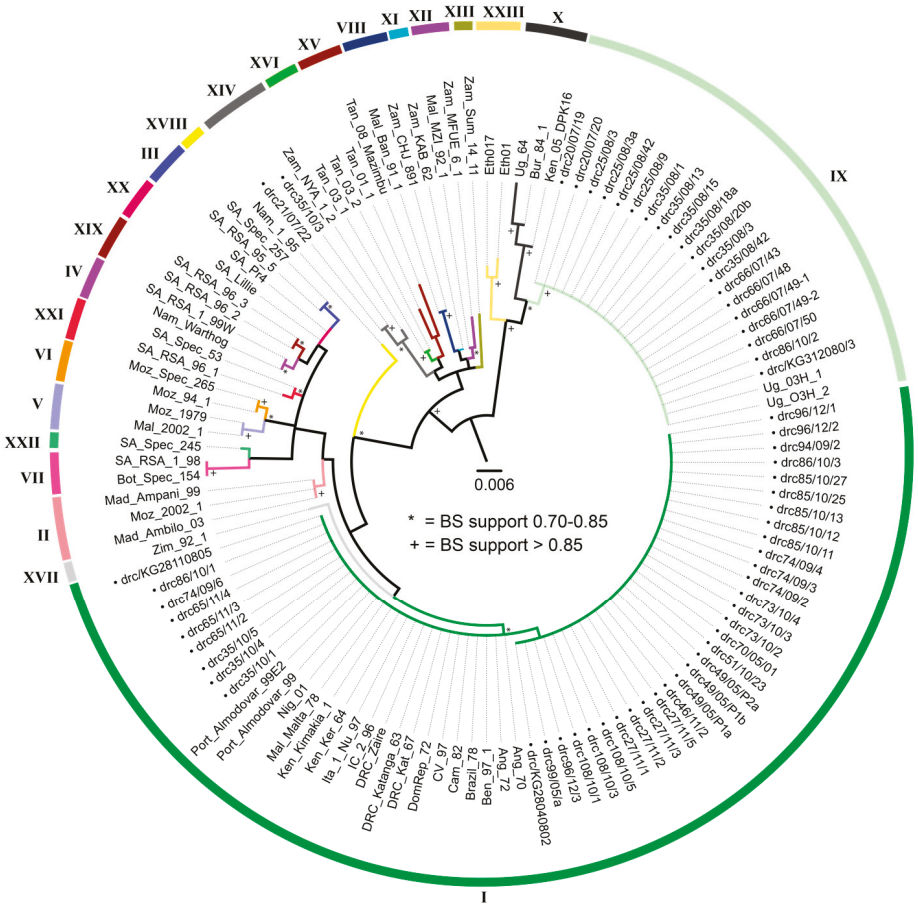

Figure 1. Maximum likelihood tree depicting genetic relationships of strains examined in this study utilizing the *p72* locus. Bootstrap support (BS) is indicated by * for values between 75% and 85%, and by + for values greater than 85% support. The scale bar indicates the number of nucleotide substitutions per site. Each color is a different genotype, indicated by the corresponding roman numerals. Labels for all strains generated by this study begin with •drc (Democratic Republic of the Congo). Strains are named in the following manner: Country_Strain Name. Acronyms used for countries of origin are as follows: Ang = Angola, Ben = Benin, Bot = Botswana, Bra = Brazil, Bur = Burundi, Cam = Cameroon, CV = Cape Verde, Dom Rep = Dominican Republic, the DRC = Democratic Republic of Congo, IC = Ivory Coast, Ita = Italy, Ken = Kenya, Mad = Madagascar, Mal = Malawi, Malt = Malta, Moz = Mozambique, Nam = Namibia, Nig = Nigeria, Port = Portugal, SA = South Africa, Tan = Tanzania, Ug = Uganda, Zam = Zambia, Zimb = Zimbabwe.

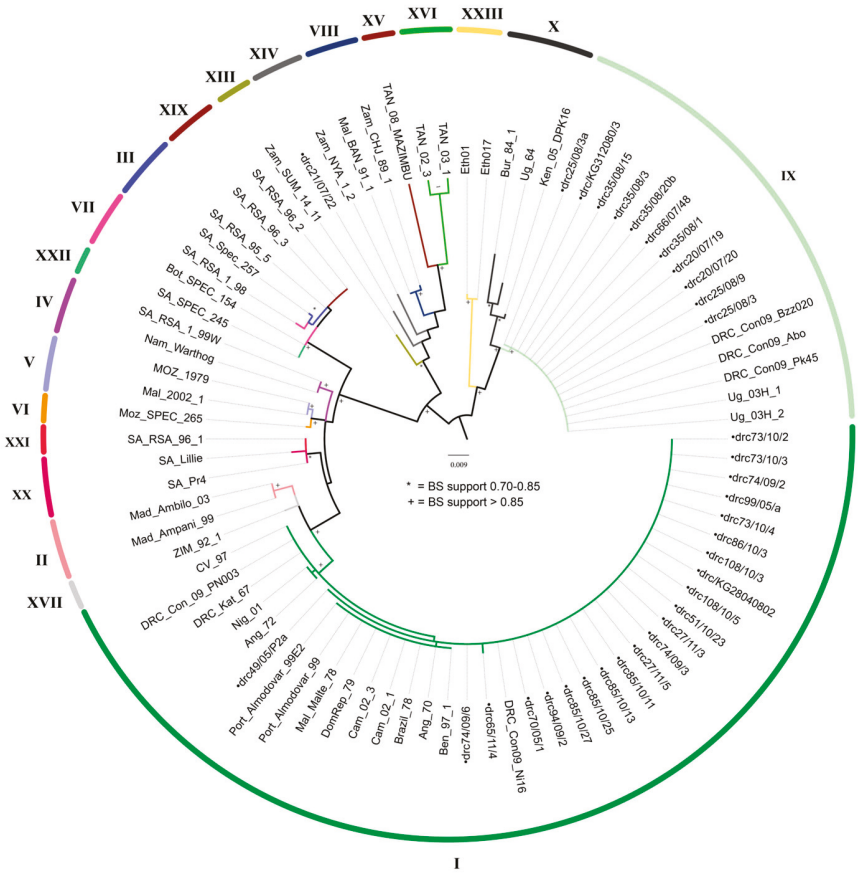

Figure 2. Maximum likelihood tree depicting genetic relationships of examined strains using the *p54* locus (*E183L* gene). Bootstrap support values greater than 75% are shown. The scale bar indicates the number of nucleotide substitutions per site. The colored clades indicate genotypes represented by strains sequenced in this study. Labels for all strains generated by this study begin with •drc. Strains are named in the following manner: Country_Strain Name. Acronyms used for countries of origin are as follows: Ang = Angola, Ben = Benin, Bot = Botswana, Bra = Brazil, Bur = Burundi, Cam = Cameroon, CV = Cape Verde, Dom Rep = Dominican Republic, the DRC = Democratic Republic of Congo, IC = Ivory Coast, Ita = Italy, Ken = Kenya, Mad = Madagascar, Mal = Malawi, Malt = Malta, Moz = Mozambique, Nam = Namibia, Nig = Nigeria, Port = Portugal, RC = Republic of Congo, SA = South Africa, Tan = Tanzania, Ug = Uganda, Zam = Zambia, Zimb = Zimbabwe.

3.4. CVR of B602L *Gene*

Sequence analysis of the CVR locus showed distinct variability in nucleotide sequence and recognized 19 unique nucleotide sequences, which were translated into amino acid sequences, and subsequently coded as amino acid tetramers (tet-types). Thirteen tet-types were detected within strains identified as belonging to *p72* genotype I, six from strains belonging to genotype IX, and two within genotype XIV strains (Table 2). All strains grouped within a tet-type contained identical CVR nucleotide sequences; therefore, no resolution was lost by converting nucleotide sequences to tetrameric repeat sequences. Tet-12 and 51 were both detected in *p72* genotype I strains, but tet-12 was also found in a *p72* genotype IX strain (drc86/10/2), and tet-51 was also found in a *p72* genotype XIV

strain (drc35/10/3). All three *p72* genotypes and 14 tet-types were identified throughout Kinshasa (Table 2, Figure 4). Regarding the five remaining provinces: Equateur presented four tet-types (within genotype IX); Bas-Congo and Maniema each had a single tet-type (within genotype I); Katanga (within genotype XIV) and Oriental each contained a single tet-type (within genotype IX), as well (Figure 3).

Table 2. Central hypervariable region (CVR) locus-based intra-genotype resolution.

Strain	Location	Year	Genotype	Tetrameric Repeats	TRS
drc35/10/1	Ngaliema *	2010	I	AAAAAAAAAAAAAAAAAAAAAAAAAAAABNAB NBTDBNAAAAAAAAAAF	51
drcKG28110805	Ngaliema *	2010	I	AAAAAAAAABNABNBTABNAAAAAAAAAAAAAAAA AAAAAAAAF	45
drc65/11/4	Nsele *	2011	I	AAAAAABNABNBTDBNAAAAAAAAF	25
drc74/09/2	Nsele *	2009	I	AAAAAAAAAAAAAAAAAAAAAF	23a
drc74/09/3	Nsele *	2009	I	AAAAAAAAAAAAAAAAAAAAAF	23a
drc74/09/4	Nsele *	2009	I	AAAAAAAAAAAAAAAAAAAAAF	23a
drc74/09/6	Nsele *	2009	I	AAAAAAAAAAAAAAAAAAAAAF	23a
drc94/09/2	Kintambo *	2009	I	AAAAAAAAAAAAAAAAAAAAAF	23a
drc27/11/3	Ngafula *	2011	I	AAAAAAAAAAAAAAAAAAAAAF	23a
drc27/11/5	Ngafula *	2011	I	AAAAAAAAAAAAAAAAAAAAAF	23a
drcKG28040802	Kasavubu *	2008	I	AAAAAAAAAAAAAAF	16
drc96/12/1	Mayanda	2012	I	AAAAAAAAAAAAAAF	16
drc96/12/2	Mayanda	2012	I	AAAAAAAAAAAAAAF	16
drc96/12/3	Mayanda	2012	I	AAAAAAAAAAAAAAF	16
drc99/05a	Ngafula *	2005	I	AAAAAAAAAAAAF	14
drc51/10/23	Ndjili *	2010	I	AAAAAAAAAAF	12
drc85/10/13	Ngafula *	2010	I	AAAAAAAAAAF	12
drc85/10/27	Ngafula *	2010	I	AAAAAAAAAAF	12
drc86/10/3	Ngafula *	2010	I	AAAAAAAAAAF	12
drc86/10/1	Ngafula *	2010	I	AAAAAAAAAAF	12
drc108/10/1	Ngafula *	2010	I	AAAAAAAAAAF	12
drc108/10/3	Ngafula *	2010	I	AAAAAAAAAAF	12
drc108/10/5	Ngafula *	2010	I	AAAAAAAAAAF	12
drc85/10/12	Ngafula *	2010	I	AAAAAAAAAF	11
drc73/10/2	Ngaliema *	2010	I	AAAAAAAAAF	11
drc73/10/3	Ngaliema *	2010	I	AAAAAAAAAF	11
drc73/10/4	Ngaliema *	2010	I	AAAAAAAAAF	11
drc49/05/P2a	Limete *	2005	I	AAAAAAAAF	10
drc85/10/25	Ngafula *	2010	I	AAAAAAAF	9
drc75/05/1	Maniema	2005	I	AAAAAAAF	9
drc49/05/p1b	Limete *	2005	I	AAAAAAAF	9
drc65/11/3	Nsele *	2011	I	AAAAAAF	8
drc49/05/p1a	Limete *	2005	I	AAAAF	6
drc70/05/1	Limete *	2005	I	AAAAF	5
Con09/Ni16	Congo [1]	2009	I	AAAAAAAAAF	10
Kat67	DRC(Zaire) [2]	1967	I	AAAAAAAABNABTDBNAAAAAAA	23
Nig13_KAF_14	Nigeria [3]	2014	I	ABNABNAAAAACBNAFA	17
drc66/07/49$_1$	Yakoma	2007	IX	AAABBAABBNABBAABBNABNABA	24a
drc66/07/43	Yakoma	2007	IX	AAABNABBBNABBAABBNABNABA	24b
drc66/07/50	Yakoma	2007	IX	AAABNABBBNABBAABBNABNABA	24b
drc66/07/492	Yakoma	2007	IX	AAABNABBBNABBAABBNABNABA	24b
drc66/07/48	Yakoma	2007	IX	AAAABNABBNABBAABBNABNABA	24c
drc35/08/p4$_2$	Boende	2008	IX	AAAABNABBNABBAABBNABNABA	24c
drc35/08/18	Boende	2008	IX	AAAABNABBNABBAABBNABNABA	24c
drc35/08/13	Boende	2008	IX	AAAABNABBNABBAABBNABNABA	24c
drc35/08/3	Boende	2008	IX	AAAABNABBNABBAABBNABNABA	24c
drc35/08/20	Boende	2008	IX	AAAABNABBNABBAABBNABNABA	24c
drc35/08/1	Boende	2008	IX	AAAABNABBNABBAABBNABNABA	24c
drc35/08/15	Boende	2008	IX	AAAABNABBNABBAABBNABNABA	24c
drc35/08/3a	Boende	2008	IX	AAAABNABBNABBAABBNABNABA	24c
drc25/08/3	Boende	2008	IX	AAAABNABBNABBAABBNABNABA	24c
drc25/08/9	Boende	2008	IX	AAAABNABBNABBAABBNABNABA	24c
drc25/08/42	Boende	2008	IX	AAAABNABBNABBAABBNABNABA	24c
drcKG31208/3	Lingwala *	2008	IX	AAAABNABBNABBAAABNABNABA	24d
drc20/07/19	Mahagi	2007	IX	AAABNABBNABBAABBNABNABA	23b
drc20/07/20	Mahagi	2007	IX	AAABNABBNABBAABBNABNABA	23b
drc86/10/2	Ngafula *	2010	IX	AAAAAAAAAAAF	12
UG03H.1	Uganda [4]	2003	IX	AAABNABBNABBAABBNABNABA	23b
Ken06.B1	Kenya [5]	2006	IX	AAABNABBNABBAABBNABNABA	23b
drc35/10/3	Ngaliema *	2010	XIV	AAAAAAAAAAAAAAAAAAAAAAAAAAAABNABNBTDBN AAAAAAAAAAAF	51
drc21/07/p22	Kipushi	2007	XIV	AVVOVAVVNBVOV	13
ETH/3	Ethiopia [6]	2011	XXIII	ABNAAAAACBNABTDBNAFA	20

Codes as labeled in previous studies: [20,26,28–30]. TRS, tetrameric repeat sequence number; *, indicates strains collected within Kinshasa Province. A = CAST, CVST, CTST, or CASI; B = CADT, CADI, CTDT, or CAGT; C = GAST or GANT; F = CANT or CAAT; N = NVDT, NVGT, NVDI, or NCDT; T = NVNT; H = RAST; S = SAST; O = NANI, NADI, or NASI; V = NAST, NAVT, NADT, or NANT; D = CASM; G = CTNT; M = NEDT; W = SADT or SVDT; U = NIDT or NTD. Additional sequences utilized in this table from previous studies: [1] [17]; [2] [26]; [3] [16]; [4] [13]; [5] [13]; [6] [14].

3.5. Democratic Republic of the Congo (DRC) ASFV Genotypes Geographical Distribution

Different ASFV strains were identified in the provinces of Bas-Congo, Equateur, Katanga, Kinshasa, Maniema, and Orientale (Figure 3). Genotype I strains were detected in Bas-Congo (Localities-Mayanda), Kinshasa (Localities-Limete, Ngafula, Ngaliema, Kasavubu, Nsele, Kintambo, Ndjili, Nsele, Kinshasa) (Figure 4) and Maniema (Locality-Maniema), whereas genotype IX strains were recovered from Equateur (Localities-Boende, Yakuma), Kinshasa (Localities-Ngafula, Lingwala), and Oriental provinces (Locality-Mahagi). Genotype XIV was detected from Katanga (Locality-Kipushi) and Kinshasa (Locality-Ngaliema).

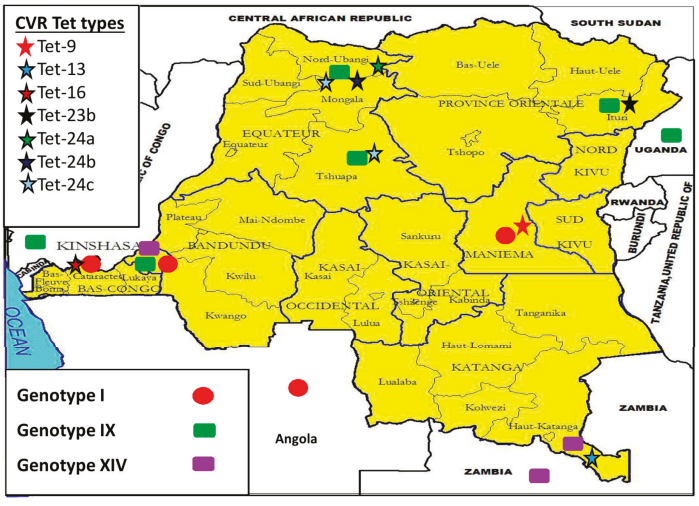

Figure 3. Provincial localization of revealed *p72* genotypes and their corresponding central hypervariable region (CVR) tet-types within the DRC, as well as some historical African swine fever virus (ASFV) genotypes from neighboring countries.

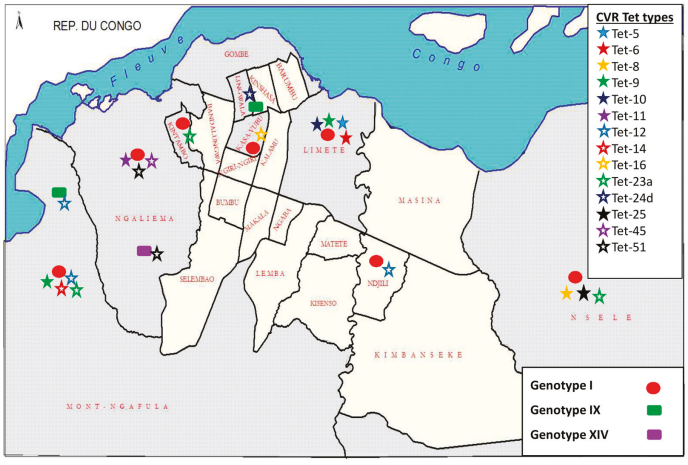

Figure 4. Localization of ASFV *p72* genotypes and the corresponding CVR tet-types in this study within the Kinshasa City Province.

4. Discussion

4.1. Molecular Characterization

This is the first extensive molecular evaluation of circulating ASFV genotypes in the DRC. Previous knowledge was based on data from single samples submitted for ASF diagnosis [9,11,26,29,31,32], but little was known about the dynamics of circulating ASFV strains in the DRC. Analysis of the *p72* gene identified three genotypes (I, IX and XIV) circulating in the DRC. Forty of 62 (64.5%) clustered with DRC historical strains (DRC_Kat63 and DRC_Kat67), as well as other strains from genotype I, confirming that genotype I is the most prevalent in the country. Additionally, DRC strains of this genotype exhibited limited genetic variability, which has been repeatedly documented and hypothesized to be predominantly a result of maintenance through the domestic pig cycle [9]. There were 19 *p72* genotype IX strains (30.6%) with no genetic variation detected. Previously undocumented within the DRC, genotype IX is much more geographically restricted, as it is endemic to East and Central Africa (Figure 5), having been reported previously in Republic of Congo, Uganda, and Kenya (Figure 5) where it is involved in sylvatic and domestic cycles [9,17]. Genotype XIV was also not previously reported in the country prior to the two (3.2%) strains reported herein. Genotype XIV was previously only reported from Zambia (Figure 5), where it was originally isolated from a tick of the genus *Ornithodoros* in 1986 [9]. In regards to the distribution of ASFV within the DRC recovered in this study, all genotypes were found near the eastern and western borders, and confirmed localities for all three genotypes occurred in the southern half of the country; however, only genotype IX viruses were collected from localities in the northern DRC (Figures 3 and 4). The presence of all three genotypes within the Kinshasa province is likely a result of pig shipments, as pork sold at markets in Kinshasa has been documented to originate from multiple regions of the country, including the provinces of Equateur, Bandundu, and Bas-Congo [33].

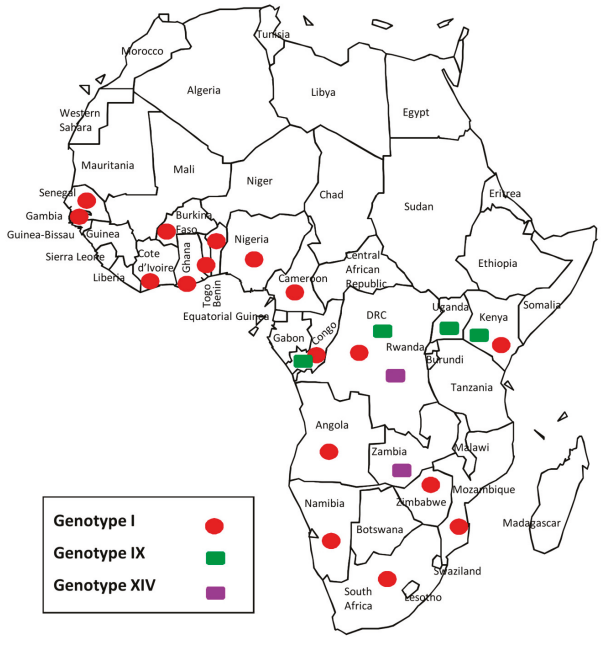

Figure 5. Continental distribution of the three *p72* genotypes revealed by this study in the DRC. Position of symbols represents the presence of a genotype within the country, and is not indicative of specific geographic localities.

Although the *p54* gene was previously determined to be a valuable locus for finer levels of discrimination [19,34,35], no additional resolution was gained for this dataset; however, the p54 locus did corroborate the topology generated by the *p72* analysis. Given the sampling scheme of this study (domestic swine only), failure to achieve higher resolution may be due to the low genetic variation consistently detected within the domestic pig cycle, when compared to the higher levels of variation previously detected within the sylvatic cycle [9].

The CVR was capable of providing further resolution than either the *p72* or *p54* genes. The pattern of genetic variability varied dependent upon the *p72* genotype examined. Within *p72* genotype I strains, genetic variation was primarily a result of variability in the number of tetramers as previously reported [36], specifically the tetrameric amino acid repeats CAST and CVST. Also of interest within genotype I, is that tet-25, 45, and 51 (also found in one genotype XIV strain) contained a conserved sequence of 11 tetramers (tetrameric repeat sequence number (TRS) ABNABNBT[D/A]BN) not found in other tetrameric sequences within this genotype. This sequence was flanked by a variable number of 'A' coded tetramers. The historical isolate Kat67 genotype I CVR was tet-23, but had a similar sequence BNAxx. Additionally, BTDBN also flanked on each end by variable repeats of 'A' [26]. The new genotype XXIII from Ethiopia had one CVR sequence, ETH/3, which also has a similar motif with xxBNABTDBxx [14]. Nigerian sequences are of genotype I and also share part of this motif in the CVR region xxABNABNxx [16] (Table 2). CVR tet-types of *p72* genotype IX consisted primarily of a more complex sequence than genotype I strains, with the exception of tet-12 (common to genotype I strains) being documented in one genotype IX strain. Interestingly, CVR tet-23b which is present in two recent DRC genotype IX strains from 2007 is identical to two genotype IX CVR sequences from Uganda in 2003 and Kenya in 2006 [13] (Table 2). Of the two tet-types detected in genotype XIV strains, the first (tet-51) was identical to a tetrameric repeat sequence found in a genotype I strain, and the second was extremely different than any other tet-types reported herein (Table 2). Several CVR tet-types are discussed below in reference to the detection of multiple strains within outbreaks, and potential links between outbreaks based on this locus.

4.2. Disease Ecology, Molecular Epidemiology and Case Investigations

The higher resolution offered by the CVR allowed for the three genotypes to be further broken down into 19 variants. The high level of variability previously noted in the CVR [9,37,38] would suggest that highly similar/identical CVRs are more closely related than more divergent CVRs; however, given the nature of nucleotide repeat regions, such as the CVR, identical sequences can occur due to homoplasy. With these possibilities in mind, a number of putative outbreak connections are proposed and discussed below, as are details of co-circulation of multiple variants.

The detection of genotype I, tet-23 strains during the 2009 outbreaks at Nsele and Kintambo, as well as the 2011 outbreak in Ngafula may suggest that these geographically proximal outbreaks were caused by closely related strains, even though they occurred over a two-year time span which could be facilitated by the asymptomatic infection of domestic pigs [39] in the area. A second potential connection is suggested by analysis of sequences from the Mahagi outbreak in April 2007 (near the Ugandan border), as they were of identical *p72* genotype IX and tet-23b to strains from Uganda (Ug03H.1, Genbank: GQ916933), and Kenya (Ken06.B1, Genbank: GQ916935 & Ken06.Bus, Genbank: GQ916940) examined previously [13]. A third connection stems from a strain from a clinically healthy pig sampled at the Kinshasa market (drcKG28040802) in 2008. This strain belonged to the same genotype I and tet-16 as samples from the 2012 outbreak in Mayanda, Bas-Congo province. The geographic proximity of these two provinces, in combination with the high level of commercial traffic between them, could easily result in the spread of ASF from one province to the other [1,20].

Again, either the ability of ASFV to persist in asymptomatic pigs (domestic or feral) or the sylvatic cycle (including ticks) could explain how closely related strains were responsible for outbreaks separated by four years, as Mayanda is a rural locality, where there is a high potential for interaction between domestic and feral swine. Another potential outbreak link was made apparent upon

examination of genotype IX strains collected from outbreaks in Yakoma (April 2007) and Boende (March and April 2008). Tet-24c strains were detected in both outbreaks, which severely affected both feral and domestic pigs [40]. The Boende outbreak was estimated to have caused more than 4500 swine fatalities [40]. Both Yakoma and Boende are forested sites, located in North Ubangi and Tshuapa Districts of the Equateur Province, respectively. The forest environment and free ranging animal husbandry practices enable interaction between domestic and wild swine, potentially allowing for crossover between infection cycles and the occurrence of multiple strains.

Another instance of variation occurred in the Ngaliema 2010 outbreak, where tet-51 was found in two strains: drc35/10/1 (genotype I) and drc/35/10/3 (genotype XIV). Co-infection of different tet-types was even documented within the same pig, when two genotype I strains, drc49/05/p1a (tet-5) and drc49/05/p1b (tet-9), were extracted from the spleen and lymph node respectively, of a pig in 2005 from Kinshasa. In similar studies conducted in Mozambique and Nigeria, individual co-infection was not observed [38,41].

Understanding the details of ASFV circulation across the DRC is clearly complex. Co-circulation of genotypes and tet-types and co-infection of multiple tet-types within a single pig suggests a high level of genetic variation and potential support of a previous hypothesis of recombination [42,43]. However, detection of conserved tet-types across large geographic areas, and over multiple years suggests that current markers can provide insight into the movement of ASFV strains. Unfortunately, connecting cases is not straight forward, as anthropogenic factors, such as trade of pigs and animal husbandry practices can play a role. Whole genome examination of these strains may provide a more definitive understanding of relationships.

As the DRC is the largest country in SSA, and borders nine countries, understanding the prevalence and distribution of ASFV genotypes within the DRC is an important step in better understanding large scale patterns of ASFV. Given the high degree of similarity, at all examined loci, between genotype IX strains collected in Mahagi, the DRC (presented herein), and Uganda strains of a previous study [13], it appears that the distribution of this strain spans the border between the DRC and Uganda, suggesting that this strain has been transmitted across boundaries by movement of either feral or domesticated swine. Two more potential cross-boundary transmissions of ASF into/out of the DRC are worth mentioning; however, their molecular evidence is less direct. The first possibility is that genotype XIV may have been transferred, between Zambia (Zam_NYA/12-(Genbank: AY351555), isolated in 1986) [9] and the DRC (drc21/07/22, strain from 2007) through Kipushi, as *p72* sequences between these strains share 99.26% nucleotide sequence identity. Unfortunately, no CVR sequence for strain Zam_NYA/12 was available for a more detailed comparison. The next putative trans-boundary migration of ASF could have occurred between Brazzaville, Republic of Congo (Con09/Ni16-(Genbank: HQ645947), isolated 2009) [17] and the DRC (drc86/10/1, strain from in 2010). The *p72* sequences were identical, and the CVR locus differed by the insertion of two amino acid tetramers coded as A (AAAAAAAAAF from the Brazzaville strain and AAAAAAAAAAAF in the DRC strain). Rapid mutation rates have been shown in vitro [44], therefore, given the highly variable nature of the CVR, it is difficult to omit the possible link between these outbreaks, especially as the boundary is a narrow aquatic border with high levels of human and animal traffic.

This first, in-depth examination of ASFV in the DRC, has provided evidence of (1) circulation of multiple genotypes previously not reported within the DRC; (2) putative links between both geographically and temporally separated outbreaks; (3) potential movement of ASFV strains across borders between the DRC and Uganda, Zambia, Congo; (4) co-circulation of multiple ASFV genotypes within outbreaks and (5) a pig co-infected with two tet-types. These data, in combination with examination of genotype relationships, will be useful for the optimization of current prevention and control strategies at the regional level given the location and size of the DRC in relation to the rest of the continent and those countries also dealing with ASF.

Acknowledgments: This work was supported by the International Atomic Energy Agency (IAEA) project "Improvement of Veterinary Laboratory Capacities in Sub-Saharan African Countries". We pay gratitude to the Wellcome Trust (WT) for its support of this research through two grants, WT075813/C/04/Z and, WT087546MAthat allowed advanced field investigations.

Author Contributions: L. K. Mulumba-Mfumu, C. Saegerman, C. E. Lamien and A. Diallo conceived and designed the experiments. J. E. Achenbach, E. Blanco, N. Moreno, G. Tshilenge, and E. Thiry performed the experiments. L. K. Mulumba-Mfumu, J. E. Achenbach, M. R. Mauldin, and C. E. Lamien analyzed the data. L. K. Dixon, A. Diallo contributed reagents/materials/analysis tools. J. E. Achenbach and M. R. Mauldin performed critical revision of the manuscript. L. K. Mulumba-Mfumu wrote the paper.

Conflicts of Interest: The authors declare no conflict of interest. The findings and conclusions in this report are those of the authors and do not necessarily represent the views of the Centers for Disease Control and Prevention.

References

1. Sánchez-Vizcaíno, J.M.; Mur, L.; Sánchez-Matamoros, A.; Martínez-López, B. African swine fever: New challenges and measures to prevent its spread. In Proceedings of the 82nd General Session World Assembly of Delegates of the World Organisation for Animal Health (OIE), Paris, France, 25–30 May 2014.
2. Montgomery, R.E. On a form of swine fever occurring in British East Africa (Kenya Colony). *J. Comp. Pathol. Ther.* **1921**, *34*, 159–191. [CrossRef]
3. Costard, S.; Mur, L.; Lubroth, J.; Sanchez-Vizcaino, J.M.; Pfeiffer, D.U. Epidemiology of African swine fever virus. *Virus Res.* **2013**, *173*, 191–197. [CrossRef] [PubMed]
4. Detray, D.E. African swine fever. *Adv. Vet. Sci.* **1963**, *8*, 299–333. [PubMed]
5. Sanchez-Vizcaino, J.M.; Mur, L.; Martinez-Lopez, B. African swine fever: An epidemiological update. *Transbound. Emerg. Dis.* **2012**, *59* (Suppl. 1), 27–35. [CrossRef] [PubMed]
6. Rowlands, R.J.; Michaud, V.; Heath, L.; Hutchings, G.; Oura, C.; Vosloo, W.; Dwarka, R.; Onashvili, T.; Albina, E.; Dixon, L.K. African swine fever virus isolate, Georgia, 2007. *Emerg. Infect Dis.* **2008**, *14*, 1870–1874. [CrossRef] [PubMed]
7. Plowright, W.; Thomson, G.R.; Neser, J.A. African swine fever. *Infect. Dis. Livest. Spec. Ref. S. Afr.* **1994**, *1*, 568–599.
8. Hess, W.R.; Endris, R.G.; Haslett, T.M.; Monahan, M.J.; McCoy, J.P. Potential arthropod vectors of African swine fever virus in North America and the Caribbean basin. *Vet. Parasitol.* **1987**, *26*, 145–155. [CrossRef]
9. Lubisi, B.A.; Bastos, A.D.; Dwarka, R.M.; Vosloo, W. Molecular epidemiology of African swine fever in East Africa. *Arch. Virol.* **2005**, *150*, 2439–2452. [CrossRef] [PubMed]
10. Dixon, L.K.; Abrams, C.C.; Bowick, G.; Goatley, L.C.; Kay-Jackson, P.C.; Chapman, D.; Liverani, E.; Nix, R.; Silk, R.; Zhang, F. African swine fever virus proteins involved in evading host defence systems. *Vet. Immunol. Immunopathol.* **2004**, *100*, 117–134. [CrossRef] [PubMed]
11. Bastos, A.D.; Penrith, M.L.; Cruciere, C.; Edrich, J.L.; Hutchings, G.; Roger, F.; Couacy-Hymann, E.; Thomson, R. Genotyping field strains of African swine fever virus by partial p72 gene characterisation. *Arch. Virol.* **2003**, *148*, 693–706. [CrossRef] [PubMed]
12. Phologane, S.B.; Bastos, A.D.; Penrith, M.L. Intra- and inter-genotypic size variation in the central variable region of the 9RL open reading frame of diverse African swine fever viruses. *Virus Genes* **2005**, *31*, 357–360. [CrossRef] [PubMed]
13. Gallardo, C.; Mwaengo, D.M.; Macharia, J.M.; Arias, M.; Taracha, E.A.; Soler, A.; Okoth, E.; Martin, E.; Kasiti, J.; Bishop, R.P. Enhanced discrimination of African swine fever virus isolates through nucleotide sequencing of the p54, p72, and pB602L (CVR) genes. *Virus Genes* **2009**, *38*, 85–95. [CrossRef] [PubMed]
14. Achenbach, J.E.; Gallardo, C.; Nieto-Pelegrín, E.; Rivera-Arroyo, B.; Degefa-Negi, T.; Arias, M.; Jenberie, S.; Mulisa, D.D.; Gizaw, D.; Gelaye, E.; et al. Identification of a New Genotype of African Swine Fever Virus in Domestic Pigs from Ethiopia. *Transbound. Emerg. Dis.* **2016**. [CrossRef] [PubMed]
15. Kouakou, K.V.; Michaud, V.; Biego, H.G.; Gnabro, H.P.; Kouakou, A.V.; Mossoun, A.M.; Awuni, J.A.; Minoungou, G.L.; Aplogan, G.L.; Awoumé, F.K.; et al. African and classical swine fever situation in Ivory-Coast and neighboring countries, 2008–2013. *Acta Trop.* **2017**, *166*, 241–248. [CrossRef] [PubMed]
16. Luka, P.D.; Achenbach, J.E.; Mwiine, F.N.; Lamien, C.E.; Shamaki, D.; Unger, H.; Erume, J. Genetic Characterization of Circulating African Swine Fever Viruses in Nigeria (2007–2015). *Transbound. Emerg. Dis.* **2016**. [CrossRef] [PubMed]

17. Gallardo, C.; Anchuelo, R.; Pelayo, V.; Poudevigne, F.; Leon, T.; Nzoussi, J.; Bishop, R.; Pérez, C.; Soler, A.; Nieto, R.; et al. African swine fever virus p72 genotype IX in domestic pigs, Congo, 2009. *Emerg. Infect. Dis.* **2011**, *7*, 1556–1558. [CrossRef] [PubMed]
18. Atuhaire, D.K.; Afayoa, M.; Ochwo, S.; Mwesigwa, S.; Okuni, J.B.; Olaho-Mukani, W.; Ojok, L. Molecular characterization and phylogenetic study of African swine fever virus isolates from recent outbreaks in Uganda (2010–2013). *Virol. J.* **2013**. [CrossRef] [PubMed]
19. Gallardo, C.; Ademun, A.R.; Nieto, R.; Nantima, N.; Arias, M.; Martín, E.; Pelayo, V.; Bishop, R.P. Genotyping of African swine fever virus (ASFV) isolates associated with disease outbreaks in Uganda in 2007. *Afr. J. Biotechnol.* **2011**, *10*, 3488–3497.
20. Misinzo, G.; Magambo, J.; Masambu, J.; Yongolo, M.G.; Van, D.J.; Nauwynck, H.J. Genetic characterization of African swine fever viruses from a 2008 outbreak in Tanzania. *Transbound. Emerg. Dis.* **2011**, *58*, 86–92. [CrossRef] [PubMed]
21. Gogin, A.; Gerasimov, V.; Malogolovkin, A.; Kolbasov, D. African swine fever in the North Caucasus region and the Russian Federation in years 2007–2012. *Virus Res.* **2013**, *173*, 198–203. [CrossRef] [PubMed]
22. Bosch, J.; Rodríguez, A.; Iglesias, I.; Muñoz, M.J.; Jurado, C.; Sánchez-Vizcaíno, J.M.; de la Torre, A. Update on the Risk of Introduction of African Swine Fever by Wild Boar into Disease-Free European Union Countries. *Transbound. Emerg. Dis.* **2016**. [CrossRef] [PubMed]
23. Gallardo, C.; Fernández-Pinero, J.; Pelayo, V.; Gazaev, I.; Markowska-Daniel, I.; Pridotkas, G.; Nieto, R.; Fernández-Pacheco, P.; Bokhan, S.; Nevolko, O.; et al. Genetic variation among African swine fever genotype II viruses, eastern and central Europe. *Emerg. Infect. Dis.* **2014**, *20*, 1544–1547. [CrossRef] [PubMed]
24. El-Sawalhy, A.; Soumaré, B.; Nouala, S.; Mukanda, B.; Wamwayi, H.; Ahmed, I.G. African Swine fever. In *Pan African Animal Health Yearbook*; Interafrican Bureau for Animal Resources, African Union: Nairobi, Kenya, 2011; pp. 16–17.
25. King, D.P.; Reid, S.M.; Hutchings, G.H.; Grierson, S.S.; Wilkinson, P.J.; Dixon, L.K.; Bastos, A.D.; Drew, T.W. Development of a TaqMan PCR assay with internal amplification control for the detection of African swine fever virus. *J. Virol. Methods* **2003**, *107*, 53–61. [CrossRef]
26. Nix, R.J.; Gallardo, C.; Hutchings, G.; Blanco, E.; Dixon, L.K. Molecular epidemiology of African swine fever virus studied by analysis of four variable genome regions. *Arch. Virol.* **2006**, *151*, 2475–2494. [CrossRef] [PubMed]
27. Tamura, K.; Stecher, G.; Peterson, D.; Filipski, A.; Kumar, S. MEGA6: Molecular evolutionary genetics analysis version 6.0. *Mol. Biol. Evol.* **2013**, *30*, 2725–2729. [CrossRef] [PubMed]
28. Boshoff, C.I.; Bastos, A.D.; Gerber, L.J.; Vosloo, W. Genetic characterisation of African swine fever viruses from outbreaks in southern Africa (1973–1999). *Vet. Microbiol.* **2007**, *121*, 45–55. [CrossRef] [PubMed]
29. Lubisi, B.A.; Bastos, A.D.; Dwarka, R.M.; Vosloo, W. Intra-genotypic resolution of African swine fever viruses from an East African domestic pig cycle: A combined p72-CVR approach. *Virus Genes* **2007**, *35*, 729–735. [CrossRef] [PubMed]
30. Misinzo, G.; Kwavi, D.E.; Sikombe, C.D.; Makange, M.; Peter, E.; Muhairwa, A.P.; Madege, M.J. Molecular characterization of African swine fever virus from domestic pigs in northern Tanzania during an outbreak in 2013. *Trop. Anim. Health Prod.* **2014**, *46*, 1199–1207. [CrossRef] [PubMed]
31. Ekue, N.F.; Wilkinson, P.J. Comparison of genomes of African swine fever virus isolates from Cameroon, other African countries and Europe. *Rev. Elev. Méd. Vét. Pays Trop.* **2000**, *53*, 229–238.
32. Mulumba-Mfumu, L.K.; Goatley, L.C.; Saegerman, C.; Takamatsu, H.H.; Dixon, L.K. Immunization of African Indigenous Pigs with Attenuated Genotype I African Swine Fever Virus OURT88/3 Induces Protection Against Challenge with Virulent Strains of Genotype I. *Transbound. Emerg. Dis.* **2016**, *63*, e323–e327. [CrossRef] [PubMed]
33. Praet, N.; Kanobana, K.; Kabwe, C.; Maketa, V.; Lukanu, P.; Lutumba, P.; Polman, K.; Matondo, P.; Speybroeck, N.; Dorny, P. Taenia solium cysticercosis in the Democratic Republic of Congo: How does pork trade affect the transmission of the parasite. *PLoS Negl. Trop. Dis.* **2010**, *4*, e817. [CrossRef] [PubMed]
34. Atuhaire, D.K.; Ochwo, S.; Afayoa, M.; Mwesigwa, S.; Mwiine, F.N.; Okuni, J.B.; Olaho-Mukani, W.; Ojak, L. Molecular characterization of African swine fever virus in apparently healthy domestic pigs in Uganda. *Afr. J. Biotechnol.* **2014**, *13*, 2491–2499.

35. Giammarioli, M.; Gallardo, C.; Oggiano, A.; Iscaro, C.; Nieto, R.; Pellegrini, C.; Dei, G.S.; Arias, M.; De Mia, G.M. Genetic characterisation of African swine fever viruses from recent and historical outbreaks in Sardinia (1978–2009). *Virus Genes* **2011**, *42*, 377–387. [CrossRef] [PubMed]
36. Goller, K.V.; Malogolovkin, A.S.; Katorkin, S.; Kolbasov, D.; Titov, I.; Hoper, D.; Beer, M.; Keil, G.M.; Portugal, R.; Blome, S. Tandem repeat insertion in African swine fever virus, Russia, 2012. *Emerg. Infect. Dis.* **2015**, *21*, 731–732. [CrossRef] [PubMed]
37. Irusta, P.M.; Borca, M.V.; Kutish, G.F.; Lu, Z.; Caler, E.; Carrillo, C.; Rock, D.L. Amino acid tandem repeats within a late viral gene define the central variable region of African swine fever virus. *Virology* **1996**, *220*, 20–27. [CrossRef] [PubMed]
38. Bastos, A.D.; Penrith, M.L.; Macome, F.; Pinto, F.; Thomson, G.R. Co-circulation of two genetically distinct viruses in an outbreak of African swine fever in Mozambique: No evidence for individual co-infection. *Vet. Microbiol.* **2004**, *103*, 169–182. [CrossRef] [PubMed]
39. Gallardo, C.; Soler, A.; Nieto, R.; Cano, C.; Pelayo, V.; Sanchez, M.A.; Pridotkas, G.; Fernandez-Pinero, J.; Briones, V.; Arias, M. Experimental Infection of Domestic Pigs with African Swine Fever Virus Lithuania 2014 Genotype II Field Isolate. *Transbound. Emerg. Dis.* **2017**, *64*, 300–304. [CrossRef] [PubMed]
40. Central Veterinary Laboratory (CVL). *Rapport Annuel D'Activites (Kinshasa/RDC)*; CVL: Kinshasa, Democratic Republic of Congo, 2010; pp. 1–52.
41. Owolodun, O.A.; Bastos, A.D.; Antiabong, J.F.; Ogedengbe, M.E.; Ekong, P.S.; Yakubu, B. Molecular characterisation of African swine fever viruses from Nigeria (2003–2006) recovers multiple virus variants and reaffirms CVR epidemiological utility. *Virus Genes* **2010**, *41*, 361–368. [CrossRef] [PubMed]
42. Smith, G.P. Evolution of repeated DNA sequences by unequal crossover. *Science* **1976**, *191*, 528–535. [CrossRef] [PubMed]
43. Blasco, R.; de la Vega, I.; Almazan, F.; Aguero, M.; Vinuela, E. Genetic variation of African swine fever virus: Variable regions near the ends of the viral DNA. *Virology* **1989**, *173*, 251–257. [CrossRef]
44. Garcia-Barreno, B.; Sanz, A.; Nogal, M.L.; Vinuela, E.; Enjuanes, L. Monoclonal antibodies of African swine fever virus: Antigenic differences among field virus isolates and viruses passaged in cell culture. *J. Virol.* **1986**, *58*, 385–392. [PubMed]

© 2017 by the authors. Licensee MDPI, Basel, Switzerland. This article is an open access article distributed under the terms and conditions of the Creative Commons Attribution (CC BY) license (http://creativecommons.org/licenses/by/4.0/).

viruses

MDPI

Article

TMPRSS2 and MSPL Facilitate Trypsin-Independent Porcine Epidemic Diarrhea Virus Replication in Vero Cells

Wen Shi [1], Wenlu Fan [1], Jing Bai [1], Yandong Tang [2], Li Wang [1], Yanping Jiang [1], Lijie Tang [1], Min Liu [3], Wen Cui [1], Yigang Xu [1,*] and Yijing Li [1,*]

1 College of Veterinary Medicine, Northeast Agricultural University, Harbin 150030, China; wenshi_china@163.com (W.S.); fanwenlu1230@163.com (W.F.); bj0815@126.com (J.B.); wanglicau@163.com (L.W.); jiangyanping2017@126.com (Y.J.); tanglijie@neau.edu.cn (L.T.); cuiwen_200@163.com (W.C.)

2 Harbin Veterinary Research Institute, Chinese Academy of Agricultural Sciences, Harbin 150001, China; tangyandong2008@163.com

3 College of Animal Science and Technology, Northeast Agricultural University, Harbin 150030, China; liumin-707@163.com

* Correspondence: yigangxu_china@sohu.com (Y.X.); liyijing@neau.edu.cn (Y.L.); Tel.: +86-451-5519-0363 (Y.L.); Fax: +86-451-5519-0363 (Y.L.)

Academic Editors: Linda Dixon and Simon Graham
Received: 17 March 2017; Accepted: 15 May 2017; Published: 18 May 2017

Abstract: Type II transmembrane serine proteases (TTSPs) facilitate the spread and replication of viruses such as influenza and human coronaviruses, although it remains unclear whether TTSPs play a role in the progression of animal coronavirus infections, such as that by porcine epidemic diarrhea virus (PEDV). In this study, TTSPs including TMPRSS2, HAT, DESC1, and MSPL were tested for their ability to facilitate PEDV replication in Vero cells. Our results showed that TMPRSS2 and MSPL played significant roles in the stages of cell–cell fusion and virus–cell fusion, whereas HAT and DESC1 exhibited weaker effects. This activation may be involved in the interaction between TTSPs and the PEDV S protein, as the S protein extensively co-localized with TMPRSS2 and MSPL and could be cleaved by co-expression with TMPRSS2 or MSPL. Moreover, the use of Vero cells expressing TMPRSS2 and MSPL facilitated PEDV replication in the absence of exogenous trypsin. In sum, we identified two host proteases, TMPRSS2 and MSPL, which may provide insights and a novel method for enhancing viral titers, expanding virus production, and improving the adaptability of PEDV isolates in vitro.

Keywords: porcine epidemic diarrhea virus; type II transmembrane serine protease; TMPRSS2; MSPL; virus replication

1. Introduction

Porcine epidemic diarrhea (PED) is caused by porcine epidemic diarrhea virus (PEDV) and is an acute and highly contagious enteric viral disease in nursing pigs. It is characterized by vomiting and lethal, watery diarrhea, and is becoming a global problem [1–7]. PED was first reported in feeder pigs and fattening swine in the United Kingdom in 1971 [8]. Since then, the disease has emerged in many pig-producing countries in Europe and Asia, resulting in tremendous economic losses to the pig industry. PEDV mainly infects the villous epithelial cells of the small intestine, which are rich in proteases, and causes atrophy of the villi, resulting in dehydration and diarrhea. Currently, although PEDV can be propagated in Vero cells treated with trypsin, which mediates the activation of virions for membrane fusion by cleaving the spike (S) glycoprotein [9,10], propagation of PEDV in vitro in a more

productive manner remains a continued challenge. Sometimes, PEDV that has been isolated from clinical samples gradually loses its infectivity during further passages in cell cultures [1]. Therefore, the development of novel strategies to control PEDV is urgently required.

PEDV is a group I coronavirus (CoV) consisting of an enveloped virus with a single-stranded, positive-sense RNA genome of approximately 30 kb [11]. The S glycoproteins of CoVs are class I fusion proteins that are generated in a locked conformation to prevent premature triggering of the fusion mechanism and are subsequently prepared for action by proteolytic processing in a step called priming [12,13]. The S protein can be cleaved by endogenous proteases, which is thought to be necessary for inducing cell–cell fusion and virus-cell fusion [12,14–17]. Some endogenous proteases present in the pig small intestine potentially facilitate the entry of PEDV virions into intestinal epithelial cells [18]. However, in vitro, PEDV-infected cells produce syncytia only after treatment with an exogenous protease such as trypsin. This exogenous protease cleavage event leads to cell–cell and virus–cell fusion [14,16,19–21]. Therefore, the proteases responsible for PEDV activation may be potential therapeutic targets.

Recently, a type of trypsin-like serine protease termed type II transmembrane serine proteases (TTSPs) was reported to cleave and activate influenza virus and coronavirus surface proteins, allowing multicycle replication in the absence of trypsin. As previously described, transmembrane protease serine 2 (TMPRSS2) and human airway trypsin-like protease (HAT) can facilitate the spread of human influenza viruses [22–25]. TMPRSS2 and TMPRSS4 play important roles in influenza virus replication, supporting the spread of influenza virus in the absence of trypsin [26]. Subsequent studies confirmed that TMPRSS2 also can activate the spike protein of human coronaviruses, such as severe acute respiratory syndrome coronavirus (SARS-CoV) [27–29] and Middle East respiratory syndrome coronavirus (MERS-CoV) [30,31]. Zmora et al. evaluated seven TTSPs previously reported to activate the surface proteins of influenza A viruses (FLUAVs), MERS-CoV, and SARS-CoV and found that mosaic serine protease large-form (MSPL) and differentially expressed squamous cell carcinoma gene 1 (DESC1) contributed to viral spread in the host [32]. Moreover, the role of TMPRSS2 in the release of PEDV from infected cells was clarified [33]. However, the effects of transmembrane serine proteases on host infection by animal coronaviruses, especially PEDV, have not been thoroughly studied thus far.

In this study, to explore the mechanism of PEDV infection, optimize culture methods, and improve the proliferation of PEDV in vitro, the TTSPs TMPRSS2, HAT, DESC1, and MSPL were assessed to determine their effects on PEDV replication in Vero cells. The results may provide a novel approach to propagating PEDV in vitro as well as potential therapeutic targets for controlling PEDV infection.

2. Materials and Methods

2.1. Plasmids and Primers

pDONR223 plasmids containing the TMPRSS2 gene (BC051839), HAT gene (BC125195), DESC1 gene (BC113412), and MSPL gene (BC114928) were kindly provided by Biogot Technology, Public Protein/Plasmid Library, Nanjing, China. Recombinant pCMV-Myc plasmids expressing human TMPRSS2, HAT, DESC1, or MSPL were constructed following gene amplification and digestion by EcoRI and BglII. All polymerase chain reaction (PCR) primers used in this study are listed in Table 1.

Table 1. Primers used in the study.

Primers	Primer Sequence (5′→3′)	Targets (ID)
Primers for the construction of TTSPs plasmids		
TMPRSS2-F	CCGGAATTCGGATGGCTTTGAACTCAGGG	TMPRSS2
TMPRSS2-R	GGAAGATCTTTAGCCGTCTGCCCTCAT	(BC051839)
HAT-F	CCGGAATTCGGATGTATAGGCCAGCACG	HAT
HAT-R	GGAAGATCTCTAGATCCCAGTTTGTTG	(BC125195)
DESC1-F	CCGGAATTCGGATGATGTATCGGCCAGATG	DESC1
DESC1-R	GGAAGATCTTTAGATACCAGTTTTTG	(BC113412)
MSPL-F	CCGGAATTCGGATGGAGAGGGACAGCC	MSPL
MSPL-R	GGAAGATCTTTAGGATTTTCTGAATCG	(BC114928)
Primers for identification of PEDV by real-time PCR		
PN-F	ACTGAGGGTGTTTTCTGGGTTGC	Nucleocapsid gene of PEDV
PN-R	GGTTCAACAATCTCAACTACACTGG	(DQ072726)
Beta-actin-F	AAGGATTCATATGTGGGCGATG	β-actin gene of Vero cells
Beta-actin-R	TCTCCATGTCGTCCCAGTTGGT	(AB004047)
Primers for identification of swine TTSPs mRNA by real-time PCR		
sw-TMPRSS2-F	CACCCGAACTATGACCCCAAGACC	Swine-TMPRSS2
sw-TMPRSS2-R	CATAGCGGCGTTCAGCACCTC	(XM_013982601)
sw-HAT-F	ACAACGCACAATAACTCCCTCTG	Swine-HAT
sw-HAT-R	GACATTGTTCTGTTGAAGGCTGG	(XM_013978756)
sw-DESC1-F	TGCTGCTGATTTTTAGATTTCGCTC	Swine-DESC1
sw-DESC1-R	AGGGGGTCCTACAGCATCTTG	(XM_013978755)
sw-MSPL-F	CCCATAAGTGGCTTCCCGTC	Swine-MSPL
sw-MSPL-R	TGTAGATGCTCTCCTGGATGGTG	(XM_013989517)
sw-GAPDH-F	AAGGTCGGAGTGAACGGATTTG	Swine-GAPDH
sw-GAPDH-R	GCCTTGACTGTGCCGTGGAAC	(XM_013991162)
Primers for identification of TTSPs in Vero cells		
m-TMPRSS2-F	ACCGCCAGGTGTTGGACCTTAC	m-TMPRSS2
m-TMPRSS2-R	GACACGCCATCGCACCAGTTAG	(XM_007968781)
m-HAT-F	AGTGTGTGTCTCCCAGCTGCTAC	m-HAT
m-HAT-R	TCGGTAGGTTGTCACTCGGGTAT	(XM_007998573)
m-DESC1-F	GGTGGAACAGAAGTAGAAGAGGG	m-DESC1
m-DESC1-R	CACATCACCTGGGTGAAACTC	(XM_007998564)
m-MSPL-F	TGACCCTGTCCGCTCACATCCAC	m-MSPL
m-MSPL-R	AAATCGCACCTCACTCTCCATCTTG	(XM_008021030)

2.2. Cell and Virus Culture

The swine intestinal epithelial cell (IEC) line [34–37] and Vero cells (ATCC, Manassas, VA, USA) were cultured in Dulbecco's modified Eagle medium (DMEM; Gibco, Grand Island, NY, USA) containing 10% fetal calf serum (FCS; Gibco). Cell-adapted PEDV strain LJB/03 from our laboratory [38–40] was propagated in Vero cells and IECs. Briefly, the confluent cell monolayer was washed once with sterile phosphate-buffered saline (PBS) and incubated at 37 °C for 1 h with PEDV LJB/03 supplemented with 21 μg/mL trypsin; then, the inoculum was removed, the cells were washed twice with PBS, and the maintenance medium (DMEM) was supplemented with 5 μg/mL trypsin. Cell cultures were harvested until the cytopathic effect (CPE) exceeded 80%. After freeze-thaw treatment, the supernatants were collected and stored at −80 °C until required.

2.3. Expression of TTSPs in Transfected Vero Cells

Vero cells were transfected with pCMV-Myc expressing TMPRSS2, HAT, DESC1, or MSPL, using Lipofectamine LTX & Plus Reagent (Invitrogen, Life Technologies, Carlsbad, CA, USA). Then, 3 μg/well of recombinant plasmid DNA was diluted into 500 μL of Opi-MEM I reduced-serum medium (Gibco) without serum and mixed with an equal volume of PLUS reagent gently. The mixture was incubated at room temperature (RT; 20–25 °C) for 5 min. Lipofectamine LTX was added, and the complexes were allowed to form by incubation for 30 min. The DNA-Lipofectamine LTX complexes

were then added to each well containing cells and medium. In parallel, Vero cells transfected with the same concentration of empty plasmid were used as a control. Post-transfection cells were cultured in 6-well plates at a density of 1.5×10^5/well and cultivated for 48 h. For analysis of TTSP expression by immunofluorescence, cells were washed three times with PBS and fixed with 4% paraformaldehyde at RT for 15 min; then, the cells were permeabilized with 0.2% Triton X-100 in PBS at RT for 10 min and blocked in PBS with 0.3% bovine serum albumin at 37 °C for 30 min. Subsequently, the cells were treated with mouse anti-Myc antibody (Sigma, St. Louis, MO, USA) and rhodamine Red-X-coupled anti-mouse (ZSGB-BIO, Beijing, China) as primary and secondary antibodies, respectively, followed by counterstaining with 4′,6-diamidino-2-phenylindole (DAPI, Beyotime, Shanghai, China). Then, a fluorescence microscope (Leica, Wetzlar, Germany) was used to visualize staining. For analysis of TTSP expression by western blot, cells were washed with PBS, and detached with 200 μL of cell lysis buffer (Beyotime) containing 1 mM phenylmethanesulfonyl fluoride (PMSF; Beyotime). Cells were subjected to sonication, mixed with 5× sodium dodecyl sulfate (SDS) loading buffer, and denatured in boiling water for 10 min. Following SDS-polyacrylamide gel electrophoresis (SDS-PAGE), proteins were transferred to a polyvinylidene fluoride membrane (Merck Millipore, Darmstadt, Germany), and immunoblots were developed using mouse anti-Myc antibody (Sigma) as the primary antibody and horseradish peroxidase (HRP)-conjugated goat anti-mouse antibody (Thermo, Waltham, MA, USA) as the secondary antibody. As a loading control, mouse anti-actin antibody (Sigma) was used. For analysis of TTSPs by flow cytometry, Vero cells transfected with TTSP-encoding plasmid were detached, washed with PBS, incubated with ice-cold ethanol for 10 min, and then stained with mouse anti-Myc primary antibodies (Sigma) followed by DyLight 647-coupled anti-mouse secondary antibodies (Dianova, BioLeaf Biotech, Shanghai, China). After three washings with PBS, cells were fixed with 2% paraformaldehyde and staining was analyzed with an Aria II flow cytometer (BD Biosciences, San Jose, CA, USA).

2.4. Quantitative Real-Time PCR Analysis

The viral RNA of PEDV propagated in Vero cells was extracted using E.Z.N.A. Total RNA Kit I (Omega Bio-Tek, Doraville, GA, USA) following the manufacturer's protocol. Complementary DNA (cDNA) was produced via reverse transcription, using oligo(dT)$_{15}$ (Takara, Tokyo, Japan) and the Superscript Reverse Transcriptase Reagent Kit (Takara) according to the manufacturer's instructions. Then, an ABI 7500 real-time PCR system (Applied Biosystems, Carlsbad, CA, USA) was used to determine viral mRNA transcript levels with SYBR Premix EX Taq II (Takara) according to the manufacturer's recommendations. The specific real-time PCR primers targeting the *N* gene of PEDV and the β-actin gene of Vero cells are described in Table 1. Real-time PCR was performed under the following conditions: 40 cycles of 30 s at 95 °C, 3 s at 95 °C, and 30 s at 60 °C. The average cycle threshold (Ct) for each individual assay was calculated from triplicate measurements using the instrument's software in "auto Ct" mode (ABI 7500 system software, version 2.3). Relative Ct values of three independent tests were calculated by the $2^{-\Delta\Delta Ct}$ method. Levels of *N* transcripts were normalized to those of β-actin transcripts in the same sample, and the $2^{-\Delta\Delta Ct}$ value of viral RNA in each sample was analyzed in parallel. There were no specific signals detected in any negative controls.

2.5. Determination of Viral Titer of PEDV Propagated in Vero Cells Expressing TTSPs

Prior to investigating the infectivity of PEDV LJB/03 propagated in Vero cells transiently expressing TTSPs, the viral titer was determined by plaque assay. In brief, after digestion, suspended Vero cells were transfected with 3 μg/well of pCMV-Myc plasmids expressing TMPRSS2, HAT, DESC1, or MSPL, with the empty pCMV-Myc plasmid used as a control. Then, the Vero cells were seeded into 6-well plates at 1.5×10^5/well, and after 24 h, the cells were infected at a multiplicity of infection (MOI) of 0.1 in an infection medium with 3 μg/mL trypsin or PBS. After 1 h of viral adsorption, the inoculum was removed, and the cells were washed twice with PBS and fixed with 3 mL of Minimum Essential Medium (MEM, Gibco) with 0.8% agarose. When CPEs appeared, cells were

stained with MEM containing 0.01% Neutral Red Solution (Sigma), and syncytia were counted as plaque under a microscope. The viral titer is expressed as plaque-forming units (PFU)/mL.

2.6. Determination of Effects of TTSPs and TTSP Inhibitor on Viral Replication

To analyze the effects of TTSPs on viral replication, the replication kinetics of intracellular viral RNA were determined by quantitative real-time PCR. Vero cells were transfected with 1 μg/well of pCMV-Myc plasmids expressing a TTSP (TMPRSS2, HAT, DESC1, or MSPL) or empty pCMV-Myc plasmid (control) and seeded in 24-well plates. Then, the cells were infected with PEDV at a multiplicity of infection (MOI) of 0.01 and supplemented with 3 μg/mL trypsin or PBS. After viral adsorption, the cells were washed twice with PBS and cultured with DMEM. At different time points post-infection, the cells were collected and subjected to quantitative real-time PCR detection as described above. To examine the viral replication in Vero cells treated with a TTSP inhibitor, TTSP-transfected Vero cells were pretreated with 200 μM or 500 μM of the TTSP inhibitor AEBSF-HCl (Sigma) or PBS for 1 h, as previously published [41]. Then, the treated cells were infected with PEDV LJB/03 at an MOI of 0.01 for 1 h; at 12 h post-infection, levels of viral replication were determined by quantitative real-time PCR.

2.7. Analysis of PEDV and TTSP Co-Localization

To determine the cellular localization of the S protein of PEDV and the TTSPs, Vero cells were transfected with pCMV-Myc plasmids expressing TMPRSS2, HAT, DESC1, or MSPL, or with empty plasmid serving as a negative control. At 24 h post-transfection, the cells were washed with PBS and infected with PEDV LJB/03 at an MOI of 1. The pCMV-Myc-transfected cells were infected with PEDV in the absence or presence of 3 μg/mL trypsin. At 24 h post-infection, the cells were fixed with 4% paraformaldehyde, permeabilized with 0.2% Triton X-100, and blocked with 0.3% bovine serum albumin. Then, the cells were incubated with mouse anti-Myc antibody (Sigma) and rabbit anti-PEDV S protein polyclonal antibody (developed in our laboratory) at RT for 1 h. After washing with PBS three times, the cells were incubated with fluorescein isothiocyanate (FITC)-conjugated goat anti-rabbit IgG (ZSGB-BIO) and Alexa Fluor 647-labeled goat anti-mouse IgG (H + L) (ZSGB-BIO) secondary antibodies at RT for 1 h. After washing, the cells were treated with DAPI (Beyotime). The coverslips were mounted on glass microscope slides in mounting buffer and examined using a laser scanning microscope (Leica TCS SP2, Wetzlar, Germany). Further image analysis, including calculation of the Pearson correlation coefficient (PCC), was performed with Image J with Just Another Colocalization Plugin [32,42].

2.8. Cleavage of PEDV S Protein by TTSPs

To determine the cleavability of S protein by TTSPs, PEDV strain LJB/03 S protein was cloned into plasmid pCMV-HA. Then, 293T cells were seeded into six-well plates at a density of 2×10^5/well and cotransfected with 2 μg/well of plasmid encoding PEDV S with a N-terminal HA tag and 2 μg/well TTSPs-expressing plasmid or an empty plasmid by using Lipofectamine LTX & Plus Reagent (Invitrogen) according to the manufacturer's protocol. At 48 h posttransfection, the cells were harvested and subjected to sonication and denatured. The lysates were separated by SDS-PAGE and blotted onto polyvinylidene fluoride membrane (Merck Millipore). The PEDV S protein with a N-terminal HA antigenic tag was detected by staining with mouse monoclonal antibody specific for the HA tag (Sigma), followed by incubation with an HRP-conjugated goat anti-mouse antibody (Thermo). As a loading control, expression of β-actin was detected with an anti-β-actin antibody (Sigma).

2.9. Analysis of TTSP Activation of PEDV for Cell–Cell Fusion

To determine the effects of TTSPs on PEDV for cell-cell fusion, the CheckMate Mammalian Two-Hybrid System (Promega, Madison, WI, USA) was used. In brief, Vero target cells were transfected with either empty pCMV-Myc plasmid or pCMV-Myc plasmids encoding TTSPs in combination with the pG5-luc plasmid, which carries the firefly luciferase reporter gene under the control of a promoter

containing five GAL4-binding sites. In parallel, Vero effector cells were transfected with the plasmids pACT (containing the herpes simplex virus VP16 activation domain upstream of a multiple cloning region) and pBind (expressing Renilla reniformis luciferase under the control of the SV40 promoter). After 24 h, the effector cells were detached, diluted in fresh medium, and added to the target cells. After 24 h of co-cultivation, the cells were washed with PBS and infected with PEDV LJB/03 at an MOI of 1 and supplemented with 1 μg/mL or 0.1 μg/mL trypsin or PBS. Cell–cell fusion was quantified by determining luciferase activity in cell lysates with a commercially available kit (Promega) after 48 h of co-cultivation.

2.10. Quantitative Analysis of TTSP Expression in the Normal and PEDV-Infected Piglet Small Intestine/IECs

Total RNA samples obtained from small intestine tissues of three normal and three PEDV-infected piglets were used to quantify gene expression levels of TTSPs. cDNA was produced using Superscript Reverse Transcriptase Reagent Kit (Takara) according to the manufacturer's instructions, and a quantitative real-time PCR assay was performed in triplicate with SYBR® Premix EX Taq II (Takara) using the *GAPDH* gene as a control. The primers used are shown in Table 1. Average Ct values calculated for *TMPRSS2*, *HAT*, *DESC1,* and *MSPL* were normalized by subtraction from the Ct values obtained for *GAPDH* as an internal control. Template-free cDNA reaction mixtures were analyzed in parallel, and no specific signal was detected in any of these experiments. The piglets were handled and maintained under strict ethical considerations according to international recommendations for animal welfare. In addition, the TTSP expression levels in the normal IECs and PEDV-infected IECs were also subjected to quantitative real-time PCR detection as described above.

2.11. Adaptation of PEDV Isolated from Clinical Samples to Vero Cells Transiently Expressing TTSPs

To analyze the adaptation of PEDV strains isolated from clinical samples to Vero cells transfected with pCMV-Myc plasmids expressing TTSPs, two PEDV-positive small intestine tissue samples (A and B) collected from outbreaks of severe acute diarrhea in suckling piglets in 2013 and 2014 in China were tested. Twenty-four hours after transfection with plasmids expressing TTSPs or empty plasmid (control), Vero cells were infected with processed viral samples supplemented with PBS or 3 μg/mL trypsin for 72 h. Following three serial passages, total RNA was extracted to assess the relative RNA levels of PEDV by qPCR.

2.12. Statistical Analysis

All experiments were repeated 3–5 times. Data were statistically analyzed by one-way ANOVA, using GraphPad Prism v5.0 software. $p < 0.05$ was considered statistically significant.

3. Results

3.1. Expression of TTSPs in Transfected Vero Cells

The genes encoding TMPRSS2, HAT, DESC1, and MSPL were cloned into pCMV-Myc plasmids and transfected to Vero cells individually. Expression of the four TTSPs in transfected Vero cells was detected via indirect immunofluorescence, western blot assay and fluorescence-activated cell sorting (FACS). As shown in Figure 1A,B, the four TTSPs were successfully expressed in Vero cells transiently transfected with pCMV-Myc plasmids expressing TMPRSS2, HAT, DESC1, or MSPL. TTSPs were expressed at the cellular plasma membrane, and the number of HAT-positive cells was lower than that for the other three TTSP-positive cells (Figure 1A). The expression of most proteases was readily detectable with the proper predicted size for each, as previously published [32], but the proteases were not expressed in Vero cells transfected with empty pCMV-Myc plasmid (Figure 1B). TTSPs are synthesized as inactive single-chain zymogens and undergo self-cleavage into active forms during or after transport to cell surfaces [43,44]. DESC1 and MSPL were found to be activated and to form bands presenting the cleaved catalytic domain of mature forms. Moreover, we analyzed TTSP

expression levels by fluorescence-activated cell sorting (FACS) of stained cells. The most prominent signal was measured in TMPRSS2-expressing cells, followed by MSPL- and DESC1-expressing cells. The fluorescence signal obtained from HAT-expressing cells was the weakest (Figure 1C).

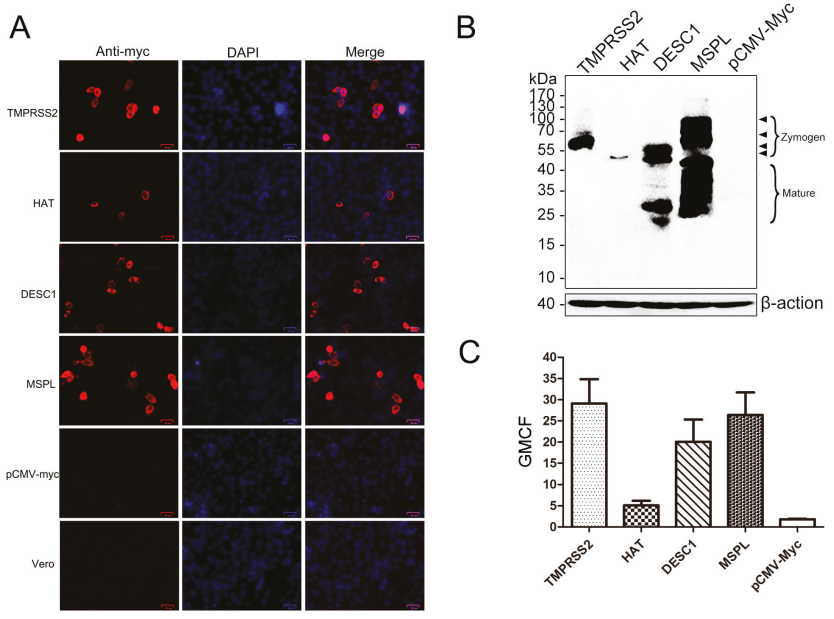

Figure 1. Expression of type II transmembrane serine proteases (TTSPs) in transfected Vero cells. (**A**) Post-transfection, the expression of TMPRSS2, HAT, DESC1, and MSPL in transfected Vero cells was detected via indirect immunofluorescence. Bar = 25 μm. Magnification, ×200; (**B**) TTSP expression in transfected Vero cells as determined by western blot. Zymogens and the mature form are indicated; (**C**) TTSPs expression was detected by FACS. The geometric mean channel fluorescence (GMCF) measured in a representative experiment performed with triplicate samples is shown. Error bars indicate standard deviations of three independent experiments.

3.2. Effects of TTSPs and TTSP Inhibitor on Viral Replication

Prior to this investigation, the presence of endogenously expressed TTSPs in Vero cells was analyzed by RT-PCR assay with primers targeting monkey-borne TMPRSS2 (XM_007968781), HAT (XM_007998573), DESC1 (XM_007998564), and MSPL (XM_008021030) genes (Table 1). No *TMPRSS2*, *HAT*, *DESC1*, or *MSPL* mRNA was detected in the Vero cells in this study. Next, the effects of these proteases on PEDV replication in Vero cells exogenously expressing TTSPs were examined. Following transfection, Vero cells were infected with PEDV in the presence or absence of trypsin. As shown in Figure 2A, in the absence of trypsin, the viral titers of PEDV propagated in Vero cells transfected with pCMV-Myc expressing TMPRSS2 and MSPL were clearly higher than those of PEDV propagated in Vero cells expressing HAT and DESC1. Among the TTSPs, the viral titers in Vero cells expressing TMPRSS2 and MSPL were almost $10^{2.5}$ to $10^{4.5}$ times higher than those in the empty-plasmid group and even 3- to 30-fold higher than those in Vero cells cultured with trypsin (3 μg/mL). Moreover, the viral RNA levels in each group were determined by qPCR at different time points post-infection. As shown in Figure 2B, at 72 h post-infection, viral RNA levels in Vero cells expressing MSPL were significantly higher than those in the other groups, and the viral mRNA relative quantity in trypsin-treated cells was slightly higher than that in TMPRSS2-transfected cells. However, the efficacy of TMPRSS2 in activating PEDV replication was almost the same as that of 3 μg/mL trypsin and was higher than that of HAT or

DESC1 at 84 h post-infection. These findings indicate that MSPL and TMPRSS2 play important roles in PEDV infection.

Furthermore, the TTSP inhibitor AEBSF-HCl was used to evaluate the effects of TTSPs on trypsin-independent PEDV entry. The cytotoxicity of AEBSF-HCl at the recommended concentrations was first tested to exclude cytotoxic effects. Then, TTSP-transfected Vero cells were treated with AEBSF-HCl and infected with PEDV. The pCMV-Myc-transfected cells were infected with PEDV in the absence of trypsin. At 12 h post-infection, viral RNA levels were determined by qPCR. As shown in Figure 2C, AEBSF-HCl induced strong inhibitory activity, resulting in dose-dependent decreases in the viral RNA levels. The viral RNA levels of PEDV in MSPL-transfected Vero cells treated with 500 μM AEBSF-HCl were significantly higher than those of cells transfected with other TTSPs. These results also indicate that TTSPs such as TMPRSS2 and MSPL play an important role in PEDV entry, suggesting that TMPRSS2 and MSPL promote PEDV replication better than trypsin.

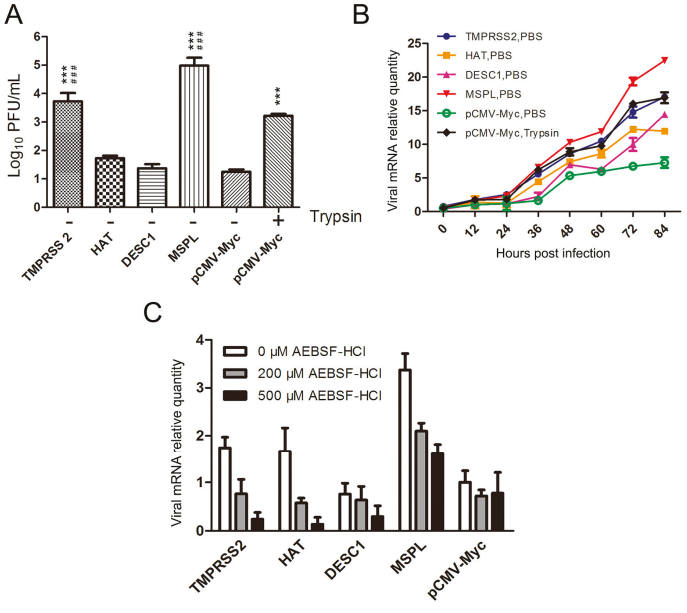

Figure 2. Effects of TTSPs and TTSP inhibitor on viral replication. (**A**) Porcine epidemic diarrhea virus (PEDV) titers following the expression of TTSPs in Vero cells. Viral titers were determined by plaque assay. *** $p < 0.001$ vs. empty pCMV-Myc plasmid; ### $p < 0.001$ vs. empty pCMV-Myc plasmid with 3 μg/mL trypsin; (**B**) Replication kinetics of intracellular viral RNA in Vero cells expressing TTSPs. Relative quantity of the empty pCMV-Myc plasmid with PBS at 0 h = 1; (**C**) Viral replication after TTSP inhibitor treatment. Error bars indicate the standard error of three independent experiments. The relative quantity of the empty pCMV-Myc plasmid with 0 μM AEBSF-HCl treatment = 1.

3.3. TTSP Activation of PEDV for Cell–Cell Fusion

We evaluated the impact of TTSP expression on PEDV-infected Vero cells, using a cell–cell fusion assay (Figure 3). Among the four TTSPs, the expression of MSPL and TMPRSS2 in Vero target cells significantly promoted fusion with Vero effector cells following PEDV infection; in particular, MSPL facilitated cell fusion better than 1 μg/mL trypsin treatment. In contrast, transfection with HAT and DESC1 did not promote cell–cell fusion that was observed with the empty plasmid control. These results indicate that MSPL and TMPRSS2 facilitate PEDV replication.

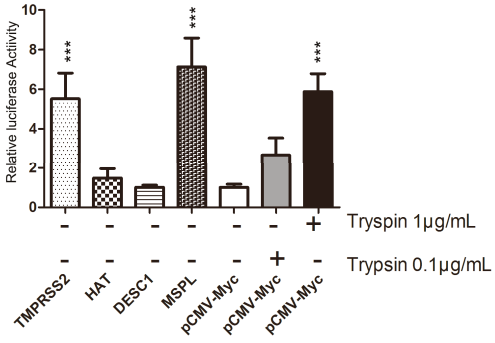

Figure 3. TMPRSS2 and MSPL activation of PEDV for cell–cell fusion. The results of a representative experiment performed with triplicate samples are shown; *** $p < 0.001$ vs. pCMV-Myc without trypsin. Relative quantity of pCMV-Myc without trypsin = 1. Error bars indicate standard error of the mean.

3.4. Co-Localization of TTSPs and PEDV

In this study, the co-localization of the four TTSPs with the PEDV S protein was investigated in infected Vero cells to determine the mechanism of PEDV activation by TTSPs. As shown in Figure 4A, immunofluorescence staining of TTSP-transfected Vero cells infected with PEDV revealed that the PEDV S protein was extensively co-localized with MSPL and TMPRSS2 but not with HAT or DESC1. This assessment was confirmed upon determination of the PCC for TTSPs and S protein signals. The S signals correlated well with those of TMPRSS2 and MSPL, indicating extensive co-localization, whereas little correlation was measured for the S protein and HAT or DESC1 signals (Figure 4B). Thus, the cellular localizations of S protein and TMPRSS2 or MSPL overlap extensively, indicating that MSPL and TMPRSS2 may interact with S protein, activating PEDV replication in Vero cells.

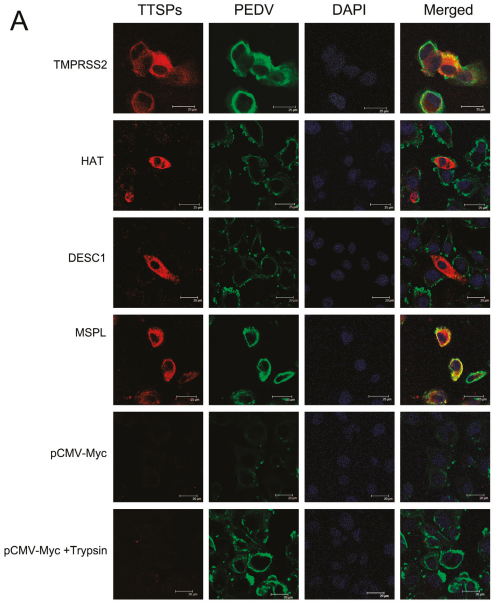

Figure 4. *Cont.*

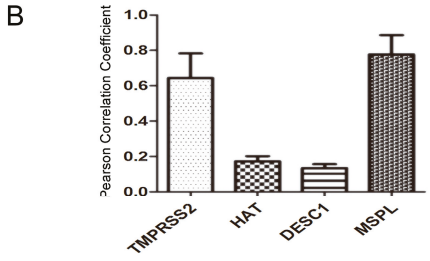

Figure 4. Analysis of TTSP and PEDV S protein co-localization. (**A**) Analysis of TTSP and PEDV S protein co-localization using a laser scanning microscope. Bar = 20–25 μm. Magnification, ×400; (**B**) The co-localization of TTSPs and S protein was determined by calculation of Pearson correlation coefficient (PCC). The average PCC measured for three to five cells from separate experiments is shown; error bars indicate the standard errors of the means.

3.5. Effects of TTSPs on PEDV S Protein Cleavage

We further assessed if the TTSPs studied were able to cleave the S protein of PEDV. As shown in Figure 5, the full-length PEDV S proteins migrating at 200 kDa were detected using anti-HA antibody reacting with the N-terminal of the PEDV S protein. Cleavage of PEDV S was detected upon the coexpression of TMPRSS2 and MSPL. The size of cleavage fragments were the same, approximately 35 kDa. In contrast, coexpressing of HAT or DESC1 did not facilitate PEDV S cleavage. Shirato et al. found that PEDV S protein could be cleaved by co-expression with TMPRSS2, the cleavage C-terminal fraction of S protein detected was 160 kDa [33]. Therefore, our study further confirmed the roles of TMPRSS2 and MSPL in the PEDV S protein activation. The effects of TMPRSS2 and MSPL on PEDV S protein cleavage may be responsible for facilitating the replication of PEDV.

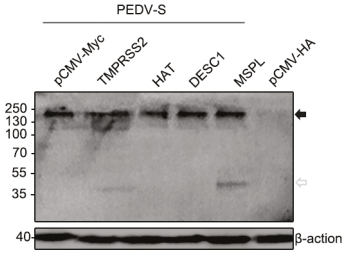

Figure 5. TMPRSS2 and MSPL cleave the PEDV S protein. Black-filled arrowheads, uncleaved S protein; white-filled arrowheads, N-terminal cleavage fragments.

3.6. Determination of TTSP Expression in the Normal and PEDV-Infected Piglet Small Intestine/IECs

We performed real-time RT-PCR analysis of the mRNA levels of TMPRSS2, HAT, DESC1, and MSPL in the small intestine tissues of normal and PEDV-infected piglets. The expression of DESC1 in the normal piglets was the highest, followed by HAT, TMPRSS2, and MSPL; moreover, the mRNA levels of all TTSPs increased in the small intestine of PEDV-infected piglets (Figure 6A). We also detected the TTSP level in IECs after PEDV infection. The endogenous TTSP level is up-regulated in IECs after PEDV infection, which was similar to that in piglet small intestine tissues infected with PEDV (Figure 6B). These results suggest that TMPRSS2, MSPL, HAT and to a higher degree, DESC1 are expressed in piglet small intestine, and that the endogenous TTSP level is up-regulated after PEDV infection. However, whether the endogenous presence of TTSPs in the small intestines of piglets contributes to viral spread in infected piglets remains to be determined.

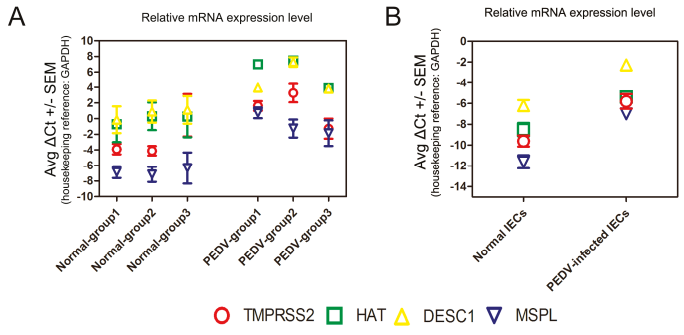

Figure 6. Expression of TTSPs in the normal and PEDV-infected porcine small intestine/intestinal epithelial cells (IECs). (**A**) Expression of TTSPs in the normal and PEDV-infected porcine small intestine; (**B**) Expression of TTSPs in the normal and PEDV-infected IECs.

3.7. TTSPs Facilitate Propagation of PEDV Isolates in Vero Cells

Two PEDV-positive piglet small intestine samples were used to test the abilities of TMPRSS2, HAT, DESC1, and MSPL to facilitate PEDV. TTSP-transfected Vero cells were infected with processed viral samples, and the relative RNA levels of PEDV propagated in Vero cells expressing TMPRSS2, MSPL, HAT, or DESC1 were determined for three serial passages. As shown in Figure 7A, TMPRSS2 and MSPL facilitated strain A replication to an almost 20-fold higher extent than the TTSP control (pCMV-Myc group) after three serial passages. Additionally, HAT could also promote culture of strain A in Vero cells. We speculate that there may be an active site of HAT on the S protein of strain A. The effect of trypsin on the isolation of strain B was not significant. However, the effect of strain B cultured in Vero cells expressing TMPRSS2 and MSPL was better than trypsin treatment; the viral mRNA level in Vero cells expressing MSPL was two times higher than that of the trypsin group after three serial passages (Figure 7B). TMPRSS2 and MSPL facilitated the propagation of the two PEDV isolates (strains A and B) in Vero cells efficiently and steadily, suggesting a promising approach for PEDV propagation of clinical samples in the absence of trypsin treatment.

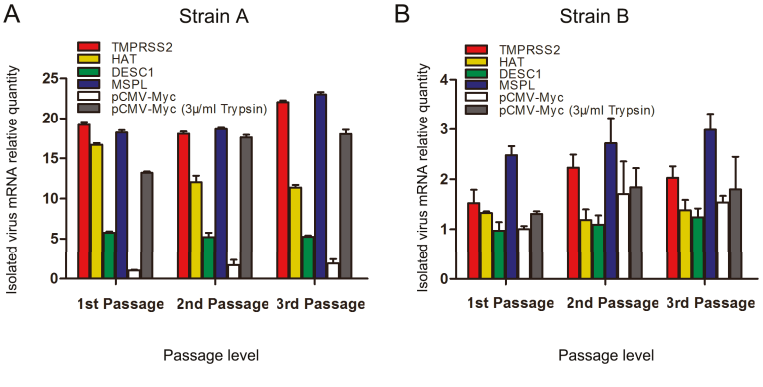

Figure 7. Culture of PEDV isolated from pig intestine in Vero cells transiently expressing TTSPs in three serial passages. (**A**) Isolation of PEDV strain A; (**B**) Isolation of PEDV strain B. The relative quantity of pCMV-Myc without trypsin at the 1st passage = 1. Error bars indicate standard error of the mean. Results shown are those of a representative experiment performed with triplicate samples.

4. Discussion

During the 1970s and 1990s, PEDV caused widespread epidemics in multiple swine-producing countries in Europe [5,45–47]. Since then, severe outbreaks have emerged in a number of Asian countries, including Japan [48], China [49], South Korea [50], and Thailand [51]. Recently, PEDV has been spreading rapidly among swine farms in the United States, resulting in high piglet mortality in more than 32 states [52,53], and similar outbreaks have also been reported in Canada and Mexico [1,3,4,6]. Currently, severe PED is one of the most important diseases affecting pig farming in China [54]. However, the effectiveness of the CV777-based vaccine has been questioned because PED outbreaks have also occurred in vaccinated herds [55]. Therefore, there is an urgent need to improve the protective efficacy of vaccines and to develop new vaccines. However, PEDV isolation in vitro remains challenging, as the isolated virus may gradually lose infectivity upon continued passaging in cell cultures supplemented with trypsin [1]. Recently, we attempted to isolate PEDV from clinical samples, using porcine intestinal epithelial cells (IECs) and found that PEDV isolates were better adapted to growth in IECs than in Vero cells [34], indicating that some trypsin-like proteases present in the IECs facilitated the propagation of PEDV. Moreover, previous research has suggested that several TTSPs located in the mucosal epithelium play critical roles in viral infectivity through the activation of viral surface proteins [23,27,31,32]. At the beginning of this study, we designed primers according to the predicted sequences of swine TTSPs from national center for biotechnology information (NCBI), and attempted to amplify the full-length TTSP genes from the trachea, bronchus, lung, and small intestine tissues of piglet and IECs. However, we failed to obtain the porcine TTSP genes. We speculate that differences may exist between the actual sequences and predicted sequences. Although TTSPs are the host proteases of respiratory and digestive tract mucosa, the TTSP expression levels may be low or limited in some conditions or over a period of time, which results in difficulty in obtaining actual porcine TTSP genes. Therefore, we studied human TTSPs (TMPRSS2, HAT, DESC1, and MSPL) to explore their effects on PEDV replication.

The TTSP family is composed of more than 20 members and divided into four subfamilies: the HAT/DESC subfamily, hepsin/TMPRSS/enteropeptidase subfamily (including TMPRSS2 and MSPL), matriptase subfamily, and corin subfamily. TMPRSS2 and MSPL are predominantly expressed in the fetal liver and kidney [56] and on the brush-border of the duodenum [57]. HAT is predominantly expressed in the trachea [58,59], whereas DESC1 is restricted to the epithelia of the skin and oral cavity [60,61]. In this study, we confirmed the presence of TMPRSS2, HAT, DESC1, and MSPL in the small intestines of normal piglets and IECs, and we also found that the mRNA levels of these TTSPs increased in PEDV-infected small intestine tissues and IECs. Whether or not the endogenous presence of TTSPs in the small intestines of piglets contributes to viral spread in infected piglets remains to be determined, and knock-out mice, as well as specific protease inhibitors, might be useful tools for these endeavors. Previous studies demonstrated that TTSPs play key roles in hormone or growth factor activation, epithelial differentiation, and the initiation of proteolytic cascades [62,63]. The mechanism underlying the effects of up-regulated TTSPs in PEDV-infected piglet small intestine tissues requires further investigation. The inhibitors of TMPRSS2 and MSPL may be potential candidates for treatment of PEDV. Moreover, according to a comparison of the promotion effects of these TTSPs on viral replication and titers in vitro, TMPRSS2 and MSPL were particularly strong, suggesting that members of the hepsin/TMPRSS/enteropeptidase subfamily may activate PEDV emergence due to their specific structure. Additional research is underway to determine whether other members of the hepsin/TMPRSS/enteropeptidase subfamily are able to activate PEDV.

The role of TTSPs in the release of PEDV from infected cells has been reported previously [33], although the mechanism by which TTSPs promote the propagation of animal coronaviruses remains unclear. In this study, to explore this mechanism, we first focused on whether TTSPs (TMPRSS2, HAT, DESC1, and MSPL) activated viral transmission via cell–cell fusion assay, and our results demonstrated that the activating effects of MSPL and TMPRSS2 were more robust than those of the other TTSPs. MSPL exhibited the strongest effect followed by TMPRSS2. It has been suggested that the addition

of trypsin mediates cell–cell fusion in PEDV-infected cells [64], thus demonstrating that TMPRSS2 and MSPL exhibit trypsin-like characteristics that facilitate cell–cell fusion. However, it should be noted that the cell–cell fusion assay allows the interaction of cell surfaces on which large amounts of receptors and proteases may be expressed, and therefore it might not fully mirror virus–cell fusion.

Although serine proteases are reportedly involved in PEDV entry, it was previously unclear which of them are most effective [41]. Thus, we used the previously published TTSP inhibitor AEBSF-HCl [41] to assess whether TTSPs (TMPRSS2, HAT, DESC1, and MSPL) activate PEDV entry into cells in the absence of trypsin. We found that viral RNA levels were decreased in a dose-dependent manner following AEBSF-HCl treatment. Additionally, we found that the level of viral mRNA increased in a dose-dependent manner in Vero cells expressing TMPRSS2 and MSPL, but not HAT and DESC1 at the stage of virus entry [65]. These results suggest that the activating effect of TMPRSS2 and, in particular, MSPL, on PEDV entry into cells was greater than that of HAT and DESC1. Although Liu et al. found that TMPRSS2 did not increase the entry of PEDV pseudoviruses into Huh-7 cells [66], several studies suggested that some candidate cellular enzymes, such as TTSPs could activate PEDV replication [41,64], and that human TMPRSS2 has been shown to enhance the multicycle replication of PEDV [33].

To explore the key role of TTSPs in facilitating PEDV replication, we speculated that the S protein of PEDV might have interacted with TTSPs located on the cell surface during viral infection. Thus, an assessment of the co-localization of TTSPs with the PEDV S protein was performed, and our results showed that the PEDV S protein co-localized extensively with MSPL and TMPRSS2, indicating that these TTSPs might interact with the PEDV S protein to promote viral entry into cells. It is worth noting that PEDV-activating TTSPs co-localized with S protein, whereas inactive TTSPs did not, despite robust expression (such as DESC1) in the cellular system analyzed. It is therefore conceivable that the cellular localization of a TTSP, apart from its substrate specificity, might determine whether the protease can activate S and other viral glycoproteins; this possibility deserves further investigation. It has been confirmed that TTSPs cleave and activate the SARS-CoV and MERS-CoV S proteins, and the cleaved fragments of the S protein may induce subtle conformational changes that increase its sensitivity for binding to its receptor [15]. We also attempted to verify the cleavage of S protein by TTSPs, and we found TMPRSS2 and MSPL could cleave PEDV S protein with the same size of cleavage fragments, but HAT and DESC1 could not. Therefore, our study further confirmed the roles of TMPRSS2 and MSPL in the PEDV S protein activation. However, the mechanisms of S protein activation by TTSPs for PEDV entry have not been clearly demonstrated, and additional research is under way to further investigate these mechanisms.

Currently, the propagation of PEDV in vitro remains a continuing challenge, as viral infectivity gradually declines during serial passages in cell cultures. In this study, we confirmed that TMPRSS2 and MSPL effectively facilitate the isolation of PEDV in vitro in the absence of trypsin. Viral adaptation and growth in Vero cells expressing TMPRSS2 and MSPL were higher than those in control cells transfected with empty plasmid control and in cells treated with trypsin. These results indicate that TMPRSS2 and MSPL might be more conducive to PEDV isolation in vitro than exogenous proteases like trypsin, suggesting a promising approach for PEDV isolation in vitro, using Vero cell lines continuously expressing TMPRSS2 or MSPL. The establishment of Vero cell lines stably expressing TMPRSS2/MSPL may facilitate the use of attenuated cell-culture-adapted PEDV strains cultured in the absence of trypsin for vaccine development, which can reduce the cost and simplify the process in the PEDV vaccine production.

In conclusion, we first demonstrated that TMPRSS2 and MSPL facilitate the replication of the animal coronavirus PEDV and play a significant role in viral infection by promoting cell–cell fusion and virus–cell fusion. Whether or not the endogenous presence of TTSPs in the small intestines of piglets contributes to viral spread in infected piglets should be determined further. This study provides insights and a novel method for enhancing viral titers, expanding virus production, and improving the adaptability of PEDV isolates in vitro.

Acknowledgments: This work was supported by the National Natural Science Foundation of China (grant 31472226), the National Key Research and Development Program of China (grant 2016YFD0500100) and the National Key Technology R&D Program of China (grant 2015BAD12B02-7). We thank the Biogot Technology, Public Protein/Plasmid Library for providing the plasmids encoding full-length human transmembrane proteases. We also thank Yandong Tang for providing the valuable suggestions to this study.

Author Contributions: Y.L. and Y.X. conceived and designed the study. W.S., W.F., J.B., Y.T., L.W., W.C. and Y.J. performed the experiments. L.T. and M.L. analyzed and interpreted the data. W.S. wrote the paper. All authors read and approved the manuscript.

Conflicts of Interest: The authors declare no conflict of interest.

References

1. Chen, Q.; Li, G.; Stasko, J.; Thomas, J.T.; Stensland, W.R.; Pillatzki, A.E.; Gauger, P.C.; Schwartz, K.J.; Madson, D.; Yoon, K.-J. Isolation and characterization of porcine epidemic diarrhea viruses associated with the 2013 disease outbreak among swine in the United States. *J. Clin. Microbiol.* **2014**, *52*, 234–243. [CrossRef] [PubMed]
2. Debouck, P.; Pensaert, M. Experimental infection of pigs with a new porcine enteric coronavirus, CV 777. *Am. J. Vet. Res.* **1980**, *41*, 219–223. [PubMed]
3. Kim, S.H.; Kim, I.J.; Pyo, H.M.; Tark, D.S.; Song, J.Y.; Hyun, B.H. Multiplex real-time RT-PCR for the simultaneous detection and quantification of transmissible gastroenteritis virus and porcine epidemic diarrhea virus. *J. Virol. Methods* **2007**, *146*, 172–177. [CrossRef] [PubMed]
4. Ojkic, D.; Hazlett, M.; Fairles, J.; Marom, A.; Slavic, D.; Maxie, G.; Alexandersen, S.; Pasick, J.; Alsop, J.; Burlatschenko, S. The first case of porcine epidemic diarrhea in Canada. *Can. Vet. J.* **2015**, *56*, 149–152. [PubMed]
5. Pensaert, M.B.; de Bouck, P. A new coronavirus-like particle associated with diarrhea in swine. *Arch. Virol.* **1978**, *58*, 243–247. [CrossRef] [PubMed]
6. Trujillo-Ortega, M.E.; Beltran-Figueroa, R.; Garcia-Hernandez, M.E.; Juarez-Ramirez, M.; Sotomayor-Gonzalez, A.; Hernandez-Villegas, E.N.; Becerra-Hernandez, J.F.; Sarmiento-Silva, R.E. Isolation and characterization of porcine epidemic diarrhea virus associated with the 2014 disease outbreak in Mexico: Case report. *BMC Vet. Res.* **2016**, *12*, 132. [CrossRef] [PubMed]
7. Wood, E.N. An apparently new syndrome of porcine epidemic diarrhoea. *Vet. Rec.* **1977**, *100*, 243–244. [CrossRef] [PubMed]
8. Oldham, J. Letter to the editor. *Pig Farming* **1972**, *10*, 72–73. [CrossRef]
9. Hofmann, M.; Wyler, R. Propagation of the virus of porcine epidemic diarrhea in cell culture. *J. Clin. Microbiol.* **1988**, *26*, 2235–2239. [PubMed]
10. Park, J.E.; Cruz, D.J.; Shin, H.J. Receptor-bound porcine epidemic diarrhea virus spike protein cleaved by trypsin induces membrane fusion. *Arch. Virol.* **2011**, *156*, 1749. [CrossRef] [PubMed]
11. Lai, M.M.; Cavanagh, D. The molecular biology of coronaviruses. *Adv. Virus Res.* **1997**, *48*, 1–100. [PubMed]
12. Bosch, B.J.; van der Zee, R.; de Haan, C.A.; Rottier, P.J. The coronavirus spike protein is a class I virus fusion protein: Structural and functional characterization of the fusion core complex. *J. Virol.* **2003**, *77*, 8801–8811. [CrossRef] [PubMed]
13. White, J.M.; Delos, S.E.; Brecher, M.; Schornberg, K. Structures and mechanisms of viral membrane fusion proteins: Multiple variations on a common theme. *Crit. Rev. Biochem. Mol.* **2008**, *43*, 189–219. [CrossRef] [PubMed]
14. Kawase, M.; Shirato, K.; Matsuyama, S.; Taguchi, F. Protease-mediated entry via the endosome of human coronavirus 229E. *J. Virol.* **2009**, *83*, 712–721. [CrossRef] [PubMed]
15. Matsuyama, S.; Taguchi, F. Two-step conformational changes in a coronavirus envelope glycoprotein mediated by receptor binding and proteolysis. *J. Virol.* **2009**, *83*, 11133–11141. [CrossRef] [PubMed]
16. Simmons, G.; Reeves, J.D.; Rennekamp, A.J.; Amberg, S.M.; Piefer, A.J.; Bates, P. Characterization of severe acute respiratory syndrome-associated coronavirus (SARS-CoV) spike glycoprotein-mediated viral entry. *Proc. Natl. Acad. Sci. USA* **2004**, *101*, 4240–4245. [CrossRef] [PubMed]
17. Spaan, W.; Cavanagh, D.; Horzinek, M.C. Coronaviruses: Structure and genome expression. *J. Gen. Virol.* **1988**, *69*, 2939–2952. [CrossRef] [PubMed]

18. Zamolodchikova, T.S. Serine proteases of small intestine mucos—Localization, functional properties, and physiological role. *Biochemistry* **2012**, *77*, 820–829. [PubMed]
19. Qiu, Z.; Hingley, S.T.; Simmons, G.; Yu, C.; Das Sarma, J.; Bates, P.; Weiss, S.R. Endosomal proteolysis by cathepsins is necessary for murine coronavirus mouse hepatitis virus type 2 spike-mediated entry. *J. Virol.* **2006**, *80*, 5768–5776. [CrossRef] [PubMed]
20. Yamada, Y.K.; Takimoto, K.; Yabe, M.; Taguchi, F. Acquired fusion activity of a murine coronavirus MHV-2 variant with mutations in the proteolytic cleavage site and the signal sequence of the S protein. *Virology* **1997**, *227*, 215–219. [CrossRef] [PubMed]
21. Yoshikura, H.; Tejima, S. Role of protease in mouse hepatitis virus-induced cell fusion. Studies with a cold-sensitive mutant isolated from a persistent infection. *Virology* **1981**, *113*, 503–511. [CrossRef]
22. Bottcher, E.; Matrosovich, T.; Beyerle, M.; Klenk, H.D.; Garten, W.; Matrosovich, M. Proteolytic activation of influenza viruses by serine proteases TMPRSS2 and HAT from human airway epithelium. *J. Virol.* **2006**, *80*, 9896–9898. [CrossRef] [PubMed]
23. Bottcher, E.; Freuer, C.; Steinmetzer, T.; Klenk, H.D.; Garten, W. MDCK cells that express proteases TMPRSS2 and HAT provide a cell system to propagate influenza viruses in the absence of trypsin and to study cleavage of HA and its inhibition. *Vaccine* **2009**, *27*, 6324–6329. [CrossRef] [PubMed]
24. Bottcher, E.; Freuer, C.; Sielaff, F.; Schmidt, S.; Eickmann, M.; Uhlendorff, J.; Steinmetzer, T.; Klenk, H.D.; Garten, W. Cleavage of influenza virus hemagglutinin by airway proteases TMPRSS2 and HAT differs in subcellular localization and susceptibility to protease inhibitors. *J. Virol.* **2010**, *84*, 5605–5614. [CrossRef] [PubMed]
25. Bertram, S.; Heurich, A.; Lavender, H.; Gierer, S.; Danisch, S.; Perin, P.; Lucas, J.M.; Nelson, P.S.; Pohlmann, S.; Soilleux, E.J. Influenza and SARS-coronavirus activating proteases TMPRSS2 and HAT are expressed at multiple sites in human respiratory and gastrointestinal tracts. *PLoS ONE* **2012**, *7*, e35876. [CrossRef] [PubMed]
26. Bertram, S.; Glowacka, I.; Blazejewska, P.; Soilleux, E.; Allen, P.; Danisch, S.; Steffen, I.; Choi, S.Y.; Park, Y.; Schneider, H.; et al. TMPRSS2 and TMPRSS4 facilitate trypsin-independent spread of influenza virus in Caco-2 cells. *J. Virol.* **2010**, *84*, 10016–10025. [CrossRef] [PubMed]
27. Glowacka, I.; Bertram, S.; Muller, M.A.; Allen, P.; Soilleux, E.; Pfefferle, S.; Steffen, I.; Tsegaye, T.S.; He, Y.; Gnirss, K.; et al. Evidence that TMPRSS2 activates the severe acute respiratory syndrome coronavirus spike protein for membrane fusion and reduces viral control by the humoral immune response. *J. Virol.* **2011**, *85*, 4122–4134. [CrossRef] [PubMed]
28. Matsuyama, S.; Nagata, N.; Shirato, K.; Kawase, M.; Takeda, M.; Taguchi, F. Efficient activation of the severe acute respiratory syndrome coronavirus spike protein by the transmembrane protease TMPRSS2. *J. Virol.* **2010**, *84*, 12658–12664. [CrossRef] [PubMed]
29. Shulla, A.; Heald-Sargent, T.; Subramanya, G.; Zhao, J.; Perlman, S.; Gallagher, T. A transmembrane serine protease is linked to the severe acute respiratory syndrome coronavirus receptor and activates virus entry. *J. Virol.* **2011**, *85*, 873–882. [CrossRef] [PubMed]
30. Gierer, S.; Bertram, S.; Kaup, F.; Wrensch, F.; Heurich, A.; Kramer-Kuhl, A.; Welsch, K.; Winkler, M.; Meyer, B.; Drosten, C.; et al. The spike protein of the emerging betacoronavirus EMC uses a novel coronavirus receptor for entry, can be activated by TMPRSS2, and is targeted by neutralizing antibodies. *J. Virol.* **2013**, *87*, 5502–5511. [CrossRef] [PubMed]
31. Shirato, K.; Kawase, M.; Matsuyama, S. Middle East respiratory syndrome coronavirus infection mediated by the transmembrane serine protease TMPRSS2. *J. Virol.* **2013**, *87*, 12552–12561. [CrossRef] [PubMed]
32. Zmora, P.; Blazejewska, P.; Moldenhauer, A.S.; Welsch, K.; Nehlmeier, I.; Wu, Q.; Schneider, H.; Pohlmann, S.; Bertram, S. DESC1 and MSPL activate influenza A viruses and emerging coronaviruses for host cell entry. *J. Virol.* **2014**, *88*, 12087–12097. [CrossRef] [PubMed]
33. Shirato, K.; Matsuyama, S.; Ujike, M.; Taguchi, F. Role of proteases in the release of porcine epidemic diarrhea virus from infected cells. *J. Virol.* **2011**, *85*, 7872–7880. [CrossRef] [PubMed]
34. Shi, W.; Jia, S.; Zhao, H.; Yin, J.; Wang, X.; Yu, M.; Ma, S.; Wu, Y.; Chen, Y.; Fan, W.; et al. Novel approach for isolation and identification of Porcine epidemic diarrhea virus (PEDV) strain NJ using porcine intestinal epithelial cells. *Viruses* **2017**, *9*, 19. [CrossRef] [PubMed]
35. Wang, J.; Hu, G.; Lin, Z.; He, L.; Xu, L.; Zhang, Y. Characteristic and functional analysis of a newly established porcine small intestinal epithelial cell line. *PLoS ONE* **2014**, *9*, e110916. [CrossRef] [PubMed]

36. Li, W.; Wang, G.; Liang, W.; Kang, K.; Guo, K.; Zhang, Y. Integrin beta3 is required in infection and proliferation of classical swine fever virus. *PLoS ONE* **2014**, *9*, e110911.
37. Xu, X.; Zhang, H.; Zhang, Q.; Dong, J.; Liang, Y.; Huang, Y.; Liu, H.J.; Tong, D. Porcine epidemic diarrhea virus E protein causes endoplasmic reticulum stress and up-regulates interleukin-8 expression. *Virol. J.* **2013**, *10*, 26. [CrossRef] [PubMed]
38. Junwei, G.; Baoxian, L.; Lijie, T.; Yijing, L. Cloning and sequence analysis of the N gene of porcine epidemic diarrhea virus LJB/03. *Virus Genes* **2006**, *33*, 215–219. [CrossRef] [PubMed]
39. Jinghui, F.; Yijing, L. Cloning and sequence analysis of the M gene of porcine epidemic diarrhea virus LJB/03. *Virus Genes* **2005**, *30*, 69–73. [CrossRef] [PubMed]
40. Mao, Y.Y.; Zhang, G.H.; Ge, J.W.; Jiang, Y.P.; Qiao, X.Y.; Cui, W.; Li, Y.J. Isolation and characteristics of virus culture of porcine epidemic diarrhea virus LJB/03. *Chin. J. Virol.* **2010**, *26*, 483–489.
41. Park, J.E.; Cruz, D.J.; Shin, H.J. Clathrin- and serine proteases-dependent uptake of porcine epidemic diarrhea virus into Vero cells. *Virus Res.* **2014**, *191*, 21–29. [CrossRef] [PubMed]
42. Bolte, S.; Cordelieres, F.P. A guided tour into subcellular colocalization analysis in light microscopy. *J. Microsc.-Oxf.* **2006**, *224*, 213–232. [CrossRef] [PubMed]
43. Afar, D.E.; Vivanco, I.; Hubert, R.S.; Kuo, J.; Chen, E.; Saffran, D.C.; Raitano, A.B.; Jakobovits, A. Catalytic cleavage of the androgen-regulated TMPRSS2 protease results in its secretion by prostate and prostate cancer epithelia. *Cancer Res.* **2001**, *61*, 1686–1692. [PubMed]
44. Miyake, Y.; Yasumoto, M.; Tsuzuki, S.; Fushiki, T.; Inouye, K. Activation of a membrane-bound serine protease matriptase on the cell surface. *J. Biochem.* **2009**, *146*, 273–282. [CrossRef] [PubMed]
45. Chasey, D.; Cartwright, S.F. Virus-like particles associated with porcine epidemic diarrhoea. *Res. Vet. Sci.* **1978**, *25*, 255–256. [PubMed]
46. Nagy, B.; Nagy, G.; Meder, M.; Mocsari, E. Enterotoxigenic *Escherichia coli*, rotavirus, porcine epidemic diarrhoea virus, adenovirus and calici-like virus in porcine postweaning diarrhoea in Hungary. *Acta Vet. Hung.* **1996**, *44*, 9–19. [PubMed]
47. Van Reeth, K.; Pensaert, M. Prevalence of infections with enzootic respiratory and enteric viruses in feeder pigs entering fattening herds. *Vet. Rec.* **1994**, *135*, 594–597. [PubMed]
48. Takahashi, K.; Okada, K.; Ohshima, K. An outbreak of swine diarrhea of a new-type associated with coronavirus-like particles in Japan. Nihon juigaku zasshi. *Jpn. J. Vet. Sci.* **1983**, *45*, 829–832. [CrossRef]
49. Xuan, H.; Xing, D.; Wang, D.; Zhu, W.; Zhao, F.; Gong, H. Study on the culture of porcine epidemic diarrhea virus adapted to fetal porcine intestine primary cell monolayer. *Chin. J. Vet. Sci.* **1984**, *4*, 202–208.
50. Kweon, C.H.; Kwon, B.J.; Jung, T.S.; Kee, Y.J.; Hur, D.H.; Hwang, E.K.; Rhee, J.C.; An, S.H. Isolation of porcine epidemic diarrhea virus (PEDV) in Korea. *Korean J. Vet. Res.* **1993**, *33*, 249–254.
51. Puranaveja, S.; Poolperm, P.; Lertwatcharasarakul, P.; Kesdaengsakonwut, S.; Boonsoongnern, A.; Urairong, K.; Kitikoon, P.; Choojai, P.; Kedkovid, R.; Teankum, K.; et al. Chinese-like strain of porcine epidemic diarrhea virus, Thailand. *Emerg. Infect. Dis.* **2009**, *15*, 1112–1115. [CrossRef] [PubMed]
52. Panel, E.A. Scientific Opinion on porcine epidemic diarrhoea and emerging pig deltacoronavirus. *EFSA J.* **2014**, *12*, 3877.
53. Song, D.; Moon, H.; Kang, B. Porcine epidemic diarrhea: A review of current epidemiology and available vaccines. *Clin. Exp. Vaccine Res.* **2015**, *4*, 166–176. [CrossRef] [PubMed]
54. Sun, R.Q.; Cai, R.J.; Chen, Y.Q.; Liang, P.S.; Chen, D.K.; Song, C.X. Outbreak of porcine epidemic diarrhea in suckling piglets, China. *Emerg. Infect. Dis.* **2012**, *18*, 161–163. [CrossRef] [PubMed]
55. Luo, Y.; Zhang, J.; Deng, X.; Ye, Y.; Liao, M.; Fan, H. Complete genome sequence of a highly prevalent isolate of porcine epidemic diarrhea virus in South China. *J. Virol.* **2012**, *86*, 9551. [CrossRef] [PubMed]
56. Dhanasekaran, S.M.; Barrette, T.R.; Ghosh, D.; Shah, R.; Varambally, S.; Kurachi, K.; Pienta, K.J.; Rubin, M.A.; Chinnaiyan, A.M. Delineation of prognostic biomarkers in prostate cancer. *Nature* **2001**, *412*, 822–826. [CrossRef] [PubMed]
57. Kitamoto, Y.; Yuan, X.; Wu, Q.; McCourt, D.W.; Sadler, J.E. Enterokinase, the initiator of intestinal digestion, is a mosaic protease composed of a distinctive assortment of domains. *Proc. Natl. Acad. Sci. USA* **1994**, *91*, 7588–7592. [CrossRef] [PubMed]
58. Yamaoka, K.; Masuda, K.I.; Ogawa, H.; Takagi, K.I.; Umemoto, N.; Yasuoka, S. Cloning and characterization of the cDNA for human airway trypsin-like protease. *J. Biol. Chem.* **1998**, *273*, 11895–11901. [CrossRef] [PubMed]

59. Yasuoka, S.; Ohnishi, T.; Kawano, S.; Tsuchihashi, S.; Ogawara, M.; Masuda, K.; Yamaoka, K.; Takahashi, M.; Sano, T. Purification, characterization, and localization of a novel trypsin-like protease found in the human airway. *Am. J. Respir. Cell Mol.* **1997**, *16*, 300–308. [CrossRef] [PubMed]
60. Hobson, J.P.; Netzel-Arnett, S.; Szabo, R.; Rehault, S.M.; Church, F.C.; Strickland, D.K.; Lawrence, D.A.; Antalis, T.M.; Bugge, T.H. Mouse DESC1 is located within a cluster of seven DESC1-like genes and encodes a type II transmembrane serine protease that forms serpin inhibitory complexes. *J. Biol. Chem.* **2004**, *279*, 46981–46994. [CrossRef] [PubMed]
61. Lang, J.C.; Schuller, D.E. Differential expression of a novel serine protease homologue in squamous cell carcinoma of the head and neck. *Br. J. Cancer* **2001**, *84*, 237–243. [CrossRef] [PubMed]
62. Bugge, T.H.; Antalis, T.M.; Wu, Q. Type II transmembrane serine proteases. *J. Biol. Chem.* **2009**, *284*, 23177–23181. [CrossRef] [PubMed]
63. Szabo, R.; Bugge, T.H. Membrane-anchored serine proteases in vertebrate cell and developmental biology. *Annu. Rev. Cell Dev. Biol.* **2011**, *27*, 213–235. [CrossRef] [PubMed]
64. Wicht, O.; Li, W.; Willems, L.; Meuleman, T.J.; Wubbolts, R.W.; van Kuppeveld, F.J.; Rottier, P.J.; Bosch, B.J. Proteolytic activation of the porcine epidemic diarrhea coronavirus spike fusion protein by trypsin in cell culture. *J. Virol.* **2014**, *88*, 7952–7961. [CrossRef] [PubMed]
65. Shi, W.; (Northeast Agricultural University, Harbin, China). TMPRSS2 and MSPL promote PEDV replication in a dose-dependent manner at the stage of virus entry. in preparations. 2017.
66. Liu, C.; Ma, Y.; Yang, Y.; Zheng, Y.; Shang, J.; Zhou, Y.; Jiang, S.; Du, L.; Li, J.; Li, F. Cell entry of porcine epidemic diarrhea coronavirus is activated by lysosomal proteases. *J. Biol. Chem.* **2016**, *291*, 24779–24786. [CrossRef] [PubMed]

© 2017 by the authors. Licensee MDPI, Basel, Switzerland. This article is an open access article distributed under the terms and conditions of the Creative Commons Attribution (CC BY) license (http://creativecommons.org/licenses/by/4.0/).

viruses

MDPI

Article

Novel Approach for Isolation and Identification of Porcine Epidemic Diarrhea Virus (PEDV) Strain NJ Using Porcine Intestinal Epithelial Cells

Wen Shi, Shuo Jia, Haiyuan Zhao, Jiyuan Yin, Xiaona Wang, Meiling Yu, Sunting Ma, Yang Wu, Ying Chen, Wenlu Fan, Yigang Xu * and Yijing Li *

College of Veterinary Medicine, Northeast Agricultural University, Harbin 150030, China; wenshi_china@163.com (W.S.); jiashuo0508@163.com (S.J.); zhywxn1925@163.com (H.Z.); neauyjy@126.com (J.Y.); xiaonawang0319@163.com (X.W.); yu19890130@126.com (M.Y.); masunting@163.com (S.M.); wuyang_neau@126.com (Y.W.); chenying_neau@163.com (Y.C.); fanwenlu1230@163.com (W.F.)

* Correspondence: yigangxu_china@sohu.com (Y.X.); yijingli@163.com (Y.L.); Tel.: +86-451-5519-0363 (Y.L.); Fax: +86-451-5519-0363 (Y.L.)

Academic Editors: Linda Dixon and Simon Graham
Received: 6 December 2016; Accepted: 17 January 2017; Published: 21 January 2017

Abstract: Porcine epidemic diarrhea virus (PEDV), which is the causative agent of porcine epidemic diarrhea in China and other countries, is responsible for serious economic losses in the pork industry. Inactivated PEDV vaccine plays a key role in controlling the prevalence of PEDV. However, consistently low viral titers are obtained during the propagation of PEDV in vitro; this represents a challenge to molecular analyses of the virus and vaccine development. In this study, we successfully isolated a PEDV isolate (strain NJ) from clinical samples collected during a recent outbreak of diarrhea in piglets in China, using porcine intestinal epithelial cells (IEC). We found that the isolate was better adapted to growth in IECs than in Vero cells, and the titer of the IEC cultures was $10^{4.5}$ $TCID_{50}$/0.1 mL at passage 45. Mutations in the S protein increased with the viral passage and the mutations tended towards attenuation. Viral challenge showed that the survival of IEC-adapted cultures was higher at the 45th passage than at the 5th passage. The use of IECs to isolate and propagate PEDV provides an effective approach for laboratory-based diagnosis of PEDV, as well as studies of the epidemiological characteristics and molecular biology of this virus.

Keywords: porcine epidemic diarrhea virus (PEDV) NJ strain; porcine intestinal epithelial cells; isolation and identification

1. Introduction

Porcine epidemic diarrhea (PED), which is caused by the porcine epidemic diarrhea virus (PEDV), is an acute and highly contagious enteric viral disease in nursing pigs. PED is characterized by vomiting and lethal watery diarrhea; and is a global problem, especially in many swine-producing countries [1–7]. PED was first reported in feeder pigs and fattening swine in the United Kingdom in 1971 [8]; since then, it has emerged in numerous European and Asian countries, resulting in tremendous economic losses to the pork industry worldwide. In 2013, the first PED outbreak was reported in the U.S.; subsequently, the outbreak spread rapidly across the country, and similar outbreaks were also reported in Canada and Mexico [4–7]. In China, PED outbreaks have occurred infrequently with only sporadic incidents [9,10]. However, in late 2010, a remarkable increase in PED outbreaks was reported in the pork-producing provinces [11,12]. In 2014, an outbreak of severe acute diarrhea, with high morbidity and mortality, occurred in sucking piglets in Nanjing, China. Herds vaccinated with the CV777-inactivated vaccine were also infected.

During this period, the effectiveness of the CV777-based vaccine was questioned as PED outbreaks also occurred in vaccinated herds [12]. PED has since become one of the most significant epidemics affecting pig farming in China [13]. PEDV is an enveloped, single-stranded, positive-sense RNA virus belonging to the genus *Alphacoronavirus*, family *Coronaviridae*, and order *Nidovirales* [14,15]. The size of its genome is approximately 28 kb, with 5′- and 3′- untranslated regions (UTRs) and seven open reading frames (ORFs) that encode four structural proteins, i.e., spike (S), envelope (E), membrane (M), and nucleocapsid (N), and three nonstructural proteins [10,16]. The S protein of PEDV is the major enveloped protein of the virion, associated with growth adaptation in vitro and attenuation in vivo [17]. In addition, the S glycoprotein is used to determine the genetic relatedness among PEDV isolates and for developing diagnostic assays and effective vaccines [18–20].

The ability to propagate the virus is critical for the diagnosis and molecular analysis of PEDV, particularly the development of inactivated or attenuated vaccine. However, propagation of PEDV in vitro is challenging. Even though PEDV may be isolated from clinical samples, it gradually loses its infectivity during further passages in cell culture [4]. Therefore, it is necessary to evaluate the disinfection efficiency in vitro viral isolates using a cell culture system that promotes growth of PEDV. Currently, several PEDV strains, such as CV777, KPEDV-9, and 83P-5, have been successfully propagated in Vero cells using media with added trypsin [21–23]. In recent years, new variants of PEDV have emerged that are difficult to isolate and propagate in Vero cells with trypsin. Researchers have attempted to use pig bladder and kidney cells to isolate PEDV, with the addition of trypsin to the medium; this is the first report of isolation of PED virus in porcine cell culture [24]. PEDV infects the epithelium of the small intestine, which is a protease-rich environment, and causes atrophy of the villi resulting in diarrhea and dehydration; this indicates that porcine intestinal epithelial cells are the target cells of this virus. In 2014, Wang et al. established a porcine intestinal epithelial cell line (ZYM-SIEC02) by introducing the human telomerase reverse transcriptase (hTERT) gene into small intestinal epithelial cells derived from a neonatal, unsuckled piglet [25]. Several studies have used this established porcine intestinal epithelial cell (IEC) line [26,27]; however, the characteristics of PEDV cultured in this cell line have not been reported.

The present study aimed to confirm and identify PEDV in samples collected from piglets with suggestive clinical signs, using the IEC line established by Wang et al. [25]. A PEDV isolate, named PEDV strain NJ, was successfully isolated. Our results show that the PEDV strain NJ is adapted to growth in IECs with media containing trypsin, suggesting a new approach for the propagation of PEDV. Furthermore, the phylogeny and mutations of the *S* gene during serial passages were analyzed to determine its genetic homology and molecular variability. A virulence experiment for IEC-adapted NJ also confirmed that the virus had a tendency towards attenuation at 45 passages.

2. Materials and Methods

All applicable international and national guidelines for the care and use of animals were followed. Approval (2016NEFU-315) was obtained from the Institutional Committee of Northeast Agricultural University for the animal experiments.

2.1. Cells and Clinical Samples

The swine intestinal epithelial cell (IEC) line established by Wang et al. was kindly provided by Prof. Yanming Zhang, College of Veterinary Medicine, Northwest A&F University, Yangling, Shaanxi, China. IEC and Vero cells (ATCC CCL-81) were cultured in Dulbecco's modified Eagle's medium (DMEM; Gibco, Grand Island, NY, USA), and supplemented with 10% fetal bovine serum (Gibco). The clinical samples (small intestine tissues) used in this study were collected from a pig farm in Nanjing, China, at which an outbreak of acute diarrhea among piglets had been reported. The virus isolated from samples was identified as PEDV by *M* gene-based reverse transcription PCR (RT-PCR). The small intestine tissue was homogenized with serum-free DMEM, and then centrifuged (Thermo Scientific Sorvall Legend Micro 17, Waltham, MA, USA) at 5000× *g* at 4 °C for 10 min. The supernatant

was filtered using 0.22-μm pore-size cellulose acetate (Merck Millipore, Darmstad, Germany), and used for virus isolation.

2.2. RNA Extraction and RT-PCR Assay

Total RNA was extracted from the clinical samples and virus cultures using the TRIzol® Plus RNA Purification Kit (Invitrogen Corp., Carlsbad, CA, USA) according to the manufacturer's instructions. Complementary DNA (cDNA) was produced via reverse transcription using the Superscript Reverse Transcriptase Reagent Kit (Takara, Tokyo, Japan) according to the manufacturer's instructions. The primer pairs of the partial *M* gene (316 bp) for identification of PEDV, 5′-TATGGCTTGCATCACTCTTA-3′ (forward) and 5′-TTGACTGAACGACCAACACG-3′ (reverse), were designed based on PEDV strain CV777, using the cDNA as a template. The PCR reaction system in a total volume of 50 μL was as follows: 5 μL of 10× buffer, 3 μL of cDNA, 1 μL of LA Taq polymerase (TaKaRa, Tokyo, Japan), 2 μL of forward primer (10 μM), 2 μL of reverse primer (10 μM), 4 μL of dNTPs mix-ture (2.5 μM), and sterile water added up to 50 μL. The cycling parameters for PCR included 95 °C for 5 min, followed by 30 cycles at 94 °C for 30 s, 55.5 °C for 30 s followed by 72 °C for 30 s, and a final extension at 72 °C for 10 min. The PCR purified products were cloned into pMD-19T vector and sequenced by Comate Bioscience Company Limited (Jilin, China).

2.3. Virus Isolation

In this study, Vero cells and IECs were used to propagate PEDV. For the propagation of PEDV using Vero cells, the confluent cell monolayer was washed once with sterile phosphate-buffered saline (PBS; pH 7.2), and incubated with 1 mL of inoculum for 1 h in a T25 flask supplemented with 21 μg/mL of trypsin (Gibco) at 37 °C under 5% CO_2. Then, the inoculum was removed and the cells were washed twice with PBS, and 4 mL of maintenance medium (DMEM, Gibco) without fetal bovine serum supplemented with 5 μg/mL trypsin was added to the flask. The propagation of PEDV using IECs was performed according to the method described above, but with the use of 10 μg/mL of trypsin during adsorption. In parallel, cells mock-inoculated with DMEM were used as control. The PEDV infected cells and viral control cells were cultured at 37 °C under 5% CO_2. The cytopathic effect (CPE) was monitored daily, and cells were harvested until the CPE exceeded 80%. After one freeze-thaw cycle, the supernatants were collected, packed separately, and stored at −80 °C until required. Virus titer was measured in 96-well plates by 10-fold serial dilution of samples at five-passage intervals. The 50% tissue culture infective dose ($TCID_{50}$) was expressed as the reciprocal of the highest dilution showing CPE by the Reed–Muench method.

2.4. Electron Microscopy Assay

The supernatants of PEDV-infected IEC cultures were centrifuged at 3000× *g* for 45 min, followed by ultracentrifugation through a 25% sucrose cushion at 30,000× *g* for 2 h at 4 °C. Virus particles were resuspended in 100 μL of DMEM and observed by transmission electron microscopy (H-7650, Hitachi, Tokyo, Japan). For imaging of virions in infected IECs, PEDV-infected cells were fixed using 2.5% glutaraldehyde at 4 °C for 8 h, washed twice with PBS, and post-fixed with 2% osmium tetroxide at room temperature (20 °C–25 °C) for 50 min. After three washes with PBS, cells were dehydrated through a graded ethanol propylene oxide series and embedded. Then, ultra-thin sections were prepared and imaged via transmission electron microscopy.

2.5. Immunofluorescence Assay

After inoculation for 24 h, mock-infected IECs and IECs infected with PEDV, at multiplicity of infection (MOI) of 0.1 were fixed with 4% paraformaldehyde at room temperature (20 °C–25 °C) for 15 min, permeabilized with 0.2% Triton X-100 in PBS at room temperature (RT) for 10 min, and blocked with 0.3% bovine serum albumin in PBS at 37 °C for 30 min. Next, mouse anti-PEDV S protein monoclonal antibody (developed in our laboratory) and fluorescein isothiocyanate (FITC)-conjugated

goat anti-mouse immunoglobulin G (IgG) (ZSGB-BIO, Beijing, China) were incubated as first and second antibodies, respectively, followed by counterstaining with 4,6-diamidino-2-phenylindole (DAPI, Beyotime, Shanghai, China). The coverslips were mounted on microscope glass slides in mounting buffer and cell staining was examined using a fluorescence microscope (Leica, Wetzlar, Germany).

2.6. Sequence Alignment and Phylogenetic Analysis of the S Gene

To monitor the amino acid variation of the S protein during the serial passaging, the parental NJ strain and the strain at different passages, i.e., NJ (15th), NJ (30th) and NJ (45th), were evaluated by RT-PCR. The *S* gene was amplified in four fragments using KOD-Plus-Neo (Toyobo, Osaka, Japan). The primers used were previously described by Zhao et al. [28]. The four fragments were amplified under same program of 2 min at 94 °C, 30 cycles of 10 s at 98 °C, 30 s at 52 °C and 1.5 min at 68 °C, and a final extension at 68 °C for 7 min. The purified PCR products were cloned into pMD-19T vector and sequenced by Comate Bioscience Company Limited (Jilin, China). The sequence analysis was performed using MegAlign in DNAStar Lasergene V 7.10 (DNAstar, Madison, WI, USA). To determine the relationships among the *S* gene of the representative PEDV isolates, phylogenetic analysis of the parent NJ strain was performed by the neighbor-joining method using molecular evolutionary genetics analysis (MEGA) software (version 4.0). Bootstrap values were estimated for 1000 replicates. The *S* gene sequences of PEDV strain NJ and the sequences of 33 known PEDV strains (listed in Table 1) retrieved from GenBank were subjected to comparative analysis.

Table 1. Reference strains of porcine epidemic diarrhea virus (PEDV) used in this study.

Strain	ID	Country	Strain	ID	Country
83P-5 (parent)	AB548618	Japan	HLJ-2012	JX512907	China
83P-5 (34th)	AB548619	Japan	IA1	KF468753	USA
83P-5 (100th)	AB548621	Japan	IA2	KF468754	USA
AD02	KC879281	South Korea	ISU13-19338E-IN-homogenate	KF650370	USA
AH2012	KC210145	China	ISU13-19338E-IN-passage3	KF650371	USA
BJ-2012-1	JX435299	China	ISU13-19338E-IN-passage9	KF650372	USA
Br1/87	Z25483	France	JS2008	KC109141	China
CH9-FJ	JQ979287	China	JS-HZ2012	KC210147	China
CH22-JS	JQ979290	China	KH	AB548622	Japan
CHGD-01	JN980698	China	LJB/03	DQ985739	China
Chinju99	AY167585	Korea	MK	AB548624	Japan
CH/S	JN547228	China	MN	KF468752	USA
CV777 vaccine	JN599150	China	NK	AB548623	Japan
CV777	AF353511	Belgium	YN1	KT021227	China
DR13	JQ023161	Korea	YN15	KT021228	China
DR13 (Attenuated)	JQ023162	Korea	YN144	KT021232	China
DX	JN104080	China			

2.7. Virulence Experiment for IEC-Adapted NJ

The in vivo swine studies were performed in a biosafety level-2 (BSL-2) laboratory. For the identification of attenuation, the pathogenicity of the lower and higher generations of NJ should be compared. PEDV NJ cultures propagated in IECs at passages 5 and 45 were used in this study. The PEDV-negative piglets as confirmed by RT-PCR method were neonatal landraces obtained from a pig farm without a PED outbreak or vaccination with PEDV vaccine. We randomly selected 20 healthy piglets as experimental animals. The piglets were divided into three groups. The two infected groups (eight pigs for each group) received an oral dose of $10^{4.5}$ median tissue culture infective dose ($TCID_{50}$)/mL of IEC-adapted NJ (5 mL) at passages 5 and 45, and the control group (n = 4) was orally administered virus-free cell culture media. The clinical signs and survival percentage of the piglets were monitored daily over a 10-day observation period, and stool samples were collected daily. The small intestine tissue samples were collected and stored at −80 °C until required. RT-PCR and immunofluorescence assays were performed to detect PEDV in the stool samples.

Necropsy was performed when the challenged piglets died post inoculation. The piglets were handled and maintained under strict ethical conditions according to international recommendations for animal welfare.

3. Results

3.1. Virus Isolation

PEDV was isolated from PEDV-positive samples collected from pig farms in China, using Vero cells and IECs, in which a severe outbreak of acute diarrhea had been reported in sucking piglets. The genomic RNA of the serially propagated virus was extracted and identified by RT-PCR. Vero cell cultures were negative for the *M* gene after two passages (Figure 1A), and no CPEs were observed in Vero cells during serial passaging (Figure 1C,D). IEC-adapted PEDV was successfully propagated (Figure 1B), and visible CPEs were observed at each passage; compared with uninfected IECs, the PEDV-infected IECs were characterized by cell fusion, syncytial and vacuole formation in the initial stage, then shrinkage, detachment, and amotic at 72 h post-inoculation (Figure 1E,F). The virus cultured in IECs and designated NJ was biologically cloned by three rounds of plaque purification in IECs prior to further virus characterization. These results demonstrate that the adaption of the PEDV strain NJ to growth in IECs was better than that in Vero cells, indicating that IECs are suitable for the isolation of PEDV from clinical samples.

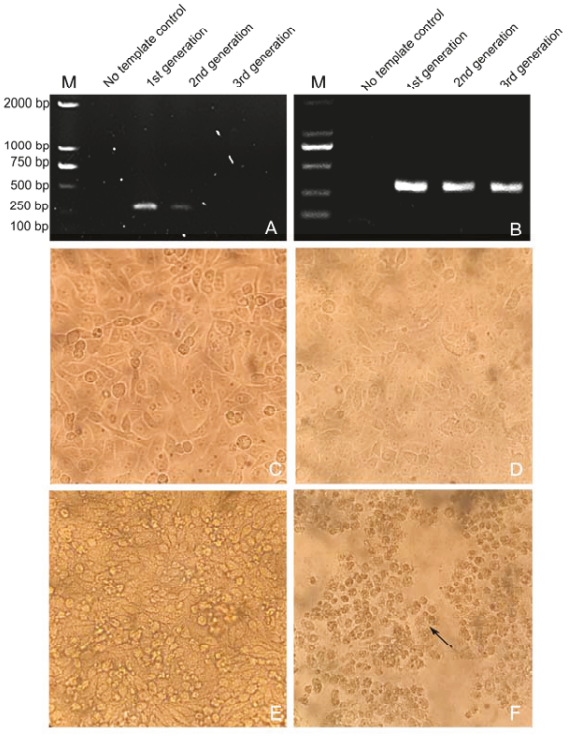

Figure 1. Isolation and identification of PEDV strain NJ in Vero cells and intestinal epithelial cell (IEC) cultures. (**A**) Identification of PEDV cultured in Vero cells at serial passages, by reverse transcription PCR (RT-PCR); (**B**) Identification of PEDV cultured in IEC at serial passages, by RT-PCR; (**C**) Control (uninfected) Vero cells; (**D**) PEDV-infected Vero cells; (**E**) Control (uninfected) IECs; (**F**) PEDV-infected IECs.

3.2. Determination of Viral Titer

The viral titer of the PEDV strain NJ propagated in IECs was determined at 5-passage intervals. The viral titer of the IEC-adapted PEDV strain NJ reached $10^{4.5}$ $TCID_{50}$/0.1 mL at passage 45 (Figure 2), suggesting that the use of an IEC culture is a promising approach for propagating PEDV.

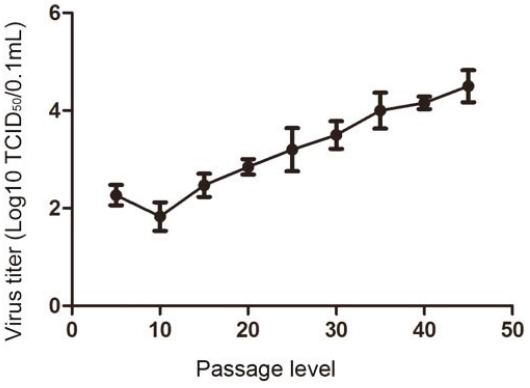

Figure 2. Viral titers of PEDV strain NJ propagated in IECs post-serial passages. All the results of a representative experiment performed with triplicate samples are shown.

3.3. Electron Microscopy

As shown in Figure 3A, the virion was circular in shape and 80–120 nm in diameter, with surface projections characteristic of coronaviruses. Thin sections of the PEDV strain NJ-infected IECs showed some of the virus particles appeared, many of the virus particles possessed a dense core, and masses of virus particles gathered in the cytoplasm at 24 h post-infection (Figure 3B).

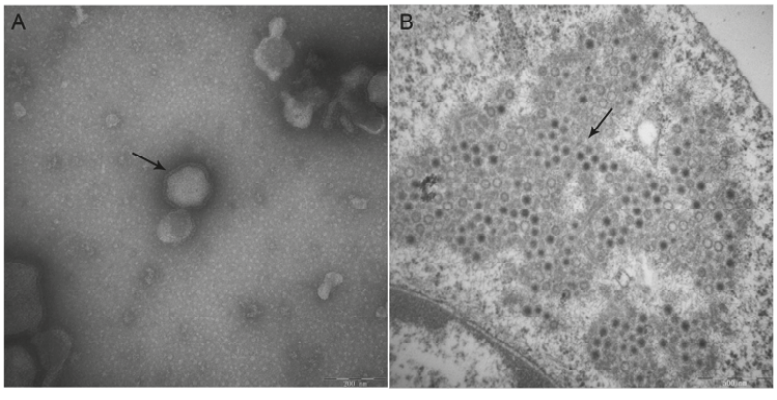

Figure 3. Images of PEDV strain NJ particles and PEDV strain NJ-infected IEC produced by electron microscopy. (**A**) Virions in culture media of IECs infected with PEDV strain NJ, as shown by the arrow; Bar = 200 nm. Magnification, ×100,000; (**B**) Thin section of IECs infected with PEDV strain NJ 24 h post-infection; many of the virus particles possessed a dense core and gathered in the cytoplasm as shown by the arrow; Bar = 500 nm. Magnification, ×50,000.

3.4. Immunofluorescence

Infection of IECs with the PEDV strain NJ was confirmed by immunofluorescence assay (Figure 4). PEDV strain NJ and cell nuclei were detected using mouse anti-PEDV S protein monoclonal antibody and 4,6-diamidino-2-phenylindole (DAPI), respectively. Specific green signals were observed in the PEDV strain NJ-infected IECs, but not in the mock-infected IECs. However, because the immunofluorescence assay was performed after inoculation for 24 h, the CPE was hard to observe during this period.

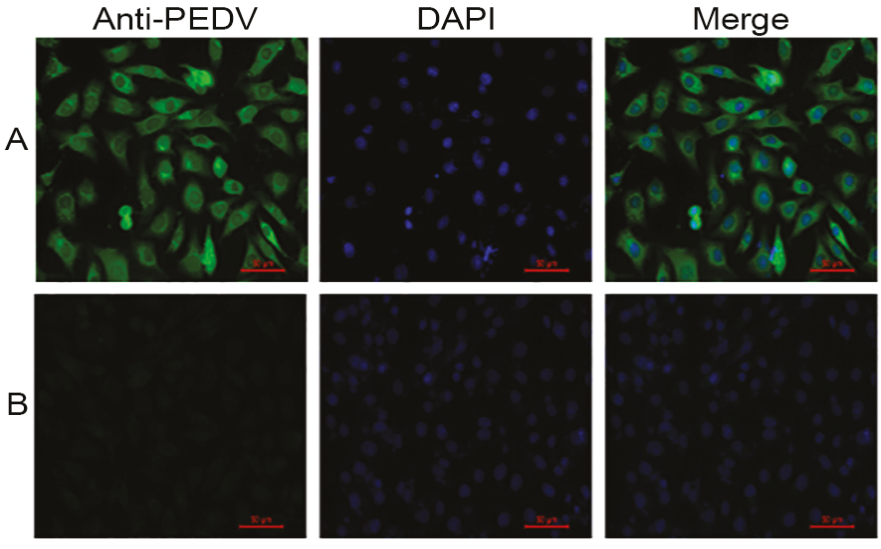

Figure 4. Detection of PEDV strain NJ in IECs by immunofluorescence assay at 24 h post-infection; mouse anti-PEDV S protein monoclonal antibody and fluorescein isothiocyanate (FITC)-conjugated goat anti-mouse immunoglobulin G (IgG) were respectively used as primary and secondary antibodies, followed by counterstaining with 4,6-diamidino-2-phenylindole (DAPI). (**A**) PEDV strain NJ-infected IECs; (**B**) Non-infected IECs.

3.5. Phylogenetic Analysis of the S Gene

The *S* gene of PEDV strain NJ was amplified by RT-PCR. Phylogenetic analysis based on the *S* gene was performed between parental PEDV strain NJ and other PEDV strains listed in Table 1. Phylogenetic analyses of *S* gene sequences revealed that all PEDV strains in this study could be separated into two groups: the NJ strain belonged to Group 1, which also contained classical PEDV CV777 and some strains isolated from China, Japan, and South Korea. As shown in Figure 5, the *S* gene of the parent NJ strain exhibited high sequence similarity with the epidemic strains CH9-FJ, CH22-JS, and DX isolated from southern China in recent years. These results suggest that the Chinese southern epidemic PEDV strains were likely derived from the same source. In addition, we did not find any insertions and deletions (INDEL) in the *S* gene compared with the Chinese PEDV *S* gene recombinant variants like IA1, IA2, and MN identified in U.S.

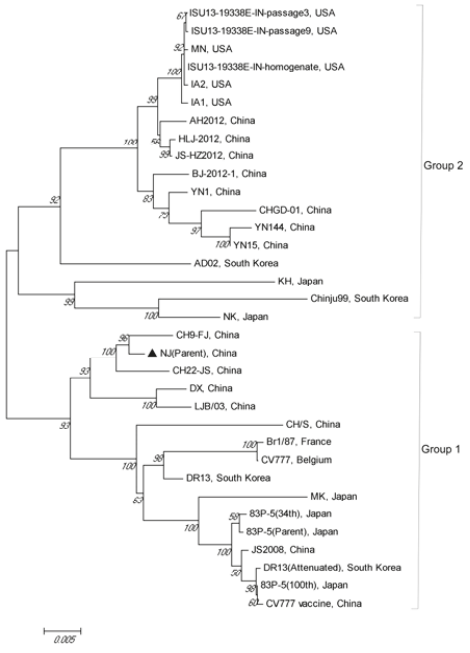

Figure 5. Phylogenetic analysis of PEDV strain NJ based on the *S* gene.

3.6. Amino Acid Variability of the S Protein of IEC-Adapted NJ after Serial Passaging

To evaluate the amino acid variability of the IEC-adapted PEDV strain NJ during serial passagings, the sequences of the *S* gene of the parent NJ and those of the virus at the 15th, 30th and 45th passage were amplified by RT-PCR. These amino acid sequences were then compared with the corresponding S protein sequences of the classical PEDV CV777 and its vaccine strain. The positions of amino acid changes were 3, 15, 70, 114, 282, 324, 378, 438, 973, 1023 and 1167 respectively (Table 2). In total, four mutations occurred at passage 15, three and four more mutations occurred at passages 30 and 45. The eight (8/11) mutations were the same as the ones occurring in the transition from classical PEDV CV777 to the CV777 vaccine strain during serial passaging, which suggested that the NJ might exhibit a tendency towards attenuation.

Table 2. The amino acid variation of S proteins during the serial passaging compared with CV777 and its vaccine strain.

Strain	Amino Acid Position										
	3	**15**	**70**	**114**	**282**	**324**	**378**	**438**	**973**	**1023**	**1167**
NJ(Parent)	S	S	A	N	L	S	N	I	Y	K	A
NJ(15th)	S	S	D	N	L	S	N	I	H	N	D
NJ(30th)	A	S	D	S	L	S	K	I	H	N	D
NJ(45th)	A	L	D	S	W	R	K	L	H	N	D
CV777	S	P	A	N	L	S	N	I	Y	K	A
CV777 vaccine	P	L	D	S	W	F	K	V	H	N	D

3.7. Pathogenicity Analysis of PEDV Strain NJ

To compare the pathogenicity of the lower-generation NJ with that of the higher-generation NJ, 5 mL of the IEC-adapted NJ culture at the 5th and 45th passage ($10^{4.5}$ $TCID_{50}$/mL) and volume-matched

virus-free cell culture medium were administrated orally to the piglets. The clinical signs and survival percentage of the piglets was monitored daily over a 10-day observation period. All piglets infected with 5th passage cultures and three (3/8) piglets infected with 45th passage cultures showed diarrheic feces, significantly emaciated body condition, and experienced severe watery diarrhea with vomiting. Abundant yellow, watery, and foul-smelling stools were also observed around the perianal region of the piglets infected with 45th passage virus (Figure 6A,B). The remaining five (5/8) piglets infected with 45th passage showed signs of mild diarrhea after inoculation that seemed to be transient. However, in the control group, the piglets were healthy without watery diarrhea (data not shown). As shown in Figure 6E, one piglet death occurred within 3 days and in total seven piglets died after the 10-day challenge in the group that received the 5th passage. However, only three piglets died in the group that received the 45th passage; although the remaining piglets had the significant clinical signs of PED, they survived the 10-day challenge. The small intestines of one of the dead piglets infected with 45th passage IEC-adapted NJ developed severe clinical symptoms, the same as those in the piglets infected with the 5th passage virus. The small intestines were typically distended with accumulation of yellow fluid and mesenteric congestion, and the small intestinal wall was thin and transparent (Figure 6C,D). The diarrheal feces and intestinal tissues collected from these piglets were analyzed by RT-PCR targeting the *M* gene, and the PCR products were found to be consistent with the expected result. Moreover, immunofluorescence analysis of the small intestine tissue revealed that the viral antigen was predominantly present in the small intestines (data not shown).

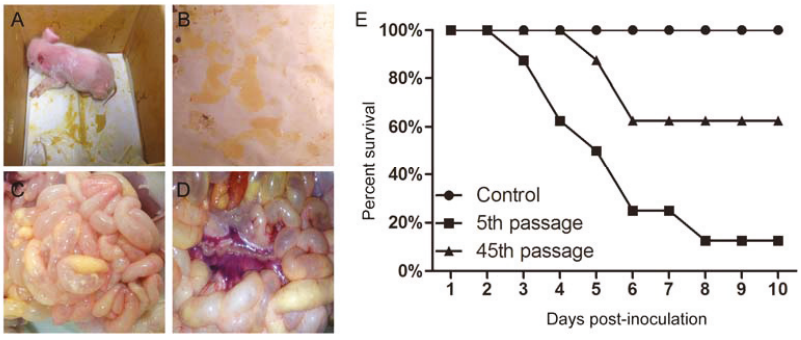

Figure 6. The clinical signs and necropsies of results of pigs infected with IEC-adapted NJ at 45th passage and the survival percentage of piglets after challenge. (**A**) Piglet with diarrhea and significantly dispirited status; (**B**) Watery diarrhea; (**C**) The intestinal tracts of infected piglets were thin and transparent; (**D**) Mesenteric congestion; (**E**) Survival percentage of piglets after challenge.

4. Discussion

The spread of PED to the U.S. and Canada has established that this viral infection represents a global epidemic [29] that has resulted in enormous economic losses to pig production. PEDV has caused similar economic losses to the pork industry in China, where frequent outbreaks have been recently reported [30]. Following the development of a CV777-based vaccine, based on the PEDV strain, and its wide application in the pig industry in China, only a limited number of incidents occurred before 2010; however, PED outbreaks have subsequently increased in frequency, particularly in pig-farming provinces. Notable, even pigs vaccinated with the CV777-based vaccine were found to be infected [31], indicating the need for the development of effective PEDV-based vaccines for the control of PED outbreaks.

To date, the propagation of PEDV remains challenging. Although Vero cells are commonly used to propagate PEDV, viral infectivity exhibits a gradual decline during serial passage in these cells. Many PEDV strains isolated from clinical samples were difficult to culture in Vero cells in recent

years [4,32,33]. The adaptability of PEDV isolate infected with cell lines was the first step to successful isolation in vitro. Thus, it is urgent to develop new methods or cell lines to improve the tropism of PEDV cultured in cells. In this study, we successfully isolated and propagated the epidemic PEDV strain using porcine intestinal epithelial cells in vitro, and demonstrated that these cells are more suitable than Vero cells for the isolation of PEDV. This is the first report on the characteristics of PEDV cultured in this cell line which was established by Wang et al. [25].

The porcine intestinal epithelial cell is recognized as the target cell of PEDV [27]. Porcine aminopeptidase N (pAPN), a functional receptor of PEDV that is highly expressed in the small intestinal mucosa, plays a critical role in PEDV infection [31]. In addition, endogenous protease in the small intestine of porcine can cleave the S protein of PEDV in vivo and facilitate entry of PEDV virions into intestinal epithelial cells, resulting in massive propagation [34]. PEDV strain NJ isolated from clinical samples was as difficult to culture in Vero cells as other isolated prevalent PEDV strains; this is mainly attributed to mutations that arise in genes encoding spike proteins during serial passage. Moreover, the low levels of pAPN in Vero cells are thought to limit the attachment and entry of variant viruses. Before this study, we compared the isolation rate of five different positive PEDV strains isolated from clinical samples cultured in IECs and Vero cells. We found all the CPEs in Vero cells were invisible in three generations, and four PEDV isolates could not be detected by RT-PCR after two generations. In contrast, porcine IECs are more suitable than Vero cells for propagating PEDV isolated from clinical samples in vitro. The CPEs in IECs could be observed at the first or the third passage, and at each passage, cultures could be detected. Due to the characteristics of coronavirus, the degradation of the virus impacts the efficiency of the infection. The S glycoprotein forms peplomers on the virion envelope and contains receptor-binding regions and four major antigenic sites [35,36]; therefore, to minimize damage to the surface projections of the virus, the infected IECs were freeze-thawed only once before inoculation. The PEDV strain NJ was detected in cell culture during serial passages, by RT-PCR as well as immunofluorescence assay, indicating that this strain adapted to infection of IECs. Owing to the sensitivity of IECs, the trypsin concentration used in IEC culture was lower than that used in Vero cells during PEDV absorption. The viral titer of the IEC-adapted PEDV strain NJ propagated in IECs increased gradually and reached $10^{4.5}$ $TCID_{50}$/0.1 mL at 45 passages.

The S protein of PEDV is known to play pivotal roles in viral entry and in inducing the neutralizing antibodies in natural hosts, which makes it a primary target for development of effective vaccines against PEDV [23,37–39]. In this study, the *S* gene of the PEDV strain NJ was amplified by RT-PCR, and its genetic diversity and phylogenetic relationships were analyzed. *S* gene-based phylogenetic analysis showed that the PEDV strain NJ is closely related to the CH9-FJ, CH22-JS, and DX strains isolated from southern China in recent years. In addition, we did not find any insertions or deletions (INDEL) in the *S* gene compared to the Chinese PEDV *S* gene recombinant variants like IA1, IA2, and MN identified in the U.S.

The differences in virulence and genome sequences between the parental strain and derived attenuated strains have been extensively studied [40,41]. To investigate the genetic variability of the S protein of the PEDV strain NJ, the *S* gene was amplified during various serial passages and analyzed. Compared with the parent NJ strain, four mutations in the S protein occurred after the 15th passage, and then another seven mutations occurred after the 30th passage. In total, 11 amino acids changed during 45 passages. The eight (8/11) mutations were the same as those occurring in the transition from the classical PEDV CV777 strain to CV777 vaccine strain during serial passaging, which suggests that the high-passage IEC-adapted NJ might show attenuation. However, the molecular basis of viral adaptation to IECs remains a subject for future investigation.

Furthermore, to identify attenuation, the pathogenicity was compared for the lower- and higher-generation NJ. The piglets were inoculated with 5 mL of the IEC-adapted PEDV strain NJ ($10^{4.5}$ $TCID_{50}$/mL) at the 5th and 45th passages. We found that all of the piglets infected with 5th passage IEC-adapted cultures showed severe watery diarrhea with vomiting, and seven (7/8) piglets died by day 10 post inoculation. However, only three (3/8) piglets infected with viral cultures at the

45th passage showed significant PED signs, such as diarrheic feces and emaciated body condition; the remaining five (5/8) piglets showed mild diarrhea after inoculation that seemed to be transient, and only three piglets died by day 10 post inoculation. The in vivo challenge experiment implied that IEC-adapted NJ at a high passage number had a tendency towards attenuation. The mutations in the S protein during serial passaging might play a major role in the attenuation of virulence, and might suggest potential genetic changes for a candidate attenuated vaccine. However, the genetic mutations in the whole genome of the NJ strain during passages needs to be investigated further.

In conclusion, we successfully isolated and identified a novel PEDV, strain NJ, from clinical samples using IECs. The adaption of the PEDV strain NJ to growth in IECs was better than that in Vero cells. To our knowledge, this is the first report to describe the isolation and characterization of the IEC-adapted PEDV strain NJ. Furthermore, the present work reveals a novel approach for the propagation of PEDV in vitro. These findings are expected to be of importance for the development and evaluation of the efficacy of vaccines against PED.

Acknowledgments: We thank Yan-Ming Zhang, College of Veterinary Medicine, Northwest A&F University, for providing the IEC line. This work was supported by the General Program of National Natural Science Foundation of China (31472226) and the National Key R & D Program (2016YFD0500100).

Author Contributions: Yijing Li and Yigang Xu conceived and designed the study. Wen Shi, Shuo Jia, Haiyuan Zhao, Jiyuan Yin, Xiaona Wang, Meiling Yu, and Sunting Ma performed the experiments. Yang Wu, Ying Chen and Wenlu Fan analyzed and interpreted the data. Wen Shi wrote the paper. All authors read and approved the manuscript.

Conflicts of Interest: The authors declare no conflict of interest.

References

1. Debouck, P.; Pensaert, M. Experimental infection of pigs with a new porcine enteric coronavirus, CV 777. *Am. J. Vet. Res.* **1980**, *41*, 219–223. [PubMed]
2. Pensaert, M.B.; de Bouck, P. A new coronavirus-like particle associated with diarrhea in swine. *Arch. Virol.* **1978**, *58*, 243–247. [CrossRef] [PubMed]
3. Wood, E.N. An apparently new syndrome of porcine epidemic diarrhoea. *Vet. Rec.* **1977**, *100*, 243–244. [CrossRef] [PubMed]
4. Chen, Q.; Li, G.; Stasko, J.; Thomas, J.T.; Stensland, W.R.; Pillatzki, A.E.; Gauger, P.C.; Schwartz, K.J.; Madson, D.; Yoon, K.-J. Isolation and characterization of porcine epidemic diarrhea viruses associated with the 2013 disease outbreak among swine in the United States. *J. Clin. Microbiol.* **2014**, *52*, 234–243. [CrossRef] [PubMed]
5. Kim, S.H.; Kim, I.J.; Pyo, H.M.; Tark, D.S.; Song, J.Y.; Hyun, B.H. Multiplex real-time RT-PCR for the simultaneous detection and quantification of transmissible gastroenteritis virus and porcine epidemic diarrhea virus. *J. Virol. Methods* **2007**, *146*, 172–177. [CrossRef] [PubMed]
6. Ojkic, D.; Hazlett, M.; Fairles, J.; Marom, A.; Slavic, D.; Maxie, G.; Alexandersen, S.; Pasick, J.; Alsop, J.; Burlatschenko, S. The first case of porcine epidemic diarrhea in Canada. *Can. Vet. J.* **2015**, *56*, 149–152. [PubMed]
7. Trujillo-Ortega, M.E.; Beltran-Figueroa, R.; Garcia-Hernandez, M.E.; Juarez-Ramirez, M.; Sotomayor-Gonzalez, A.; Hernandez-Villegas, E.N.; Becerra-Hernandez, J.F.; Sarmiento-Silva, R.E. Isolation and characterization of porcine epidemic diarrhea virus associated with the 2014 disease outbreak in Mexico: Case report. *BMC Vet. Res.* **2016**, *12*, 132. [CrossRef] [PubMed]
8. Oldham, J. Letter to the editor. *Pig Farming* **1972**, *10*, 72–73. [CrossRef]
9. Bi, J.; Zeng, S.L.; Xiao, S.B.; Chen, H.C.; Fang, L.R. Complete Genome Sequence of Porcine Epidemic Diarrhea Virus Strain AJ1102 Isolated from a Suckling Piglet with Acute Diarrhea in China. *J. Virol.* **2012**, *86*, 10910–10911. [CrossRef] [PubMed]
10. Chen, J.; Wang, C.; Shi, H.; Qiu, H.; Liu, S.; Chen, X.; Zhang, Z.; Feng, L. Molecular epidemiology of porcine epidemic diarrhea virus in China. *Arch. Virol.* **2010**, *155*, 1471–1476. [CrossRef] [PubMed]
11. Li, W.; Li, H.; Liu, Y.; Pan, Y.; Deng, F.; Song, Y.; Tang, X.; He, Q. New variants of porcine epidemic diarrhea virus, China, 2011. *Emerg. Infect. Dis.* **2012**, *18*, 1350–1353. [CrossRef] [PubMed]

12. Luo, Y.; Zhang, J.; Deng, X.; Ye, Y.; Liao, M.; Fan, H. Complete genome sequence of a highly prevalent isolate of porcine epidemic diarrhea virus in South China. *J. Virol.* **2012**, *86*, 9551. [CrossRef] [PubMed]
13. Sun, R.Q.; Cai, R.J.; Chen, Y.Q.; Liang, P.S.; Chen, D.K.; Song, C.X. Outbreak of porcine epidemic diarrhea in suckling piglets, China. *Emerg. Infect. Dis.* **2012**, *18*, 161–163. [CrossRef] [PubMed]
14. Duarte, M.; Gelfi, J.; Lambert, P.; Rasschaert, D.; Laude, H. Genome organization of porcine epidemic diarrhoea virus. *Adv. Exp. Med. Biol.* **1993**, *342*, 55–60. [PubMed]
15. Spaan, W.; Cavanagh, D.; Horzinek, M.C. Coronaviruses: Structure and genome expression. *J. Gen. Virol.* **1988**, *69*, 2939–2952. [CrossRef] [PubMed]
16. Song, D.; Park, B. Porcine epidemic diarrhoea virus: A comprehensive review of molecular epidemiology, diagnosis, and vaccines. *Virus Genes* **2012**, *44*, 167–175. [CrossRef] [PubMed]
17. Sato, T.; Takeyama, N.; Katsumata, A.; Tuchiya, K.; Kodama, T.; Kusanagi, K. Mutations in the spike gene of porcine epidemic diarrhea virus associated with growth adaptation in vitro and attenuation of virulence in vivo. *Virus Genes* **2011**, *43*, 72–78. [CrossRef] [PubMed]
18. Lee, S.; Lee, C. Outbreak-related porcine epidemic diarrhea virus strains similar to US strains, South Korea, 2013. *Emerg. Infect. Dis.* **2014**, *20*, 1223–1226. [CrossRef] [PubMed]
19. Lee, D.K.; Park, C.K.; Kim, S.H.; Lee, C. Heterogeneity in spike protein genes of porcine epidemic diarrhea viruses isolated in Korea. *Virus Res.* **2010**, *149*, 175–182. [CrossRef] [PubMed]
20. Gerber, P.F.; Gong, Q.; Huang, Y.W.; Wang, C.; Holtkamp, D.; Opriessnig, T. Detection of antibodies against porcine epidemic diarrhea virus in serum and colostrum by indirect ELISA. *Vet. J.* **2014**, *202*, 33–36. [CrossRef] [PubMed]
21. Hofmann, M.; Wyler, R. Propagation of the virus of porcine epidemic diarrhea in cell culture. *J. Clin. Microbiol.* **1988**, *26*, 2235–2239. [PubMed]
22. Kusanagi, K.; Kuwahara, H.; Katoh, T.; Nunoya, T.; Ishikawa, Y.; Samejima, T.; Tajima, M. Isolation and serial propagation of porcine epidemic diarrhea virus in cell cultures and partial characterization of the isolate. *J. Vet. Med. Sci.* **1992**, *54*, 313–318. [CrossRef] [PubMed]
23. Kweon, C.H.; Kwon, B.J.; Lee, J.G.; Kwon, G.O.; Kang, Y.B. Derivation of attenuated porcine epidemic diarrhea virus (PEDV) as vaccine candidate. *Vaccine* **1999**, *17*, 2546–2553. [CrossRef]
24. Shibata, I.; Tsuda, T.; Mori, M.; Ono, M.; Sueyoshi, M.; Uruno, K. Isolation of porcine epidemic diarrhea virus in porcine cell cultures and experimental infection of pigs of different ages. *Vet. Microbiol.* **2000**, *72*, 173–182. [CrossRef]
25. Wang, J.; Hu, G.; Lin, Z.; He, L.; Xu, L.; Zhang, Y. Characteristic and functional analysis of a newly established porcine small intestinal epithelial cell line. *PLoS ONE* **2014**, *9*, e110916. [CrossRef] [PubMed]
26. Li, W.; Wang, G.; Liang, W.; Kang, K.; Guo, K.; Zhang, Y. Integrin beta3 is required in infection and proliferation of classical swine fever virus. *PLoS ONE* **2014**, *9*, e110911.
27. Xu, X.; Zhang, H.; Zhang, Q.; Dong, J.; Liang, Y.; Huang, Y.; Liu, H.J.; Tong, D. Porcine epidemic diarrhea virus E protein causes endoplasmic reticulum stress and up-regulates interleukin-8 expression. *Virol. J.* **2013**, *10*, 26. [CrossRef] [PubMed]
28. Zhao, P.D.; Tan, C.; Dong, Y.; Li, Y.; Shi, X.; Bai, J.; Jiang, P. Genetic variation analyses of porcine epidemic diarrhea virus isolated in mid-eastern China from 2011 to 2013. *Can. J. Vet. Res.* **2015**, *79*, 8–15. [PubMed]
29. Kim, S.H.; Lee, J.M.; Jung, J.; Kim, I.J.; Hyun, B.H.; Kim, H.I.; Park, C.K.; Oem, J.K.; Kim, Y.H.; Lee, M.H.; et al. Genetic characterization of porcine epidemic diarrhea virus in Korea from 1998 to 2013. *Arch. Virol.* **2015**, *160*, 1055–1064. [CrossRef] [PubMed]
30. Gao, Y.; Kou, Q.; Ge, X.; Zhou, L.; Guo, X.; Yang, H. Phylogenetic analysis of porcine epidemic diarrhea virus field strains prevailing recently in China. *Arch. Virol.* **2013**, *158*, 711–715. [CrossRef] [PubMed]
31. Li, B.X.; Ge, J.W.; Li, Y.J. Porcine aminopeptidase N is a functional receptor for the PEDV coronavirus. *Virology* **2007**, *365*, 166–172. [CrossRef] [PubMed]
32. Oka, T.; Saif, L.J.; Marthaler, D.; Esseili, M.A.; Meulia, T.; Lin, C.M.; Vlasova, A.N.; Jung, K.; Zhang, Y.; Wang, Q. Cell culture isolation and sequence analysis of genetically diverse US porcine epidemic diarrhea virus strains including a novel strain with a large deletion in the spike gene. *Vet. Microbiol.* **2014**, *173*, 258–269. [CrossRef] [PubMed]
33. Lee, S.; Kim, Y.; Lee, C. Isolation and characterization of a Korean porcine epidemic diarrhea virus strain KNU-141112. *Virus Res.* **2015**, *208*, 215–224. [CrossRef] [PubMed]

34. Shirato, K.; Matsuyama, S.; Ujike, M.; Taguchi, F. Role of proteases in the release of porcine epidemic diarrhea virus from infected cells. *J. Virol.* **2011**, *85*, 7872–7880. [CrossRef] [PubMed]
35. Correa, I.; Jiménez, G.; Suñé, C.; Bullido, M.J.; Enjuanes, L. Antigenic structure of the E2 glycoprotein from transmissible gastroenteritis coronavirus. *Virus Res.* **1988**, *10*, 77–93. [CrossRef]
36. Gebauer, F.; Posthumus, W.; Correa, I.; Suné, C.; Sánchez, C.; Smerdou, C.; Lenstra, J.; Meloen, R.; Enjuanes, L. Residues involved in the formation of the antigenic sites of the S protein of transmissible gastroenteritis coronavirus. *Virology* **1991**, *183*, 225–238. [CrossRef]
37. Sun, D.; Feng, L.; Shi, H.; Chen, J.; Cui, X.; Chen, H.; Liu, S.; Tong, Y.; Wang, Y.; Tong, G. Identification of two novel B cell epitopes on porcine epidemic diarrhea virus spike protein. *Vet. Microbiol.* **2008**, *131*, 73–81. [CrossRef] [PubMed]
38. Park, S.J.; Moon, H.J.; Yang, J.S.; Lee, C.S.; Song, D.S.; Kang, B.K.; Park, B.K. Sequence analysis of the partial spike glycoprotein gene of porcine epidemic diarrhea viruses isolated in Korea. *Virus Genes* **2007**, *37*, 321–332. [CrossRef] [PubMed]
39. Chang, S.H.; Bae, J.L.; Kang, T.J.; Kim, J.; Chung, G.H.; Lim, C.W.; Laude, H.; Yang, M.S.; Jang, Y.S. Identification of the epitope region capable of inducing neutralizing antibodies against the porcine epidemic diarrhea virus. *Mol. Cells* **2002**, *14*, 295–299. [PubMed]
40. Song, D.S.; Yang, J.S.; Oh, J.S.; Han, J.H.; Park, B.K. Differentiation of a Vero cell adapted porcine epidemic diarrhea virus from Korean field strains by restriction fragment length polymorphism analysis of ORF 3. *Vaccine* **2003**, *21*, 1833–1842. [CrossRef]
41. Song, D.S.; Oh, J.S.; Kang, B.K.; Yang, J.S.; Moon, H.J.; Yoo, H.S.; Jang, Y.S.; Park, B.K. Oral efficacy of Vero cell attenuated porcine epidemic diarrhea virus DR13 strain. *Res. Vet. Sci.* **2007**, *82*, 134–140. [CrossRef] [PubMed]

© 2017 by the authors. Licensee MDPI, Basel, Switzerland. This article is an open access article distributed under the terms and conditions of the Creative Commons Attribution (CC BY) license (http://creativecommons.org/licenses/by/4.0/).

MDPI AG
St. Alban-Anlage 66
4052 Basel, Switzerland
Tel. +41 61 683 77 34
Fax +41 61 302 89 18
http://www.mdpi.com

Viruses Editorial Office
E-mail: viruses@mdpi.com
http://www.mdpi.com/journal/viruses

MDPI AG
St. Alban-Anlage 66
4052 Basel
Switzerland

Tel: +41 61 683 77 34
Fax: +41 61 302 89 18

www.mdpi.com

ISBN 978-3-03842-473-4